Lecture Notes in Physics

125

Nonradial and Nonlinear Stellar Pulsation

Proceedings of a Workshop
Held at the University of Arizona
in Tucson, March 12 – 16, 1979

Edited by
H. A. Hill and W. A. Dziembowski

Springer-Verlag
Berlin Heidelberg New York 1980

Editors

Henry Allen Hill
Department of Physics, The University of Arizona, Tucson, AZ 85721/USA

Wojciech A. Dziembowski
Centrum Astronomiczne PAN, ul Bantycka 18, 00–716 Warszawa/Poland

ISBN 3-540-09994-8 Springer-Verlag Berlin Heidelberg New York
ISBN 0-387-09994-8 Springer-Verlag New York Heidelberg Berlin

Printing and binding: Beltz Offsetdruck, Hemsbach/Bergstr.
2153/3140-543210

FOREWORD

A workshop was held in Tucson at the University of Arizona from March 12 through March 16, 1979 to furnish a forum for both theorists and observers to study and exchange ideas on some of the current problems in nonradial and nonlinear stellar pulsation. This workshop, sponsored by the Department of Physics in conjunction with Steward Observatory was organized into morning sessions of invited and contributed papers and into afternoon sessions of discussions and informal contributions. This structure was quite successful with many of the contributions to these workshop proceedings motivated by interactions at these sessions. The scientific success of the workshop must in large measure be the result of the strong international character of the list of participants and the constructive mode in which they worked together.

The idea for the work grew out of discussions with Drs. Robert A. Rosenbaum, former President of Wesleyan University and John P. Schaefer, President of the University of Arizona, on the scientific program at SCLERA and on how the scholarship and teaching in each of these two respective institutes might be brought closer together. The financial support which made the workshop and these proceedings possible was furnished by President Schaefer. In the planning and execution stages of the workshop, the advice and counsel of Dr. Robert H. Parmenter, Head of the Department of Physics, was frequently sought.

The Scientific Organizing Committee was Drs. W. Dziembowski, W. Fitch, H. Hill, E. Nather, S. Starrfield, H. Van Horn and R. White. The aim of the organizing committee was to maintain a balance between theory and observation and through the organization of the meeting, encourage the interaction of those working in these more often than not isolated areas of science.

The local organizing committee consisted of Drs. T. Caudell, W. Dziembowski, W. Fitch, H. Hill and R. White, and Mr. R. Bos. They were all helped during the running of the symposium by J. Logan and R. Rosenwald and by J. Brown, conference coordinator.

I would also like to thank MacMillan Journals LTD for granting permission to reprint the material in the Introduction from the workshop review by Douglas Gough in Nature.

The scientific editing was performed at the University of Arizona and in part at Wesleyan University in collaboration with visiting professor Dr. W. Dziembowski. His broad knowledge of the field of stellar pulsation was invaluable. The editing of the manuscript was performed primarily by Ms. A. Whitehead with some of the responsibility being shared by Dr. G. Harwood. The final production, supervised by Dr. T. Caudell, was a collaborative effort of all of us at SCLERA. In addition to the SCLERA staff, a significant contribution was made to the final production by Ms. J. Twehous. I express my sincere personal thanks to each person who helped complete this project.

Henry A. Hill
Tucson, Arizona
March, 1980

TABLE OF CONTENTS

INTRODUCTION*

D. Gough
University of Cambridge
United Kingdom

In recent years considerable attention has been devoted to the observation and theoretical description of variable stars. In this context the term "variable" should be taken to mean pulsating or oscillating as opposed to cataclysmic or nova. The distinction here is important; when a system is observed to oscillate, be it a star or a molecule, there exists then the potential of probing the workings of that system in a quantitative manner. It is in this spirit that the following summary of the workshop, both discussions and papers, is presented.

* * * * *

Over the past two decades the theory of the pulsation of the Classical Cepheid and RR Lyrae stars has reached a high degree of sophistication. This kind of pulsation is the simplest mode of oscillation a star can undergo: it is periodic and the motion is purely in the radial direction. Although there remain some niggling discrepancies between theory and observation, the agreement is sufficient to convince most astrophysicists that our ideas are basically correct. Thus we seem to have a firm foundation from which to extend our studies to stars whose oscillations are nonradial and nonperiodic.

Walter Fitch (Steward Observatory) reviewed observations of variable stars of δ Scuti and related type. These stars pulsate at low amplitude, and many exhibit two characteristic frequencies which bear a ratio close to that of two small integers. Consequently much of the subsequent discussion concerned direct resonances between two modes of oscillation. Arthur Cox (Los Alamos Scientific Laboratories) reported his failure to reproduce this behavior theoretically from initial value integrations even when the resonance conditions had been carefully engineered, and Robert Stellingwerf (Rutgers University), who had analyzed the stability of pairs of singly periodic limit cycles of potential double mode Cepheid models, never found both cycles to be simultaneously unstable to linear perturbations. The double mode behavior remains unexplained. During discussions of parametric resonances, it was pointed out that many of these stars seem to exhibit characteristics of strange

*Reprinted from Nature, 278, 685(1979)

attractors. Some δ Scuti stars appear to pulsate in many modes simultaneously; Wojciech Dziembowski (Copernicus Astronomical Center) estimated that nonlinearities developed by any one mode alone were too small to limit its amplitude to a value as low as those observed, and concluded that mode interactions must be responsible. Definitive calculations have not yet been performed, but techniques developed for studying oceanic gravity wave interactions and plasma turbulence are available for tackling problems of this kind. We can therefore anticipate considerable advances in this study in the near future.

A class of stars for which there is no convincing explanation is characterized by β Cephei. Myron Smith (University of Texas at Austin) reviewed the observations. The stars are of spectral type B, and lie in a strip in the Hertzsprung-Russell diagram a little above the main sequence. Mike Jerzykiewicz (Wroclaw University Observatory) and C. Sterken (Free University of Brussels) reported new observations and pointed out that almost all stars in the β Cephei strip show signs of variability. They appear to pulsate in both radial and nonradial modes. As with the β Scuti stars simple period ratios are found, which suggest again that resonance mechanisms are operating. Frequency splitting, presumably by rotation, has been measured, which offers the exciting prospect of trying to infer the angular velocity within these stars. Unfortunately we are not yet in a position to do this because the modes of oscillation have not been unambiguously identified; different workers expressed contradictory opinions about the modes they thought were responsible for the variability.

An intriguing property of some β Cephei stars is that they switch from one mode of oscillation to another on a timescale of no longer than about 10 periods. Smith argued that this is evidence that the oscillations are confined to a rather thin outer layer of the star, because otherwise it would be difficult to envision how dissipative processes could effect the enormous energy transfer that would be involved. Others contradicted that claim, citing simple nonlinear oscillators that can alter their character on a dynamical timescale. It is unlikely that it will be established in the near future whether such oscillators actually represent the behavior of β Cephei stars in any way, because the basic physics of the variability is not yet understood.

How are the oscillations driven? Morris Aizenman (National Science Foundation) reviewed the many ingenious ideas that have been proposed in the past, all of which have failed. A recent suggestion by Stellingwerf that the mechanism is no more than the Eddington valve that drives classical Cepheids and RR Lyrae stars was debated. He proposed that interpolation in opacity tables on too coarse a grid had led to an underestimate of the efficacy of the valve, but Arthur Cox, one of the chief suppliers of opacity data to the astrophysical community, claimed that though finer resolution decreased the stability of the theoretical models it was never

sufficient to render them unstable. The suggestion was made that if all the mechanisms reviewed by Aizenman were operating in unison the sum of their contributions might be sufficient to maintain the pulsations against dissipation. This idea, which is reminiscent of an early suggestion for solving the solar neutrino problem, was unenthusiastically received.

A significant fraction of the workshop was devoted to discussing oscillations of the sun. First, Henry Hill (University of Arizona) reviewed the observations spanning the period range 3^{min}-160^{min} and discussed the evidence already in the literature for the oscillations in the data being of solar origin. There followed a sequence of presentations of new observations and discussions of the longer period oscillations in the upper atmosphere and the evidence for phase coherence.

By comparing different diameter measurements made at the Santa Catalina Laboratory for Experimental Relativity by Astrometry (SCLERA), Hill argued that the amplitudes of oscillation rise more steeply with height above the photosphere than can be comfortably accommodated within the framework of linear theory. At first sight this should be no cause for alarm, because the amplitudes thus inferred in the low chromosphere are so great that nonlinearities must surely be important. Nonetheless several participants were uneasy with the result, because in the photospheric regions, where presumably linear theory is valid, the eigenfunctions have the appearance of waves penetrating an evanescent region from above yet having frequencies characteristic of the resonating cavity beneath. Tuck Stebbins (Sacramento Peak Observatory) presented measurements of relative oscillation amplitudes at different positions in the wings of a spectrum line which support Hill's conclusion, and Timothy Brown (High Altitude Observatory) found contradictory evidence from shape changes of the limb darkening function. The issue is currently unresolved.

For many people, the most convincing evidence that the oscillation data arise from genuine dynamical solar vibrations is their phase coherence. Peter Worden (Sacramento Peak Observatory) criticized early analyses of the SCLERA data, but Thomas Caudell (University of Arizona) presented new measurements of solar equatorial diameter variations which, it was finally agreed, convincingly maintained phase over an interval of 23 days. This did not terminate the discussion, however, because as Maurice Gabriel (Universite de Liege) pointed out, unless there were a considerable difference in the amplitudes of eastward and westward propagating waves one would not expect phase coherence over a period longer than half the mean rotation of the sun. The details of the phase data may indeed be consistent with beating phenomena induced by rotation, but further analysis must be done. Polar diameter measurements, which have not yet been analyzed, are not subject to this criticism.

One of the most exciting aspects of solar oscillations is their potential for providing diagnostics of the solar interior. To realize this potential it is

essential to examine the theory quite meticulously to ensure that the physics is well understood, and that measurable properties of the oscillations of theoretical models can be computed accurately. In this respect, greatest attention has been paid to the five-minute oscillations, because it is of these that the most refined measurements have been made. Investigations by groups at the University of California at Los Angeles and the Observatoire de Nice have revealed that of the uncertainties beneath the photosphere only the value of the adiabat deep in the convection zone substantially influences the oscillation frequencies; in addition, the Nice group have found that the frequencies of all but the chromospheric modes are insensitive to variations in the structure adopted for the solar atmosphere, within the framework of the usual linearized theory. The results of both groups seem to imply that the adiabat must be that of a convection zone whose depth is at least 20% of the solar radius. This conclusion is similar to the findings of Beckers and Gilman, who reported at the EPS Workshop on Solar Rotation in Catania [Publication No. 162 of the Astrophysical Observatory of Catania (Eds. Belvedere and Paterno) 1978] that they could not explain the observed absence of a polar vortex unless the depth of the convection zone were at least of the order of 40% of the sun's radius.

The case for so deep a convection zone is not completely closed. Participants of the workshop were reminded of the EPS conference on solar physics [Pleins feux sur la physique solaire (Ed. Rosch) CNRS, Paris, 1978] held in Toulouse last year, where Dziembowski and Pamjatnykh pointed out that the observations by Hill and Caudell (Mon. Not. R. astron. Soc., 186, 327; 1979), apparently of solar g modes of degree about 30, are difficult to explain in terms of the so-called standard solar model (see Nature, 274, 739; 1978). At the Arizona workshop Jorgen Christensen-Dalsgaard (Universite de Liege) presented computations of g modes in a solar model with low interior heavy element abundance Z; such models have shallow convection zones through which modes of the kind reported by Hill and Caudell can penetrate with ease. Solar models with low Z also predict low neutrino fluxes in agreement with Davis' measurements, but they do pose many problems, such as how to explain the frequencies of the five-minute oscillations. Ross Rosenwald (University of Arizona) pointed out that if the claim of the SCLERA group concerning the nonlinear behavior of the oscillations high in the solar atmosphere were correct, the linear calculations performed to date may not be relevant, and this problem may disappear. The claim has not yet been substantiated.

Another new observation which may shed light on this issue was reported by George Isaak (University of Birmingham). His group has measured variations in the Doppler shift of a potassium line in light integrated from the entire solar disk, and have measured discrete frequencies of what appear to be acoustic oscillations of low degree with periods of about 5 minutes. Unlike the most common 5-minute modes, these penetrate beneath the convection zone and provide an integral measure of the

structure deep in the solar interior. A preliminary theoretical analysis favored a model with a somewhat lower value of Z than that of the standard model, and a shallower convection zone. This model lies between the two extremes discussed above, and so serves to remind us how uncertain we are of the sun's internal structure.

The final day of the meeting was devoted to degenerate variables. Edward Robinson (Univeristy of Texas at Austin) gave a stimulating review of the observations, many of which have been obtained only in the past few years. Most of these variables appear to be DA white dwarfs lying in a narrow range of specral type with B-V ≈ 0.2, though John McGraw (University of Arizona) in particular has observed variable white dwarfs of different colors. Of the DA dwarfs, about 25% are observed to be variable, and aside from their variability show no other distinguishing feature. Luminosity amplitudes range from a few tenths of a magnitude down to the limit of detectability.

The low amplitude variables have stable periods; one such star, R548 is even more stable than the Crab pulsar. The larger the amplitude the longer the period, and the less stable the power spectrum of the pulsations. It is not unusual for the stars with larger amplitudes also to switch entirely from one mode to another.

Oscillation periods range between about 100 s and 1,000 s, which are much too long to be p modes. Explanations in terms of g modes have been attempted, but it is sometimes difficult to fit the periods satisfactorily. Moreover, with the longer period variables it is difficult to explain why neighboring g modes in the densely spaced spectrum are not observed, a problem faced also by those who argue that the 2^{h} 40^{min} oscillation of the sun is a g mode. Carl Hansen (Joint Institute for Laboratory Astrophysics) suggested that perhaps the oscillations were toroidal elastic modes of a rather mushy material, but reliable estimates of the elastic properties of these degenerate stars are not available to test this hypothesis. In any case it was difficult to explain why only oscillations of the periods observed should be driven, and the others damped. Arthur Cox pointed out that (with the eye of faith) one could imagine the region in the HR diagram where pulsating white dwarfs have been found to be an extension of the classical Cepheid instability strip. He found models that were unstable to radial pulsations, but the periods of such modes are only about 1 s.

In summary it seems that both theory and observation are getting to a crucial point where tentative inferences are being made which are not all in the same direction. There is evidence that these contradictions arise from a lack of understanding of the physics. Time was, therefore, very ripe for the experts in the field to get together and discuss the assumptions on which these inferences are based, to discuss the accuracy and the implications of the observations and to decide which observations and which theory should be done in the immediate future to clarify the most outstanding of the uncertainties.

OBSERVATIONAL EVIDENCE OF RADIAL MODE RESONANCES AND OF NONSPHERICAL SYMMETRY IN SOME VARIABLE STARS OF δ SCUTI AND RELATED TYPES

W.S. Fitch
Steward Observatory
University of Arizona
Tucson, Arizona

ABSTRACT

(1) For 29 (and possibly 30) multimode radial variables in the Cepheid instability strip I suggest that necessary and sufficient conditions for the existence of their multimode excitation may be that the excited periods be close to a direct resonance with each other and that their excitation growth rates be relatively small. (2) Discussion of the observational evidence on nonradial modes observed in δ Scuti and β Cephei stars suggests that radial mode excitation is always dominant when nonspherical perturbations are small or variable and that nonradial modes only appear when figure perturbations are significant, so that one seldom (or perhaps never) observes in these stars the first order m-splitting discussed by Ledoux for the case of slow rotation.

1. INTRODUCTION

We address in the following sections the more general aspects of nonradial and nonlinear stellar pulsation problems rather than the particular stellar types in which they occur. In connection with nonlinear problems the observational evidence of radial mode resonances in Cepheid strip stars will be discussed first; consideration will be given to nonradial oscillations in δ Scuti and β Cephei stars in succeeding sections.

2. SIMPLE RESONANCES IN MULTIMODE RADIAL PULSATORS

Double (or occasionally triple) radial mode excitation is fairly common in the Cepheid strip at fundamental periods of less than approximately 6-7 days. Following especially Christy's (1966a,b) now classical work, theoretical investigations have been very successful in elucidating the properties of single mode radial pulsators. With regard to double mode excitation, Stellingwerf (1975) has constructed a model with two simultaneously excited radial modes; unfortunately, with a more realistic interior boundary condition, neither he nor anyone else could later

reproduce this result. This strongly suggests that, in order for a star to exhibit double radial mode excitation, it must possess some unique properties. Quite recently, Simon (1978) has proposed that the double mode state (fundamental frequency f_0 and first overtone frequency f_1) requires a resonance with a higher mode of frequency f_k, such that $f_0 + f_1 \approx f_k$; he also identified f_k with the third overtone f_3 for the 2-6 day double mode or beat Cepheids and with the fourth overtone f_4 for the dwarf Cepheids or AI Velorum stars. Petersen (1978) has enthusiastically seconded this suggestion, but neither Simon nor Petersen have been completely successful in reproducing the observed periods and period ratios for reasonable mass models.

These resonances pose an exciting possibility, but can be criticized for the invocation of an unobserved (and therefore ad hoc) mode to explain the presence of the observed modes. Simon and Petersen both considered only double mode Cepheid and RRs-type variables. There are now at least 29 (and provisionally 30) stars in the Cepheid strip known to show double radial modes, and if the work reported in § 3.4 on 4 CVn is not erroneous, there are 34 observed radial mode period ratios, 31 of which now seem securely established. Some of these ratios of observed periods are obviously very sharp low order simple resonances, such as 3/5, 4/5 and 3/4, suggesting that <u>all</u> of the ratios should be examined from this viewpoint. Simon (1978) has pointed out the importance of the second order coupling frequency $f_1 + f_0$ when discussing the nonlinear coupling of f_0 and f_1, but to be theoretically consistent, one should also examine the other cross coupling term in second order, $f_1 - f_0$. If for generality we consider two radial modes j and k, where $k > j$, and if we assume a nonlinear coupling leading to a resonance where $nf_j \approx mf_k$ (m, n being small integers with $m < n$), then obviously there must also be approximate resonances where f_j, f_k, $f_k + f_j$, and $f_k - f_j$ are commensurable. Following Simon, we denote the distances from each exact resonance assumed as

$$d_{j,k} = 1 - (nf_j)/(mf_k) \quad , \qquad d_{j,k+j} = 1 - (n+m)f_j/m(f_k+f_j) \quad ,$$

$$d_{j,k-j} = 1 - (n+m)f_k/n(f_k+f_j) \quad , \qquad d_{j,k-j} = 1 - (n-m)f_j/m(f_k-f_j) \quad ,$$

$$\text{and} \qquad d_{k,k-j} = 1 - (n-m)f_k/n(f_k-f_j) \quad .$$

In Figure 1 we illustrate seven different resonances as horizontal lines in a plot of observed period ratio versus log P_0 (day). Here the solid circles are observed ratios. The triangle is also an observed value for CY Aqr which was considered an uncertain value prior to the Comm. 27 IBVS No. 1537 announcement that EH Lib has a beat period yielding a period ratio of 0.7559. The plus signs represent our new provisional values of period ratios for 4 CVn. The 6-17 day bump Cepheids (Simon and Schmidt 1976), involving the basic 1/2 resonance for P_2/P_0, are only

indicated schematically. The fractions in brackets are the five assumed direct resonances involved. Please note how the difference frequency determines the lowest order resonance possible. An example of this is provided by the $P_2/P_0 \approx 3/5$ line, where the 3/8 and 5/8 resonances arise from the sum frequency while the 3/2 and 5/2 ratios arise from the difference frequency. If we adopt the provisional ratios for 4 CVn, then the top line for $P_2/P_1 \approx 4/5$ is represented by the δ Scuti star 4 CVn, the AI Velorum star VZ Cnc, and the RR Lyrae star AC And. At $P_1/P_0 \approx 7/9$ we have the δ Scuti star 44 Tau and 7 AI Velorum stars. At $P_1/P_0 \approx 3/4$ are the AI Velorum stars CY Aqr and EH Lib, the δ Scuti stars 4 CVn and 21 Mon, and the RR Lyrae stars AQ Leo and AC And. For the beat Cepheids we chose $P_1/P_0 \approx 5/7$ for the 3 shortest period stars and $P_1/P_0 \approx 7/10$ for the remaining 8. At $P_2/P_0 \approx 3/5$ are AC And and the 5 δ Scuti stars CC And, 1 Mon, δ Del, δ Sct, and 4 CVn. Table 1 lists the stars, their fundamental radial mode periods, identifications of the excited radial modes, the observed period ratios, and the assumed resonance ratios. The last 5 columns of Table 1 provide the 5 distances d from the assumed exact resonances. It will be noted that generally, for the direct resonance $P_k/P_j = f_j/f_k = \omega_j/\omega_k \approx m/n$ and the two resonances with the sum frequency $f_k + f_j$, the distances from resonance are quite small whereas the distances from resonances with the difference frequency $f_k - f_j$ are distinctly larger. The larger distances in this latter case may account for the fact that, when the observed nonlinear coupling of f_k and f_j in light and/or velocity measures on large amplitude variables is analyzed into its harmonic components, the amplitude of the second order difference term is usually smaller than that of the sum term.

The associations of P_2/P_0 with the 1/2 and 3/5 ratios, of P_1/P_0 in some cases with the 3/4 ratio, and of P_2/P_1 with the 4/5 ratio seem inescapable. By extension, the remaining associations of P_1/P_0 with the 7/9, 5/7 and 7/10 resonances appear quite plausible. The main shortcoming of this type of argument is that no a priori upper limit is set with respect to invoked resonance. If we adopt $P_1/P_0 \approx 17/22$ instead of $\approx 7/9$ for the AI Velorum stars, or $P_1/P_0 \approx 12/17$ instead of $\approx 5/7$ and 7/10 for the beat Cepheids, we get better representations, i.e., smaller distances from resonance, for these groups already discussed by Simon (1978) and by Petersen (1978). If we keep our adopted resonances for P_1/P_0, then examination of Figure 1 and Table 1 shows that we have nearly exhausted the low order resonances possible for the range of period ratios expected from model calculations. Finally, in order for any resonance such as 7/9 or 7/10 to be effective, the excitation growth rates must be small, since the system must "remember" what happened as long ago as 7 fundamental periods. In fact, all normal evolutionary mass models of δ Scuti and AI Velorum stars (cf. Dziembowski 1977; Stellingwerf 1979; Cox, King and Hodson 1978b) list kinetic energy growth rates $\Delta E/PE \approx 10^{-3} - 10^{-5}$ per period for the strongest excited modes. Cox, King and Hodson (1978a) do not list growth rates for their most recent 3

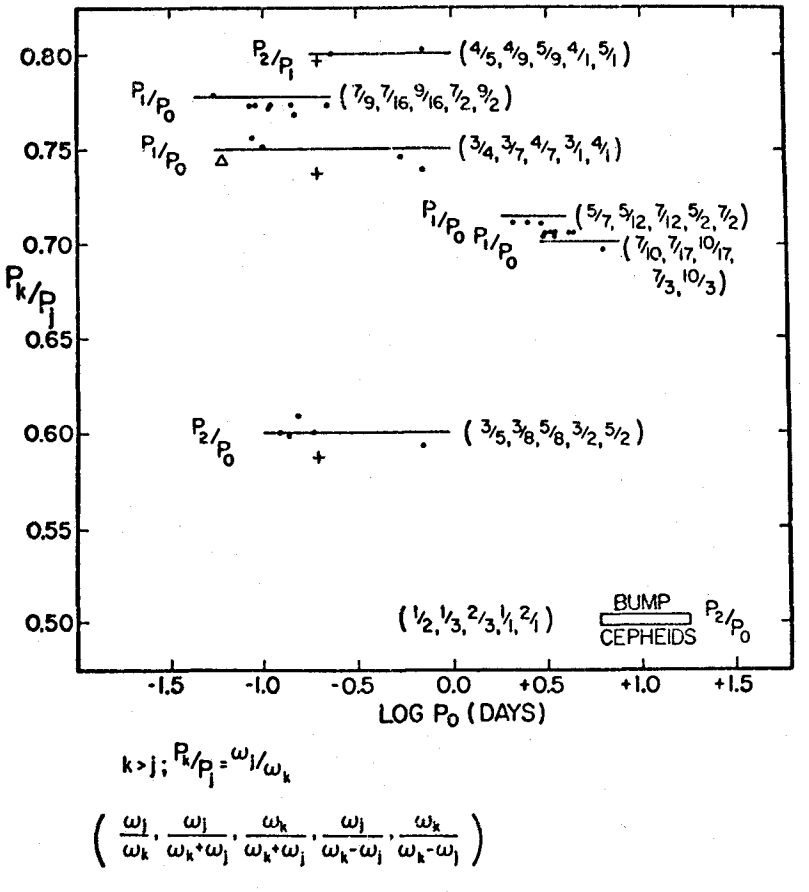

Figure 1. Observed period ratios as functions of log P_0(day). The horizontal lines represent the assumed direct resonance ratios, which are also given as the first fraction in the parentheses. The remaining fractions are the corresponding resonances of the lower and higher mode with the sum frequency and with the difference frequency, respectively. Individual stars are plotted as solid circles. The open triangle represents CY Aqr and the plus signs are provisional values for 4 CVn (see text).

Table 1. Radial Mode Period Resonances

Notes	Star	P_o(day)	j,k	P_k/P_j	m/n	$d_{j,k}$	$d_{j,k+j}$	$d_{k,\ k+j}$	$d_{j,k-j}$	$d_{k,k-j}$
B	SX Phe	0.0550	0,1	0.7782	7/9	-0.0005	-0.0003	+0.0002	-0.0024	-0.0019
	CY Aqr	0.0610	0,1	0.7443	3/4	+0.0076	+0.0044	-0.0033	+0.0297	+0.0223
	AE UMa	0.0860	0,1	0.7734	7/9	+0.0056	+0.0032	-0.0025	+0.0248	+0.0193
	EH Lib	0.0884	0,1	0.7559	3/4	-0.0079	-0.0045	+0.0034	-0.0322	-0.0242
	RV Ari	0.0931	0,1	0.7726	7/9	+0.0067	+0.0038	-0.0029	+0.0293	+0.0228
δN	21 Mon	0.0999	0,1	0.7507	3/4	-0.0009	-0.0005	+0.0004	-0.0037	-0.0028
	BP Peg	0.1095	0,1	0.7715	7/9	+0.0081	+0.0046	-0.0035	+0.0353	+0.0275
	AI Vel	0.1116	0,1	0.7727	7/9	+0.0065	+0.0037	-0.0029	+0.0287	+0.0223
δB	CC And	0.1249	0,2	0.5999	3/5	+0.0002	+0.0001	-0.0001	+0.0004	+0.0002
δBN	1 Mon	0.1361	0,2	0.5984	3/5	+0.0027	+0.0017	-0.0010	+0.0066	+0.0040
δ	44 Tau	0.1449	0,1	0.7729	7/9	+0.0063	+0.0035	-0.0028	+0.0276	+0.0215
	V703 Sco	0.1500	0,1	0.7683	7/9	+0.0122	+0.0069	-0.0054	+0.0526	+0.0409
δN	δ Del	0.1568	0,2	0.6093	3/5	-0.0155	-0.0096	+0.0058	-0.0397	-0.0238
δN	δ Sct	0.1938	0,2	0.6005	3/5	-0.0008	-0.0005	+0.0003	-0.0021	-0.0013
δB:	4 CVn	0.1981	0,1:	0.7368	3/4	+0.0176	+0.0101	-0.0076	+0.0669	+0.0502
δB:	4 CVn	0.1981	0,2:	0.5874	3/5	+0.0210	+0.0132	-0.0079	+0.0509	+0.0305
δB:	4 CVn	0.1981	1,2:	0.7972	4/5	+0.0035	+0.0019	-0.0016	+0.0173	+0.0138
	VX Hya	0.2234	0,1	0.7732	7/9	+0.0059	+0.0033	-0.0026	+0.0260	+0.0202
:	VZ Cnc	0.2323:	1,2	0.8006	4/5	-0.0008	-0.0004	+0.0003	-0.0038	-0.0030
	AQ Leo	0.5498	0,1	0.7461	3/4	+0.0052	+0.0030	-0.0022	+0.0205	+0.0154
	AC And	0.7112	0,1	0.7383	3/4	+0.0156	+0.0090	-0.0067	+0.0596	+0.0447
	AC And	0.7112	0,2	0.5920	3/5	+0.0133	+0.0084	-0.0050	+0.0327	+0.0196
	AC And	0.7112	1,2	0.8018	4/5	-0.0023	-0.0012	+0.0010	-0.0114	-0.0091
	TU Cas	2.1393	0,1	0.7097	5/7	+0.0064	+0.0038	-0.0027	+0.0221	+0.0158
	U TrA	2.5684	0,1	0.7105	5/7	+0.0053	+0.0031	-0.0022	+0.0183	+0.0131
	VX Pup	3.0117	0,1	0.7090	5/7	+0.0074	+0.0043	-0.0031	+0.0254	+0.0182
	AP Vel	3.1278	0,1	0.7031	7/10	-0.0044	-0.0026	+0.0018	-0.0149	-0.0104
	BK Cen	3.1739	0,1	0.7047	7/10	-0.0067	-0.0039	+0.0028	-0.0227	-0.0159
	UZ Cen	3.3344	0,1	0.7063	7/10	-0.0090	-0.0053	+0.0037	-0.0306	-0.0215
	Y Car	3.6398	0,1	0.7031	7/10	-0.0044	-0.0026	+0.0018	-0.0149	-0.0104
	AX Vel	3.6731	0,1	0.7059	7/10	-0.0084	-0.0049	+0.0035	-0.0287	-0.0201
	GZ Car	4.1588	0,1	0.7052	7/10	-0.0074	-0.0044	+0.0030	-0.0252	-0.0176
	BQ Ser	4.2707	0,1	0.7053	7/10	-0.0076	-0.0044	+0.0031	-0.0257	-0.0180
	V367 Ser	6.2931	0,1	0.6967	7/10	+0.0047	+0.0028	-0.0019	+0.0155	+0.0109
					Max |d|	0.0210	0.0132	0.0079	0.0669	0.0502
					Mean |d|	0.0070	0.0041	0.0029	0.0249	0.0180

Notes: δ = δ Scuti type; N=nonradial modes also excited; B=close binary; :=provisional mode identification for 4 CVn; :=estimated value of P_o for VZ Cnc.

References: SX Phe, Kozar 1978; EH Lib, Karetnikov and Medvedev 1979; 1 Mon, this paper; 44 Tau, Wizinowich and Percy 1978; δ Del, this paper; 4 CVn, this paper; AQ Leo, Jerzykiewicz and Wenzel 1977. References for the other stars are given in Fitch and Szeidl 1976 or in Stobie 1977.

$M_\odot$ model of AC And, but it seems probable that these growth rates are much smaller than those of, for instance, the Christy models of RR Lyrae stars. It therefore seems reasonable to suggest that the RR Lyrae star AQ Leo, the 2-6 day double mode Cepheids, and the 6-17 day bump Cepheids may also have relatively low growth rates for radial mode excitation. This condition, together with the existence of nonlinear coupling leading to a resonance, may constitute the necessary and sufficient conditions for the excitation of double mode radial pulsation. Stockman (1979) of Steward Observatory recently made an excellent suggestion regarding the testing of Simon's (1978) resonance hypothesis or that discussed here by artificially "tweaking" appropriate nonlinear models to force a resonance and then observing whether this produced double mode excitation.

3. NONRADIAL MODE EXCITATION IN δ SCUTI AND β CEPHEI STARS

3.1 Preliminaries

In considering nonradial mode excitation, it should first be noted that, of the 17 radial mode variables in Table 1 with $P_0 < 0.25$ day, 7 are δ Scuti stars and 10 are AI Velorum or RRs stars. Further, 6 of the 7 δ Scutis are either in binaries (CC And, 1 Mon, 4 CVn) and/or also exhibit nonradial modes (21 Mon, 1 Mon, δ Del, δ Sct). Only 44 Tau, which Wizinowich and Percy (1978) recently showed to have $P_1/P_0 = 0.7729$, does not display these additional complications. In 6 of these 7 stars the strongest excited mode is the radial fundamental. However, if the present work proves correct, in 4 CVn the strongest excited mode is the second radial overtone P_2, with P_1 second and P_0 the weakest of these three. In addition, 4 CVn also appears to be an eclipsing binary with an orbital period $P_{orb} \approx 13.6$ day, and it may have tidal modulation of P_0 and P_1 but not of P_2.

Before taking up the general question of nonradial mode excitation, new results on 1 Mon, δ Del and 4 CVn will be discussed in some detail.

3.2 1 Monocerotis

Miller (1973) obtained 17 nights of V-filter photometry on 1 Mon and, upon finding a very strong beat period of 7.7455 day, attributed this to the simultaneous excitation at nearly equal amplitudes of periods $P_1 = 0.13377$ and $P_2 = 0.13613$ day. Because I thought the star interesting but didn't agree with his conclusions, Wisniewski and I placed 1 Mon on our observing program. Five nights of Stromgren b-filter measures had already been obtained when we received from Shobbrook and Stobie (1974) a preprint of their excellent paper in which they discussed both the 25 nights of V-filter measures they had obtained and the 17 nights by Millis. We then dropped 1 Mon from our own observing program as being a needless waste of available time.

Shobbrook and Stobie (1974) showed that the variations of 1 Mon could be

explained either as the resultant of nonlinear coupling of three nonlinearly excited equidistant frequencies f_1 = 7.346132, f_2 = 7.475281, and f_3 = 7.21718 cycles/day (hereafter c/d), or as the tidal modulation of f_1 by a companion in a nearly circular orbit of frequency F = 0.064555 c/d (P_{orb} = 15.4907 ± 0.0036 day). In the former case, which they preferred, the three modes would result from first order rotational perturbations of a nonradial mode, lifting the m-degeneracy according to the theory introduced by Ledoux (1951), with an observed splitting $\Delta f = f_2 - f_1 = f_1 - f_3$ = 0.12911 c/d (= 2F for the tidal case). However, the observed period ratio $P_2/P_0 \approx$ 3/5 (cf. Table 1), a ratio which one would expect for two radial modes where rotational splitting is not possible. For this reason, we consider the nonradial mode m-splitting explanation for f_0 (f_1 of Shobbrook and Stobie 1974) to be questionable.

Their objections to a tidal modulation in 1 Mon were (a) that no odd harmonic combinations of F with f_1 (our f_0) are present, and (b) that, if a binary, 1 Mon should show an orbital velocity variation, K_1, of the order of 100 km s^{-1}, whereas the limited velocity data available indicate $K_1 \approx 4$ km s^{-1}. We here demonstrate that their basis for objection (a) is incorrect and that objection (b) is not necessarily valid.

Shobbrook and Stobie (1974) found that there is no measurable phase difference between variations in yellow and blue light, so in discussing the phase variations it is possible to combine the measures of Fitch and Wisniewski (1979) for five nights with theirs. By using the least squares method, sine curves in the fundamental radial mode f_0 (f_1 of Shobbrook and Stobie 1974) and its second harmonic $2f_0$ have been fitted to determine the nightly mean values of the amplitudes A and phases ϕ on each of the 17 nights by Millis, 24 of the 25 nights by Shobbrook and Stobie (1974) (1 night has too few measures), and the 5 nights by Fitch and Wisniewski (1979). To combine the phase variations ϕ_0 in f_0 and ϕ_{20} in $2f_0$, each night's ϕ_{20} is first divided by 2 and then added to a mean zero-point phase correction of 0.5806 cycles appropriate to our chosen time zero-point T_0 = Hel. J. D. 2439000.0. Shobbrook and Stobie (1974) demonstrated that $\Delta\phi_{20} = 2\Delta\phi_0$ in 1 Mon, just as Fitch (1967, 1976) had earlier found in CC And. In other words, in both stars one observes a real variation in the time of occurrence of a nonlinearly excited mode. In Figure 2, ϕ_0 is plotted as solid circles and $0.5\phi_{20}$ + 0.5806 as plus signs against the nightly mean phases of F = 0.064555 and 2F = 0.12911 c/d. Suggestive smooth curves have not been drawn through the points, but it seems obvious that the double cycle interval of 15.491 days (F = 0.064555 c/d) gives a much better representation of the observed phase variations than does the half period (2F = 0.12911 c/d). Further, when we fit to all the yellow measures a single expansion involving just jf_0 + kF, where j and k are selected integers including odd values of k (-5, -4, -3, -2, -1, 0, +1, +2, +3, +4, +5 when j = 1), a much better representation of the combined

Millis and Shobbrook and Stobie (1974) data is obtained than if only the even k integers, such as those adopted by Shobbrook and Stobie (1974), are used. This formed the basis for their first objection to the presence of tidal modulation in 1 Mon. When the Millis and Shobbrook and Stobie data are combined, the $f_4 \approx 12.105$ c/d of Shobbrook and Stobie are resolved into our $f_2 = 12.2741$ (or 12.2771) c/d and $f_{N1} = 13.0621$ c/d, where f_2 (uncertain by 1 cycle/yr) is the second radial overtone and f_{N1} is a presently unidentified nonradial mode of very small amplitude ($A_0 = 0.0866 \pm 0.0003$, $A_{20} = 0.0158 \pm 0.0003$, $A_2 = 0.0026 \pm 0.0003$, and $A_{N1} = 0.0028 \pm 0.0003$, in units of the mean light level).

The second objection raised by Shobbrook and Stobie (1974) to the tidal modulation of f_1 was based upon the uncharacteristically low value for K_1, thereby raising doubts as to 1 Mon's binary status. In considering the orbital velocity of 1 Mon on the binary hypothesis, several points must be addressed.[1] The notation used in the following discussion will be that of Fitch and Wisniewski (1979).

First, because of the small differences in successive half cycles of F, the orbital eccentricity e must be small. In the circular orbit approximation, if we start from Kepler's harmonic law and the definition of the center of mass, we obtain the following expression for the orbital velocity of the primary mass M_1:

$$V_1 = V_\oplus \, q^{1/3} \, (1+q)^{-2/3} \, (FP_\oplus)^{1/3} \, (M_1/M_\odot)^{1/3} \quad ,$$

where $V_\oplus = 29.86$ km s^{-1} for the orbital speed of the earth and $P_\oplus = 365.25$ day for its sidereal period. With $F = 0.064555$ c/d as the orbital frequency of 1 Mon, we have $V_1(\text{km s}^{-1}) = 85.6 \, q \, (1+q)^{-2/3} \, (M_1/M_\odot)^{1/3}$. If for illustrative purposes we adopt $M_1 = 2.0 \, M_\odot$ and $M_2 = 0.1 \, M_\odot$, so that $q = 0.05$, then $V_1 = 5.2$ km s^{-1}. This is not in serious disagreement with the observational $K_1 = 4.0$ (± 2.7) km s^{-1} determined by fitting F, f_0, $f_0 + 2F$, and $2f_0$ to the 19 velocities obtained on 4 nights by Jones (1971). The difficulty here is that one should employ a much more complicated frequency set to accurately represent the actual velocity variation, and there are not enough measures available to permit such a fitting.

In an earlier presentation to this workshop, equations (24), (26) and (27) of Fitch and Wisniewski (1979) were used, together with an observational value of $A_{2F} = 0.0045 \pm 0.0003$, to derive $q < 0.2$. However, a fundamental error existed in the assumption that A_{2F} represents an ellipticity effect. Using equations (24) and (26) together with the definition of the pulsation constant Q_0 (≈ 0.033 day for the fundamental radial mode), one can show that with $M_1 = 2.0 \, M_\odot$, $q = 0.05$ (as above), x_1

[1]The first discussion of this problem at the workshop was in error due to the inadvertent use of the constant in equation (27) of Fitch and Wisniewski (1979), which contained the orbital frequency of 14 Aur A rather than 1 Mon.

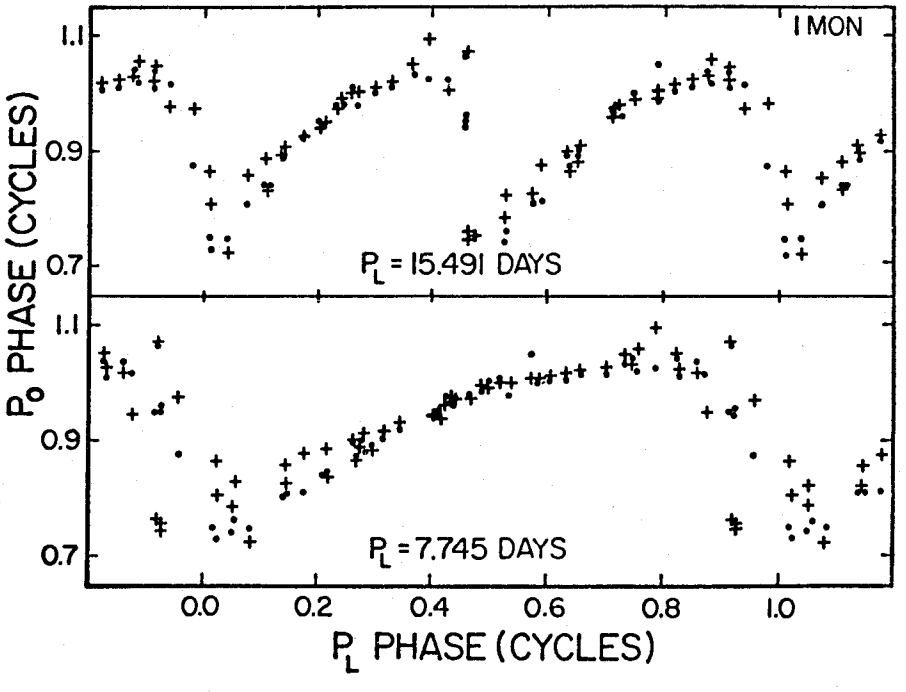

Figure 2. Observed variations of ϕ_0 (solid circles) and of $0.5\phi_{20} + 0.5806$ (plus signs) against nightly mean phases of the two possible long periods in 1 Mon. One pair of symbols is obtained by a least squares fit of $f_0 = 7.346132$ c/d and $2f_0$ to the data of each night separately.

= 0.55 for an F2 star in the V-filter, y_1 = 1.0, f_0 = 7.346132 c/d, F = 0.064555 c/d, and for the amplitude of concern, $A_{2F} \leq 8.6 \times 10^{-5}$ as compared to the observational value of 0.0045 ± 0.0003. That is, the observed variation in mean light level cannot be an ellipticity variation if the orbital velocity is small, but it can arise from nonlinearity effects in large amplitude beats as pointed out by Shobbrook and Stobie (1974). Much more extensive velocity measures, uniformly distributed over the phases of F, are needed, but we believe the present evidence favors a tidal modulation model for 1 Mon.

3.3 δ Delphini

Leung and Wehlau (1967) analyzed the B-filter photometric measures of δ Del which they had obtained on 33 nights in 1962-63. They described the variation they found as being due to the resultant of 3 frequencies centered around 6.4 and 2 around 12.7 c/d, with a single additional frequency at 10.4686 c/d. None of the frequencies they listed can be described as simple combinations or multiples of others. Because their analysis seemed questionable and because Preston (1966) had announced δ Del to be a binary in a very eccentric orbit of 40.5 day period, δ Del was included in our δ Scuti star observing program. On 29 nights between August 1972 and September 1974, 5431 b-magnitude measures were obtained covering 114.8 hours of the variation, and to date the only result has been a confirmation of the 4 lowest frequencies already found by Leung and Wehlau. Following an independent analysis of their data as well as an analysis of our own, the elements of the light variation of δ Del in 1962-63 and in 1972-74 are presented in Table 2. For the first two frequencies f_0 and f_{N1} phase-locking has been forced between the two data sets, even though there is a suggestion that all frequencies have changed very slightly during the interval between these two sets. Because of these apparent small changes and the subsequent ambiguities in cycle counts, different frequencies for f_{N2} and f_2 were adopted in the two sets. In each set, the estimated uncertainty in any frequency is ± 0.0002 c/d, so that any real frequency changes are only marginally apparent. In both sets, more periodicities are present near 12-13 c/d, but the precise values of these periods differ. No harmonic or sum or difference frequencies appear to be present. Further, in both sets the fundamental radial mode f_0 is the dominant excited mode; the second radial overtone f_2 is also present; at least two nonradial modes f_{N1} and f_{N2} are excited; and no possibility exists of invoking a constant frequency difference a la Ledoux (1951) to explain the nonradial mode excitation. δ Del appears to be very similar to δ Scuti in overall pulsation behavior (Fitch 1976).

3.4 4 Canis Venaticorum

On 36 nights between February 1974 and April 1976 Wisniewski, Bell and Fitch obtained 7984 b-magnitude measures covering 202.0 hours of the light variation of 4

Table 2. Adopted Solutions For The Blue Light Variation Of δ Delphini*

	Leung and Wehlau, 1962-63 B Measures					Our 1972-74 b-Measures				
Name	f_i(c/d)	A_i	σ_A	ϕ_i	σ_ϕ	f_i(c/d)	A_i	σ_A	ϕ_i	σ_ϕ
f_0	6.377893	0.0278	±0.0005	0.306	±0.003	6.377893	0.0263	±0.0003	0.307	±0.002
f_{N1}	6.55814	0.0056	±0.0005	0.319	±0.013	6.55814	0.0049	±0.0003	0.318	±0.009
f_{N2}	6.6328	0.0046	±0.0005	0.635	±0.017	6.6331	0.0042	±0.0003	0.562	±0.011
f_2	10.4682	0.0052	±0.0005	0.054	±0.014	10.4684	0.0043	±0.0003	0.501	±0.011
	Comparison = ζ Del σ(1 obs) = ± 0.0112 mag 1018 measures, compressed from 1596 measures on 33 nights. Δm_0 = -0.0815 ± 0.0003 mag					Comparison = ζ Del σ(1 obs) = ± 0.0069 mag 1211 measures, compressed from 5431 measures on 29 nights. Δm_0 = -0.1197 ± 0.0002 mag				

*$m_\delta = m_\zeta + \Delta m_0 - 2.5 \log [1 + \Sigma A_i \sin 2\pi (f_i t + \phi_i)]$

t = Hel.J.D. - 2437840.0

CVn. As we have stated earlier (Fitch and Szeidl 1976; Fitch 1976), the Fourier transform frequency spectra are extremely complex. At present it appears most probable that in 4 CVn the 3 radial modes f_0 = 5.0489, f_1 = 6.85225 and f_2 = 8.5949 c/d are all excited with f_2 the strongest and f_0 the weakest of the three. Further, the apparent presence of additional frequencies at 1.3270, 1.4016, 4.5292 and 7.3751 c/d can be rationalized by noting that 1.4016/19 = 0.07377 and 1.3270/18 = 0.07372 c/d, while (5.0489 - 4.5292)/7 = 0.07424 and (7.3751 - 6.85225)/7 = 0.07469 c/d. That is, there are 5 apparent combinations which all suggest the presence of a low frequency F ≈ 0.0737 - 0.0747 c/d and a modulation period P_{orb} ≈ 13.6 - 13.4 day. In addition, there are present a number of other low harmonics of a frequency F near this value, such that when a 9 term expansion in selected harmonics of F = 0.07379 c/d was fitted to the complete data set and then the mean light variation calculated over one long period according to these harmonics, a very strong indication was obtained that 4 CVn has an orbital period P_{orb} ≈ 13.6 day and undergoes two shallow eclipses per period (depths ≈ 0.04 mag), but that these eclipses are not equidistant. The time intervals between successive mid-minima are about 6.1 and 7.5 days, respectively, so that if this interpretation is correct the orbit must be significantly noncircular. In this picture, all the low frequency terms arise from the attempt to describe eclipses by Fourier expansions in the orbital period, while the terms at f_0 - 7F and f_1 + 7F are attributed to orbital modulation of the fundamental and first overtone radial modes. A more complicated possibility is that, since the two eclipse minima appear to be of approximately equal depth, the binary members are of nearly equal T_e and <u>both</u> may be δ Scuti variables. In that case it may be that f_0' = 4.5292 and f_2' = 7.3751 c/d are the radial fundamental and second overtone modes of the second star, with f_0'/f_2' = 0.6141 and with F ≈ 0.07374 c/d (P_{orb} ≈ 13.56 day).

Because the strongest pulsation frequency in 4 CVn, which we have termed f_2 = 8.5949 c/d, is clearly present in each of our 6 data subsets as well as in the fit to the complete data base, we do not agree with the conclusions of Warman, Pena and Arellano-Ferro (1979). They analyzed 5 closely spaced nights of V and B photometry which they had obtained in 1977, and proposed that the first 4 radial modes are excited in 4 CVn, with f_0 = 4.796, f_1 = 6.540, f_2 = 7.942 and f_3 = 8.636 c/d. However, we find none of these frequencies. Whatever may be the correct solution to the problems posed by the very complex but periodic behavior of 4 CVn, it now seems certain that there is <u>no</u> observational evidence connecting this behavior with first order rotational perturbation theory.

3.5 <u>Nonradial Mode Excitation</u>

In most well-observed δ Scuti stars the light variation is quite complex, and in many of these stars the observed frequency splittings are sufficiently small that

some nonradial mode excitation must be present. However, as already pointed out in § 3.1, when radial modes are also present the fundamental f_0 is usually the most strongly excited of all, and the nonradial modes are usually an order of magnitude weaker than f_0 (cf. 1 Mon, δ Del, δ Sct). The only δ Scuti stars in which constant frequency difference spacing has been demonstrated are CC And and 1 Mon, and it now seems apparent that they are both binaries with the radial fundamental being tidally modulated. Because of the alternating character of even and odd half-cycles of the long beat period, both of these stars must have elliptical orbits. In addition, the β Cephei stars σ Sco and α Vir are both binaries in elliptical orbits and both show tidal modulation of the dominant pulsation frequency.

By contrast, the δ Scuti stars Y Cam and 14 Aur and the β Cephei star 16 Lac are all binaries in circular orbits and all have excited nonradial modes that are not tidally modulated and that are also not separated by constant frequency differences. Y Cam is an eclipsing binary (Broglia and Conconi 1973), 16 Lac is a spectroscopic and an eclipsing binary (Jerzykiewicz et al. 1978), and 14 Aur is a spectroscopic and an ellipsoidal binary (Fitch and Wisniewski 1979). Jerzykiewicz (1978) has recently reanalyzed the published observations of the β Cephei star 12 Lac, and has concluded from the existence of constant Δf steps in the frequency spectrum that in this case Ledoux's theory of first order rotational splitting does apply. However, we must point out that the 4 frequencies (his f_1, f_3, f_4 and f_5) for which he makes this identification may just as easily be described as f_1, $f_1 + 2F$, $f_1 + F$, and $2f_1 + F$, where $F = 0.15537$ c/d implies an orbital period $P_{orb} = 6.4362$ day. Further, as he admits, the mean light level varies from night to night. We suggest that when adequate observations become available the light level variation will be found to be periodic with period $0.5P_{orb} = 3.2181$ day, as expected for a close binary subject to the ellipticity effect. The other two frequencies f_2 and f_6 do not fit this simple splitting pattern and at least f_2 must be a nonradial mode.

The suggestion that duplicity effects may commonly complicate the behavior of a pulsating star has met with a great deal of resistance, the basis of which is difficult to understand. If one recalls that about half of all stars occur in binary or multiple systems, and that the β Cephei and δ Cephei instability strips represent normal stages in the evolutionary life histories of stars of various masses, then it is to be expected that about half of all these variables will have physical companions that will in many cases be close enough to influence the outer structure of the pulsating star. If one insists that CC And, 1 Mon and 12 Lac are not binaries but rather that the strongest pulsation mode (which we identified as f_0 in CC And and 1 Mon) is a nonradial mode with first order m-splitting, then one requires ad hoc explanations for the following points: (a) In CC And, 1 Mon, δ Del, δ Sct and AC And, we find $P_2/P_0 \approx 3/5$, with P_0 the strongest excited pulsation mode and, in AC And, definitely the radial fundamental mode. On the nonbinary hypothesis, P_0 is not

a radial mode in CC And and 1 Mon, but shows an m-splitting not seen in δ Del, δ Sct and AC And. (b) From a study of the statistics of binary orbits, we expect to see a number of pulsators with close companions in noncircular orbits. If CC And and 1 Mon are not representative of this type of system, why have stars such as this not been found and how will their pulsational behavior differ from that observed in CC And and 1 Mon? (c) CC And and 1 Mon both show a pulsation behavior which alternates in character between even and odd cycles of the m-splitting beat period. This is not predicted by Ledoux but is consistent with tidal modulation in an elliptical orbit. (d) Both CC And and 1 Mon are relatively large amplitude nonlinear pulsators, with significant second harmonic content in the light variations due to the dominant mode (our P_0 in each). If these are nonradial modes, then they must in both cases be surface harmonics with $\ell \geq 5$, since for both stars the accurate analytic representation of the observed light variations requires terms to at least $f_0 \pm 5F$. To interpret such terms as m-splitting requires that $m \geq 5$, however, since $|m| \leq \ell$, it follows that $\ell \geq 5$, a result which is unreasonable for a large amplitude pulsator viewed in light integrated over the apparent disk.

From the preceding discussion, it appears that the observational evidence implies that nonradial mode excitation in stars above the main sequence will usually occur only in those stars with significant departures from spherical symmetry, due either to high rotation or to close companions. If this inference is correct, and if the theoretical investigations of nonradial pulsations are to have any relevance to the real world, then the model builders will have to accept the rather grim problems posed by the abandonment of simple spherical models.

* * * * *

This work has been supported in part by a National Science Foundation grant GP-38739.

REFERENCES

Broglia, P. and Conconi, P. 1973, Pub. Osserv. Astr. Milano-Merate, Nuova Serie, No. 27.

Christy, R.F. 1966a, Ap. J., 144, 108.

Christy, R.F. 1966b, Ann. Rev. Astr. and Ap., 4, 353.

Cox, A.N., King, D.S. and Hodson, S.W. 1978a, Ap. J., 224, 607.

Cox, A.N., King, D.S. and Hodson, S.W. 1978b, preprint.

Dziembowski, W. 1977, Acta. Astr., 27, 95.

Fitch, W.S. 1967, Ap. J., 148, 481.

Fitch, W.S. 1976, in Proc. IAU Colloquium No. 29, Multiple Periodic Variable Stars, ed. W.S. Fitch (Budapest: Akademiai Kiado), Vol. 1, p. 167.

Fitch, W.S. and Szeidl, B. 1976, Ap. J., 203, 616.

Fitch, W.S. and Wisniewski, W.Z. 1979, Ap. J., 231, No. 3.

Jerzykiewicz, M. 1978, preprint.

Jerzykiewicz, M. and Wenzel, W. 1977, Acta. Astr., 27, 35.

Jerzykiewicz, M., Jarzebowski, T., Musielok, B. and Le Contel, J.M. 1978, IAU Commission 27, Information Bull. No. 1508.

Jones, D.H.P. 1971, Royal Obs. Bull., No. 163.

Karetnikov, V.G. and Medvedev, Yu. A. 1979, IAU Commission 27, Information Bulletin No. 1537.

Kozar, T. 1978, Acta. Astr., 28, 131.

Ledoux, P. 1951, Ap. J., 114, 373.

Leung, K.C. and Wehlau, W. 1967, Ap. J., 149, 39.

Millis, R.L. 1973, Pub. A.S.P., 85, 410.

Petersen, J.O. 1978, preprint.

Preston, G.W. 1966, Kleine Veröff, Remeis-Sternw. Bamberg, No. 40, p. 163.

Shobbrook, R.R. and Stobie, R.S. 1974, Mon. Not. R. Astr. Soc., 169, 643.

Simon, N.R. 1978, preprint.

Simon, N.R. and Schmidt, E.G. 1976, Ap. J., 205, 162.

Stellingwerf, R.F. 1975, Ap. J., 195, 441.

Stellingwerf, R.F. 1979, Ap. J., 227, 935.

Stobie, R.S. 1977, Mon. Not. R. Astr. Soc., 180, 631.

Stockman, P. 1979, personal communication.

Warman, J., Peña, J.H. and Arellano-Ferro, A. 1979, A. J., 84, 109.

Wizinowich, R. and Percy, J.R. 1978, preprint.

δ SCUTI VARIABLES: THE LINK BETWEEN GIANT- AND DWARF-TYPE PULSATORS

W. Dziembowski*
Department of Physics
University of Arizona
Tucson, Arizona

ABSTRACT

An attempt is made to interpret the differences in pulsational behavior between horizontal branch and main sequence (or early post-main sequence) variables. Results of linear stability studies for δ Scuti stars are reviewed and supplemented with new calculations. The function of the opacity mechanism in generating instability to a variety of radial and nonradial modes is discussed. The highest excitation rates for these variables, though still much lower than in the case of Cepheids, are found in fundamental modes with higher spherical harmonic orders, ℓ, and among higher overtones with low values of ℓ. It is argued that amplitudes in δ Scuti stars are limited by nonlinear mode coupling, resulting in lower amplitudes and multiperiodicity, rather than by saturation of the opacity mechanism as is the case with horizontal branch variables.

1. INTRODUCTION

The discoveries of many low amplitude variables made in recent years and the demonstration that the sun is an oscillating star strongly suggest that stellar oscillations must be very common. Understanding of this phenomenon may furnish insight into the mechanics of atmospheric turbulence and heat balance; it may also provide a means of probing stellar interiors.

Most low amplitude pulsators fall into the three following types:

1. ZZ Ceti,
2. β Cephei and related early type variables, and
3. δ Scuti.

In all cases, these are stars characterized by dwarf-like or only slightly developed giant-like structure. This is in contrast to classical pulsating stars, such as

---

*Visiting Professor on leave-of-absence from the Copernicus Astronomical Center, Warsaw, Poland.

Cepheids and RR Lyrae, that are helium-burning stars in advanced evolutionary stages. It now appears likely that there is one common cause of variability in all the above stars, namely the familiar opacity mechanism. There are, however, striking differences in the pulsation properties of giants and dwarfs, respectively, which are listed below:

1. Pulsations detected in giants are usually of high amplitude, while dwarfs are usually low amplitude pulsators.
2. The number of modes excited in giants is one or, in rare cases, two; a large number of excited modes is found in pulsating dwarfs.
3. There is no evidence for the existence of nonradial modes in giants. However, nonradial modes are clearly indicated in many dwarfs studied.
4. The instability strip in giants is well-defined but poorly defined in dwarfs.

Our understanding of the pulsation phenomenon in Cepheids has reached a very satisfactory level since it is, by astrophysical standards, remarkably simple. Small amplitude variables present a much more complicated problem due both to a lack of spherical symmetry of the motion and to multiperiodicity. The nature of these differences between giants and dwarfs in their pulsational behavior will be discussed using δ Scuti variables as an example. This type of variable star comprises both main sequence stars and early post-main sequence (thick shell phase) stars.

Two factors complicate consideration of these variables as members of a homogeneous group. One is the problem of whether large amplitude variables classified as RR_S types, which overlap genuine δ Scuti stars in their range of periods and spectral types, are in the same evolutionary phase as the δ Scuti stars. There is no consensus on this question. However, it is more in the spirit of this paper to assume that these are more evolved objects having low mass and that they therefore should not be considered in the same group. This question will be addressed in § 5 where the possible existence of large amplitude variables among main sequence stars will be discussed.

The other complicating factor is metallicity. In his recent review,[1] Breger (1979) concludes that variability and strong metallicity are mutually exclusive for main sequence variables, but not for post-main sequence variables. It has been speculated (Vauclair, Vauclair and Pamjatnykh 1974) that since metallicity may be treated as evidence for unsuppressed diffusion, the settling of helium relative to hydrogen should occur. Because most of the driving is due to the He II ionization layer, depletion of helium from this zone due to settling may prevent pulsational instability. Recently, Cox, King and Hodson (1979) made an extensive survey of linear stability in models with a reduced helium content in their outer layers. They

[1]Readers are referred to this excellent review for a complete survey of the properties of δ Scuti stars.

showed that the extent of the instability strip is very sensitive to the amount of helium and that the complete depletion of helium in the outer layers results in stabilizing the models.

Although this effect is unquestionably important for understanding pulsation properties of δ Scuti stars, it seems doubtful that it can account for the essential differences between these stars and Cepheids. This is especially borne out by the fact that many normal main sequence stars which lie within the instability strip still fail to pulsate with large amplitudes.

2. CHANGES IN PULSATION PROPERTIES IN THE COURSE OF STELLAR EVOLUTION

Development of a condensed core and extended envelope during evolution causes drastic changes in the propagation properties of acoustic and gravity modes in the stellar interior. An oscillatory mode characterized by its frequency, ω, and spherical harmonic order, ℓ, has almost all of its energy confined to the layers where it can propagate, thereby becoming a trapped acoustic or gravity wave. From the point of view of pulsational instability, the location of the propagation zones and hence the evanescent zones is important because (1) it tells what portion of the stellar mass is engaged in the motion, and (2) the driving via the opacity mechanism depends on the evanescent (non-propagating) behavior of the oscillations in the driving zone. Discussions of the propagation properties of various stellar models may be found in the following papers: Scuflaire (1974); Dziembowski (1975); Osaki (1975); and Unno (1975).

Approximate criteria for propagation can be written (cf. Dziembowski 1975) as

$$\omega \gtrsim c(\ell + 1)/r,\ \omega \gtrsim g/c \quad \text{for acoustic waves, and} \tag{1}$$

$$\omega \lesssim ng/c,\ \omega \lesssim n\ell c/r \quad \text{for gravity waves} \tag{2}$$

where c is the speed of sound, g is the local gravitational acceleration and

$$n^2 = -\left(\frac{\partial \ln \rho}{\partial \ln T}\right)_{P,M}\left[\left(\frac{\partial \ln T}{\partial \ln P}\right)_{ad} - \frac{d\ln T}{d\ln P}\right] + \left(\frac{\partial \ln \rho}{\partial \mu}\right)_{P,T}\frac{d\mu}{d\ln P} \tag{3}$$

where ρ, T, P and μ denote density, temperature, pressure and the mean molecular weight, respectively, and the derivative $\frac{d\mu}{d\ell nP}$ is calculated in the equilibrium model. The Brunt-Väisälä frequency, ng/c, is frequently denoted by N. The above criteria provide, in an approximate way, the necessary and sufficient conditions for propagation. They differ in this respect from those obtained by Scuflaire (1974) which, although rigorous, represent only necessary conditions.

The radial behavior of the parameters g^2/c^2 and c^2/r^2, which enter into the above criteria, are shown schematically in Figure 1 for an evolved stellar model. The characteristic feature for such stars is a pronounced hump in g/c which is nonexistent or barely present in zero age main sequence (ZAMS) stars. This hump

prevents the penetration of radial modes into the deep interior and, as a result, the propagation zone in evolved stars contains a smaller fraction of the total mass. The upper boundary of the propagation zone is also moved outward in evolved stars because, for a given mode, ω varies as $R^{-3/2}$ and the surface g varies as R^{-2}.

This effect has another interesting consequence: higher order acoustic modes may be evanescent in the driving region for stars with higher surface g. It has indeed been found by Castor (1970) and confirmed later in several papers that, with respect to radial pulsations, δ Scuti stars are unstable to high order overtones with considerably higher growth rates than those of the fundamental mode or the first overtone.

Consequences of the development of the g/c maximum are different in the case of the nonradial modes because these modes may propagate in the interior as gravity waves. As shown in Figure 1, there is an intermediate frequency range where modes have mixed character; those in the envelope are acoustic-type waves, while gravity-type waves are found in the interior. This gives rise to a new set of modes and modifies the properties of previously existing modes.

The propagation zones are separated by an evanescent zone where the amplitude changes monotonically with r. For modes with high values of ℓ, the increase of the amplitude in the envelope for the trapped modes is so large that their properties are not affected by the changes in the interior (Shibahashi and Osaki 1976). On the other hand, the properties of low ℓ modes are always strongly affected. In the case of such stars as RR Lyrae or the Cepheids, such modes either experience a reduction in growth rate by orders of magnitude or are entirely damped. It has been found, for example, that as soon as $\ell \gtrsim 6$, the growth rates are reduced to the same order of magnitude (and remain always less) than those for the radial modes (Dziembowski 1977; Osaki 1977).

Similar, though much smaller, effects are present in the evolutionary phases of δ Scuti stars. In Figure 2, taken from Dziembowski (1977), the growth rates for low ℓ modes are compared in two models of a 1.5 $M_\odot$ star. In the ZAMS star model, a weak maximum of g/c establishes the inner propagation zone. In the frequency range considered, however, only for $\ell = 4$ is a mode trapped in this zone. Except for this mode, the growth rates of nonradial modes are essentially the same as those for radial modes, both being determined almost exclusively by frequency.

A much larger number of modes is present in the second model which represents the phase immediately following hydrogen exhaustion in the center. Most of these modes are trapped in the interior and, therefore, have much smaller growth rates than the radial modes. The modes with frequencies close to those of the ZAMS model are not trapped within the envelope to a very great extent. This is especially true for modes with $\ell = 2$ or 3, a factor which brings about a noticeable decrease in the growth rates of nonradial, relative to radial, modes.

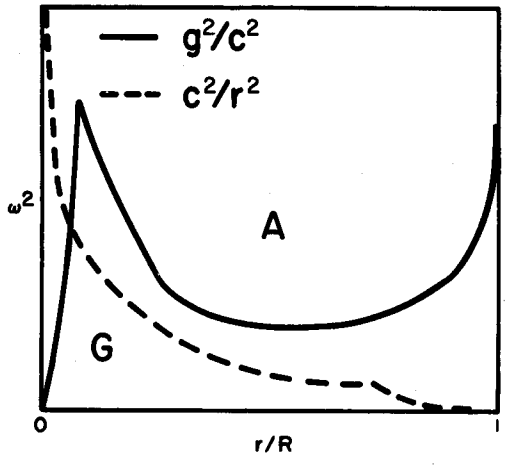

Figure 1. Regions of acoustic (a)- and gravity (g)-wave propagation in the interior of a giant. Critical lines are drawn schematically. Factor n has to be used to determine the critical frequencies for gravity-waves, while factors $\ell + 1$ and ℓ must be used to determine the critical frequencies for acoustic- and gravity-waves, respectively. Note that if ℓ is large, there are two g-regions.

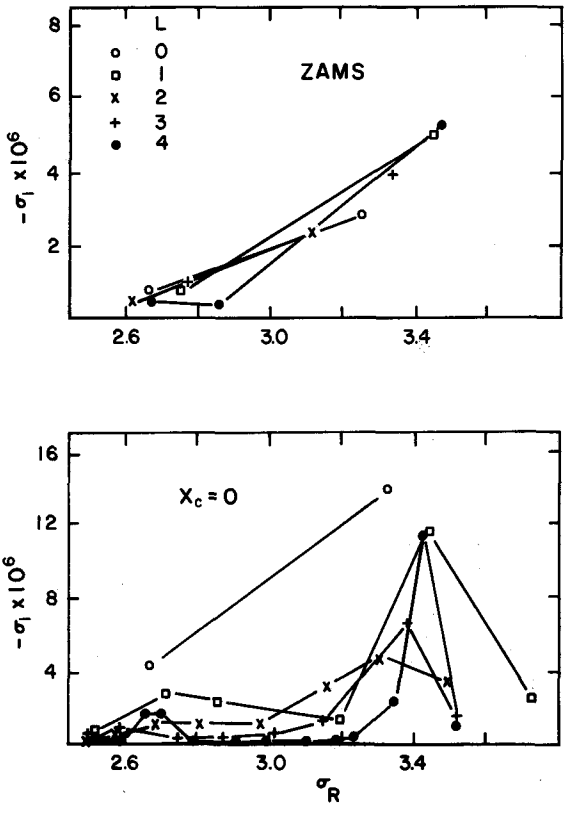

Figure 2. Growth rates ($-\sigma_I$) and frequencies (σ_R) in units of $(4\pi G\langle\rho\rangle)^{1/2}$ for modes in the range of frequencies corresponding to the two first overtones of the radial pulsations. The graphs are for two models of a 1.5 $M_\odot$ star.

It should be noted that the modes with the highest growth rates tend to cluster close to the frequencies of the radial modes. This may explain the closely spaced spikes frequently seen in the periodogram for δ Scuti variables.

3. SOME RESULTS OF LINEAR STABILITY SURVEYS FOR MODELS OF δ SCUTI STARS

Several surveys concerning linear stability have been made, the most recent and complete one for radial modes being that of Stellingwerf (1979). The current discussion is based primarily upon the results of this survey and, in addition, upon some new calculations pertaining to nonradial modes.

All stellar models which lie within the range of effective temperatures for δ Scuti variables are unstable to some modes of radial and nonradial pulsations, assuming a standard helium content. The instability is due to the opacity mechanism with the He II ionization zone playing the dominant role in driving.

The highest pulsational energy growth rates per period ($\eta = -4\pi\omega_I/\omega_R$, where ω_I and ω_R are the real and imaginary parts of ω) are found for the fourth overtone, where they reach values of about 10^{-3}. The growth rates for the fundamental and the first overtone modes are at least two orders of magnitude lower. Let us recall that in Cepheids and RR Lyrae stars only fundamental, first overtones, and occasionally second overtones can be driven but the typical growth rates, η, are between 0.05 and 0.2.

Though, in all cases, the He II ionization zone provides the major driving, there are differences in details of the opacity mechanism. In the case of δ Scuti stars, H I and He I ionization zones play virtually no role in driving radial pulsations. Instead, the significant contribution to driving comes from the zone located at $T \simeq 1.5 \times 10^5$ K. This driving zone acts only in stars with high surface g; it is caused by an opacity bump which occurs when the location in frequency of the Planck function maximum coincides with the frequency of the He II ionization edge (Stellingwerf 1979).

Results are similar for nonradial modes associated with spherical harmonics of moderately low order ($\ell \lesssim 50$). Figure 3 gives a comparison of the driving (or damping) rates for radial and nonradial modes. Only those modes that are effectively trapped in the envelope were included in this survey. Modes corresponding to ℓ lower than 10 have somewhat reduced driving (or damping) rates due to imperfect trapping, as discussed in the previous section. It is clear that linear theory predicts no preference for radial over nonradial mode excitation for a wide range of ℓ values. In driving fundamental modes associated with high ℓ values, the H I ionization zone is important and becomes dominant at ℓ = 80-100.

Linear theory locates the blue boundary of the instability strip for main sequence stars at spectral type A3 in agreement with observations. Driving of high ℓ modes by this instability is expected in much earlier types, but this cannot result

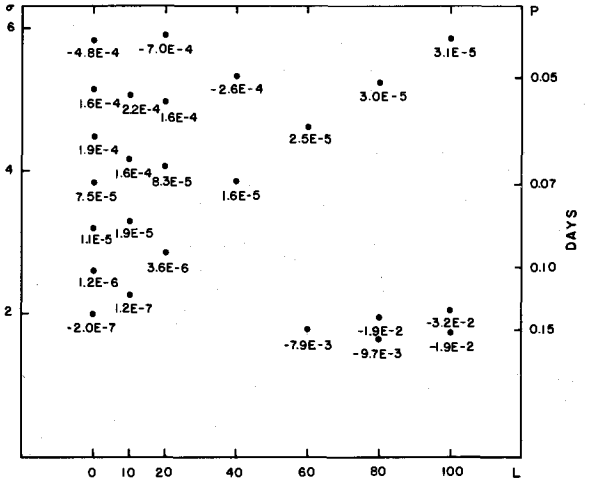

Figure 3. Periods and excitation rates for envelope oscillation of a δ Scuti star model with $M = 2\ M_\odot$, $L = 31.3L_\odot$, $\log T_e = 3.887$ and standard Population I composition. Frequency σ is in $(4\pi G\langle\rho\rangle)^{1/2}$ units and the numbers at the points indicating mode location are growth rates $(-\sigma_+)$ in the same units. Modes lying on the diagonal are f-modes. The upper left corner contains p-modes while g-modes are located in the lower right corner.

in observable variability. In addition, the shortest period theoretically predicted for δ Scuti stars is somewhat less than 30m, a figure which coincides with the observational evidence. This theory also provides an explanation of why nonradial modes are observed in δ Scuti stars but not in Cepheids.

The latter point is, however, only one of the differences between giant- and dwarf-type pulsators discussed in the introduction. It is tempting to relate lower amplitudes in dwarfs to lower growth rates, but predictions based on linear growth rates are subject to a great deal of uncertainty. This may be appreciated by noting that we have firm evidence of fundamental mode excitation in δ Scuti stars in spite of the fact that the undetected overtones have growth rates which are at least two orders of magnitude larger than the fundamental mode. Thus, the major differences between δ Scuti stars and giant pulsators can be understood only by studying nonlinear effects leading to amplitude limitation.

4. LIMITATION OF PULSATION AMPLITUDES

Christy (1966), in his celebrated paper on nonlinear pulsations of RR Lyrae stars, showed that in these stars pulsation amplitudes are limited by saturation of the driving mechanism. This occurs when the flux carried by pulsation in the driving zone amounts to about 10 percent of the total luminosity. Is the amplitude limiting process the same in δ Scuti stars? The answer is that it is almost certainly different.

By applying the same numerical technique as used in the case of RR Lyrae stars to δ Scuti stars, Stellingwerf (1980) has shown conclusively that these stars should have very large (> 1 mag) amplitudes, a finding which is in obvious conflict with the observations. One may speculate that driving is saturated by a large number of nonradial modes which correspond to large ℓ-values and are therefore invisible in the form of light variability. However, an inspection of numerical data on linear nonradial modes leads to the prediction of root mean square macroturbulence velocities in the range 10^1 - 10^2 kms^{-1}, assuming these modes carry 10 percent of total luminosity. This result apparently rules out the possibility of this form of saturation, since the observed macro- and micro-turbulence velocities are only a few kms^{-1}.

The conclusion must be that the opacity mechanism is not saturated in δ Scuti stars and, consequently, that there must be an efficient mechanism that removes energy from linearly driven modes. This situation is apparently similar to that of convection in subphotospheric layers, in which case radiative losses prevent the temperature gradient from approaching its adiabatic value. It seems most likely that, in our case, energy is driven out from the mode as a result of its nonlinear interactions with other modes. In Stellingwerf's model, the number of possible modes available for interaction was grossly reduced by the assumption of spherical

symmetry.

When considering low amplitude oscillations, only three (and in special cases two) mode resonant interactions are important. Such interactions take place between any (j, k, m) modes if $\omega_j = \omega_k + \omega_m + \Delta\omega$ with $\Delta\omega$ much smaller than any of the three ω's involved and if the projection of the nonlinear terms resulting from interaction between one pair of the modes onto the eigenfunction of the third mode is non-zero.

If we write the displacement vector $\vec{\xi}$ in the form

$$\vec{\xi}_i = A_i(t)\vec{h}_i \sin\left[\phi_i + (\omega_i + \Delta\omega)t\right]$$

where h_i is the normalized eigenvector, then by standard techniques known in various fields of physics (see, for example, Davidson 1972) we have

$$\frac{dA_i}{dt} = \lambda_i A_i + C_i A_p A_q \cos\Phi$$

where i, p, and q are any of j, k, m; C_i is the projection of interaction terms for the p- and q-modes onto the i-mode eigenfunction; λ_i is the linear growth rate (if > 0); $\Phi = \phi_j - \phi_k - \phi_m$ and

$$\frac{d\Phi}{dt} = \Delta\omega + \left(C_j \frac{A_k A_m}{A_j} - C_k \frac{A_j A_m}{A_k} - C_m \frac{A_j A_k}{A_m}\right)$$

Several special cases of mode interaction have been studied in the past. Vandakurov (1965, 1967) investigated the decay instability of a radial mode (j) into two gravity modes (k,m). If nonadiabatic effects are ignored, then instability occurs if

$$4\vec{h}_j^2 C_k C_m > \Delta\omega^2$$

In the case considered, $C_k = C_m$ and, consequently, the above inequality defines an instability band for each value of the radial mode amplitude.

This instability is prevented by damping of the nonradial modes if $-\lambda_k \gtrsim 2|\vec{h}_j C_k|$. On the other hand, if λ_j is large, the growth of the radial mode may not be disturbed by possible growth of the nonradial modes. This is one reason why this instability is not likely to be important in the case of giants. The other reason is that, in giants, radial modes tend to be trapped in the envelope, while gravity modes tend to be trapped in the deep interior which results in very low values of the projection C. For δ Scuti stars, however, the decay instability is likely to be very important.

In an attempt to interpret amplitude modulation in RR Lyrae stars, Kluyver (1935) studied high frequency mode driving using the resonance $\omega_j - 2\omega_k$, a special

case of the more general resonance considered here. Papaloizou (1973) studied the limiting action of such a resonance on pulsation amplitudes in massive stars which are vibrationally unstable due to the ε mechanism. It is likely that, in δ Scuti stars, this phenomenon is responsible for limiting amplitudes of higher overtones.

The effects of mode coupling in limiting amplitudes have thus far been considered only for linearly driven modes. However, the possibility of the existence of opposite effects emerges from the work of Simon (1978) and the discussion presented by Fitch (1980), which indicate that short period variables that are characterized by rather large amplitudes show evidence of resonances in their frequency distributions. Amplitude amplification as a result of resonant mode interaction is known in plasma theory (Davidson 1972) and occurs if $C_k = C_m = -C_j$. In the case of oscillation mode interactions in a star, this remains an intriguing possibility. Quantitative studies of mode coupling in δ Scuti stars and other stars are now in progress.

5. CONCLUSION

The preceding discussion suggests the following interpretation of the differences listed in the introduction between dwarf- and giant-type pulsators:

1. Amplitudes in dwarfs are smaller because they are limited by nonlinear mode coupling which becomes important before the driving mechanism is saturated. The greater importance of mode coupling in dwarfs than giants is related both to lower excitation rates and lower values of coupling coefficients. These two effects may be understood in terms of differences between propagation mode properties in giants and dwarfs.
2. Multiperiodicity in dwarfs is caused by the fact that the driving mechanism is not saturated and by the fact that there are many nonradial modes associated with low ℓ harmonics having very similar properties.
3. Nonradial modes are not observed in giants because, for low ℓ harmonics, they are either damped or their excitation rates are so low that the driving mechanism is saturated by the radial modes. The latter modes saturate in driving before nonradial modes grow to any observable amplitude). Again, the difference in growth rates between $\ell = 0$ and $\ell > 0$ modes, in the case of giants, is easily understood in terms of propagation properties.
4. In addition to the fact that dwarfs tend to be low amplitude pulsators, gravitational settling of helium in dwarfs may contribute to poorer definition of the instability strip.

* * * * *

It is a pleasure to express my thanks to Professor Henry A. Hill, head of the SCLERA group at the Department of Physics of the University of Arizona, and to other members of this group for their hospitality during my stay with them. Helpful

conversations with Walter Fitch, Henry Hill, Antoni Kuszell, Bob Stellingwerf, and Yuri Vandakurov are gratefully acknowledged.

This work was supported in part by the National Science Foundation.

REFERENCES

Breger, M. 1979, Pub. A. S. P., 91.

Castor, J.L. 1970, B. A. A. S., 2, 302.

Christy, R.F. 1966, Ap. J., 144, 108.

Cox, King and Hodson 1979, (in press).

Davidson, R.P. 1972, Methods in Nonlinear Plasma Theory, (Academic Press).

Dziembowski, W. 1975, Mem. Soc. Roy. Liege, 6^{e}s VIII, 287.

Dziembowski, W. 1977, Acta Astr., 27, 95.

Fitch, W.S. 1980, these proceedings.

Kluyver, H.A. 1935, Bull. Astron. Inst. Neth., 7, 265.

Osaki, Y. 1975, Publ. Astron. Soc. Japan, 27, 237.

Osaki, Y. 1977, Publ. Astron. Soc. Japan, 29, 235.

Papaloizou, J.P.B. 1973, Mon. Not. R. Astr. Soc., 162, 143.

Scuflaire, R. 1974, Astr. Ap., 36, 107.

Shibahashi, H. and Osaki, Y. 1976, Publ. Astron. Soc. Japan, 28, 199.

Simon, N.R. 1978, preprint.

Stellingwerf, R.F. 1979, Ap. J., 227, 935.

Stellingwerf, R.F. 1980, these proceedings.

Unno, W. 1975, Publ. Astron. Soc. Japan, 27, 81.

Vandakurov, U.V. 1965, Proc. Acad. Sci. USSR, 164, 525.

Vandakurov, U.V. 1967, Ap. J., 149, 435.

Vauclair, G., Vauclair, S. and Pamjatnykh, A. 1974, Astr. Ap., 31, 63.

NONLINEAR CALCULATIONS FOR BUMP CEPHEIDS

S.W. Hodson and A.N. Cox
Theoretical Division
Los Alamos Scientific Laboratory of the University of California
Los Alamos, New Mexico

ABSTRACT

Using the von Sengbusch-Stellingwerf relaxation method, hydrodynamic calculations have been made to find strictly periodic solutions for the fundamental mode pulsations of 7 $M_\odot$ models. These models have a helium enrichment in the surface convection zones up to Y = 0.78. From the linear theory period ratio Π_2/Π_0 and the Simon and Schmidt resonance hypothesis, the observed Hertzsprung progression of light and velocity curve bump phase with period should result. These surface helium enhanced models show the proper nonlinear bump phase behavior without resort to any mass loss before or during the blue loop phases of yellow giant evolution. At 6000 K and the luminosity of 4744 $L_\odot$ given by evolution theory for 7 $M_\odot$ (that is, at a fundamental mode period of 8.5 day), the velocity curve bump is well after the maximum expansion velocity. At 5400 K and the same luminosity (period of 12.5 day), the bump on the velocity curve occurs well before maximum expansion velocity time. The Christy echoes appear to be exhibited in the latter case but not in the former. The echo interpretation may not be appropriate for these masses which are larger than the anomalous masses used by Christy (1975); Stobie (1969a, 1969b); and Adams (1978). Resonance of the fundamental and second overtone modes should not necessarily show echoes of surface disturbances from the center. The conclusion is that helium enrichment in the surface convection zones can adequately explain observations of bump Cepheids at evolution theory masses.

* * * * *

Our calculations deal with the so-called bump Cepheids which have periods between about 5.5 and 13 days. Chemically homogeneous models were considered in some detail by Christy (1974), Stobie (1969a, 1969b); King et al. (1973); and most recently by Adams and Davis (1978). The Goddard model, calculated by a large number of computer programs, also possesses a velocity and light curve bump. Until 1977, a model mass of about 2/3 the evolutionary theory value was required in order to give the proper bump phase and its variation with the fundamental radial pulsation mode.

All Cepheid mass anomalies can be resolved if one adopts models with helium enriched convection zones and, for modes with periods between 0.7 and 4 days, a

deeper helium enriched zone constituting possibly 10^{-3} of the stellar mass (Cox et al. 1977). This strategy has had successes in explaining the double-mode Cepheids and the sole triple-mode Cepheid, AC Andromedae, in terms of normal evolution theory masses. This paper addresses only the bump Cepheids; results for AC Andromedae and double-mode Cepheid models are discussed by Cox, King and Hodson (1978) and by Cox, Hodson and King (1979) respectively.

In bump Cepheids, helium enrichment is necessary only in the thin convection zones which comprise less than 10^{-4} of the stellar mass. The cause of this enrichment may be some fractionation process that operates through a solar-type wind, leaving the helium behind (Cox, Michaud and Hodson 1978). The mass loss rate of about 10^{-10} $M_\odot$/yr is probably unobservable, and certainly the mass of the yellow giants, pulsating or not, is not significantly affected in the 10^6 - 10^7 years needed for their blue loops in the Hertzsprung-Russell diagram. The helium enhancement requires time and cannot operate in fast-evolving stars of mass greater than 8 $M_\odot$.

A question relevant to the helium enhancement hypothesis is: Can this tremendous helium mass fraction, Y = 0.75, be detected in the stellar spectrum? Kamp and Deupree (1979); Sonneborn, Kuzma and Collins (1979); and Kurucz (1978) have considered the spectrum of yellow giants. The only effects noted with Y = 0.75 are a reduced Balmer jump, a large strengthening of the weak metal lines that is probably unobservable, and a moderate strengthening of the strong temperature sensitive lines. All the authors feel that the enhanced helium may not be detected, especially since all blue looping yellow giants should show the same helium enhancement regardless of their pulsation. More work is in progress.

Another unanswered question is: Will the inverted μ gradient due to the helium enhancement mix downward rapidly enough to destroy the enriched layer, during which time fractionation is being brought about by the wind? Two-dimensional calculations are currently being made to study this question. A smooth gradient in a 7 $M_\odot$ 5900 K Cepheid from Y = 0.30 at 90,000 K and 8×10^{-8} g/cm^3 ($1 - q = 3 \times 10^{-4}$) to Y = 0.72 at 60,000 K and 2×10^{-8} g/cm^3 ($1 - q = 6 \times 10^{-5}$) has been studied for a very short run (less than a year of star time). The small effects noted indicate a mixing timescale of at least 10^5 years, but this number is still very tentative. A mixing time of 10^6 - 10^7 years would serve to keep the helium in the convection zones for bump Cepheids; this would also allow a slight downward leakage to give correct period ratios for the slower evolving double-mode and triple-mode Cepheids.

Simon and Schmidt (1976) have enabled us to study the bump phase using only the linear theory. From the extensive Stobie (1969b) nonlinear results and their linear adiabatic periods, Simon and Schmidt have shown that bumps occur for Cepheid models when Π_2/Π_0 lies between 0.46 and 0.53. At $\Pi_2/\Pi_0 = 0.53$, the bumps are located far on the descending sides of the light and velocity curves while, at 0.50-0.46 for Π_2/Π_0, they are on the rising parts. Figure 1 (from Cox, Michaud and Hodson 1978)

plots Π_2/Π_0 versus Π_0.

Consider first the results in Figure 1 for the homogeneous models at 7 $M_\odot$ using the King IVa composition (X = 0.70, Z = 0.02). On the basis of these linear results, there should be no light or velocity curve bumps for those models between the blue (B) and red (R) edge, a finding which is inconsistent with the results of nonlinear calculations. If the mass is reduced to 5 $M_\odot$ but the luminosity for 7 $M_\odot$ retained, the corresponding curve in Figure 1 indicates that one can presumably get bumps for periods like 10 days or longer. The curve near to the one just discussed was obtained using Carson opacities in homogeneous evolutionary mass models for 7 $M_\odot$ and evolutionary luminosity. A nonlinear calculation at the tip of the extension at 8.7 days and 6000 K, with slightly lower Π_2/Π_0, gives no bumps if the pulsation amplitude is a normal one such as 30-40 km/s. If the amplitude is made slightly larger by a reduced artificial viscosity, one gets amplitudes like 45 km/s. Because of the stronger helium driving, Vemury and Stothers (1978) have found bumps. Surface helium enriched models at 6, 7 and 8 $M_\odot$ show the proper observed Hertzsprung progression of the bumps.

A few words about the Vemury and Stothers (1978) result are in order. First, the Carson opacities used by them differ greatly from the opacities that have been found in other work. The bumps seen in Figure 2 (taken from Vemury and Stothers 1978) do <u>not</u> seem to be like the well-known echoes from the central regions discussed extensively by Christy (1974). We propose that they are surface disturbances, perhaps shock waves, due to the large velocity gradients at the surface, and not the bumps observed in the Cepheid light and velocity curves.

Setting aside the Vemury and Stothers results, for which only the opacities used are disputed, the question is whether nonlinear calculations can actually confirm the observed Hertzsprung progression of the bump phase with period for our inhomogeneous models. Surface helium enhanced models for Y_S = 0.78 have been calculated at 7 $M_\odot$ for the evolution theory blue loop luminosity of 1.85×10^{37} erg/s. Results for the cool T_e of 5400 K, near the red edge or possibly just beyond it, are given in Figure 3. This model has fundamental mode period of 12.5 days. The period ratio, according to the Simon and Schmidt (1976) hypothesis, should give a bump on the rising part of the light curve and on the falling part of the observer's radial velocity curve. This is seen for this red model where radial velocity variations at every one of our 49 levels, each differently amplified and slightly displaced from its neighbors, are plotted against time for five periods. The Christy (1974) echo can be seen clearly, which simultaneously verifies the Christy (1975); Simon and Schmidt (1976); and Cox et al. (1977) concepts on, respectively, echoes, period ratios and enhanced helium. This case is analogous to the Cepheid Z Sct (12.9d). Note that mass loss in early red giant stages, forbidden to us by stellar evolution research, is not required to give the bumps at the proper phase.

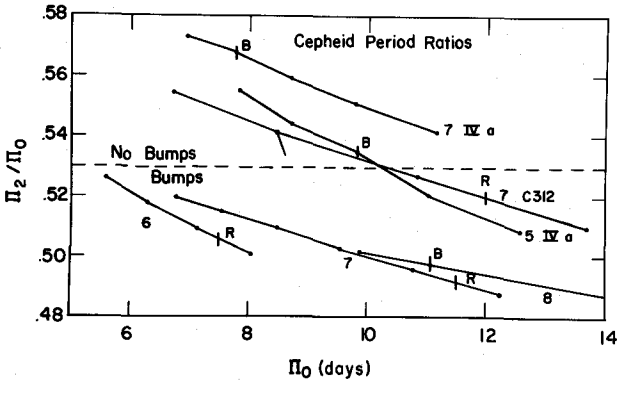

Figure 1. Plot of Π_2/Π_0 versus Π_0 for various Cepheid masses and compositions, from linear theory. Fundamental blue and red edges are indicated by B and R, respectively. Homogeneous envelopes are indicated for three cases; 7 $M_\odot$ - King IVa (7 IVa), 7 $M_\odot$ - Carson 312 (7 C312), and 5 $M_\odot$ - King IVa (5 IVa). From nonlinear calculations all surface helium enriched models at 6, 7, and 8 $M_\odot$ show bumps with the observed Hertzsprung progression. For the homogeneous models, no bumps are found unless the luminosity becomes too large for a given mass (5 IVa) or an extreme velocity gradient (7 C312). (Ap. J., June 1, 1978).

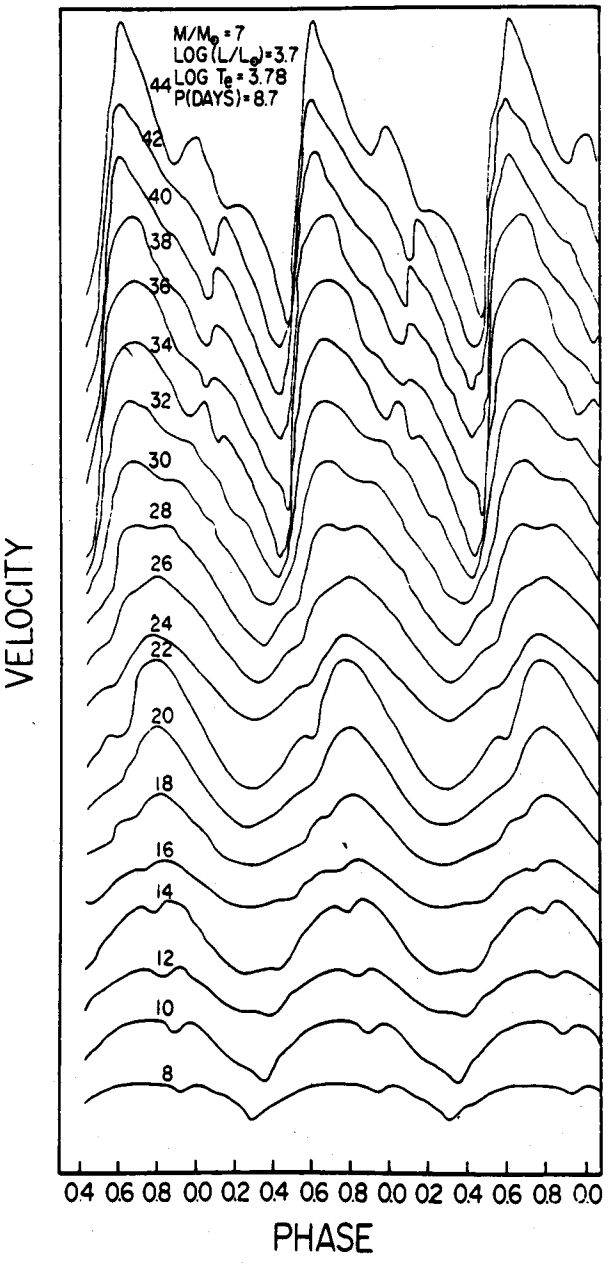

Figure 2. Plot of radial velocity versus phase for various levels in the 8.7^{d} model by Vemury and Strothers (1978). The bump on the descending side of the surface velocity curve appears to be a surface disturbance and not a well defined echo from the core obtained by Christy (1975).

A hotter, bluer model is shown in Figure 4. With mass, luminosity and composition structure the same as the model used in Figure 3, this 6000 K, 8.5 day case, near the fundamental-first overtone transition line, gives the bump on the rising part of the velocity curve like the Cepheids DL Cas (8.00d) and η Aql (7.18d).

All is not perfect, though. The Christy echo is absent and the bump appears at all levels. However, it is at least more systematic than the bump of Vemury and Stothers (1978) and is comparable to that found in Christy's models with similar periods. The Π_2/Π_0 period ratio of 0.51 is correct for the Simon and Schmidt (1976) hypothesis. The second overtone is indeed unstable for both the 5400 K and 6000 K models if one feels that Π_2 should occur naturally rather than be induced.

Two final points should be noted. A prediction might be made that, for Cepheids which are in the proper period range and could have bumps, perhaps one in ten actually do not have them because they are on the rapid first evolutionary crossing of the instability strip, before any helium enhancement can be established. As discussed by Cox, Michaud and Hodson (1978), examples of this type of Cepheids may be X Sgr (7.01d) and FN Aql (9.48d). For these homogeneous stars the bumps should occur for much longer periods, from 13 to possibly 30 days, as for RU Sct (19.7d), AZ Pup (23.2d) and X Pup (26.0d).

The proposed helium enhancement in yellow giants maintained by a helium poor stellar wind, if stable enough against downward mixing, offers an adequate explanation of the masses and behavior of bump Cepheids.

REFERENCES

Adams, T.F. and Davis, C.G. 1978, B.A.A.S. 10, 401.

Christy, R.F. 1968, Quart. J.R.A.S. 9, 13.

Christy, R.F. 1974, in Cepheid Modeling, NASA SP-383, ed. D. Fischel and W.M. Sparks, p. 85.

Cox, A.N., Deupree, R.G., King, D.S. and Hodson, S.W. 1977, Ap. J. (Letters), 214, L127.

Cox, A.N., Hodson, S.W. and King, D.S. 1979, Ap. J. (Letters), 230, L109.

Cox, A.N., King, D.S. and Hodson, S.W. 1978, Ap. J., 224, 607.

Cox, A.N., Michaud, G. and Hodson, S.W. 1978, Ap. J., 222, 621.

Kamp, L.W. and Deupree, R.G. 1979, Pub. A.S.P., in press.

King, D.S., Cox, J.P., Eilers, D.D. and Davey, W.R. 1973, Ap. J., 182, 859.

Kurucz, R.L., 1978, private communication.

Simon, N.R. and Schmidt, E.G. 1976, Ap. J., 205, 162.

Sonneborn, G., Kuzma, T.J. and Collins, G.W. 1979, Ap. J., in press.

Stobie, R.S. 1969a, M.N.R.A.S. 144, 485.

Stobie, R.S. 1969b, M.N.R.A.S. 144, 511.

Vemury, S.K. and Stothers, R. 1978, Ap. J., 225, 939.

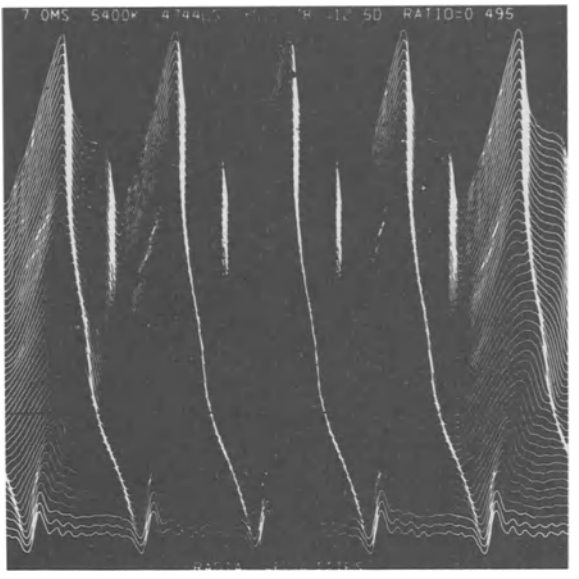

Figure 3. Plot of observer's radial velocity versus time for each level of a surface helium enhanced model (Y_s = 0.78) at 7 $M_\odot$, 4744 $L_\odot$, and T_e = 5400 K, near the fundamental red edge. Each level has been amplified and displaced from neighboring levels. With Π_0 = 12.5^d and Π_2/Π_0 = 0.495, a well defined bump is evident on the falling side of the curve (rising side of light curve) as predicted by Simon and Schmidt.

Figure 4. Plot of observer's radial velocity curve versus time for each level of a surface helium enhanced model (Y_s = 0.78) at 7 $M_\odot$, 4744 $L_\odot$, and T_e = 6000 K, near the fundamental first overtone transition line. Each level has been amplified and displaced from neighboring levels. With Π_0 = 8.5^d and Π_2/Π_0 = 0.508, a well defined bump is evident on the rising side of the curve (falling side of light curve).

A NONLINEAR STUDY OF AI VELORUM

A.N. Cox and S.W. Hodson
Theoretical Division
Los Alamos Scientific Laboratory of the University of California
Los Alamos, New Mexico

ABSTRACT

Using results from earlier studies of double-mode dwarf Cepheids by Cox, King and Hodson (1979), hydrodynamic calculations have been undertaken for AI Vel. The evolution theory mass of 1.8 $M_\odot$ previously derived, together with a luminosity of 23 $L_\odot$ and a T_e of 7500 K, give the observed period of 0.11 day and the observed period ratio Π_1/Π_0 = 0.773. Although the observed T_e was 7620 K, a cooler T_e is used due to the former's location at the fundamental pulsation mode blue edge. The composition used is X = 0.70, Z = 0.01--a Z value lower than normal in order to make the period ratio as large as that observed. The goal is to see if double-mode behavior, due to either mode switching or a permanent state, can be predicted for the model. Progress in converging the model to a periodic pulsation solution by the von Sengbusch-Stellingwerf relaxation method is discussed.

* * * * *

Earlier studies of double-mode dwarf Cepheids by Cox, King and Hodson (1979), have proposed that the observed period ratios of the two simultaneously pulsating modes could be correctly predicted theoretically for stars of mass 1.1 to 2.2 $M_\odot$ in their normal giant evolution. Some authors such as Bessell (1969); Petersen and Jorgensen (1972); Jones (1975); Dziembowski and Kozlowski (1974); and Simon (1979a) have concluded that the dwarf Cepheids are low mass stars, probably in a post-red giant evolutionary stage. In most recent work, Breger (1976); Bessell (1974); and McNamara and Langford (1975) suggested that the dwarf Cepheids or AI Velorum stars were merely large amplitude δ Scuti variables. Many observed quantities, such as period distributions, Wesselink radii, space motions, metal abundances, gravities, etc., support this suggestion. A further problem was that the period ratios were more typical of the low mass population II stars. Our work (Cox, King and Hodson 1979) and that by Stellingwerf (1979) showed that the large observed period ratios of 0.763 to 0.778 could be obtained even with the normal heavy element composition, Z = 0.02. For AI Vel, which is the prototype variable with a fundamental period of 0.11 day, Cox, King and Hodson (1979) found that the best linear theory period ratio fit of 0.773 is obtained with a 1.8 $M_\odot$, 23 $L_\odot$, 7500 K stellar model having a composition

X = 0.70 Z = 0.01. These parameters are consistent with both normal post-main sequence evolution and linear pulsation theories.

Table 1 shows various physical parameters for all the known double-mode dwarf Cepheids including our star AI Vel, which will be used for this nonlinear study. The T_e for AI Vel, 7620 K, is exactly at the fundamental radial mode blue edge. In order to obtain a non-zero fundamental mode growth rate (cf. Cox, King and Hodson 1979), we have used a T_e of 7500 K in this sutdy.

Period ratios for masses and compositions of interest are also found in Cox, King and Hodson (1979) and are reproduced here in Table 2. The period ratios were obtained for a constant period of 0.11 day, which represents a line of almost constant radius for each mass in the Hertzsprung-Russell diagram. This line of constant period is also a line of constant period ratio, and that ratio is given for T_e values all across the instability strip between 7000 K and 8000 K.

The compositions that give the observed period ratio of 0.773 are the Carson C312, Deupree IV, Deupree V and Cogan II mixtures. The observed period ratio can also be obtained through depletion of the helium content by gravitational settling in these high-gravity, slowly evolving stars. A value of Z = 0.01 seems required for all except the controversial Carson C312 mixture; the Cox-Davis VI mixture has the period ratio too low. Thus in our 50 zone model for nonlinear studies we have used the Deupree IV composition with no surface helium depletion.

It is the purpose of this study to demonstrate double-mode behavior by periodic nonlinear calculations. Linear theory analysis of the nonlinear periodic solutions should show whether a given full amplitude mode is stable or unstable against decay to another. As Stellingwerf (1975a,b) has discovered for RR Lyrae variables and some 1.6 $M_\odot$ models, a region in the H-R diagram may exist where the fundamental and first overtone modes have a tendency to decay to each other, resulting in a mixed mode pulsation. However, permanent double-mode behavior (changing only on an evolutionary timescale) for the 1.6 $M_\odot$ case could not be confirmed by Hodson and Cox (1976). Further, the RR Lyrae permanent double-mode domain is clearly beyond the red edge. Therefore, we currently expect that mode switching from F to 1H or vice versa alone could cause two simultaneous radial pulsation modes for any double-mode variable such as the dwarf Cepheid AI Vel.

A problem exists in the use of mode switching as an explanation for the behavior of the double-mode Cepheids. The switching time is approximately 10^2 years while the evolution time as pulsators is 10^6 years, leading to an estimate of only 10^{-4} of the Cepheids which should exhibit double-mode behavior. However, about 25 percent of these stars actually do. A domain of instability toward each mode one quarter the width of the instability strip is indicated, but no domain at all has been found by nonlinear periodic calculations as yet. The latest deep helium enrichment models for the double-mode classical Cepheids may give such a domain but

Table 1. Theoretical Masses, Radii, And Luminosities For Double-Mode Dwarf Cepheids

Variable	Π_0(d)	Π_1/Π_0	T_e(K)	$M_T/M_\odot$	$R_T/R_\odot$	$L_T/L_\odot$	Q_0(d)
SX Phe*	0.05496	0.778	7850	1.1 ± 0.1	1.3 ± 0.1	5 ± 1	0.0325
CY Aqr**	.06104	.744:	7930	1.4 ± 0.1	1.7 ± 0.1	10 ± 1	.0326
ZZ Mic	.0654	.763	7500	1.4 ± 0.1	1.8 ± 0.1	10 ± 1	.0327
AE U Ma	.08602	.773	7500	1.6 ± 0.1	2.2 ± 0.3	14 ± 4	.0328
RV Ari	.09313	.773	7500	1.6 ± 0.1	2.3 ± 0.3	14 ± 4	.0328
BP Peg	.10954	.772	7500	1.8 ± 0.1	3.0 ± 0.3	25 ± 5	.0328
AI Vel	.11157	.773	7620	1.8 ± 0.1	2.9 ± 0.3	25 ± 5	.0328
V703 Sco	.14996	.768	7000	1.9 ± 0.1	3.9 ± 0.5	33 ± 8	.0329
VX Hya	0.22339	0.773	6980	2.2 ± 0.1	4.8 ± 0.4	48 ± 8	0.0330

* 1st crossing assumed

** 1st or third crossing

T_e values for SX Phe, CY Aqr, AI Vel, and VX Hya from McNamara and Feltz (1978). For V703 Sco, T_e is from Jones (1975). For all variables the deep interior composition is Z = 0.01 with Y between .2 and .3 except for SX Phe with Z = 0.001 with interior Y between .2 and .3.

Table 2. Double-Mode Dwarf Cepheid Period Ratios

$\Pi_0 = 0^d.11$ $\quad 7000 \leq T_e \leq 8000$ K

	Compositions (Y_S,Z)					
$M/M_\odot$	C 312	C-D VI	D IV	D V	D IV I*	C II
	(.25, .02)	(.28, .02)	(.29, .01)	(.24, .01)	(.10, .01)	(.195, .005)
1.5	0.768	0.765	0.770	0.770	0.773	0.773
2.0	.774	.764	.770	.773	.769	.771
2.5	0.786	0.768	0.776	0.776	0.774	0.780

*Y_S down to 250,000 K

the calculations have not yet been done. Certainly the resonance concepts of Simon (1979b), if correct, also give very narrow double mode regions in the instability strip.

To illustrate this situation, let us examine the best available picture for RR Lyrae variables. Figure 1 gives Stellingwerf's (1975a) graph of growth rate versus T_e. These data are very similar to the earlier results of von Sengbusch (1974). The linear theory curves, based on studies of equilibrium models, are very familiar, giving blue edges of the instability strip for the first two radial modes similar to those of Iben (1971); Cox, King and Tabor (1973) and others. The stability of the nonlinear solution is given for the overtone growing out of the fundamental and for the fundamental growing out of the overtone. In a small region either mode can exist at full amplitude. Except for those obtained in the red region beyond the Deupree (1977) red edge at 6350 K, the full amplitude solutions are never simultaneously unstable to switching from one to another.

The linear theory growth rates for AI Vel are given in Figure 2; the log T_e for our nonlinear model is 3.875.

With a growth rate of only a few parts in a million per period, really tight convergence by the periodic Stellingwerf method has not been obtained. The velocity curve at the limiting amplitude is given in Figure 3 for three of the last trial periods calculated. The velocity amplitude is about 7 km/s. The light curve is given in Figure 4 for these same three trial periods with a M_{bol} range of 1.28 to 1.48. The stability of these solutions against decay to the overtone is -0.1% per fundamental period.

Calculations for the overtone show that it is also stable, rejecting the fundamental mode at a rate of 0.1% per overtone period. Thus, at 7500 K, either F or 1H behavior is possible.

What fraction of the δ Scuti variables exhibit two or more modes? Nine double-mode dwarf Cepheids are listed in Table 1. Fitch does not believe ZZ Mic should be on the list so there are probably only eight. Although more double-mode stars exist among the δ Scuti variables, they are difficult to detect and then they often display nonradial modes such as those found in 1 Mon. Fitch (1980) lists nine of these. This provides a numerator total of approximately 20, with the denominator being the number of all δ Scuti variables. Breger's (1979) latest review gives only 130 variables, but actually 1/3 of all stars between A2 V and F0 V vary. Thus, the denominator should perhaps be in the thousands. The fraction of δ Scuti variables which exhibit two modes is probably less than 10^{-2}. This indicates a much different case than that of the more luminous classical Cepheids, one-quarter of which exhibit double-mode variability.

Mode switching timescales for an evolving AI Vel variable can be obtained from the formula given by Stellingwerf (1975b), corrected by a factor of $\sqrt{2}$:

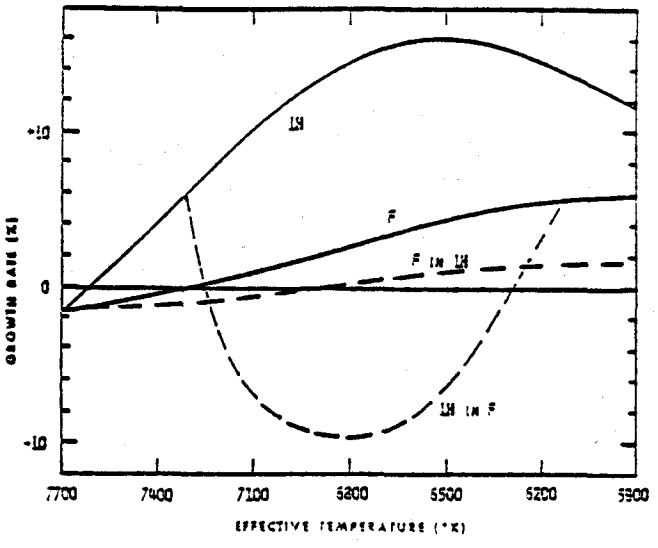

Figure 1. Composite growth rate diagram for a sequence of RR Lyrae models with M = 0.578 $M_{\odot}$, X = 0.7, Z = 0.001 and L = 2 x 10^{35} ergs/sec.

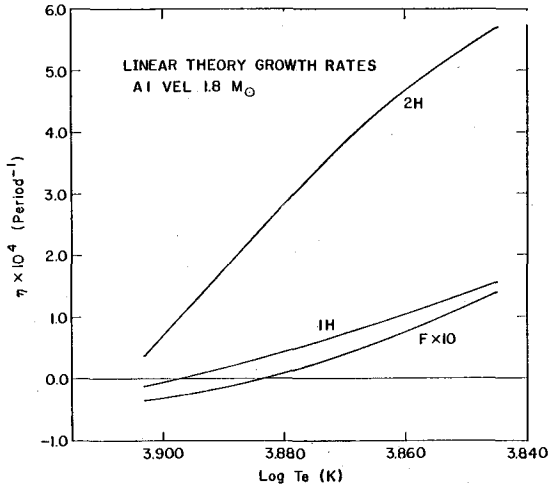

Figure 2. The growth rate for AI Vel calculated from linear theory.

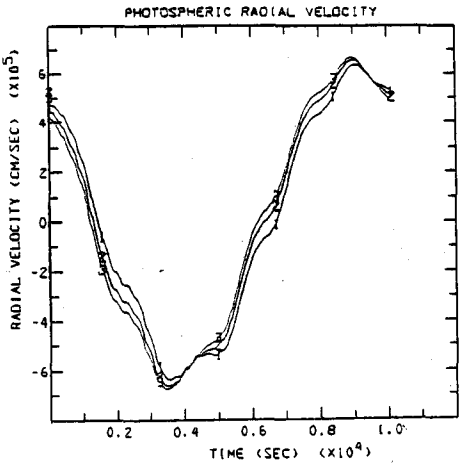

Figure 3. The limiting velocity amplitude of the periodic Stellingwerf method for AI Vel. The last three trial periods are given.

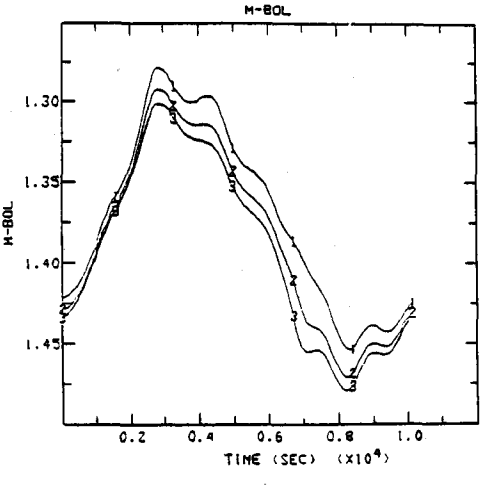

Figure 4. The limiting light curves of the periodic Stellingwerf method for AI Vel. The last three trial periods are given.

$$\tau = \sqrt{\frac{2}{\left(\frac{\partial \eta}{\partial T_e}\right)\left(\frac{\partial T_e}{\partial t}\right)}} \quad , \qquad (1)$$

where η is the switching rate from one mode to another. Here we estimate the mode switching rate for the kinetic energy to change from $-2 \times 10^{-3}/\Pi_0$ to $+3 \times 10^{-5}/\Pi_0$ as T_e changes from 7500 K to 7620 K (the F blue edge where Figure 2 data obtains). In the $1H \rightarrow F$ case, this rate may be ten times slower per Π_1, as shown in the RR Lyrae models given in Figure 1. This implies that the $\partial \eta/\partial T_e$ rate for redward evolution ($1H \rightarrow F$) is 6×10^{-6} per K per year for our 0.086 day Π_1. From evolution tracks, $\partial T_e/\partial t$ is about 5×10^{-4} K per year. Evaluation of the formula gives a mode switching time scale of about 2.6×10^4 years.

With evolution times like 2×10^6 years to cross the instability strip, it appears that 10^{-2} of all δ Scuti stars might be seen in two modes simultaneously. Those with larger periods should be going redward with increasing periods and increasing Π_0 amplitude. At shorter periods, either Π_0 or Π_1 amplitudes could be growing, depending on the evolution direction in the S-shaped tracks on the H-R diagram. The very rough theoretical expectation that 10^{-2} of all δ Scuti variables exhibit two modes agrees with the rather approximate fraction gleaned from observations. No amplitude changes should be detectable over the available time span of less than 50 years.

More study is needed in order to understand the double-mode behavior of AI Vel and others like it. Preliminary work indicates that they are all mode switching at transition lines which, due to the differing surface helium content of the stars, occur all across the instability strip.

REFERENCES

Bessell, M.S. 1969, Ap. J. Suppl., 18, 195.

Bessell, M.S. 1974, in IAU Symposium 59 Stellar Instability and Evolution, ed. Ledoux, Noels and Rodgers, p. 63.

Breger, M. 1976, in Proc. Los Alamos Solar and Stellar Pulsation Conference, ed. A.N. Cox and R.G. Deupree, LA-6544-C, p. 47.

Breger, M. 1979, Pub. A.S.P., 91, 5.

Cox, A.N., King, D.S. and Hodson, S.W. 1979, Ap. J., 228, 870.

Cox, A.N., King, D.S. and Tabor, J.E. 1973, Ap. J., 284, 201.

Deupree, R.G. 1977, Ap. J., 214, 502.

Dziembowski, W. and Kozlowski, M. 1974, Acta Astr., 24, 245.

Fitch, W. 1980, these proceedings.

Hodson, S.W. and Cox, A.N. 1976, in Proc. Los Alamos Solar and Stellar Pulsation Conf., ed. A. N. Cox and R. G. Deupree, LA-6544-C, p. 202.

Iben, I. 1971, Ap. J., 168, 225.

Jones, D.H.P. 1975, in IAU Symposium 67, Variable Stars and Stellar Evolution, ed. Sherwood and Plaut, p. 243.

McNamara, D.H. and Langford, W.R. 1975, Pub. A.S.P., 89, 505.

Petersen, J.O. and Jorgensen, H.E. 1972, Astr. Ap., 17, 367.

Simon, N.R. 1979a, Astr. Ap., 74, 30.

Simon, N.R. 1979b, Astr. Ap., in press.

Stellingwerf, R.F. 1975a, Ap. J., 195,441.

Stellingwerf, R.F. 1975b, Ap. J., 199, 705.

Stellingwerf, R.F. 1975c, personal communication.

Stellingwerf, R.F. 1979, Ap. J., 227, 935.

von Sengbusch, K. 1974, in Cepheid Modeling, ed. D. Fischel and W.M. Sparks, NASA SP-383, p. 129.

NONLINEAR δ SCUTI MODELS: THE MAIN SEQUENCE CATASTROPHE?

R.F. Stellingwerf
Department of Physics and Astronomy
Rutgers University
New Brunswick, New Jersey

ABSTRACT

For nonlinear models of 0.4 $M_\odot$ and 2.0 $M_\odot$ δ Scuti stars, pulsation amplitudes obtained in this region depend critically upon artificial viscosity parameters. Models with limited viscosity attain huge amplitudes. Furthermore, it is found that nonlinear stability properties depend primarily upon the amplitude. Determination of the actual dissipation mechanism is thus crucial to our understanding of these objects, and probably other main sequence pulsators as well. At present the most likely mechanisms appear to be 1) dissipation in the atmosphere, corona and wind; 2) turbulent dissipation in the convective zones; 3) magnetic fields.

1. INTRODUCTION

Observed stars in the lower Cepheid strip generally show very complicated behavior. Pulsation in a complex mixture of modes is not uncommon. Linear (small amplitude) nonadiabatic stellar models indicate that as many as six radial modes are expected to be unstable (Stellingwerf 1979) and nonradial modes are probably present as well.

As an initial step towards understanding this phenomenon, several nonlinear models have been studied in some detail. The final result is not encouraging: some basic physical dissipation mechanism seems to be missing. The evidence for this conclusion and various potential solutions to this dilemma are discussed below.

2. NONLINEAR MODELS

A low mass model was computed with the parameters M = 0.4 $M_\odot$, M_{bol} = 2.55, T_e = 7400 K, X = 0.7, Y = 0.295, Z = 0.005. This model provides a period ratio Π_1/Π_0 = 0.773 as observed in AI Vel. The lowest four modes are unstable at small amplitudes; periods and growth rates are given in Table 1 (cf. Stellingwerf 1979).

Periodic limit cycles were obtained in the fundamental and first overtone modes. The fundamental limit cycle had amplitudes of 2K = 114 km/s, and ΔM_{bol} = 1.51 magnitudes. The limiting amplitude was caused by saturation of the He^+ driving, but this amplitude is too large by about a factor of two. A nonlinear stability analysis

indicated the presence of a slowly growing instability associated with the inner boundary condition -- also found by Christy (1974) -- but showed no tendency to mode switching.

The first overtone limit cycle had amplitudes of 2K = 92 km/s and ΔM_{bol} = 1.3 magnitudes, and was found to be stable, aside from the inner boundary condition problem.

In this model the viscosity is that described in Stellingwerf (1975) with C_Q = 4, α = 0.1. This form effectively restricts the viscous dissipation to regions of strong shock formation. As a test of how additional viscosity might affect the amplitude, the model was rerun in the first overtone with C_Q = 1, α = 0 (i.e., the classical "Christy" form). The limiting amplitude in this case was 2K = 40 km/s, ΔM_{bol} = 0.36. The viscous term contributed roughly one third of the total dissipation and affected the amplitude profoundly. The amplitude now agrees with observations, but is entirely arbitrary, and the viscous dissipation is unphysical. A stability analysis of this limit cycle showed a positive switching rate of 0.12% per period toward the second overtone, the most unstable mode. It seems unlikely that this result is independent of the unreal dissipation.

A second model was run with the parameters M = $2M_\odot$, M_{bol} = 0.89, T_e = 7000, X = 0.7, Y = 0.28, Z = 0.02. This model resembles δ Scuti, and is unstable in four modes as shown in Table 2.

Table 1. Linear Periods and Growth Rates

Mode	Period (d)	Growth Rate (%/cycle)
0	0.1132	0.13
1	0.0875	0.72
2	0.0705	1.80
3	0.0591	0.90
4	0.0502	-2.20
5	0.0434	-5.70

The variation of driving and damping as a function of period was determined by integrating one period at various initial amplitudes (F-mode). The results are shown in Figure 1. Although these crude estimates suggest a limiting amplitude of about 30 km/s (2K = 60 km/s), this is not caused by saturation of driving, but by an increase in the damping. Both H and He^+ driving continue to increase at large amplitudes.

Table 2. Linear Periods and Growth Rates

Mode	Period (d)	Growth Rate (%/cycle)
0	0.1889	0.0013
1	0.1456	0.0168
2	0.1183	0.0621
3	0.0988	0.1072
4	0.0848	-0.3800
5	0.0744	-0.7200

Relaxation to the limit cycle showed that the model can readjust to avoid the increase in deep dissipation. The amplitude increased to 2K = 160 km/s, ΔM_{bol} = 2.7, but did not fully converge since the outer layers were approaching escape velocity. Clearly some mechanism other than saturation must limit the amplitude to the observed values ($0^m.1$-$0^m.2$). This "limit cycle" was found to be stable. The huge amplitudes could not result from a failure of the iterative scheme since a positive total work integral was found at each stage of the calculation. A time integration would yield the same result, even after roughly ten million periods.

Decrease of the viscous shift parameter α from 0.1 produced no effect until a value of about 0.01 was reached. At this point, strong, deep damping is present and the final amplitude drops to well below 10 km/s.

Decrease of the helium abundance to Y = 0.18 failed to reduce 2K below 50 km/sec.

The behavior of this model indicates a very serious deficiency in the theory, a deficiency not apparent in linear analyses. Clearly, realistic amplitudes can be obtained through manipulation of the viscosity, but this tells us nothing. What is the actual mechanism?

3. DISCUSSION

Since growth rates for δ Scuti models are very small, even a small amount of dissipation, increasing with amplitude, could limit the pulsations. In terms of growth rate, an additional contribution of $\eta = -1.0 \times 10^{-6}$ per period would suffice. In view of this, many normally negligible effects must be considered. A few of these were checked with numbers taken from the δ Scuti model discussed above. The results, presented when appropriate as the ratios of the corresponding η to the $\eta = -1.0 \times 10^{-6}$ above are as follows:

1. Molecular viscosity, atmospheric; fails by 10^{-10}.
2. Radiative viscosity; fails by 10^{-7}.

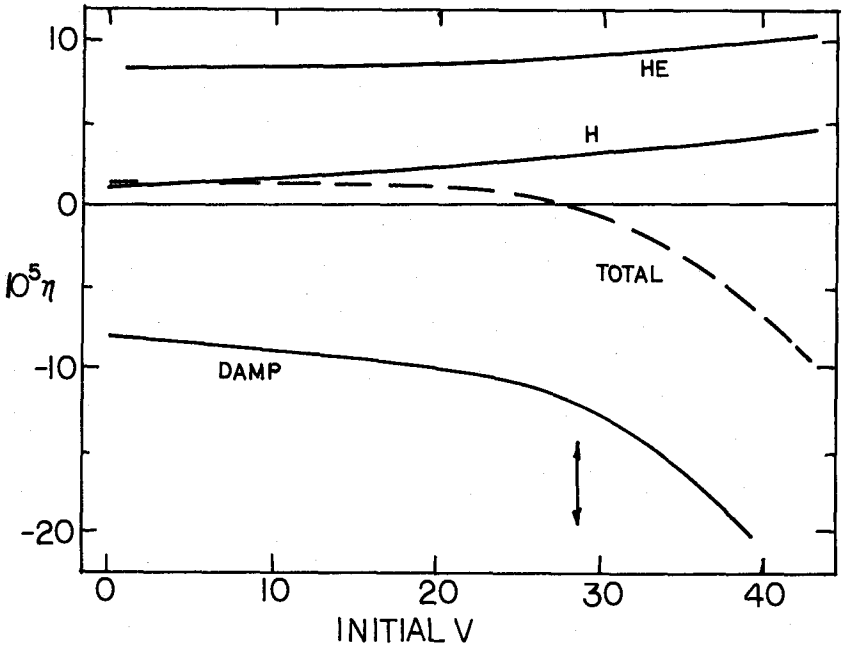

Figure 1. Driving and damping terms as a function of amplitude for the 2 $M_\odot$ δ Scuti model discussed in the text. Here η = work in units of total K.E., and is shown separately for the hydrogen ionization region, helium ionization region, and interior ("damp"). The dashed line is the sum of these three contributions.

3. Bulk viscosity, ionization zones; fails by 10^{-4} as long as photoionization dominates. It could contribute if the collisional term becomes important, since this is a slower process.
4. Reynolds stresses. In turbulent convective regions; estimates show that this effect could be important. However, models have so far failed to support this, as the convection is very weak.
5. Shocks, atmospheric dissipation. Again, this is a possibility, but models have not clearly demonstrated that shock heating and emission high in the atmosphere can stabilize the envelope.
6. Winds. A more promising idea is the direct loss of energy via waves propagating into a stellar wind. Supersonic winds are exceedingly stable and can convect energy very efficiently.
7. Magnetic fields. The amplitude-limiting effect of magnetic fields has probably already been observed as the Blashko effect (long period modulation of the light curve) in RR Lyrae stars. If true, then a more pronounced influence would be expected in stars with lower pulsational excitation.

Many of these mechanisms represent very difficult mathematical problems. It is, nonetheless, of some importance that this point be resolved. Not only does our understanding of the lower Cepheid strip variables rest upon it, but it could affect other problems as well. A small reduction of the amplitudes of Cepheids, for example, is certain to assist in computations of double mode stars. Accurate RR Lyrae amplitudes are needed for comparison with globular clusters, etc. Until this issue is resolved, accuracy cannot be claimed for either the computed amplitudes or the computed modes of the lower Cepheid strip variables.

* * * * *

This work is supported in part by NSF grant number AST 79-01165.

REFERENCES

Christy, R.F. 1974, Cepheid Modeling, G.S.F.C. publication, NASA-SP-383, p. 85.
Stellingwerf, R.F. 1975, Ap. J., 195, 441.
Stellingwerf, R.F. 1979, Ap. J., 227, 935.

A PROGRAM TO OBSERVE VERY LOW AMPLITUDE RADIAL VELOCITY VARIATIONS IN δ SCUTI STARS

W.D. Heacox
Lunar and Planetary Laboratory
University of Arizona
Tucson, Arizona

ABSTRACT

The University of Arizona Radial Velocity Spectrometer is probably capable of attaining a resolution of 100 m/s or less on slowly rotating stars of blue magnitude 5.5 or brighter and pulsation periods of 0.02 days or greater in the δ Scuti instability region of the H-R diagram. Such performance is approximately equivalent to a photometric resolution of 10^{-3} magnitudes, and thus represents a possible means of improving the detectability of δ Scuti pulsations by an order of magnitude. The instrument is briefly described and a high priority observing program is outlined.

1. INTRODUCTION

The University of Arizona Radial Velocity Spectrometer has been designed with the goal of detecting the reflex orbital motion of solar-type stars due to the presence of Jupiter-like planets. The required precision is about 10 m/s, representing an improvement over existing instruments of more than an order of magnitude. The applicability of this instrument to δ Scuti observations derives from the pulsation amplitude leverage of about 90 km/s/magnitude in such stars (Breger 1979), so that a radial velocity precision of 10 m/s would be approximately equivalent to a photometric precision of 10^{-4} magnitudes, greatly exceeding the abilities of existing photometric instrumentation. We anticipate that the precision actually obtainable on δ Scuti-type stars will be only about 100 m/s for slowly rotating stars and for pulsation periods no less than 0.02 days. This nonetheless represents an improvement of an order of magnitude in the detectability of δ Scuti pulsations, and suggests that application of our instrument to δ Scuti stars may help to elucidate mechanisms responsible for pulsational instabilities in this region of the H-R diagram.

2. THE INSTRUMENT

The University of Arizona Radial Velocity Spectrometer is described briefly

in the following paragraphs; more complete descriptions have been published by Serkowski (1978) and by Serkowski et al. (1979a, 1980).

The instrument is a slitless echelle spectrograph preceded by an exceptionally stable Fabry-Perot interferometer of finesse 10. The primary purpose of the Fabry-Perot is the definition of well-separated spectral resolution elements (i.e., transmission maxima) with well-defined wavelengths. The spectrum is scanned by tilting the Fabry-Perot. The instrument is coupled to the Cassegrain focus via a single fused silica optical fiber about 10 m in length subtending 2.5 arc seconds on the sky, mechanically isolating the spectrograph from the telescope. The optical fiber coupler is described in detail by Heacox (1980). The detector is a GE charge injected device (CID) of narrow aspect ratio (TN 2201) preceded by an ITT proximity focused intensifier (F-4111). Eight echelle orders, corresponding to a spectral bandwidth of about 250 A centered at 4250 A, are focused on the detector. The spectral resolution of the instrument is about 0.065 A.

Wavelength calibration is provided by a hollow cathode discharge tube and by an NO_2 absorption cell illuminated by a point source lamp. The image scrambling properties of the optical fiber coupler ensure illumination of the spectrograph by the calibration sources that is nearly identical to that of starlight. Additional calibration will be provided by daily observations of integrated sunlight; according to the observations reported by Brookes et al. (1978) and Claverie et al. (1980) in these proceedings, the radial velocity of integrated sunlight should be sufficiently stable for this purpose.

In a prototype configuration mounted at the Cassegrain focus, the spectrometer has observed the radial velocities of Arcturus and Venus with a precision of between 10 and 25 m/s (Serkowski et al. 1979b). When the improved instrument is completed in 1980 we expect to achieve a precision of 10 m/s in a single 40 minute observation on a 1.5 m telescope of a slowly rotating G0 dwarf of blue magnitude 5.5 or brighter. Since stars of earlier spectral type contain less radial velocity information in our passband than do solar-type stars, this precision will be degraded somewhat in observations of stars as hot as δ Scuti stars. In summary, we expect the instrument to achieve a precision of 50-100 m/s in a 15 minute observation on a 1.5 m telescope of a slowly rotating ($v \cdot \sin i < 20$ km/s) dwarf or subgiant of blue magnitude 5.5 or brighter in the spectral range A8-F5. This precision will be further reduced by an uncertain amount in observations of dwarfs earlier than A8 and of luminosity classes III and II.

3. A PROPOSED OBSERVING PROGRAM

Both photometric and radial velocity variations are observed in δ Scuti stars. For stars showing detectable variations of both types and with the same period, the amplitudes in radial velocity (km/s) are considerably larger than the

corresponding photometric amplitudes (magnitudes), probably by a factor of between 60 and 100 (Frolov 1975; Breger, Hutchins and Kuhi 1976; Breger 1979). It is not certain that this relation can be extrapolated to the very small amplitude pulsations considered here, although Breger, Hutchins and Kuhi (1976) argue that the mean ratio of these amplitudes may be even higher for the intrinsically small amplitude main sequence δ Scuti stars. In any event, it seems likely that a radial velocity resolution of ∿ 100 m/s will constitute an improvement of an order of magnitude in the sensitivity of measurements of δ Scuti pulsations.

We propose to extensively observe selected known δ Scuti stars to this precision for at least two reasons. First, we would like to know the relation between radial velocity and photometric amplitudes and phases for the different frequencies observed in stars showing multiple modes in photometric variations. We expect that such observations will shed some light on the mode identifications and, in particular, on the question of the existence of nonradial modes. Second, we hope to discover new modes with amplitudes too small to be detected photometrically with current instrumentation. This would at the very least help resolve the conflict over the existence of rotational m-splitting as opposed to perturbations due to duplicity. While relatively bright, slowly rotating δ Scuti stars are rather rare, there are candidates available for such observation (e.g., 44 Tau).

We also propose to conduct a systematic search for δ Scuti stars in an unbiased sample of bright, sharp-lined stars which lie in the δ Scuti instability region of the H-R diagram. We estimate that nearly 100 such stars will be available to our instrument, about half of them dwarfs or subgiants. We hope that the results of such a survey will address the following subjects, among others:

1. The fraction of slowly rotating stars in this region of the H-R diagram that pulsate;
2. The fraction of such stars that show pulsation modes of various types and multiplicities;
3. The duplicity rate amongst slowly rotating δ Scuti stars;
4. The correlations (if any) of pulsation characteristics with stellar physical parameters in slowly rotating, low amplitude δ Scuti stars.

We anticipate that such a search will reveal that the δ Scuti phenomenon is much more common in slowly rotating stars than had been previously apparent. The results of the search should be particularly valuable in determining the extent to which diffusion is the mechanism responsible for the distinction between pulsating and non-pulsating stars of otherwise similar characteristics.

Thus far, limited telescope time and the necessity of extensive instrumental development and testing efforts have precluded the possibility of applying the spectrometer to any observational program other than that for which the instrument has been specifically developed. If all goes well we hope to initiate a pilot program of observations of a selected δ Scuti star in 1980 and, if the results are

encouraging, to expand to a program similar to that outlined above shortly thereafter.

REFERENCES

Breger, M., Hutchins, J. and Kuhi, L. V. 1976, Astrophys. J., 210, 163.

Breger, M. 1979, Pub. Astron. Soc. Pacific, 91, 5.

Brookes, J.R., Isaak, G.R., McLeod, C.P., van der Raay, H.B. and Roca Cortes, T. 1978, Mon. Not. R. Astr. Soc., 184, 759.

Claverie, A., Isaak, G.R., van der Raay, H.B. and Roca Cortes, T. 1980, these proceedings.

Frolov, M.S. 1975, in Pulsating Stars, ed. B.V. Kukarkin, p. 201, Wiley.

Heacox, W.D. 1980, in Optical and Infrared Telescopes of the 1990's, ed. D. Hewitt, in press.

Serkowski, K. 1978, in High Resolution Spectroscopy, ed. M. Hack, p. 245, Trieste.

Serkowski, K., Frecker, J.E., Heacox, W.D. and Roland, E.H. 1979a, Proc. SPIE, 172, 130.

Serkowski, K., Frecker, J.E., Heacox, W.D. and Roland, E.H. 1979b, Astrophys. J., 228, 630.

Serkowski, K., Frecker, J.E., Heacox, W.D. and Roland, E.H. 1980, in An Assessment of Ground-Based Techniques for Detecting Other Planetary Systems, ed. D.C. Black and W.E. Brunk, in press (NASA Conference Proceedings).

PULSATION MODES IN B STARS WITH VARIABLE LINE PROFILES

M.A. Smith
Department of Astronomy
University of Texas at Austin

ABSTRACT

In this paper several observational characteristics of the line profile variable B stars ("53 Persei variables") are discussed. These stars reside between O8 and B5 on the main sequence and extend perhaps to class I. We believe the 53 Per variables are a separate group related to the classical β Cephei variables.

Line profiles of 53 Per variables exhibit periodic changes in line width and asymmetry but not in radial velocity. These and various photometric signatures are attributed to g-mode nonradial pulsations. Unlike the β Cephei variables the 53 Per variables exhibit highly unstable periods which frequently change from one value to another in a few days. Ratios of 2:1 among these periods are especially common, and the total range in period can exceed a factor of ten in a single star.

Recently it has become possible to make a physical mode identification for a pair of m-modes in 53 Per: $\ell = 3$, $m = -2$ and -3. Additionally, there are indications that the nonradial oscillations in these stars are excited in the envelope rather than in the core. If so, an opacity-related mechanism might be responsible.

Among the classical β Cephei variables, our profile observations of a few of them can be simulated only by radial pulsation models. Spectra of several, if not all, members of this group exhibit periodic "bouncing shells" in visible and/or ultraviolet lines. The detection of these shells promises to furnish us with an additional means of distinguishing between radial and nonradial pulsations in B-stars.

1. INTRODUCTION

Two separate but related groups of stars, the line profile variable B stars (hereinafter referred to as "53 Per variables") and the classical β Cephei stars will be considered here. Both types of variables exhibit profile variations through a pulsation cycle, but differences between the characteristics of these two groups are great enough to minimize problems in classifying a particular star.

The β Cephei stars have pulsation periods in the range of 3.5 to 6 hours; these periods are so stable that an ephemeris may be set up for them over decades or

longer. Spectroscopically, the β Cephei variables exhibit variations in line asymmetry. However, contrary to some earlier reports, many do not show variations in line width; in those stars that do exhibit width variations, they occur nonuniformly with phase.[1] The β Cepheids show conspicuous light, color and radial velocity variations. Many show periodic modulations of their light and velocity curves, indicating the presence of stable multiple periods (cf. Lesh and Aizenman 1976).

In contrast the 53 Per variables show smooth profile variations which alternate in line width and line asymmetry. They exhibit smaller light variations than do the β Cephei stars, and still smaller variations in color and radial velocity. Their periods are long, ranging from 3.6 hours to 2.0 days, and are highly unstable.

With the exception of the final section, this discussion will be limited to various observational results obtained for the 53 Per variables and their theoretical implications. However, details of modeling the profile variations with a nonradial pulsation velocity field will not be presented, nor will a mountain of profile fitting results which either have already been discussed elsewhere (e.g., Smith and McCall 1978a; Smith 1978a,b) or soon will be.

2. INCIDENCE OF THE 53 PER VARIABLES

As Figure 1 indicates, our high resolution (0.1 A) Reticon observations show[2] that profile variability exists on the main sequence from O8 or O9 (10 Lac) to B5 (53 Per, HR 7119), i.e., from about 7 to 22 $M_{\odot}$. In terms of luminosity such stars as ι CMa (B3 II), and possibly Deneb (Lucy 1976; A2 Ia) and ρ Leo (B1 Iab). 53 Per variables may or may not be members of binary systems.

Unfortunately, it is possible to search for line profile variations only in slowly rotating stars, since rotational broadening does not totally dominate the profile. Photometric determinations of variability in faster rotators may be undertaken at some future date.

Among the sharp-lined stars in the domain just described, all non-β Cephei stars but two show variable profiles. One of these two profile-constant stars, 3 Cen A, is the prototype ^{3}He-rich star. Its constancy, along with the lack of variables

---

1. Nonuniform variations have been noted with photoelectric equipment in BW Vul (Goldberg et al. 1974), 12 Lac (Allison et al. 1977) and σ Sco (Smith 1980). An interpretation of the line width changes, apart from nonradial pulsations, is given in Section 7-2.

2. All observations have been carried out using the coudé Reticon system on the 107-inch telescope at McDonald Observatory, or photographically on the 82-inch coudé photographic system. A number of 1979 profiles reported in Table 1 were also obtained on the new coudé Reticon system attached to the 82-inch telescope. The two Reticon systems have comparable speeds.

among late B stars, hints at an exclusion between chemical peculiarities due to diffusion (Hartoog and Cowley 1979) and nonradial pulsations. The other profile-constant star is the quintessential BO V standard, τ Sco, which may be a pulsating star simply viewed pole-on.

3. 53 PER VARIABLES AS NONRADIAL PULSATORS

The following evidence supports the classification of 53 Per variables as nonradial pulsators:

1. The detailed line profile variations are smooth and periodic in time and agree very well with predictions of a traveling wave model. This is an enormous accomplishment of the traveling wave model. It should be noted for these profile variations that free parameters cannot be continually adjusted to fit the different line shapes. Smith and Stern (1979) have recently performed an extensive set of quality control experiments to show that periods can be determined reliably from data of this quality.

2. The periods are too long to arise from radial or pressure (p)-type nonradial modes. They are also too short to be consistently explained by orbital motion in a marginal SB2 binary. The periods in 53 Per exhibit a range of a factor of fourteen. However, a large period range can be incorporated within nonradial pulsation theory for gravity (g)-modes if one is willing to accept singly-excited high overtones.

3. The dominant period appears to shift approximately every month to another value. Period ratios of 2:1 are especially common, a fact which points to resonance-coupling between pulsation modes. The nonradially pulsating ZZ Ceti variables exhibit very similar characteristics.

4. There is spectroscopic evidence that, as periods increase, the horizontal motions on the disk of the star become more and more dominant, as expected for nonradial g-modes (note the extended line wings in long-period profiles in Figure 2).

5. The presence of a pair of close frequencies in the light curve of 53 Per in late 1977 suggests the rotational splitting of modes with two different values of m (Buta and Smith 1979). The degree of this splitting agrees well with the observed rotational velocity of the star.

6. The low color-to-light ratio in 53 Per suggests the dominance of a nearly color-free contribution to the light curve. The nonradial geometric contribution, caused by the distortion of the star from a spherical shape, is the obvious candidate.

4. PERIOD ANALYSIS

Any remarks about periods must be prefaced by stating that our spectroscopic profile-variation analysis technique does not discriminate low-amplitude secondary modes. However, because our single-mode solutions generally fit the data so well, it

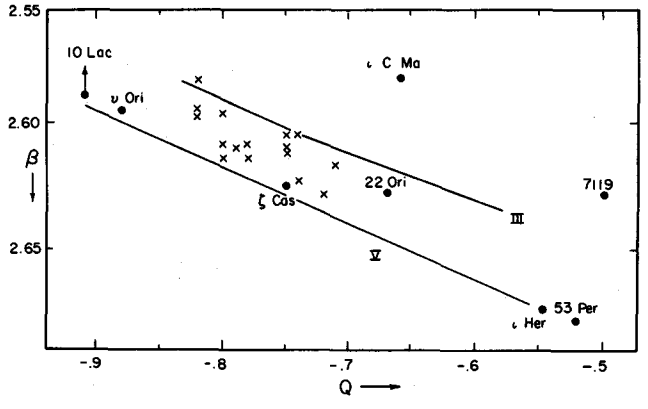

Figure 1. The β vs. Q photometric diagram for the 53 Per variables. For reference, crosses are classical β Cephei stars.

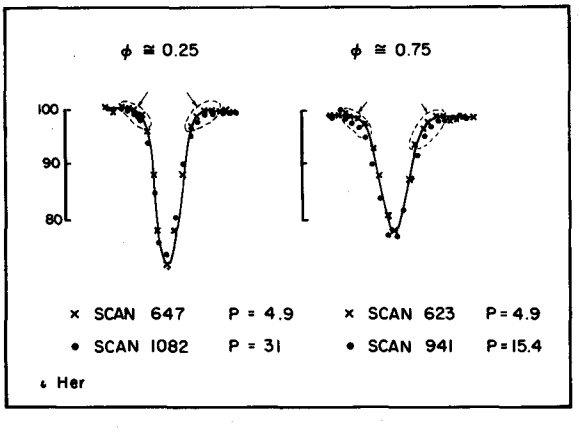

Figure 2. The effect of horizontal motions with increasing periods in the λ4130 profile of ι Her. Note the persistently broader wings in long-period profiles of a particular phase. Short period (crosses) and long period (dots) observations are shown near phases 0.25 and 0.75.

is probable that most of the pulsational energy in the outer stellar envelope is usually restricted to one (k,ℓ) mode.

Table 1 summarizes the current status of the period determinations for the six best observed variables. With the possible exception of 10 Lac, the noteworthy characteristic of these variables is that their periods change every month or so. Smith and McCall (1978a) first pointed out this period transience for 53 Per but on the basis of only ∿ 6 profiles per three day observing run. While we have no reason to deny any of the periods quoted therein, we have been very closely monitoring the behavior of another variable, ι Her, to confirm the existence of this transience and to see whether it extends to low amplitude stars as well. As Table 1 shows, the transience is indeed ubiquitous. Even in a small amplitude star like ι Her, five different periods have been found over a total of two observing seasons; four periods have been observed on at least two runs.

At present period changes have also been followed during an observing run three or four times. Each time a change occurs, it does so over a time span of two or three days (e.g., Smith 1978a).

The extreme range of the periods is a second remarkable characteristic. The median period in Table 1 is 11.5 hours. About half of all the detected periods lie in the range of 7.3 to 15.4 hours. Theoretically, fairly high overtone values (up to $k \approx 25$) are indicated by these long periods. Periods longer than approximately 15 hours require observations over several contiguous nights and are more difficult to determine accurately. Still, periods on the order of a day have been found on several occasions. Very short periods (< 3.5 hours) cannot be determined from our data because of the phase-smearing that goes on during the finite observation time. However, shorter periods than this would be unlikely because the limiting g-mode period of a B star lies in this approximate area (Osaki 1976).

A third remarkable characteristic of these periods, already noted, is the near-integral period ratios that frequently occur. 53 Per itself shows several such coincidences, e.g., $4\omega_0$, $2\omega_0$, ω_0 and $\omega_0/3$, if ω_0 corresponds to P = 14.6 hours. There is also a slight preference for oscillations to change directly from a frequency ω_0 to $\omega_0/2$ or to $2\omega_0$.

Not all period ratios involve magic numbers. For example, consider the behavior of ι Her during the spring of 1978. In April and July it showed its familiar 13.9 hour period. In May and June it showed a 15.4 hour period for two months or longer. These two periods are too far apart to arise from rotational splitting, and too close together for one mode to be a harmonic of the other. A possible explanation within the context of nonradial pulsation theory involves mode-switching. For example, a change in the overtone value may be occurring (e.g., if $\ell = 2$, $k = 6 \rightarrow 7$). A picture begins to emerge in which oscillations rapidly transfer energy from one mode to another for some inexplicable reason. However, they prefer

Table 1. Summary of Observations on Several Line Profile Variables

Star	Obs'd Periods (hr)	P-Quality (Scale 1-3)	No. Runs/No. Profiles	Ampl. (km/sec)
53 Per	3.59*	1	1/5	8
(B45IV)	4.50:	1/2	1/3	12
	7.29	2	2/4,5†	9-12
	11.43	2	1/7	12
	14.6	2	2/8,8	7-10
	45	3+	2/7,7	10-12
		Total:	9/49	
ι Her	4.92	2	1/15	5
(B3V)	9.9	3	4/2,6,15,18	4-6
	13.9	3	6/5,13,18,10	4-5
	15.4	3	2/17,8	4
	31	2	2/5,3	4
		Total:	13/102	
10 Lac	4.9	3	6/4,5,15,5,9,6	4-10
(O9V)	?		1/2	28?
		Total:	7/46	
22 Ori	- 8.95	3	3/8,4,11	5
(B2IV)	- 4.5	3	4/5,11,3:,3	3-5
	+14.1	2	3/3,3,7	5-7
	+22.5	2	1.5/9	
		Total:	10.5/56	
υ Ori	11.5	3	3/4,4	5
(BOV)	23.5	2	1.5/10	4
	?		1/7	~ 2
		Total:	5.5/25	
ζ Cas	21.5	2	2/11,2	4
(B2V)	?		2/18,7	
		Total:	4/38	

GRAND TOTAL: 316 OBSERVATIONS (as of February 1979)

Minus sign denotes retrograde mode.

"1.5" indicates two observing runs on the same month.

† An underlined entry implies two periods were found in one set of observations.

* Period once observed simultaneously with another.

to transfer this energy to some stray mode having a (sub)-integral value of the initial frequency.

The transient behavior of modes in 53 Per is reminiscent of the large-amplitude ZZ Ceti stars. As Robinson and McGraw (1976) and McGraw (1978) have pointed out, these stars also exhibit transient long-period oscillations as well as period ratios of 2:1. These authors have built a convincing case supporting nonlinear coupling for mode-switching on short timescales. Perhaps these attributes are common to all overdriven, nonradially pulsating stars.

There is also another property of these periods which may be worth noting. This concerns the trend in the average periods in two well-observed stars, 53 Per and ι Her, during the last 2-1/2 years. As Figures 3 and 4 indicate, their periods were rather short when observations began. As time progressed, the periods tended to longer values. Obviously, we are dealing with an insufficient time base yet. However, because both stars display these tendencies, they might be indicative of an important pattern.

5. CONSTRAINTS ON THE ORIGIN OF THE PULSATIONS

The ultimate favor the observer can do for the theoretician is to furnish clues as to why the observed phenomenon occurs at all. In this vein, it is suggested that the nonradial g-modes are excited in the envelopes of B stars and not in their cores.

Consider first the energy involved in a typical g_1-oscillation. Given the surface amplitudes observed in 53 Per and the eigenfunctions of Osaki (1975), Smith and McCall (1978a) pointed out that the vibrational energy of a 10 $M_\odot$ ZAMS star can be as large as a few tenths of a percent of its gravitational energy. As an additional complication, there exists the rapid change-over from one mode to another. In order for the star to conserve its pulsational energy, one expects the amplitude at the surface to be very different for different modes (i.e., the modes should occupy very different energy states). However, it is an observational fact that the pulsational velocity amplitude of a star remains the same at different times to within 50 percent, regardless of its period. The implication is that the oscillations themselves are localized and require less energy to shift from one state to another. It also seems easier to understand the transience of the oscillations if they are confined to the outer tenuous layers of the star.

An additional argument against a core-instability mechanism may be found in the behavior of a very young nonradial pulsator, υ Ori. This star has been observed to have periods of either 11.5 or 23 hours on a few different occasions. According to Osaki's (1975) propagation diagrams, the entire inner 50 percent of the mass of a zero age main sequence B star is evanescent as far as the propagation of any nonradial modes goes. It would therefore be difficult for oscillations in υ Ori to be propagated, to say nothing of being excited, in the star's core. However, one

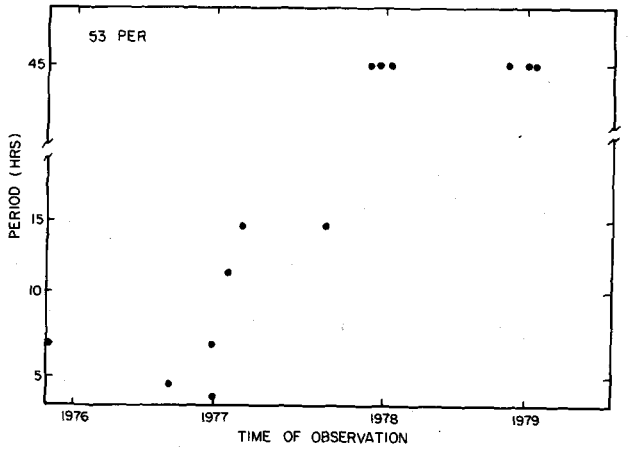

Figure 3. The observed period of 53 Persei as a function of observing epoch.

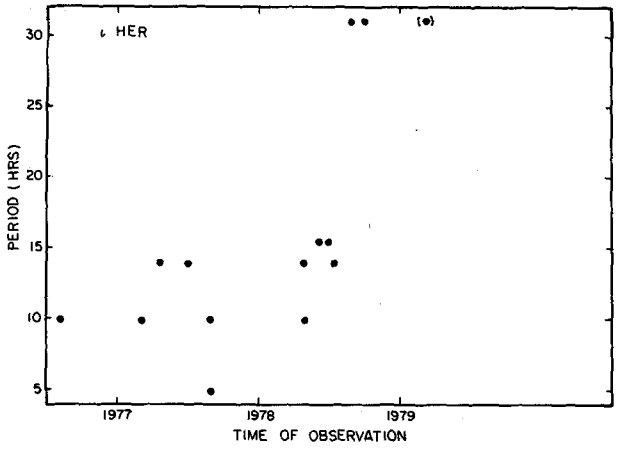

Figure 4. The observed period of ι Her as a function of observing epoch.

possible alternative explanation must be explored before the existence of core-excited oscillations can be ruled out. Just as in quantum mechanics, the eigenfunctions might still "tunnel" for some distance through an evanescent region, particularly if $\ell = 1$ (Osaki, personal communication). Therefore, no firm conclusions can be reached until the spherical harmonic index ℓ that is present in υ Ori can be identified, presumably through the use of photometry and spectroscopy. Still, the probable existence of nonradial oscillations in υ Ori puts core-related pulsation mechanisms on the defensive. It is time for the theoretician to begin scrutinizing envelope-related processes, such as a modified κ-mechanism.

6. MODE IDENTIFICATIONS

Last year Aizenman and Lesh (1978) concluded that it was not yet possible to identify the pulsation modes in β Cephei stars. Under normal circumstances the same cautionary notes apply for the 53 Per variables. One cannot merely match theoretical periods to observations and so determine k and ℓ values for an observed oscillation; theoretical uncertainties in period estimates are legion, and the masses and ages of field B stars are not known with accuracy. However, one clue concerning the identification of the modes became apparent from the initial discovery of the 53 Per variables: variations in line asymmetry and line width <u>without</u> concomitant radial velocity changes are a signature of a sectorial traveling wave ($m = \pm\ell$). The sense of the profile variations with time (except for 22 Ori in 1977-78) indicates a preference for $m < 0$. [3,4] Altogether, the observations consistently point to $m \approx -\ell$, where ℓ is necessarily a small integer.

By combining light and color curves with the spectroscopy, as has recently been done for 53 Per by Buta and Smith (1979) and Smith and Buta (1979), complementary information can be used to identify the physical mode of an oscillation. This is possible because the hills and valleys of a nonradially pulsating object tend to <u>cancel</u> variations in light, while causing a <u>smearing</u> of the spectroscopic line profile. Moreover, photometry provides the displacement produced by a traveling wave, whereas spectroscopy furnishes its time derivative, the pulsation velocity. Therefore, simultaneous observing programs are worth the difficulty of implementation.

Next consider that light variations are caused primarily by pressure and temperature changes. In most pulsating objects the geometric effects are small.

---

3. It is pertinent to note that Hansen, Cox and Carroll (1978) have found that rotation produces a greater tendency to instability for the $m = \underline{-\ell}$ modes in a nonradially pulsating star.

4. However, we now have a well documented case (22 Ori) (Smith 1980) of a star pulsating in a $m = +\ell$ mode (1977-78) changing to the $m = -\ell$ mode, a reversal of the direction of the traveling waves. Perhaps the potential well for $m = +\ell$ modes exists but is simply too shallow for the star to continue in that mode for an extended period of time.

However, in 53 Per the period-pair observed by Buta and Smith (1979) is sufficiently long, and the amplitudes sufficiently large, that nonadiabatic effects might well render the temperature variations small compared to the geometric ones. Let us examine the behavior of 53 Per in late 1977 and 1978 (Buta and Smith 1979; Smith and Buta 1979). During that time this star showed a period of nearly two days. It also showed a low color-to-light ratio, $\Delta(v - y)/\Delta v = 0.10$, rather than the well-determined value of 0.18 which is characteristic of $\ell = 0$ or $\ell = 1$ pulsations. If the geometric effects upon color changes are assumed to be small, it can be shown that the geometric component is in fact responsible for most or all of the light variations. It is then possible to integrate the spectroscopic amplitude and compute a photometric amplitude which can be compared to the observed photometric amplitude. Good agreement between the observed and computed photometric amplitude was found only if $\ell = 3$; other ℓ values produced light amplitudes which were incorrect by a factor of three or more or even possessed the wrong sign. The obvious conclusion is that $\ell = 3$ alone fits the light and profile data for 53 Per at that time.

Another aspect of the behavior of 53 Per during this time concerns its light curve, which demonstrated the presence of two closely spaced frequencies. This is reasonable if the pair is assumed to represent two rotationally-split modes. For the splitting of modes, one can write (in the usual notation):

$$\Delta\omega = \Delta m \, (1 - C) \, \frac{(V_{rot} \sin i)}{R_o \sin i} \quad .$$

If Δm is known, this equation can be used to compare the frequency splitting $\Delta\omega$ with the spectroscopically determined rotational velocity, $V_{rot} \sin i$. For 53 Per only one value works: $\Delta m = 1$. This value gives complete agreement between the observed values $\Delta\omega$ and $V_{rot} \sin i$ if $i = 60°$, a reasonable inclination value. Values of $\Delta m > 1$ lead to nonphysical values for sin i and can be ruled out.

The above exercise does not merely provide a consistency check for the hypothesis of rotational splitting of modes. It, and the clues furnished above, lead to a complete description of the nonradial surface indices for the two observed oscillations: $\ell = 3$, $m = -2$ and -3. In view of the considerable prejudice against odd ℓ-values, it is ironic that the first mode identification of a nonradially pulsating B star should prove to be just such a value, rather than a more widely supported one such as $\ell = 2$.

7. RECENT DEVELOPMENTS ON β CEPHEI STARS

Two interesting developments have recently arisen from studies of line profiles of β Cephei variables (Campos and Smith 1980):

1. (At least) many β Cephei stars are radial pulsators. It was initially

expected that nonradial pulsations would explain the large line asymmetries observed in β Cephei stars, but this was not found to be the case. Profiles that exhibit asymmetry changes but small width changes over the pulsation cycle are the result of rotation in the star enhancing small asymmetries due to radial pulsation (see Duval and Karp 1978). β Cephei, δ Ceti and γ Peg are examples of stars which show this property. Figure 5 depicts these variations and the fits for β Cep assuming a radial pulsation. Profiles of δ Cet and γ Peg have been modeled after radial pulsators as well. However, no common set of nonradial parameters appears capable of reproducing the detailed changes in shape and radial velocity. (A slightly different result reported for β Cephei in Smith (1977) probably results from the use of data reproduced on a poor scale.) Figures 6 and 7 show the effect of increasing radial pulsation amplitude and of rotational velocity on the profile at maximum radial velocity (maximum blue asymmetry). Note in Figure 6 that at radial velocity maximum (minimum), the blue (red) wing becomes more and more depressed with increasing amplitude. The radial velocity range increases at the same time. In Figure 7, note that increasing the rotational velocity produces a broader, more asymmetric line whose radial velocity measurement will not be changed much. When the limit of large rotational velocity is approached, the asymmetries decrease in size once again.

Based on color-to-light amplitudes, Stamford and Watson (1978a) have also come to the conclusion that main β Cephei stars have active radial modes. None of these findings dispute the possibility that nonradial pulsation may also be going on in β Cephei stars, especially in those with multiple periods. Indeed the close period pairs in several β Cephei stars that exhibit beating suggest that one of the oscillations is nonradial. Moreover, the surrounding in the H-R diagram of the β Cephei stars by the 53 Per variables suggests an underlying instability to nonradial pulsation in this entire range of the H-R diagram. It is quite possible that nonradial pulsation actually excites radial pulsation in the β Cephei stars but that the amplitude of the nonradial pulsation is exceeded by that of the radial pulsation at the surface.

2. Bouncing shells are common in β Cephei stars. LeContel (1968) and Smith and McCall (1978b) have reported the presence of weak shell components in the blue spectral lines of γ Peg. This shell appears to resonate regularly with the pulsation cycle. Our Reticon observations indicate that a much stronger shell is present in σ Sco and is responsible for much of its profile variation. As Figure 8 shows, this shell exhibits a redward emission component at some phases and grossly distorts the underlying photospheric profile of Si III lines. The shell is also present in ultraviolet spectra (Campos and Smith 1980).

There are several other β Cephei stars which show shell components in the ultraviolet range (see the spectra of Lesh 1978). The following evidence from Copernicus UV data is presented here for the first time and suggests the presence of

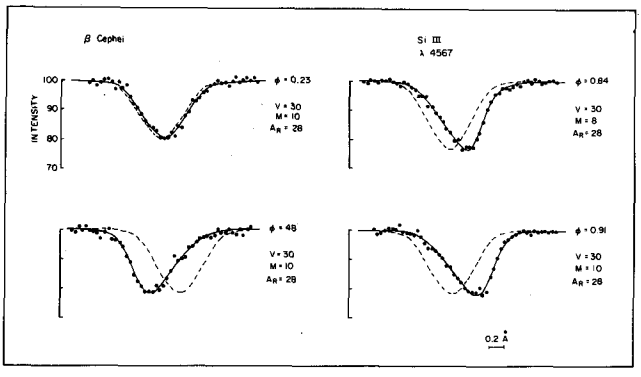

Figure 5. A series of Reticon observations of Si III λ4567 in β Cep. The solid line is a radial pulsation fit using the parameters indicated.

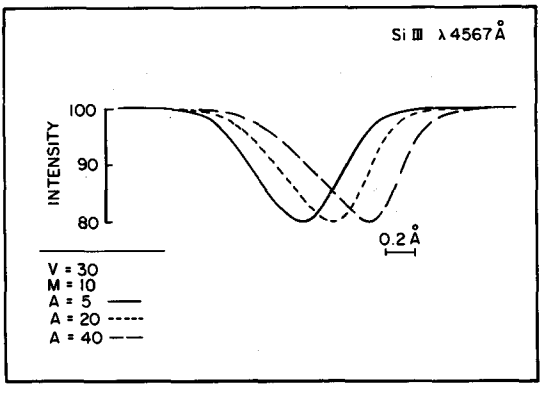

Figure 6. The effect of increasing radial pulsation amplitude on a λ4567 line profile computed at maximum velocity phase (uniformly expanding atmosphere assumed).

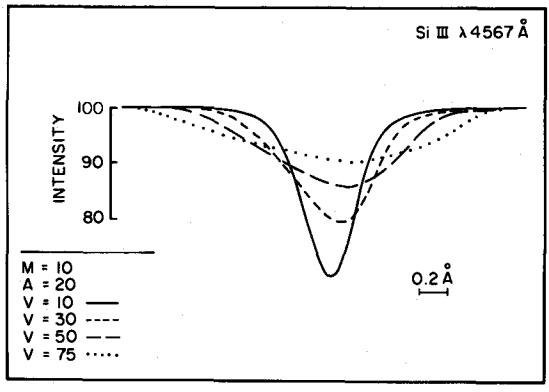

Figure 7. The effect of increasing rotational velocity on a λ4567 line profile at maximum velocity phase. Note the increasing asymmetry of the line with increased rotational velocity.

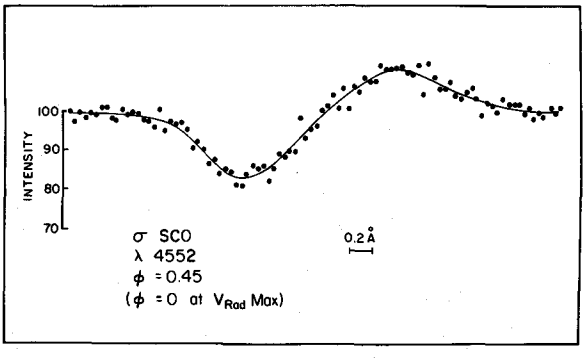

Figure 8. A Reticon observation of Si III λ4552 in σ Sco showing a strong shell component in emission. (Solid line represents only a smoothed fit to the data.)

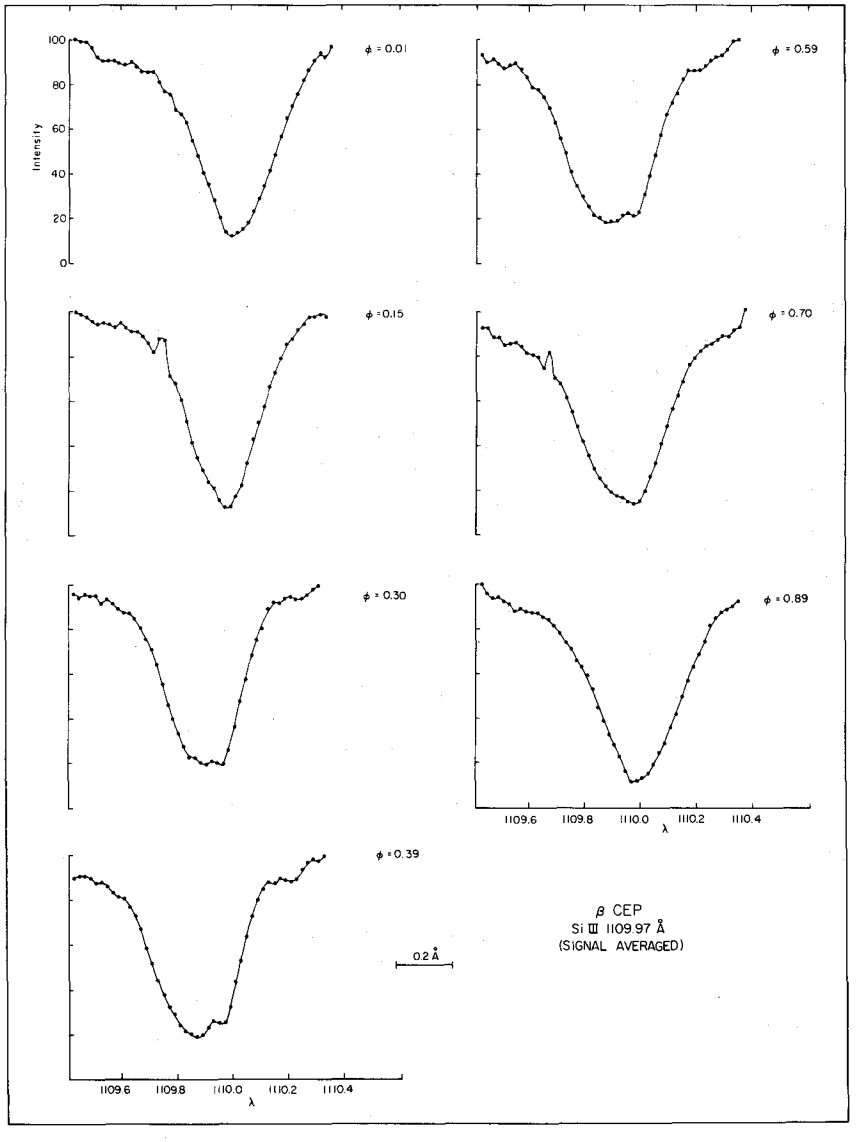

Figure 9. Signal-averaged Copernicus observations of λ1110.96 in β Cep through a pulsation cycle. Note the persistent blue asymmetry.

a shell in β Cephei itself. As Figure 9 shows, strong ultraviolet profiles show only blue asymmetries and no red ones at opposite phases (in contrast to the behavior of visual line profiles). Moreover, at certain phases, fine structure components appear in the core of the line and remain there during the time the main shell component moves upwards.

Stamford and Watson (1978b) have computed some promising models suggesting that the profile variations of BW Vul (including its double-lobed structure at certain phases) can be produced by a large amplitude "piston" in the subphotosphere that drives shocks through the line formation region.

The relevance of shells to the study of nonradial pulsation is that they may help discriminate which B-type variables do not exhibit nonradial pulsation signatures at their surface. A picture is emerging in which shell ejection seems to be closely linked to radial pulsation. If so, observations of key UV lines will provide an opportunity to test for surface dominance of radial modes independently of the analysis of photospheric profile variations. In summary, three criteria -- color-to-light ratios, the character of photospheric profile variations, and the detection of shells in the UV -- may soon be used to characterize the general type of pulsational instability in the β Cephei stars.

* * * * *

I am indebted to Messrs. Buta and Campos for permitting me to exhibit results of unpublished thesis work.

REFERENCES

Allison, A.M., Glaspey, J.W. and Fahlman, G.G. 1977, Ap. J., 82, 283.

Aizenman, M.L. and Lesh, J.R. 1978, Goddard Conf. on Solar and Stellar Pulsation, ed. D. Fischel, W. Sparks and J. Lesh, June 1-2, 1978.

Buta, R.J. and Smith, M.A. 1979, Ap. J., 232, 213.

Campos, A.J. and Smith, M.A. 1980, Ap. J., 238, in press.

Duval, P. and Karp, A.H. 1978, Ap. J., 222, 220.

Goldberg, B.A., Walker, G.A.H. and Odgers, G.J. 1974, Astr. Ap., 32, 355.

Hansen, C.J., Cox, J.P. and Carroll, B.W. 1978, Ap. J., 226, 210.

Hartoog, M.R. and Cowley, A.P. 1979, Ap. J., 228, 229.

LeContel, J.-P. 1968, in 4th Colloq. Multiperiodic Variable Stars, (ed. L. Detre; Budapest: Academic), p. 298.

Lesh, J.R. 1978, Trieste Conference on Astrophysics: High Resolution Spectroscopy, ed. M. Hack, July 2-7, 1978, 34.

Lesh, J.R. and Aizenman, M.L. 1976, Multiple Periodic Variable Stars, IAU Colloq. 29, (ed. W.S. Fitch; Budapest: Academic), p. 11.

Lucy, J.B. 1976, Ap. J., 206, 449.

McGraw, J.T. 1978, Goddard Conf. on Solar and Stellar Pulsation, ed. D. Fischel, W. Sparks and J. Lesh, June 1-2, 1978.

Osaki, Y. 1975, Pub. A.S.J., 27, 237.

Osaki, Y. 1976, Pub. A.S.J., 28, 105.

Osaki, Y. 1978, personal communication.

Robinson, E.L. and McGraw, J.T. 1976, Los Alamos Conf. on Solar and Stellar Pulsation, ed. A. Cox and R.G. Deupree, Aug. 3-5, 1976, p. 98.

Smith, M.A. 1977, Ap. J., 215, 574.

Smith, M.A. 1978a, Ap. J., 224, 927.

Smith, M.A. 1978b, Goddard Conf. on Solar and Stellar Pulsation, ed. D. Fischel, W. Sparks and J. Lesh, June 1-2, 1978.

Smith, M.A. 1980, Ap. J. Supp. (in press).

Smith, M.A. and Buta, R.J. 1979, Ap. J., 232, L193.

Smith, M.A. and McCall, M.L. 1978a, Ap. J., 221, 861.

Smith, M.A. and McCall, M.L. 1978b, Ap. J., 223, 221.

Smith, M.A. and Stern, S.A. 1979, Ap. J., (in press).

Stamford, P.A. and Watson, R. 1978a, I.A.U. Colloq. 46, Hamilton, New Zealand.

Stamford, P.A. and Watson, R. 1978b, Proc. Astr. Soc. Australia, 3, 273.

THE STABILITY OF THE β CEPHEI STARS

M.L. Aizenman
Division of Astronomical Sciences
National Science Foundation
Washington, D.C.

1. INTRODUCTION

From an observational point of view, the β Cephei stars appear to be well-understood, ordinary blue stars. Their spectral types range from BO.5-B2. Their luminosity classes lie in the range (II-III)-IV. The stars are, in general, slow rotators. Both the light and radial velocity periods of these stars lie between three and seven hours, with the amplitude of the light variation usually less than 0.1 mag in the visible, and with radial velocity variations of less than 50 km/sec. The light curve lags the radial velocity curve by one-quarter period. If the variation in luminosity is interpreted as being due to a periodic change in the radius of the star, this phase lag means that these stars are brightest when the radius is at a minimum. Conversely, minimum brightness would correspond to maximum radius of the star. The periods of the radial velocity and luminosity variations are identical. In about half of the known β Cephei stars, a modulation of the light and radial velocity variations is observed, and this has been interpreted as an interference between two nearly equal periods. Changes in line width are observed in all of the multiply periodic β Cephei stars and in some of the singly periodic stars. The lines are broadest on the descending branch of the radial velocity curve and narrowest on the ascending branch. Approximately twenty β Cephei stars are now known, and a complete observational review of these stars has been published by Lesh and Aizenman (1978).

This class of stars occupies a well-defined "instability strip" in the Hertzsprung-Russell diagram. Figure 1 shows the location of these stars in a theoretical HR diagram computed by Lesh and Aizenman (1973). It is apparent that the strip is approximately parallel to the main sequence. This strip is, in fact, coincident with a region known as the "core-collapse zone," the "S-bend," or the "hydrogen exhaustion phase." This is a region which is traversed by a star three times in its evolution away from the main sequence: first in the core hydrogen burning phase, again in the secondary contraction phase as the star adjusts its structure to that of a thick hydrogen burning shell, and once more during the initial phases of hydrogen shell burning. This region is also traversed by stars contracting

towards the main sequence.

Despite the abundant observational knowledge available on the β Cephei stars, they remain in some ways an enigma. The interest of these stars for theoretical studies is obvious: we do not know why they vary. The early B stars have been considered relatively simple and well understood. Models can be computed readily enough. Nevertheless, we have been unable to obtain a consistent, simple explanation for the variability of these stars.

2. THE INTERNAL STRUCTURE OF B STARS

From a comparison with evolutionary tracks, it is found that the masses of the β Cephei stars lie between 10 and 20 $M_\odot$. The only observational mass for a β Cephei star was obtained by Herbison-Evans et al. (1971) for α Vir A, who found a mass of 10.9 ± 0.9 $M_\odot$. They also found a radius of 8.1 ± 0.5 $R_\odot$ and a log $(L/L_\odot)$ = 4.17 ± 0.10.

In this mass range, hydrogen is converted into helium via the CN cycle in a convective core. As the star evolves away from the main sequence, the mass fraction in the core decreases. Because of this, the star has a region of spatially varying mean molecular weight. For stars in this mass range, material in such a region maintains neutral equilibrium towards convection. There are problems, however, as to what criterion one uses to identify neutral stability in a region of varying mean molecular weight. In a region of constant chemical composition, neutral stability against convection means the actual temperature gradient is equal to the adiabatic temperature gradient. In a region where there is a gradient in the mean molecular weight, neutral stability occurs only when

$$\nabla = \nabla_{ad} + \frac{\beta}{4 - 3\beta} \frac{d\ell n\mu}{d\ell nP} \quad ,$$

where the symbols have their usual meanings. In constructing a stellar model, a question exists as to whether one should use this criterion or simply

$$\nabla = \nabla_{ad} \quad .$$

Consider a situation wherein the actual temperature gradient lies between the values given by these two equations. Addressing such a situation by using a local, linear stability analysis, Kato (1966) showed that the material was unstable to small perturbations. He argued that such an instability would mix the material, making the second equation the relevant one to use. Both Gabriel (1969) and Aure (1971) argued that these conclusions applied only on a local scale, and that a full global analysis was required before one could draw such conclusions. They believed radiative damping in the exterior layers of the star could effectively cancel any destabilizing effects from the interior. Mixing would not take place, and the first equation would then be

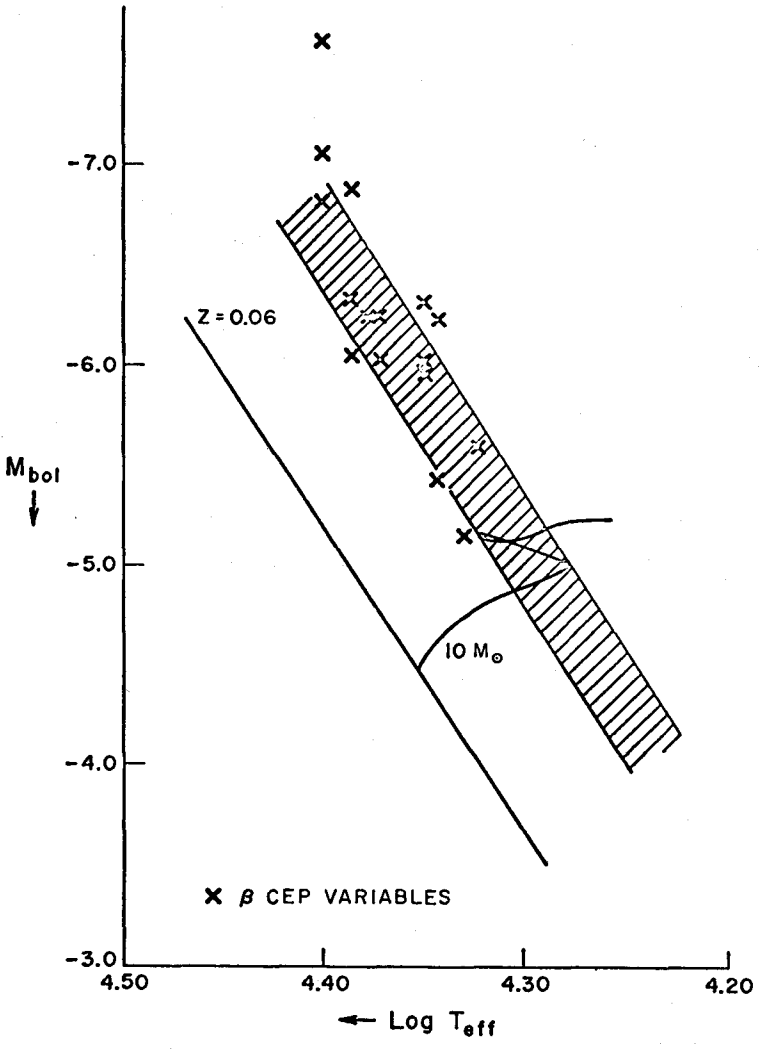

Figure 1. The location of the β Cephei stars in the theoretical HR diagram. The zero-age main sequence for a composition of (X = 0.69, Y = 0.25, Z = 0.06) and the evolutionary track for a 10 $M_\odot$ model are shown. The hatched area is the region traversed three times by a star in the course of its early post-main sequence evolution. After Lesh and Aizenman (1973).

the appropriate form to use in massive stellar models. The question, however, remains open.

The existence of the semi-convective region does not change the general features of the evolution of the star from the main sequence. As the central core decreases in mass, the overall radius and luminosity of the star increase. When the mass fraction in the convective core drops to 0.03-0.05, the entire star begins to contract, and during this contraction the increase in luminosity is almost entirely due to conversion of gravitational potential energy into radiative energy. During the latter stages of this contraction, nuclear energy generation shifts from the center of the star to a thick shell: The inner core of the star begins to contract more quickly than before and hydrogen-rich material in the outer layers moves in towards higher densities and temperatures. This material begins to burn and results in an expansion of material above the energy source. The expansion uses energy, resulting in a slight drop in luminosity. As the shell establishes itself and begins to move outward through the star, the star evolves towards lower effective temperatures at an essentially constant luminosity.

3. ROTATION, MASS LOSS, AND THEIR EFFECT ON THE SEMI-CONVECTIVE REGIONS

There are a number of ways in which rotation may affect our calculations of stellar structure. Rotation reduces the effective gravity at any point which is not on the axis of rotation. Equipotential surfaces are no longer spheres because of this centrifugal force. The radiative equilibrium equations change because the radiative flux is not constant on an equipotential surface; this in turn can affect stability towards convection. Finally, Cowling (1951) found that rotation can affect the criterion for convective stability.

Kippenhahn, Meyer-Hoffmeister and Thomas (1970), in an examination of the effects of slow rotation on a 9 $M_\odot$ star, tested the consequences of two different assumptions about the distribution of angular momentum during evolution. In the first case, local conservation of angular momentum was assumed in all radiative regions, while solid body rotation and overall conservation of angular momentum were assumed in the convective layers. In the second case, local angular momentum conservation was assumed in regions of varying chemical composition while overall conservation of angular momentum and solid body rotation were assumed in all chemically homogeneous regions. The models were started on the main sequence with the maximum angular velocity ($\Omega = 1.55 \times 10^{-4}$ rad/sec) consistent with the equilibrium of a 9 $M_\odot$ star. The effect of the centrifugal force was equivalent to a reduction in the stellar mass. The main sequence lifetime slightly increased (about 4%). In the second case, where Ω was assumed constant in the hydrogen-rich envelope (which slowly expands during the main sequence phase), the angular velocity decreased

with time but the radius of the star increased. Since the ratio of centrifugal to gravitational forces at the equator is proportional to $\omega^2 R^3$, there was a slight increase in the angular velocity which resulted in mass loss near the end of the main sequence phase. This was suggested as a possible explanation for phenomena observed in Be stars. The total mass loss was small, however, and could be avoided with a slightly smaller initial velocity.

Endal and Sofia (1976, 1978) studied rotation on the post-main sequence stages. A number of different assumptions were made concerning the redistribution of angular momentum in the models. However, the angular momentum was assumed in all cases to be constant on equipotential surfaces. The models were chosen so as to bracket sets of physically plausible rotation laws. All the models were started with solid body rotation and an angular velocity characteristic of main sequence stars; none of the models was in rapid rotation. Results were as follows: Rotation lengthened the timescale of evolution. All the models were slightly less luminous and redder than the nonrotating sequences. There was little noticeable effect in the HR diagram.

Several attempts at understanding the problem of mass loss have been made in the past five years. We know that the hot luminous stars are losing mass, as evidenced by resonance lines in the ultraviolet spectrum or the presence of hydrogen emission in the visible spectrum. A paper by de Loore, De Greve and Lamers (1977) analyzed the effects of various rates of mass loss, bracketing the observational estimates, on massive stars.[1] Irrespective of the mass loss rate, the evolution of the star losing mass occurred at lower luminosity than that of a star that did not lose mass. Furthermore, the end of core hydrogen burning occurred at lower effective temperatures. The net effect was that the hydrogen core burning phase covered a wider strip of the HR diagram. De Loore, De Greve and Lamers (1977) also found that stars that lose mass enter the Hertzsprung Gap overluminous by factors of 1.3 to 5. This difference was due to the fact that such a star has a different chemical composition from a star of the same mass and effective temperature which has not lost mass. In the hydrogen shell burning phase, evolution is so rapid that the stars lose very little mass, and they move toward the red giant region at nearly constant luminosity. At a given luminosity, the masses are much lower than those without mass loss.

Sreenivasan and Wilson (1978a) calculated nine evolutionary sequences for a 15 $M_\odot$ star. These included evolution for various rates of mass loss, with and

---

[1]The mass loss rates of early type giants and dwarfs are, however, very uncertain. Snow and Morton (1976) suggest that stars with $\log (L/L_\odot) < 4.3$ do not, with the exception of the Be stars, show significant mass loss. For example the BOV star τ Sco shows a mass loss rate of only 7×10^{-9} $M_\odot$/yr.

without semi-convection. They found that, because of the long lifetime of the central hydrogen burning phase, most of the mass loss occurred between the zero age main sequence and the onset of the hydrogen burning shell phase. Without semi-convection, the rate of evolution was slowed. The mass loss shifted the evolutionary tracks to lower luminosities and effective temperatures. The luminosity of the point where shell burning occurred dropped. The mass contained in the hydrogen convective core was smaller at a given central hydrogen content for sequences which were losing mass, and this effect increased with increasing mass loss. The mass fraction of the core was altered only slightly.

When semi-convection was included, this zone formed outside and in contact with the convective core as soon as the model evolved away from the main sequence. The mass fraction of this semi-convective zone reached a maximum of 0.12 when that of the convective zone was 0.26. The semi-convective region disappeared shortly before central hydrogen exhaustion.

Sreenivasan and Wilson noted that as the convective core died out, a detached semi-convective zone formed and quickly grew to a maximum size of $q \sim 0.25$. The hydrogen-burning shell source became established below this zone. After the hydrogen burning shell source had formed, the model evolved towards the red giant branch on a nuclear timescale, this contrasts with models without mass loss or semi-convection which moved to the red giant branch on a Kelvin timescale. Sreenivasan and Wilson also considered the effect of mass loss on the semi-convective region. They found that mass loss greatly reduced the extent of both phases of semi-convection and the effects of semi-convection were quite small.

The effects of rotation in addition to mass loss, and semi-convection were also considered by Sreenivasan and Wilson (1978b) for the same 15 $M_{\odot}$ star discussed above. The authors explicitly incorporated the loss of angular momentum due to enhanced mass loss caused by the centrifugal forces. The effect of rotation increased the mass loss rate by a factor of 1.2 on the main sequence. As was to be expected, the larger mass loss led to a luminosity even lower than in the model without rotation, and increased the timescale of evolution. At the end of central hydrogen burning, the enhanced mass loss factor decreased to 1.1. This was because the rotational velocity had decreased from 350 km/sec on the zero age main sequence to 150 km/sec at the shell burning phase. This decrease was caused by mass loss and the net increase in the stellar radius.

Effects of the larger mass loss rate on the semi-convective regions were demonstrated in an even greater decrease in the size of the semi-convective region in contact with the convective core. There was also a decrease in the size and effect of the detached semi-convective zone. Rotation appeared to increase the rate of mass loss by about 20% in the early evolutionary phases.

4. EVOLUTIONARY THEORIES OF β CEPHEI INSTABILITY

We have noted that the β Cephei variables lie in a region that is traversed by a star three times during its evolution away from the main sequence. Because of this, it is tempting to ascribe the instability of the Cephei stars to something that happens during normal stellar evolution and to assume that an internal change in the structure of the star is the cause of its variability. For example, Schmalberger (1960) speculated on the possibility that the β Cephei variables were stars in the overall contraction phase of evolution, and that it was the readjustment of the star's internal structure during this phase that led to the observed variability.

The only self-consistent method of examining such a hypothesis is to construct a set of equilibrium models and test them for stability. This was done by Davey (1973) for 10 $M_\odot$ and 15 $M_\odot$ stars, from stages before the zero age main sequence to hydrogen exhaustion in the core, and through the early hydrogen shell development stages. He made a complete nonadiabatic, linear analysis of the models and tested the fundamental mode and the first overtone of each model for stability. While the periods obtained from his models agreed with the periods of β Cephei stars (a situation yielded by all models), no instability could be found in either the pre- or post-main sequence phases. The fact that the star was not in strict thermal equilibrium during the overall contraction phase was allowed for in the calculations, but it had a negligible destabilizing effect.

Aizenman and Weigert (1977) tested a number of different models which simulated contraction toward the main sequence. In the models, they varied the initial abundances of He_3 and C_{12}, small abundances of which can halt the contraction of the star towards the main sequence. This can occur in the region of the β Cephei strip. In fact, He_3 abundances ranging from 0.001 to 0.005 by mass (homogeneously distributed throughout the star) define He_3 burning main sequences which pass directly through the region occupied by the β Cephei stars. Nonradial, quasi-adiabatic calculations were performed on the models, and they were found to be completely stable. In all instances it was found that the radiation damping of the external layers completely dominated the effects of local nuclear driving in the exterior.

Thus calculations of the stability of ordinary stars evolving toward or away from the main sequence and crossing the β Cephei region have not succeeded in explaining the variability. More exotic models have been attempted. Forbes (1968) pointed out that highly evolved stars which have lost considerable mass during the red giant stages of evolution can return to the main sequence during the core helium burning stage. Such stars are greatly overluminous for their mass. Davey (1973) modeled a 10 $M_\odot$ star with a helium burning shell source containing 0.1 $M_\odot$ and "removed" 75% of the mass from the outer regions to obtain a converged model of 2.5 $M_\odot$. The evolution of this star toward higher effective temperatures was

characterized by two effective nuclear energy sources: a helium burning convective core and a thin, hydrogen burning shell. An analysis of this model, however, showed no tendency towards instability. Aizenman and Weigert (1977) also considered a model in the vicinity of the β Cephei strip which had experienced mass loss and was overluminous for its mass. A nonradial analysis showed that it was completely stable. In fact the model with mass loss, because of its higher central condensation, was more stable than models without mass loss.

An extensive set of calculations was carried out by Osaki (1975, 1976). In his first paper, Osaki (1975) studied nonradial oscillations of a 10 $M_\odot$ star in the core hydrogen burning stage. He examined both the radial and the nonradial quadrupole oscillations and found no instability. However, after reports of instabilities found to high-order g-modes during the overall contraction phase (Chiosi, 1974) and the initial shell burning phase (Aizenman, Cox, and Lesh 1975a), Osaki (1976) undertook an analysis of this section of the HR diagram for high-order g-modes. He did not find any instability for the low-order p-, f-, and g-modes, nor did he find the instabilities claimed by Chiosi (1974) or Aizenman et al. (1975a). He did, however, note that a spurious vibrational instability of the higher-order g-modes occurred in evolved models as a result of a numerical inaccuracy. The eigenfunctions of high g-modes in evolved models oscillate very rapidly and have many nodes in the chemically inhomogeneous zone just outside the convective core. In evaluating the stability integral, it is necessary to compute the term $d(\delta T/T)/d \ln r$; if this is done by direct numerical differentiation at discrete mesh points in the region of varying chemical composition (where there are many nodes), numerical inaccuracy results. Osaki proceeded to derive an expression for this term, thus removing the need for numerical differentiation. His results did not show any instability for the overall contraction or initial shell-burning stage. Aizenman, Cox, and Lesh (1975b) applied Osaki's technique to their results and found that models which had previously been found to be unstable were stable. The difference could be traced to the numerical differentiation technique that had been used earlier.

Osaki carried his analysis beyond these numerical results. He noted that eigenmodes of low frequency behave like gravity waves in the region of varying molecular weight, and have large amplitudes in this region. Thus the question was whether or not these large amplitudes, combined with nuclear driving in the shell, could overcome radiative dissipation. He found, however, that the least stable modes were those such as g_{10}, and that even for such modes the damping was ten times as large as the nuclear driving. The damping for these modes arose near the shell. The lower-order g-modes had acoustic propagation properties in the envelope. As a result, these modes were stable because of radiative dissipation in the envelope. Osaki analyzed his results and found that the growth rate for a mode in the shell

region was always negative if there was no nuclear burning and the temperature gradient was subadiabatic. If there was a source of nuclear energy, there was large radiative dissipation in the region of varying molecular weight for short-wavelength modes. The longer wavelengths could be driven in this region, but they faced the radiative dissipation in the envelope. Osaki concluded that nuclear-driven vibrational instability of nonradial g-modes was unlikely, provided that the temperature gradient was subadiabatic.

It is clear then that the region of varying molecular weight is of prime interest in this discussion. It is a region that forms immediately after the star leaves the main sequence, it is the region where nuclear burning begins to take place, and it is a region where destabilization effects can occur.

Discussions of the semi-convective region began with Schwarzschild and Harm (1958), who showed that, for stars with masses greater than 10 $M_\odot$, the temperature gradient became superadiabatic in the zone of varying chemical composition as the star evolved away from the main sequence. They treated this zone by adjusting the chemical composition to make the actual temperature gradient equal to the adiabatic temperature gradient (Schwarzschild criterion). However, in determining the onset of convection in a zone of varying chemical composition one must take into account the effect of a gradient of mean molecular weight (μ); this changes the criterion for convective neutrality (Ledoux criterion). There has been considerable discussion as to which criterion should be used. This problem of convection is, moreover, intimately related to the stability of g-modes. As we mentioned earlier, while Kato (1969) argued in favor of g-mode oscillations causing a mixing of the inhomogeneous region, Gabriel (1969) and Aure (1971) argued that on a global scale such oscillations would not occur because they would be damped by the outer radiative region. This problem was reanalyzed by Shibahashi and Osaki (1976a). In the local analysis of Kato, the inhomogeneous region was stable against ordinary convection. In the regions outside this zone there was very strong damping. A straightforward analysis showed that the conclusions of Gabriel and Aure must hold for g-modes having low ℓ and low frequency. However, the possibility existed that an eigenmode that was trapped in the semi-convective region would become overstable if its value of ℓ was high enough. In the analysis by Shibahashi and Osaki of a 15 $M_\odot$ and 30 $M_\odot$ star, some modes were found to be unstable. For the 15 $M_\odot$ star, all modes with $\ell < 15$ were stable. For the 30 $M_\odot$ star, all modes with $\ell < 8$ were stable. The e-folding times of these oscillations were found to be of the order of 10^3 to 10^4 years. Some mixing could be expected to occur, since the e-folding was shorter than the evolutionary timescale of the stars. As a general rule, the modes having higher ℓ were more unstable. Shibahashi and Osaki suggested that some form of overstable convection exists for stars more massive than 15 $M_\odot$ in the core hydrogen burning phase, since molecular and radiative viscosities are not important. Thus, in their opinion, the

Schwarzschild criterion would be preferable to the Ledoux criterion. But eveything depends on the particular model in question, and they believe that the correct physical criterion for convection cannot be expressed uniquely in the form of a local criterion.

Gabriel et al. (1975) and Scuflaire et al. (1976) have found unstable g-modes for a 30 $M_\odot$ star evolving away from the main sequence. Their unstable modes have ℓ = 1 and ℓ = 2. The cause of this difference is not known. The question now arises as to whether this instability is the cause of the variability seen in β Cephei stars. The periods can be matched easily enough. But the only unstable modes, those trapped in the μ-gradient zone, possess amplitudes which are extremely small at the stellar surface.

Shibahashi and Osaki (1976b) extended their calculations to the stage at which a hydrogen burning shell developed in the star. In this case, nuclear burning was taking place inside the semi-convective region, and the stability of such a situation was examined. Their analysis led them to expect overstability only for low order g-modes with moderately large ℓ, and indicated that overstability could occur only in the earliest stages of shell hydrogen burning, if at all. A few modes for 11 $< \ell <$ 14 were found to be unstable for the 40 $M_\odot$ star. A single mode was unstable for the 20 $M_\odot$ star.

Van der Borght (1978) also considered this problem and did a detailed local analysis of the stability of a semi-convective nuclear burning shell. His conclusions were that the onset of nuclear reactions in hydrogen burning shells could be responsible for overstable oscillations which would cause periodic variations in luminosity.

Of course, arguments concerning semi-convection lose much of their impact if mass loss is a factor in the β Cephei stars. The papers by the groups in Italy and Canada have shown that, irrespective of the way in which semi-convection is treated, it disappears in models that are losing mass in the early evolutionary stages. Therefore, if mass loss is a factor, Sreenivasan and Wilson (1978c) conclude that the β Cephei phenomenon cannot be attributed to the presence of semi-convection.

What can we conclude from the discussion of the semi-convective zone and the hydrogen shell? Essentially, the idea that these zones are the cause of the instability looks extremely promising at first glance. The detailed calculations do not seem to bear this out. While these zones may be destabilizing if one uses a local analysis, radiative damping appears to remove any hope of actually obtaining an unstable mode which would fit into the observational framework. Nevertheless, further calculations on the effects of semi-convection combined with the hydrogen burning shell are needed before this idea can be conclusively excluded from further consideration.

5. ROTATION

The effects of rotation on the vibrational frequencies of a star have been studied for quite some time and a number of general results are known. Essentially, there are two main cases of interest to us: If the perturbations are such that the configuration maintains axial symmetry (i.e., $\partial f'/\partial\phi = 0$), then the effects of rotation are always proportional to Ω^2 (Ledoux and Walraven 1958). A more interesting case, however, occurs when the perturbations are not axially symmetric. Here, there are terms that are linear in the angular rotation frequency and, if the rotation is slow enough, terms involving the square of this frequency can be neglected.

The best known result for axially symmetric perturbations is the one concerning the "pseudo-radial oscillation." Here one assumes that the fundamental mode of pulsation for the homologous, compressible, uniformly rotating star can be approximated by holding the relative radial component ($\delta r/r$) constant in space, obtaining the well-known result

$$\sigma^2 = \frac{4\pi G\rho}{3}(3\gamma - 4) + \frac{2}{3}\Omega^2(5 - 3\gamma)$$

(Ledoux and Walraven 1958).

For non-axially symmetric oscillations, we have the result concerning the splitting of the degeneracy that exists for nonradial oscillations in the nonrotating case. For slow rotation the vibrational eigenfrequencies become

$$\sigma_m = \sigma_0 + \frac{m\Omega(2\omega^2 + 1)}{\omega^4 + \ell(\ell + 1)} \quad , \qquad \omega^2 = \frac{3\sigma_0^2}{4\pi G\rho} \quad ,$$

where σ_0 is the frequency of oscillation. The results can be generalized to more realistic stellar models. A recent paper by Hansen, Cox and Van Horn (1977) has extended the non-axially symmetric case to include the effects of differential rotation. They find that (in the inertial frame)

$$\sigma = \sigma_0 - m(1 - C - C_1)\Omega_0$$

where σ_0 is the rest frequency, the quantity C is an integral which represents the behavior of the eigenfunctions in the nonrotating star, Ω_0 is the angular velocity of rotation, and C_1 is a term which can account for small effects arising from differential rotation. This analysis also assumes that the rotation of the star is sufficiently slow that centrifugal forces can be neglected (Ω^2 terms are dropped), implying implies that the equilibrium and pulsation properties of the nonrotating model can be used.

In a second paper, Hansen, Cox and Carroll (1978) have computed (using the Cowling approximation) the vibrational stability of nonradial modes of rotating stars. The approximations made are the same as in the earlier paper. Their result is extremely interesting. They find that prograde modes ($m < 0$), which travel in the same direction as the star's rotation, are less stable than when rotation is not occurring. On the other hand, retrograde modes ($m > 0$), which travel in a direction opposite to that of rotation, are more stable when rotation is included. The reason for this difference is not clear at the present time. It is quite possible that this effect is relevant to the explanation of the line profile variable B stars.

A paper which has provoked considerable discussion since its publication is that of Papaloizou and Pringle (1978). They addressed the effects of rotation on nonradial modes, and specifically considered the low frequency g-modes through the use of a method of successive approximations. Rotation introduces a new set of modes, known as the toroidal modes, which have frequencies approximately equal to the rotation frequency (the frequency is zero in the nonrotating case). In fact, to first order, the eigenvalues of these modes are

$$\sigma = -m\Omega + \frac{2m\Omega}{\ell(\ell + 1)} \quad .$$

In this approximation, one assumption is that $\xi = p' = 0$ (i.e., the radial component of displacement and the Eulerian pressure variation are zero). The next order of approximation yields

$$\sigma = -m\Omega + \frac{2m\Omega}{\ell(\ell + 1)} + O(\Omega^3) \quad .$$

Thus, the actual structure of the star does not affect the eigenvalues until terms of order Ω^3 are included in the calculations. For slow rotation, the frequencies of the toroidal modes are essentially independent of the structure of the model.

It is interesting to note a comment made by Ledoux (1958). In analyzing the results of the compressible model, he stated that for the axially symmetic mode there is an additional solution which is directly proportional to the angular rotation frequency. He discarded this solution as spurious and referred to an earlier analysis (Ledoux 1949). The spurious solution is, in fact, the toroidal solution obtained by Papaloizou and Pringle. The result Ledoux obtained in 1949 is consistent with that of Papaloizou and Pringle because the solution is independent of structure through terms including Ω^2.

It is not clear what role the toroidal modes play in the pulsation of early type stars, but Papaloizou and Pringle believed that they may be widely applicable. For example, they suggested that these modes may be the ones observed in the ZZ Ceti stars.

Papaloizou and Pringle also carried out a similar analysis of the effects of

rotation on the asymptotic g-modes. Here the only assumption made in the zero order approximation was that p' = 0. The calculation yielded (in the rotating frame), for high ℓ, with $\Omega >> \sigma_0$

$$\sigma = -m\Omega \pm 2\sqrt{\Omega\sigma_0}$$

where σ_0 is the eigenfrequency of the nonrotating star. If the rotation frequency was such that $\Omega << \sigma_0$, the usual result was obtained:

$$\sigma \sim \sigma_0 \pm m\Omega$$

In both the toroidal and the g-modes, the Eulerian pressure, density and temperature variations are zero to order Ω. To this order, there would be no light variations seen in the star. Higher order approximations have $p' \neq 0$. However, the problem must be analyzed in more detail. It is still too early to attempt to make an identification of modes or even periods based on this analysis.

In considering the β Cephei phenomenon, Papaloizou and Pringle suggested that an instability in these stars could be driven by a particular type of Kelvin-Helmholtz instability. This instability arises in the region in which the angular velocity of the rotating material changes rapidly over a short radial distance. The authors argued that such a shear in the angular momentum profile could be maintained by evolutionary effects and/or tidal interactions, making possible the driving of the observed oscillations by this instability. They did not expand on this hypothesis, so it is difficult to see if this effect could actually occur. Sreenivasan and Wilson (1978c) used this idea to suggest that the β Cephei stars have lost a significant amount of rotation in their outer surface layers, have been subject to the Papaloizou and Pringle Kelvin-Helmholtz instability, and have subsequently ejected a shell or lost enough mass to form a shell. They suggested that the β Cephei stars are precursors of the Be shell stars.

Finally, we turn to a theory, proposed by Osaki (1974), that attempts to explain the β Cephei stars in quite a different way. This theory makes use of the fact that, if a convective region is in rotation, the nonradial modes associated with this region (known as g minus modes) are complex. In the absence of rotation, these modes hve an exponential growth rate. If the rotating star has a normal mode of oscillation whose eigenfrequency matches the oscillatory behavior of the convective region, the energy of the overstable convective motion may be coupled to the entire star. Osaki found that a resonance could take place with the nonradial f-mode. The period of this mode was close to that observed in the β Cephei stars. Another requirement of the theory was that the rotation period of the convective core be of the order of a quarter of a day. Osaki concluded that this mechanism could explain some of the characteristics of the β Cephei stars. While the theory has certain

attractive features, its requirements have to be considered as "ad-hoc" in nature, for this reason, this theory has never been generally accepted as a viable explanation of the β Cephei stars.

6. THE BEAT PHENOMENON

As we have noted in our introduction, approximately half of the β Cephei stars exhibit the beat phenomenon. Chandrasekhar and Lebovitz (1962) suggested that this phenomenon might be due to the effects of rotation on the oscillations that were the cause of the light and velocity variations. They proposed that if the ratio of specific heats in the star had a certain value, then a degeneracy (i.e., resonance) could occur between the fundamental radial mode of oscillation and the nonradial quadrupole oscillation modes. If rotation were taken into account, one would have two nonradial modes characterized by slightly different frequencies. These two frequencies would be the ones observed in the beat β Cephei stars.

In a series of papers, Clement (1965a, 1965b, 1966, 1967) examined this suggestion and found that if one assumed uniform rotation, the mechanism gave a frequency much too small to match the observations. This mechanism required angular velocities that were three to four times larger than the observed velocities. But if a reasonable differential rotation law, such as that given by Stoeckly (1965), was used, the existence of the two frequencies could indeed be explained by this rotation effect. Clement found that surface velocities of the order of 40 kms/sec would match the observations. He concluded that while the particular rotation law chosen had no special validity, the hypothesis of differential rotation was not inconsistent with the observations.

Osaki (1971) also suggested a variation of the basic Chandraskhar-Lebovitz mechanism. The beat phenomenon was interpreted as being due to the interaction of a $\ell = 2$, $m = 2$ nonradial mode and a radial mode. Deupree (1974a) analyzed models of 8 $M_\odot$, 10 $M_\odot$, and 12 $M_\odot$ and found that one could expect a degeneracy to exist between the radial fundamental and at least one higher nonradial overtone. In comparing the results with observations, he found that the stars which gave no indication of being binaries seemed to match the Chandrasekhar-Lebovitz hypothesis quite well. However, those stars that were binaries could not be explained on this basis (τ Sco and 16 Lac).

We also note that Deupree (1974b) carried out an analysis that examined nonlinear nonradial adiabatic pulsations of a 10 $M_\odot$ star. Of interest to us here are his results for two modes with nearly equal periods. Deupree examined a model which had solid body rotation with a surface equatorial velocity of 5 km/sec. The initial velocity distribution was taken to resemble either the radial fundamental mode or the nonradial $\ell = 2$ f-mode. His numerical analysis showed that the two modes maintained approximately equal amplitudes, which was interpreted as being indicative of the

existence of an energy interchange between the two modes.

Fitch (1967, 1969) suggested that the beat phenomenon is due to a modulation of the radial pulsation by a tidal deformation.

An interesting explanation of the double periodicity was proposed by Kato (1974). Since most of the stars that exhibit double periodicity are spectroscopic binaries, he wondered if the binary nature of these stars has something to do with the presence of a double period. We should note that it is not true that all of the double period variables are binary systems (β Canis Majoris is a good counterexample). Kato considered a situation where the difference of the frequencies of the normal modes is close to the frequency of the tidal wave induced by the secondary. In such a case, a resonance interaction and excitation of oscillations could be expected. Specifically, Kato considered quadrupole oscillations ($\ell = 2$) which have slightly different frequencies associated with $m = 2$, 0, or -2. The choice of these particular values of m was governed by the tidal deformation effects. The resonance condition was that the difference between the $m = +2$ and $m = 0$ frequencies must equal twice the frequency of the tidal wave. It must be remembered that if this type of resonance is being considered, and if both of the nonradial oscillations are stable, then energy cannot be supplied to the system by the tidal effects of the secondary. However, if one of the two oscillations is excited by some mechanism, then the other can be amplified by the tidal resonance.

Another type of resonance occurs when two completely unrelated modes of oscillation happen to have frequencies very close to one another. An example of such a situation would be the fundamental radial mode and gravity modes having $\ell = 2$. The theory also requires that the difference in the azimuthal "quantum number" between the modes be two, this being a consequence of the fact that the tidal wave induced by the secondary has two components. We know that this coincidence of frequencies takes place in the late core hydrogen burning phases. Under these circumstances it is possible for the pulsation modes and the tidal wave to interact. Kato (1974) derived the above conditions under which energy can be supplied to the pulsation modes from the tidal wave.

The latter mechanism depends explicitly on the requirement that the β Cephei stars which exhibit the beat phenomenon be members of binary systems. This is clearly not the case. Kato recognized this problem but argued that this mechanism would work even if the mass of the secondary was small, opening up the possibility that it simply had not been detected. But, as the author noted in his review of this theory (Kato, 1975), a remaining weakness is that there is no explanation of why the mechanism works preferentially at any particular evolutionary stage of the star.

In conclusion, it appears that the beat phenomenon seen in many β Cephei stars remains unexplained.

7. INSTABILITIES IN THE OUTER ATMOSPHERE

In the preceding sections we have discussed mechanisms that are associated with the interior of the star. As has been previously shown, these are not the instability mechanisms responsible for the variability of the classical Cepheids and RR Lyrae stars.

The mechanism which drives these stars is the envelope ionization mechanism. This mechanism has its origin in the following physical concept: If, at some instant, the luminosity in the interior of the star is decreasing outward, then more heat is flowing into the bottom of a shell than is flowing out of the top. This means that the shell is gaining heat. If the phasing of these heat gains is phased properly, a Carnot heat engine results which can drive an oscillation. It can be shown that regions in the stellar envelope containing hydrogen and helium in different stages of ionization can have the proper phasing for driving pulsations. The theory is completely discussed by Cox (1974). The results, however, are readily summarized: Oscillations are primarily driven by the HeII ionization zone in the envelope, with some contribution from hydrogen ionization.

When we turn to the β Cephei stars, we find that this mechanism simply does not work, probably because the temperatures of the β Cephei stars are too high. The HeII ionization zone lies too close to the surface to be very effective. Underhill (1966) suggested that the ionization zones of heavier elements such as carbon, nitrogen and oxygen might play a role, but the abundances required for this to work make it appear unlikely.

One would think that the envelope ionization mechanism had been thoroughly examined and that little more would have to be said about it with regard to the β Cephei stars. This is not the case. There have been a number of recent studies concerning the outer envelope and the possibility that it could be the region which harbors the basic destabilization mechanism. In a rather general fashion, Aizenman and Weigert (1977) noted that the treatment of the HeII ionization region and the envelope opacities had a strong effect on the results they obtained for their nonradial analysis. In their paper they made the following comment: "It is evident, therefore, that a careful treatment of the outer envelope is required. In fact, a nonadiabatic treatment is absolutely necessary. We have found that changes in the manner in which the outer convective zone (He II ionization) is treated, shallow though it may be, have a decisive effect on the stability results." They found that this region could make some of the lower g-modes unstable. Stability was also strongly affected by the the opacity and its thermodynamic derivatives. Essentially, the point was that the accuracy of quantities such as opacity and its thermodynamic derivatives, while quite adequate for computing the equilibrium configuration, was not sufficient for pulsational studies.

A similar effect had already been noted by Stothers (1976b), who calculated

the stability of both radial and nonradial modes for stars of 10.9 $M_\odot$ and 15 $M_\odot$. He used the Carson opacities in his calculations because these opacities exhibit a "bump" due to the ultimate ionization of the CNO elements at moderate temperatures and densities. In an earlier paper, Stothers (1976a) found that this bump excited radial pulsations in high mass main sequence stars. Since this bump was more prominent at lower densities, he thought that lower mass stars might also lose stability as they evolved away from the main sequence. To test this hypothesis, he calculated new equilibrium models using the Carson opacities and found that, if these opacities were correct, the β Cephei stars would have to be in the core hydrogen burning phase. Also, his stability results differed very little from results found by many others using usual opacities. If the observed pulsations were assumed to be radial oscillations, se of either the Carson or the Cox-Stewart opacities indicated that the β Cephei stars were first overtone oscillators.

Stothers found that none of the radial or nonradial modes were unstable. He did find a tendency for a beat phenomenon to exist in the sense that the two lowest nonradial p-modes fo$_\ell$ ℓ = 2 had rather close periods. His conclusion was that semi-convection did not seem to play a role in destabilizing modes if the Carson opacities were used. However, Stothers pointed out that future improvements in stellar opacity calculations might lead to larger CNO bumps in the intermediate mass range, and this would enhance the κ (opacity) mechanism in some of the models.

Stellingwerf (1978) recently put forth an interesting proposal concerning helium ionization driving in β Cephei stars. Essentially, Stellingwerf suggested that the actual driving mechanism for the β Cephei stars may be the presence of a slight "bump" in the opacity which occurs at 1.5×10^5 °K. He argued that this bump represents the coincidence of the frequency maximum of the radiation flux and the opacity edge due to HeII ionization. Since the radiation field at this temperature is optimum for HeII ionization, an opacity bump can occur even though HeII is nearly ionized. The driving is caused by the variation of the opacity temperature derivative. In the models which Stellingwerf computed, there was a clear tendency for driving, but he found no destabilization of the stars. An examination of this mechanism throughout this region of the HR diagram, indicated that the instability increased at lower luminosities, with maximum driving occurring at lower effective temperatures for lower luminosities. The locus of maximum driving was shown to run parallel tc the observed β Cephei variables, but about 0.1 in log T_{eff} to the red. Stellingwerf believed that improved models could easily remove a shift of this magnitude.

Periods given by Stellingwerf's models were too long for a radial fundamental mode. He noted that his mechanism would not work on overtone pulsations, but argued that the results of Jones and Shobbrook (1974) could reconcile the observations with his theory. However, the work of Jones and Shobbrook does not explain this

discrepancy. It almost certainly contains a systematic error since it is based on an astrometric distance to the Scorpio Centaurus association which has been criticized on statistical grounds. Stellingwerf also offered the work of Watson (1972) as a possible substantiation of his theory. This can be questioned, however, on the basis of Watson's Q values, which are much higher than those found by any more recent authors. They may have resulted from the manner in which Watson treated the hydrogen line profiles used to drive his abnormally high values of log g. In any case, at the present time the observations are not consistent with a radial fundamental oscillation driven by the proposed Stellingwerf mechanism.

Recent work by Cox and Stellingwerf (1979) about the role of radiation pressure in determining the position of driving regions in the HR diagram is of interest here. The study was motivated by HeII ionization effects on the opacity derivatives described above. The authors concluded that, if the β Cephei stars are indeed destabilized by an envelope mechanism, there would be an instability strip for these stars which would be more vertical than the Cepheid strip due to radiation pressure. In fact, the slope of such a strip could even have the same sign as that of the main sequence. The authors also showed that a period-luminosity relation would exist in which the increase in the luminosity with increasing period would be enhanced by radiation pressure.

The important point to note here is that the presence of an envelope ionization mechanism would indeed give a slope that would be parallel to the main sequence. However, other mechanisms could also account for this phenomenon. Any destabilizing mechanisms that were a function of the evolutionary stage of the star (such as the presence of a shell source) would also result in an instability strip that would be parallel to the main sequence. The fact that the envelope ionization mechanism and radiation effects predict a strip with possible slope does not argue in favor of preferring this mechanism to any other.

We conclude this section by mentioning the "μ-mechanism" proposed by Stothers and Simon. According to this theory, the β Cephei stars are members of close binary systems in which the original, more massive star, having evolved and expanded during core hydrogen burning, has reached its Roche lobe. It then begins to lose mass to the secondary star. The secondary first accretes the envelope material and then the helium-rich material from the core. If sufficient helium is available and if the mass of the secondary exceeds 6 $M_{\odot}$, this layer of helium raises the effective temperature. Radial pulsations can, in fact, be energized by the hydrogen reactions taking place in the core. The instability results from the fact that the addition of heavier material on the outside of the star leads to a lower mass concentration. The central pulsation amplitude is then increased and the nuclear driven pulsations at the center of the star become sufficient to destabilize the star. The mechanism, if applied to all β Cephei stars, requires that all of them be binaries.

This particular theory has been the subject of considerable criticism. Plavec (1971) found that many of the binaries suggested as possible β Cephei candidates on the basis of this theory would not be satisfactory. The star α Virginis, which is a β Cephei star, does not satisfy the criteria required by this theory (Smak 1970). Also, the abundances of the β Cephei stars seem completely normal (Watson 1971). The conclusion is that there is no evidence to indicate that the Stothers and Simon mechanism actually takes place in the β Cephei stars.

8. SUMMARY

We have presented a short summary of the observed properties of the β Cephei stars and discussed recent analytical work dealing with them. In spite of the intensive efforts by a number of independent groups, the origin and cause of the β Cephei phenomenon remain unknown.

REFERENCES

Aizenman, M.L., Cox, J.P. and Lesh, J.R. 1975a, Ap. J., 197, 399.

Aizenman, M.L., Cox, J.P. and Lesh, J.R. 1975b, Multiple Periodic Variable Stars, IAU Colloquium no. 29, Budapest.

Aizenman, M.L., Weigert, A. 1977, Astron. Astrophys., 56, 459.

Aure, J.-L. 1971, Astron. Astrophys., 11, 345.

Chandrasekhar, S. and Lebovitz, N.R. 1962, Ap. J., 136, 1105.

Chiosi, C. 1974, Astron. Astrophys., 37, 237.

Clement, M.J. 1965a, Ap. J., 141, 210.

Clement, M.J. 1965b, Ap. J., 141, 1443.

Clement, M.J. 1966, Ap. J., 144, 841.

Clement, M.J. 1967, Ap. J., 150, 589.

Cowling, T.G. 1951, Ap. J., 114, 272.

Cox, J.P. 1974, Reports on Progress in Physics, 37, 565.

Cox, J.P. and Stellingwerf, R.F. 1979, preprint.

Davey, W.R. 1973, Ap. J., 179, 235.

de Loore, C., De Greve, J.P. and Lamers, H.J.G.L.M. 1977, Astron. Astrophys., 61, 251.

Deupree, R.G. 1974a, Ap. J., 190, 631.

Deupree, R.G. 1974b, Ap. J., 194, 393.

Endal, A.S. and Sofia, S. 1976, Ap. J., 210, 184.

Endal, A.S. and Sofia, S. 1978, Ap. J., 220, 279.

Fitch, W.S. 1967, Ap. J., 148, 481.

Fitch, W.S. 1969, Ap. J., 158, 269.

Forbes, J.E. 1968, Ap. J., 153, 491.

Gabriel, M. 1969, Astron. Astrophys., 1, 321.

Gabriel, M., Noels, A., Scuflaire, R. and Boury, A. 1975, Mem. Soc. Roy. Sci. Liege,

6 Serie., 8, 273.

Hansen, C.J., Cox, J.P. and Carroll, B.W. 1978. Ap. J., 226, 210.

Hansen, C.J., Cox, J.P. and Van Horn, H.M. 1977, Ap. J., 217, 151.

Herbison-Evans, D., Hanbury Brown, R., Davis, J. and Allen, L.R. 1971, Mon. Not. R. Astr. Soc., 151, 161.

Jones, D.H.P. and Shobbrook, R.R. 1974, Mon. Nat. R. Astr. Soc., 166, 649.

Kato, S. 1966, Publ. Astron. Soc. Japan, 18, 374.

Kato, S. 1974, Publ. Astron. Soc. Japan, 26, 341.

Kato, S. 1975, Multiple Periodic Variable Stars, IAU Colloquium no. 29, Budapest.

Kippenhahn, R., Meyer-Hoffmeister, E. and Thomas, H.C. 1970, Astron. Astrophys., 5, 155.

Ledoux, P. 1949, Mem. Soc. Roy. Sci. Liege 9, Chapter V, Section 4.

Ledoux, P. and Walraven, Th. 1958, Handb. Phys., (Berlin: Springer), 51, 353

Lesh, J.R. and Aizenman, M.L. 1973, Astron. Astrophys., 22, 229.

Lesh, J.R. and Aizenman, M.L. 1978, Ann. Rev. Astron. Astrophys., 16, 215.

Osaki, Y. 1971, Publ. Astron. Soc. Japan, 23, 485.

Osaki, Y. 1974, Ap. J., 189, 469.

Osaki, Y. 1975, Publ. Astron. Soc. Japan, 27, 237.

Osaki, Y. 1976, Publ. Astron. Soc. Japan, 28, 105.

Papaloizou, J. and Pringle, J.E. 1978, Mon. Nat. R. Astr. Soc., 182, 423.

Plavec, M. 1971, PASP, 83, 144.

Schmalberger, D.C. 1960, Ap. J., 132, 591.

Schwarzschild, M. and Harm, R. 1958, Ap. J., 128, 348.

Scuflaire, R., Noels, A., Gabriel, M. and Boury, A. 1976, Astrophys. Space Science, 39, 463.

Shibahashi, H. and Osaki, Y. 1976a, Publ. Astron. Soc. Japan, 28, 199.

Shibahashi, H. and Osaki, Y. 1976b, Publ. Astron. Soc. Japan, 28, 533.

Smak, J.I. 1970, Acta Astron., 20, 75.

Snow, T.P. and Morton, D.C. 1976, Ap. J. Suppl., 32, 429.

Sreenivasan, S.R. and Wilson, W.J.F. 1978a, Astrophys. and Space Science, 53, 193.

Sreenivasan, S.R. and Wilson, W.J.F. 1978b, Astron. Astrophys., 70, 755.

Sreenivasan, S.R. and Wilson, W.J.F. 1978c, NASA/Goddard and Los Alamos Conference on Stellar Pulsation Instabilities.

Stellingwerf, R.F. 1978, A. J., 83, 1184.

Stoeckly, R. 1965, Ap. J., 142, 208.

Stothers, R. 1976a, Ap. J., 204, 853.

Underhill, A. 1966, The Early Type Stars. Dordrecht.

Van der Borght, J. 1978, personal communication.

Watson, R.D. 1971, Ap. J., 169, 343.

Watson, R.D. 1972, Ap. J. Suppl., 24, 167.

MULTIPERIODICITY AND NONRADIAL OSCILLATIONS OF THE β CEPHEI STAR 12 LACERTAE

M. Jerzykiewicz
Wroclaw University Observatory
Poland

1. INTRODUCTION

Over a quarter of a century ago Ledoux (1951) made an attempt to explain the complex radial-velocity and line-profile variations of β Canis Majoris, a classical "beat" β Cephei star, in terms of the first order rotational splitting of an $\ell = 2$ nonradial oscillation mode. He identified the longer of the two periods observed in this star with the $m = 2$ retrograde traveling wave and the shorter one with the $m = 0$ stationary oscillation. However, this model was not entirely successful. Although it accounted for the close frequency beating and the line profile variations, the phase relation was wrong in that the computed lines turned out to be broadest on the ascending branch of the corresponding velocity curve, and not on the descending branch as observed (the $m = -2$ prograde wave yielded the correct phase relation, but associated the broadening with the shorter period, contrary to what is observed.)

In spite of this difficulty, Osaki (1971) further investigated the possibility that the "beat" phenomenon and the line profile variations in the multiperiodic β Cephei stars might be due to $\ell = 2$ oscillations in the presence of slow rotation. He confirmed Ledoux's result that a superposition of a stationary oscillation upon a traveling wave produced modulation of the velocity amplitude in the "beat" period, with the line profile variation caused mainly by the traveling wave. Osaki computed rotational velocities for several β Cephei variables from the observed "beat" periods under the assumption that the $\ell = 2$, $m = -2$ and $m = 0$ oscillations were both excited. He found them to be consistent with the measured $v \sin i$ values, provided that the stars were seen nearly equator-on. However, there was an exception: for β Canis Majoris, the computed v was 9 km/sec, while the observed $v \sin i$ has been found to be 28 km/sec (McNamara and Hansen 1961), a difference which is difficult to explain.

Thus, the evidence that multiperiodic β Cephei stars are undergoing nonradial oscillations has been somewhat circumstantial. A proof that one of these variables, 12 Lacertae, is indeed a nonradial oscillator was recently provided by Jerzykiewicz (1978) through a frequency analysis of the star's light and radial velocity variations. The present paper summarizes work which has led to two additional

conclusions: a demonstration that at least two modes of different ℓ are simultaneously excited in 12 Lacertae, and the identification of one of them as a rotationally split $\ell = 3$ oscillation.

2. FREQUENCY ANALYSIS OF THE LIGHT VARIATION

12 Lacertae shows cyclic variations in brightness, radial velocity and line profiles. The average cycle-length is equal to about $^{d}.19309$. The amplitude varies smoothly from one cycle to another. In each cycle the light maximum occurs near the middle of the descending branch of the velocity curve. At the same phase, the spectral lines are most diffuse, while on the ascending branch they are sharpest.

The first modern frequency analysis of the light variation of 12 Lacertae was carried out by Barning (1963). He used blue magnitude observations secured by a number of workers in the course of the international campaign organized in 1956 by de Jager (1963). Barning was able to represent the light variation of the star as a sum of four sine-wave components with periods of $^{d}.193089$, $^{d}.197358$, $^{d}.182127$, and $29^{d}.85$ (the first two of these were already known). The relative amplitudes amounted to 1.000, 0.337, 0.315, and 0.319, respectively. The first three components accounted for the cycle-to-cycle amplitude variation, while the last one arose from long-term changes in the mean brightness of the star. However, the standard deviation computed after the data were whitened with the four components was approximately $^{m}.02$, a value considerably larger than the mean error of a single observation, estimated by de Jager to be between $^{m}.005$ and $^{m}.010$. From this, Barning postulated the presence of other periodicities or, in addition to the regular pattern, erratic changes in the brightness of 12 Lacertae.

In order to determine which of these two possibilities is correct, the 1956 international campaign observations have been re-analyzed in the present work. Several data of poor quality were eliminated from the 1956 observations, and yellow rather than blue magnitudes were used for this analysis as they are less subject to the effects of systematic errors. In all, 909 observations taken on 25 nights over an interval of 75^{d} were selected. The data were reduced to a common zero point by adding carefully determined nightly corrections. From an inspection of this material, the mean error of a single measurement was estimated to be between $^{m}.005$ and $^{m}.010$.

The results of the analysis, schematically shown in Figure 1, can be summarized as follows. At least six sine-wave components are present in the light variation of 12 Lacertae, so that the star's frequency spectrum is in fact much more complex than has been hitherto realized. Frequencies of the three strongest components are very nearly identical to those found by Barning (1963), but the remaining three frequencies represent new findings. Simple relationships were also found to exist between some of the frequencies. For example, the primary, the

fourth, and the tertiary frequencies (ω_1, ω_4, and ω_3, respectively) form an equidistant triplet. Moreover, the fifth component frequency, ω_5, turns out to be equal to $\omega_1 + \omega_4$. No obvious relations were found between ω_2 or ω_6 and the corresponding remaining frequencies.

A comparison of the six-term synthetic light-curve with observations showed a satisfactory agreement for all nights. The sample displayed in Figure 2 includes the first night, JD 2435683, and also the last one, JD 2435758. On JD 2435708 one can see a skew light curve, with a steeper descending branch adequately represented by the solution. The largest amplitude of the light variation occurred on JD 2435710, while on JD 2435757 the amplitude was the smallest observed in 1956. The nights JD 2435722 and JD 2435752 are shown as examples of a poor fit and of a rather large scatter, respectively.

The standard deviation of the six-term solution is equal to $^m.0088$, falling within the range of the mean error of a single observation as estimated above. Thus, short-period components fainter than about $^m.0030$, which might still be present in the data, would be very difficult to separate from the periodogram noise. It should also be noted that the present analysis could not yield any periods longer than about $^d.5$ due to the nightly data corrections mentioned above.

3. THE RADIAL VELOCITY VARIATION

The most extensive spectrographic investigation of 12 Lacertae was carried out by Struve (1951). On twenty nights during the interval from July 16 to September 24, 1950 he secured 258 spectrograms of the star. Nearly one-half of these were obtained with the coudé spectrograph of the 100-inch Mount Wilson reflector at a dispersion of 10 A/mm, and over sixty with the Mills three-prism spectrograph of the Lick Observatory at about the same dispersion but with lower resolving power. The remaining spectrograms were taken at a dispersion of about 50 A/mm with Cassegrain instruments of the Mount Wilson and McDonald Observatories. All spectrograms were measured by Struve and radial velocities were derived.

In order to determine whether the sine-wave components found in the light variation of 12 Lacertae have their counterparts in the star's radial velocities, a six-term trigonometric polynomial, with the same frequencies as obtained in the preceding paragraphs, was fitted to the above-mentioned data by the method of least squares. The velocity amplitudes resulting from the solution are shown as a function of frequency in Figure 1 (bottom) for ease of comparison.

The five strongest components present in the light variation can be seen to occur in the radial velocities with amplitudes considerably greater than their mean errors. However, the faintest component has an amplitude of only twice the mean error, making its presence in the data questionable. As with the light variation, the primary component is about three times stronger than the secondary one. However,

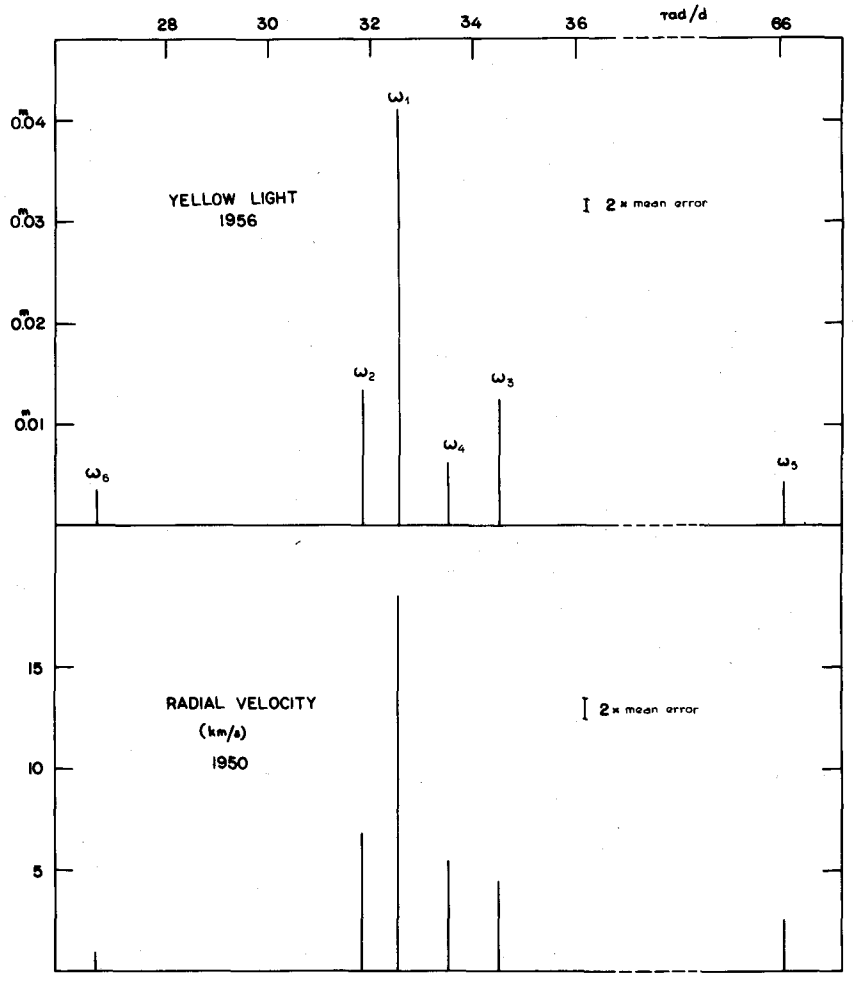

Figure 1. The frequency spectra of 12 Lacertae determined from the 1956 international campaign yellow magnitude photometry (top), and from the 1950 radial velocity observations of Struve (1951) (bottom). The frequencies are numbered in order of decreasing light amplitude.

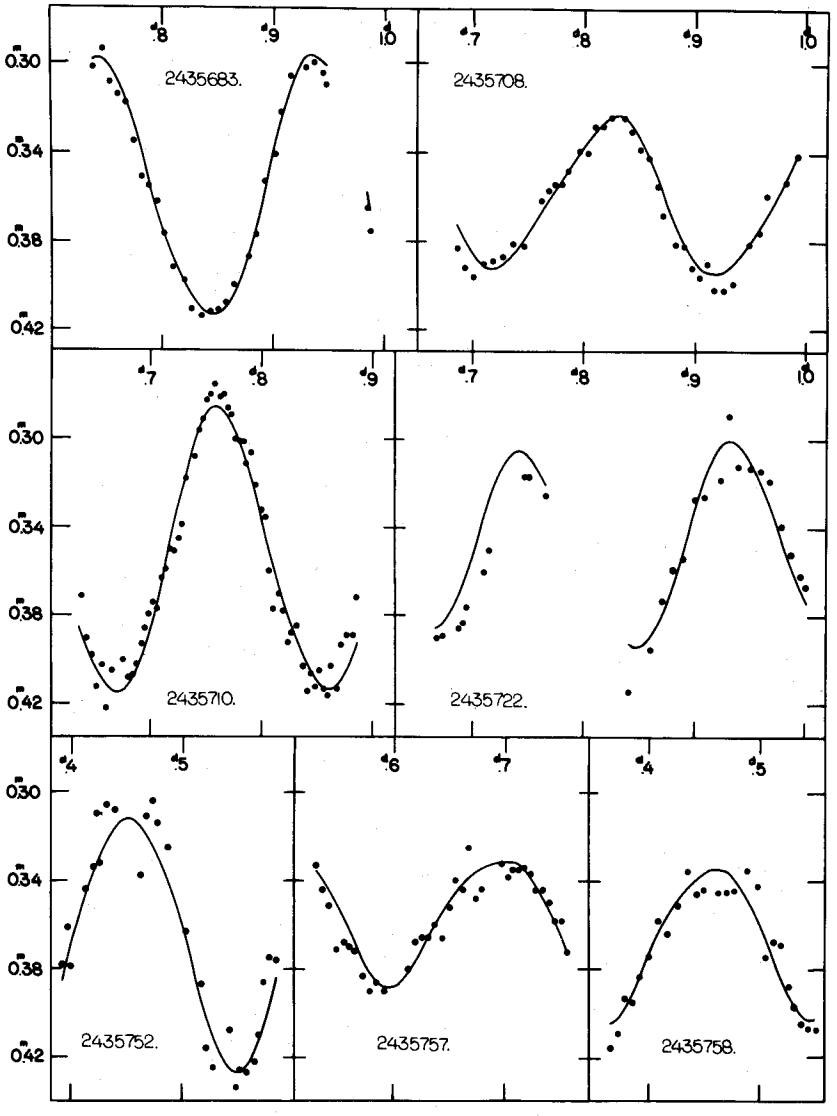

Figure 2. A sample comparison of the observed (points) and computed (solid lines) light curves of 12 Lacertae.

the second component in the velocity variation is somewhat stronger than the fourth with the fourth somewhat stronger than the tertiary. This is unlike the relationships exhibited in the light variation, wherein the secondary and tertiary components were roughly equal, with the fourth being much fainter. These differences indicate that the velocity to light amplitude ratios are, perhaps, not the same for all components. However, the differences may have been caused by a small change of the frequency spectrum of 12 Lacertae between 1950 and 1956. They might also be due to the fact that the observed radial velocities are not properly averaged over the stellar disc because of the difficulties of measuring the wavelength shifts from spectral lines with asymmetric and variable line profiles. Also, the observed differences between the velocity and light cycles may have resulted from a combination of the above effects.

The standard deviation of the six-term radial velocity solution equaled 5.1 km/sec. This value resulted from observational errors, including the unknown systematic effects caused by Struve's (1951) use of four different spectrographs, and from any radial velocity changes not taken into account in the solution, e.g., possible long-term velocity variations. Unfortunately, it does not seem possible to determine the relative importance of these factors. However, the amplitude of any unevaluated velocity variation is probably not greater than 2 km/sec.

4. IDENTIFICATION OF THE FREQUENCIES: THE TRIPLET

A natural explanation for the ω_1, ω_4, ω_3 equidistant triplet is that it corresponds to first order rotational splitting of an $\ell \leq 3$ mode with three values of m forming an arithmetic progression. As Dziembowski (1977) has shown, the $\ell > 3$ oscillations produce little light and radial velocity variation because of averaging over the stellar disc, and therefore can be excluded. Even so, for $\ell \leq 3$ fourteen possible rationales exist for the ω_1, ω_4, ω_3 triplet. Fortunately, the line profile observations of 12 Lacertae can be used to limit the number of possibilities. Osaki (1971) found that a phase relation between the radial velocity and line width variations consistent with the observations (cf. § 1) could be obtained if the dominant oscillation in 12 Lacertae was prograde. Osaki favored an $\ell = 2$, $m = -2$ interpretation, but offered no proof of the uniqueness of this solution.

It can be demonstrated that, out of the fourteen above-mentioned possibilities, the strongest component in the light and radial velocity variations of 12 Lacertae corresponds to a prograde wave only in the case of the $\ell = 3$ mode for which all $m < 0$ oscillations are excited and all $m \geq 0$ ones are quiescent. In the remaining thirteen cases, particularly those with $\ell = 2$, there is either no profile variation associated with the ω_1 component (if this component is identified with the stationary oscillation, $m = 0$), or the phase relation between the radial velocity and line profile variations is wrong (a retrograde wave, $m > 0$). Consequently, the

frequencies ω_1, ω_4, and ω_3 should be identified with $\ell = 3$, $m = -1$, -2, and -3, respectively.

This identification of the ω_1, ω_4, ω_3 frequencies rests on the assumption that the ω_1 component, the strongest one in both light and radial velocity frequency spectra (cf. §§ 2 and 3), also dominates the line profile variation. This assumption is strongly supported by the observations. In fact, should the line profiles vary mainly with one of the other frequencies, including ω_2, their much smaller radial velocity amplitudes (cf. Figure 1) would cause the phases of, for example, the most diffuse lines to slide all over the velocity curve. This is not borne out by the observations, which consistently show these phases to be near the middle of the descending branch.

Given the above identification of the triplet frequencies, the angular velocity of rotation (Ω) of 12 Lacertae can be obtained from the observed values of the frequencies using Ledoux's (1951) first order rotational splitting formula. It turns out to be $\Omega = 1.085$ rad/d, if the splitting coefficient C is assumed to be equal to 0.1. Some justification for this choice is furnished by the work of Hansen, Cox and Van Horn (1977), who computed C for massive zero age main sequence models. In the case of a 10 $M_\odot$ model and $\ell = 2$, they obtained $C = 0.104$ for the p_1 mode and $C = 0.067$ for the p_2 mode. For the evolved models, which are more nearly applicable to the β Cephei variables, and for $\ell \neq 2$, these coefficients can be expected to be somewhat different, making the above-mentioned value of Ω uncertain. Despite the uncertainties, however, and using the radius of 8.8 $R_\odot$ derived from the star's position in the H-R diagram (Sterken and Jerzykiewicz 1980), one gets $v = 77$ km/sec for the equatorial velocity of rotation of 12 Lacertae. Then, from $v \sin i = 29$ km/sec, as observed by McNamara and Hansen (1961), it follows that the aspect angle $i = 22°$. However, since McNamara and Hansen obtained $v \sin i$ from measurements taken at the sharp-line phases, $i = 22°$ is probably a lower limit. In any case, it can be concluded that 12 Lacertae is seen more nearly pole-on than equator-on. Finally, it should be pointed out that, with $\Omega = 1.085$ rad/d, the ratio of the oscillation frequency to the angular velocity of rotation is approximately 30. Thus, the rotation is indeed slow, justifying the assumption of first order splitting.

5. THE REMAINING FREQUENCIES

The position of the ω_2 frequency in the frequency spectra described in §§ 2 and 3 indicates that it must correspond to a different harmonic mode than the ω_1, ω_4, ω_3 triplet. It can therefore be due to either a radial mode ($\ell = 0$), or to a nonradial mode with $\ell \leq 2$, and any value of m, i.e., $|m| \leq 1$ for $\ell = 1$, or $|m| \leq 2$ for $\ell = 2$.

One possibility, viz., $\ell = 1$, $m = -1$, might bring some order into an otherwise rather confused picture. If this identification was true, all waves

traveling in the direction of the star's rotation and corresponding to odd $\ell \leq 3$ would be excited. Why $\ell = 2$, $m < 0$ oscillations, among others, should remain quiescent is not at all clear, however. Perhaps the $\ell = 2$, $m < 0$ traveling waves are, in fact, excited in 12 Lacertae, but the small value of the aspect angle (cf. § 4) reduces the corresponding component amplitudes, rendering their detection difficult.

The identification of the two faintest components is also somewhat uncertain. The fact that the combination frequency $\omega_5 = \omega_1 + \omega_4$ was found in the light and radial velocity variations of 12 Lacertae, rather than the usual $2\omega_1$, $\omega_1 + \omega_2$, etc., may be due to a geometric effect of the aspect angle or to an accidental resonance between $\omega_1 + \omega_4$ and an eigenfrequency. If the former effect is responsible for the relationship, a determination of the aspect angle could be attempted. However, nonlinear calculations to at least the second order in the displacement would be necessary to evaluate the latter possibility.

The faintest component frequency, ω_6, probably corresponds to an overtone oscillation. Unfortunately, this identification cannot be entirely conclusive because, at this time, the only extensive calculations of nonradial eigenfrequencies for evolved massive models (Baker and Dziembowski 1969) do not include $\ell = 3$ modes.

6. SUMMARY

12 Lacertae undergoes nonradial oscillations in the presence of slow rotation. Moreover, oscillations of two different harmonic degrees, ℓ, are seen to be simultaneously excited in this star. These conclusions were derived solely from the frequency spectra of the light and radial velocity variations. A definite identification of the ω_1, ω_4, and ω_3 frequencies in terms of spherical harmonics has been made by making use of the line profile observations. These frequencies correspond to $\ell = 3$, $m = -1$, -2, and -3 oscillations, respectively. Therefore, by identifying the ω_2 frequency with an $\ell = 1$, $m = -1$ harmonic mode, which is one of several possibilities, all prograde oscillations with odd $\ell \leq 3$ are found to be excited in 12 Lacertae.

Furthermore, from the value of the rotational splitting in the ω_1, ω_4, ω_3 triplet, and the observed projected velocity of rotation, the aspect angle is estimated to be 22°. Although this result is somewhat uncertain, primarily because accurate values of the splitting coefficient C for massive evolved stars are not available, it indicates that 12 Lacertae is seen more nearly pole-on than equator-on.

In view of these results, a simple solution to the discrepancies that have been encountered in the case of β Canis Majoris (cf. § 1) can be suggested: the two short periods (P_1 and P_2 in the notation of Struve 1950) correspond to oscillation modes of different ℓ. Since it is the period of the line profile variations, and because of the observed phase relation with the corresponding radial velocity curve,

P_2 should be identified with a prograde wave. However, the $\ell = 2$, $m = -2$ mode, as suggested by Osaki (1971), is only one of several possibilities. In a recent study of the light and radial velocity variations of β Canis Majoris, Shobbrook (1973) found a faint short period component in addition to P_1 and P_2; this component, if confirmed, may help to limit the number of these possibilities.

The lack of detailed calculations for nonradial oscillations of evolved massive stars has hampered the explicitness of much of the above discussion. It is also because of this circumstance that no attempt was made here to determine the classification of the vertical properties of the modes which may correspond to the frequencies observed in 12 Lacertae.

* * * * *

The author gratefully acknowledges financial support from the University of Arizona during his stay in Tucson.

REFERENCES

Baker, N. and Dziembowski, W. 1969, personal communication.
Barning, F.J.M. 1963, B. A. N., 17, 22.
de Jager, C. 1963, B. A. N., 17, 1.
Dziembowski, W. 1977, Acta. Astr., 27, 203.
Hansen, C.J., Cox, J.P., and Van Horn, H.M. 1977, Ap. J., 217, 151.
Jerzykiewicz, M. 1978, Acta. Astr., 28, 465.
Ledoux, P. 1951, Ap. J., 114, 373.
McNamara, D.H. and Hansen, K. 1961, Ap. J., 134, 207.
Osaki, Y. 1971, Publ. Astr. Soc. Japan, 23, 485.
Shobbrook, R.R. 1973, Mon. Not. R. Astr. Soc., 161, 257.
Sterken, C. and Jerzykiewicz, M. 1980, these proceedings.
Struve, O. 1950, Ap. J., 112, 471.
Struve, O. 1951, Ap. J., 113, 589.

NEW β CEPHEI STARS AND THE β CEPHEI INSTABILITY STRIP

C. Sterken
Astrofysisch Instituut
Free University of Brussels
Belgium

M. Jerzykiewicz
Wroclaw University Observatory
Poland

1. INTRODUCTION

As a result of a photoelectric search program carried out among bright early B stars (Jerzykiewicz and Sterken 1977), and a subsequent detailed photometric and spectrographic investigation (Jerzykiewicz and Sterken 1978), four new β Cephei variables have been found. A list of β Cephei stars has also been compiled (Jerzykiewicz and Sterken 1978), including variables discovered recently by Balona (1977); Haug (1977); and Jakate (1978a). Using the published uvby and β photometry, the positions of these stars in the c_0 - β and the log P - β planes, it was demonstrated that the β Cephei variables fall within a well defined instability strip and that they do not obey a unique period-luminosity relation.

In §§ 2 and 3 of the present paper the main results of Jerzykiewicz and Sterken (1978) are briefly reviewed. The β Cephei instability strip in the log T_e - M_{bol} diagram is defined in § 4. A comparison with the theoretical evolutionary tracks is made in § 5. Finally, in § 6 the earlier conclusion of Jerzykiewicz and Sterken (1978) concerning the period-luminosity relation is confirmed.

2. THE NEW β CEPHEI VARIABLES

A summary of observational results on the four new β Cephei variables is given in Table 1. The stars are arranged in order of increasing primary photometric period. The MK classification in column four is from Hiltner, Garrison and Schild (1969).

The results listed in columns five and six are based on the photometric observations obtained on 15 nights during the interval from 27 November to 15 December 1977 at the European Southern Observatory, Cerro La Silla, Chile. The instrumentation used was the simultaneous four-channel uvby spectrograph-photometer, attached to the Danish national 50 cm reflecting telescope. The spectrographic observations, the results of which are summarized in the last two columns of Table 1,

Table 1. Observed Properties of the New β Cephei Stars

HD	HR	m_v	MK	Primary Period	$\underline{u}$ Range	Lines	2K km/s
68324	3213	$5^m.4$	B1 IVn	$0^d.108 \pm 0^d.0005$	$0^m.005 - 0^m.018$	very broad	20
64722	3088	5.7	B1.5 IV	0.1154 ± 0.0001	0.014 - 0.035	very broad	?
63949	3058	5.8	B1.5 IV	0.1182 ± 0.0001	0.008 - 0.015	?	?
64365	3078	6.0	B2 IV	0.1927 ± 0.0001	0.010 - 0.040	sharp	9.5

were taken on two nights, 27/28 and 28/29 November 1977, at the coudé focus of the ESO 152 cm telescope. The dispersion was 12.3 A/mm. Baked Kodak IIaO plates were used. The spectrograms were measured with the Grant spectrocomparator of the Max Planck Institut fur Astrophysik in Heidelberg.

The u observations of HD 68324 are shown in Figure 1 as a function of heliocentric Julian day. The light amplitude is variable from night to night. The primary period can be estimated as $0^d.108 \pm 0^d.0005$. The change of the mean brightness, seen on JD 2443482, may be due to light-variability of the comparison star, HD 68243.

The spectrum of HD 68324 is characterized by very broad H and HeI lines. Campbell and Moore (1928) noted the broadness of the lines and the probable variability in velocity. In Figure 2 the radial velocities of HD 68324 on JD 2443476, determined from the hydrogen lines H_γ to H_{10}, are plotted against heliocentric Julian day. Although the scatter is rather large, variation on a time scale close to the primary photometric period can be seen clearly. The 2K range can be estimated at 20 km/s and the γ-velocity equals 38 km/s. The CaII K line yields a mean velocity of 12.9 ± 1.0 km/s.

The b observations of HD 64722, the second variable in Table 1, are displayed as a function of heliocentric Julian day in Figure 3. The least-squares frequency analysis of these data gave $0^d.1154 \pm 0^d.0001$ (estimated mean error) for the primary period of the light variation. A unique figure could not be obtained for the secondary period, however. Two values, which are separated from each other by one cycle per sidereal day, fit the data equally well: $0^d.1168 \pm 0^d.0002$ and $0^d.1323 \pm 0^d.0002$. More observations are needed to decide which of these periods is the correct one. It should also be kept in mind that more than two sine-wave components may be present in the variation of HD 64722.

Figure 4 gives the radial velocities of the star on JD 2443475, determined from the mean of the hydrogen lines H_{10}, H_9, H_ϵ, H_γ and H_β. The uncertainty of these values is rather high, approximately 4 km/s, because the broadness of the lines renders them difficult to measure. Even so, the data shown in Figure 4 indicate that the radial velocity of HD 64722 varies on a short time scale. Unfortunately, these observations were taken on the night when the star's light variation was at a minimum (cf., Figure 3) and therefore it should not be surprising that no well-defined radial velocity curve can be seen.

The third star in Table 1, HD 63949, was found by Jerzykiewicz and Sterken (1978) to be constant in b light to within $0^m.010$, and was therefore used as one of the comparison stars for HD 64365. As it turned out, however, the star is certainly variable on a time scale of about three hours, with the maximum u range equal to $0^m.015$. The u observations of HD 63949 are shown in Figure 5, plotted against

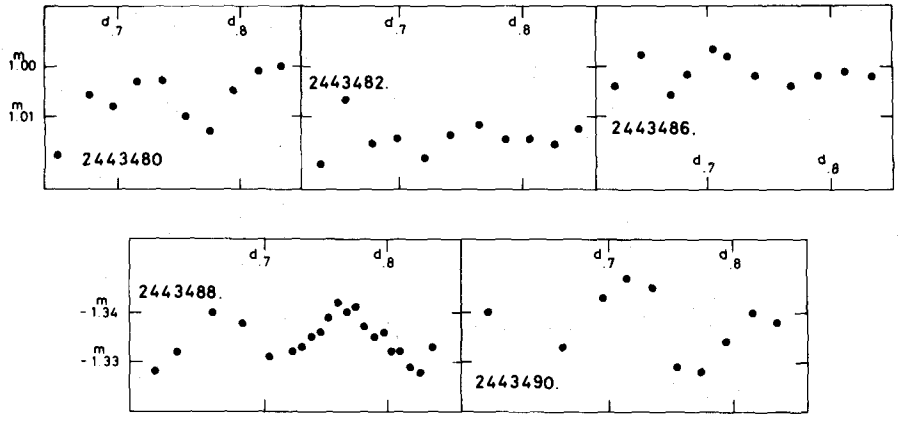

Figure 1. The u observations of HD 68324. On the first three nights (top) the comparison star is HD 68243, while on the last two nights (bottom) the star's brightness is compared to that of HD 67341.

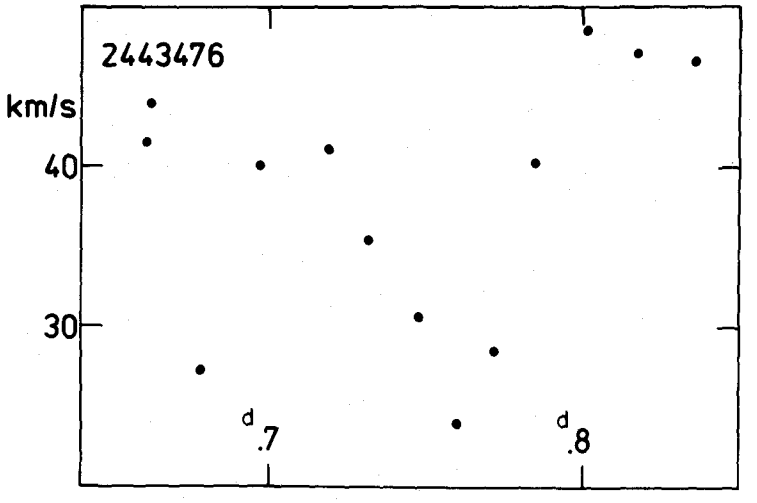

Figure 2. The radial velocities of HD 68324 on JD 2443476.

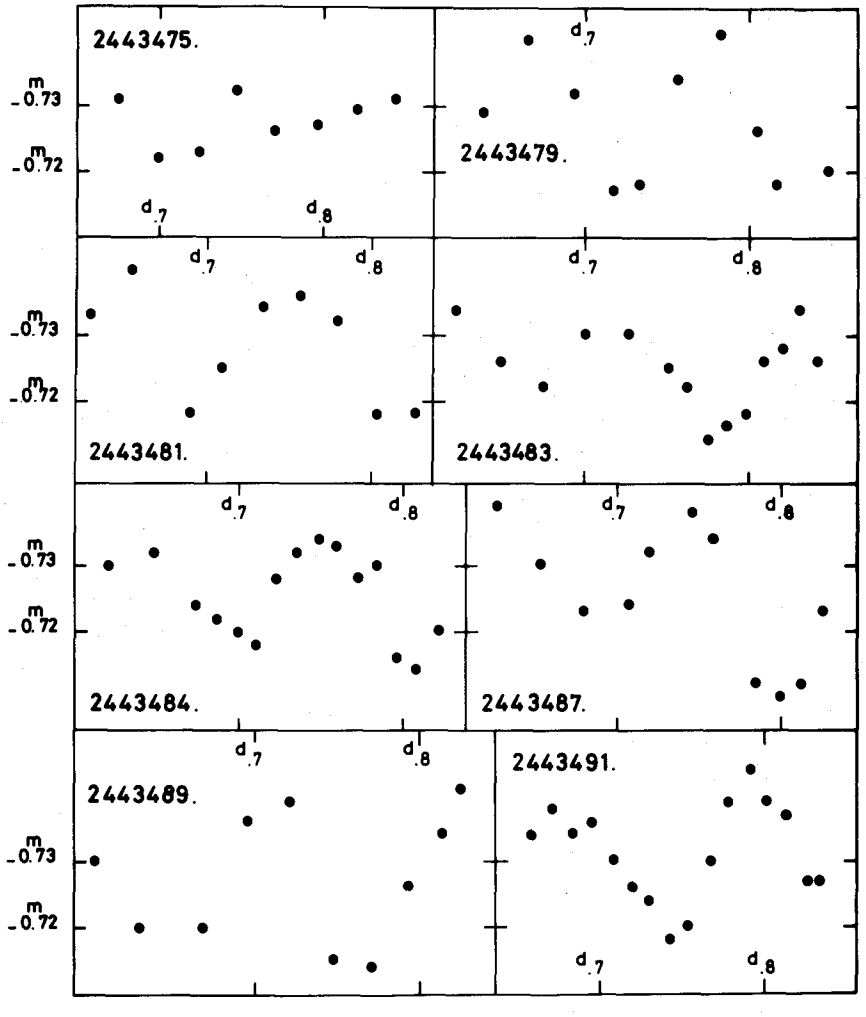

Figure 3. The b magnitude differences, HD 64722 minus HD 62758.

heliocentric Julian day. The variation can be seen clearly on all nights. The range is not constant; it seems to reach a minimum of $0^m.008$ on JD 2443490.

From all u observations we determined the primary period of the light variation of HD 63949 to be $0^d.1182 \pm 0^d.0001$. No attempt has been made, however, to derive the secondary period, since the data are probably not extensive enough for this purpose.

The last star in Table 1, HD 64365, shows a spectacular amplitude modulation. This can be seen from Figure 6, where the u observations of the star are displayed as a function of heliocentric Julian day. The least-squares frequency analysis of these data yielded $0^d.1927 \pm 0^d.0001$ as the best value of the primary period. The secondary period is equal to either $0^d.1680 \pm 0^d.0003$ or $0^d.2019 \pm 0^d.0003$. Clearly, more observations are needed before any extensive frequency analysis of the star's light variation can be undertaken.

The spectrum of HD 64365 shows a large number of well-defined sharp lines. The radial velocities of the star obtained from spectrograms taken on JD 2443476 are displayed in Figure 7 as a function of phase of the primary photometric period. Phase zero was arbitrarily set at JD 2443476.0. All velocities shown are mean values from about 30 lines of HeI, NII, CII, SiIII, OII and H, except one value (open circle in Figure 7), which was determined from a broken plate on which not all of the lines could be measured.

As can be seen from Figure 7, the velocity curve of HD 64365 on JD 2443476 is very nearly sinusoidal in shape. The 2K range is 9.5 km/s, and the γ-velocity is equal to about 31 km/s. The CaII K line yields the mean velocity of 21.1 ± 0.7 km/s.

Since no photometry of HD 64365 was obtained on JD 2443476, little can be said about phase relation between the light and radial velocity variations of the star. The vertical arrow in Figure 7 indicates the phase of maximum light, computed according to the following elements:

$$\text{Max. } \underline{u} \text{ light} = \text{JD}_\odot\ 2443480.713 + 0^d.1927\ E, \qquad (1)$$

which best fit the observed u light maxima. The horizontal bar shows an estimated uncertainty of this computed phase.

Thus, all these new β Cephei stars display variable light ranges. Three of them exhibit primary periods which are considerably shorter than any of the hitherto known objects of this type. However, they are "normal" as far as their MK type is concerned. The two of them for which we have high dispersion spectra show very broad lines, while HD 64365 is a sharp-line star.

3. THE c_0 - β AND log P - β DIAGRAMS

Jerzykiewicz and Sterken (1978) presented a list of β Cephei stars, compiled

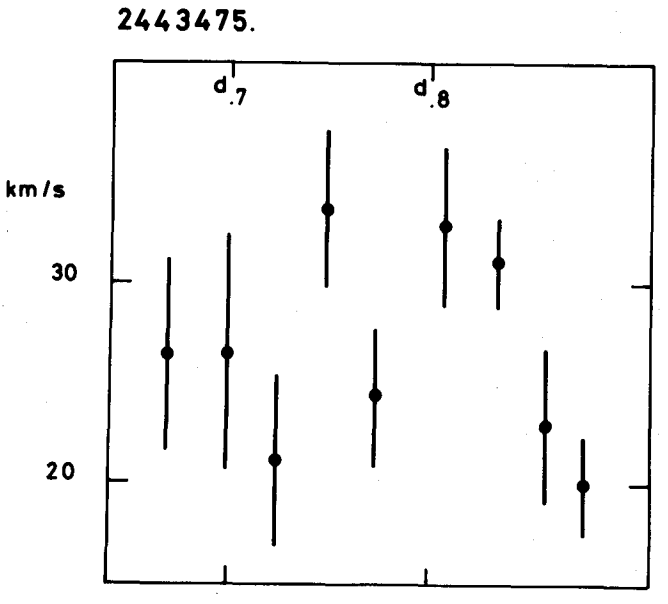

Figure 4. Radial velocities of HD 64722 on JD 2443475. The vertical bars are equal to twice the mean error.

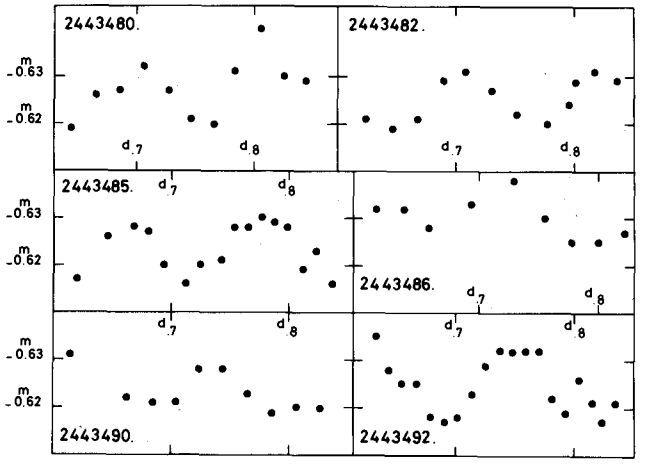

Figure 5. The u magnitude differences, HD 63949 minus HD 64287, plotted as a function of heliocentric Julian date.

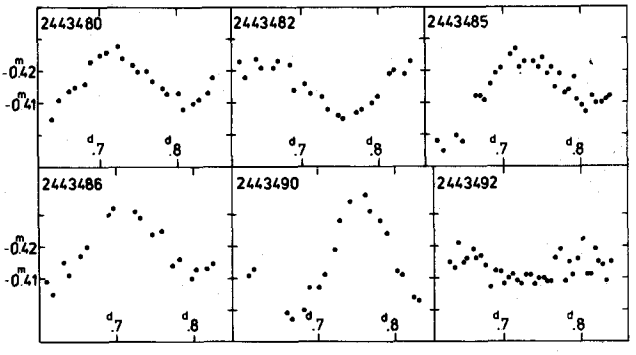

Figure 6. The u observations of HD 64365 referred to HD 64287.

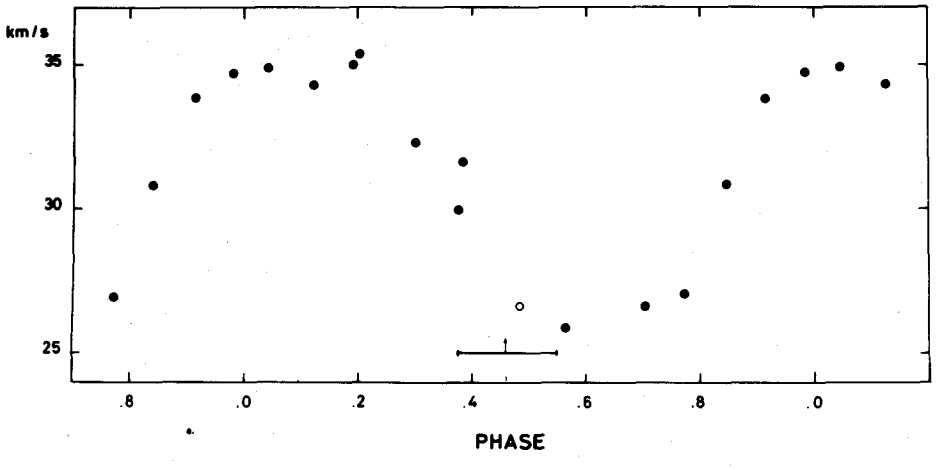

Figure 7. The radial velocity variation of HD 64365 on JD 2443476, plotted as a function of phase of $0^d.1927$, the primary photometric period. Zero phase is arbitrarily chosen at JD 2443476.0. The open circle denotes an observation obtained from a broken plate. Computed phase of light maximum is indicated with an arrow, and the horizontal bar shows the estimated uncertainty of this value.

according to the following criteria: (1) convincing evidence of light variability within a period shorter than nine hours, and (2) spectral type B3 or earlier, with supergiants and emission line objects excluded. The list is reproduced here in Table 2. One variable, HD 61068, which was discovered recently by Lesh and Wesselius (1978) from satellite UV observations, has been added. The stars are arranged in order of increasing right ascension. The MK classification in column five is from Lesh (1968); or Hiltner, Garrison and Schild (1969) for the Catalogue of Bright Stars objects; from Feast (1958) for NGC 3293 variables; from Schild (1970) for NGC 4755-F; and from Garrison, Hiltner and Schild (1977) for HD 80383. The sixth column of Table 2 provides the primary photometric period P according to the most recent work, which is referenced in the last column.

The β Cephei stars are plotted in Figure 8 in the c_0 - β plane; the four NGC 3293 variables are excluded, as uvby photometry is not available. In addition, 25 early-type stars found to be non-variable by Lynds (1959), Jerzykiewicz (unpublished), and Jerzykiewicz and Sterken (1977, 1978) are shown. The c_0 indices were computed by means of the iterative procedure of Crawford (Crawford and Barnes 1974). All published uvby data were taken into account; if two or more sets of uvby colors were available for the same star, a straight mean of the corresponding c_0 indices was computed. Likewise, all available β values were used in forming a mean for each star. In a number of cases the data used by Jerzykiewicz and Sterken (1978) were supplemented by β values of Deutschman, Davis and Schild (1976). No corrections for duplicity were applied to either c_0 or β, except for β Crucis (see below).

As can be seen from Figure 8, the β Cephei stars occupy a well-defined strip in the c_0 - β plane, approximately parallel to the zero age main sequence. The ridge line of the strip runs about $0\overset{m}{.}025$ in β above the zero age relation of Crawford (1978). Except for V986 Ophiuchi, the β Cephei stars fall within the interval $-0\overset{m}{.}07 < c_0 < +0\overset{m}{.}13$. The low luminosity end of the strip seems to be well-defined. However, the position of the high luminosity end depends on whether V986 Ophiuchi is considered to be the same type of object as the remaining ones.

The boundaries of the β Cephei strip in the interval $-0\overset{m}{.}07 < c_0 < +0\overset{m}{.}13$ are shown in Figure 8 by broken lines. The upper boundary is defined, in order of decreasing luminosity, by 19 Monocerotis and α Lupi, and the lower one by HD 63949 = HR 3058, HD 80383, and 16 Lacertae. The overall width of the strip, measured in β from the lower to the upper boundary, is $0\overset{m}{.}025$.

Perhaps the most striking feature of Figure 8 is that only seven constant stars are contained within the β Cephei strip, as compared to the 33 β Cephei variables. Moreover, in the interval $-0\overset{m}{.}07 < c_0 < +0\overset{m}{.}13$, where most of these variables are located, the constant stars which lie inside the strip fall close to the strip's boundaries. The only exception is HD 74273 = HR 3453. However, the range of published β values for this star (Lindemann and Hauck 1973; Deutschman,

Table 2. The β Cephei Stars

HR	HD	Name	m_V	MK	P	Source of P
39	886	γ Peg	$2^m.8$	B2 IV	$0^d.15175$	Sareyan, Valtier and Le Contel (1975)
779	16582	δ Cet	4.1	B2 IV	0.16114	Jerzykiewicz (1971a)
1072	21803	KP Per	6.4	B2 IV	0.20175	Jerzykiewicz (1971b)
1463	29248	ν Eri	4.0	B2 III	0.17351	van Hoof (1961)
1679	33328	λ Eri	4.3	B2 IVn	0.240	Balona (1977)
2294	44743	β CMa	2.0	B1 II-III	0.25130	Shobbrook (1973a)
2387	46328	ξ^1 CMa	4.3	B1 III	0.20958	Shobbrook (1973b)
2571	50707	15 CMa	4.8	B1 III	0.18456	Shobbrook (1973b)
2648	52918	19 Mon	5.0	B1 IV	0.175	Balona (1977)
2670	53755	-	6.5	B0.5 IVn	0.180	Balona (1977)
2928	61068	-	5.7	B2 III	0.1612	Lesh and Wesselius (1978)
3058	63949	-	5.8	B1.5 IV	0.1182	this paper
3078	64365	-	6.0	B2 IV	0.1927	this paper
3088	64722	-	5.7	B1.5 IV	0.1154	this paper
3213	68324	-	5.2	B1 IVn	0.108	this paper
-	80383	-	9.1	-	0.1842	Haug (1977)
-	92024	NGC 3293-5	9.1	B1 III	0.17	Balona (1977)
-	-	NGC 3293-24	9.2	B1 III	0.188	Balona (1977)
-	-	NGC 3293-26	9.3	B1 III	0.175	Balona (1977)

HR	HD	Name	m_v	MK	P	Source of P
-	-	NGC 3293-27	9.0	B0.5 III	0.236	Balona (1977)
-	-	NGC 4755-F	9.0	B2 III	0.203	Jakate (1978a)
4853	111123	β Cru	1.3	B0.5 III	0.1605	Pagel (1956)
5056	116658	α Vir	1.0	B1 IV	0.17379	Shobbrook, Lomb and Herbison-Evans (1972)
5132	118716	ε Cen	2.3	B1 III	0.16961	Shobbrook (1972)
5267	122451	β Cen	0.6	B1 III	0.30	Balona (1977)
5395	126341	τ^1Lup	4.6	B2 IV	0.17735	van Hoof, Pretorius and Pikoos (1964)
5469	129056	α Lup	2.3	B1.5 III	0.25988	Lesh (1978)
6084	147165	σ Sco	2.9	B1 III	0.24684	Sterken (1975)
6453	157056	θ Oph	3.3	B2 IV	0.14053	Briers (1967)
6527	158926	λ Sco	1.6	B1.5 IV	0.21370	Shobbrook and Lomb (1972)
6580	160578	κ Sco	2.4	B1.5 III	0.19987	Shobbrook and Lomb (1972)
6684	163472	V2052 Oph	5.8	B2 IV-V	0.13989	Morton and Hansen (1974)
6747	165174	V986 Oph	6.1	B0 IIIn	0.2907	Jerzykiewicz (1975)
8007	199140	BW Vul	6.4	B2 III	0.20103	Valtier (1976)
8238	205021	β Cep	3.2	B1 III	0.19049	Gray (1970)
8640	214993	12 Lac	5.2	B1.5 III	0.19308	Jerzykiewicz (1978)
8725	216916	16 Lac	5.6	B2 IV	0.16917	Jerzykiewicz (unpublished)

Davis and Schild 1976; and Shobbrook 1978a) is nearly $0^m.030$, making the mean rather uncertain. The conclusion, as previously stated by Jerzykiewicz and Sterken (1978), is that, in the interval $-0^m.07 < c_0 < +0^m.13$, the constant stars are probably separated from the β Cephei variables. In other words, the β Cephei strip may well represent an instability region in the sense that all stars which fall within it become β Cephei variables.

The fact that a number of stars plotted in Figure 8 are double does not change the above conclusions. In the c_0 - β plane, a duplicity correction moves a point along a line very nearly parallel to the ridge line of the β Cephei strip (cf., the arrow in Figure 8). Moreover, of all variables located close to either end of the $-0^m.07 < c_0 < +0^m.13$ interval, only β Crucis is double. A duplicity correction was applied to this star, using the value computed by Shobbrook (1978a).

The β indices of the β Cephei stars are plotted in Figure 9 against log P, where P is the primary photometric period. The filled circle farthest to the right corresponds to β Centauri and the open circle indicates where this star would fall if the radial velocity period determined by Lomb (1975) was used instead of Balona's (1977) photometric period. Stars which were discovered to be β Cephei variables by Jerzykiewicz and Sterken (1978) (cf. Table 1) are represented by filled triangles.

The diagram shows a considerable amount of scatter. As can be easily seen, a number of points would deviate by more than $0^m.010$ from any straight line fit. Moreover, the difference in β between stars occupying the extremes of the period range is probably insignificant, especially if V986 Ophiuchi is disregarded. From these facts Jerzykiewicz and Sterken (1978) concluded that the concept of a unique period-luminosity relation appears to be inapplicable to the β Cephei variables, and that it should be abandoned.

4. THE β CEPHEI STARS IN THE THEORETICAL H-R DIAGRAM

In order to get the effective temperature scale for the c_0 colors, a linear relation was derived between c_0 and $\Theta_e = 5040/T_e$ from stars for which Code et al. (1976) have determined empirical effective temperatures. Stars with $T_e > 12200$ K were used, but supergiants were omitted. The c_0 indices were computed from the uvby colors taken out of the Lindemann and Hauck (1973) catalogue. Duplicity corrections as determined by Davis and Shobbrook (1976) were applied to the c_0 values of β Crucis, α Virginis, and δ Scorpii. Assuming that the c_0 indices are error-free and assigning weights to Θ_e according to the mean errors given by Code et al. (1976), the following equation was obtained by means of the least-squares method:

$$\begin{matrix}\theta_e = 0.282\ c_0 + 0.203, \\ \pm 0.014 \quad \pm 0.004\end{matrix} \qquad (2)$$

where the numbers underneath the coefficients indicate their mean errors. Equation

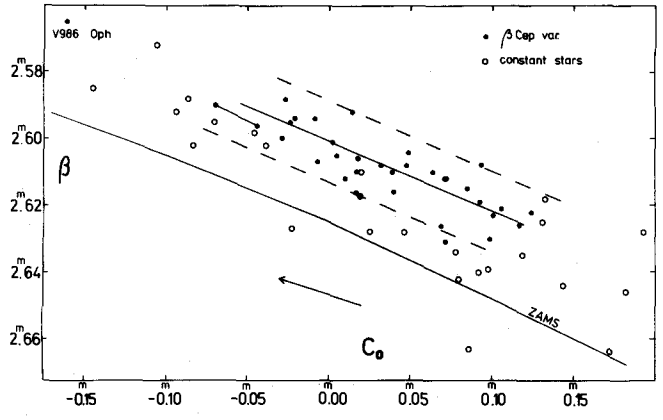

Figure 8. The β Cephei variables (filled circles) and constant early B stars (open circles) in the c_0 - β plane. The arrow indicates a maximum duplicity correction, as estimated by Shobbrook (1978a). The two filled circles at the left and right ends of the short straight line segment correspond to β Crucis, corrected and uncorrected for duplicity, respectively. The lower solid line is the zero age main sequence according to Crawford (1978), and the upper one defines the ridge line of the β Cephei strip. The broken lines indicate the boundaries of the strip.

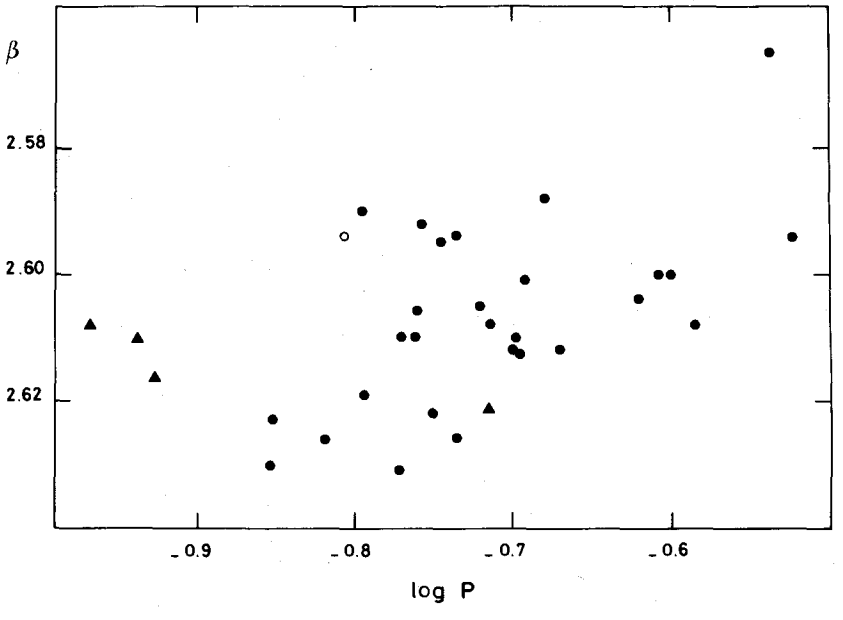

Figure 9. The β indices of the β Cephei variables plotted against log P, where P denotes the primary photometric period. The four new β Cephei stars are shown as filled triangles. The open circle corresponds to β Centauri, if the radial velocity period was used instead of the photometric one.

(2) agrees well with the mean relation between c_0 and Θ_e derived by Davis and Shobbrook (1976).

From Equation (2) and the mean c_0 indices effective temperatures of the β Cephei and constant stars were computed; however, for β Canis Majoris, β Crucis, α Virginis and ε Centauri, T_e values were taken directly from Code et al. (1976).

The visual absolute magnitudes M_V were derived from the mean β indices using the calibration of Crawford (1978). Finally, the bolometric absolute magnitudes were computed as $M_{bol} = M_V + BC$, with the bolometric corrections obtained from the above-mentioned effective temperatures and the empirical calibration, BC versus T_e, of Code et al. (1976).

The β Cephei variables (filled circles) and constant stars (open circles) are plotted in the theoretical H-R diagram in Figure 10. Also shown are Crawford's (1978) zero age main sequence, the ridge line of the β Cephei instability strip (rightmost solid line), and its boundaries (broken lines), all transformed from Figure 8. V986 Ophiuchi (log T_e = 4.506 and $M_{bol} = -9\overset{m}{.}25$) is not shown.

As can be seen from Figure 10, the β Cephei instability strip in the theoretical H-R diagram extends over M_{bol} from $-5\overset{m}{.}0$ to $-7\overset{m}{.}5$. Only V986 Ophiuchi has luminosity considerably exceeding the latter limit. The ridge line of the strip runs approximately $1\overset{m}{.}25$ above Crawford's zero age main sequence. The width of the strip in log T_e is approximately 0.055.

Thus, the extent and location of the β Cephei phenomenon in the temperature-luminosity plane seems to be quite well defined. This is not a new conclusion, of course. However, this definition may be more precise, as it is based on more numerous samples of β Cephei stars and on more recent temperature and luminosity calibrations than those of Percy (1970); Watson (1972); Lesh and Aizenman (1973a); and Balona and Feast (1975).

5. THE EVOLUTIONARY STATUS OF THE β CEPHEI STARS

Watson (1972) and Lesh and Aizenman (1973a), using evolutionary tracks computed with Cox-Steward opacities, found that the β Cephei variables occupy a region in the H-R diagram traversed three times by a 10 to 15 $M_\odot$ star in its early evolution: once in the core hydrogen-burning phase, once in the secondary contraction phase, and once in the shell hydrogen-burning phase. Although, Lesh and Aizenman concluded that the β Cephei stars are in one of the two later stages of evolution, Watson maintained that most β Cephei stars are core hydrogen-burning objects. This difference of opinion has been caused by the fact that Lesh and Aizenman found many non-variable B stars in their β Cephei region, whereas Watson believed that β Cephei variables and constant stars separate in the H-R diagram. Watson's work was criticized by Lesh and Aizenman (1973b) on the grounds that, of his 28 non-variable stars, only four fall in the same spectral-type range as the β Cephei

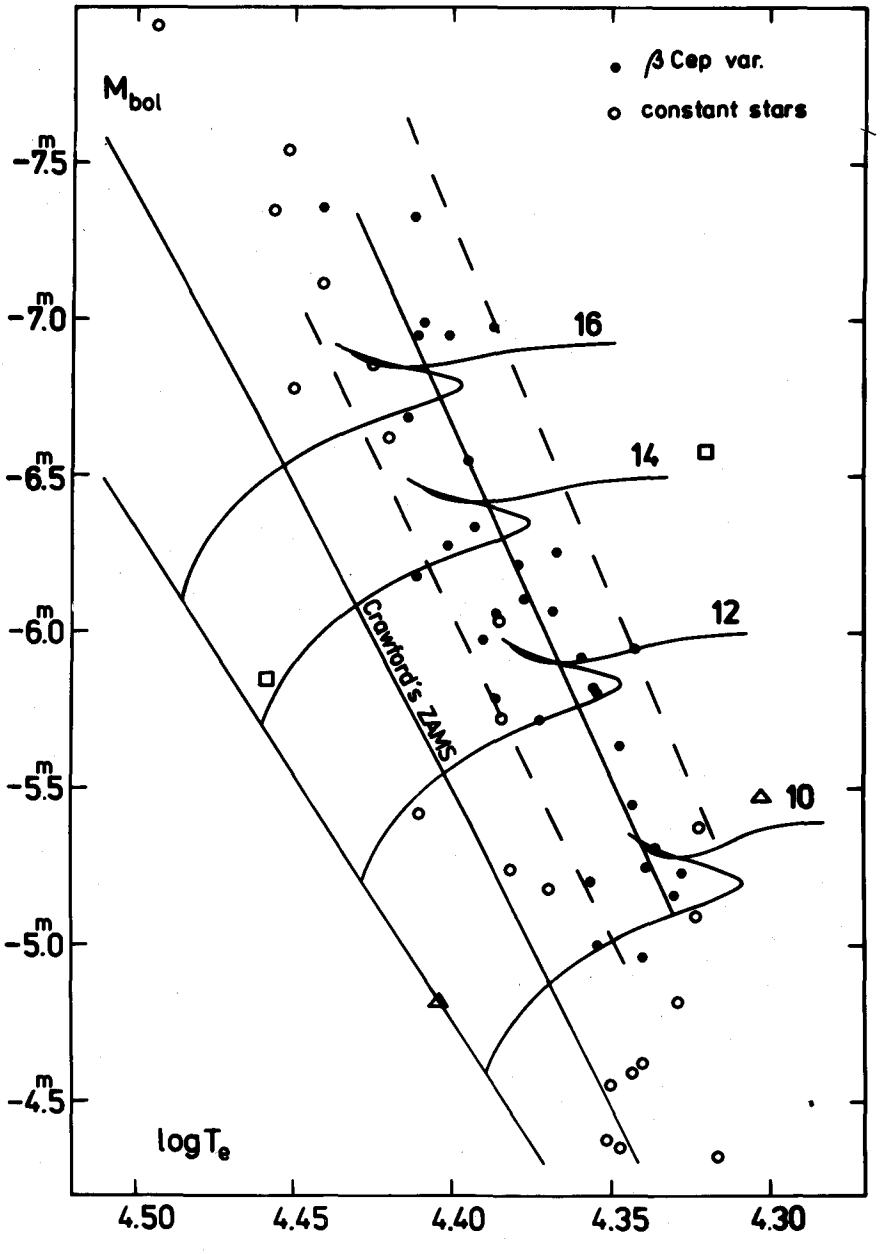

Figure 10. The β Cephei variables (filled circles) and constant early B stars (open circles) in the theoretical H-R diagram. V986 Ophiuchi (log T_e = 4.506 and M_{bol} = -9.25) is not shown. See § 5 for explanation of the remaining symbols.

variables. However, the conclusion of Lesh and Aizenman (1973a) is also questionable, because their non-variable stars were objects which have never been checked for light variability. The result that constant stars do avoid the β Cephei strip in the H-R diagram (cf., Jerzykiewicz and Sterken 1978 and also § 3 and Figure 10 of the present paper) appears to be the first one of this kind based on an extensive sample of stars that have been carefully investigated photometrically for variability. A similar conclusion has been reached recently by Jakate (1978b), who investigated the position of a number of β Cephei and constant stars in the [u - b] - β plane. However, Jakate's results with respect to the extent and position of the instability strip (cf. Jakate and Sterken 1979) differ from those of Jerzykiewicz and Sterken (1978).

The determination of the evolutionary status of the β Cephei stars is further complicated by the circumstance that the position of the β Cephei strip in relation to the theoretical evolutionary tracks depends on the opacities used, as has been pointed out by Lesh and Aizenman (1973a), Stothers (1976), and others. Figure 10 illustrates the evolutionary tracks of 10, 12, 14 and 16 $M_\odot$ models with an initial chemical composition of X = 0.70 and Z = 0.03, computed by de Loore et al. (1978). A modification of Paczynski's (1970) stellar evolution program, using Cox-Steward opacity tables, was employed. The leftmost open triangle and open square represent the zero age models of Stothers (1976) for M equal to 10.9 and 15 $M_\odot$, respectively. In these models Carson's radiative opacities were used and the composition was X = 0.73 and Z = 0.02. The rightmost open symbols indicate the evolution of the corresponding models to a point near the end of the core hydrogen-burning phase (X_c = 0.064).

As can be seen from Figure 10, it is not possible to infer which of the three above-mentioned evolutionary phases most β Cephei stars are currently in, assuming the adequate representation of early B star evolution by the tracks of de Loore et al. (1978). If, on the other hand, Stother's (1976) evolutionary tracks are more nearly appropriate, a number of β Cephei variables would be found in the core hydrogen-burning phase. In both these cases, however, the zero age models fall considerably below the observed zero age main sequence of Crawford (1978). It is thus clear that, until this discrepancy is removed, any conclusion concerning the evolutionary status of the β Cephei stars will be somewhat questionable. One consequence of this problem is the uncertainty by at least $2M_\odot$ of masses for β Cephei stars obtained from a comparison with the presently available theoretical models.

It should be mentioned that Lesh and Aizenman (1973a) used Z = 0.06 in their model calculations in order to increase the opacity. This removed the discrepancy between the theoretical and observed zero age main sequences. By following the same procedure, most β Cephei stars are found to be in the core hydrogen-burning phase.

Attempts to determine the evolutionary status of the β Cephei variables have

been often made in the hope of unearthing clues to the unknown excitation mechanism presumably operating inside them. We would like to point out that, in view of the observed separation of their locations in the H-R diagram, the evolutionary history of the β Cephei variables may be relevant in this context only insofar as it results in carrying their progenitors into the instability strip. In other words, we believe that the search for a possible excitation mechanism should be concentrated in the envelopes of the β Cephei stars, and not in their cores.

An investigation of the evolutionary status of the β Cephei variables has been recently carried out by Shobbrook (1978a,b). Shobbrook (1978a) maintains that in the c_0 - β plane the width of the β Cephei strip does not exceed $0^m.003$ in β, i.e., $0^m.15$ in luminosity, a value very much smaller than $1^m.25$ we found. The main reason for this discrepancy comes probably from the fact that Shobbrook could not take into account most of the variables which we used for determining the boundaries of the β Cephei strip, because they were discovered after his analysis had been completed. Moreover, Shobbrook believes that there are constant stars within the β Cephei strip. This conclusion is also contradicted by our results. Therefore, Shobbrook's (1978b) statement that all these variables must be very near the end of the core hydrogen burning phase appears to be unfounded.

6. THE PERIOD-LUMINOSITY RELATION

In Figure 11 the absolute bolometric magnitudes of the β Cephei stars are plotted as a function of log P, where P is the primary photometric period. A straight line, fitted to the data by the method of least-squares, is also shown. It has the following equation:

$$\begin{array}{llll} -3.9 \log P & - 9.0 = M_{bol}, & & (3) \\ \pm 1.3 & \pm 1.0 & \pm 0.8 & \end{array}$$

where the numbers underneath the coefficients indicate their mean errors, while the one beneath the righthand side is the standard deviation of the solution. After adding a log T_e term we obtained the following equation:

$$\begin{array}{llll} -0.05 \log P & - 0.042 \log T_e + 4.08 = M_{bol} & & (4) \\ \pm 0.03 & \pm 0.003 & \pm 0.04 & \pm 0.14 \end{array}$$

These results clearly confirm our earlier conclusion (cf. Jerzykiewicz and Sterken 1978 and § 3 of the present paper) that the β Cephei stars do not obey a period-luminosity relation. Indeed, in the case of equation (3) the standard deviation is much greater than any reasonable estimate of the mean error of the M_{bol} values. Adding a log T_e term results in decreasing the standard deviation considerably; however, the coefficient of log P then turns out to be of the same

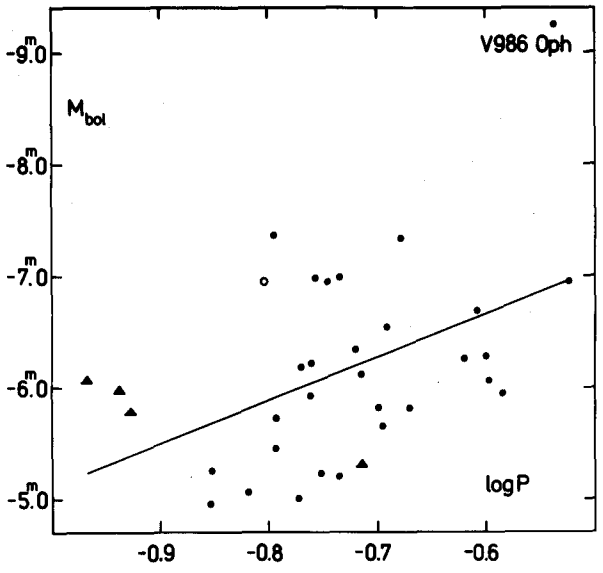

Figure 11. The β Cephei stars in the M_{bol} - log P plane. The symbols are the same as in Figure 9. The straight line was fitted to the data by the method of least squares.

order of magnitude as its mean error, so that equation (4) actually represents the ridge line of the β Cephei strip, and not a log P - log T_e - M_{bol} relation. As we have already pointed out (Jerzykiewicz and Sterken 1978), the lack of a period-luminosity relation lends support to the idea that the primary photometric periods of β Cephei variables may correspond to a variety of nonradial oscillation modes.

REFERENCES

Balona, L.A. 1977, Mem. R. Astr. Soc., 84, 101.

Balona, L.A. and Feast, M.W. 1975, Mon. Not. R. Astr. Soc., 172, 191.

Briers, R. 1967, Inf. Bull. Var. Stars, no. 200.

Campbell, W.W. and Moore, J.H. 1928, Publ. Lick Obs., 16.

Code, A.D., Davis, J., Bless, R.C. and Brown, R.H. 1976, Ap. J., 203, 417.

Crawford, D.L. 1978, Astr. J., 83, 48.

Crawford, D.L. and Barnes, J.V. 1974, Astr. J., 79, 687.

Davis, J. and Shobbrook, R.R. 1976, Mon. Not. R. Astr. Soc., 178, 651.

de Loore, C., De Greve, J.P., Packet, W. and Vanbeveren, D. 1978, personal communication.

Deutschmann, W.A., Davis, R.J. and Schild, R.E. 1976, Ap. J. Suppl., 30, 97.

Feast, M.W. 1958, Mon. Not. R. Astr. Soc., 118, 618.

Garrison, R.F., Hiltner, W.A. and Schild, R.E. 1977, Ap. J. Suppl., 35, 111.

Gray, D.F. 1970, Astr. J., 75, 958.

Haug, U. 1977, The Messenger, no. 9, 14.

Hiltner, W.A., Garrison, R.F. and Schild, R.E. 1969, Ap. J., 157, 313.

Jakate, S.M. 1978a, Astr. J., 83, 1179.

Jakate, S.M. 1978b, a preprint.

Jakate, S.M. and Sterken, C. 1979, these proceedings.

Jerzykiewicz, M. 1971a, Lowell Obs. Bull., 7, 199.

Jerzykiewicz, M. 1971b, Acta Astr., 21, 501.

Jerzykiewicz, M. 1975, Acta. Astr., 25, 81.

Jerzykiewicz, M. 1978, Acta. Astr., 28, in press.

Jerzykiewicz, M. and Sterken, C. 1977, Acta. Astr., 27, 365.

Jerzykiewicz, M. and Sterken, C. 1978, I.A.U. Colloq. No. 46, in press.

Lesh, J.R. 1968, Ap. J. Suppl., 17, 371.

Lesh, J.R. 1978, Ap. J., 219, 947.

Lesh, J.R. and Aizenman, M.L. 1973a, Astr. Ap., 22, 229.

Lesh, J.R. and Aizenman, M.L. 1973b, Astr. Ap., 26, 1.

Lesh, J.R. and Wesselius, P.R. 1978, Astr. Ap., in press.

Lindemann, E. and Hauck, B. 1973, Astr. Ap. Suppl., 11, 119.

Lomb, N.R. 1975, Mon. Not. R. Astr. Soc., 172, 639.

Lynds, C.R. 1959, Ap. J., 130, 577.

Morton, A.E. and Hansen, H.K. 1974, Pub. Astr. Soc. Pacific, 86, 943.

Paczynski, B. 1970, Acta. Astr., 20, 47.

Pagel, B.E.J. 1956, Mon. Not. R. Astr. Soc., 116, 10.

Percy, J.R. 1970, Ap. J., 159, 177.

Sareyan, J.-P., Valtier, J.-C. and Le Contel, J.-M. 1975, Astr. Ap., 44, 215.

Schild, R.E. 1970, Ap. J., 161, 855.

Shobbrook, R.R. 1972, Mon. Not. R. Astr. Soc., 157, 5P.

Shobbrook, R.R. 1973a, Mon. Not. R. Astr. Soc., 161, 257.

Shobbrook, R.R. 1973b, Mon. Not. R. Astr. Soc., 162, 25.

Shobbrook, R.R. 1978a, Mon. Not. R. Astr. Soc., 184, 43.

Shobbrook, R.R. 1978b, Mon. Not. R. Astr. Soc., 184, 825.

Shobbrook, R.R. and Lomb, N.R. 1972, Mon. Not. R. Astr. Soc., 156, 181.

Shobbrook, R.R., Lomb, N.R. and Herbison-Evans, D. 1972, Mon. Not. R. Astr. Soc., 156, 165.

Sterken, C. 1975, Astr. Ap., 43, 321.

Stothers, R. 1976, Ap. J., 210, 434.

Valtier, J.-C. 1976, Astr. Ap., 51, 465.

van Hoof, A. 1961, Z. Ap., 53, 106.

van Hoof, A., Pretorius, W.S. and Pikoos, C. 1964, Inf. Bull. Var. Stars, no. 63.

Watson, R.D. 1972, Ap. J. Suppl., 24, 167.

16 LACERTAE: AN ECLIPSING SYSTEM WITH A β CEPHEI PRIMARY

M. Jerzykiewicz
Wroclaw University Observatory
Poland

ABSTRACT

A model is presented of the 16 Lacertae system which is shown to be an eclipsing variable with a β Cephei primary.

1. INTRODUCTION

The $12^{d}.097$ single-line spectroscopic binary 16 Lacertae, the primary component of which is a well-known β Cephei star, was recently found by Jerzykiewicz et al. (1978) to be an eclipsing variable. In the present paper a model of the system of 16 Lacertae is derived from observations. Moreover, it is shown that fairly accurate values of the primary component's radius and mass can be obtained from precise photometry of the eclipse.

2. OBSERVATIONS

The discovery that 16 Lacertae is an eclipsing system was a by-product of frequency analyses of two extensive series of photoelectric observations of the star. The first series consisted of over one thousand B magnitudes obtained by the author on 31 nights in the summer and autumn of 1965 at the Lowell Observatory. The second series included about five hundred blue-color observations secured by Jarzebowski, Jerzykiewicz, Le Contel and Musielok in the autumn of 1977 at the San Pedro Martir Observatory of the National University of Mexico, the Mt. Chiran station of the Haute Provence Observatory, and the Bialkow station of the Wroclaw University Observatory. Both these data series can be represented by synthetic light-curves, having the form of a sum of three sine-wave components with frequencies of 5.9112, 5.8551 and 5.5032 cycles/day. However, in 1965 the component amplitudes were equal to $0^{m}.020$, $0^{m}.010$ and $0^{m}.011$, respectively, whereas in 1977 they amounted to only $0^{m}.008$, $0^{m}.005$, and $0^{m}.007$. It is unclear whether this result indicates that the oscillations of 16 Lacertae are dying out, or that in 1977 we observed a minimum in a long-term variation of the oscillation amplitudes. This question can only be answered by future observations.

The eclipse of 16 Lacertae can be seen clearly after the intrinsic light-variations are removed. This is shown in Figure 1, where the deviations from the above-mentioned 1965 and 1977 synthetic light-curves are plotted as a function of the orbital phase, computed according to the following elements:

$$\text{Minimum light} = JD_{\odot}\ 2439054.575 + 12^{d}.09684\ E \qquad (1)$$
$$\pm.005 \quad \pm.00003$$

All observations with orbital phase within the interval 0.95 to 0.05 are shown. Points represent the 1965 data obtained on seven nights, while open circles correspond to observations taken on one night in 1977 at Mt. Chiran and San Pedro Martir (left and right of the mid-eclipse phase, respectively). The improved value of the orbital period in equation (1) was derived by forcing the 1965 and 1977 data to agree along the ascending branch of the light-curve.

It can be estimated from Figure 1 that the total duration of the eclipse is somewhere between $0^{d}.34$ and $0^{d}.40$, and that the depth of the eclipse amounts to $0^{m}.037 \pm 0^{m}.003$.

According to the spectroscopic orbital elements of Fitch (1969), the orbit of 16 Lacertae is very nearly circular ($e = 0.035 \pm 0.03$), with $K_1 = 23.0 \pm 0.6$ km/sec, $a_1 \sin i = 3.82 \times 10^6$ km, and the mass-function $f(M) = 0.0152\ M_{\odot}$. From this value of the mass-function one gets the mass ratio $M_2/M_1 < 0.2$, if $i > 55^{o}$ and $M_1 > 6\ M_{\odot}$. Thus, for any value of M_1 even remotely consistent with the primary's MK type of B2 IV, it follows that the mass of the secondary is approximately 1 $M_{\odot}$, and that $a_1 + a_2$ amounts to at least 3.0×10^7 km. Consequently, unless the radii of the components are very much greater than their main-sequence values, it can be concluded that the system is a detached one with the secondary contributing a negligible fraction of the total light.

3. A MODEL OF THE SYSTEM OF 16 LACERTAE

In view of the preceding conclusions regarding the secondary component's mass and the dimensions of the system, a solution based on a simple spherical model was attempted. The contribution of the secondary to the total light of the system was neglected. The mean radius of the primary was taken to be $R_1 = 5.8\ R_{\odot}$, which is consistent with $\log T_e = 4.354$ and $M_{bol} = -5^{m}.00$. These values were obtained for 16 Lacertae by Sterken and Jerzykiewicz (1979) from the photometric indices c_0 and β using recent empirical calibrations of the temperature, bolometric correction, and absolute magnitude scales for the early-type stars. The mass of the primary, $M_1 = 10\ M_{\odot}$, also used in the solution was derived (Sterken and Jerzykiewicz 1979) by comparing the star's position in the H-R diagram with Population I evolutionary tracks. This comparison showed that the primary is still in the core hydrogen-burning phase. Finally, a cosine law of limb darkening was assumed, with the limb darkening coefficient equal to 0.4.

From these data it is possible to get a unique solution for a given R_2 and Δt, i.e., the secondary component's radius and the duration of the eclipse,

respectively, provided the spectroscopic orbital elements are considered. The procedure is as follows. A rough initial value of i, the inclination angle of the orbit, is assumed. This allows computation of approximate mass ratio and dimensions of the orbit, a_1 and a_2, from the spectroscopic elements and M_1. A better value of i is then obtained from the equation:

$$\cos^2 i = \frac{R^2}{a^2} - \frac{(\Delta t)^2 \pi^2}{P^2} \quad , \qquad (2)$$

where $R = R_1 + R_2$, $a = a_1 + a_2$, and P is the orbital period. Equation (2) holds for spherical components in a circular orbit, so that it is appropriate in the present context. With this better value of i the calculations are repeated. It was found that the solution converges very rapidly for almost any initial value of i.

A number of solutions were obtained in this way for different R_2 and Δt. The results are summarized in Figure 2, where computed depth of the eclipse (at the mid-eclipse phase) is shown plotted against the ratio of the radii, $k = R_2/R_1$, for three values of Δt: $0^d.35$, $0^d.37$ and $0^d.40$. As expected, for a given k the depth of the eclipse increases with Δt. Moreover, for each of the three Δt, the depth of the eclipse increases rapidly, until k equal to about 0.25 is reached; at this point the eclipse depth becomes insensitive to k. For $\Delta t = 0^d.35$ none of the solutions is deep enough to represent satisfactorily the observed $0^m.037$ eclipse. On the other hand, the computed $0^m.037$ eclipse for $\Delta t = 0^d.40$ turned out to have a flat bottom, contrary to what is observed. The solution for $\Delta t = 0^d.37$ and $k = 0.22$ (filled circle in Figure 2) fits the observations quite well. This can be seen from Figure 1, in which the solution is shown with a solid line.

A model of the system of 16 Lacertae corresponding to this solution is illustrated in Figures 3 and 4. In Figure 3 the position of the inner Lagrangian point is also indicated. Clearly, the system is a detached one. The eclipse is a partial transit. At the mid-eclipse phase (cf. Figure 4), about 80 percent of the disc of the secondary is projected onto the primary. The secondary, having a mass of 1.25 $M_\odot$ and radius of 1.28 $R_\odot$, is probably a normal late F or early G dwarf. Unfortunately, there is little hope that its spectrum will ever be seen.

As far as the author is aware, the system of 16 Lacertae has by far the smallest mass ratio among all presently known unevolved binaries.

4. DISCUSSION

The accuracy of the model derived in the preceding paragraph is difficult to ascertain. Much depends on the precision of the photometry, but errors in the spectroscopic elements are also a factor. The situation is further complicated by the circumstance that the photometric and spectrographic observations had to be freed

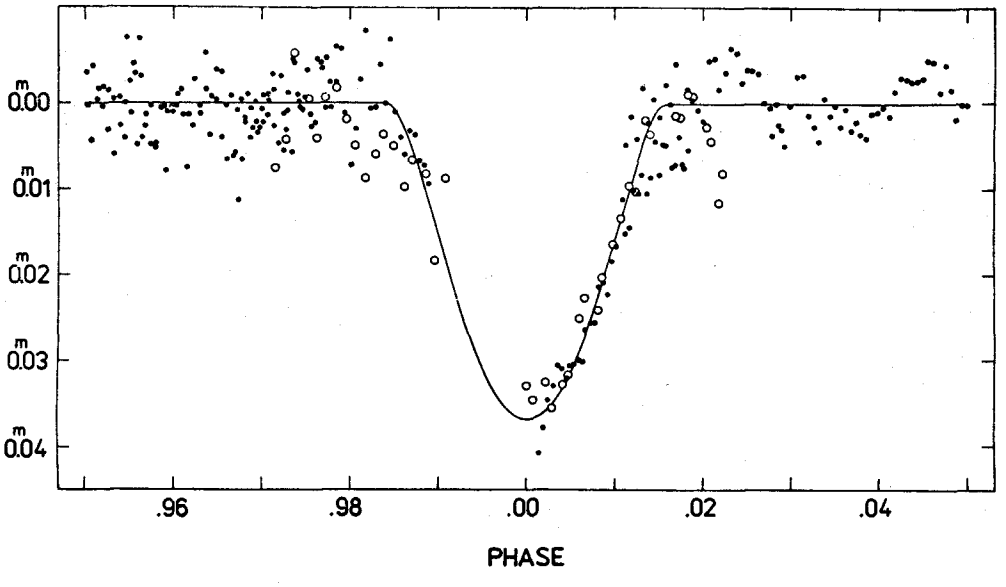

Figure 1. The primary eclipse of 16 Lacertae. The deviations from the intrinsic light-variations are plotted against phase of the $12^{d}.09684$ orbital period. All observations were taken in the blue region of the spectrum. The 1965 and 1977 data are shown with points and open circles, respectively. The line corresponds to the solution derived in § 3.

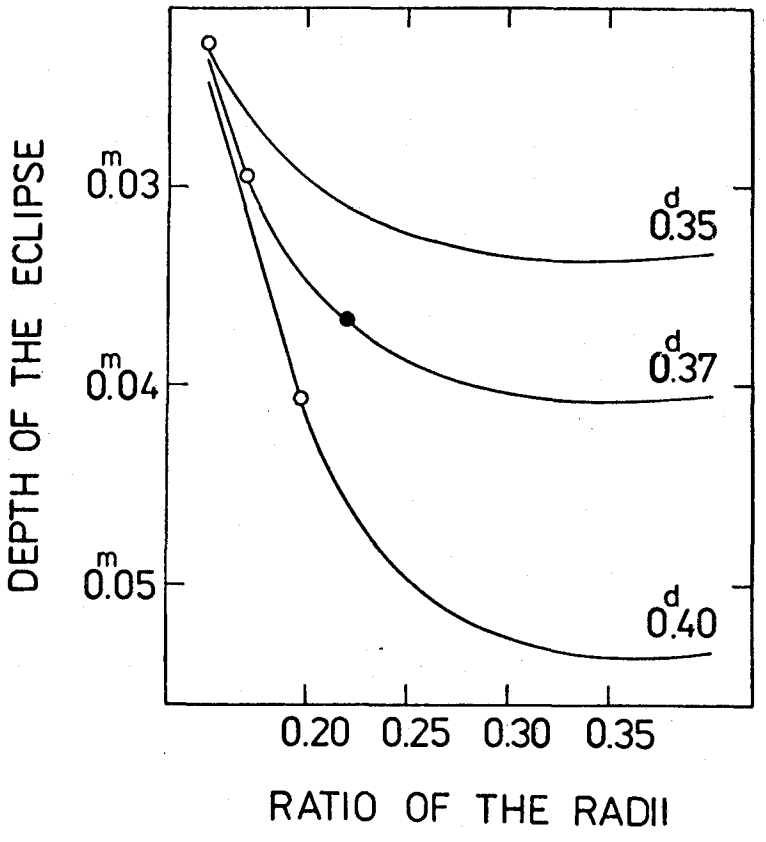

Figure 2. The computed depth of the eclipse of 16 Lacertae at the mid-eclipse phase for three values of the total duration of the eclipse. This depth is shown as a function of R_2/R_1, the secondary to primary radius ratio. The calculations were performed with the primary component's mass and radius equal to 10 $M_\odot$ and 5.8 $R_\odot$, respectively. A cosine law of limb darkening was assumed, with a limb darkening coefficient of 0.4. Solutions left of the open circles correspond to total eclipses. The filled circle indicates the adopted solution.

Figure 3. The system of 16 Lacertae in projection on the tangent plane of the sky. The secondary is shown at the greatest elongation (left) and in the conjunction with the primary at the mid-eclipse phase (right). The dimensions of the system are a_1 = 3.84 x 10^6 km and a_2 = 30.7 x 10^6 km. The inner Lagrangian point is indicated with a cross.

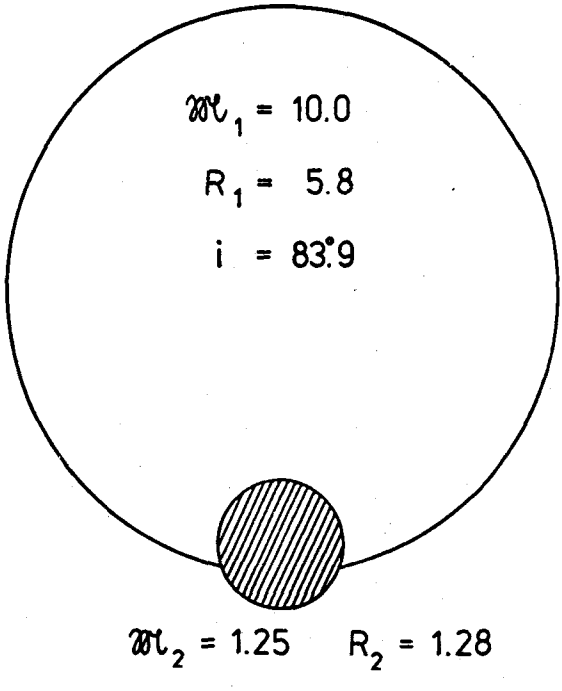

Figure 4. The system of 16 Lacertae at the mid-eclipse phase. The components' masses and radii are in solar units, and i is the inclination of the orbit to the tangent plane of the sky.

from the intrinsic variations, due to the oscillations of the primary, before they could be used to investigate the eclipse and the orbital radial-velocity variation.

In addition to these observational errors, the radius and mass of the primary, used as data in the solution, are also subject to a number of uncertainties. Most important of these are probably the systematic effects in the empirical calibrations of the temperature, bolometric correction, and absolute magnitude scales. The mass of the primary also depends on the reliability of the theoretical evolutionary tracks used to derive it. Unfortunately, there is no straightforward way to quantify all these uncertainties. What can easily be done, however, is to examine how the solution would change if the values of radius and mass of the primary were arbitrarily taken to be somewhat different than those used in the preceding paragraph.

Figure 5 shows how the computed depth of the eclipse depends on R_1. The calculations were performed with $\Delta t = 0\overset{d}{.}37$ and $M_1 = 10\ M_\odot$. The limb darkening coefficient was assumed to be 0.4. As can easily be seen, the solutions are rather sensitive to R_1. In fact, if the eclipse photometry was the main source of errors, the radius of the primary could be determined to within $\pm 0.2\ R_\odot$.

The sensitivity of the computed depth of the eclipse to M_1 is less pronounced. This is shown in Figure 6, which is based on computations with $\Delta t = 0\overset{d}{.}37$, $R_1 = 5.8\ R_\odot$, and a limb darkening coefficient of 0.4. However, the mass of 10 $M_\odot$ for the primary is probably correct to within $\pm\ 1\ M_\odot$, if all the other parameters of the system are not very much in error.

Thus, if R_1 or M_1 were changed by more than about ±4 and ±10 percent, respectively, the solution would no longer fit the observations. Since the radius and mass of the primary, estimated from its position in the H-R diagram, are probably much less certain than this, the problem can be reversed: values of R_1 and M_1 should be assumed that make it possible to derive a satisfactory model of the system. However, R_1 and M_1 are not independent parameters of the model, e.g., if the mass of the primary was increased by as much as $2\ M_\odot$, a satisfactory solution could still be obtained, provided that R_1 was also increased. Therefore, the above-mentioned values of $\pm 0.2\ R_\odot$ and $\pm 1 M_\odot$ are lower limits of the actual uncertainties with which the radius and mass of the primary can be determined by comparing the observed eclipse with the computed solution. Hopefully, future observations, especially photometric, will bring these uncertainties close to their lower limits.

Once this is accomplished, accurate photometry of the eclipse of 16 Lacertae could be used to investigate the variations of the star's radius due to its oscillations. In conjunction with simultaneous radial velocity measurements, such

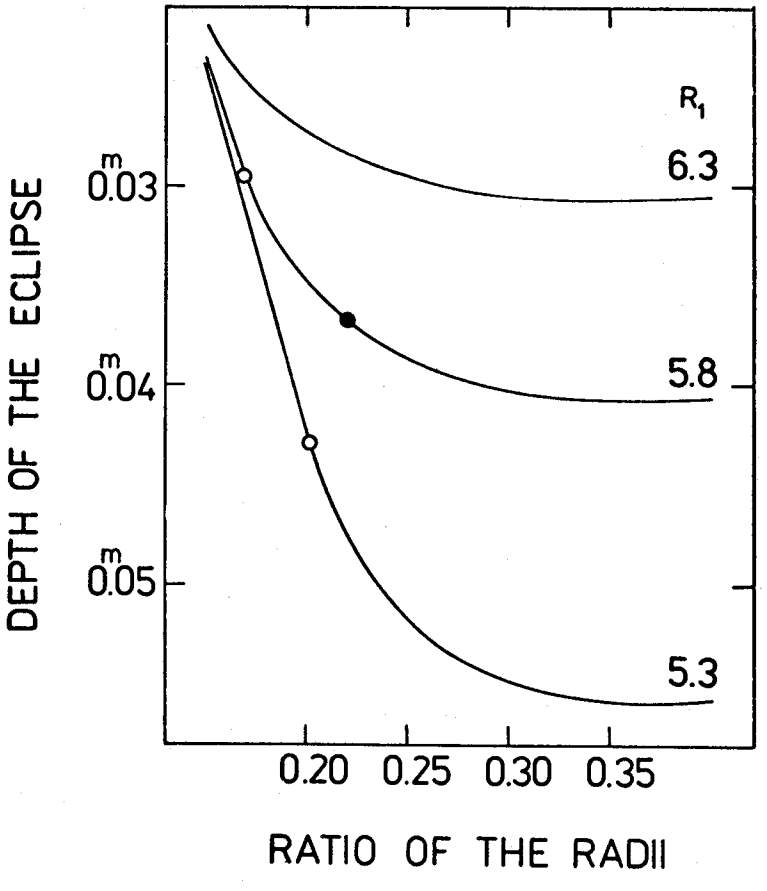

Figure 5. The computed depth of the eclipse of 16 Lacertae at the mid-eclipse phase shown as a function of R_2/R_1, for three values of R_1. Symbols are the same as in Figure 2.

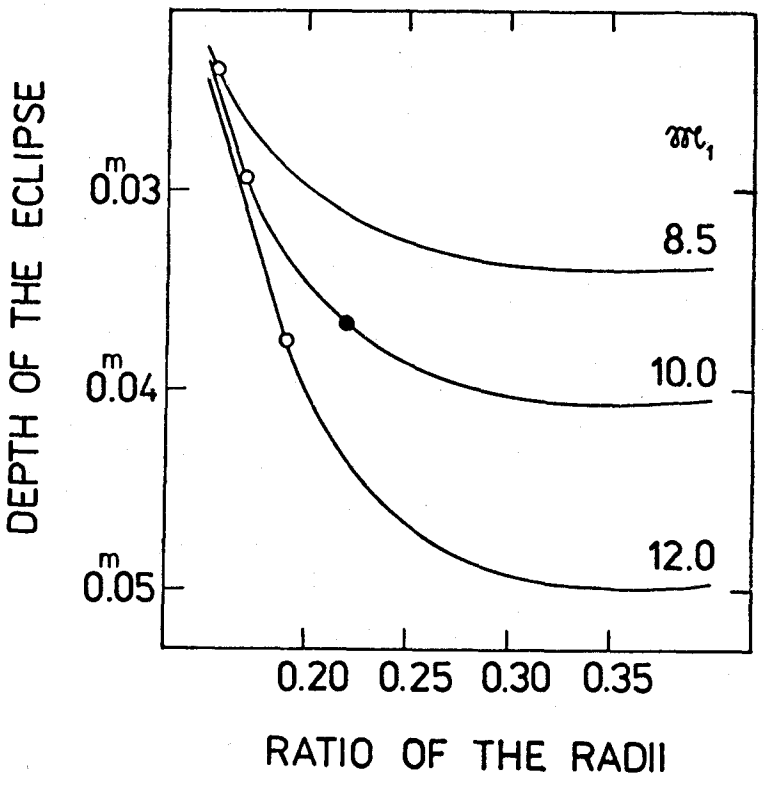

Figure 6. The computed depth of the eclipse of 16 Lacertae for different values of M_1, the primary component's mass.

observations may yield data to study the temporal changes of the surface geometry of the star, making possible the determination of its oscillation mode.

* * * * *

The author acknowledges financial support from the University of Arizona during his stay in Tucson.

REFERENCES

Fitch, W.S. 1969, Ap. J., 158, 269.

Jerzykiewicz, M., Jarzebowski, T., Le Contel, J.-M. and Musielok, B. 1978, Comm. 27 I.A.U. Inf. Bull. Var. Stars, no. 1508.

Sterken, C. and Jerzykiewicz, M. 1979, these proceedings.

LINEAR, NONADIABATIC PULSATION CALCULATIONS FOR MODELS OF UPPER MAIN SEQUENCE AND β CEPHEI STARS

H. Saio, J.P. Cox, C.J. Hansen and B.W. Carroll
Joint Institute for Laboratory Astrophysics
National Bureau of Standards and University of Colorado

ABSTRACT

Equations for linear nonadiabatic pulsation and the method of their solution are discussed in some detail. The numerical results presented concern mainly 7 $M_\odot$ stellar models in early evolutionary phase. A driving zone at a temperature of 1.5 x 10^5 K was found to be present for both radial and nonradial modes, but no net pulsational instability was observed. Effects of rotation on pulsation frequencies and on stability are also discussed.

1. INTRODUCTION

We have considered the general problem of small nonradial, nonadiabatic oscillations of spherical stars. Such oscillations must obey the mass, momentum, energy, and flux equations and the two equations which, together, comprise Poisson's equation. For spherical stars, it is both customary and adequate to assume a separation of the pulsation variables into spherical harmonics, as follows:

$$\begin{Bmatrix} f'(r,\theta,\phi,t) \\ \delta f(r,\theta,\phi,t) \end{Bmatrix} = \begin{Bmatrix} f'(r) \\ \delta f(r) \end{Bmatrix} Y_\ell^m(\theta,\phi) e^{i\sigma t} \qquad (1)$$

where f represents any physical variable; a prime denotes the Eulerian variation; δf denotes the Lagrangian variation; r, θ and ϕ are the usual spherical polar coordinates; Y_ℓ^m denotes a spherical harmonic; and σ denotes the (complex) pulsation angular frequency. The real component σ, σ_R, gives the pulsation period for the mode considered:

$$\Pi = \frac{\pi}{\sigma_R} \qquad (2)$$

The imaginary component of σ, σ_I, gives the "damping time" τ_e for the perturbation ($|\delta f| \propto e^{-\sigma_I t}$):

$$\tau_e = \frac{1}{\sigma_I} \tag{3}$$

Three vectors are involved in the analysis: δr (Lagrangian displacement); $\nabla\psi'$ (negative of the Eulerian variation of the force per unit mass, with ψ' being equal to the Eulerian variation of the gravitational potential ψ), and F' (Eulerian variation of the net energy flux). Assuming the separation of variables described in equation (1), the two transverse components of each of these vectors involve only algebraic relations. Therefore, each vector differential equation (momentum, flux, and force per unit mass) becomes a scalar differential equation. The resulting system of differential equations is of the sixth spatial order in, for example, the dependent variables P' (Eulerian variation of total pressure), ρ' (Eulerian variation of density ρ), δr (radial component of δr), ψ', $d\psi'/dr$ (spatial derivative of ψ'), and δs (Lagrangian variation of specific entropy s). However, in nonadiabatic oscillations, each dependent variable is complex, resulting in a system of the sixth order in complex variables.

In treating radiative transfer, a type of Eddington approximation (Unno and Spiegel 1966) has been used which yields

$$\vec{F}'_{rad} = -\left(\frac{4\pi}{3\kappa\rho}\nabla J\right)' \tag{4}$$

where

$$\vec{F}' = \vec{F}'_{rad} + \vec{F}'_{conv} \quad , \tag{5}$$

κ is the opacity, and J is the mean intensity, given by

$$J = \frac{ac}{4\pi}T^4 + \frac{1}{4\pi\kappa}\frac{ds}{dt} \tag{6}$$

Here T is the local temperature, a and c are the radiation constant and velocity of light, respectively, and t is the time. The following assumption was made regarding F'_{conv}, the Eulerian variation of the convective flux:

$$\delta(\nabla \cdot F_{conv}) = 0 \quad . \tag{7}$$

The variables actually used in the calculations were the Dziembowski-like variables

$$y_1 = \frac{\delta r}{r} \quad , \quad y_2 = \frac{1}{gr}\left(\frac{P'}{\rho} + \psi'\right) \quad ,$$
$$y_3 = \frac{1}{gr}\psi' \quad , \quad y_4 = \frac{1}{g}\frac{d\psi'}{dr} \quad , \tag{8}$$
$$y_5 = \frac{\delta S}{C_p} \quad , \quad y_6 = \left[\frac{\delta L(r)}{L(r)}\right]_{rad}$$

where g is the local gravitational acceleration, c_p is the specific heat per unit mass at constant pressure, and $\delta L(r)$ is the Lagrangian variation of the radiative interior luminosity L(r). The differential equations are then

$$\frac{dy_i}{dr} = f_i\ (r;\ y_1,\ldots,y_6),\ i = 1,\ldots,6 \quad , \tag{9}$$

where f_i are complicated functions which will not be reproduced here. In place of the actual angular oscillation frequency, σ, a dimensionless frequency, ω, was used. The relationship of these two quantities is given by:

$$\omega^2 = \frac{\sigma^2 R^3}{GM} \tag{10}$$

There are six boundary conditions, three at the center and three at the surface. Physically, the three central boundary conditions are that the three divergences involved, $\nabla \cdot \delta \underline{r}$, $\nabla \cdot \nabla\psi'$, and $\nabla \cdot \underline{F}'$, all remain finite. A similar situation is found with respect to the first two divergences when considering linear, nonradial, adiabatic oscillations. The three surface boundary conditions are that $\delta P/P$ be finite; that ψ' and $\nabla\psi'$, the gravitational force per unit mass and its gradiant, be continuous across the (perturbed) surfaces; and that there be no incident flux on the top of the atmosphere, as discussed by Ando and Osaki (1975). Again, the first two of these are the same as for linear, nonradial, adiabatic oscillations.

The normalization adopted is

$$y_1 = 1 \tag{11}$$

at the surface.

The above equations and boundary conditions, together with the above normalization condition, constitute an eigenvalue problem for the (complex) eigenvalue σ (or ω).

As a check on the accuracy of the numerical calculations that were performed, the work integral was also evaluated. Agreement with σ_I to 0.5% was obtained.

The surface phase lags were also computed for the various modes investigated. It was found for all the modes that maximum light coincided very closely with the instant of minimum stellar radius, as is actually observed in the β Cephei stars.

The results of the calculations have been expressed in terms of a "normalized growth rate," η'. This quantity, introduced by Stellingwerf (1978), is defined as follows:

$$\eta' = \frac{\int_M \oint PdV\, dm}{\int_M \left|\oint PdV\right| dm} = \frac{W_+ - W_-}{W_+ + W_-} \tag{12}$$

where W_+ and W_- (both > 0) are, respectively, the areas under the positive and negative portions of the work curve. Thus, if driving alone was occurring with no damping, $\eta' = +1.00$; conversely, in a situation of damping only, with no driving, $\eta' = -1.00$.

The above techniques have been applied to several kinds of stars, as discussed below.

2. UPPER ZERO AGE MAIN SEQUENCE MODELS

Several models of the upper zero age main sequence have been examined for linear, nonradial, nonadiabatic pulsations using the techniques described in § 1. (A previous investigation by Aizenman, Hansen and Ross (1975) was made using an adiabatic analysis and a simple opacity; this analysis yielded quasi-adiabatic stability results.) The models examined here had masses of 7 $M_\odot$, 12 $M_\odot$, and 20 $M_\odot$. The modes investigated were: p_2, p_1, f, g_1^+, and g_2^+ for $\ell = 2$; p_1 and g_1^+ for $\ell = 1$; and p_1, f and g_1^+ for $\ell = 3$.

The opacity was obtained through the use of Stellingwerf's (1975) formula for $T < 10^6$ K, and Iben's (1975) formula for $T > 10^7$ K; for 10^6 K $\leq T \leq 10^7$ K, the two formulae were smoothly joined together. The nuclear reaction rates were those of Fowler, Caughlan and Zimmerman (1975). The Schwarzschild criterion was used in semiconvective regions.

The periods were found to be the same as those computed adiabatically when calculations were taken to five significant figures. Also, throughout almost the entire model, the eigenfunctions were practically the same as those computed adiabatically.

As we had expected, the models were found to be stable in all cases.

3. MODELS FOR β CEPHEI STARS

In 1979, Stellingwerf discovered a new driving mechanism that is operative for radial pulsations and possibly other modes. Called the "bump mechanism," it is based on a local change in slope or "wiggle" of the opacity as a function of temperature at a given density. This wiggle occurs approximately at a temperature where the peak of the Planck function is observed to coincide with the ionization potential of He^+ (54.4 ev). This coincidence occurs at about 1.5×10^5 K; this is

near the temperature required for an ionization zone to produce pulsational instability in the β Cephei stars (Cox 1967). Stellingwerf (1979) showed that this bump mechanism would be more effective for stars with small mass concentrations than for highly centrally concentrated stars.

Using models of β Cephei stars, Stellingwerf (1978) calculated their stability against radial pulsations using the bump mechanism as the destabilizing mechanism. Although he found that driving occurred in the vicinity of 1.5×10^5 K. The bumb mechanism did not quite destabilize the models when currently estimated opacities were used. However, by artifically enhancing the opacities in the relevant region (to a degree well within the presently estimated uncertainties), he was able to produce pulsational instability in his models.

One of Stellingwerf's (1978) most interesting results was his finding that the locus of maximum instability on the Hertzsprung-Russell (H-R) diagram had a "backward" slope (opposite in sign to the slope of the Cepheid instability strip) almost exactly parallel to the mean line defined by the observed β Cephei variables. Stellingwerf (1978) suggested that this "backward" slope was a result of radiation pressure, a conjecture which proved to be correct (see below). However, his locus of maximum instability is lower by ~ 0.1 in log T_e than that observed for the β Cephei variables (T_e = effective temperature); this is illustrated in Figure 1, on which are also plotted some evolutionary tracks and the positions for some observed β Cephei stars.

In a subsequent investigation it was shown by Cox and Stellingwerf (1979) that the "backward" slope was actually a result of radiation pressure. Since the bump mechanism is an "envelope ionization mechanism" (Cox 1974), all the usual principles relating to this kind of process should apply. It is particularly important that the internal energy lying above the driving region be of the same order as the energy radiated by the star in a pulsation period:

$$\frac{\langle c_v T \rangle \Delta m}{\Pi L} \sim 1, \tag{13}$$

where c_v is the specific heat per unit mass at constant volume, T denotes the temperature in the driving region, Δm is the mass lying above the driving region, Π is the pulsation period of the star, and L is the equilibrium luminosity of the star. Radiation has a marked effect upon c_v, as is shown by the relation (Cox and Giuli 1968):

$$c_v = c_{v,g} \frac{8 - 7\beta}{\beta} \tag{14}$$

where $c_{v,g}$ is the contribution to c_v due only to gas, and $\beta = P_g/(P_g + P_r)$ is the ratio of gas to total (gas plus radiation) pressure. Thus, a radiation pressure of

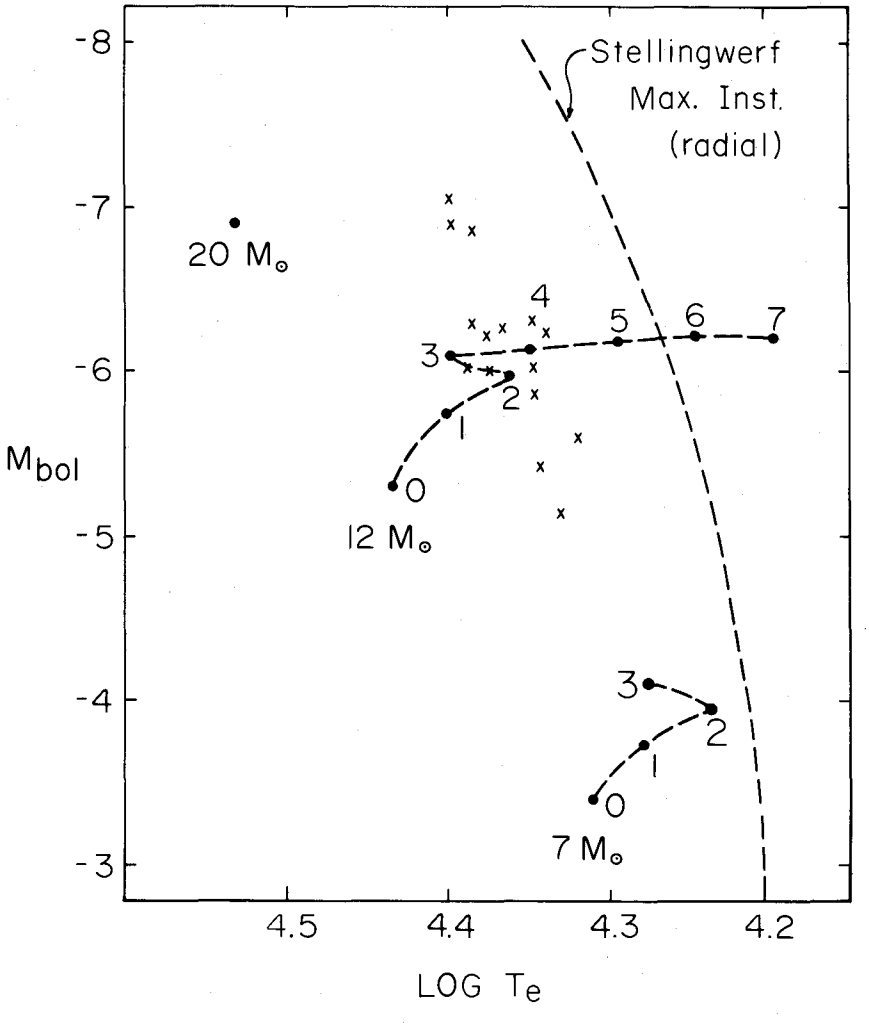

Figure 1. The locus of maximum instability of observed β Cephei variables along with evolutionary tracks for several models.

only 10 percent ($\beta \simeq 0.90$) can almost double c_v. Adopting equation (13) as the instability condition, and making a few other simplifying assumptions, Cox and Stellingwerf (1979) derived the following relation for the slope of the locus of maximum instability on the H-R diagram:

$$\frac{\partial \ell n L}{\partial \ell n T_e} = \frac{2\mu(4 - \zeta)}{(\mu - 1)(\alpha\delta + \gamma) + \mu + 1 - \eta - \mu(2 - \zeta/2)} \tag{15}$$

where

$$\alpha\delta + \gamma = \gamma \frac{-7\beta^2 + 16\beta - 8}{\beta(8 - 7\beta)} \tag{16}$$

The quantities μ, ξ, η and γ are defined by the following proportionalities and relations:

$$\Pi \propto \frac{R^{\zeta}}{M^{\eta}},$$

$$L \propto M^{\mu}, \tag{17}$$

$$\gamma = \frac{1}{1 + \left(\frac{\partial \ell n \kappa}{\partial \ell n \rho}\right)_T}$$

It is apparent that, for values of β only slightly less than unity, the quantity $\alpha\delta + \gamma$ becomes small or negative which can render $\frac{\partial \ell n L}{\partial \ell n T_e}$ positive, in agreement with Stellingwerf (1978).

Physically, radiation pressure puts more internal energy above any given level in the envelope. This consequently permits the condition for instability, equation (13), to be satisfied at a smaller radius and higher effective temperature than if radiation were not taken into account.

Cox and Stellingwerf (1979) also discussed the period-luminosity (Π-L) relationship which should apply to the β Cephei stars if these pulsations are "driven" by an envelope ionization mechanism. Because observations have shown that several periods may occasionally be present in any one β Cephei star, Cox and Stellingwerf (1979) suggested that the bump mechanism might also drive certain nonradial oscillations in this class of stars. The primary intent of this portion of our investigation was to test this conjecture.

The vibrational stability of some of the evolutionary models against small, nonradial oscillations was tested by the methods described in § 1. In particular,

the 7 $M_\odot$ and 12 $M_\odot$ models were examined in evolutionary stages 0, 1 and 2 as shown in Figure 1. An attempt was made to test a 12 $M_\odot$ model in stage 5 or 6; however, in these stages, the models had become so centrally concentrated that those calculations which had yielded results for the less centrally concentrated models failed to converge in this case. This may be due to the fact that the structure of the eigenfunctions becomes very complicated in such highly centrally concentrated models (Osaki 1977), particularly in the inner region where many nodes appear. Consequently, we have no results from our models in the interesting region occupied by 12 $M_\odot$ models in stage 5 or 6.

Of the successful calculations, the 7 $M_\odot$ model in stage 2 comes closest to the Stellingwerf maximum instability locus shown in Figure 1. Accordingly, we have presented some results for this model (stages 0, 1 and 2, for the p_1, f, and g_1^+ modes) in Table 1. Values of the normalized growth rate η' are given and estimated corresponding values for purely radial oscillations are provided for comparison.

On the basis of these results, nonradial modes appear to be driven by the bump mechanism about as strongly (or as weakly, depending on one's viewpoint) as the purely radial modes. However, until further results are available, particularly for stage 5 and 6 of the 12 $M_\odot$ model, this must be an extremely tentative conclusion. At least the 7 $M_\odot$ models in stages 0, 1 and 2 showed definite driving in the vicinity of 1.5×10^5 °K, where the bump mechanism is located (see Figure 2).

One point seems relatively clear: the 12 $M_\odot$ model in stages 0, 1 and 2 showed very little driving of nonradial oscillations due to the bump mechanism. We may therefore conclude that any driving of nonradial oscillations due to the bump mechanism is likely to be bound closely to the dashed line in Figure 1 applying to radial oscillations. Thus, the widespread excitation of nonradial oscillations in the general regions of the β Cephei stars found by Smith and McCall (1978) probably cannot be accounted for by this mechanism. [M. Smith (e.g., Buta and Smith 1979 or Smith 1980 paper presented at this conference) has referred to these stars as the "53 Persei variables."]

4. EFFECTS OF SLOW ROTATION ON NONADIABATIC, NONRADIAL FREQUENCIES

It is well known that slow rotation will cause those frequencies of non-axisymmetric modes which are characterized by a given "latitudinal" spherical harmonic to be split into $2\ell + 1$ "sublevels." If the angular rotation velocity Ω is constant throughout the star, this splitting is usually expressed as follows:

$$\omega = \omega_0 + \omega' \tag{18}$$

$$\omega' = -m\Omega(1 - C), \tag{19}$$

where subscript o denotes the nonrotating fraction and the magnitude of the quantity

Table 1. β Cephei Partial Results (Nonradial)

$7\ M_\odot$, $\ell = 2$

Stage	M_{bol}	Mode	Per. (hr.)	η'	η' (radial)
0	-3.4	p_1	1.613	-0.58	~ -0.3
		f	2.110	-0.59	
		g_1^+	3.499	-0.79	
1	-3.7	p_1	2.441	-0.56	~ -0.4
		f	3.103	-0.51	
		g_1^+	4.506	-0.58	
2	-3.96	p_1	3.668	-0.61	~ -0.4
		f	4.515	-0.46	
		g_1^+	5.826	-0.41	

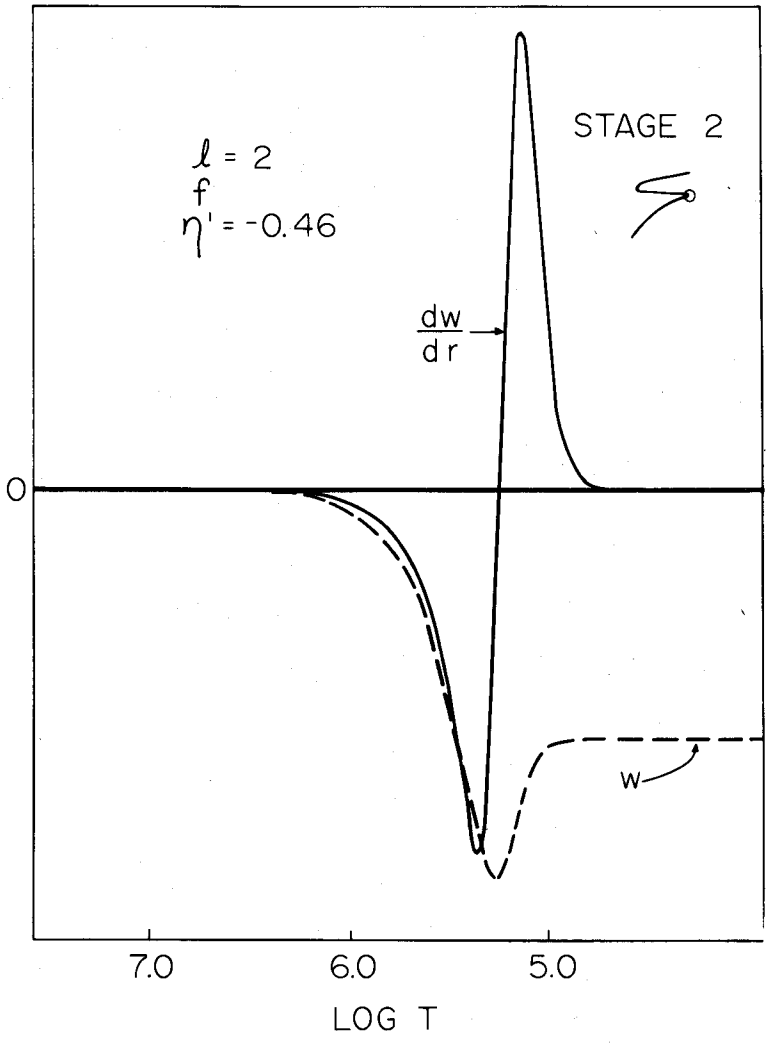

Figure 2. Calculation showing driving in the vicinity of the location of the bump mechanism for a 7 $M_\odot$ model.

C depends upon the structure of the star. The value of C also depends on the eigenfunction appropriate for the particular mode of oscillation; this eigenfunction may be derived entirely on the basis of adiabatic theory (i.e., no nonadiabatic effects need be taken into account). In addition, it can be shown that C can be calculated by use of the eigenfunctions appropriate to the nonrotating state of the star. This fact derives ultimately from the existence of a variational principle for linear, adiabatic, nonradial oscillations. In other words, an error of order ε in the eigenfunctions will only produce an error of order ε^2 in the eigenvalue.

The above splitting arises solely from the Coriolis forces, and would be present even in a star that is rotating so slowly that departures from sphericity are negligible.

The question then arises as to the relative stability of these various sublevels, a question which does involve nonadiabatic effects. An attempt to answer this question was made by Hansen, Cox and Carroll (1978), who calculated the appropriate stability coefficients by use of quasi-adiabatic approximation involving only the adiabatic eigenfunctions. Interestingly enough, they found that the sublevels corresponding to prograde ($m < 0$) azimuthal running waves were slightly less stable than retrograde ($m > 0$) waves.

In an attempt to improve upon this situation, we have tried to compute this splitting and the associated stability of the sublevels on the basis of nonadiabatic, nonradial oscillation theory. However, attempts to derive an integral expression analogous to C in equation (19), but involving only the nonadiabatic, nonrotating eigenfunctions have been relatively unsuccessful. We suspect that the reason for this failure is that a variational principle for nonadiabatic, nonradial oscillations does not exist. Therefore, we fear that the nonadiabatic eigenfunctions for the (slowly) rotating configuration must first be computed in order to obtain the desired stability information. Nevertheless, an integral expression, such as that referred to above, should serve as a valuable check on the final results. Work is now in progress on this project.

REFERENCES

Aizenman, M.L., Hansen, C.J. and Ross, R.R. 1975, Ap. J., 201, 387.

Ando, H. and Osaki, Y. 1975, Publ. Astron. Soc. Japan, 27, 581.

Buta, R.J. and Smith, M.A. 1979, Ap. J., in press.

Cox, J.P. 1967, in Aerodynamic Phenomena in Stellar Atmospheres (I.A.U. Symp. No. 28), (ed. R.N. Thomas; London: Academic Press).

Cox, J.P. 1974, Rep. Prog. Phys., 37, 563.

Cox, J.P. and Giuli, R.T. 1968, Principles of Stellar Structure (New York: Gordon and Breach).

Cox, J.P. and Stellingwerf, R.F. 1979, Publ. A.S.P., (in press).

Fowler, W.A., Caughlan, G.R. and Zimmerman, B.A. 1975, Ann. Rev. Astron. Astrophys.,

13, 69.
Hansen, C.J., Cox, J.P. and Carroll, B.W. 1978, Ap. J., 226, 210.
Iben, I., Jr. 1975, Ap. J., 196, 525.
Osaki, Y. 1977, Publ. Astron. Soc. Japan, 29, 235.
Smith, M.A. 1980, these proceedings.
Smith, M.A. and McCall, M.L. 1978, Ap. J., 223, 221.
Stellingwerf, R.F. 1975, Ap. J., 195, 441.
Stellingwerf, R.F. 1978, Ap. J., 83, 1184.
Stellingwerf, R.F. 1979, Ap. J., 227, 935.
Unno, W. and Spiegel, E.A. 1966, Publ. Astron. Soc. Japan, 18, 85.

IMPORTANCE OF STUDYING β CEPHEI STARS IN OPEN CLUSTERS AND ASSOCIATIONS

S.M. Jakate and C. Sterken†
†Astrofysisch Instituut
University of Brussels
Belgium

ABSTRACT

Beta Cephei stars which are located in clusters and associations can be used to gather information on their evolutionary phase when they are placed on the color-magnitude diagram. A tentative study is presented which attempts to use this idea to answer several important questions concerning β Cephei stars.

1. INTRODUCTION

Beta Cephei stars in clusters and associations are of special interest because the position in the color-magnitude diagram of these variables may provide information about their phase of evolution.

Jakate (1978) demonstrated that the position of the small "gap" in luminosity vs. temperature graphs, which corresponds to the core hydrogen exhaustion phase in the post main-sequence evolution of an open cluster, could be used to determine the evolutionary state of the β Cephei stars belonging to the cluster. He applied this technique to NGC 4755 and NGC 3293 and found that the β Cephei stars belonging to these clusters lie below the gap observed by Feast (1958). From this, he concluded that these β Cephei stars are in the core-hydrogen burning phase of their evolution.

Although there are only two such open clusters known which contain β Cephei stars, eight of these variables are found within approximately five associations and subgroups. Jakate's technique could not be applied to these associations, because of the difficulty of determining the position of the gap in their thinly populated color-magnitude diagrams. Therefore, it was decided to determine the luminosity level of the gap theoretically from published evolutionary tracks. This allows a comparison of the positions of the β Cephei stars belonging to the associations.

Several attempts have been made in the past to find observational parameters that can be used to separate β Cephei stars from non-variables in various planes (e.g., Lesh and Aizenman 1973; Watson 1972; Jones and Shobbrook 1974; Shobbrook 1978). In a recent review paper, Lesh and Aizenman (1978) concluded that there is no obvious observational parameter that uniquely separates the variables. Part of the reason for this failure could be that the "other B stars" used for this purpose were

never checked for constancy. For example, several of the "other B stars" of Shobbrook's (1978) sample have been identified as "slow" variables in recent surveys (Balona 1977, Jerzykiewicz and Sterken 1977).

Jerzykiewicz and Sterken (1978) and Jakate (1979) plotted the positions of known β Cephei stars and of several stars verified to be constant in the c_0-β and [u-b]-β planes respectively. It is evident from these plots that the β Cephei instability strip has a finite width and that constant stars, in general, seem to lie outside this strip. These diagrams are analyzed further in Section 4 and are used to list some associations and clusters which should be searched for new β Cephei stars.

2. ISOCHRONES AND NGC 4735

Evolutionary tracks of stars between 5 and 20 $M_\odot$ (X,Z = 0.70, 0.03), as calculated by de Loore et al. (1979), were used to obtain three sets of isochrones of ages 5, 7, and 9 x 10^6 years. These isochrones were then used to establish the luminosity level of the beginning of the "gap" or, in other words, the end of the core hydrogen burning phase. This level was assumed to be the point at which the first increase in temperature takes place during the post main-sequence evolution of a star. Isochrones obtained on the log Te-M_{bol} plane were converted to the c_0-β plane using a linear relation between c_0 and $\Theta_e = 5040/T_e$; this relation was given by stars for which Code et al. (1976); Schild, Peterson and Oke (1971); and Underhill, Divan, and Prevot-Burnichon (1979) determined effective temperatures. A linear relation between Θ_e and the bolometric correction was determined with the data of Code et al. (1976), and the β-M_V relation given by Crawford (1978) was used. These isochrones extend only to the beginning of the gap.

Figure 1 shows the comparison of NGC 4755 and the isochrones on the c_0-β plane. The position of the gap, as given by Feast (1958), is also indicated. The uvbyβ photometry data for the cluster is from Perry et al. (1976), who estimated its age (from three data/information sources) to be 7 ± 1 x 10^6 years. The observational zero age main sequence (ZAMS) (Crawford 1978) lies considerably above the theoretical main sequence, a discrepancy which has been discussed by Lesh and Aizenman (1973); Shobbrook (1978) and others.

It is clear from Figure 1 that the two β Cephei stars, F and IV-18, are below the observational and theoretical gap. This finding confirms the results of Jakate (1978), who concluded that the β Cephei stars in NGC 4755 are going through their core hydrogen burning phase.

3. β CEPHEI STARS IN ASSOCIATIONS

Table 1 lists associations and clusters known to contain β Cephei stars. NGC 3293 (Balona 1977) was omitted because no uvbyβ photometry is available. With the exception of NGC 4755, the stars in Table 1 were derived from the list of confirmed β

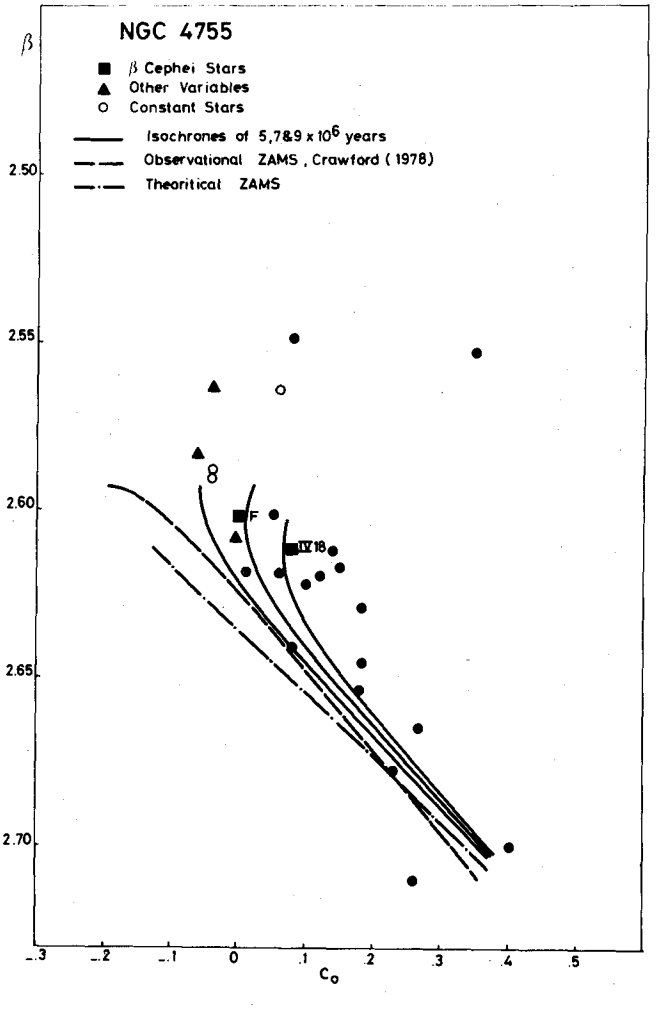

Figure 1. The c_0-β plane for NGC 4755.

Cephei variables given by Shaw (1975); NGC 4755 was taken from Jakate (1978). The quantity $\Delta\beta_a$ is the difference in β between the brightest and faintest β Cephei members of an individual association or cluster; Δc_{0_a} is defined in a similar manner. Masses, determined by comparing the evolutionary tracks with the location of the β Cephei stars, are given in the next column. The last column gives the masses for some of these β Cephei stars as determined by Lesh and Aizenman (1978).

The sources of uvbyβ photometry and membership criteria in Table 1 are: Glaspey (1971) for Upper Sco, Lower Cen and Upper Cen; Perry et al. (1976) for NGC 4755; and Crawford and Warren (1976) for the Lacerta OBI associations. The associations, subgroups and clusters listed in Table 1 are given in order of increasing age, as determined by comparison of their c_0-β diagrams; generally, this order is in agreement with comments found in the three sources mentioned above. However, the overall age spread of these associations is small; in particular, Upper Sco, Lower Cen and NGC 4755 seem to be of about the same age.

Figures 2 and 3 show c_0-β diagrams for the individual associations; a comparison with the set of isochrones is also provided. The positions of the β Cephei stars are indicated for each case. All of the fainter β Cephei members of these associations are clearly below the gap including some of the brighter members. In these diagrams, the brighter β Cephei member of an association is expected to occupy an ambiguous position very close to the gap; this is because it is the star which could be at the end of the core hydrogen burning phase (e.g., α Lup and β Cru).

The quantity $\Delta\beta_a$ seems to be constant ($\Delta\beta_a = .015 \pm .003$); this is probably a reflection of the mass range, at a given cluster age, of stars going through the β Cephei phase. If, in fact, these β Cephei stars are in their core hydrogen burning phase of evolution, it can be assumed that there are two definite points (arbitrarily designated a and b) on the evolutionary track of a massive star between which it goes through the β Cephei phase; the later point is probably close to the end of the core hydrogen burning phase. It must be noted that this conclusion is based upon a relatively small number of associations and clusters, but the fact that this quantity ($\Delta\beta_a$) seems consistent with the width of the observational instability strip is striking.

Accepting this hypothesis, an estimation of the duration of the β Cephei phase as suggested by this data on clusters and associations may be attempted. Let us assume the mean age of the cluster to be 7×10^6 years and the mean mass of its faintest β Cephei member to be 13 $M_\odot$. If we further assume that this faintest member is at position "a" in its β Cephei phase, then it has 2.5×10^6 years before reaching position "b" or the end of its core hydrogen burning phase. It is interesting to note that, with reference to its mean mass of 13 $M_\odot$, this is about 25% of its total lifetime off the main sequence. This estimate is in agreement with the frequency of occurrence of β Cephei stars determined for a complete mass range of 8 to 20 $M_\odot$

Table 1.

	Beta * Cephei Members	$\Delta\beta_a$	Δco	Mass	Mass From Lesh and Aizenman (1978)
Upper Sco	σ Sco	.017	.127	16	14
	θ Oph			12	12
Lower Cen	β Cru	.016	.083	17	> 15
	ε Cen			13	
NGC 4755	F	.01	.080	16	
	IV-18			13	
Lacerta OB Ib	12 Lac			14	13
Lacerta OB Ia	16 Lac			12	14
Upper Cen	α Lup	.012	.011	14	14
	δ Lup			12	

* From the list of confirmed Beta Cephei stars, Shaw (1975) except for NGC 4755 (Jakate 1978).

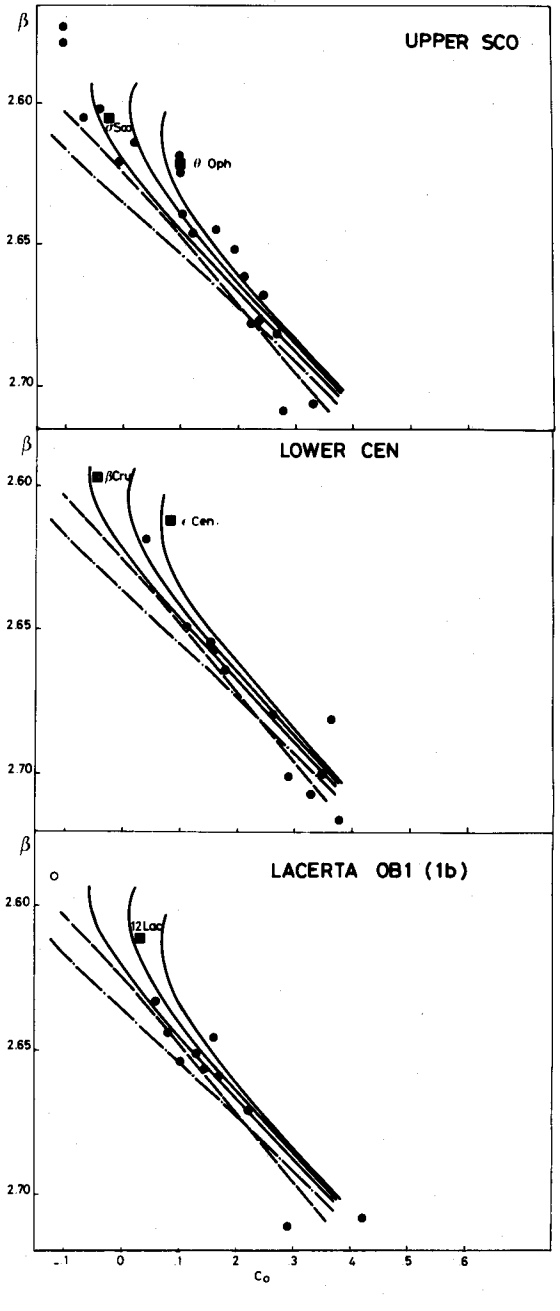

Figure 2. c_0-β diagram for Upper Sco, Lower Cen and Lac OB1 (1b) associations.

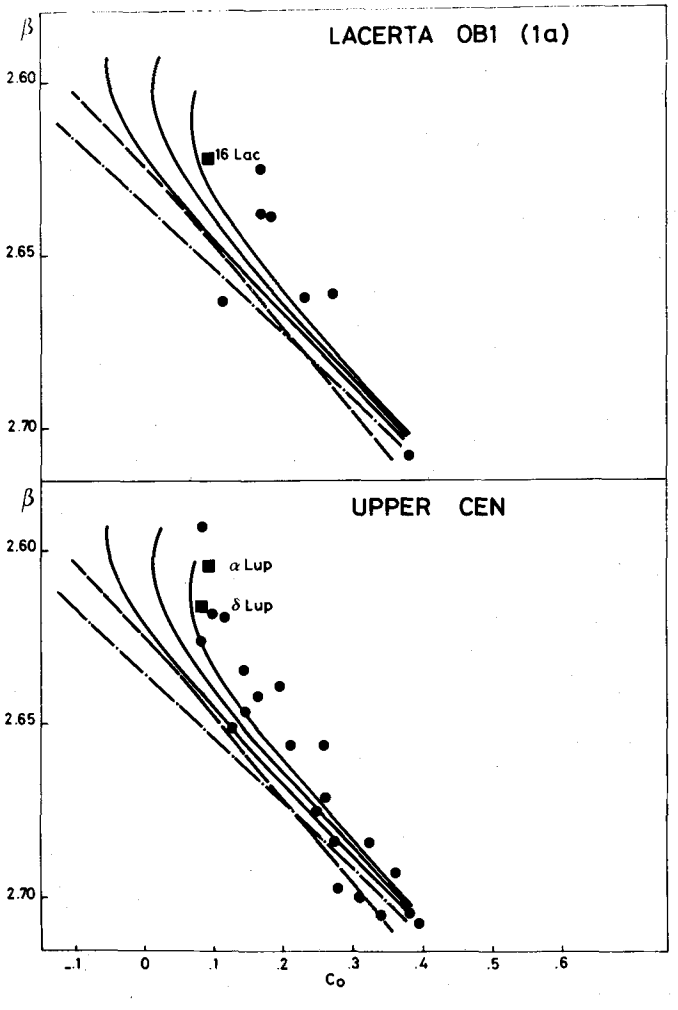

Figure 3. c_0-β diagram for Lac OB1 (1a) and upper Cen association.

(e.g., Percy 1974 and Shaw 1975).

The above discussion should be considered to be preliminary because of limited data available. However, it should be sufficient to further stress the importance of studying β Cephei stars in open clusters and associations.

4. OBSERVATIONAL INSTABILITY STRIP

Two aspects of the observational instability strip for β Cephei stars are discussed in the literature: the width of the strip and the presence of non-variables within it. Due to the existence of different kinds of variables in this part of the H-R diagram (Smith 1977), it is rather important that the non-variables used to define the strip are constant stars and not just "other B stars" or "non-β Cephei" variables.

The [u-b]-β and c_0-β diagrams (Jakate 1979; Jerzykiewicz and Sterken 1978; Sterken and Jerzykiewicz 1980) have demonstrated the finite width of the observational instability strip and the visual location of the constant stars outside of this region. It was thought that the separation obtained between the β Cephei stars and the constant stars was not related to the indices employed in these cases, but was instead due to the fact that "constant stars" were used rather than "other B stars." This procedure was justified mainly because both c_0 and [u-b] are reddening-free indices and are related to the effective temperature of B stars. However, the instability strip, in the case of the c_0-β diagram, is significantly wider ($\Delta\beta$ = .025) than the strip on the [u-b]-β plane ($\Delta\beta$ = .015). This prompted us to check for the eventual "discrimination" property of the c_0-β, Q-β and [u-b]-β planes.

This test was attempted for two clusters: NGC 4755 and h and χ Persei. Figure 4 shows plots of c_0-β, Q-β and [u-b]-β for NGC 4755. The photometry data are from Perry et al. (1976) and the information on constant stars and on β Cephei and other variables is from Jakate (1978). The number of β Cephei stars expected on the basis of c_0-β and Q-β diagrams is significantly larger than that expected from the [u-b]-β diagram. It is again evident that the instability strip in the c_0-β and Q-β diagrams is more densely populated and includes approximately three times more constant stars than the [u-b]-β strip. The information on the variability of the stars in NGC 4755 is based on only two nights of observations (Jakate 1978).

Similar diagrams are presented for stars in h and χ Persei (Figure 5). The photometry information is from Crawford (1970) and that on the nature of the variability is from Percy (1972). However, the errors on the indices used are large (see error bars in the figure).

We could not find an explanation of the apparently greater efficiency of the [u-b]-β diagram, particularly when the errors in c_0, Q and [u-b] do not differ significantly and both are good indicators of effective temperature. The verification of [u-b] as a more selective parameter for characterizing β Cephei stars could have large implications for the study of these stars. For example, the

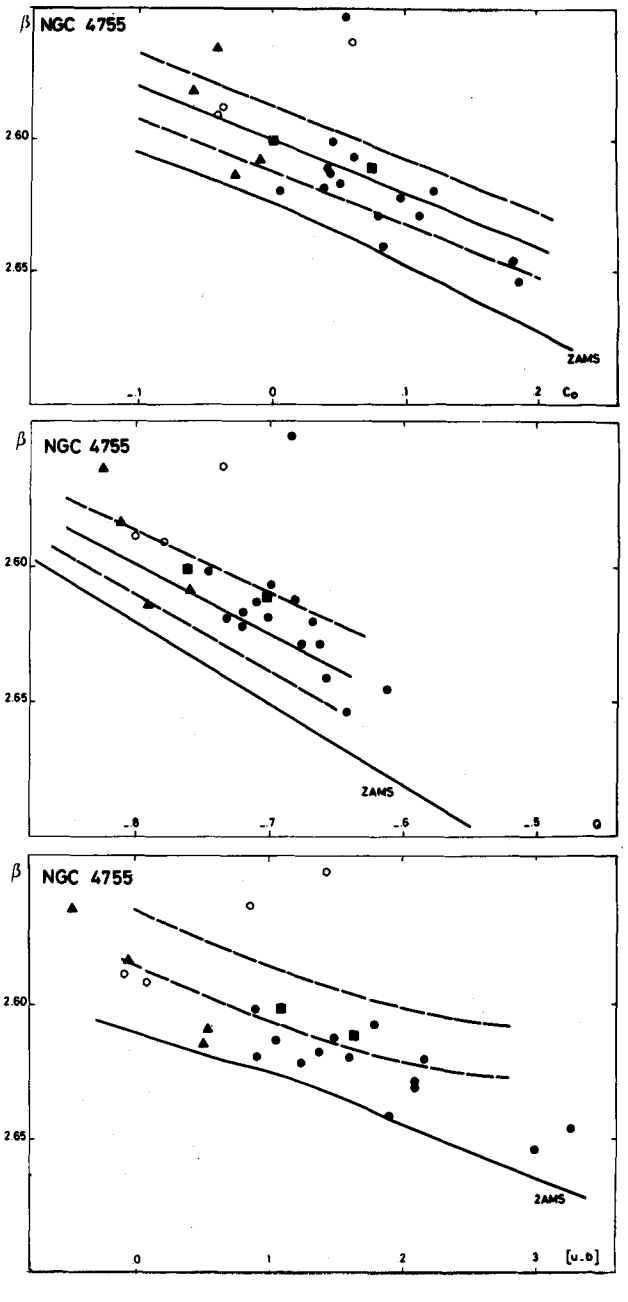

Figure 4. c_0-β, Q-β and [u-b]-β diagrams for NGC 4755.

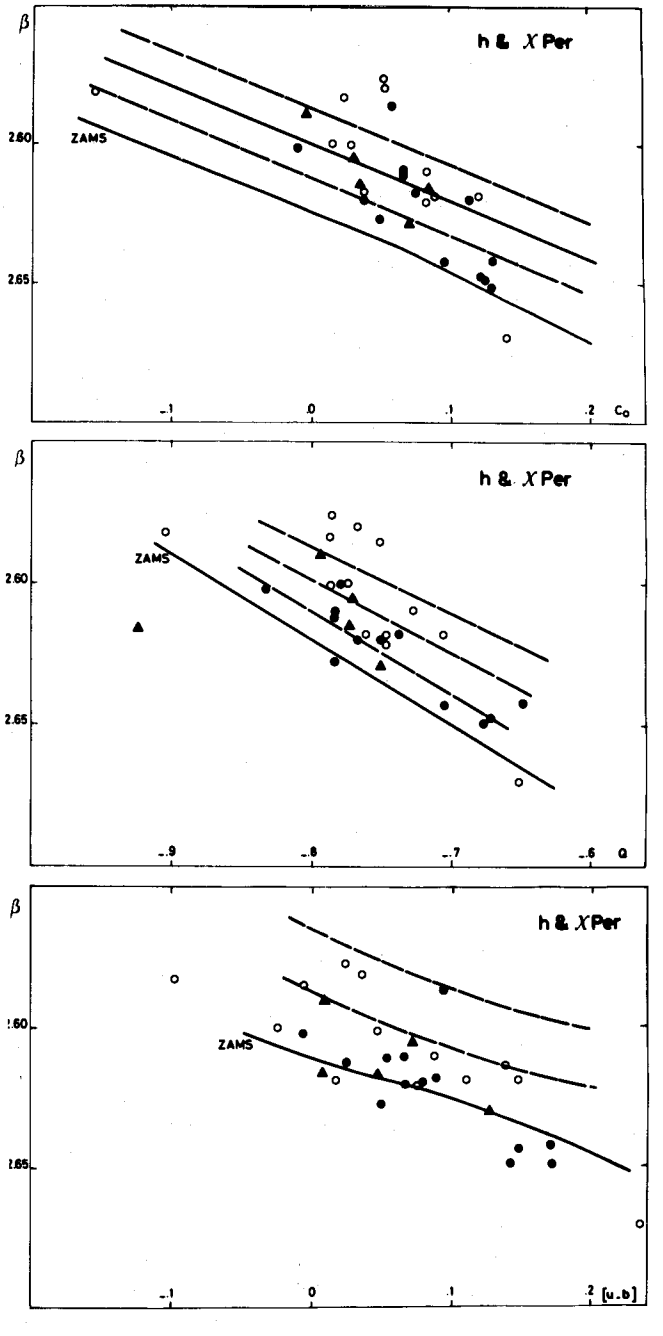

Figure 5. c_0-β, Q-β and [u-b]-β diagrams for h and χ Per.

traditional technique for determining β Cephei evolutionary phases by comparing the theoretical evolutionary tracks with the location of the instability strip (Lesh and Aizenman 1973) depends not only upon the chemical composition and the opacities used (Stothers 1976), but also upon the form of the H-R diagram used to represent the strip.

The purpose of this paper was to stress the importance of studying β Cephei stars in clusters and associations for various reasons. We believe that a systematic study of stellar variability in open clusters and associations will provide insight into the following questions:

Are all the β Cephei stars in the core hydrogen burning phase of evolution?

Where does the β Cephei phase begin and end?

Does the [u-b] index really discriminate better than other formerly used indices?

The results presented in this paper should be considered as tentative due to insufficient data. Figures 6, 7, 8, and 9 give [u-b]-β diagrams for some interesting clusters and associations in which we plan to search for β Cephei stars.

* * * * *

This investigation was supported by the National Foundation of Collective Fundamental Research of Belgium (F.K.F.O.) under no. 2.9009.79 (SMJ) and no. 2.0028.79 (CS).

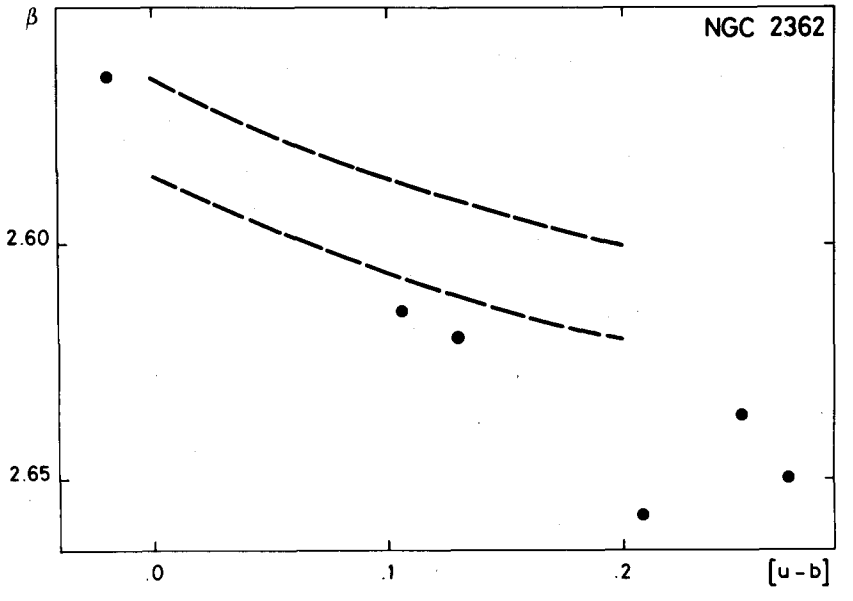

Figure 6. [u-b]-β diagrams for stars in NGC 2362.

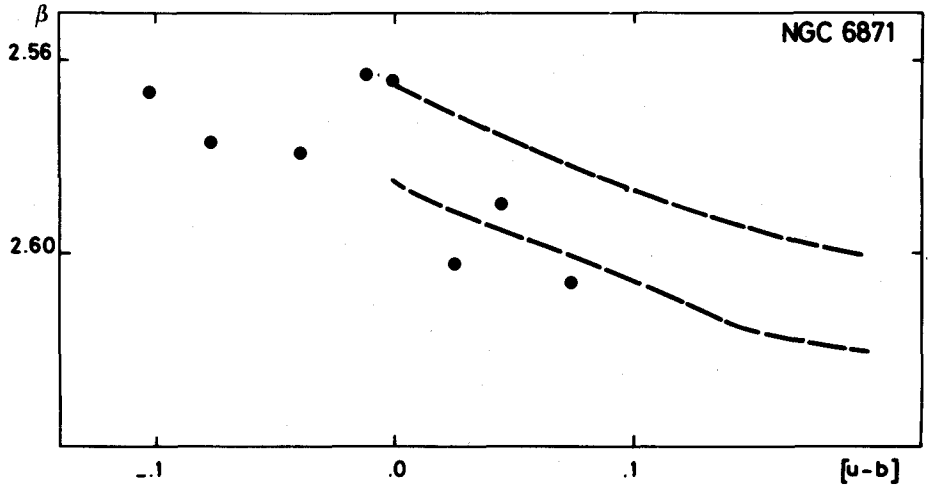

Figure 7. [u-b]-β diagrams for stars in NGC 6871.

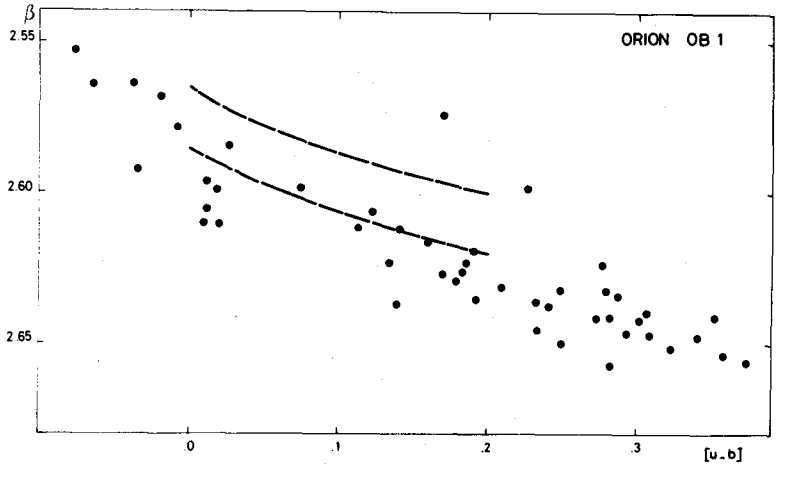

Figure 8. [u-b]-β diagrams for Ori OB1 association.

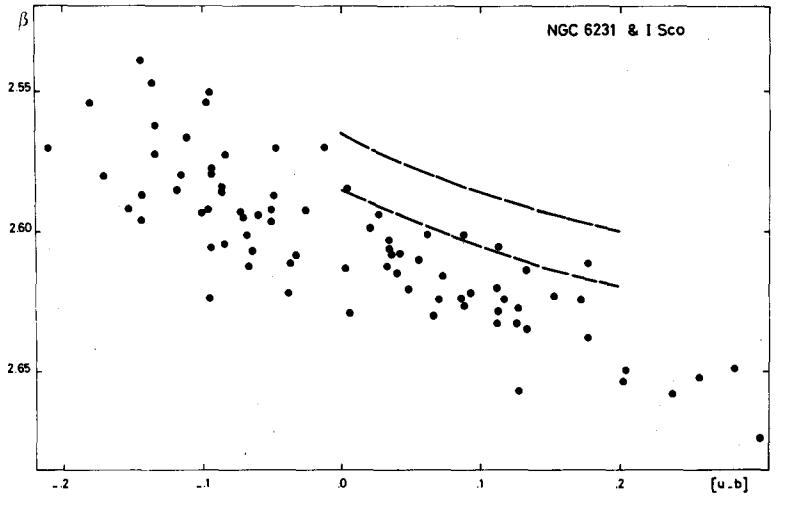

Figure 9. [u-b]-β diagrams for NGC 6231 and I Sco association.

REFERENCES

Aizenman, M.L. and Lesh, J.R. 1978, Goddard Conf. on Solar and Stellar Pulsation, ed. D. Fischel, W. Sparks, J. Lesh, June 1-2.

Balona, L.A. 1977, Mem. R. Astr. Soc., 84, 101.

Code, A.D., Davis, J., Bless, R.C. and Brown, H.B. 1976, Astrophys. J., 203, 417.

Crawford, D.L. 1978, Astron. J., 83, 48.

Crawford, D.L., Barnes, J.V. and Hill, G. 1977, Astrophys. J., 8L, 606.

Crawford, D.L., Barnes, J.V., Hill, G. and Perry, C.L. 1971, Astron. J., 76, 1048.

Crawford, D.L., Barnes, J.V. and Warren, W.H. 1974, Astron. J., 79, 623.

Crawford, D.L., Glaspey, J.W. and Perry, C.L. 1970, Astron. J., 75, 822.

Crawford, D.L., and Warren, W.H., Jr. 1976, Publ. Astr. Soc. Pac., 88, 930.

de Loore, C., De Greve, J.P., Packet, W. and Vanbeveren, D. 1979, personal communication.

Feast, M.W. 1958, Mon. Not. R. Astr. Soc., 118, 618.

Glaspey, JW. 1971, Astron. J., 76, 1041.

Jakate, S.M. 1978, Astron. J., 83, 1179.

Jakate, S.M. 1979, Astron. J., in press.

Jerzykiewicz, M. and Sterken, C. 1977, Acta. Astr., 27, 365.

Jerzykiewicz, M. and Sterken, C. 1978, IAU Colloq. 46, in press.

Jones, D.H.P. and Shobbrook, R.R. 1974, Mon. Not. R. Astr. Soc., 166, 649.

Lesh, J.R. and Aizenman, M.L. 1973, Astr. Astrophys., 22, 229.

Percy, J.R. 1972, Publ. Astr. Soc. Pac., 84, 420.

Percy, J.R. 1974, Astron. Astrophys., 30, 465.

Perry, C.L. 1973, IAU Symp. 50, 192.

Perry, C.L., Franklin, C.B., Jr., Landolt, A.U. and Crawford, D.L. 1976, Astron. J., 81, 632.

Schild, R., Peterson, D.M. and Oke, J.B. 1971, Astrophys. J., 166, 95.

Shaw, J.S. 1975, Astron. Astrophys., 41, 367.

Shobbrook, R.R. 1978, Mon. Not. R. Astr. Soc., 185, 825.

Smith, M.A. 1977, Astrophys. J., 215, 574.

Sterken, C. and Jerzykiewicz, M. 1980, these proceedings.

Stothers, R. 1976, Astrophys. J., 210, 434.

Underhill, A.B., Divan, L. and Prevot-Burnichon, M.-L. 1979, preprint.

Warren, W.H., Jr. and Hesser, J.E. 1977, Astrophys. J. Suppl., 34, 115.

Watson, R.D. 1972, Astrophys. J. Suppl., 24, 167.

PULSATION OF HIGH LUMINOSITY HELIUM STARS

D.S. King
Department of Physics and Astronomy
University of New Mexico
and
Los Alamos Scientific Laboratory
University of California

J.C. Wheeler
Department of Astronomy
University of Texas at Austin
and
Joint Institute for Laboratory Astrophysics
University of Colorado
and
National Bureau of Standards

J.P. Cox
Joint Institute for Laboratory Astrophysics
University of Colorado
and
National Bureau of Standards

A.N. Cox and S.W. Hodson
Theoretical Division
Los Alamos Scientific Laboratory
University of California

ABSTRACT

A discussion of the long period R Coronae Borealis stars is presented. The constraints on theoretical models imposed by their age, kinematics and distribution led to difficulties in formulating an evolutionary sequence to the formation of this type of star. Several types of models are investigated and the results given.

1. INTRODUCTION

The R Coronae Borealis stars and other hydrogen-deficient carbon stars (Hd C stars) are usually assumed to have masses less than or approximately equal to one solar mass in order to be consistent with their extreme old disk/bulge kinematics and distribution. The common presumption is that mass loss which bares the helium core has been important in the evolution of these stars; binary mass transfer is the suspected mechanism, despite the lack of any evidence for duplicity in these stars.

Paczynski (1971) argued that RCrB stars cannot result from ordinary evolution and mass loss (whatever the mechanism). His structural studies gave two requirements: the total mass, carbon core plus helium envelope, must be in the range

0.8 $M_\odot$ to 2 $M_\odot$ ($M_\odot$ = solar mass). To provide a core at any stage of ordinary evolution which has the requisite total mass and which has a sufficiently massive helium envelope (or the potential for it) requires an initial total mass $\gtrsim 5\ M_\odot$. Such a mass is in severe contradiction with the kinematics. Paczynski (1978) suspects a process involving a hot bottom envelope (Scalo, Despain and Ulrich 1975) wherein the hydrogen-rich red giant envelope is convected downward to the vicinity of the hydrogen-burning shell and converted entirely to helium. When occurring quickly at an advanced stage of evolution, such a process would not affect the net lifetime of the star appreciably and would accommodate a low mass consistent with the kinematics.

An important question thus arises as to whether the masses of RCrB stars are $\lesssim 1\ M_\odot$ or significantly above that limit. In the latter case, the evolution is even more anomalous than suggested by Paczynski. The RCrB stars must actually have lived longer than indicated by their kinematics. Wheeler (1978, 1979) has suggested that excess helium and an increased lifetime may be related phenomena and that these shared properties may be traced from blue stragglers through helium stars to Type I supernovae.

One of the most effective ways to establish the mass of the RCrB stars, and hence the existence of an anomalously long lifetime, is through an examination of the observed pulsational properties. Preliminary studies of the linear and nonlinear pulsations of helium stars have been undertaken by Trimble (1972) and by Wood (1976). We are systematically restudying this problem, using more recent and higher estimates of the effective temperature (RY Sgr) and of the high carbon abundance. The requirements that the stars have the proper pulsation period ($\sim$ 40 days) while being both pulsationally unstable and dynamically stable (see § 3 for meaning of this term) may give tight theoretical constraints on the mass, luminosity and effective temperature of these stars. Of the approximately thirty known RCrB stars, at least three of them are observed to have Cepheid-like pulsations superimposed on their longer period brightness variations. These are RY Sgr, UW Cen and RCrB.

2. LINEAR MODELS

Envelope models of stars with masses between 0.8 $M_\odot$ and 3 $M_\odot$ and with luminosities in the range from $3 \times 10^3\ L_\odot$ to $2 \times 10^4\ L_\odot$ ($L_\odot$ = solar luminosity) have been investigated. Linear nonadiabatic calculations with the techniques described by Castor (1971) have been used to identify a number of these models with periods close to the observed values. The full hydrodynamic equations with radiation flow treated in the diffusion approximation were used. Opacity and equation of state data are taken from the Huebner et al. (1977) opacity library for a mixture of 0.90 helium and 0.10 carbon by mass (referred to as HE9C1). Since these library opacities are available only for temperatures of 12,000 K or greater, the Stellingwerf (1975)

opacity formula has been used for lower temperatures. Because of the small amount of mass contained in these low temperature layers, the use of this formula should have little effect on periods and stability, but could have some effect on the limiting amplitude of light and velocity variations.[1]

Figure 1 is a plot of $\log \Pi_0$ (Π_0 = fundamental period) as a function of $\log T_{eff}$ (T_{eff} = effective temperature). The approximate locations of two of the variable stars, RY Sgr and RCrB, are indicated. We note that it is only for the higher luminosities that we are able to attain the observed periods near the effective temperatures for these stars. The T_{eff} value for RY Sgr (7100 K ± 500 K) was recently determined by Schonberner (1975). Even at the higher luminosities, we would predict a somewhat lower effective temperature than those observed.

Figure 2 summarizes the linear fundamental blue edge data. For comparison, the fundamental blue edge for normal composition Cepheids (X = 0.70, Z = 0.02) with evolutionary masses is approximately 700 K cooler than the edge indicated for the 2 $M_\odot$ and 3 $M_\odot$ models. The important thing to note is that, for large L/M (as in the 1 $M_\odot$ case), the blue edge is considerably bluer than for the higher masses. This leads to a rather extensive range in T_{eff} for which pulsational instability might be expected. As we will see, however, it may well be that at these large L/M values the models may, in fact, be unstable in the sense that they tend to throw off the outer envelope. This will be discussed in § 3. For the models that are pulsationally unstable, the growth rates tend to be quite large, with kinetic energy e-folding times that are typically one period or even less.

3. NONLINEAR MODELS

A sequence of models at $L/L_\odot = 1.13 \times 10^4$ ($M_{bol} = -5.38$) was studied, using the nonlinear theory. The masses investigated were 1.2 $M_\odot$, 1.4 $M_\odot$, 1.6 $M_\odot$ and 2.0 $M_\odot$. The T_{eff} was fixed at 6300 K. This value, although somewhat lower than that observed for RY Sgr, was chosen in order to assure that the models were to the red of the blue edge of the instability strip. In all cases, a velocity distribution was imposed on the equilibrium model which had the same radial distribution as the linear model adjusted to give 10 km/s at the photosphere. Table 1 lists the models along with their periods and limiting amplitude behavior.

The 1.2 $M_\odot$ and 1.4 $M_\odot$ models were dynamically unstable in the sense that the pulsations grew rapidly and appeared to lead to ejection of some of the mass. Unfortunately, it was not possible to follow this process since the large compressions in the outer layers caused a reduction of the integration timestep to

[1] Subsequent calculations have shown that the opacity and equation of state in these outer regions can have a fairly important effect on periods.

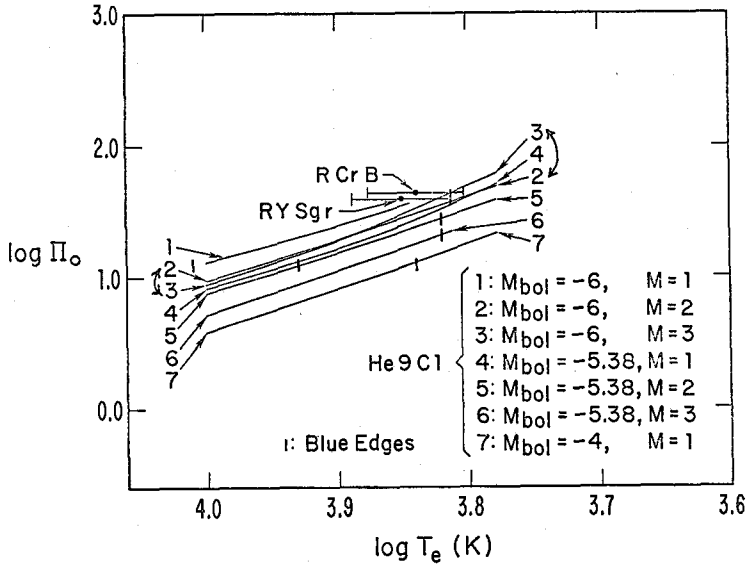

Figure 1. The log of the linear fundamental period as a function of log of the effective temperature for a variety of stellar masses and luminosities. The composition of HE9C1, Y = 0.9 and X_c = 0.10 is used for all models. Approximate blue edges are indicated and the positions of two of the pulsating RCrB stars are shown.

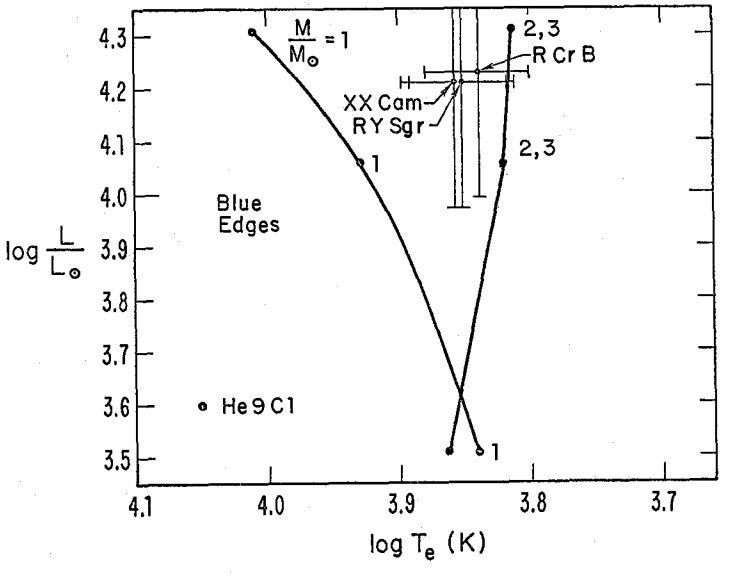

Figure 2. Blue edges are shown on the Hertzsprung-Russell diagram. Three of the RCrB stars are indicated. Although XX Cam is not known to pulsate like RY Sgr and RCrB, its position in the H-R diagram seems to be quite close to that of RY Sgr.

Table 1. Nonlinear Models at $L/L_\odot = 1.13 \times 10^4$ and $T_{eff} \approx 6300$ K

Mass	Π(days)	ΔM_{bol}	$\Delta R/R$	ΔV_{radial} (km/s)
1.2 $M_\odot$	44	-	-	-
1.4	43	-	-	-
1.6	39	$2\overset{m}{.}0$	0.17	27
2.0	36	$2\overset{m}{.}2$	0.23	40

such an extent that the calculation could not proceed. Figure 3 shows the growth of the photospheric radius variation for the 1.4 $M_\odot$ model. The radial velocity of the photosphere reached a maximum value of about 50 km/s. The escape velocity for this mass and radius is about 80 km/s. Figure 4 shows the radial velocity behavior of the 1.6 $M_\odot$ model. For this model and the 2 $M_\odot$ case a stable limit cycle is attained. We note that the variations are not as smooth as those of the more massive Cepheids (for example, see King et al. 1973). The magnitude of the radius and velocity variations are in reasonable agreement with observations; however, the light variation is considerably larger than observed and quite ragged in appearance, as noted by Trimble (1972). This may be due to an incorrect treatment of radiation in the outer layers, or may suggest the existence of running waves which, if taken into account, could lead to a decrease in the light variation. These questions remain for future investigation.

4. CONCLUSIONS

There are several interesting results to be found in these preliminary calculations: (1) there is qualitative agreement between these results using newer opacities and the earlier ones of Trimble (1972) and Wood (1976); (2) models with sufficiently large L/M have a very hot blue edge for their instability strip; (3) very large L/M values lead to dynamically unstable models which appear to eject mass and therefore may not be realistic descriptions for the pulsating RCrB stars; and (4) for the sequence studied, it appears that a reasonable mass could be $\sim 1.5\ M_\odot$. The fact that this is above the Chandresekhar limit strengthens the suggestion made by Wheeler (1978) that these hydrogen-deficient carbon stars may indeed by among the precursors of Type I Supernovae.

REFERENCES

Castor, J.I. 1971, Ap. J., 166, 109.

Huebner, W.F., Merts, A.L., Magee, N.H. and Argo, M.F. 1977, Los Alamos Scientific Laboratory report LA-6760-M.

King, D.S., Cox, J.P., Eilers, D.D. and Davey, W.R. 1973, Ap. J., 182, 859.

Paczynski, B.E. 1971, Acta. Ast., 21, 1.

Paczynski, B.E. 1978, private communication.

Scalo, J.M., Despain, K.H. and Ulrich, R.K. 1975, Ap. J., 196, 805.

Schonberner, D. 1975, Astron. Ap., 44, 383.

Stellingwerf, R.F. 1975, Ap. J., 195, 441.

Trimble, V. 1972, Mon. Not. R. Astr. Soc., 156, 411.

Wheeler, J.C. 1978, Ap. J., 225, 212.

Wheeler, J.C. 1979, Ap. J., 234, 000.

Wood, P.R. 1976, Mon. Not. R. Astr. Soc., 174, 531.

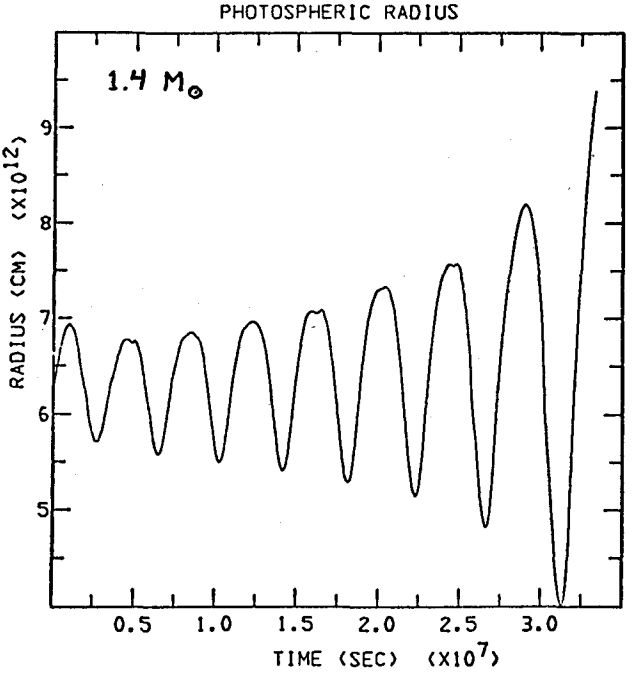

Figure 3. The photospheric radius variation for a 1.4 $M_\odot$ model with $M_{bol} = -5^m.38$, T_{eff} = 6300 K and the HE9C1 composition. This model becomes violently unstable near the end of the run.

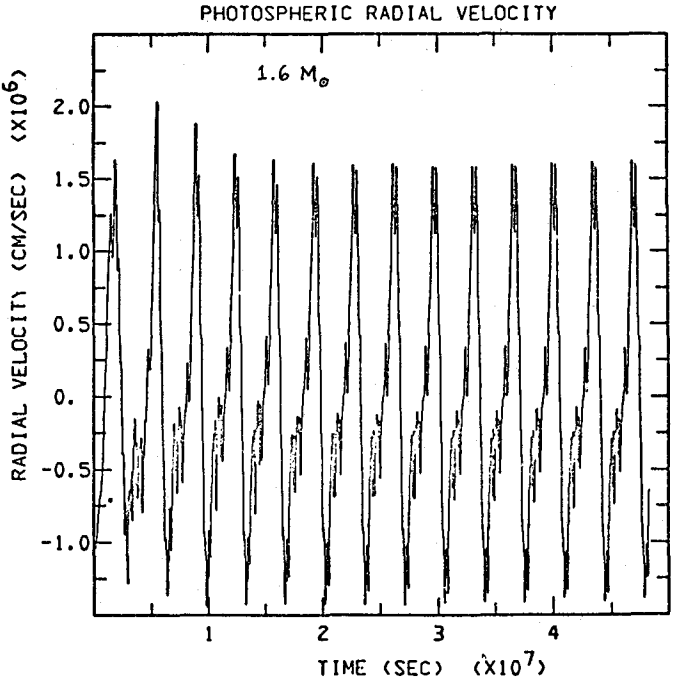

Figure 4. The photospheric radial velocity variation for a 1.6 $M_\odot$ model with the same parameters as those in Figure 3. This model reached a stable limit cycle.

SOME COMMENTS ABOUT β CEPHEI STARS

H. Saio and J.P. Cox
Joint Institute for Laboratory Astrophysics
National Bureau of Standards and University of Colorado

The excitation mechanism of β Cephei stars has been an enigma for a long time. We will discuss here a few conjectures in connection with this problem.

Some β Cephei stars are plotted in a period luminosity plane (Figure 1) where periods, effective temperatures and absolute magnitudes were obtained from Lesh and Aizenman (1978), and bolometric corrections were obtained from the table by Code et al. (1976). The periods belonging to a multiperiod β Cephei star are connected with a horizontal line. Theoretical relations for some modes of oscillation in the instability strip are also described (lines of constant Q, where Q is the "constant" in the period-mean density relation). This figure shows that several modes of oscillation are probably excited in many cases and that many of those have Q values less than that of the fundamental radial oscillation.

Recently, Stellingwerf (1978) suggested that a possible driving mechanism might be found in the opacity bump near the He ionization zone. Although driving by this opacity bump is not great enough to excite radial oscillations (Stellingwerf 1978) or nonradial oscillations (Saio et al. 1980) in the massive stars, the locus of maximum instability of this mechanism in the H-R diagram is almost parallel to the β Cephei instability strip. The effective temperatures in this locus for the fundamental radial mode are, however, lower than the effective temperatures in the instability strip of β Cephei stars by about 0.1 in the logarithm.

Cox and Stellingwerf (1979) discussed some consequences of the condition of maximum instability by this driving mechanism in the envelope. After some manipulation of equation (1) in their paper, we have for a given equilibrium luminosity:

$$QT_e^5 \sim \text{constant}, \qquad (1)$$

for maximum instability. Equation (1) suggests that, in the H-R diagram the locus of maximum instability for the bump mechanism has a higher effective temperature for the modes with smaller Q values. The smallest Q value in Figure 1 is less than that of the fundamental radial pulsation by a factor of approximately 2. Therefore, the locus of maximum instability for the modes with the smaller Q values has a higher effective temperature than that for the fundamental radial mode by 0.06 in the

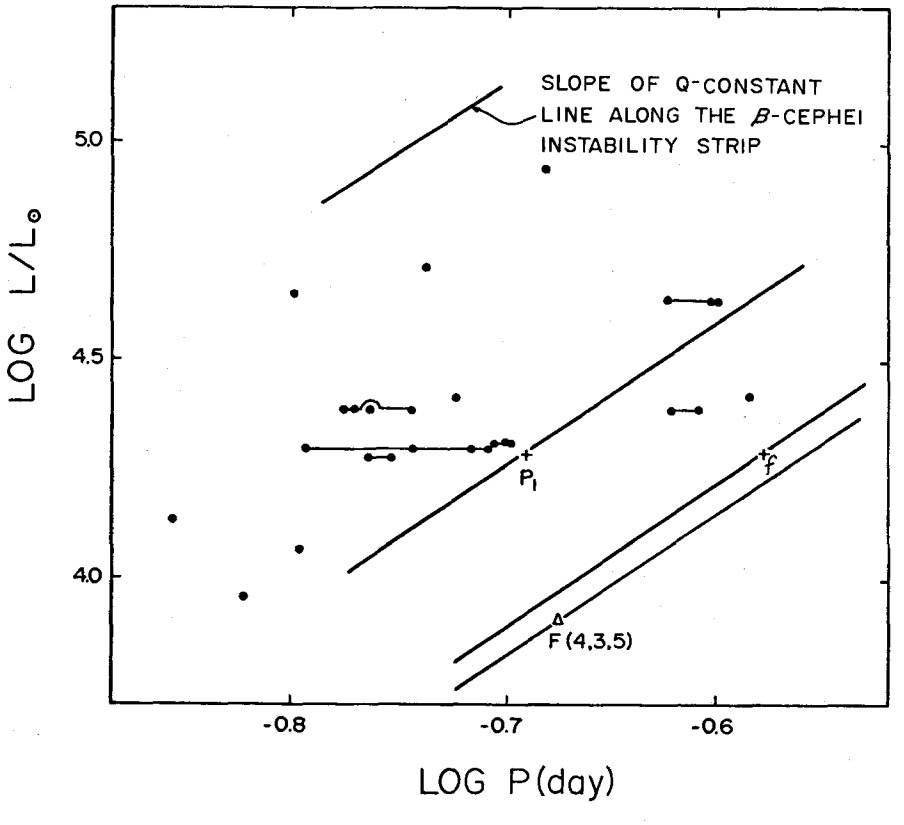

Figure 1. Several β Cephei stars placed in the period luminosity plane. The range of periods for multiperiodic β Cephei stars are indicated by the short horizontal lines.

logarithm. This may imply that β Cephei stars prefer modes with smaller Q values than the Q value for the fundamental radial oscillation.

If the oscillations of β Cephei stars are excited only by the bump mechanism in the envelope of the star, the width of the instability strip might be as large as $\Delta \log T_e \gtrsim 0.06$ as discussed above; this is contrary to the observed narrowness of the instability strip for β Cephei stars (e.g., Lesh and Aizenman 1978; Sterken and Jerzykiewicz 1980). Moreover, the observed instability strip shows the existence of a lower limit to the luminosity of β Cephei stars which cannot readily be explained by an envelope driving mechanism.

Comparison of the instability strip with evolutionary models in the H-R diagram suggests that the instability strip almost coincides with the location of the hydrogen exhaustion phase ("S-bend" phase), and that the lower limit to the luminosity of β Cephei stars corresponds to the evolutionary track of $\sim 10\ M_\odot$ models. In the hydrogen exhaustion phase of stars with $10\ M_\odot$ to $\sim 20\ M_\odot$, semiconvective and fully convective zones appear and grow rapidly in the region with a gradient of mean molecular weight (e.g., Simpson 1971, Sreenivasan and Wilson 1978). As pointed out by Sreenivasan and Wilson (1978), the appearance of these zones modifies the chemical composition in this region and hence causes a rapid change of structure. The interesting coincidence between the observed instability strip of β Cephei stars and the rapid appearance of semiconvective and fully convective zones in the hydrogen exhaustion phase tempts us to conjecture that the oscillations of β Cephei stars may be excited by a combination of the bump mechanism in the envelope and the rapid change of structure caused by the appearance of a convection zone in the hydrogen exhaustion phase. With this conjecture we can explain the narrowness and lower luminosity cutoff of the instability strip because of the requirement of the evolutionary phase and the associated lowest mass.

Also, this conjecture may suggest the existence of an upper limit to the luminosity of β Cephei stars; the extent of this limit is presently uncertain. The evolutionary models with $30\ M_\odot$ by Simpson (1971) and with $20\ M_\odot$ by Chiosi and Summar (1970) show that, for stars with such high masses, a semiconvection zone appears in the early phase of core hydrogen burning and exists continuously also in the hydrogen exhaustion phase. Since in these stars the rapid appearance of convective and semiconvective zones does not occur, we can expect that oscillation is not excited in these stars. It is interesting to note that the luminosity of ξ^1 CMa (the most luminous β Cephei variable in the 1978 H-R diagram by Lesh and Aizenman) is nearly equal to the luminosity at the "S-bend" phase of the models with $\sim 20\ M_\odot$.

In summary, we are suggesting that the instability of the β Cephei stars may be due to a combination of envelope driving (perhaps via the "bump" mechanism) and driving (in some manner, such as that suggested by Vandakurov 1977) in the deep interior due to a rearrangement of the internal structure.

REFERENCES

Chiosi, C. and Summa, C. 1970, Ap. Space Sci,. 8, 478.

Code, A.D., Davis, J., Bless, R.C. and Hanbury Brown, R. 1976, Ap. J., 203, 417.

Cox, J.P. and Stellingwerf, R.F. 1979, Publ. A.S.P., in press.

Lesh, J.R. and Aizenman, M.L. 1978, Ann. Rev. Astr. Ap., 16, 215.

Saio, H., Cox, J.P., Hansen, C. and Carroll, B. 1980, these proceedings.

Simpson, E.E. 1971, Ap. J., 165, 295.

Sreenivasan, S.R. and Wilson, W.J.F. 1978, Ap. Space Sci., 53, 193.

Stellingwerf, R.F. 1978, Astr. J., 83, 1184.

Sterken, C. and Jerzykiewicz, M. 1980, these proceedings.

Vandakurov, Yu.V. 1977, Sov. Astron. Lett., 3 (5), 249.

OBSERVATIONAL EVIDENCE FOR GLOBAL OSCILLATIONS OF THE SUN: A REVIEW

H.A. Hill
Department of Physics
University of Arizona
Tucson, Arizona

ABSTRACT

The results of many observations have been interpreted as evidence for global oscillations of the sun. The periods found in these analyses range from minutes to hundreds of years. The shorter period oscillations are usually interpreted as the normal modes proper whereas the longer period features may be manifestations of superpositions and/or nonlinear coupling of these normal modes. The work done to date in this broad area is reviewed.

1. INTRODUCTION

The general consensus is that phenomena exist on the sun which are to varing degrees periodic in time. There have been investigations where the periods considered range from minutes (Deubner 1976) to hundreds of years (Wolff 1976) and include the well known eleven year solar cycle. Over the various subsets of this period range, evidence has been put forth, at differing confidence levels, in support of conjectures that global oscillations are manifested in the various observations. In each case, the sought after signature in the observations is the exceedingly long term stability expected for such global oscillations.

The demonstration of the existence of global oscillations has been quite difficult for several reasons. In the case of very short period and the well observed five minute mode, it has not been possible to observe the phase of these oscillations over long enough times to clearly establish a global character (cf. Gough 1980a). At the other end of the spectrum, a long period phenomenon observed in, say sunspot number, may be understood as the result of beats between individual global oscillations. This leads to the unsettling situation where the postulated global oscillations producing the beats are not directly observed and furthermore, for these types of phenomena it is currently not understood how such oscillations affect the primary observable. In the intermediate range where one presumably has a better chance of directly detecting an oscillation directly over long periods of time, the observations are extremely difficult. This is because any global oscillations present in this period range must have small amplitudes.

A discussion of the observational evidence for global oscillations can be conveniently broken into two parts: 1) a discussion of the long term stability of a periodic phenomenon and, 2) the solar origin of the phenomenon. The latter problem has arisen because of the apparent small signals associated with global oscillations in the intermediate period range. In some cases, it is quite apparent that the phenomenon is solar but it is difficult to identify the global character. In others, it has been easier to establish the long term stability of a periodic feature but quite difficult to establish the origin as solar. During the latter part of the seventies, both of these general problems have received considerable attention and many interesting developments have been reported. It is these developments that are addressed in the following sections.

2. REPEATED PHENOMENA

The number of reported periodic features with apparent long term stability in the period range from five minutes to $\sim$ 100 years is quite large. Should a significant fraction of these be real, then the oscillation spectrum is very rich and bodes well for the seismic sounding of the sun. The period range has been extended to several hundred years because such an observed period could possibly be the direct manifestation of a global mode or possibly beats between two or more shorter period global modes.

3. FIVE MINUTE OSCILLATIONS

Those solar oscillations having a period of around five minutes are the best documented. The initial evidence for their existence was first reported at the I.A.U. Symposium no. 12 in 1960 (Leighton 1960). They may be observed by monitoring brightness changes of the continuum radiation (i.e., the radiation not associated with spectral lines), by observing intensity changes in the spectral lines (which could be due to temperature changes in the atmosphere produced by the oscillations), or by studying surface velocities using the Doppler shifts of spectral lines.

These solar oscillations typically manifest themselves as a small scale (less than 5000 km) velocity field in the solar photosphere and low chromosphere. The motions are predominantly radial with a period of about 300 sec. The lifetime of a given oscillation, as measured by the decay of the velocity-time autocorrelation function, is only about two periods of oscillation.

The five minute oscillations have often been analyzed theoretically as a purely atmospheric phenomenon (Noyes and Leighton 1963; Souffrin 1966; Stein 1967; Kahn 1961; Whitaker 1963; Uchida 1967; Thomas, Clark and Clark 1971). These analyses have treated the photosphere as a rigid boundary or as a layer with an imposed turbulent boundary condition. Within the atmosphere both acoustic waves and gravity waves have comparable frequencies although the spatial characteristics are distinct;

because most observational work has dealt primarily with frequency characteristics of the five minute oscillation, some controversy over the actual nature of the waves has resulted. Interpretation of these particular oscillations as acoustic modes is presented in the first four of those papers mentioned above while the last three have treated the oscillations as gravity modes. Frazier (1968) first offered persuasive evidence that at least a major portion of the oscillating power of the five minute oscillations is in the form of acoustic modes.

A different class of models based upon trapping of acoustic waves below the photosphere has been considered in some detail by Ulrich (1970), Leibacher and Stein (1971), and Wolff (1972). These models offer an explanation for the existence of wave motions in a layer of the quiet solar atmosphere and in a frequency band where waves are essentially nonprogressive. Similar results have been obtained by Ando and Osaki (1975), who treated these oscillations as global nonradial modes.

The "modal" character of these overstable subphotospheric oscillations is theoretically characterized as a concentration of power along ridges in a figure where the axes are k and ω (referred to as the k-ω diagram), k representing the horizontal wavenumber and ω the eigenfrequency. Despite extensive work, this "modal" character has only recently become evident in observations, primarily because of the large accumulation of data necessary for the computation of k-ω spectra with adequate statistical stability.

The first clear resolution of the observed power into ridges on the k-ω plane is found in the work by Deubner (1975). On the basis of further work of this nature, Rhodes, Ulrich and Simon (1977) have concluded that the five minute oscillations clearly represent nonradial p mode oscillations in the solar envelope.

Are these five minute oscillations global modes? Deubner, Ulrich and Rhodes (1979) and Claverie et al. (1980) have examined observationally the long term stability of these modes and found coherence times at least as long as the length of the observation (i.e., 9 hours). However, as discussed by Gough (1980a) this is not sufficiently long to demonstrate the global character of these modes. More observational work is required before this question can be answered.

4. OSCILLATIONS WITH PERIODS BETWEEN FIVE MINUTES AND ONE HOUR

The proof of the existence of solar oscillations with periods between five minutes and approximately one hour would be significant since these oscillations might represent low order p and g modes. With the introduction of a new observational technique used at SCLERA[1], the first evidence was obtained which indicated that large scale oscillations in this period range could be detected (Hill

[1]SCLERA is an acronym for the Santa Catalina Laboratory for Experimental Relativity by Astrometry jointly operated by the University of Arizona and Wesleyan University.

and Stebbins 1975). Observations at SCLERA using these techniques (basically time sequences of solar diameter measurements) have continued to indicate the existence of oscillations of this character (Hill, Stebbins and Brown 1976; Brown, Stebbins and Hill 1978; Hill and Caudell 1979; Caudell et al. 1980).

These periodic phenomena have proven difficult to study. The oscillations in the observables are relatively small making it quite difficult to confirm the SCLERA results by alternate observational techniques and also quite difficult to discriminate against various sources of noise (for review, see Hill 1978). The long term stability or more exactly, phase coherence, has been fairly well established observationally (Hill and Caudell 1979; Caudell and Hill 1980; Caudell et al. 1980) and discussed by Gough (1980a). This result has been interpreted as strong evidence for the solar origin and global character of the oscillations.

Confirmation of the results from SCLERA have been sought by several investigations (cf. Hill 1978 for review). It now appears that the work of Claverie et al. (1980) does represent a confirmation at the shorter end of this period range. The mean spacing of the periods from 6 to 9 minutes reported by Hill, Brown and Stebbins (1976), (published in Table 2.1 of Hill 1978) agrees within an experimental error of 3% with the mean spacing reported by Claverie et al. (1980) [taking into account the sensitivity of the SCLERA work to only even ℓ in contrast to both even and odd ℓ sensitivity of the results of Claverie et al. (1980)].

It has been possible to demonstrate phase coherency for a number of the modes in this period range (Hill and Caudell 1979; Caudell and Hill 1980; Caudell et al. 1980). To date the phase coherency has been established for 12 modes over a period of 23 days. This coherency in phase is the best evidence currently available which simultaneously points to the solar origin of the oscillations and the global character. Particularly it is quite difficult for effects in the earth's atmosphere to produce such phase coherency. In this regard it has been possible to make use of the phase coherence to measure the contributon of the earth's atmospheric differential refraction to these observations (Knapp, Hill and Caudell 1980) and to show that this noise is an order of magnitude below the observed oscillations.

5. OSCILLATIONS WITH PERIODS NEAR 2^h40^m

Oscillations with periods near 2^h40^m have been detected using velocity observations by Severny, Kotov and Tsap (1976) and Brookes, Isaak and van der Raay (1976). The reported amplitude is of the order of 1m/sec which is near the limit of observing technology. This has posed considerable difficulty in clearly establishing the oscillation as a solar feature.

The primary thrust in this region has been furnished by the group at the Crimean Observatory. They reported in 1978 (Kotov, Severny and Tsap 1978) that the oscillations were observed in 1974, 1975, and 1976 and shown to be phase. The

initial attempts at Stanford (Dittmer 1977) to confirm these results from the Crimea were unsuccessful. After the initial work, staff from these two observatories have worked together in an effort to resolve their divergent results. This collaborative effort has been successful to date with the publication in 1979 (Scherrer et al. 1979) of a cautious announcement of the confirmation of the oscillation at 2^h40^m. This is indeed a significant result.

Scherrer et al. (1979) published a rather impressive figure which suggests the phase coherence of the oscillations from 1974 through 1978. This is strongly suggestive of a solar phenomenon, i.e., not the manifestation of the earth's atmosphere, and a global mode or modes of oscillation.

6. PERIODIC FEATURES WITH PERIODS AT TWELVE DAYS

Periodic features with periods around 12 days have shown up in the analysis of solar oblateness observations (Dicke 1977), of Zurich daily sunspot numbers (Knight, Schatten and Sturrock 1979) and of spectroscopic differential rotation data and sunspot drift velocity measurements (Kuhn and Worden 1979). In this period range, the identification of an oscillation as being global may pose problems more difficult than the ones encountered in actually detecting the oscillation. However, it is quite feasible to expect to see in this period range the manifestations of global oscillations particularly in the form of beats (see Gough 1980b), and as such, these results are considered here.

Dicke (1977) has reported evidence for oscillations in the solar oblateness data obtained during the summer of 1966 (Dicke and Goldenberg 1974). Dicke's view in 1977 as to the period of this oscillation was 12.64 days (synodic). Knight, Schatten and Sturrock (1979) analyzed 44520 daily sunspot numbers and found a peak in the spectrum at 12.07 days (synodic). Kuhn and Worden (1979) have found in their analysis of spectroscopically derived differential rotation coefficients an oscillation at 16.7 days. They also note that many frequencies in the sunspot drift velocity measurements have periods which are multiples of 4.2 days.

It remains for further work to ascertain whether these particular oscillations are the same or closely related. However, there does appear to be periodic features in this period region which may prove quite interesting in terms of solar seismology (Gough 1980b; Knight, Schatten and Sturrock 1979).

7. THE SOLAR CYCLE AND LONGER PERIOD FEATURES

Global oscillations of the sun may well be responsible to some extent for the very long period structures with time scales $\geq$ 10 years. Wolff (1976) using a model with interacting of modes, has put forth an interpretation of the structure found by Currie (1973) in the power spectrum of the Zurich relative sunspot number. This pioneering work in this period domain has produced intriguing results.

In the spirit of Wolff's model, the spectrum analyses by Dicke (1979) of the daily sunspot number and the deuterium/hydrogen ([D/H]) ratio from two bristle cone pines is included here. Dicke has reported a very narrow peak at 22 years in both spectrum analyses, suggesting a stable clock inside the sun. This is just the property expected from global oscillations.

These are just the beginnings of developments in this period range. New work should increase our insight into the mechanisms responsible for these long term periodic structures.

8. SUMMARY

Viable interpretations of observations have been put forth as evidence for global oscillations of the sun and many fundamentally important results have consequently been obtained. It is apparent from this review that much work remains to be done to fully ascertain the practical value of solar seismology. However, enough independent work is currently available to indicate that solar seismology programs can be mounted during the 1980's with a reasonable expectation of obtaining new information about the solar interior.

* * * * *

This work was supportd in part by the National Science Foundation and the Air Force Office of Scientific Research.

REFERENCES

Ando, H. and Osaki, Y. 1975, Publ. Astron. Soc. Japan, 27, 581.

Brookes, J.R., Isaak, G.R. and van der Raay, H.B. 1976, Nature, 259, 92.

Brown, T.M., Stebbins, R.T. and Hill, H.A. 1978, Ap. J., 223, 324.

Caudell, T.P. and Hill, H.A. 1980, Mon. Nat. R. Astr. Soc., in press.

Caudell, T.P., Knapp, J., Hill, H.A. and Logan, J.D. 1980, these proceedings.

Claverie, A., Isaak, G.R., McLeod, C.P., van der Raay, H.B. and Roca Cortes, T. 1980, these proceedings.

Currie, R.G. 1973, Astrophys. and Spa. Sci., 20, 509.

Deubner, F.-L. 1975, Astr. Ap., 44, 371.

Deubner, F.-L. 1976, Astron. Astrophys., 51, 189.

Deubner, F.-L., Ulrich, R.K. and Rhodes, E.J., Jr. 1979, Astron. Astrophys., 72, 177.

Dicke, R.H. 1977, Ap. J., 218, 547.

Dicke, R.H. 1979, Nature, 280, 24.

Dicke, R.H. and Goldenberg, H.M. 1974, Ap. J. Suppl., 27, 131.

Dittmer, P.H. 1977, Ph.D. Dissertation, Stanford University.

Frazier, E.N. 1968, Z. F. Astrophys., 68, 345.

Gough, D.O. 1980a, these proceedings.

Gough, D.O. 1980b, Mon. Not. R. Astr. Soc., in press.

Hill, H.A. 1978, The New Solar Physics, (ed. J.A. Eddy; Boulder: Westview Press), Chapter 5.

Hill, H.A. and Caudell, T.P. 1979, Mon. Not. R. Astr. Soc., 186, 327.

Hill, H.A. and Stebbins, R.T. 1975, Ann. N.Y. Acad. Sci., 262, 472.

Hill, H.A., Stebbins, R.T. and Brown, T.M. 1976, Atomic Masses and Fundamental Constants, 5, (ed. J.H. Sanders and A.H. Wapstra; New York: Plenum), p. 622.

Hill, H.A., Brown, T.M. and Stebbins, R.T. 1976, The Observatory, 96, 130.

Kahn, F.D. 1961, Ap. J., 134, 343.

Knapp, J., Hill, H.A. and Caudell, T.P. 1980, these proceedings.

Knight, J.W., Schatten, K.H. and Sturrock, P.A. 1979, Ap. J. Letters, L153, 16.

Kotov, V.A., Severny, A.B. and Tsap, T.T. 1978, Mon. Not. R. Astr. Soc., 183, 61.

Kuhn, J.R. and Worden, S.P. 1979, Ap. J. Letters, L119, 30.

Leibacker, J.W. and Stein R.F. 1971, Ap. Lett., 7, 191.

Leighton, R.B. 1960, Proc. IAU Symposium no. 12, 321 (Nuovo Cimento Suppl., 22, 1961).

Noyes, R.W. and Leighton, R.B. 1963, Ap. J., 138, 631.

Rhodes, E.J., Jr., Ulrich, R.K. and Simon, G.W. 1977, Ap. J., 218, 901.

Scherrer, D.H., Wilcox, J.M., Kotov, V.A., Severny, A.B. and Tsap, T.T. 1979, Nature, 277, 635.

Severny, A.B., Kotov, V.A. and Tsap, T.T. 1976, Nature, 259, 87.

Souffrin, P. 1966, Ann. d'Ap., 29, 55.

Stein, R.F. 1967, Solar Phys., 2, 385.

Thomas, J., Clark, P.A. and Clark, A., Jr. 1971, Solar Phys. 16, 51.

Uchida, Y. 1967, Ap. J., 147, 181.

Ulrich, R.K. 1970, Ap. J., 162, 193.

Whitaker, W.A. 1963, Ap. J., 137, 914.

Wolff, C.L. 1972, Ap. J. Letters, 177, L87.

Wolff, C.L. 1976, Ap. J., 205, 612.

THE LATEST RESULTS OF THE VELOCITY SPECTROSCOPY OF THE SUN[1]

A. Claverie, G.R. Isaak, C.P. McLeod and H.B. van der Raay
Department of Physics
University of Birmingham, UK

T. Roca Cortes
Instituto de Astrofisica de Canaries

As part of a study designed to obtain an overall view of the solar surface through examination of low ℓ value oscillations, it was found that high sensitivity Doppler spectroscopy of integral sunlight in the 769.9 nm line of neutral potassium reveals several equally spaced lines of high Q centered on the well known period of five minutes. These lines are interpreted as low ℓ, high n overtones of the entire sun.

Recent work incorporating high spatial resolution for study of five minute oscillations in the solar photosphere has indicated a concentration of narrow ridges in the k,ω diagram. Most of these oscillations are global in nature, and are low n and high ℓ value acoustic modes.

Doppler shift measurements of integral solar light indicated several discrete lines of amplitude 0.1 to 0.3 ms^{-1} within the main peak of the power spectrum of the five minute oscillation. These lines are found to have, on average a uniform spacing of 67.8 μHz. Line of sight velocity measurements of the whole solar disk were made using optical resonance spectroscopy comparing the position of the Fraunhofer absorption line of neutral potassium at 769.9nm with that of the same line in the laboratory.

The observations were made during 1976, 1977 and 1978 at Izana, Tenerife and simultaneously in 1978 at Pic du Midi in the Pyrenees; the two sites, some 2300 km apart, were assumed to be meteorologically and observationally independent. The data analysis was based upon 33, 35 and 7 days of observation, respectively, in the three years of the study period.

The daily data consisted of a mean line of sight velocity determined every 42

---

[1]This paper is an abstract of a talk presented at this workshop by G. Isaak. The details of the observations were summarized from a longer paper published in Nature (Claverie et al. 1980). The theoretical implications of this work as proposed by Christensen-Dalsgaard and Gough at the workshop are presented in the following paper.

seconds (100 seconds on Pic du Midi) for the entire observing day. Residuals corresponding to velocity amplitudes of less than 3 m/s appeared after subtraction of the observer's velocity relative to the centroid of the sun due to the spin and orbital velocities of the earth. Small allowances for residual curvature effects were made.

Analysis, using standard power spectrum techniques, of simultaneous data from the two sites substantiated the solar origin of the observed oscillations and indicated the existence of a series of well defined peaks. Averaging the power spectra for individual days over the 3 year period clearly indicated the presence of peaks with an apparent constant spacing. Further analysis of data strings of different lengths had no effect on the observed spacing.

The constancy of the peak spacing was demonstrated first by plotting the order of the peaks against the observed frequencies and second by screening the mean power spectra data with a high pass filter, by subtracting a moving mean over three points and then subjecting the resulting points to an autocorrelation and power spectrum analysis. Mean line spacings of 67.6, 67.4 and 67.6; and 67.8, 68.0 and 68.0 μHz were found, respectively, by the two analytical methods for each of the three observational years. A cross correlation analysis of the 1976 and 1977 power spectra yielded a correlation coefficient of 0.87 with a maximum at zero lag, indicating the consistency of the lines over the two year period.

The 1978 data, obtained by improved experimental technique, were subjected to a superimposed epoch analysis. The frequency range was restricted to that covered by the power spectrum analysis and the same peak structure was found. Straight line fits to these plots yielded mean line spacings of 67.4 ± 0.5 and 67.9 ± 0.2 μHz, respectively.

A power spectrum analysis of two consecutive days of data was made with zeros inserted in the data string at the times when actual data were not available. This produced a 32 hour data string whose power spectrum demonstrated the usual peaks in the power spectrum. Sine waves of the indicated frequencies were subtracted from the original data by using a least squares procedure which optimized the frequency, phase and amplitude of the fitted wave. The resulting power spectrum clearly demonstrated the coherency of the oscillations over the 32 hour data string with a value of Q in excess of 400.

The authors suggest that these lines correspond to normal modes of vibration of the whole sun, but note that their definitive identification will necessitate acquisition of information on their spatial structure. Since integral light spectrometers tend to average out modes of high ℓ value with many peaks and troughs across the visible disk of the sun, the observations are strongly biased toward low ℓ value modes. This analysis indicates that these modes are of low ℓ value which may supply constraints on the solar interior.

REFERENCE

Claverie, A., Isaak, G.R., McLeod, C.P., van der Raay, H.B. and Roca Cortes, T. 1979, Nature, 282, 591.

IMPLICATIONS OF THE WHOLE-DISK DOPPLER OBSERVATIONS OF THE SUN

J. Christensen-Dalsgaard
Astronomisk Institut, Aarhus Universitet, Denmark
and Institut d'Astrophysique, Universite de Liege, Belgium

D. Gough
Institute of Astronomy, and Department of Applied Mathematics
and Theoretical Physics, University of Cambridge, UK

ABSTRACT

Isaak's announcement (Claverie et al. 1980) of the discovery by his group of distinct, approximately evenly spaced peaks in the power spectra of whole-disk Doppler measurements immediately raised the issue of what they imply about the structure of the solar interior. Here we report our immediate reactions, and infer that the observations seem to imply a lower sound speed, appropriately averaged throughout the interior, and probably a lower mean temperature than standard solar models predict.

1. INTRODUCTION

Taken at face value, the observations reported by Isaak and his colleagues (Claverie et al. 1980) provide a very important addition to the solar oscillation data. It appears that the peaks in the power spectra are produced by p modes of low degree, as Isaak has proposed, because it is to such modes that the measuring technique is most sensitive. Unlike the more common five minute oscillations of high degree that have been measured carefully by Deubner (1975, 1977), Rhodes, Ulrich and Simon (1977) and Deubner, Ulrich and Rhodes (1979), these modes penetrate deeply into the sun and so provide us with direct information about the solar interior. It is of considerable interest, therefore, to analyze these oscillations, and to ask what they imply.

2. INTERPRETATION OF THE DATA

Isaak has suggested that the peaks in his power spectra might arise from a single spectrum of modes of like degree, such as the radial pulsations. If one compares the mean frequency separation between those peaks with the differences in neighbouring frequencies of a single spectrum of modes of a typical standard solar model (e.g., Iben and Mahaffy, 1976; Christensen-Dalsgaard, Gough and Morgan 1979) one finds that the latter exceeds the former by a little more than a factor 2.

Isaak's interpretation would therefore imply that the internal structure of the sun is very different from that of the usual models.

To see just how different the sun would have to be, let us note that for periods near five minutes the order n of the modes of a standard solar model is about 20, provided the degree ℓ is about unity, and the asymptotic formula valid for $n >> \ell$ for the cyclic frequency difference $\Delta\nu$ between modes n and n + 1 is a good approximation (Christensen-Dalsgaard, Gough and Morgan 1979). Thus

$$\Delta\nu \approx \left(2\int_0^R \frac{dr}{c}\right)^{-1} , \qquad (1)$$

(e.g., Vandakurov 1967), where r is a radial distance coordinate, c is the local adiabatic sound speed and R is the solar radius. We can see, therefore, that a halving of $\Delta\nu$ implies a halving of an appropriate mean of the sound speed. If one ignores uncertainties in composition, it would be necessary for the sun to have a mean temperature only 70 percent of that of the standard models. The problems this idea poses are tremendous, if one wishes to accept the atomic and nuclear physics upon which the theory depends. Moreover, it raises the question of why only a single spectrum of oscillations is excited.

A more likely explanation, perhaps, is that contributions from modes of all degrees are present in the data. It is a property of modes with $n >> \ell$ that the frequencies of modes with even ℓ almost coincide; so do the modes with odd ℓ, their frequencies lying approximately midway between those of their even counterparts. Only when ℓ becomes comparable with n do the frequencies fail to coincide, but then ℓ is so great that the sensitivity of the measuring technique is extremely small. To counter somewhat the decrease in instrumental sensitivity, however, is the fact that there are present in the sun a very large number of modes of high degree. Thus one might expect to see in the power spectrum of the five minute oscillations a continuum produced by the majority of the modes, upon which is superposed the discrete spectrum arising from all the modes of low degree. To assess whether this idea is plausible, we shall discuss in the next section the dependence of the instrumental sensitivity on the degree of the modes.

3. STRUCTURE OF THE POWER SPECTRUM

Let $V_{n\ell}$ be the surface velocity amplitude of the modes characterized by (n,ℓ): we shall assume that the $2\ell + 1$ modes of degree ℓ are on average excited to the same amplitude. Then if actual and instrumental broadening are ignored, one would expect the observed mean power spectrum to be of the form:

$$P(\nu) = \sum_{n,\ell} (2\ell + 1) S_\ell^2 V_{n\ell}^2 \delta(\nu - \nu_{n\ell}) \quad , \tag{2}$$

assuming random phases, where ν is frequency, $\nu_{n\ell}$ is the frequency of the mode (n,ℓ), S_ℓ is the mean instrumental sensitivity (spatial filter function) for the modes of degree ℓ, and δ is the Dirac delta function. Note that because the oscillations under consideration are p modes, their velocities are almost radial. Hence S_ℓ depends only on the structure of the surface harmonics of degree ℓ, and not on the order n of the modes.

Spatial filter functions for p modes of low degree have been computed by Hill (1978). First the surface harmonics are expressed in terms of the usual polar angles (θ,ϕ). Because the mean power spectrum presented by Claverie et al. (1980) is an average of spectra each of which is computed from only a single day's observing, rotational splitting can be ignored and the oscillations have no preferred direction. Hence it is immaterial in which direction one chooses the polar axis to be. It seems most expedient to choose it to lie along the line of sight, so that the mean velocity observed, if one neglects limb darkening, is given by

$$\bar{V}_{n\ell m} = \frac{V_{n\ell} \int_0^{\pi/2} P_\ell^m(\cos\theta) \cos^2\theta \sin\theta \, d\theta \int_0^{2\pi} \sin \cos m\phi \, d\phi}{\left\{ \frac{\pi}{4} \int_0^{\pi} \left[P_\ell^m(\cos\theta) \right]^2 \sin\theta \, d\theta \int_0^{2\pi} \sin^2 \cos^2 m\phi \, d\phi \right\}^{1/2}} \equiv S_{\ell m} V_{n\ell}$$

where P_ℓ^m is the associated Legendre function. The normalization has been chosen such that $V_{n\ell}$ is the root-mean-square velocity over the entire surface of the sun. In this coordinate system $S_{\ell m} = 0$ if $m \neq 0$, so that the mean spatial filter function S_ℓ, averaged amongst all the modes of degree ℓ (with respect to any coordinate system), is simply

$$S_\ell = (2\ell + 1)^{-1/2} S_{\ell 0} = \frac{\pi^{1/2}}{2\Gamma(2 - \ell/2)\,\Gamma(5/2 + \ell/2)} \quad , \tag{3}$$

where Γ is the gamma function.

Values of the functions S_ℓ and the weights $(2\ell + 1)S_\ell^2$ appearing in equation (1) are presented in Table 1 for the modes of lowest degree; $S_\ell = 0$ for all even ℓ greater than 2. Hill (1978) presents in his Table 4.1 values of filter functions comparable with $S_{\ell m}$, the only difference being that his functions are referred to a polar axis perpendicular to the line of sight. It should be the case that the root-mean-square of all Hill's values corresponding to a particular ℓ should simply be S_ℓ, but there appears to be some discrepancy.

Of course the actual power spectrum is not quite of the form (2), because broadening merges groups of discrete but almost coincident delta functions into a

Table 1.

ℓ	S_ℓ	$(2\ell + 1)S_\ell^2$
0	0.667	0.444
1	0.500	0.750
2	0.267	0.356
3	8.33×10^{-2}	4.86×10^{-2}
5	-1.04×10^{-2}	1.19×10^{-3}
7	3.13×10^{-3}	1.46×10^{-4}
9	-1.30×10^{-3}	3.22×10^{-5}

sequence of almost evenly spaced peaks. Nevertheless the positions of the centers of each peak could be estimated by averaging the eigenfrequencies contributing to that peak with weights $(2\ell + 1)S_\ell^2 V_{n\ell}^2$. This task is not simple because we do not know the relative amplitudes $V_{n\ell}$. It is evident from Table 1, however, that unless the surface amplitudes increase rapidly with ℓ, the data are dominated by contributions from only the first few spectra of modes. It is interesting to note that the sum of those values in the third column of Table 1 corresponding to the modes of even degree is the same as that from the modes of odd degree. Hence if all the low degree modes were excited to comparable surface amplitudes, one would not expect to find a systematic alternation in the heights of the peaks in the mean power spectra of the observations.

4. IMPLICATIONS CONCERNING THE SOLAR STRUCTURE

Given a sequence of solar models, with known pulsation frequencies, one can in principal use the whole-disk five minute power spectra to choose that model which most closely fits the data. The first step is to obtain a rough estimate by comparing the observed mean spacing of the peaks with that of the models. Hopefully this would be sufficiently accurate to associate with each peak in the spectrum the order of the mode of a particular degree whose frequency should correspond to the position of that peak. Having thus identified the modes, a finer adjustment could then be made by aligning the actual values of the eigenfrequencies with the positions of the peaks.

Let us compare the mean peak separation in the Birmingham data, about 0.0680 mHz, with the predictions of a standard solar model. Christensen-Dalsgaard, Gough and Morgan (1979), for example, present mean eigenfrequency separations of several spectra of modes of low degree of a solar model with uniform heavy element abundance $Z = 0.02$, the mean being taken in the period range 280s - 350s. We quote 0.137 mHz, 0.138 mHz, 0.139 mHz and 0.139 mHz for the spectra with $\ell = 0$, 2, 3 and 4 respectively. Note that all these values exceed twice the observed spacing. Consequently, as can be seen from equation (1), the observations imply that the mean sound speed in the interior of the standard model is too high. It is interesting to note that lowering the sound speed in the interior generally implies a lowering of the neutrino flux.

In addition to the model with uniform Z, Christensen-Dalsgaard, Gough and Morgan (1979) examined two models with low initial Z that have been contaminated during their main-sequence evolution at rates such as to raise their surface heavy element abundances to $Z = 0.02$ at the present time. They found, in accord with previously computed metal deficient models with uniform Z, that the frequency spectrum for modes of like degree becomes less densely spaced as the value of Z in the interior decreases (cf. Iben and Mahaffy 1976). Such a model might therefore

reproduce the Birmingham data. Indeed, if we assume that the centers of alternate peaks in the power spectra are given approximately by the average of the frequencies of the $\ell = 0$ and $\ell = 2$ modes, the model with $Z = 0.004$ has the same mean spacing as the mean power spectrum of the observations; this model has a neutrino flux of 2.3 SNU, which is within two standard deviations of Davis's (1978) mean value.

It would be rash to conclude from this exercise that the sun has a low heavy element abundance in its interior. The frequency separation obtained from the whole-disk observations provides a complicated average of the internal sound speed, not the composition. Although the contaminated solar models reproduce some of the observed features of the sun, acceptance of them probably poses more problems than it appears to solve. In particular the model with $Z = 0.004$ has a convection zone only 120,000 km deep, too shallow to explain the frequencies of the five minute oscillations of high degree (Berthomieu et al. 1980; Lubow, Rhodes and Ulrich 1980), and not shallow enough to provide a natural explanation of the claim of Hill and Caudell (1979) that g modes of moderate degree have significant amplitudes in the photosphere (Christensen-Dalsgaard, Dziembowski and Gough 1980). Other possibilities exist for reducing the sound speed in a solar model, such as upsetting the thermal energy balance (e.g., Dilke and Gough 1972). It remains to be seen whether such models can reproduce the Birmingham data.

* * * * *

We are grateful to A.J. Cooper for pointing out an error in the original manuscript.

REFERENCES

Berthomieu, G., Cooper, A.J., Gough, D.O., Osaki, Y., Provost, J. and Rocca, A. 1980, these proceedings.

Christensen-Dalsgaard, J., Gough, D.O. and Morgan, J.G. 1979, Astron. Astrophys., 73, 121-128.

Christensen-Dalsgaard, J., Dziembowski, W. and Gough, D.O. 1980, these proceedings.

Claverie, A., Isaak, G.R., McLeod, C.P. van der Raay, H.B. and Roca-Cortes, T. 1980, these proceedings.

Davis, F., Jr. 1978, Proc. informal conference on 'Status and future of solar neutrino reasearch', (ed. G. Friedlander, US Technical Information Service BNL 50879, Springfield, VA), Vol. 1, pp. 1-54.

Deubner, F.-L. 1975, Astron. Astrophys., 44, 371-375.

Deubner, F.-L. 1977, Proc. IAU Colloq. No. 36, (ed. R.M. Bonnet and Ph. Delache; G. de Bussac, Clermond-Ferrand), 45-68.

Deubner, F.-L. Ulrich, R.K. and Rhodes, E.J., Jr. 1979, Astron. Astrophys., 72, 177-185.

Dilke, F.W.W. and Gough, D.O. 1972, Nature, 240, 262-264 and 293-294.

Hill, H.A. 1978, in The new solar physics, (ed. J.A. Eddy; Boulder: Westview Press) p. 135-214.

Hill, H.A. and Caudell, T.P. 1979, Mon. Not. R. Astr. Soc., 186, 327.
Iben, Jr., I. and Mahaffy, J. 1976, Astrophys. J. Lett., 209, L39-L43.
Lubow, S., Rhodes, E. and Ulrich, R. 1980, these proceedings.
Rhodes, E.J., Jr., Ulrich, R.K. and Simon, G.W. 1977, Astrophys. J., 218, 901-919.
Vandakurov, Yu. V. 1967, Astron. Zh., 44, 786-797.

OBSERVATIONS OF LONG PERIOD OSCILLATIONS IN THE SOLAR LIMB DARKENING FUNCTION

R.T. Stebbins
Sacramento Peak Observatory[1]
Sunspot, New Mexico

1. INTRODUCTION

The most interesting region of the sun's normal mode spectrum lies between $\sim$ .1 mHz and $\sim$ 2 mHz. Theoretical predictions of the spectrum (Hill 1978, Figure 2.2) show the high frequency extreme of the g modes to lie near .4 mHz, the band becoming increasingly dense toward lower frequencies. The fundamental modes overlap the g modes slightly and extend upward to .45 mHz. The p modes extend from .25 mHz up to higher frequencies with increasing density. The g modes are of interest because they probe the deep solar interior. The period of the fundamental radial mode is very sensitive to envelope structure. The p modes probe the envelope and may be expected to be most readily observable. The rotational sidebands of any mode at any depth reflect the internal rotation at that depth.

In the region of the spectrum where the modes are least dense (.45 - .6 mHz), there are 110 modes/mHz; ignoring rotational sidebands the spectral resolution of the elusive 12-hour uninterrupted observation is 23 μHz, encompassing 2-3 modes in the sparsely populated region. Resolution of rotational sidebands would require a 600 hour uninterrupted observation. By comparison, p modes in the five minute band are roughly a nanohertz apart. The extreme density and complexity of the sun's acoustic spectrum coupled with the signal weakness in the interesting .1 - 2 mHz region make observations of this phenomena extremely challenging.

2. BACKGROUND

The original measurements of oscillations in the .1 - 2 region stem from the oblateness measurements of Hill and Stebbins (1975b). The early serendipitous work in this area (Hill and Stebbins 1974, 1975a) culminated in a concerted effort (Brown, Stebbins and Hill 1978) to demonstrate the reality of solar oscillations in a spectral regime where none had been seen previously. The method used, a product of the oblateness effort, was a novel one: the shape of the limb darkening function was

[1]Operated by the Association of Universities for Research in Astronomy, Inc. under contract AST 78-17292 with the National Science Foundation.

analyzed by a finite Fourier transform to locate a point, called the "edge" of the sun as defined by the Finite Fourier Transform Definition (FFTD). The FFTD located at an edge of the sun which was extremely precise, affected by motion of the solar limb and certain forms of limb brightening, and very insensitive to seeing changes. Oscillations, reported as motion of the FFTD edge, could have been due to limb motion and/or a pulsating limb brightening of the requisite form.

This work was met with skepticism (see Hill 1978 for summary). The sun was presumed not to be a pulsator. The FFTD was not widely understood. Conventional methods, such as Doppler techniques and intensity measurements, did not produce corroborating results. Two classes of explanations for the FFTD pulsations were advanced: the spectra were basically noise, or some systematic effect, other than global pulsations, gave rise to the observed spectra. In the latter case, explanations ranged from instrumental to atmospheric differential refraction to the rotation of small brightness features (e.g., granules) through the aperture.

Deubner's work (1975) on the five minute oscillation now is commonly taken to demonstrate that the sun is a pulsator. Intercomparisons between different types of observations seem to fail in a variety of circumstances (Hill 1978), including the easily observed and robust five minute oscillations. Alternate explanations of the long period oscillations, as detected by the limb analysis method, are rarely accompanied by the appropriate careful observation. Brown, Stebbins and Hill (1978) have made the most extensive statistical analysis of the FFTD spectra, which they offer as the fundamental arguments for the reality of the oscillations. Phase coherence demonstrated by Brown, Stebbins and Hill (1978), and of late more strongly by Hill and Caudell (1979), Caudell and Hill (1980), and Caudell et al. (1980), add credence to the solar global pulsation interpretation and are inconsistent with instrumental, atmospheric, or granule interpretations. In short, the case for the existence of long period solar oscillations is growing stronger.

3. GOALS

To reap the potential rewards of solar seismology will require more than establishing the existence of the long period oscillations. Considering the faintness of even the FFTD signnal, some improvements in observational techniques are called for. Although Brown, Stebbins and Hill (1978) did not take advantage of it, the FFTD is capable of distinguishing between limb motion and limb brightening. Indeed, it was employed to just that end in the oblateness measurements. By a twist in the application of the FFTD, it can be used to test the character of the oscillatory signal, thereby distinguishing between possible origins of the signal. Moreover, the observed character, should it prove to be that of global oscillations, should be predictable by pulsation theory.

Further, the work reported here was conducted on a different instrument than

all previous FFTD work. Another data base is also highly desirable for a novel phenomena such as global pulsations. The goals here, then, are an improved detection technique, an elucidation of signal character, further tests of the pulsation interpretation, and an expanded data base.

4. METHOD

Despite its novelty, the FFTD still seems to be the most effective way to detect oscillations between .2 and 1.5 mHz. The details of the FFTD and its properties have been described, studied, and tested extensively (Hill, Stebbins and Oleson 1975). Briefly, a weighting function, defined in an interval of predetermined width, is multiplied by the observed limb darkening function and the results are summed. The interval is translated across the limb darkening function until the sum goes to zero, i.e., a balance point is found. That point, the center of the interval, is called the edge. The weighting function, a Chebyschev polynomial, is chosen so that the edge location is insensitive to seeing changes and sensitive to certain forms of change in the limb darkening function.

The interval width, half of which is called the scan amplitude, is an adjustable parameter. Changing the scan amplitude changes the sensitivity to limb brightening. Therefore, subtracting the motion of an FFTD edge defined by a small interval from another FFTD edge defined by a large interval measures the difference in sensitivities to limb brightening. If the pulsation manifests itself by limb motion alone, the subtraction yields zero. If the shape of the limb darkening has a pulsating component, the subtraction should be non-zero. The results of this subtraction will be called the brightness signal. By forming many brightness signals with a referenced edge defined by a large interval and many edges defined by progressively smaller intervals, one has a characterization of the limb brightening signal, a signature. That signature can be calculated from an intensity eigenfunction through application of the FFTD formalism. This signature can be the point of comparison between pulsation theory and observation.

In the past, the FFTD has been applied directly to a digitized limb profile from a scanning photomultiplier. An error signal was used to serve the center point of the scan. This transpired simultaneously at two diametrically opposed limbs, and the recorded data was the solar diameter, i.e., the separation of the photomultipliers. The interval size was established by the mechanical scan amplitude (hence the terminology). The innovation in this work was to record the digitized limb profile and compute a family of FFTD edges by numerically setting the scan amplitude to several values. In this way, many FFTD edges could be followed simultaneously. Another difference in the present work is the fact that only one limb is used. Although this restriction is imposed by the available equipment, it does eliminate the possibility of atmospheric differential refraction effects and the

measurement of limb motions. This measurement responds only to brightness oscillations.

The data were acquired with the Diode Array on the Vacuum Tower Telescope at the Sacramento Peak Observatory. The Echelle spectrograph was made to pass a narrow band of clean continuum near 6430 A. The diodes were set up to digitize a 96" x 96" patch astraddle the west limb at the equator. The sample interval in the radial dimension was 1". The data was averaged in the tangential direction to reduce the effects of granules in the aperture. The patch was digitized by sweeping the image past the line of diodes in the tangential direction. Digitization and flyback took slightly less than 16 seconds and was repeated every 16 seconds for as long as possible without interruption. This observing program was pursued as often as daylight, telescope scheduling, weather, breakdown, and other calamities would allow from March 1977 to October 1979. Data sets represented here are tabulated in Table 1. Of the 53 data sets, these 16 have been selected for length (none shorter than 8.0 hours) and paucity of interruptions.

The data reduction begins by computing a family of FFTD edges for each time step. Eighteen edge signals are followed with scan amplitudes (interval halfwidth) ranging from 6" to 44". The family of 18 edge time strings is converted to a family of 17 brightness signal time strings by subtracting all others from the edge signal with the largest scan. This subtraction removes all limb motions whether oscillatory or telescope pointing errors. The family of brightness signals is transformed to a family of Fourier transforms by the usual methods. (Mean and quadratic removal, windowing, extension with zeros, and transformation follow the advice of Brault and White 1971.) Finally, the amplitude and phase of each brightness signal at each frequency point are computed. This result can be thought of as a two-dimensional surface. Frequency and scan size are the independent variables; the amplitude of oscillation is the dependent variable. The signature is seen by taking a constant frequency cut through this surface.

This report will henceforth concern itself with an examination of the signature, the amplitude of oscillation versus scan. This function can be influenced by several factors. First is the limb brightening caused by a particular global mode. p and g modes exhibit different limb brightenings (Hill and Caudell 1979), and in frequency increments where both are present, there will be superposition to confuse the observer. Secondly, within a frequency resolution element, the observer will see a superposition of all the active modes. The frequency resolution is one over the length of the data set; the beat period is equal to or greater than the length of the data set--which hampers day-to-day comparisons. Thirdly, an FFTD edge defined by a particular scan will have a dependence on ℓ, the principal index of a mode's spherical harmonic. Consequently, the signature may change if the dominant mode in the frequency interval changes to one with a different ℓ value.

Table 1.

Date	Starting Time (UT)	Length (Hours)	Limb
29 September 1977	13:46:32	10.08	West Equator
30 September 1977	13:36:16	10.08	"
6 April 1978	13:46:48	11.16	"
7 April 1978	13:49:00	8.06	"
11 April 1978	13:51:08	10.78	"
12 April 1978	13:23:04	9.22	"
29 September 1978	13:57:16	10.17	"
1 October 1978	13:51:28	10.35	"
2 October 1978	13:56:28	10.22	"
3 October 1978	13:57:52	10.49	"
13 May 1979	15:54:24	9.38	"
7 October 1979	15:50:00	8.27	"
8 October 1979	14:20:12	9.39	"
10 October 1979	15:03:52	9.21	"
11 October 1979	13:47:48	10.34	"
12 October 1979	14:40:24	8.96	"

To examine the signature, the analysis is restricted to .45 - .6 mHz where theory predicts a sparsely populated region of only p modes. To determine what the signature looks like, and how reproducible it is, the signature is averaged over this frequency band in all 16 data sets and the standard deviation of the averages is computed.

5. RESULTS

The empirical signature is shown in Figure 1. One can see the variation of oscillatory amplitude with scan. The standard deviations of the mean are shown at each of the scan values used. In computing these, account has been taken of the fact that the time strings were extended with zeros to 18.2 hours, and consequently the frequency points are not independent measurements.

There is a significant signature, peaked toward smaller scans. This is direct evidence that oscillations detected by FFTD limb analysis are brightness changes at least in part. There may or may not be motion of the limb for Doppler detection, but there are brightening changes. This is a systematic effect, not the result of random noise in 17 different channels. What are the possible sources of this systematic signature ?

Changes in atmospheric seeing have a signature peaked toward smaller scans. However that signature should have a minimum near a scan 1.8 times the full-width-at-half-maximum of the atmospheric transfer function. With seeing 5" or less, that minimum would be found at a scan of $\sim$ 8", if the signal were due to seeing fluctuations. There is no minimum to be seen. But this result is consistent with the known properties of the FFTD; the most sensitive FFTD edge (6" scan) would move about 1 milli sec for a 20% change in the full-width-at-half-maximum. Considering that seeing fluctuations have a broadband character, one would not expect to see an atmospheric signature here--and one does not.

Instrumental sources and atmospheric differential refraction are ruled out by the nature of the measurement. The differential aspect of the brightness signal removes telescope problems. Esoteric diode misbehavior (selected oscillating gains carefully arranged about the limb to look like the limb darkening changes) would be averaged out by telescope pointing errors.

The casual rotation of surface brightness features through the aperture can be ruled out by two tests: similar data taken at the pole has the same signature, and the brightness signals all have very similar phases. Since different granules are passing into the different FFTD intervals, the FFTD signals should not enjoy any phase relation.

Global pulsations, on the other hand, may indeed have this signature. This signature suggests limb brightening sharply peaked toward the intensity onset. Conventional linear pulsation theory does not predict such an intensity

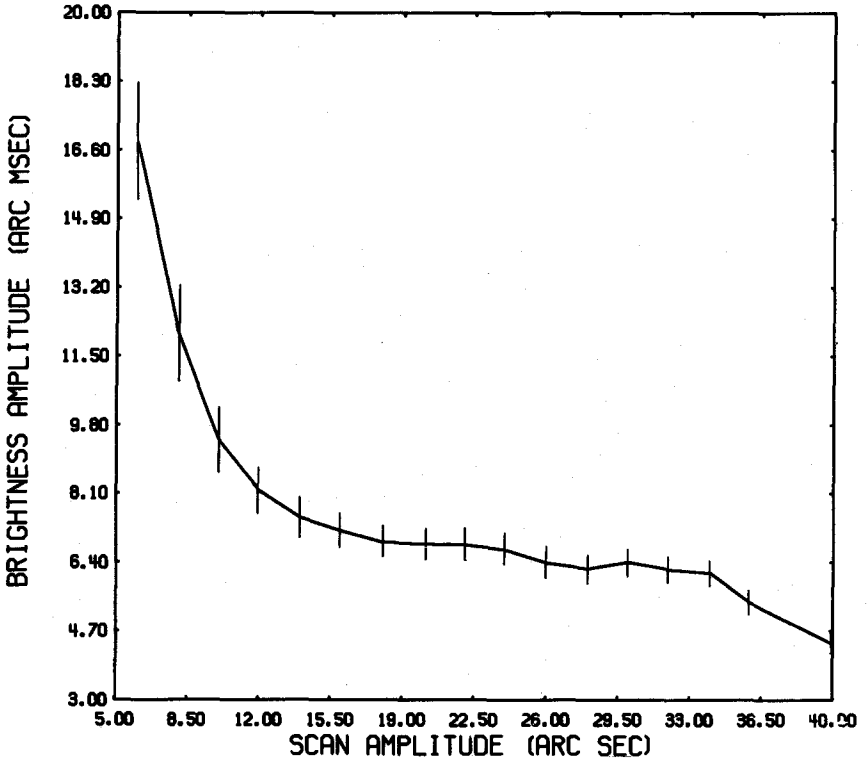

Figure 1. The signature, the oscillatory amplitude versus FFTD scan amplitude, has been averaged from .45 to .6 mHz and over all data sets. The reference edge has a scan amplitude of 44 arc sec. The brightness amplitude is the Fourier amplitude of the brightness signal, the separation between the FFTD edge with the associated scan size and the reference edge. The error bars are the standard deviation of the average.

eigenfunction, but then, as the paper in these proceedings by Stebbins et al. (1980) shows, conventional linear pulsation theory is inconsistent with the observed behavior at five minutes. There is evidence of nonlinearity there, suggesting the sort of mechanism necessary to produce the required temperature structure. Knapp, Hill and Caudell (1980) show evidence for a limb brightening sharply peaked toward the intensity onset. Considering that the average spans two years of observations, this signature would appear to be an enduring characteristic of the sun.

6. CONCLUSIONS

The evidence presented here demonstrates the reality of long period brightness oscillations in the solar limb darkening function. This extension of the FFTD, the simultaneous application of multiple edge definitions, provides another test for establishing the reality of long period solar oscillations. Additional information, namely the signature, characterizes the signal measured, and can be used to enhance detection of these faint and complex signals. In essence, brightness oscillations can be detected without relying on the broadband statistics of spectra. This is essential for study of small bands in highly resolved spectra. The signature information also affords a vehicle for comparison to pulsation theory, another step toward seismology.

* * * * *

The observing staff of the Tower telescope, Horst Mauter, Dick Mann and Gary Phillis, deserve special mention for the perseverance demanded by the exacting setups and the long tedious observing runs; they made it possible. Timothy Brown and Henry Hill contributed useful comments throughout. I am especially indebted to Henry for pointing out a flaw unwittingly introduced into the analysis after it was originally avoided. The forbearance of the editors and the typist, Ms. Christy Ott, in tardy preparation of the report are also acknowledged.

REFERENCES

Brault, J. and White, O.R. 1971, Astron. Ap., 13, 169.

Brown, T.M., Stebbins, R.T. and Hill, H.A. 1978, Ap. J., 223, 324.

Caudell, T.P. and Hill, H.A. 1980, Mon. Not. R. Astr. Soc., in press.

Caudell, T.P., Knapp, J., Hill, H.A. and Logan, J.D. 1980, these proceedings.

Deubner, F.-L. 1975, Astr. Ap., 44, 371.

Hill, H.A. 1978, The New Solar Physics, (ed. J.A. Eddy; Boulder: Westview Press), Chap. 5.

Hill, H.A. and Caudell, T.P. 1979, Mon. Not. R. Astr. Soc., 186, 327.

Hill, H.A. and Stebbins, R.T. 1974, The Seventh International Conference on General Relativity and Gravitation, Tel-Aviv University, June 23-28.

Hill, H.A. and Stebbins, R.T. 1975a, Ann. N. Y. Acad. Sci., 262, 472.

Hill, H.A. and Stebbins, R.T. 1975b, Ap. J., 200, 471.

Hill, H.A., Stebbins, R.T. and Oleson, J.R. 1975, Ap. J., 200, 489.
Knapp, J., Hill, H.A. and Caudell, T.P. 1980, these proceedings.
Stebbins, R.T., Hill, H.A., Zanoni, R. and Davis, R.E. 1980, these proceedings.

SOLAR CONTINUUM BRIGHTNESS OSCILLATIONS: A PROGRESS REPORT

T.M. Brown
High Altitude Observatory
Boulder, Colorado

R.L. Harrison
Department of Physics and Astronomy
University of New Mexico
Albuquerque, New Mexico

During the last few years a controversy has grown up surrounding the proper treatment of boundary conditions for oscillations in the solar atmosphere. Hill, Caudell and Rosenwald (1977) have pointed out that by observing two oscillating dynamic variables simultaneously, it is in principle possible to determine the relative contribution of two independent solutions to the wave equation. These solutions are conventionally denoted ξ_- and ξ_+, corresponding respectively to waves that are of roughly constant amplitude at all heights in the solar atmosphere, and to those that grow exponentially with height, on a scale comparable to the pressure scale height. These arguments are plausible, but they lead to a surprising result: using available measures of velocity and intensity amplitudes in several frequency regimes, together with a detailed nonadiabatic model to generate the required eigenfunctions, Hill, Rosenwald and Caudell (1978) concluded that the amplitudes of the ξ_- and ξ_+ solutions are approximately equal in the upper photosphere. This conclusion has stirred much criticism, since there is no a priori reason to expect the ξ_+ solution to be in any way significant. A more direct objection is that at each frequency there are exactly as many parameters to be fitted (the two wave amplitudes) as there are observations available (a velocity and intensity amplitude). There is thus no meaningful way to cross-check the theory's predictions with other observations. This situation has led us to seek other sets of observations which are more informative than those currently available, so that the notion of a large contribution from the ξ_+ solution can be checked for self-consistency. Although we have not yet succeeded in this aim, some progress has been made, and we can now judge where the effort will lead and begin to draw some tentative conclusions.

Our approach has been similar to that of the SCLERA group in that we intend to combine observations of velocity and intensity amplitude at the various frequencies of interest. It differs, however, in that we wish to use observations with high resolution in both the spatial and temporal frequency domains (henceforth

termed "wavenumber" and "frequency"). There are two principal advantages to using observations of this sort. First, with adequate resolution it is possible to distinguish between p and g modes of oscillation, or, in the case of the five minute oscillations, between different radial modes. It thus becomes possible to compare modes with the same radial mode number but different frequencies, or with different mode numbers and the same frequency. As long as the effects of varying wavenumber are not large, such comparisons can be made in a straightforward way. The second advantage found in the use of high-resolution data is that the importance of any time delay between the velocity and intensity observations is reduced. Since almost all of the incoherence in early observations of the five minute oscillations comes from beating between the various modes, resolving the modes leads to a much more stable power spectrum. Thus, it seems likely that the use of this technique will produce good velocity-intensity ratios regardless of the amount of time which elapses between the two sets of observations.

The problem of obtaining k-ω diagrams of velocity, though still calling for careful work, now seems to be well in hand (Deubner 1975, 1977; Rhodes, Ulrich and Simon 1977). For this reason we addressed the development of methods for obtaining data of the same quality on intensity oscillations. This proved to be a more difficult problem for a variety of reasons. The most serious impediments were the small amplitude expected for the intensity fluctuations (in the entire 5-minute band, rms $\delta I/I$ of about 2×10^{-3}), coupled with the large background power to be expected from non-oscillatory sources like granulation. Further, the intensity oscillations represented a small perturbation within a large constant background, meaning that any change in detector sensitivity or atmospheric transmission would appear strongly in the fluctuating intensity signal. All of this suggested that large amounts of data and sophisticated reduction techniques would be needed to attain the desired accuracy, and that the optical setup used for the observations should be as simple and stable as possible. For these reasons we chose to observe the brightness oscillations in the continuum, a decision that was reinforced by the comparative simplicity of radiation transfer in the continuum.

To date we have observations of two distinct sorts, one dealing with oscillations at the extreme solar limb and the other with those at disk center. The former consist of photoelectric observations taken with the vacuum tower telescope and echelle spectrograph at Sacramento Peak Observatory. The data were processed in such a way that the effects of atmospheric seeing and transparency changes were negligible but, unfortunately, the frequency and wavenumber resolution were at best marginally adequate for the purposes outlined above. For a full discussion of these observations, see Brown (1979). The disk center observations were photographic, also obtained at the Sacramento Peak tower telescope, but using the Universal Birefringent Filter (UBF). These observations cover a much larger field of view than do the limb

observations, resulting in considerable improvement in the wavenumber resolution obtainable. In addition, the large number of pixels per frame significantly increased the signal-to-noise ratio. The registration problems inherent in disk-center observations were solved by superimposing images of a small sunspot that were brought in by periscope from another part of the solar disk. We analyzed these frames by digitizing the entire time series, converting photographic density to intensity, and correcting for sky transparency and similar effects in such a way that the integrated sunlight in each frame appeared constant. We then integrated each frame along one spatial dimension to produce a two-dimensional data array, with space and time constituting the coordinate axes. Finally, using conventional fast transform techniques, we produced two-dimensional power spectra from these data. The analysis of these data is not yet complete, and our attempts at interpretation have barely begun. Nevertheless, it is possible to make a few statements based on a comparison between the two data sets, as well as on the more complete analysis of the limb observations.

The k-ω diagram derived from the limb observations is shown in Figure 1. Especially at the higher contour levels, the power is located in two well-separated frequency regions, corresponding to periods of five minutes and periods of fifteen minutes and longer. Some of the low-frequency power undoubtedly comes from the granulation intensity field, but by far the largest part of the observed power lies at wavenumbers of less than 0.5 Mm^{-1}, corresponding to features of roughly supergranule size or larger. Exactly what physical process is responsible for these large-scale intensity perturbations is not clear. Several interesting conclusions may be reached by studying the way in which the k-ω diagram varies with μ in the neighborhood of the extreme limb. In particular, the analysis of low-wavenumber fluctuations below frequencies of .004 s^{-1} (Brown 1979) indicates three things:

(1) The amount and radial distribution of power in this band is sufficient to cause the apparent diameter fluctuations reported by Brown, Stebbins and Hill (1978). This verifies that the diameter variations are indeed caused by changes in the detailed shape of the limb darkening function.

(2) The amplitudes of the fluctuations tend to increase with increasing distance from the limb, unlike the relationship predicted by Brown, Stebbins and Hill (1978). This implies that most of the fluctuations originate comparatively deep in the photosphere, and not in a high, optically thin shell.

(3) There is no sign of a narrow spike in oscillating intensity at the extreme limb. This spike was a prominent characteristic of the models of Hill, Rosenwald and Caudell (1978) and, although the limb observations were not well suited to detect such a feature, it should have appeared in some measure.

Figure 2 shows a k-ω power plot derived from the disk-center observations. The differences between this plot and that given in Figure 1 are immediately apparent. Most notably, the region of low-frequency power has grown until there is no clear distinction between it and the five minute oscillations, at least at low

wavenumbers. On the other hand, the resolution has improved so that, at higher wavenumbers (above 0.8 Mm^{-1} at .02 s^{-1}), the ridge structure of the five minute oscillations can be clearly distinguished. The ridges corresponding to radial numbers of 0 and 1 are particularly well shown, and those corresponding to 2 and 3 are discernible. The apparent noise level in this region of the k-ω diagram is extremely low, corresponding to a value for $(\delta I/I)^2$ of less than 5 x 10^{-14} per frequency-wavenumber bin. Evidently photographic techniques are very effective in this area of the diagram. Unfortunately, their performance along the axes k = 0 and ω = 0 is less inspiring. Stationary imperfections in the image (dirt on the optics, internal reflections) cause spurious power at ω = 0. Similarly, variations over time in the development process tend to cause low-wavenumber fluctuations at all frequencies. It will thus be difficult to use this technique to learn much about oscillation modes with periods comparable to the length of a timestring, or with wavelengths comparable to the size of the photographic frame. Further, the difficulty of obtaining accurate photometric calibration at any period or wavenumber may cause some uncertainties in the derived velocity/intensity ratios. In spite of these difficulties we can tentatively conclude that the intensity amplitudes of the five minute oscillations are larger at the limb than at disk center, while for fluctuations at low frequencies and wavenumbers this trend is reversed. These facts suggest that the intensity fluctuations responsible for the observed power arise high in the photosphere for the five minute oscillations, and much lower for oscillations of lower frequency and wavenumber.

Work is continuing on the analysis of these observations with two chief aims. The first of these is to determine, for a number of regions within the range occupied by the five minute oscillations, the ratio of rms amplitudes for velocity and intensity. For this purpose the velocity measurements will not be simultaneous with the intensity measurements, since the former must be taken from the literature. Our second goal is improvement in observing and averaging techniques so that k-ω diagrams of intensity may be obtained more conveniently and with improved noise levels and resolution. Once such methods are available, it should be possible to refine the estimates of velocity/intensity ratios, extend these estimates to larger areas in the k-ω plane, and perhaps obtain these ratios using simultaneous observations of velocity and intensity.

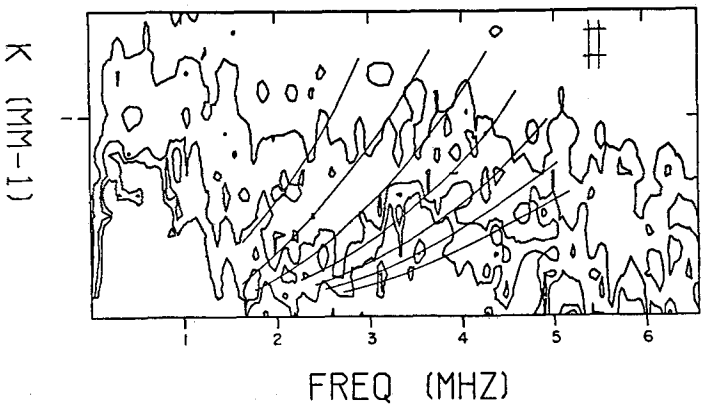

Figure 1. The k-ω diagram derived from limb intensity observation.

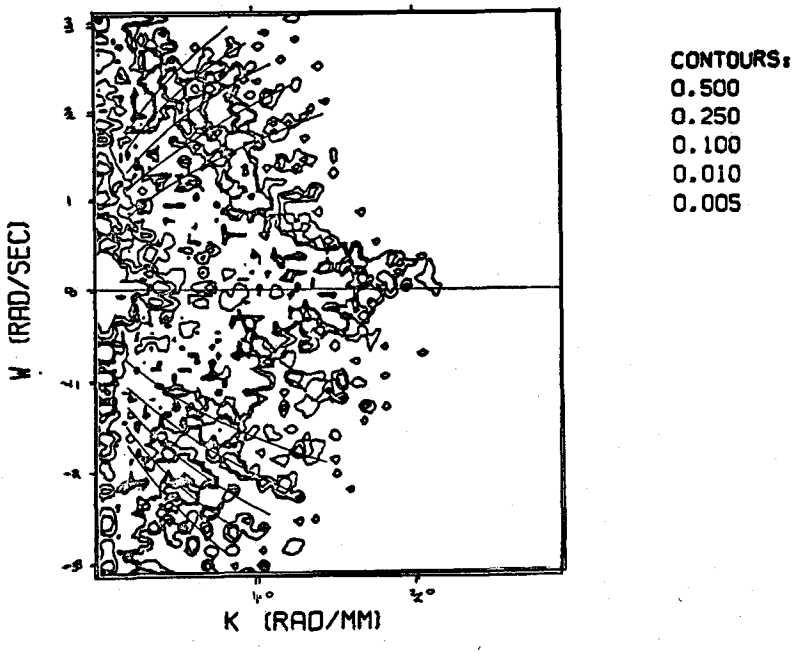

Figure 2. The k-ω diagram derived from disk-center intensity observation.

REFERENCES

Brown, T.M. 1979, Ap. J., 230, 255.

Brown, T.M., Stebbins, R.T. and Hill, H.A. 1978, Ap. J., 223, 324.

Deubner, F.-L. 1975, Astr. Ap., 44, 371.

Deubner, F.-L. 1977, Astron. Astrophys., 57, 317.

Hill, H.A., Caudell, T.P. and Rosenwald, R. 1977, Ap. J. (Letters), 213, L81.

Hill, H.A., Rosenwald, R. and Caudell, T.P. 1978, Ap. J., 225, 304.

Rhodes, E.J., Jr., Ulrich, R.K. and Simon, G.W. 1977, Ap. J., 218, 901.

RECENT OBSERVATIONS OF SOLAR OSCILLATIONS AT SCLERA

T.P. Caudell, J. Knapp, H.A. Hill and J.D. Logan
Department of Physics
University of Arizona
Tucson, Arizona

ABSTRACT

This work deals with the subject of global solar oscillations. These oscillations are observed as fluctuations in the diameter of the sun. A diameter is determined by a mathematical solar edge definition at the SCLERA[1] instrument. The oscillations have periods ranging from a few minutes to several hours and have amplitudes measured in millionths of a solar radius. These small amplitudes are observable only due to the unique properties of the edge definition. The properties of the observed solar oscillations are determined from the data; their statistical significance and repeatability are then tested.

1. INTRODUCTION

The reported discovery of global long period solar oscillations has raised many questions among the scientific community, some expressing doubt as to their existence, others expressing uncertainty as to their origin. The previous works of Hill and Stebbins (1976); Brown, Hill and Stebbins (1978); Hill and Caudell (1978) have categorically addressed the problems of defining the edge of the sun, sources of noise in diameter measurements and alternate interpretations of the results as well as the statistical significance of the global oscillation interpretation. In this paper we discuss the current set of solar diameter measurements, their analysis and their significance.

The observations discussed within this work were gathered at the SCLERA facility, a telescope located in the Santa Catalina Mountains northeast of Tucson. This instrument has been described in much detail elsewhere (Stebbins 1975) and therefore will not be readdressed here. A new set of solar oscillation measurements which were obtained in the spring of 1978 are presented. Comparison with previous

---

[1]SCLERA is an acronym for Santa Catalina Laboratory for Experimental Relativity by Astrometry, jointly operated by the University of Arizona and Wesleyan University.

data is made and the repeatability of the phenomena demonstrated. The temporal phase coherency of the newly observed oscillations is examined and the statistical significance determined.

2. OBSERVATIONS

The raw oscillation data consists of time strings of relative solar diameters; relative in the sense that no absolute diameter is measured. A mathematical definition of the solar edge, referred to as the finite Fourier transform definition (Hill, Stebbins and Oleson 1975) or FFTD hereafter, was applied to diametrically opposite limbs. This edge definition has several important properties. The first is that the FFTD has a vastly decreased sensitivity to atmospheric "seeing" compared to other definitions. The second is that the FFTD has enhanced sensitivity to intensity fluctuations which peak sharply at the limb and manifest these fluctuations as diameter changes (see paper by Knapp et al. in this work.) These two properties conspire together to allow the detection of solar oscillations from earth-based observatories.

3. DATA ANALYSIS

In detail, the new observations consist of 18 days of equatorial diameter measurements interspersed between May 21 and June 12, 1978. A diameter was recorded digitally every 8 seconds after being filtered by a digital low pass R.C. type filter with a time constant of 16 seconds. These were later averaged together in groups of 8 to form a time string sample of every 64 seconds. Corrections for atmospheric refraction were calculated and made to the data followed by a least squares fit parabola. The resulting time strings, which ranged between 200 and 500 points, were multiplied by a cosine bell apodizing function which tapered the first and last 10 percent to zero and padded zeros out to 2048 points. Standard fast Fourier transforms were then computed, normalized to the number of points in the actual data string and stored.

4. INTERCOMPARISON OF OBSERVATIONS

For the 13 longer time strings, power spectra were computed and a 13 day average was formed. This average is plotted in Figure 1 as a function of frequency in milliHertz. Note the general character; a series of peaks with varying heights superimposed on a variable background. There is a larger than average feature at the very low frequencies which partially results from incomplete atmospheric refraction correction, but otherwise the average peak plus background height remains nearly constant. How does this spectra compare to those obtained previously; that is, how repeatable is this result?

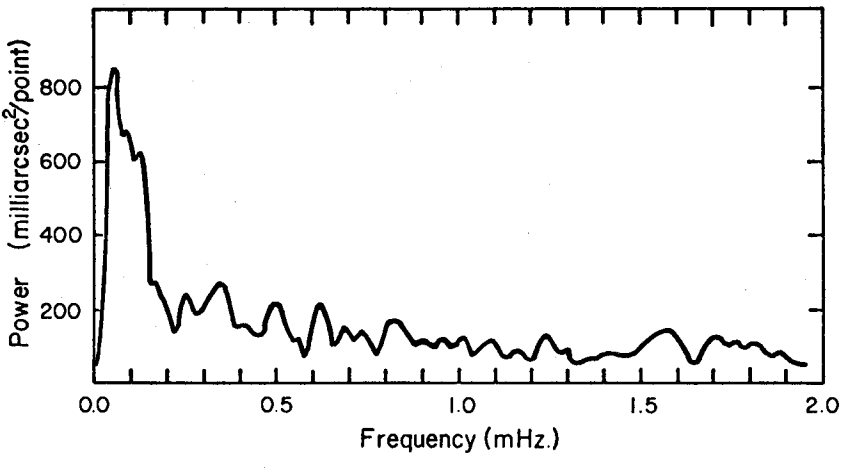

Figure 1. The average of 13 daily power spectra.

To answer this important question we have made a thorough comparison between the newest data and that of Brown et al. (1978) taken in the fall of 1975. The two aspects considered are (1) the repeatability of the frequencies present in the spectrum, and (2) a comparison of the peak heights to background ratio, a measure of the noise both solar and nonsolar. We will address these tests in order and place the results in Table 1. In the final section, the phase coherence of the new observations will be discussed along with their statistical significance.

To begin with, the two sets of observations are listed as the first item in Table 1. Note that the 1975 set was mixed between solar equator and pole whereas the 1978 data was taken entirely at the equator. As the second item in the table we give the average length of the daily observing run with the standard deviation of each average following the appropriate time. Third in the list is the FFTD scan amplitude used for the data sets. This amplitude specifies the amount of the solar limb used in the computation of the edge definition and dictates the sensitivity of the observations to variable sized spatial structures (Hill 1978) which may be present on the solar surface. This property will be examined more closely in a later paragraph. We now turn to the comparison of average power spectra.

When comparing power spectra, a peak will be defined as a low-high-low combination of contiguous points in power and we will call frequency alignment of peaks between the two separate spectra the instance when the maximum power occurs in the same 30 microHertz wide frequency bin (the resolution of the data sets). When all peaks are considered under the above criteria, 20 peaks are in frequency alignment between the 1975 and 1979 spectra. For a purely random source of diameter fluctuations, one expects approximately one-third of the total number of peaks to be in alignment by this selection criteria. The reason for this is simply that it takes three frequency bins to define a peak, one high and two low, yielding a one in three chance for a random alignment between another set of three bins. To calculate more carefully the probability that the alignment of 20 peaks could be of random origin a numerical simulation has been used. This is because the 1975 spectrum has 29 peaks where the 1978 spectrum has 36, giving trouble in the standard binomial coefficient technique.

To simulate the comparison process, a Monte-Carlo calculation was performed. The method was to generate a large number of pairs of spectra, 1.0×10^5 in this case, each with 29 and 36 peaks respectively placed at random frequencies within the 93 frequency bins in the interval of interest. The number in alignment is counted for each random pair and sorted into an accumulating histogram. The resulting histogram is given in Figure 2 where the area under the curve has been normalized to unity. This should be interpreted as the probability of n peaks aligning as a function of n for a totally random source. Taking the integral of this curve from n = 20 to 29, the maximum possible number in alignment, we find for the probability

Table 1. Comparison of Observations in Summary

Data Sets		1975	1978
1.	No. of days	11	13
	Equator	5	13
	Pole	6	0
2.	Ave. data length	$7^h \pm 1\overset{h}{.}6$	$6\overset{h}{.}2 \pm 1\overset{h}{.}9$
3.	FFTD scan amp.	13.6 arc sec	27.2 arc sec
4.	Number of peaks in frequency range 0.2 - 3.0 mHz	29	36
5.	Ave. peak to peak plus background heights ratio	35.8% ± 15.4%	33.8% ± 15.5%

$P(n \geq 20) = 9.4 \times 10^{-4}$. For a Gaussian distribution with half width equal to σ, this probability represents a 3.8 σ result away from such a random origin and is statistically a good indication of the repeatability of the phenomenon in nature.

One obvious question raised by this comparison is: Although the number of peaks in alignment appears to be statistically significant, should we not expect better agreement? Since we now have observational evidence that each peak in the spectrum is a superposition of several eigenstates of the sun each characterized by a different spatial structure on the surface, the filtering due to differing aperture size and the location of the aperture on the solar edge (i.e., pole or equator) will alter the average peak location (see Hill 1978). Also, over a period of time the mixture of states within a particular peak is likely to change depending on the nature of the driving mechanism. Any change in mixture (i.e., in amplitude of an eigenstate) will alter the combined power level of a peak as well as change its average location by small but significant amounts. With this understanding of the processes, the agreement between the two average power spectra must be considered good.

To address the second test enumerated above we must again go to the 1975 and 1978 average power spectra. Comparing the mean ratio of peak height to peak plus background height for the two averages gives an indication of differences in signal and noise. For the 1975 observations of Brown, Stebbins and Hill (1978) this mean was found to be 36%, to be compared with 34% for the new observations in the frequency range between 0.20 and 3.00 mHz and is listed as item 5 in Table 1. The second moment of the distributions of the ratios is examined by comparing the standard deviations for these ratios which are 15% and 16%, respectively. From this it can be concluded that the character of the two sets of data are quite similar and that the signal to background ratio has remained nearly the same.

5. PHASE COHERENCY

We now turn to the subject of phase coherency in the observed oscillations, a matter which has received much attention in the literature (Hill and Caudell 1979; Brown, Stebbins and Hill 1978; Keil and Worden 1980; Caudell and Hill 1979; Grec and Fossat 1979). Phase coherency has been reported in two previous works, inconclusively at first by Brown, Hill and Stebbins (1978) and more clearly by Hill and Caudell (1979) in a new analysis of the SCLERA 1973 oblateness data. In this latter paper, six oscillations were found to display coherence on 7 days' data spanning a 13 day period. The statistical significance of this result was examined more carefully by Caudell and Hill (1979). They concluded that the probability of producing these six phase solutions by random noise was 3.8×10^{-5} compared to 1.6×10^{-2} for a completely random signal. A similar phase analysis is performed with the new observations; a considerably more convincing result is found. The phases referred

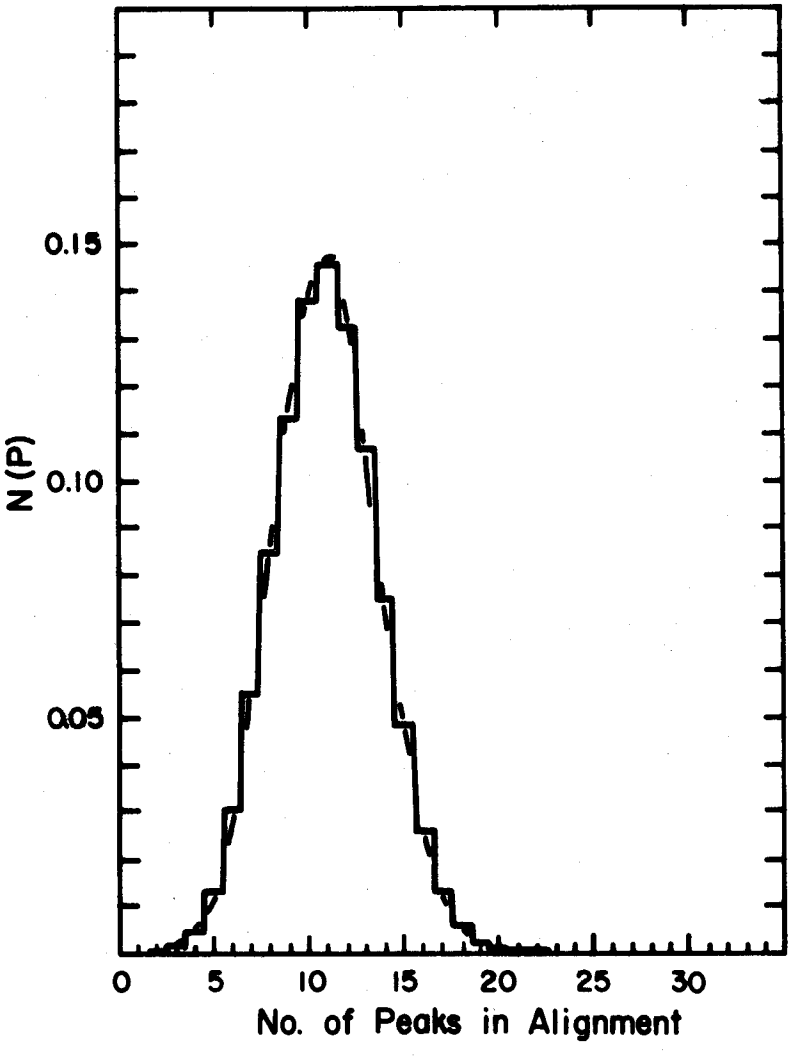

Figure 2. The Monte-Carlo generated probability density function for estimation of the likeliness that N peaks will randomly align when comparing two power spectra containing 29 and 36 peaks respectively.

to are determined from the daily Fourier transforms of time strings of fluctuation in the observed solar diameter. Since these are, by definition, only determinable to within a multiple of 2π on each day, coherence is found when a relatively straight line can be produced by the addition of certain multiples of 2π to each day's phase. The statistical significance of a phase solution is judged by the size of the residuals around the straight line, that is, the standard deviation, σ, of the linear fit.

For the peaks in power confined to the frequency range 0.2 to 1.05 milliHertz, all 18 days of 1978 data were analyzed for phase coherency. This was achieved through the use of an automatic procedure which, when given the 18 daily phases over the 23 day span, would sweep a least squares fit straight line through individual multiples of 2π until the best fit was found. Each solution found in this way was then manually confirmed to be indeed the best. This was repeated for the 12 peaks in the frequency range under study. The final solutions for these oscillations have been plotted in Figures 3, 4, and 5 with the multiples of 2π added in as a function of day number. The σ for these linear fits range between 0.6 rad and 1.0 rad. Note that like the work of Hill and Caudell (1979), the phase solutions have been iterated to bring consistency between the frequency and the slope of the phase solution. The question now is what is the probability that this level of coherency is produced by a random source?

The estimation of probabilities concerning the statistical significance of natural phenomena can be difficult in certain instances, particularly when small samples are concerned. Analytical techniques usually involve a model of the statistics, including the assumption of a probability distribution, based on the apparent "noise" in the data. Probabilities calculated from models like these are inherently sensitive to the assumptions and, therefore, may lead to differing results. An example of a phenomenon where this has proved a problem is discussed by Caudell and Hill (1979). Here, we again use a more direct approach and resort to a Monte-Carlo numerical simulation. The problem of statistical modeling is then alleviated at the sacrifice of large amounts of computer time. For this calculation, a set of 18 random phases was chosen between 0 and 2π. These were then placed in the daily arrangement indicated by the data set over the 23 day span. These random phases were then given to the same automatic solution finding routine used on the real data, the best linear fit found and the σ computed. This sigma was then stored in the appropriate bin of an accumulating histogram and the automatic procedure repeated with the choice of 18 new random phases. The resulting histogram generated from 5,000 trials is given in Figure 6 where a bin size of 0.03 radians was used. The area under the curve has been normalized to unity. Care must be taken in not performing too few trials in any Monte-Carlo simulation and, therefore, stability of the result must be empirically determined.

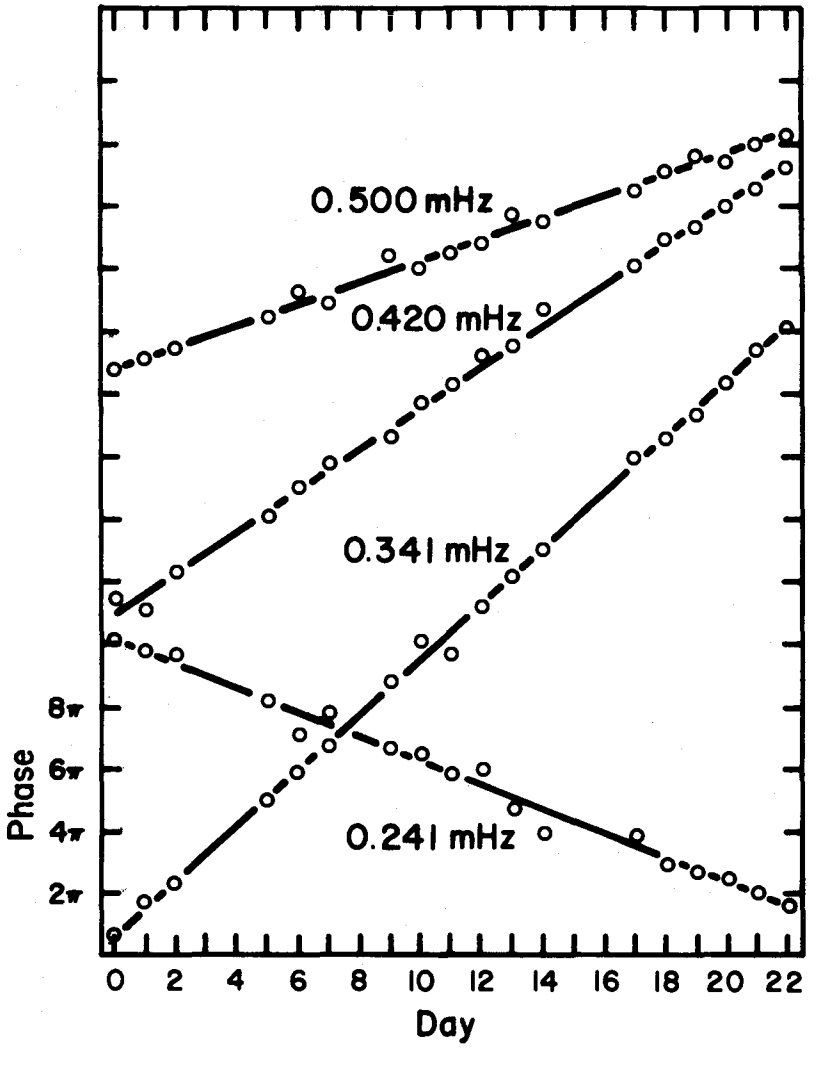

Figures 3. The phase solutions for 12 frequencies plotted against day number. A least squares fitted line has been drawn through the phases. The individual frequencies are placed on the plots.

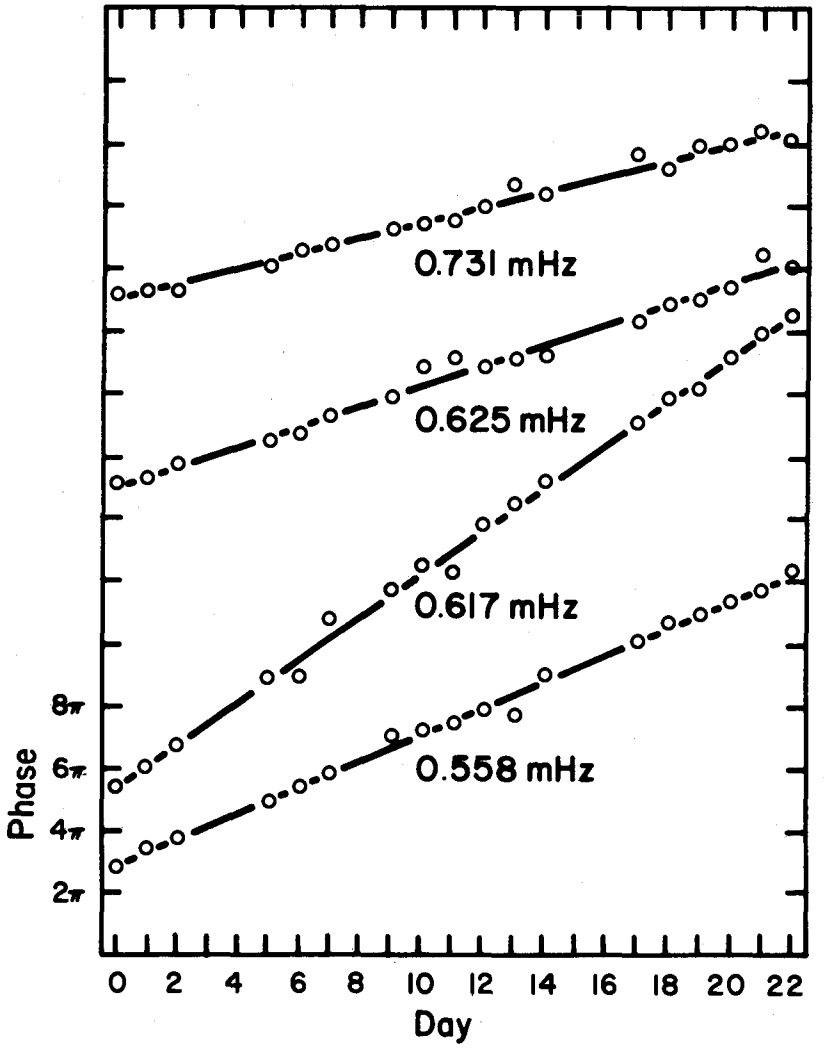

Figures 4. The phase solutions for 12 frequencies plotted against day number. A least squares fitted line has been drawn through the phases. The individual frequencies are placed on the plots.

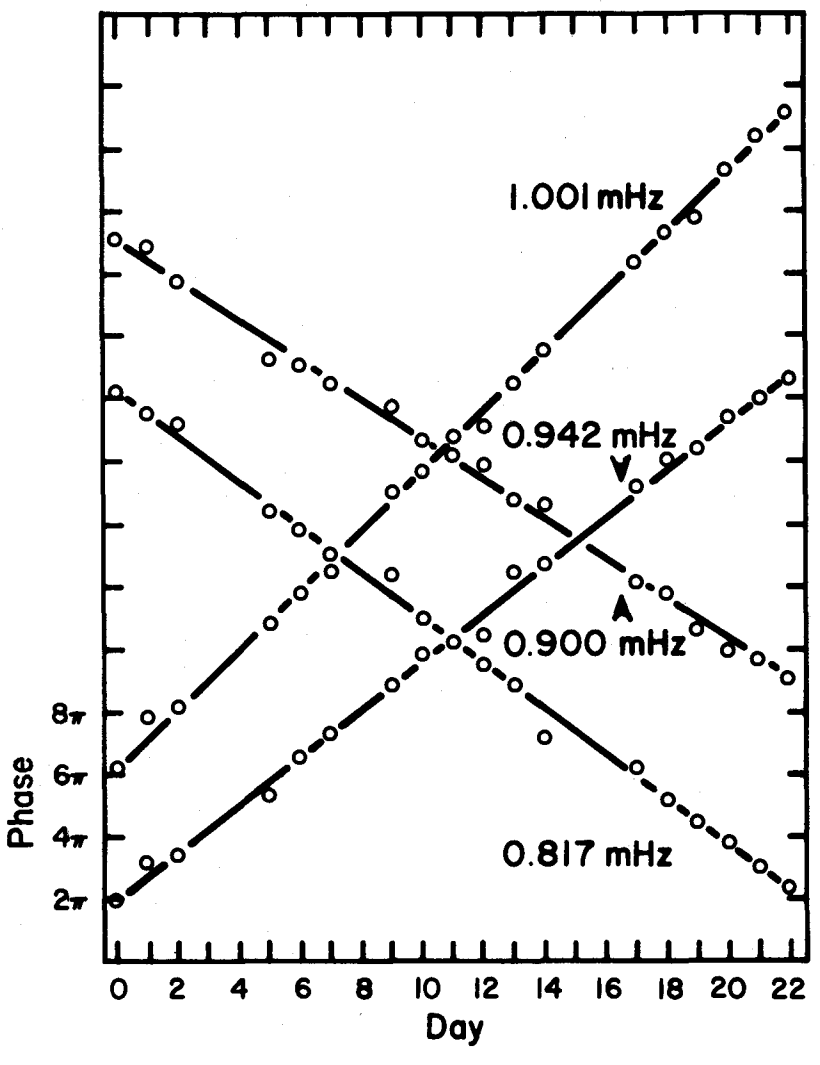

Figures 5. The phase solutions for 12 frequencies plotted against day number. A least squares fitted line has been drawn through the phases. The individual frequencies are placed on the plots.

Upon examining Figure 6 we see that the sigmas associated with the real data fall well away from the peak, which occurs near 1.2 rads. In fact, there are several instances where the σ obtained from the observations are sufficiently low that the Monte-Carlo simulation with 5,000 trials failed to yield a non-zero result in the histogram. To evaluate the randomness of a particular linear fit to the phase data we compute the probability that a random noise source will lead to a sigma less than or equal to the observed value. This probability is given by the integral of the distribution in Figure 6 from zero to the observed sigma. This function is plotted in Figure 7 as a function of a particular sigma. The range of observed sigmas is plotted on Figure 7. From this we conclude that on an individual basis the probability that a single phase solution is produced by a random noise source is on the average 4×10^{-3} compared to an expected value for pure randomness of 0.5. Taken as a set of 12 independent observations the resultant probability would be the product of these 12 individual probabilities, producing an incredibly small probability. This phase data constitutes one of the strongest pieces of evidence for the global nature of the solar oscillations to date.

In summary, the new set of solar diameter measurements made at SCLERA confirms the existence and repeatability of the solar oscillations and lends strong evidence to their global nature.

* * * * *

The authors wish to acknowledge many helpful discussions with Douglas Gough, Jørgen Christensen-Dalsgaard, W. Dziembowski, Randall Bos and Raymond Zanoni and also the help of Paul Ballard and Robert Snyder in preparing certain aspects of the SCLERA instrument for this data run.

This work was supported in part by the National Science Foundation and the Air Force Geophysical Laboratory.

REFERENCES

Brown, T.M., Stebbins, R.T. And Hill, H.A. 1978, Ap. J., 223, 324.

Caudell, T.P. and Hill, H.A. 1979, Mon. Not. R. Astr. Soc., Short Communications (submitted).

Grec, G. and Fossat, E. 1979, Mon. Not. R. Astr. Soc., Short Communications (in press).

Hill, H.A. 1978, in The New Solar Physics, (ed. J.A. Eddy; Boulder: Westview Press), Chapter 5.

Hill, H.A. and Caudell, T.P. 1978, Mon. Not. R. Astr. Soc., 186, 327.

Hill, H.A., Stebbins, R.T. and Oleson, J.R. 1975, Ap. J., 200, 484.

Keil, S.L. and Worden, S.P. 1980, these proceedings.

Knapp, J., Hill, H.A. and Caudell, T.P. 1980, these proceedings.

Stebbins, R.T. 1975, Ph.D. thesis.

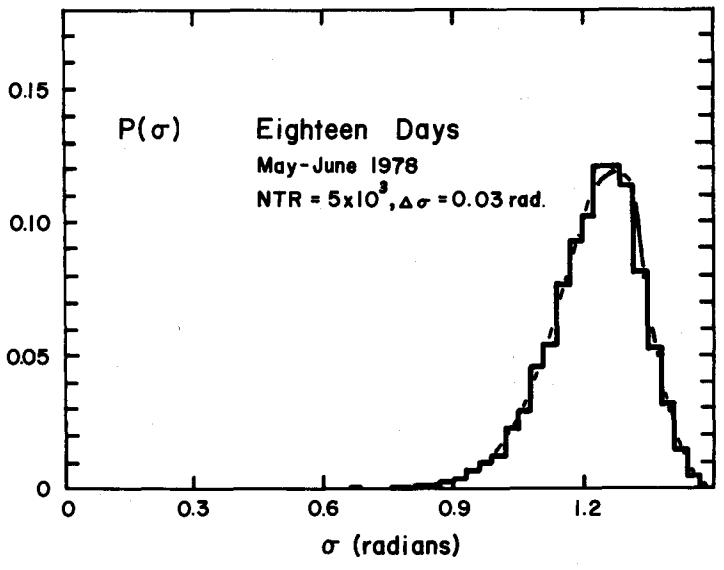

Figure 6. The Monte-Carlo generated probability density function. Random phases are used to compute the distribution of standard deviations, σ, expected for pure noise in phase solutions like those in Figures 3, 4, and 5.

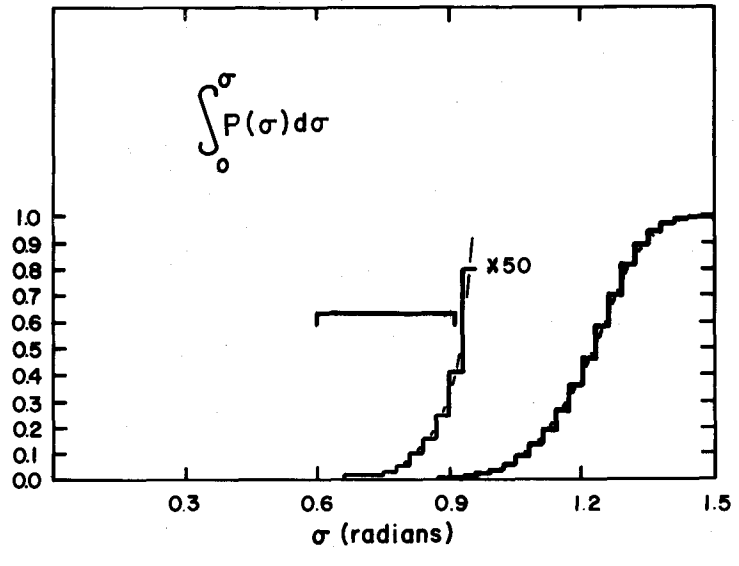

Figure 7. The integral of the distribution in Figure 6 from zero to a particular value of σ as a function of that σ. From this the probability that the phase solution fits in Figures 3, 4, and 5 and might be produced by pure noise may be estimated.

SOURCES OF NOISE IN SOLAR LIMB DEFINITIONS

S.L. Keil[1] and S.P. Worden
Air Force Geophysics Laboratory
Sacramento Peak Observatory[2]
Sunspot, New Mexico

ABSTRACT

We postulate that the rotation and evolution of solar surface structure can function as a source of noise in solar limb definition measurements. To test this hypothesis, we have produced a time series of 216 spectroheliograms taken at two minute spacings. These spectroheliograms were obtained in an Fe I line, formed at a depth similar to optical depth unity at the limb. We foreshortened this data in order to simulate the solar limb brightness profile and passed it through the finite Fourier transform definition (FFTD) algorithm used by Hill and his collaborators at SCLERA. In this work we were able to determine the amount of variation in solar limb position which is attributable to evolutionary changes in solar surface structure. We also artificially rotated one of these surface structure functions in order to determine the effects which surface structure rotation might have on limb position. In this paper, we conclude that rotation alone can produce power only at low frequencies ($\omega \lesssim 1$ mHz). However, the evolution of solar surface structure exhibits a power spectrum which is similar to that observed with the SCLERA instrument at all of the frequencies. We also show that standing surface structure patterns can produce phase for a period of seven days such as the phase coherence found in the observations at SCLERA, although in the case of the latter, the periods are significantly longer.

1. INTRODUCTION

Periodic changes in the apparent solar diameter have been observed by Hill and his co-workers (Brown, Stebbins and Hill 1978; Hill, Stebbins and Brown 1975) at the Santa Catalina Laboratory for Experimental Relativity by Astrometry (SCLERA); these are thought to result from global oscillations of the entire sun. Other workers, attempting to observe similar periodicities in large-scale velocity patterns (Grec and Fossat 1976; Brookes, Isaak and van der Raay 1976; Dittmer, Scherrer and

---

[1]NAS/NRC Resident Research Associate.

[2]Operated by the Association of Universities for Research in Astronomy, Inc. under contract AST 78-17292 with the National Science Foundation.

Wilcox 1977; Dittmer 1978), and intensity (Musman and Nye 1977; Livingston, Milkey and Slaughter 1977; Beckers and Ayers 1977) have had little success. Brown, Stebbins and Hill (1978) point out that interpretation of the latter observations and their comparison with diameter measurements are difficult. In fact, apparent solar diameter oscillations can result from a number of sources. Using Hill's limb position definition, changes in opacity or temperature structure can lead to an apparent change in the solar diameter without the presence of any mass motion; thus, the unsuccessful search for velocity oscillations does not confirm or refute the diameter measurements. Similar problems occur in the interpretation of intensity observations; consequently, the inability of other observers to find brightness oscillations does not negate the SCLERA results. Several investigators have examined the possibility that the SCLERA results may, in part, be attributable to changes in the earth's atmospheric transmission (Fossat and Ricort 1975) or to changes in solar surface structure (Worden and Simon 1976).

We have computed the effect of evolutionary changes in solar intensity patterns upon measurements of the apparent solar diameter which use the finite Fourier transform definition (FFTD) of the solar limb position (Hill, Stebbins and Brown 1975). The properties of the FFTD limb position definition are discussed by Hill, Stebbins and Brown (1975) and Brown, Stebbins and Hill (1978). To briefly review the FFTD, the limb position is obtained from the transform:

$$F(G;\ r,a) = \int_{-1/2}^{1/2} G(r + a \sin \pi s) \cos (2\pi s)\, ds \qquad (1)$$

where r is the radial distance from the center of the sun, a the distance over which the slit is scanned, and G(r) is the limb darkening profile. With a fixed value for the scan amplitude a, the limb position is that value of r for which F = 0. In practice, the definition is implemented by scanning a slit sinusoidally across the solar limb. By varying the scan amplitude a, and making scans both at the equator and pole, effects due to solar oblateness can be separated from brightness effects (changes in the limb darkening function). By observing for periods lasting from 7 to 9 hours on 11 different days, Brown, Stebbins and Hill (1978) have generated a mean power spectra of the limb position which shows periodicities at a number of frequencies. Their data have also been tested for peak repeatability. They found that approximately 2/3 of the stronger peaks were coincident between the first and second halves of their data. The SCLERA investigators have also shown that a degree of phase coherence may exist for many of these frequencies (see Figure 1 of Hill and Caudell 1979). The coherence is manifested as a constant phase drift in time shown over a number of days. Their measurements were made with a 100" long slit oriented parallel to the solar limb and a scan amplitude (a) of 13."6. The observed periodicities compare well with those predicted by Christensen-Dalsgaard and Gough

(1976) based upon models of the solar interior.

In order to test how evolutionary changes in solar intensity patterns affect the zero point of equation (1), and thus the limb position, we observed intensity patterns at disk center over a period of several hours in a line formed at an optical depth similar to an optical depth of unity at λ5500 A in the continuum near the solar limb. These observations were artificially rotated to the limb in order to generate a time-dependent limb darkening function $G_t(r)$ which was then used in equation (1). A time-dependent solar limb position, $r_{limb}(t)$, was thus generated as a function of both evolutionary and rotational changes in solar surface structure. We then searched $r_{limb}(t)$ for periodicities and have compared our results with those of Brown, Stebbins and Hill (1978).

In § 2 we describe the observations, their subsequent reduction and some of the problems that arise in their interpretation. Section 3 considers periodicities in the data and their origins. Finally, in § 4, we discuss the implications of our findings for experiments designed to measure the solar limb position using the FFTD definition.

2. OBSERVATIONS AND REDUCTION

The observations consist of a time sequence of spectroheliograms made at disk center, using the universal birefringent filter on the Sacramento Peak Tower Telescope (30-inch aperture). They were made in the core of Fe I 5171 which has a mean height of formation approximately 450 km above optical depth unity at λ = 5500 A. A filtergram was taken every two minutes during a period of 7.2 hours. Other relevant data pertaining to these filtergrams are: bandpass - 1/8 A; exposure time 1/4 sec; image scale .102 mm/arcsec; image size 215" x 147" on the sun. One such filtergram is shown in Figure 1 along with a similar filtergram taken simultaneously in the continuum.

Each frame was digitized, using the Sacramento Peak fast microphotometer, sampling every 1/2" (360 km) along both axes with a Gaussian spot whose FWHM was 1."5. The characteristic curve of the film, obtained from step wedges and calibration spots, was used to convert microphotometered film densities to intensities. Thus the observations are reduced to two-dimensional intensity patterns, $I_t(x,y)$, obtained at 216 points in time, each separated by two minutes. The x axis is 215" long and parallel to the equator; the y axis is 147" long and perpendicular to the equator. The effect of the slit used in the FFTD limb position definition is to integrate the light along the y-axis with equal weighting, and along the x-axis with weighting determined by equation (1). Thus the intensity pattern at each time t was averaged over the y axis to obtain

$$I_t(x) = 1/N_y \sum_{i=1}^{N_y} I_t(x,y_i) \qquad (2)$$

where N_y is the number of digitized points along the y axis.

To remove the effects of sky transparency changes, uneven exposure and development and large-scale changes caused by film irregularities over distances on the order of the frame size, we fit a second order polynomial to $I_t(x)$ at each time t, using least squares. If $I_t(x)$ is the fitted polynomial at time t, we then compute

$$I'_t(x) - I_t(x)/\tilde{I}_t(x) \quad . \qquad (3)$$

Thus any real change in the average solar intensity from one frame to the next is lost, as well as any spatial changes with dimensions on the order of the frame size.

Variation in transmission from point to point on the filter will be independent of time. Thus, by averaging $I'_t(x)$ over all of the frames, we can obtain the filter profile and remove it from the data. Another set of data is thereby generated; this is given by:

$$I''_t(x) = I'_t(x)/\frac{1}{N_t} \sum_{i=1}^{N_t} I'_{t_i}(x) \qquad (4)$$

where $N_t = 216$ is the total number of frames. The suppression of intensity variations that are caused by local film irregularities is perhaps the most difficult problem. In order to get an estimate of their contribution to the data, a final set of data is generated in which adjacent frames are averaged together so that

$$I'''_t(x) = \frac{1}{2}\left[I''_t(x) + I''_{t+\Delta t}(x)\right] \quad , \qquad (5)$$

where $\Delta t = 2$ minutes. Besides averaging out film irregularities, this 2 minute sampling rate may also suppress contributions from the 5 minute oscillations.

The time dependence of the limb darkening function G(r) is next obtained from the observed intensity fluctuations $I_t^P(x)$, where P can represent one or more primes. This is done by artificially rotating $I_t^P(x)$ to the limb. We assume that G(r) will undergo variations similar to those observed at disk center, where the variations are reduced by foreshortening and by horizontal transfer. Since we have chosen a line formed at approximately the same height as the continuum at the limb, horizontal transfer will affect the contrast of very small features such as granulation; however, large-scale features will be affected only at the extreme limb, where foreshortening has already dropped the contrast to almost zero. Variations in G(r) may also be produced at the equator by rotation of the observed intensity patterns

through the field of view.

The artificial rotation is accomplished by rotating the first point in $I_t^P(x)$ to a position near the limb, such that the remainder of the data string extends just beyond the limb. This process is shown schematically in Figure 2 where the original data, lying between points A and B, is rotated to lie between points A'' and B''. The data is then resampled in equal increments of solar radius (Δr) near the limb. All of the elements of $I_t^P(x)$ falling into a given Δr increment are then averaged, thereby accounting for foreshortening. The data is next multiplied by a time independent limb darkening function $G_0(r)$ to produce

$$G_t^P(r) = G_0(r) I_t^P(r) \tag{6}$$

where $I_t^P(r)$ is obtained by the resampling of $I_t^P(x)$. An example of the reduction process for one frame is shown in Figure 3.

The apparent FFTD limb position $r_{limb}(t)$ is then generated as a function of time by substituting $G_t^P(r)$ into equation (1) and searching for the value of r for which the integral in equation (1) is zero.

In order to determine the relative contributions of large or small-scale fluctuations in $I_t(x)$ to variations in $r_{limb}(t)$, and thus the importance of including smearing due to horizontal transfer, $I'_t(x)$ is smoothed to suppress intensity variations smaller than 12,000 km. The variations greater than 12,000 km are also divided out so that only small- scale fluctuations remain. This procedure showed that almost all of the observed signal comes from features larger than 12,000 km; furthermore, horizontal transfer is only of minor importance in suppressing the limb position fluctuations generated by changes in the limb darkening profile. Calculations designed to simulate horizontal transfer were performed and it was found that the fluctuations in $I'_t(x)$ were suppressed by factors of 0.5 and 0.1.

The significance of our results was examined by looking at purely random signals. Using a random number generator, we have generated sets of data, $I_t^R(x)$, and passed them through the analysis described above. The random data were multiplied by factors which gave them the same rms variations as our observational data. Random data which fluctuated over both large and small scales were tested in this manner.

In addition to intensity changes which occur during the course of solar evolution, the intensity pattern at the limb may be altered by the effects of solar rotation upon the equatorial regions. To test the effects of solar rotation alone, one of the aforementioned solar limb profiles was artificially rotated across the limb at intervals corresponding to three minutes of rotation. The rotated profile was then passed through the FFTD as described above to determine the possible variation in limb position produced solely by the rotation of a fixed solar intensity

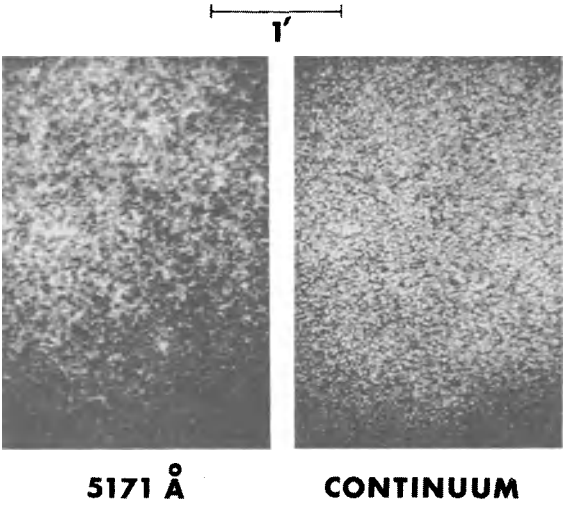

Figure 1. Sacramento Peak filtergrams obtained in the Fe I 5171 A line and simultaneously in the continuum showing surface structure. A sequence of 216 of these were used in this analysis.

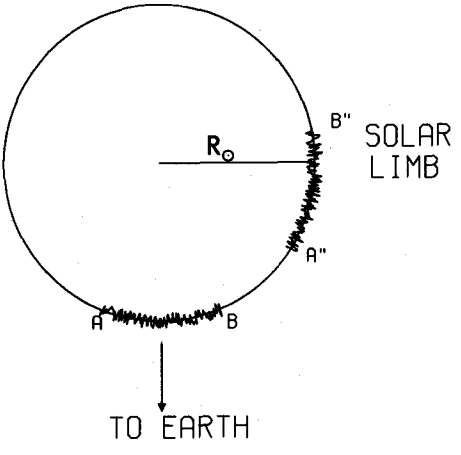

Figure 2. A schematic representation of the sun (not to scale). The filtergrams shown in Figure 1 are obtained between points A and B. The data is then rotated artificially to lie between A'' and B'' and then resampled to take foreshortening into account.

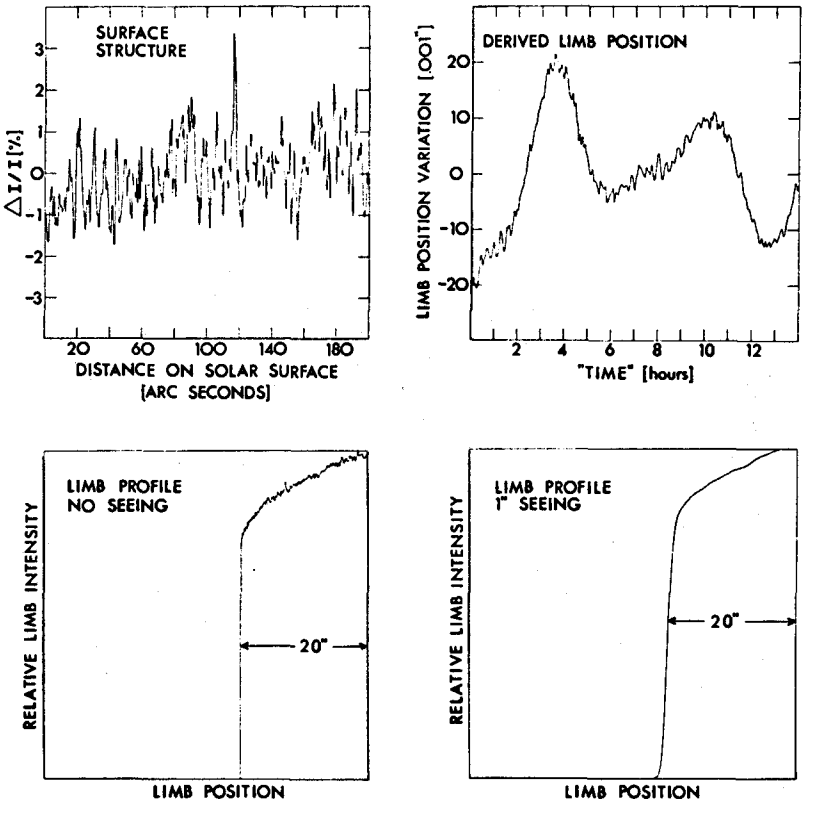

Figure 3. A filtergram such as that shown in Figure 1 reduced to one dimension (upper left), foreshortened and limb darkened to represent the actual intensity at the solar limb; without seeing (lower left), with 1" seeing (lower right). In the upper right is an example of variations in the derived FFTD limb position when this pattern is allowed to rotate around the limb.

pattern around the solar limb. The simulated rotation was computed for 256 time steps, effectively modeling the solar rotation for 13 hours. The variations in limb position, generated by both evolutionary and rotational changes, were then Fourier analyzed. An example of the limb position changes generated by rotation is given in Figure 3 along with illustrations of various steps in the reduction process.

3. RESULTS

3.1. Observed Periodicities

Figure 4 shows the temporal power spectra of limb position fluctuations, $r_{limb}(t)$, generated from: (a) $I'_t(x)$ $[r'_{limb}(t)]$; (b) $I''_t(x)$ $[r_{limb}(t)]$; (c) $I_t(x)$ smoothed over 31 spatial points in order to remove features smaller than 12,000 km; and (d) $I'_t(x)$ divided by a 31 point running mean of $I_t(x)$ so that only features smaller than 12,000 km remain. Figures 4c and 4d show that most of the fluctuations generated by the raw data result from large-scale features, affirming the proposition of Brown, Stebbins and Hill (1978) that small-scale features will have a negligible effect.

The average power levels for $r'_{limb}(t)$ [$\sim$ 40 (milliarcsec)^2] and for $r_{limb}(t)$ [$\sim$ 30 (milliarcsec)^2] are higher than the value of 25 (milliarcsec)^2 observed by Brown, Stebbins and Hill (1978). If we multiply the fluctuations in $I_t'(x)$ by 0.5 to simulate the effect of horizontal transfer, the average power level of the fluctuations in $r'_{limb}(t)$ drops to $\sim$ 12 (milliarcsec)^2. Since we have shown that most of the signal comes from large scale features, this may overestimate the effect of horizontal transfer on the fluctuations.

Table 1 offers a comparison of the periods of some of the stronger peaks shown in Figure 4a with the observations of Brown, Stebbins and Hill (1978) and with the predicted radial p-mode frequencies of Christensen-Dalsgaard and Gough (1976). Deubner (1977) has pointed out that, because of the almost continuous range of predicted periods, such a comparison cannot be used to prove that global oscillations have been observed. One must spatially resolve the various modes in order to make a meaningful comparison. Nevertheless, our calculation shows that many of the periods observed by Brown, Stebbins and Hill (1978) could originate from changes in solar intensity patterns. The source of these intensity changes, however, has not yet been addressed.

To test the effects of atmospheric seeing, we have convoluted the time-dependent limb darkening function $G'_t(r)$ with both 1/2 arcsec and 1 arcsec seeing before computing $r'_{limb}(t)$ from equation (1). Seeing of 1/2 arcsec increases the power by approximately 5% while 1 arcsec seeing decreases it by about 10%. This result confirms that the FFTD is largely independent of the effects of seeing.

The statistical reliability of the data shown in Figure 4 is very low. In order to increase the reliability, we have subdivided our data first into two

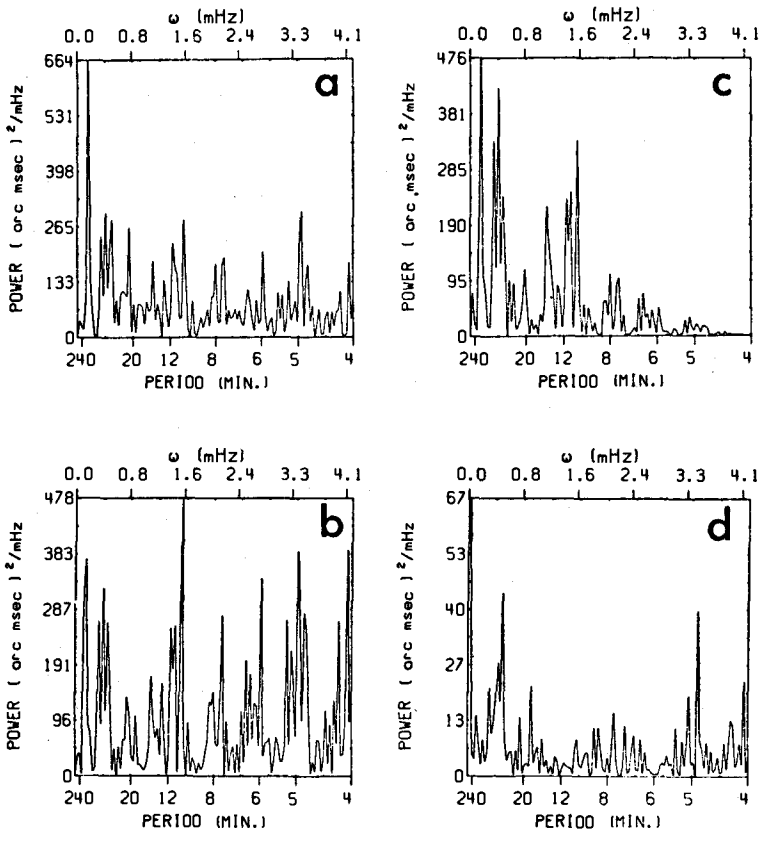

Figure 4. Temporal power spectra of limb position fluctuations found by passing the 216 limb intensity functions, such as shown in Figure 3, through the FFTD formalism. Before computing the FFTD limb positions used to generate each figure, we (4a) removed a second order polynomial from the intensity fluctuations (equation 3); (b) averaged together the intensity fluctuations on temporally adjacent frames (equation 5); (c) smoothed the intensity fluctuation over 31 spatial points to suppress features smaller than 12,000 km; and (d) removed features larger than 12,000 km by dividing each set of intensity fluctuations by a 31 point spatial running mean.

Table 1.

Observed Period (min)		Predicted Period (min)
This Study	Hill et al.	Christensen-Dalsgaard & Gough
	(above 95% conf)	
102.0		
	66.2	62.22
46.0	44.7	41.98
39.4	39.0	
32.0	32.1	32.32
	28.7	
		26.00
	24.8	
23.0		
21.3	21.0	21.51
	19.5	18.33
		15.95
14.6	13.3	14.13
12.8	12.1	12.64
11.6	11.4	11.54
10.4	10.7	10.60
	9.9	9.81
	9.3	9.12
	8.5	8.52
8.0	7.8	7.94
7.5	7.6	7.53
	6.9	7.12
	6.7	6.75
6.5	6.5	6.41
6.0		
5.2		
4.9		

subsets, each 3.6 hours long, and then into three subsets each 2.4 hours long. In the first case, our effective resolution is changed from .0386 mHz to .0772 mHz and in the second, to .115 mHz. The upper limit on periods that can be easily observed drops from approximately two hours to one in the first case and to approximately 45 minutes in the second. The positions of peaks with frequencies higher than $\sim$ .35 mHz are affected very little by the sectioning. The fact that many of the peaks survive the sectioning of the data indicates that they are of solar origin, and attributable to long-lived solar phenomena. The average power drops from 40 (milliarcsec)^2 to $\sim$ 25 (milliarcsec)^2 in the first case and to 16 (milliarcsec)^2 in the second. To make a quantitative estimate of the stability of the power spectra, similar observations over a period of several days are necessary.

Figure 5a shows the power spectrum which would result solely from rotation. Also shown is the average power spectrum observed by Brown, Stebbins and Hill (1978). We can immediately see that rotation produces almost no high frequency power. Once again, this is in line with the contention of Brown, Stebbins and Hill (1978) that small scale features (granulation) will have minimal effects on the FFTD. However, at frequencies less than 1 mHz, the mean power level is between 5 and 40 (milliarcsec)^2; this is clearly compatible with the SCLERA results and demonstrates that rotation of solar features alone can be a substantial source of noise. However, since the SCLERA results for the solar equator are very similar to those for the pole, where rotation has no effect, the indication is that the rotation of solar surface structure is not a dominant effect.

Spatial and temporal variations in $I_t(x)$ may arise from several sources. Changes in the average sky transparency, differential changes in the sky transparency across the aperture, uneven exposure or development of the film, changes in the film emulsion from one point to the next, variations in the transmission across the filter, and actual changes in the solar intensity pattern will all produce fluctuations in $I_t(x)$. In attempting to isolate true solar effects from other sources, some of the actual solar variations must also be suppressed. We may also underestimate some of the non-solar sources of intensity fluctuations. These two problems place a fundamental limit on the accuracy of our measurements, the magnitude of which is difficult to determine. Thus, these calculations should be interpreted as only a rough estimate of the possible solar effects on limb position determinations which use the FFTD definition. Nevertheless, the results are quite dramatic and show that the interpretation of apparent limb shift measurements is not a straightforward exercise.

3.2. Random Data and Phase Coherence

We have generated ten sets of random data for $I_t^R(x)$ (R = 1 - 10) and have used them to generate FFTD limb position fluctuations for which power and coherence

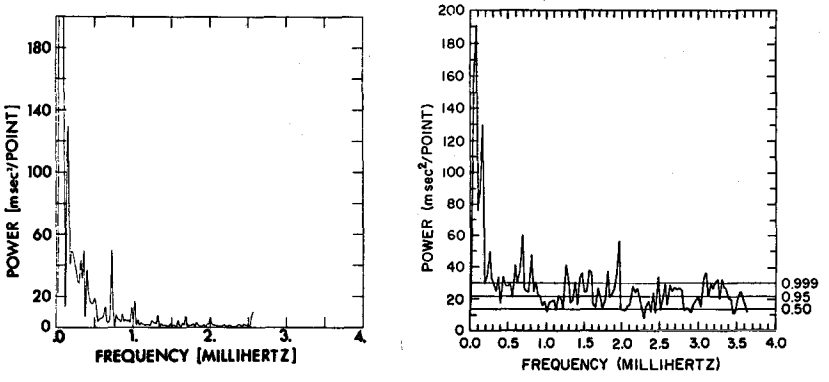

Figure 5. (a) Temporal power spectrum of limb position fluctuations that were generated by rotating a single limb intensity profile such as shown in Figure 3 around the limb. Each time step is generated by rotating the intensity profile an appropriate distance; thus excluding evolutionary changes in the surface intensity pattern.

(b) The temporal power spectra of limb position variations observed by Brown, Stebbins and Hill (1978).

spectra have been computed.

Each set of data was generated such that the mean spatial scale of the fluctuation is approximately 12,000 km and the rms variance is approximately 1%, in agreement with the observations. The individual power spectra have average power levels near 40 $(\text{milliarcsec})^2$ with several peaks well above this level. The positions of the peaks vary randomly from one spectrum to the next. All but one or two peaks for each of the ten spectra were removed by subdividing the data into three shorter sections and averaging together the resulting spectra.

In Figure 6a, we plot the coherence and phase spectra between two of the random data sets. Before computing the coherence spectra, the real and imaginary parts of the cross-power spectra and the individual power spectra were smoothed over five frequency points using rectangular weighting. Figure 6b shows the coherence and phase spectra obtained by averaging 9 separate spectra obtained from 9 different pairs of the random data. Figure 6a indicates that, with a limited data sample, some frequency ranges exhibit substantial coherence even though the data is random. A mean coherence of approximately 30%, shown in Figure 6b, could be expected from a large number of random data samples. This result shows that some "phase coherence" may result from purely random noise sources and that observed coherence should be interpreted with caution.

Hill and Caudell (1979) have found a constant phase drift at several different frequencies in data taken on seven different days; they argue that this supports the conclusion that their data is of solar origin and results from global oscillations. The fact that high coherence (60-80%) can be found in several frequency bands for random data indicates that caution is necessary in interpreting phase and phase changes. To test whether their technique for fitting a straight line through phases found on different days would produce similar results for random data, we generated seven random phases between 0 and 2π and assumed that the phases were measured on the days corresponding to their observations (i.e., the 8, 9, 10, 11, 19, 20, 21 of September, 1973). Following Hill and Caudell (1979), we held the phase on the first day constant and added multiples of 2π to the other phases until we obtained the best fit to a straight line. This process was repeated several hundred times so as to build up a statistical distribution of fits and rms error.

Table 2 gives the slope and rms error (σ) of the fitted lines found by Hill and Caudell (1979) at the six different frequencies. The average value of σ for the fits at the six frequencies is $\sim$ 0.75 radians. Figure 7 gives the distribution of σ's we found by fitting 300 different sets of random phases. The average slope of our fitted straight line was 1.63 radians/day with a standard deviation of 0.85 radians/day. The average value of σ was 0.756 radians and the standard deviation about the mean was 0.157 radians. Four of the values measured by Hill and Caudell fall within, and one value just outside, one standard deviation of our figure. The

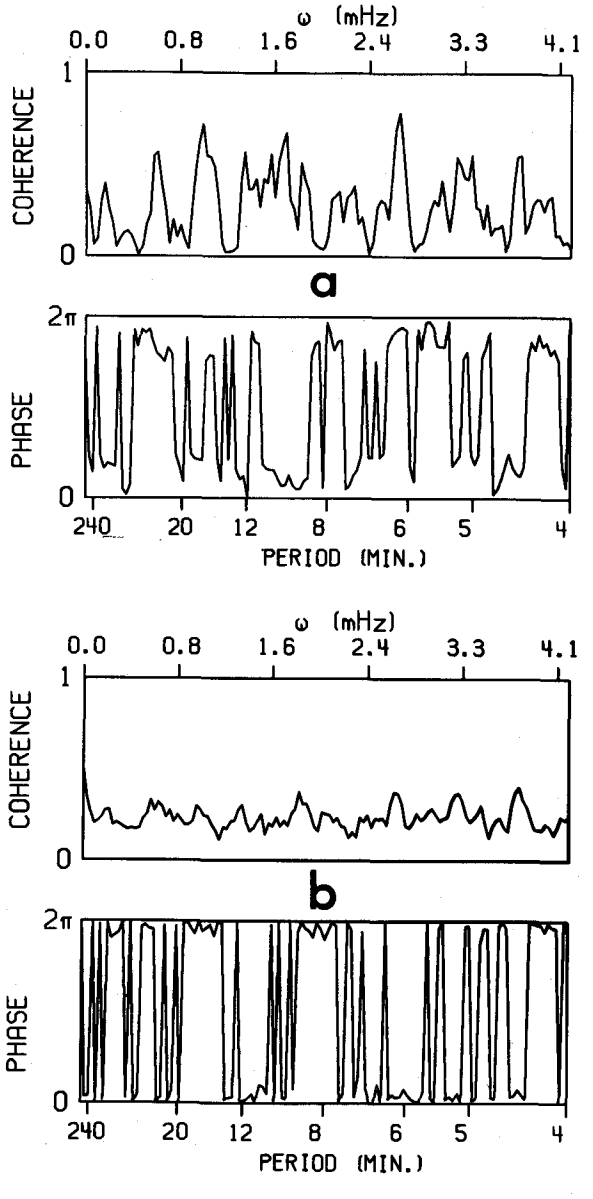

Figure 6. (a) Coherence and phase spectra between limb position fluctuations generated by passing two independent random data sets through the FFTD formalism.

(b) Coherence and phase spectra found by averaging together results such as those shown in Figure 6a for 9 pairs of random data.

value of σ they found at 0.606 mHz, which is much larger than expected from random data, is strongly influenced by one stray data point taken on the 21st of September (see Figure 1 of Hill and Caudell 1979).

Five of the values of σ found by Hill and Caudell are smaller than the average of our random distribution. They estimated the probability to be 3×10^{-12} that random data could exactly produce their result. However, the important question is not whether random data reproduces their particular results but whether it can produce or do better (smaller σ) than their results. Thus, the pertinent question is as follows: In six trials with random phases, what is the probability that five of the trials will give an error less than or equal to about 0.74 radians (their largest value excluding that found at 0.606 mHz)? From the distribution shown in Figure 7, we compute that the probability of getting a value of σ less than or equal to 0.74 radians in a single trial is 0.43. If we consider six trials with five outcomes resulting in σ's of this magnitude, the probability computed from the binomial distribution is 0.052. Furthermore, the probability that random phases would produce one fit better than 0.59 radians (their best fit) is 0.4. The chance that random numbers could produce the findings of Hill and Caudell is much higher than the 3×10^{-12} they quote. Indeed, their results differ by just one standard deviation from what could be expected if all of the phases they measured were random. Thus, constant phase drift is not a conclusive argument for the solar origin of their data.

Recently, Caudell et al. (1980) have found similar phase coherence for 18 days of data. While this result tends to indicate that a coherent phenomenon is present, we feel that caution should be taken before ascribing it solely to a global solar oscillation. Solar surface features, which can produce the type of power spectra we have shown here, are also long-lived. Livingston and Orrall (1974) have shown that supergranular patterns may exist for 3-5 days in some cases. Distortion of a standing supergranular pattern caused by differential rotation may produce phase drifts of the type seen in the SCLERA data. This would indicate that solar surface structure may not be a truly random noise source in limb definition measurements. We have run preliminary tests on data in which one day's phase is partially dependent on the previous day's phase. In a series extending over 18 days, we find that the mean value of σ can be lowered by 10-20% by assuming some form of partial coherence.

4. CONCLUSIONS

We must first note that our calculations and observations have been exploratory in nature and that further work is necessary to clearly separate all of the phenomena that can affect solar limb measurements. Nevertheless, we have shown that solar intensity patterns could substantially influence limb position determinations. We feel that the following conclusions are possible:

(1) Changes in the apparent solar limb position, as determined from the FFTD

Table 2.

Frequency (mHz)	Slope (radian/day)	rms error (radians)
0.248	2.75	0.74
0.366	4.16*	0.65*
0.414	4.76	0.59
0.463	0.01	0.66
0.539	3.72	0.64
0.606	2.80*	1.25*
average	3.04	0.77

* These values were estimated from Figure 1 of Hill and Caudell (1979). The other values were sent to us by T. Caudell.

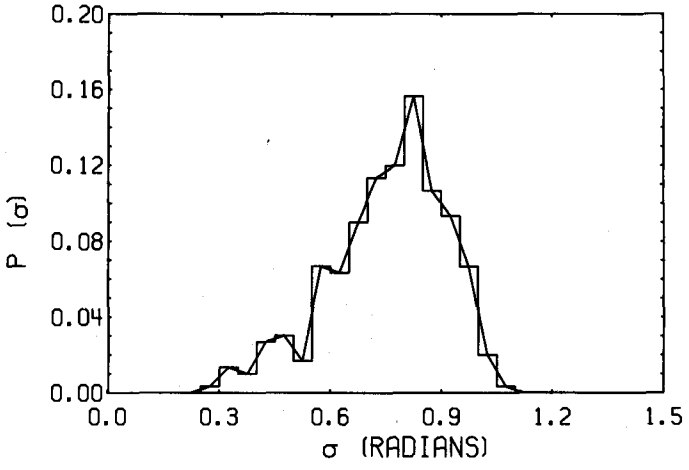

Figure 7. Sigma is the rms variation of the residuals obtained when a set of seven totally independent phases are fit with a straight line. Each phase is allowed to change by multiples of 2π until the best fit (smallest sigma) is found. The process was repeated for 300 independent sets of random phases. $P(\sigma)$ is the probability that a certain sigma will have a value that falls in a bin $\Delta\sigma = 0.05$ radians about this value of sigma.

formalism (equation 1), can result from evolutionary and rotational changes in solar intensity patterns. The magnitude and periodicities generated by the intensity variations are similar to those measured by Brown, Stebbins and Hill (1978). Further work, which is needed to conclusively determine the effect of these phenomena, should include photoelectric measurements in order to eliminate some of the problems produced by the use of films and observations on a large number of days. Such work is currently in progress.

(2) It has not been demonstrated conclusively that the relationship between phases observed at the same frequencies on different days reflects the origin of the data. We have shown that random data can produce phase relationships that mimic the observations; further work is therefore necessary to correctly interpret the phase.

We conclude that evolution and rotation of solar intensity patterns may be a substantial source of noise in solar limb position measurements. We do wish to note, however, that this does not indicate that the SCLERA results are statistically insignificant. Indeed, the SCLERA oscillations may be the source of the changes in the solar intensity pattern which we are observing. Ultimately, the determination of the relative contributions of solar oscillations and random noise sources to the SCLERA results will be made through studies of phase coherence over long periods of time. We feel that this is a problem which warrants significant additional study and one to which we are devoting considerable time.

* * * * *

We would like to thank Dr. T. Caudell for providing us with the SCLERA phase coherence results. We would also like to thank Dr. H.A. Hill and his collaborators at the University of Arizona who organized an excellent and useful symposium during which these problems were discussed.

REFERENCES

Beckers, J.M. and Ayres, T.R. 1977, Ap. J., 217, L69.

Brookes, J.R., Isaak, G.R. and van der Raay, H.B. 1976, Nature, 259, 92.

Brown, T.M., Stebbins, R.T. and Hill, H.A. 1978, Ap. J., 223, 324.

Caudell, T.P., Knapp, J., Hill, H.A. and Logan, J.D. 1980, these proceedings.

Christensen-Dalsgaard, J. and Gough, D.O. 1976, Nature, 259, 89.

Deubner, F.-L. 1977, Mem. S. A. It., 48, 499.

Dittmer, P.H. 1978, Ap. J., 224, 265.

Dittmer, P.H., Scherrer, P. and Wilcox, J.M. 1977, Book of Abstracts, Topical Conference on Solar and Interplanetary Phys., January 12-15, Tucson, p. 16.

Fossat, E. and Ricort, G. 1975, Astron. Astrophys., 43, 243.

Grec, G. and Fossat, E. 1976, Astron. Astrophys., 55, 411.

Hill, H.A. and Caudell, T.P. 1979, Mon. Not. R. Astr. Soc., 186, 327.

Hill, H.A., Stebbins, R.T. and Brown, T.M. 1975, in Atomic Masses and Fundamental Constants, (ed. J.H. Sanders and A.H. Wapshal;New York: Plenum), p. 622.

Livingston, W., Milkey, R. and Slaughter, C. 1977, Ap. J., 211, 281.
Livingston, W.C. and Orrall, F.Q. 1974, Solar Phys., 39, 301.
Musman, S., Nye, A. 1977, Ap. J., 212, L95.
Worden, S.P. and Simon, G.W. 1976, Ap. J., 210, L163.

OBSERVATIONS WITH HIGH TEMPORAL RESOLUTION OF THE SOLAR Ca^+ K LINE

T. Duvall, W. Livingston, and C. Mahaffey
Kitt Peak National Observatory
Tucson, Arizona

ABSTRACT

High time resolution ($\Delta t = 10^s$) photometric scans of chromospheric Ca^+ K are examined for evidence of propagating waves. The scans refer to a quiet area (1 x 7 arc seconds) near disk center. Diagnostics include line profile movies, time sequence spectrograms and power spectra. Both upward and downward (reflected?) disturbances having lifetimes $\sim$ 1-2 minutes are seen.

1. INTRODUCTION

It has long been known that calcium K spectroheliograms display bright points that are a few arc seconds in size and have a transitory lifetime of approximately a minute (Jensen and Orrall 1963). These bright points are especially evident in the violet reversal feature in the core of Ca II K 3933 A, usually designated K_{2V}. One may speculate that these K_{2V} bright points represent a manifestation of outward propagating waves--suddenly enhanced by the chromospheric density gradient. In this preliminary study we attempt to better define the temporal nature of the bright points and look for evidence of waves in the time domain from 20^s to 10^m.

2. THE OBSERVATIONS AND REDUCTION PROCEDURE

On a day of "good" seeing ($\sim$ 2 arc seconds), the 82 cm image of the sun produced by the McMath Telescope was centered over the entrance slit of the 13.5 m spectrometer, positioned so as to avoid any "network" or "plage." The slit dimension was equal to 1.0 x 7.5 arc seconds, and the image was driven to remove the mean component of solar rotation. For this experiment the double-pass spectrometer was operated in single-pass in order to improve the signal to noise ratios and because only temporal changes were of interest. A wavelength interval of 5 A was scanned by the spectrometer in $1\overset{s}{.}6$, with 4 scans being summed to constitute a single record having a repetition time of $9\overset{s}{.}5$. Thus the Nyquist frequency is 0.053 Hz (period $\sim$ 20^s). This process was continued for 80^m after which the system noise was determined by inserting a lens into the beam, reducing the spatial resolution to approximately 1 x 2 arc minutes. Another 80^m run was then performed. Observations were made on two

days, 11 and 14 December 1978. An additional similar run was made on 26 December 1978 for purposes of comparison, using Mg b 5183, a line formed in the low chromosphere.

Each record was normalized to a local "continuum" window and adjusted in wavelength to a fixed photospheric reference line in order to eliminate the effects of transparency change and spectrograph drift (for procedural details see White and Livingston 1978). Examples of line profile variations that remain after the above adjustments are displayed in Figure 1. (Movies of these profile variations, accelerated x 40, have also been produced.)

A quadratic fit was made to the extreme absorption core of the Ca^+ K line, K_3, and the residual intensity, I_{K3}, and relative wavelength, reduced to velocity, V_{K3}, were determined. Average power spectra for I_{K3} and V_{K3} were calculated as follows. The observation length of $\sim$ 414 points was padded to 512, then broken into 3 overlapping segments of 256 points, each of which, suitably apodized, was padded to 512 points. The 3 spectra were then averaged together. Figure 2 shows the low frequency end of these average power spectra. The dominant periods and relative power are given in Table 1. Power spectra made with the integrating lens in place showed that system noise, with the possible exception of the "seeing" component, was negligible.

Sou-Yang Liu (1974) has reported that intensity perturbations sometimes propagate from the far wing of K into the core K_{232}. The profile movies previously mentioned show these effects rather inadequately due to unavoidable image-motion disturbances. A more useful tool is a "time sequence spectrogram," a pictorial representation of the line profile as a function of time. Each spectrum scan is converted back to intensity on a CRT picture with wavelength as the abscissa and time the ordinate. Figure 3 is such a display confined to near line core. The rather impulsive nature of the intensity and velocity disturbances is clearly visible, although occasionally there is a suggestion of a near sinusoidal event (e.g., at the top of the figure). The power spectrum provides a quantitative description of the frequency content of the picture ignoring phase. But phase information is needed to see the wave phenomena that Liu found. In Figure 3 the arrows point to a bright feature that moves from the wing to the line core with time. To accentuate such features we have subtracted the time-averaged profile from the data set to produce Figure 4. Now one sees a multitude of tilted features, mostly pointing toward the line core, suggesting propagation both upward and downward. Downward manifestations seem confined to very near the core.

3. DISCUSSION

The time sequence spectrogram (Figure 3) displays three phenomena. The very narrow horizontal streaks arise from image motion; these are spurious and should be

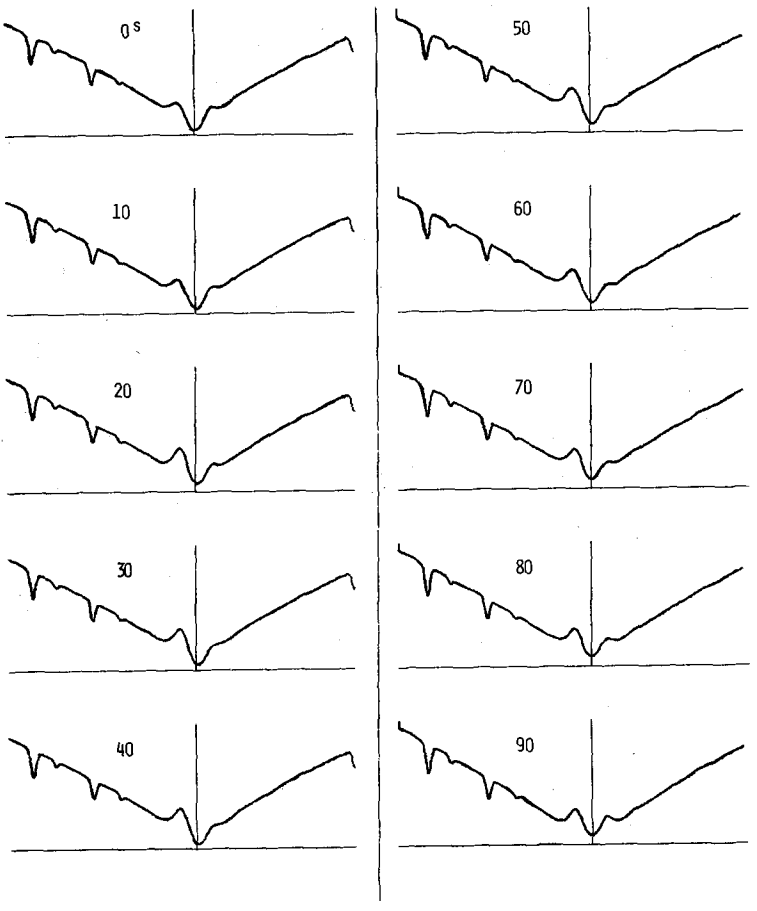

Figure 1. A segment of the line profile movie showing the development and decay of a K_{2V} bright point. The vertical fiducial is fixed with respect to the photospheric lines. As the intensity of K_{2V} increases, an apparent velocity shift is induced in K_3, producing a pseudo correlation.

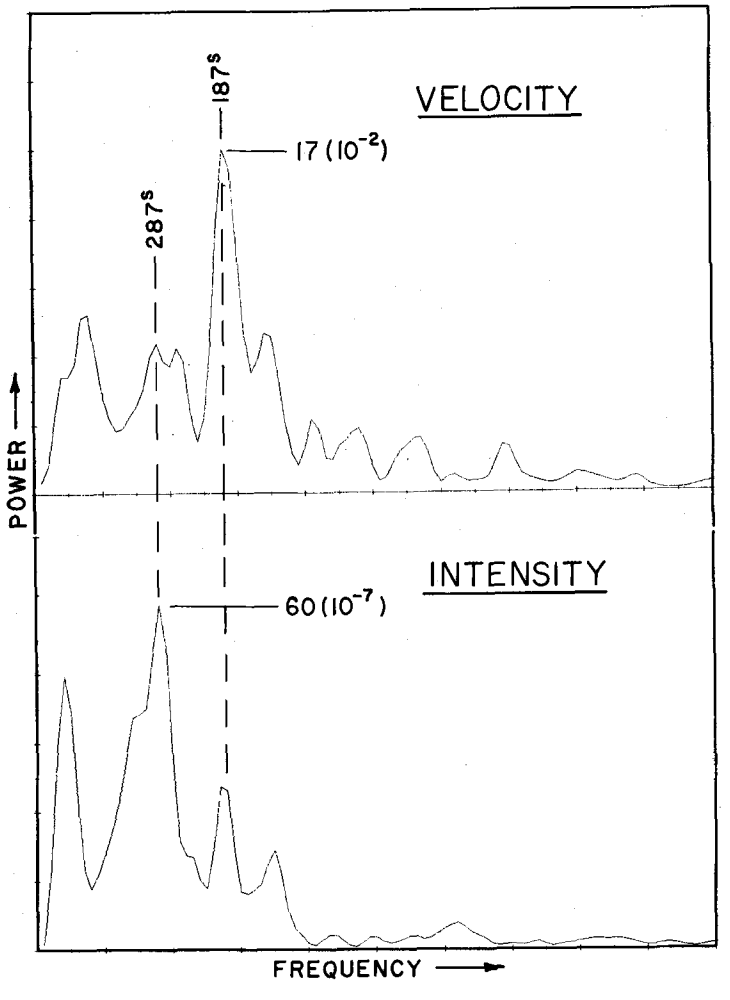

Figure 2. Power spectra for the Ca^+ K run on 11 December 1978. Velocity and intensity both refer to K_3. The strong peak at 187 sec may be due to the induced correlation illustrated in Figure 1.

Table 1. Dominant Period(s) and Relative Power for I_{K3}, V_{K3}, I_{Mg}, and V_{Mg}

	Periods	
	Intensity	Velocity
Ca^+ K_3	285 (185) (141)	(325) (244) 187 (146)
Mg 5183	363-262 a broad feature (155)	295 (157)
	Power	
Ca^+ K	$60(10^{-7})$	$17(10^{-2})$
Mg 5183	$1(10^{-7})$	$5(10^{-2})$

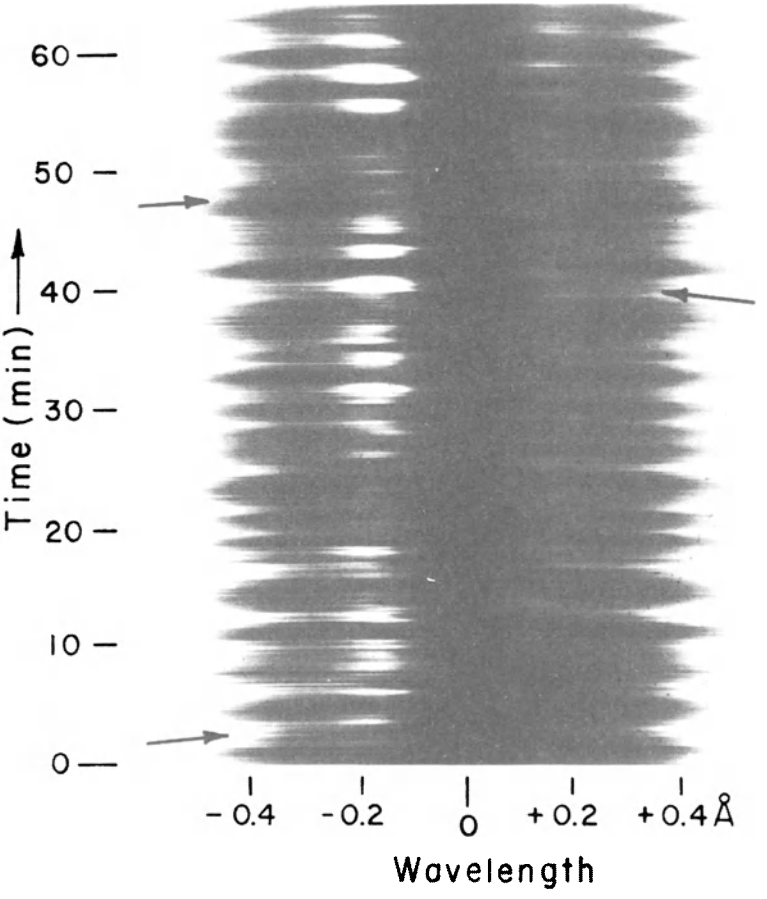

Figure 3. A time sequence spectrogram for 11 December 1978. The wavelength scale is set by photospheric lines outside the region displayed and refers to center disk value of Ca^{+} K (3933.682 A). Arrows point to tilted intensity patterns indicating upward propagating disturbances.

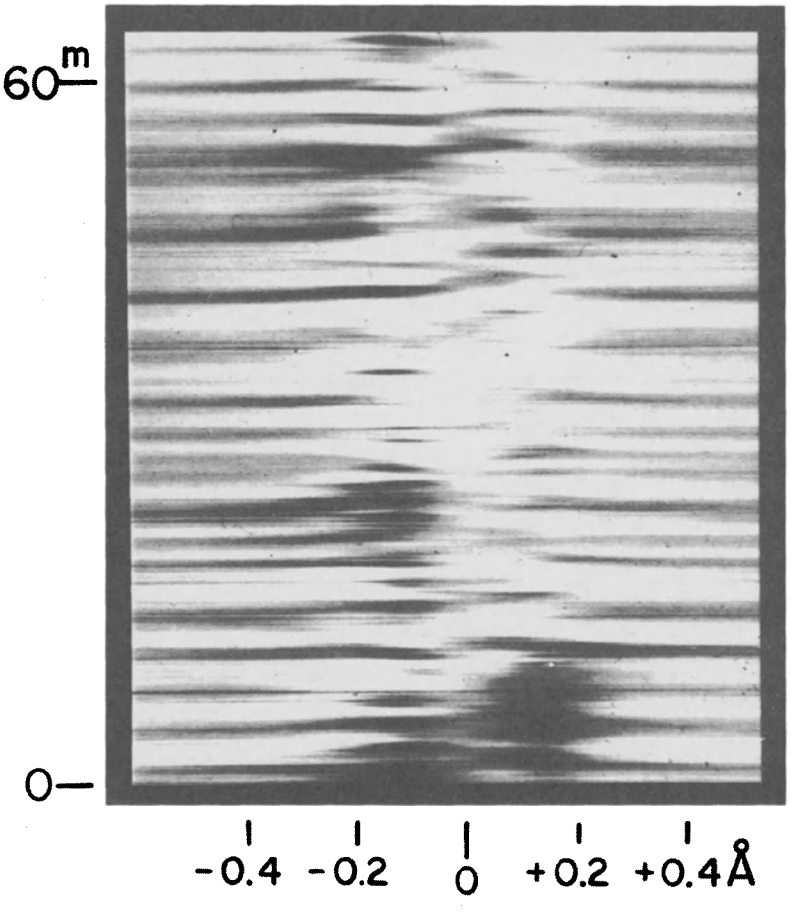

Figure 4. A time sequence spectrogram for 11 December 1978, with the time average profile removed. The V-shaped patterns centered on $\lambda = 0$ suggest both upward and downward propagating disturbances.

ignored. The second feature is the horizontal banded structure corresponding to the five minute and 180 second "oscillations." Liu proposes that the five minute component originates with "network" fragments while the 180 second power is confined to the K_{2v} points. The evident randomness of this pattern suggests either a short coherence time or a continuous mixing of the oscillation trains. The third phenomenon found in the spectrogram is the tilted features best seen in Figure 4. According to Liu, as we go from $\Delta\lambda \pm 0.3$ A to K_2 to K_3 we move upward from 350 Km to 700 Km to 1580 Km respectively. Thus a bright feature which moves with time consecutively through these spectral regions represents direct evidence for an outward propagating disturbance which produces local heating, presumably through (shock?) dissipation. By the same reasoning, downward propagating waves are also seen; we may speculate that these arise from reflection.

In summary, we have illustrated that the solar chromosphere contains oscillatory and transitory phenomena having time scales of seconds to minutes. No single diagnostic is completely sufficient and we point to the utility of profile movies, time sequence spectra, and power spectra for analyzing these motions.

REFERENCES

Jensen, E. and Orrall, F.Q. 1963, Ap. J., 138, 252.
Liu, S.-Y. 1974, Ap. J., 189, 359.
White, O.R. and Livingston, W. 1978, Ap. J., 226, 679.

EXCITATION OF SOLAR G MODES WITH PERIODS NEAR 160 MINUTES

D. Keeley
Science Applications, Inc.
Palo Alto, California

ABSTRACT

Solar g modes with ℓ = 1 to 4 and periods near 160 minutes have been investigated using a solar model with normal structure. Radiative dissipation in the region below the convection zone is much greater than the driving provided by nuclear reactions or the opacity mechanism. A crude treatment of convection suggests that it also is not an important source of driving. The damping due to turbulent viscosity is also small. Excitation of these modes by coupling to convective turbulence is substantial in terms of the rms energy of the modes, but the surface velocity is very small because of the large amount of mass involved in the oscillation.

1. INTRODUCTION

The $2^h\ 40^m$ period first reported by Severny, Kotov and Tsap (1976) and by Brookes, Isaak and van der Raay (1976) has been supported by more recent observations (Scherrer et al. 1979). In this paper, properties of modes in this period range are examined in the context of a conventional solar model, and their stability investigated as described below.

A model representing the sun was obtained by evolving a homogeneous 1 $M_\odot$ model from the zero age main sequence until it resembled closely the present sun. The properties of the model were as follows: $L = 3.83 \times 10^{33}$ erg sec^{-1}, $R = 6.9136 \times 10^{10}$ cm, Z = .02, Y(surface) = .244, X(center) = 0.39. The mixing length was 1.238 pressure scale heights. The convection zone included about 1.2×10^{31} grams and extended down to a temperature of about 1.5×10^6 K.

The differential equations for adiabatic eigenfunctions were written in the form used by Osaki (1975), and solved by the method of inverse iteration. The damping (or excitation) was then determined by perturbation theory, using the adiabatic eigenfunctions. The turbulent excitation energy and viscous damping were calculated as described by Goldreich and Keeley (1977), except for an improvement in the integral over the wave numbers in the turbulent spectrum.

2. LINEAR STABILITY ANALYSIS

The condition for linear instability is that a net positive amount of PdV work be done during one cycle of the oscillation. In calculating growth rates according to perturbation theory, only the nonadiabatic part of the pressure perturbation can contribute to the work integral. If the time dependence is assumed

to be exp(iωt), then the nonadiabatic pressure perturbation is

$$\delta P_{na} = - \frac{(\Gamma_3 - 1)\rho}{i\omega} \delta\left(\frac{\nabla . \vec{F}}{\rho} - \varepsilon\right) \qquad (1)$$

in which δ denotes a Lagrangian perturbation, and all other symbols have their usual meaning. For a given mass element, there is a positive contribution to the driving if

$$\nabla . \vec{\xi}\ \delta\left[\frac{\nabla . \vec{F}}{\rho} - \varepsilon\right] > 0 \quad , \qquad (2)$$

in which ξ is the displacement.

2.1. Radiative Contribution

The equations used for the radiative flux $\vec{F}_r$ are

$$\vec{F}_r = - \frac{4\pi}{3\kappa\rho} \nabla J \qquad (3)$$

$$J - B = - \frac{1}{4\pi\kappa\rho} \nabla . \vec{F}_r \qquad (4)$$

in which J is the mean intensity, B is the Planck function, and κ is the absorption coefficient. Since the perturbation of the scalar quantity $\nabla \cdot \vec{F}_r$ is required in equation (2), it is convenient to write an equation for it directly:

$$\nabla . \vec{F}_r - \frac{1}{3} \nabla . \left[\frac{1}{\kappa\rho} \nabla \left(\frac{1}{\kappa\rho} \nabla . \vec{F}_r\right)\right] = - \frac{4\pi}{3} \nabla . \left(\frac{1}{\kappa\rho} \nabla B\right) \qquad (5)$$

The second term on the left is usually omitted in calculations of both the hydrostatic model and the damping. Its effect on hydrostatic models is normally small, but for some oscillation modes its perturbations have a large effect on the damping. It is especially important at the outer boundary of the solar convection zone.

It is customary to do Eulerian perturbations in nonradial calculations because they commute with spatial derivatives; this problem is more difficult to deal with in these circumstances than it is for radial motions. However, in regions where κ or other quantities vary very rapidly in space, the Eulerian perturbations are very much larger than Lagrangian perturbations. Because it is ultimately necessary to construct the Lagrangian perturbation for use in equation (2), the cancellation of

several significant digits, which could result when going from Eulerian to Lagrangian at the outer edge of the convection zone, could have a serious effect. Numerical errors due to noise in the eigenfunctions could occur in this potentially important driving region. Even if the eigenfunctions are not noisy, possible systematic effects due to the grid structure could introduce significant errors. For these reasons, Lagrangian perturbations were used throughout, and terms which were cancelled in part or totally by similar terms from the convective flux perturbation were handled explicitly. The final expression for the perturbation of $\nabla \cdot \vec{F}_r \equiv D$ is EQUATION 6

$$\delta D - \frac{1}{3}\left[\beta(\beta\delta D);K\right]_{;K} = -\frac{4\pi}{3}\left[\beta(\beta\delta B);K\right]_{;K} + \frac{1}{3}\left[\beta(\delta\beta D);K\right]_{;K} + \left(\frac{\delta\beta}{\beta} F_{r\,K}\right)_{;K} - \left(\xi_{J;K}F_{r\,J}\right)_{;K} - \xi_{J;K}F_{r\,K;J} \qquad (6)$$

in which $\beta \equiv (\kappa\rho)^{-1}$. Index notation has been used because ordinary vector notation is somewhat ambiguous for the last two terms. The semicolons denote covariant derivatives.

2.2. Convective Contribution

An equation for the time-dependent convective flux was written in the form given by Cox et al. (1966):

$$\frac{d\vec{F}_c}{dt} = \frac{\vec{F}_c^{(i)} - \vec{F}_c}{\tau} \quad , \qquad (7)$$

in which the timescale τ is taken to be the mixing length divided by the local convective velocity, and $\vec{F}_c^{(i)}$ is the convective flux as calculated from mixing length theory. The perturbed form of the equation is

$$\delta\vec{F}_c = \frac{\delta\vec{F}_c^{(i)}}{1 + i\omega\tau} \quad . \qquad (8)$$

The Lagrangian perturbation of the instantaneous flux was taken to be

$$\delta\vec{F}_c^{(i)} = \delta\left(-F_c^{(i)} \frac{\nabla P}{|\nabla P|}\right) \quad , \qquad (9)$$

in which a unit vector in the direction of $-\nabla P$ is taken as the direction of the convective flux, and $F_c^{(i)}$ is the magnitude of the flux as calculated in the usual way. Equation (9) expands out to the form

$$\delta\vec{F}_c(i) = \delta F_c{}^i\hat{r} - \frac{F_c{}^i}{r}\left(H\frac{\delta P}{P} - (\xi_\perp - \xi_r)\right)\nabla_\perp Y_{\ell m} \quad , \tag{10}$$

in which H is the pressure scale height,

$$\nabla \equiv \hat{r}\frac{\partial}{\partial r} + \frac{1}{r}\nabla_\perp \quad , \text{ and } \quad \vec{\xi} = \xi_r \hat{r} Y_{\ell m} + \xi_\perp \nabla_\perp Y_{\ell m} \quad .$$

The perturbation of the divergence of $\vec{F}_c$ is given by

$$\delta(\nabla.\vec{F}_c) = \nabla.(\delta\vec{F}_c) - \nabla\vec{\xi}:\nabla\vec{F}_c \quad , \tag{11}$$

in which the last term is the same form as in equation (6) for the radiative flux, and is partly cancelled by it.

2.3. Nuclear Contribution

The energy generation rate has been written in the usual form:

$$\varepsilon = \varepsilon_0 \rho^\eta T^\nu \quad , \tag{12}$$

from which the perturbation in the adiabatic approximation is obtained:

$$\frac{\delta\varepsilon}{\varepsilon} = -\nabla.\vec{\xi}\left[\eta + (\Gamma_3 - 1)\nu\right] \quad . \tag{13}$$

Constant values for η and ν were used throughout the energy-generating region. Since $\Gamma_3 - 1$ is quite constant also, the nuclear contribution can easily be scaled to any desired values of the exponents η and ν. For the results given in Table 1, the values $\eta = 1$, $\nu = 15$ were used. The high value for ν was used because the nuclear reactions cannot maintain the equilibrium abundance of products in the PP chain for which the exponent $\nu \sim 4$ or 5 is appropriate. Since nuclear driving did not appear to be an important effect, it was not considered necessary to treat this contribution in more detail.

2.4. The Condition for Local Driving

With the approximations discussed above, the condition for driving of the instability (equation 2) becomes

$$\nabla.\vec{\xi}\left\{\frac{\delta(\nabla.\vec{F})}{\rho} + \nabla.\vec{\xi}\varepsilon + \varepsilon\nabla.\vec{\xi}\left[\eta + (\Gamma_3 - 1)\nu\right]\right\} > 0 \quad . \tag{14}$$

The nuclear reactions always contribute to instability, as does the density perturbation in a region where $\nabla \cdot \vec{F} > 0$.

Table 1

TABLE 1. g Modes Near 2^h40^m = 9600s

ℓ =	1	2	3	4
Period (s)	10196	9473	9840	9647
Nodes	6	10	15	19
Amplitude ratio	12	10	22	36
Radiative damping rate (s^{-1})	1.40-13	4.02-13	9.16-13	1.49-12
Convective damping rate	8.80-17	-1.38-15	-4.26-15	-5.75-15
Turbulent damping rate	1.92-15	1.50-14	2.61-14	2.85-14
Nuclear excitation rate	1.29-14	1.33-14	1.37-14	1.38-14
Radiative damping below convection zone	99%	98%	96%	96%
Turbulent excitation energy (ergs)	9.3+25	1.6+26	1.3+26	7.9+25
Energy for 1 cm/sec at surface (ergs)	1.1+33	5.8+32	8.7+32	1.4+33

3. RESULTS AND CONCLUSIONS

Adiabatic eigenfunctions and frequencies were calculated for several modes at each value of ℓ in the range ℓ = 1 to 4, and the work integral was calculated as described in § 2 above. The results are summarized in Table 1 for the 4 modes with periods closest to 160 minutes. In addition, the radial and transverse components of $\vec{\xi}$ are shown in Figure 1 for the ℓ = 1 mode. The 200 point grid resolved the 6 nodes of the ℓ = 1 mode quite well, but resolution was not as good for the 19 nodes at ℓ = 4. However, it is unlikely that errors large enough to alter the conclusions are present.

Except for the ℓ = 1 mode, the ratio of the maximum radial displacement to the surface displacement increased strongly with ℓ, as indicated in Table 1. Radiative damping was by far the dominant dissipative mechanism, and most of that damping occurred below the convection zone. Convective flux transport provided driving near the surface of the convecton zone in an amount comparable to the radiative driving there. The energy expected in these modes as a result of nonlinear coupling to convective turbulence was $\sim 10^{26}$ ergs, whereas the energy required for a surface velocity of 1 cm/sec is $\sim 10^{33}$ ergs. In any case, the turbulent excitation mechanism would not be a satisfactory one unless the observations eventually show that many modes are excited.

The observations are not easily understood in terms of the conventional considerations discussed in this paper.

REFERENCES

Brookes, J.R., Isaak, G.R. and van der Raay, H.B. 1976, Nature, 259, 92.

Cox, J.P., Cox, A.N., Olsen, K.H., King, D.S. and Eilers, D.D. 1966, Ap. J., 144, 1038.

Goldreich, P. and Keeley, D.A. 1977, Ap. J., 212, 243.

Osaki, Y. 1975, Publ. Astron. Soc. Japan, 27, 237.

Scherrer, P.H., Wilcox, J.M., Kotov, V.A., Severny, A.B. and Tsap, T.T. 1979, Nature, 277, 635.

Severny, A.B., Kotov, V.A. and Tsap, T.T. 1976, Nature, 259, 87.

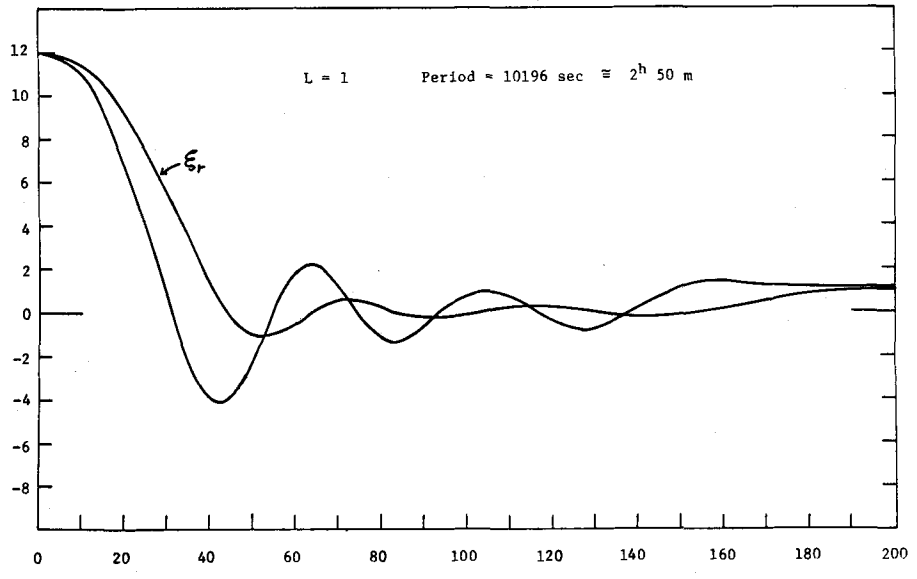

Figure 1. The radial and transverse components of the displacement vector for the $\ell = 1$ mode. The eigenfunctions are normalized so that $\xi_r = 1$ at the surface. The abscissa is the grid point number. The lower boundary of the convection zone is at point 173.

THE COLLECTIVE EXCITATION OF g-MODES IN THE SUN

C.L. Wolff
NASA-Goddard Space Flight Center
Greenbelt, Maryland

ABSTRACT

Oscillations of the solar interior (linear g-modes) may be strongly driven by the collective influence of all the modes upon the nuclear reactions in the core. This heretofore neglected effect could couple the modes, reduce the effective amplitudes near the center, and spatially concentrate most of the oscillation energy into just a portion of the radiative interior. If operating at sufficient strength, this can reverse the conventional conclusion, drawn from single mode calculations, that almost all solar g-modes are damped. Furthermore, it would put the theory into rough harmony with three otherwise troubling observations: (1) the "low" neutrino flux measured by Davis (1978), (2) the high correspondence found by Wolff (1976) between recurrence periods in solar activity and the rotational beat periods of g-modes, and (3) the fluctuations in the sun's diameter which imply g-mode activity at high angular harmonics (Hill and Caudell 1979). A nonlinear expression is derived for the local rate of work done on an array of oscillation modes by the nuclear reactions. Three additional tests of the model are suggested.

1. INTRODUCTION

There is evidence that g-modes are excited in the sun at angular harmonic numbers $\ell >> 1$ (Hill and Caudell 1979; Wolff 1976). This consists of a direct detection of oscillatory power in the correct frequency range, a demonstration that particular oscillations display phase coherence over many days, and a detection of the long beat periods implied by the rotation of g-modes. This evidence is discussed in detail in § 5. A likely consequence of the excitation of high harmonic modes is that a very large number of modes will be active. As I wrote in 1974, "There is not much physical difference between the properties of two high-order modes of similar order. If one high harmonic mode is excited by the star and maintained against dissipating mechanisms, we must therefore expect that a whole range of neighboring harmonics will also be driven to comparable steady amplitudes." As an example, let us take just the five angular orders (ℓ = 6 to 10) for which good evidence was given by Wolff (1976). For each value of ℓ, there are $\ell + 1$ different standing waves corresponding to the possible azimuthal harmonic numbers. Adding these gives 45

different angular states. But each angular harmonic can exist in numerous radial harmonics. If only five radial harmonics are active for the typical angular state, one has 5 x 45 = 225 different standing waves possible in this small range, $\Delta k = \Delta \ell = 5$. Hundreds or thousands of linear g-modes are not unreasonable to expect. Because of this, I feel that conventional calculations of growth rates (which consider each mode as though no others were present) are in serious risk of missing interactions which may be of major importance.

In contrast to the observations, linear theories find that g-modes of high ℓ value are damped and, therefore, are not expected to be observed. There is even some ambiguity as to whether the lowest angular harmonics ($\ell \leq 3$) can be excited. Christensen-Dalsgaard, Dilke, and Gough (1974) found several such modes with a net excitation but, in slightly different solar models, Dziembowski and Sienkiewicz (1973) and Shibahashi, Osaki, and Unno (1975) found all such modes to be damped. However, many of the modes are so slightly damped that they lose only $\sim 10^{-10}$ of their energy during each cycle. For these, not much additional driving is needed to change the damped mode into one that is excited. Furthermore, if there is a way to increase by an order of magnitude the ratio of driving to damping, a very large array of linear modes now thought to be damped would become excited.

In this paper, a way of obtaining increases of this magnitude is described. It depends upon nonlinear coupling of modes by the nuclear term. This causes individual modes to receive perturbations from all the other modes which outweigh the weak driving and damping terms of conventional linear theory. Temperature fluctuations in parts of the core are assumed to exceed 5% (rms) due to the combined action of many g-modes. Moderately high harmonic modes are expected since they have relatively smaller amplitudes at the surface, thus reducing the energy losses there. Radiative losses very close to the center of the sun are reduced by the partial cancellation of the many modes involved. This picture of the solar core also differs from the conventional one in that the occasionally large local oscillation amplitudes would almost certainly keep the inner core well mixed. As discussed in § 5, mixing is a known way to solve the solar neutrino problem.

2. SPATIAL REDISTRIBUTIONS OF AMPLITUDE

Several members of the workshop were quite skeptical that the consideration of ensembles of modes could avoid the large amplitudes and heavy radiation damping which are known to occur in most individual linear modes near the center of a star. For this reason, two elementary examples are presented here of situations in which a group of modes can have strength in the central regions which is less than that found if the linear modes were computed one at a time in the usual manner.

The first example does not even require coupling between the linear modes. Those modes, which have antinodes in the vicinity of the shell (mean radius, $r_\varepsilon \simeq 0.1$

R_θ) where nuclear burning makes its greatest contribution toward the driving of most g-modes, are especially well situated to be driven by the nuclear mechanism. It is not unlikely that many of these modes will have larger amplitudes than others. For simplicity then, let us consider an ensemble of modes each of which has an antinode at r_ε. Let us write the local temperatue fluctuation due to the i^{th} mode as $\theta_i \sin \omega_i t$ where,

$$\theta_i \equiv \left(\frac{\delta T}{T_o}\right)_i \quad , \tag{1}$$

δT is the Lagrangian perturbation in the mean temperature T_o, and ω_i is the oscillation frequency. The rms amplitude of a typical linear mode is,

$$\bar{\theta}_i \equiv \left(\frac{1}{N} \sum_{i=1}^{N} \theta_i^2\right)^{1/2}$$

In these terms, the time average of the squared fluctuation due to N modes is,

$$\theta^2 = < \left[\sum_{i=1}^{N} \theta_i \sin\omega_i t \right]^2 > = \frac{N}{2} \left(\bar{\theta}_i\right)^2 \quad . \tag{2}$$

where all ω_i are assumed incommensurate. Closer to the stellar center by at least one radial wavelength of a typical mode, the radial phase can be taken as random. The typical mode, then, has a local amplitude of $\theta_i / \sqrt{2}$, where θ_i is the amplitude at the nearest antinode of that mode. Now, the mean squared temperature fluctuation is only

$$\theta^2 = \frac{N}{4} \left(\bar{\theta}_i\right)^2 \quad . \tag{3}$$

Comparison of equations (2) and (3) shows that the squared fluctuation due to all the modes is twice as large at $r = r_\varepsilon$ as it is far from r_ε when each is compared to $\bar{\theta}_i$ which is the appropriate quantity for conventional, single mode calculations. The above conclusion is unchanged after integrating over all angles, which affects (2) and (3) by the same factor. Finally, a difference of more than a factor of two can occur if θ becomes finite and attention is shifted to a highly nonlinear function of the temperature, such as the nuclear term.

The second example gives larger effects. To illustrate the point, we need only two groups of modes whose oscillation frequencies are about the same and whose radial harmonic numbers, k, differ by two. There are many such cases (see Figure 1). Most of these lie above 0.29 mHz, where the many curves are converging on the figure, but there are some cases which fall as low as 0.18 mHz. Any pair with $\Delta k = 2$ will

do, but we will choose a case where $|k| >> 1$ so that simple asymptotic forms can be used for the eigenfunctions. The two groups of modes near 0.18 mHz with (k, ℓ, m) = (-9, 4, m) and (-11, 5, m) have radial eigenfunctions which are adequately approximated in the g-region by the sine waves plotted in Figures 2a and 2b. In the exponential regions, the behavior is indicated schematically by the dashed curves. The ordinates are $S^{-1/4} Q$ in which variable the eigenfunctions approach pure sine waves when plotted on a logarithmic distance scale, provided $|k|$ is large enough (see Wolff 1979, especially equation (19) and Figure 4). The sum of the two curves is given in Figure 2c and immediately suggests a way in which the star can concentrate oscillatory motion in the vicinity of the strongest nuclear driving, $r = r_\varepsilon$, and diminish its exposure to radiation losses near the center and in the envelope. The star need only couple the approximately equal oscillation frequencies of the two groups so that they are exactly the same; the distribution in Figure 2c can then continue for roughly half a year until rotation separates the groups. It is important to note that the concentration shown in Figure 2c cannot apply to all angular directions. This is obvious in linear theory where the modes are orthonormal spherical harmonics and imply a total cancellation of the concentration when integrated over a spherical surface. But, in nonlinear theory, oscillation energy can be concentrated into a small fraction of all possible directions. Wolff (1974) derived a way of doing this by coupling all the linear modes of a given value of ℓ. He showed that this could proceed in the sun if nonlinear coupling was able to make fractional changes of $\sim 10^{-5}$ in the oscillation frequencies of the linear modes. We can reasonably assume that coupling is adequate to make these changes since our model already requires much larger fractional perturbations ($\sim 10^{-3}$, as deduced from the spacing of eigenvalues in Figure 1) to achieve the radial concentrations illustrated in Figure 2c. In summary, the solar core can develop, from time to time, very interesting nonlinear modes whose amplitudes are concentrated in all three spatial dimensions, provided that the nonlinear driving term is strong enough to couple the oscillation periods of appropriate groups of modes. The simplest illustration of the method may probably be found when only two groups of linear modes are used with radial harmonic numbers differing by two.

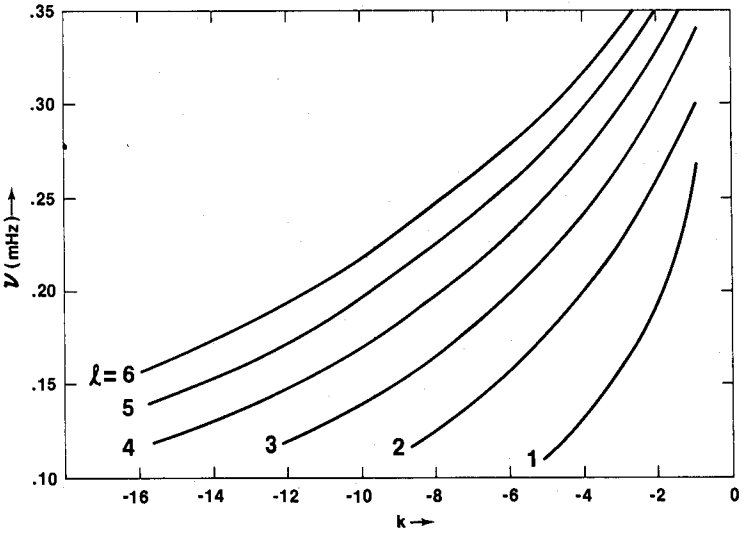

Figure 1. The distribution of linear g-mode oscillation frequencies, $\nu = \omega/2\pi$, in a standard solar model. The curves are labeled by ℓ, the principal index of the spherical harmonic. The abscissa is k, the radial harmonic index. Acceptable oscillation frequencies whose modes satisfy the required physical boundary conditions occur for integer values of k and ℓ. On the scale of this figure, the frequencies of linear modes are independent of the azimuthal number, m, because of the sun's very slow rotation.

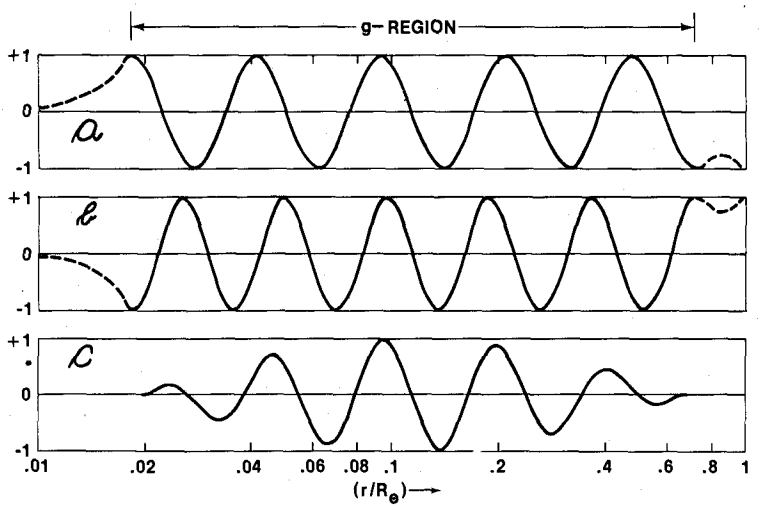

Figure 2. The effect of coupling the oscillation frequencies of two similar modes. (a) The approximate radial dependence of oscillation amplitude for a mode, k = -9 and ℓ = 4. (b) The same for a mode, k = -11 and ℓ = 5. The ordinates are in a natural variable related to energy. (c) The sum of (a) and (b). This gives a new mode whose amplitude is diminished by a factor of five, both in the central regions and near the base of the convective envelope ($\simeq$ 0.7 $R_\odot$ in this model). All curves have been normalized to one at their largest maximum. For the curve in (c), the larger amplitudes lie in layers where nuclear driving has its greatest effect on the oscillations.

3. DEPARTURE FROM LINEAR THEORY

The unlinearized fluid equations commonly used in pulsation theory are

$$\frac{d\rho}{dt} + \rho\nabla.\vec{v} = 0 \tag{4a}$$

$$\frac{d\vec{v}}{dt} + \frac{\nabla p}{\rho} + \nabla W = \text{(turbulent forces)} \tag{4b}$$

$$\frac{1}{\gamma - 1}\ \frac{d}{dt}\left(\frac{p}{\rho}\right) + \frac{p}{\rho}\nabla.\vec{v} = \varepsilon - \frac{\nabla.\vec{F}}{\rho} + \text{(turbulent viscosity)} \tag{4c}$$

where ρ, p, and v are the density, pressure, and velocity of the fluid, and d/dt stands for $(\partial/\partial t + \vec{v} \cdot \nabla)$. Perturbations of the gravitational potential, W, will be neglected because high harmonics will be of interest. Left members of the equations contain the adiabatic terms. The right members have the nonadiabatic terms which will be discussed later. For g-modes in the solar core, the total pulsational energy greatly exceeds the nonadiabatic losses per cycle so that the familiar quasiadiabatic approximation is valid. Using equation (1) this can be written as

$$\frac{\delta\rho}{\rho_0} = b\theta \tag{5}$$

and

$$\frac{\delta p}{p_0} = \gamma b\theta \tag{6}$$

where $\delta\rho$ and δp are the Lagrangian perturbations in the density and pressure, $b = (\gamma - 1)^{-1}$, and $\gamma = 5/3$ in the solar core.

We need an order of magnitude estimate of how the adiabatic terms of (4) depart from linearity as the relative temperature perturbation, θ, becomes large. To obtain this, we will first write,

$$p \equiv (p_0 + \delta p) = p_0(1 + \gamma b\theta) \simeq p_0(1 + \theta)^{\gamma b} \tag{7}$$

and similarly,

$$\rho \simeq \rho_0(1 + \theta)^b \tag{8}$$

The indicated approximations are fairly good since b and γ are of order unity and θ is not expected to exceed a few tenths. - Using (7) and (8) to eliminate ρ and p, we see that the velocity in equation (4a) must balance terms $\sim (1 + \theta)^b$. In the adiabatic members of (4b) and (4c), the velocity balances terms $\sim (1 + \theta)$. Very

roughly then, the velocity field will solve these equations if its dependence on θ has exponents, b and 1, comparable to the other terms. Assuming this holds well enough for our purposes, no term in the left members of equations (4) varies with θ at a rate faster than $(1 + \theta)^{2b} = (1 + \theta)^3$. The lower curves in Figure 3 show the function,

$$\frac{(1 + \theta)^{\beta}}{1 + \theta\beta} \tag{9}$$

for two values of β. Since the denominator is merely the linearized form of the numerator, the ratio represents the fractional departure from linearity of any term in the equations of motion whose dependence at some value of θ approximates $(1 + \theta)^{\beta}$. The curve $\beta = 2$ typifies the behavior of the adiabatic terms in (4) while the $\beta = 4$ curve is a generous upper limit. From the figure, errors would not be expected to approach $\sim$ 10% until the local temperature fluctuation exceeds a few tenths.

Unlike the preceding situation, highly nonlinear behavior is common for the nonadiabatic terms. The turbulence is usually discussed in terms of a generalized pressure tensor and is thought to be negligible in our problem. But a unique form of turbulence will be suggested in § 4.2 as the ultimate limit on the growth of pulsational amplitudes. The radiative exchange term, $\rho^{-1}(\nabla \cdot \vec{F})$, contains two strongly nonlinear functions in the radiative flux,

$$\vec{F} = \text{constant} \cdot \frac{\nabla T^4}{\rho\kappa} \quad ;$$

namely, the opacity κ and the temperature to the fourth power. Using equation (8) and the opacity tables of Cox and Stewart (1970) for solar core conditions, one can show that there is considerable cancellation between the variations of $\rho\kappa$ and T^4. This is not true in the outer envelope of the sun. However, in the core, the overall temperature dependence of the radiative term turns out to be quite slow, corresponding to $\beta < 2$ in Figure 3. The order of magnitude proof is too long to include here but it depends on two approximations: (1) the distance between nodes of the oscillation is taken to be much shorter in at least one dimension than the local temperature scale height; and (2) the gradient and divergence operators are replaced by π/L, where L is the shortest of the 3 internodal distances.

The nuclear burning term, ε, is notoriously sensitive to temperature. For pulsations of infinitesimal amplitude, $\beta \simeq 12$. This comes primarily from the reaction, $^3He + {}^3He \rightarrow {}^4He + 2\ {}^1H$, as pointed out by Dilke and Gough (1972) and by Unno (1975). For finite amplitude pulsations, β varies during the cycle and the following procedure was used. The conventional interpolation formula for the rate

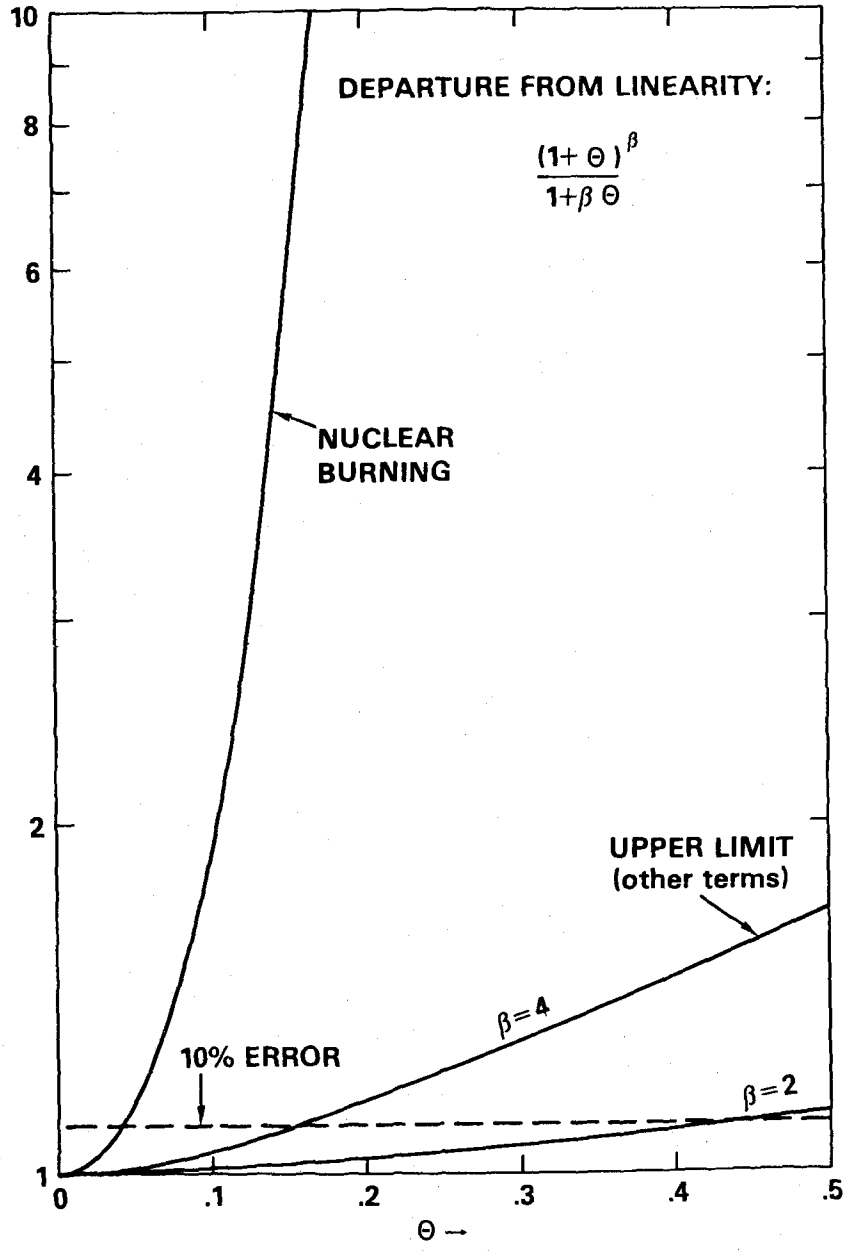

Figure 3. The fractional departure from linearity of $(1 + \theta)^{\beta}$ as a function of the relative temperature change, θ. The behavior of most terms in the pulsation equations is typified by the curve for $\beta = 2$. The curve for $\beta = 4$ is an upper limit for all terms except those for nuclear heating and turbulence. The nuclear curve is drawn for material at a temperature of 9×10^6 K and containing 75% hydrogen by mass.

per unit mass of nuclear energy generation is:

$$\varepsilon = \varepsilon_0(1 + \delta\rho/\rho_0)(1 + \theta)^n \qquad (10)$$

Using equations (5) and (8), this becomes

$$\varepsilon \simeq \varepsilon_0(1 + \theta)^\beta \qquad (11)$$

where $\beta = n + b$ here. In order for equation (11) to typify the true energy released over an oscillation cycle, ε_0 and n must be numerically determined for each mean temperature, T_0, and each range, $\pm\ \theta$, of the fluctuation. For this purpose, a matrix of ε values was calculated using the expressions of Fowler, Caughlin, and Zimmerman (1975) for the 9 reactions of the proton-proton chain. A well-mixed core was assumed with a hydrogen mass fraction of 75%. The calculations were made for a density of 100 g cm^{-3}, a grid of mean temperatures (6, 7, 8, ... 15) x 10^6 K, and an array of θ values. The abundances of ^{7}Be and ^{3}He were in equilibrium with the local mean temperature while the abundances of deuterium and ^{7}Li were allowed to fluctuate during the oscillation cycle. By interpolating within the ε matrix and constructing the appropriate derivative, the exponent in equation (11) becomes a known function of θ and T_0, permitting a plot of the departure from linearity of the nuclear heating term. It is shown in Figure 3 for a mean temperature of 9 x 10^6 K. When the local temperature fluctuations are only a few percent, linear theory holds very well. As the fluctuations grow larger, increases of an order of magnitude will occur in the nuclear term before any serious error arises in the other terms of equation (4). Thus, a range exists for θ from approximately 0.04 to 0.2 where linear theory remains valid except that the nuclear term is underestimated. I suggest that portions of the solar core are pulsing in this range for three reasons. (1) There are many truly linear modes ($\theta \to 0$) for which the total damping exceeds the driving by less than an order of magnitude. More and more of these modes would become excited as θ exceeded 0.1 and the enhancement of the nuclear term became greater. (It is necessary to treat the modes in groups, as in § 2, to avoid the large amplitudes near the center which would disrupt the oscillatory motion, but this also further improves the prospects for excitation by significantly reducing radiation damping.) (2) The combination of groups of modes to produce a spatially concentrated, nonlinear mode is a step in the direction of existing local treatments of the problem. Dilke and Gough (1972) and Unno (1975) have already demonstrated that linear g-modes can be excited when the envelope of the star is neglected. By appropriate coupling of modes similar to theirs, nonlinear modes could probably be formed with reduced envelope activity. (3) Large amplitude oscillations in the core can resolve three discrepancies between observations and conventional theory (§ 5) while maintaining small enough surface

amplitudes to remain consistent with other measurements.

4. COLLECTIVE EXCITATION AND DAMPING

4.1. Collective Effects on the Nuclear Excitation Term

It may be hereafter assumed that parts of the sun's core are occasionally oscillating in the range of temperature fluctuations just given. A lower limit to the nonlinear driving term is now derived. The rate of mechanical work done on the pulsations by the nuclear reactions is given by the integral over the stellar mass of

$$dU = dm \langle \theta \delta\varepsilon \rangle$$

where dm is the mass element, $\delta\varepsilon$ is the Lagrangian perturbation of ε, and the indicated averaging is taken over time. By equation (11) this becomes

$$dU \simeq dm\, \varepsilon_0 \langle \theta \cdot \left[(1+\theta)^{\beta} - 1\right] \rangle \ .$$

For integer values of β, this has an exact expansion in terms of binomial coefficients, $C_j^{\beta} \equiv \beta![(\beta-j)!\ j!]^{-1}$. It is

$$dU \simeq dm\, \varepsilon_0 \sum_{j=1}^{\beta} C_j^{\beta} \langle \theta^{j+1} \rangle \ . \tag{12}$$

Since there will always be an integer within 4% of the desired value of β (recall that $\beta \geq 12$), interpolation between these is probably easier than use of the noninteger form of equation (12). In conventional growth rate calculations, equation (12) is approximated by $dU_1 = dm\, \varepsilon_0\, \beta\, \langle \theta^2 \rangle$. Although this first order approximation to the work integral will not be used, it is instructive to divide equation (12) by dU_1 to emphasize how this paper departs from conventional work:

$$\frac{dU}{dU_1} = 1 + \frac{(\beta-1)!}{(\beta-3)!\ 3!} \frac{\langle \theta^4 \rangle}{\langle \theta^2 \rangle} + \frac{(\beta-1)!}{(\beta-5)!\ 5!} \frac{\langle \theta^6 \rangle}{\langle \theta^2 \rangle} + \ldots \ . \tag{13}$$

The omitted odd powers of θ will be shown to have zero time averages in our model.

The collective influence of all the modes enters equation (13) directly only in the time averages of even powers of θ. It also enters indirectly, when θ is large, by affecting β as mentioned earlier. If there are a large number N of individual modes and none has more than a small fraction of the energy, then the amplitude of the i_{th} mode, θ_i, is much less than $|\theta|$. By Figure 3, each mode has nearly perfect linear behavior so that its time dependence is sinusoidal. Thus,

$$\theta = \sum_{i=1}^{N} \theta_i \sin\omega_i t \tag{14}$$

will hold until the mode approaches its limiting amplitude. In the following calculation, all oscillation frequencies ω_i will be assumed to be independent and incommensurate. This gives a lower limit to the overall nuclear driving but does not revise our belief that, in fact, some of these frequencies will couple. It follows from equation (14) that the time average of θ raised to any odd power must vanish. For even powers, an amplitude distribution must first be assumed. For brevity, the simplest useful one will be chosen; however, more realistic distributions are expected to give comparable results until the ratio in equation (13) becomes much greater than 1. All the stronger modes are assumed to have the same amplitude A and the weaker ones are set equal to zero. In the limit of a large number, N_s, of strong modes, it can be shown that

$$<\theta^{2q}> = (2q - 1)!!\ (<\theta^2>)^q \qquad , \text{ or}$$

$$= (2q - 1)!!\ (\theta_{rms})^{2q}$$

where $\theta_{rms} = (1/2\ N_s\ A^2)^{1/2}$ in this case and $(2q - 1)!!$ stands for the product, $1 \cdot 3 \cdot 5 \cdots (2q - 1)$. The factorial can increase the nuclear energy generation by much more than one might have guessed from knowledge only of the rms amplitude. Physically, this increase reflects the fact that, when the modes interfere constructively, they enhance the nuclear burning much more than they reduce it during destructive interference. The ratio dU/dU_1 can now be numerically evaluated and it is plotted in Figure 4. The figure shows how the nuclear portion of the work integral departs from its linear value as the rms temperature fluctuation rises. Two different equilibrium temperatures were used for the solar material, 9 and 12 x 10^6 K, roughly bounding the layers in a mixed model where nuclear reactions are important to the pulsation. From the figure one sees that this driving is greater than linear theory would give by factors of 3 to 10 in the range of fluctuations, $0.10 < \theta < 0.14$. Actually, this range will be more like $0.06 < \theta < 0.08$ because the plotted curves considerably underestimate the enhancements. (That is because a constant β was used, appropriate to the location $\theta = \theta_{rms}$, whereas an averaging over a statistical distribution of β values would describe better the true situation.) Nevertheless, it is already clear from the figure that many modes can be expected to switch from a damped condition to one of excitation under the combined effects of the extra driving in this range and the reduced damping caused by the spatial concentration. The following limitations should be kept in mind.

4.2. Limitations on Harmonic Numbers and Amplitudes

Very high radial harmonics cannot be making the main contribution to the enhanced nuclear driving. The nodes of such harmonics are too closely spaced in the radial direction, placing a limit on how far the fluid can move in an oscillation

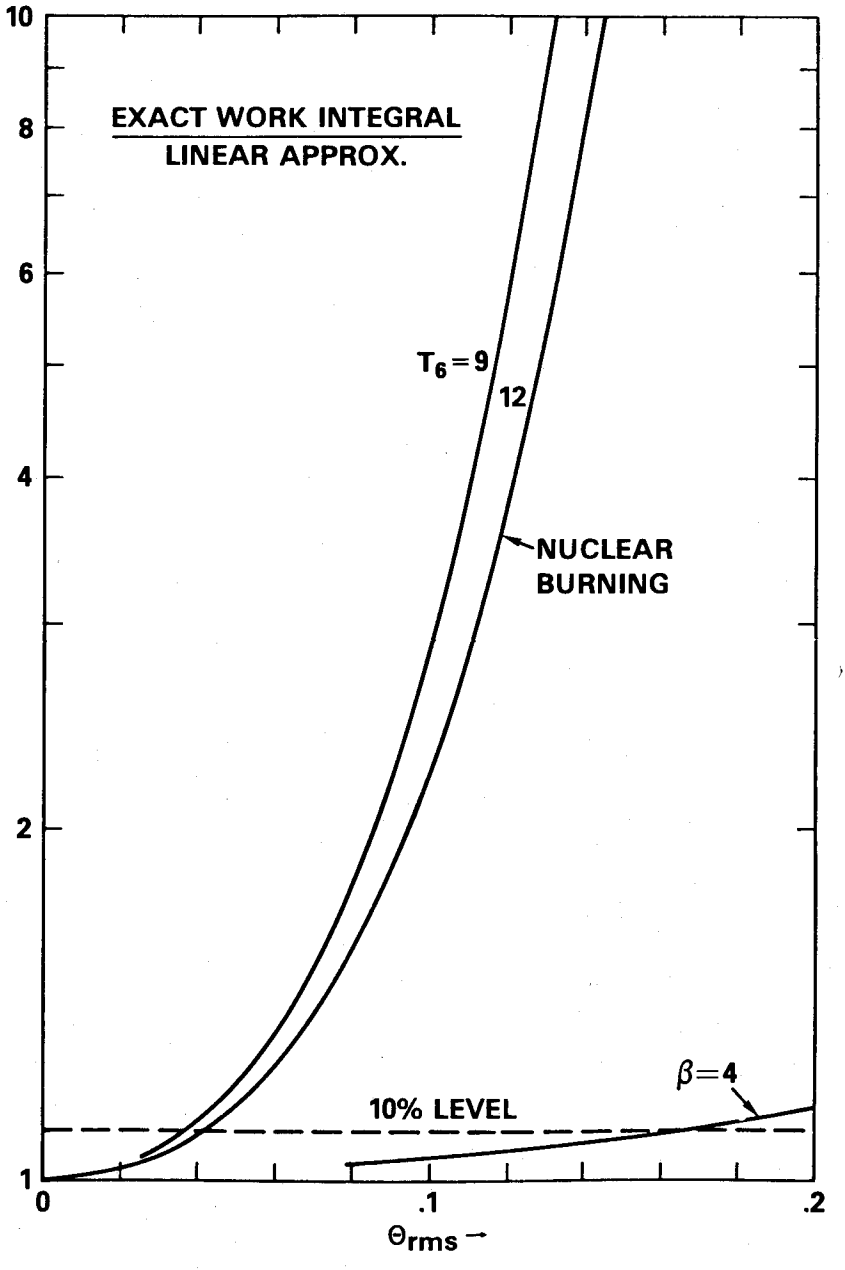

Figure 4. A lower limit to the exact work integral for nuclear driving divided by its conventional linear approximation, dU_1. The abscissa, θ_{rms}, represents the root mean square value of the local relative temperature fluctuation. The curves are computed for the temperatures of 9 and 12 million kelvin in material which is 75% hydrogen. The $\beta = 4$ curve from Figure 3 is included for reference since it serves as a generous upper limit to the behavior of the radiation damping term in the core.

cycle. In turn, that limits the total temperature fluctuation available since the motion is curl-dominated. In order to obtain temperature fluctuations exceeding ± 5% near r_ε, the typical linear modes being coupled must have harmonic numbers, $-k < 15$ for low values of ℓ. For $\ell = 10$, the condition becomes $-k \leq 10$ and there is little further change for higher ℓ values.

The second limitation applies to the angular harmonics of the g-modes with oscillation periods ≃ 1 hour seen by the SCLERA telescope. These limb measurements by Hill and Caudell imply motions of the photosphere and subsurface layers in which $(\delta r/r) \sim 10^{-6}$. Fairly large ℓ values are required to make such a small surface motion consistent with a large amplitude in the core. Figure 5 shows how much the radial motion is diminished as it traverses the convection zone from r_b, the base of the zone, to 0.98 $R_\odot$, a subsurface layer. Th solid lines come from the relation, $\delta r\, \rho_0^{1/2}\, r^{\ell^* + 1.5}$ = constant, where $\ell^* = [\ell(\ell + 1)]^{1/2}$. The lines are dashed where this ceases to be a good approximation. Three plausible base levels have been used, $(r_b/R_\odot) = 0.5$, 0.6, and 0.7. Reductions $\sim 10^{-4}$ are needed in Figure 5 in order that the surface amplitudes will imply motions at r_b for which $(\delta r/r) \sim 10^{-2}$. Motion of this order of magnitude can lead to the large temperature fluctuations at greater depth required by our model. Therefore, our model could conveniently explain the SCLERA observations with ℓ values greater than about 15. This is certainly consistent with the measured range, $20 < \ell < 40$, but more detailed measurements and modeling will both be required before a stronger statement can be made.

Finally, the maximum displacement of the fluid at an antinode must be less than half the distance between the nodes. To exceed this would produce unphysical amplitudes. The condition for oscillatory motion would thereby be violated and a partial transition to circulatory motion would occur locally. Significant energy losses would result because of the failure of part of the fluid to return smoothly after such an extreme excursion. This is a form of turbulence, of course, but it may not be useful to try to describe it by the conventional expressions normally inserted into equations (4) by pulsation theorists. Rather, the phenomenon is more analogous to the droplets expelled from a pond after a pebble has been thrown in. I believe that this mechanism limits the size of the oscillations described in this paper. Each nonlinear mode should grow until the antinodes having the most extreme motion begin to throw off "droplets" at an average rate comparable in energy content to the nuclear driving. Since this phenomenon should occur most often at the most centrally located antinodes, an adiabatic stratification may develop in a tiny core (radius, $\sim 10^{-2}\ R_\odot$) due to the frequent mixing. (Incidentally, shock phenomena are not expected in our model because the high sound speed in the core keeps $v/c < 10^{-2}$ throughout the star.)

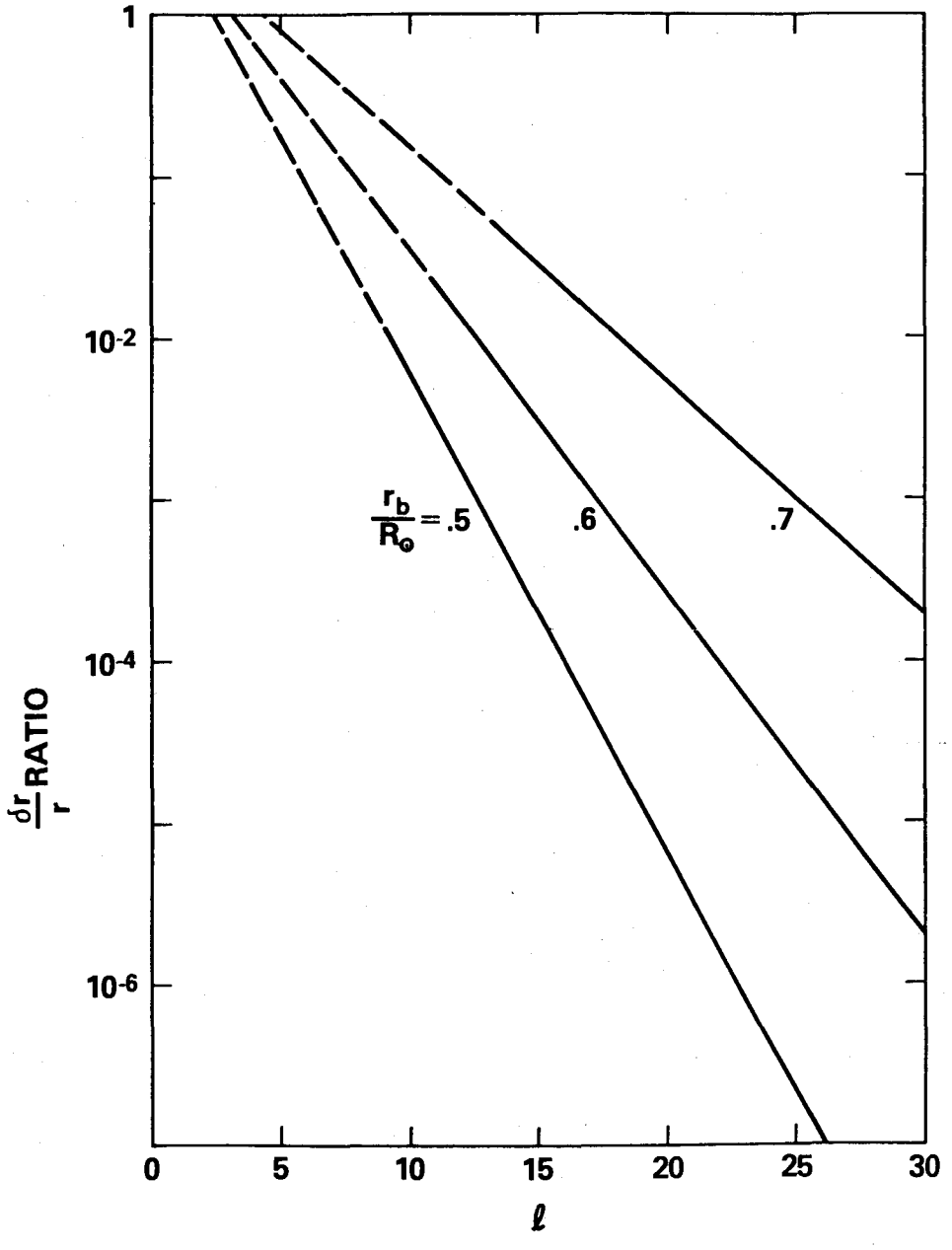

Figure 5. The ratio of $(\delta r/r)$ at a subsurface layer, $r = 0.98\ R_\odot$, and $(\delta r/r)$ at the base of the convection zone, r_b. Very strong reductions in subsurface amplitudes occur for all modes with high angular harmonic numbers, ℓ. The stronger reductions occur for the thicker convection zones. The small limb excursions measured by Hill and Caudell are roughly consistent with the large core amplitudes advocated herein at ordinate values on this figure $\sim 10^{-4}$. This implies that high ℓ harmonics are needed in our model and this is consistent with the measurements.

5. OBSERVATIONAL TESTS OF THE MODEL

5.1. Existing Evidence

In the preceding sections, theoretical means are described by which g-modes may be excited in the sun. Present day uncertainties concerning stellar interiors prevent anyone from demonstrating more than the plausibility of a purely theoretical argument about the excitation of g-modes in the solar core. But there are three sets of observations which, taken all together, form a fairly strong case against the standard, unmixed solar models. These observations are all consistent with the pulsating mixed model described herein.

Numerous radial velocity measurements taken in this decade have shown oscillatory power in the range (15 minutes to 1 hour) appropriate to g-modes; among the earliest are those of Durasova, Kobrin, and Yudin (1971) and Deubner (1972). However, these measurements failed to display precise, reproducible periods and angular harmonic structure, leaving most people in doubt as to whether they represented global modes. The first good evidence of g-modes in the sun was Wolff's (1976) indirect detection of their rotation periods; this exercise was undertaken because of the likelihood that these periods might be easier to detect than the much more numerous oscillation periods. Under appropriate nonlinear coupling stronger than about one part in 10^5, Wolff (1974) demonstrated that large numbers of solar g-modes can couple to form a small number of rigidly rotating modes, each having an array of oscillation periods but just one rotation period. The set of theoretical rotation periods derived can be regarded as a unique signature of coupled g-modes. Later, the not unreasonable assumption was put forth by Wolff (1974) that oscillatory power in the solar core and therefore in the lower convection zone would modulate solar activity. To a remarkable degree, the periodicities in two centuries of sunspot data matched the beat periods between g-mode rotation periods. Since the detected beat periods had been derived from modes with angular harmonic numbers ℓ = 6, 7, 8, 9, 10, and one higher order mode, the agreement was strong indirect evidence that many g-modes with $\ell \geq 6$ are excited. It further implied that groups of linear modes with a single value of ℓ had become coupled so as to concentrate their oscillatory power in longitude; these particular beats could not otherwise have been observed. These observations support the present paper because they strongly indicate that high ℓ modes are excited and concentrate their power in at least one spatial dimension.

In their solar diameter measurements, Hill and Caudell (1979) achieved the first direct detection of g-modes, represented by oscillatory power at periods of 45 and 67 minutes. These periods are too long to be p-modes whether the standard solar model or a mixed one is used. The measurements were taken by Hill and Caudell at two different scan amplitudes, providing a rough measurement of the typical horizontal wavelengths involved. These are referred to in terms of a range of spherical

harmonics, $20 < \ell < 40$. Finally, the modes display phase coherence over the two-week observational interval, proving that they are global modes.

Continued confirmation of these measurements will have major consequences for the study of solar interiors. The high angular harmonics detected by Hill and Caudell are all damped by radiation losses near the solar center under standard calculations. Also, when a standard extrapolation is made of the surface amplitudes, these measurements imply impossibly large motion in the interior unless an exceptionally thin convection zone is assumed. Thus, the Hill and Caudell observations are not consistent with conventional, uncoupled g-modes in a standard solar model. The conventional approach provides neither an excitation mechanism nor acceptable central amplitudes. Both difficulties could be avoided by the scheme proposed in this paper. Finally, a well-known problem of the standard model is its inability to explain the low value of the neutrino flux seen in the Davis (1978) experiment. Unless there is an undetected error in the nuclear physics, Davis' measurements imply the standard model is incorrect in at least the central tenth of the solar radius since that is where virtually all the detected neutrinos are generated. As many authors have noted (e.g., Bahcall 1977), thorough mixing of the core material could alleviate this problem. Mixing increases the hydrogen mass fraction from 0.5 to 0.75, thereby lowering the central temperature by several million kelvins. Because of the extreme temperature sensitivity of the relevant reactions, the mixed models have neutrino fluxes which are lower than those predicted by the standard model by a factor of 3, putting them in agreement with the Davis experiment. The large amplitude pulsations limited by turbulent losses as proposed herein would almost certainly mix the central parts of the core in a time much shorter than 10^9 years. (The turbulent limit discussed in § 4.2 takes place at antinodes whose dimensions are $\sim 10^{-2}$ or 10^{-3} $R_\odot$. This means that diffusion lengths are of comparable size, giving adequately rapid mixing.) By providing a mixing mechanism, our model is consistent with Davis' (1978) neutrino flux to the currently achieved levels of accuracy.

5.2. Future Tests

The model has several consequences which can be searched for in data now being accumulated. First of all, the sun's nuclear burning rates vary in this model, resulting in a modulation of the neutrino flux on time scales of months and years. This variation in burning rates follows from the fact that many nonlinear modes with different ℓ values are active. The modes rotate at different rates in the sun, causing enhanced burning as the longitudes into which their oscillatory power is concentrated rotate past each other. In addition to directly modulating the neutrinos, the extra burning is associated with slight mixing events in directly changing the neutrino rate. It is not clear whether the direct or indirect effect

will be the larger.

Secondly, upwellings of huge scale are to be expected in the convective envelope from time to time. These are caused by the occasional high concentrations of oscillatory power at certain latitudes and longitudes, heating the base of the convection zone asymmetrically. Transport of the extra heat to the surface would seem to be accomplished most efficiently by flow patterns on scales comparable to those of the oscillations. (Of course, there would also be a local increase in the intensity of small scale convection, carrying off part of the heat with no net upward mass flux.) The large scale upwellings seem to me to be unavoidable in an adiabatically stratified layer and have played a part in all my solar papers since 1974. The more interesting question is their intensity. In particular, will they reach the surface with velocities that are detectable? This can only be answered by observation in view of the uncertainties in the theory of astrophysical convection.

Thirdly, an asymmetric flow like the above must increase the surface brightness in and near the upwelling region. Thus, the sun's intensity as seen at the earth will vary sometimes with a period of roughly 27 days. This small effect may be detectable by experiments that are, or shortly will be, in space.

Detection of any of the above three effects would lend support to our model. But the most convincing confirmation would come if appropriate recurrence tendencies were proven. Variability on definite time scales of months and years is predicted by this model (Wolff 1976) on the basis of the easily calculable rotation periods of most solar g-modes. The standard picture of the sun would be inconsistent with a neutrino flux proven to be variable but it might be able to accommodate upwelling and luminosity changes by means of more realistic treatments of flow in convective envelopes.

6. SUMMARY

A method was described for exciting g-modes in the sun at the high angular harmonic numbers required by the observations. Qualitatively, it can resolve three serious discrepancies between conventional theoretical work and solar measurements. It proposes a new picture of the solar interior wherein the core of the sun is in a quite different state from the almost peaceful condition envisioned by most solar physicists.

The key theoretical feature of this paper was that it noted the very large number of linear modes which are probably active (hundreds or thousands) and assumed that they will occasionally combine to produce large temperature fluctuations exceeding 5% in various small regions of the sun's core. Such large fluctuations produce strong nonlinear effects through the nuclear reactions. An illustration was given on how this could concentrate the oscillation energy into layers favorable to excitation and diminish the exposure to losses near the center and in the envelope.

A set of nonlinear modes would result which formed at fairly regular intervals and grew until their amplitudes became large enough for turbulence to limit their further growth. The type of turbulence thought to be significant (§ 4.2) stirs the inner core material with mixing lengths $\sim 10^{-3}\ R_{\odot}$, guaranteeing a well-mixed core. The most important unproven aspect of this model was the assumption that perturbations of $\sim 10^{-3}$ in the oscillation frequencies will occur during mode coupling so that spatial concentration in the radial dimension can be achieved.

Today, pulsation theory cannot make definitive predictions about the sun because of major unknowns like the composition and temperature gradient in the core, the true importance of turbulence, and the detailed nature of coupling among linear modes. Therefore, it is especially dangerous to ignore inconvenient observations. There are now three groups of observations weighing against the conventional view of an unmixed solar core pulsating only in very low angular harmonics at infinitesimal amplitude, if at all. It is possible to avoid the negative implications of each group of observations by either questioning its validity or by making special revisions to the theory, but it is not encouraging when so many special arguments are needed. In contrast to this, the model advocated in this paper seems to be compatible with all three groups. These groups are: (1) the observation by Hill and Caudell that solar g-modes are active at high ℓ values; (2) the indirect detection by Wolff (1976), implying that nonlinear coupling is operating among g-modes, concentrating their oscillatory power in the angular dimensions; and (3) the unexpectedly low measurement by Davis (1978) of the low solar neutrino flux. The neutrino problem has received much attention and numerous solutions have been proposed. In his review, Bahcall (1979) has described all solutions depending on solar model revisions as "ad hoc." It is possible that the model presented herein is the first exception: it explains three troublesome data sets, not just that of the neutrinos, and it is a fairly plausible outcome of the presence of many high order g-modes in a fluid containing an extremely nonlinear driving mechanism.

Finally, the model implies several other things which can be tested in the coming years. It predicts time variability on certain definite time scales (measured in months and years) for the phenomena modulated by the g-modes; specifically, these are the solar neutrino flux, upwellings of global scale in the convective envelope, and rotationally asymmetric brightness of the sun. See § 5.2 for details. With appropriate adjustments for the different physics involved and the shorter data sets available, many of these future tests may be similar in principle to that given by Wolff (1976) using the extensive records of solar activity variations.

REFERENCES

Bahcall, J.N. 1977, Ap. J. (Letters), 216, L115.

Bahcall, J.N. 1979, Space Sci. Rev. (to be published).

Christensen-Dalsgaard, J., Dilke, F.W.W., and Gough, D.O. 1974, Mon. Not. R. Astr. Soc., 169, 429.

Cox, A.N. and Stewart, J.N. 1970, Ap. J. Suppl. No. 174, 19, 243.

Davis, R., Jr. 1978, Proceedings of the Brookhaven Solar Neutrino Conf., 1, 1.

Deubner, F.-L. 1972, Solar Physics, 22, 263.

Dilke, F.W.W. and Gough, D.O. 1972, Nature, 240, 262.

Durasova, M.S., Kobrin, M.M., and Yudin, O.I. 1971, Nature Phys. Sci., 229, 82.

Dziembowski, W. and Sienkiewicz, R. 1973, Acta Astr., 23, 273.

Fowler, W.A., Caughlan, G.R., and Zimmerman, B.A. 1975, Ann. Rev. Astron. Ap., 13, 69.

Hill, H.A. and Caudell, T.P. 1979, Mon. Not. R. Astr. Soc., 186, 327.

Shibahashi, H., Osaki, Y., and Unno, W. 1975, Publ. Astron. Soc. Japan, 27, 401.

Unno, W. 1975, Publ. Astron. Soc. Japan, 27, 81.

Wolff, C.L. 1974, Ap. J., 193, 721.

Wolff, C.L. 1976, Ap. J. 205, 612.

Wolff, C.L. 1979, Ap. J., 227, 943.

COMMENTS ON GRAVITY MODE EXCITATION MECHANISMS

W. Dziembowski[1]
Department of Physics
University of Arizona
Tucson, Arizona

Studies of nonlinear effects in solar oscillations may help us identify a mechanism for gravity mode excitation. However, we do not expect that nonlinearities in the perturbation of nuclear energy generation rate as discussed by Wolff (1980) are indeed relevant. Nonadiabatic effects for gravity modes trapped in the interior are quite small: typical linear growth or damping rates are in the range of 10^{-9} - 10^{-10} per pulsation period (see e.g., Keeley 1980). In such a situation energy exchange between modes due to three-mode resonant coupling (see Dziembowski 1980) will certainly be important at the amplitude level well between the onset of the nonlinear effects discussed by Wolff.

Thus, for the hypothesis that long-period solar variability is the manifestation of gravity modes, we attach more promise to the investigation of three-mode resonant interactions. Moreover, nonlinear mode interaction may account in a natural way for amplitude decline of 2^h40^m oscillations occurring on the time scale of few years (Kotov, Severny and Tsap 1978). Decay due to radiative damping occurs on the time scale by at leave five orders of magnitude longer.

REFERENCES

Dziembowski, W. 1980, these proceedings.
Keeley, D.A., 1980, these proceedings.
Kotov, V.A., Severny, A.B. and Tsap, T.T. 1978, Mon. Not. R. Astr. Soc., 183, 61.
Wolff, C.L. 1980, these proceedings.

---

[1]Visiting Professor on leave-of-absence from the Copernicus Astronomical Center, Warsaw, Poland.

SOME THEORETICAL REMARKS ON SOLAR OSCILLATIONS

D. Gough
Institute of Astronomy, and Department of Applied Mathematics
and Theoretical Physics, University of Cambridge, UK

ABSTRACT

The properties of the linear modes of oscillation of a nonrotating nonmagnetic star, with particular reference to the sun, are briefly described. The most likely mechanisms by which they might be excited are reviewed, and it is concluded that stochastic excitation by turbulence is probably the dominant mechanism that drives the solar five minute oscillations. Phase coherence of one of the components of the SCLERA diameter data is illustrated, and the new five minute oscillations in the Birmingham whole-disk Doppler data are discussed. Finally some of the problems raised by conflicting evidence concerning the structure of the sun are aired, but not resolved.

1. INTRODUCTION

From the properties of linear eigenmodes and the values of the oscillation amplitudes that are observed at the solar surface, it is consistent to suppose that the amplitudes of most of the modes are small throughout the sun, except possibly in the upper atmosphere. Though it is a circular argument to conclude from this that the amplitudes really are small, the present discussion is nonetheless based towards linearized theory. Such theory may prove to be inadequate for a complete description of solar oscillations, but it is no doubt useful in providing us with an understanding of much of the essential physics.

Interest in solar oscillations extends beyond the phenomenon itself. The modes experience conditions inside the sun, and thus provide us with the opportunity to perform a seismological inversion on the solar interior. Because linear eigenmodes of a given model of the sun can be computed with relative ease and certainty, and because there exists a considerable body of inverse theory developed chiefly by geophysicists, one has reason to anticipate at least a modicum of success. At present the quality of the data is probably inadequate to warrant using the entire mathematical machinery that has been developed for studying the earth, but the information we do have available is sufficient to have posed several problems worthy of discussion.

Before such discussion is possible, it is necessary to establish the basic properties of the linear eigenmodes. This will be done briefly, after which some of the issues that have been raised in other contributions to this workshop will be addressed.

2. CLASSIFICATION OF LINEAR NORMAL MODES

The following discussion will concentrate on the most commonly encountered modes of oscillation that can exist in a nonrotating nonmagnetic star. These were classified by Cowling (1941) into p, f, and g modes for adiabatic oscillations of a polytrope; it is believed that a formal classification of this type is possible for adiabatic oscillations of any stellar model. Since the equilibrium model is essentially spherically symmetrical--at present the inhomogeneities produced by convection will be ignored--a linear mode is separable in radial and angular spherical polar coordinates and time, with sinusoidal time dependence and an angular dependence that is proportional to a tesseral harmonic. The mode can be characterized by three integers n, ℓ, m, where ℓ and m denote the degree and order of the tesseral harmonic and n is usually called the order of the mode. The oscillating frequency is independent of m. It is convenient to regard n as being negative for the g modes, zero for the f modes and positive for the p modes.

Broadly speaking, as $|n|$ increases so does the number of nodes in the radial component of the displacement eigenfunction. Indeed, for smoothly varying stellar models such as a polytrope of low index, $|n|$ is equal to the number of nodes in the radial displacement,[1] as is also the case for any realistic stellar model when $|n|$ is sufficiently large. Otherwise the situation is rather more complicated. The algebraic method of node counting described by Eckart (1960), and employed by Scuflaire (1974) and Osaki (1975) for stellar oscillations in which perturbations in the gravitational potential are ignored, breaks down when gravity is correctly taken into account. Nevertheless, it seems that the symmetry of the governing equations is such that eigenfrequencies cannot cross under continuous transformations of the equilibrium model. Thus it seems likely that a value of n can be uniquely assigned to any mode of a stellar model in such a way that it agrees with Cowling's classification when the equilibrium model is transformed continuously by any path to a polytrope of low index. However, this has not been proved.

Strictly speaking, this discussion applies only to adiabatic oscillations subject to perfectly reflecting boundary conditions. These have real eigenfrequencies and eigenfunctions. The linear nonadiabatic oscillations, possibly with leaky boundary conditions, are not purely oscillatory and the problem of their

---

[1] In the case $\ell = 0$ alone, the center of the star is considered to be a node.

classification is more complicated (cf. Christensen-Dalsgaard 1980), though for most modes the eigenfrequency is almost real. In the following discussion I shall loosely call such an oscillation a normal mode. Because the quality Q, which is the ratio of the damping or growth time of the oscillation to its period, is high, the deviations of the basic properties of the oscillation from the adiabatic normal modes are generally small; therefore, adiabatic and nonadiabatic approximations will not be differentiated except where such distinction is important.

3. NATURE OF THE OSCILLATIONS

A precise formal classification of modes of the kind described above would provide a useful means of specifying the mode unambiguously and concisely, but a more physical description is often much more informative. In simple situations, such as that discussed by Cowling, p modes are stationary acoustic waves, f modes are surface waves and g modes are internal gravity waves. In more realistic models of the sun, the local character of a mode can change with depth. In some places the dynamics of a mode might resemble that of a gravity wave, whereas elsewhere the motion might be characteristic of a surface wave or an acoustic wave. It is simplest to recognize the local behavior when $|n|$ is large and eigenfunctions vary with radius much more rapidly than the equilibrium model. In that case the JWKB approximation, or even the plane wave approximation, can be made. Several examples of solar modes are discussed in this way by Christensen-Dalsgaard, Dziembowski and Gough (1980) and Christensen-Dalsgaard and Gough (1980a) in these proceedings.

The p modes of low degree exist with substantial amplitude throughout the entire body of the sun. When n is large they may be regarded as ordinary sound waves propagating almost radially, and in this limit the energy density per unit radial distance is constant. The modes of high degree and low order propagate obliquely; these are confined in the surface layers by refraction resulting from the increase with depth of the sound speed. The principal restoring force in an acoustic oscillation is the pressure fluctuation produced by compression. Thus the velocity field has a high divergence, and is almost irrotational. Typically most of the kinetic energy is associated with the vertical component of the motion.

When n is large the wavelength is small, and the speed of propagation is hardly influenced by the stratification of the star. The eigenfrequencies $\omega_{n\ell}$ approach a harmonic sequence as n increases, with frequencies given by (e.g., Vandakurov 1967)

$$\omega_{n\ell} \sim \tfrac{\pi}{2}(2n+\ell+\varepsilon)\left(\int_0^R \frac{dr}{c}\right)^{-1} \quad \text{as } n \to \infty \quad , \tag{3.1}$$

where r is the radial coordinate, R is the radius of the sun, c is the sound speed

and ε is a constant which depends on the equilibrium solar model. As is the case with solutions of the pure wave equation in a spherical cavity, $\omega_{n,\ell} \sim \omega_{n-1,\ell+2}$ and $\omega_{n,\ell+1} \sim 1/2(\omega_{n,\ell} + \omega_{n,\ell+2})$ as $n \to \infty$. Though equation (3.1) is correct in the limit $n \to \infty$ at fixed finite ℓ, it is useful to regard the formula as an approximation at finite n, in which case the condition $n >> \ell$ must be satisfied.

If $\ell >> 1$ and n is large, but not much greater than ℓ, the eigenfrequencies may be estimated by ray theory. The period of oscillation is the time taken for an oblique wave initially propagating downwards from the surface to return to the surface. The dispersion relation is found by noting that in order for a sequence of such waves to interfere constructively to form a stationary wave pattern of order n, each ray must return to the surface n horizontal wavelengths displaced from its origin. One finds in this way that if the region of the sun occupied by the wave is approximatd by a polytrope of index μ,

$$\omega_{n\ell} \simeq 2n \frac{\gamma g k}{\mu+1} \quad , \tag{3.2}$$

where $g = GM/R^2$ is the surface gravity and $\gamma = (d\ln p/d\ln\rho)_s$, with p being pressure, ρ density and derivative being taken at constant specific entropy, and where $k = [\ell(\ell + 1)]^{1/2}/R$ is the horizontal wavelength. Moreover the penetration depth is found to be $2nk^{-1}$, which is simply the level at which waves of frequency $\omega_{n\ell}$ have a total wavelength k and therefore propagate horizontally. Equation (3.2) is correct for values of large n; when n is small, one must take more careful account of the boundary conditions, which add the constant μ to the factor 2n. There is also a modification due to buoyancy if the polytrope is not adiabatically stratified. The complete formula is given, for example, by Gough (1978).

It is clear from equations (3.1) and (3.2) that $\omega_{n\ell}$ increases with ℓ and n when n or ℓ is large, and numerical solutions always exhibit this property regardless of the values of n and ℓ. Thus one would expect p-mode frequencies to be bounded below by that of the radial pulsation of order unity, although it does not appear that this has been proved. This mode of a typical solar model has a period of about one hour.

The f mode, or fundamental mode, is essentially a surface wave. The restoring force is provided by gravity, and were it not for the curvature of level surfaces in the unperturbed star and the variation of gravity with depth, the velocity field would be both irrotational and solenoidal and the frequency would be that of a deep water wave: $\omega = (gk)^{1/2}$, irrespective of the stratification of the unperturbed state. The waves are concentrated in a layer of thickness k^{-1} immediately beneath the surface. Thus when $\ell >> 1$, the deep water wave frequency is an accurate approximation. The kinetic energy is approximately equally shared between the horizontal and vertical components of the motion.

Internal gravity waves can exist if there is a region of the star which is

stably stratified. The restoring force is provided by negative buoyancy which generates vorticity, giving rise to an array of oscillating eddies. The frequency is lower than that of a p mode of the same degree, and consequently there is more time for pressure to adjust across the eddy. As a result, the dilatation of the flow is determined almost completely by the unperturbed density stratification, and is such that the momentum density field is almost solenoidal (cf. Ogura and Phillips 1962).

Oscillatory g modes tend to be confined to stably stratified regions, and are evanescent in convection zones. Thus in the sun there are at least two classes of such modes: those confined to the interior beneath the convection zone, and those in the atmosphere. Their frequencies are controlled by the buoyancy frequency N which is given by

$$N^2 = g\left(\frac{1}{\gamma}\frac{d\ell n p}{dr} - \frac{d\ell n \rho}{dr}\right) \quad . \tag{3.3}$$

This would simply be the frequency of a small oscillating fluid parcel that remains in pressure balance with its surroundings and which is imagined to drive no horizontal flow. Note, therefore, that because the motion of an actual g mode cannot be purely vertical, the extra inertia provided by the horizontally moving fluid reduces the frequency of the mode below N. A formal proof of this statement is given by Christensen-Dalsgaard (1979). As $\ell \to \infty$ at fixed n, the eddies become elongated in the radial direction and the horizontal components of velocity approach zero. The eddies become trapped near the maxima N_{max} of N, and $\omega_{n,\ell} \to N_{max}$ from below. As $|n|$ increases at fixed ℓ, the eddies become more flattened in the vertical direction, and the flow is predominantly horizontal. The gravitational potential energy that can be drawn on by an eddy decreases in comparison to its inertia and the frequency diminishes. Indeed, $\omega \to 0$ and $|n| \to \infty$ at fixed ℓ. When $|n|$ and ℓ are comparable, the kinetic energy is shared about equally between the horizontal and vertical components of the motion. Note that, unlike the p modes, the f modes and the g modes depend on the presence of horizontal variations in the perturbations, and so do not exist when $\ell = 0$.

Throughout most of the inner half by radius of the sun, N is probably of order 0.4 mHz which estimates, to within geometrical factors, the frequencies of internally trapped g modes with order not greatly in excess of degree. The dependence of N^2 on radius is depicted in these proceedings in Figure 1 of Christensen-Dalsgaard, Dziembowski and Gough (1980) for two solar models. The buoyancy frequency never exceeds about 0.45 mHz, which implies that these g modes cannot have periods less than about half an hour. Further details of the properties of the modes also are presented in Christensen-Dalsgaard, Dziembowski and Gough (1980).

The frequencies of the atmospheric g modes can be rather greater than those

of the interior modes. If the atmosphere is approximated by a perfect isothermal gas of molecular weight μ at temperature T, equation (2.3) reduces to

$$N^2 = \left(1 - \frac{1}{\gamma}\right)\frac{g}{H} \quad , \tag{3.4}$$

where $H = \mathcal{R}T/\mu g$ is the scale height of the atmosphere, $\mathcal{R}$ being the gas constant. Taking μ = 1.2 and T = 5800 K, the effective temperature of the sun, a value of about 4 mHz is obtained for N. Thus one expects atmospheric g modes to have periods greater than or approximately equal to 4 minutes.

Note than in the corona the buoyancy frequency is less than one tenth that in the photosphere and low chromosphere. Thus the higher frequency g modes are trapped between the corona and the top of the convection zone. If the height of the base of the corona above the top of the convection zone is h, the g mode frequencies are approximately given by

$$\omega^2 \simeq \frac{k^2N^2}{k^2 + (n\pi/h + \delta)^2 + 1/(2H)^2} \quad , \tag{3.5}$$

where δ is a finite phase factor that depends weakly on conditions in the corona and the convection zone and on k and n.

It should perhaps be added that formally there is a class of linear g modes that are trapped in the convection zone. These have $\omega^2 < 0$, and so grow exponentially with time. They are sometimes called g^- modes, to distinguish them from the oscillatory modes described above, which are then labeled g^+. If an initial equilibrium state of no motion was imagined, g^- modes would grow if a region existed where $N^2 < 0$. Their amplitudes would soon become large, and nonlinear effects would become important. This is convection, and it is not clear whether the linear modes have much direct relevance to the final state.

Other forms of oscillations are also possible. In particular, rotation and magnetic fields modify the waves described above, and also add new spectra of modes: the inertial oscillations and the Alfven modes. Moreover, oscillatory dynamo modes in some form or other are presumably responsible for the solar cycle, and thermally controlled oscillations with much longer periods arising from the coupling between the convective and radiative zones may be operative. These modes will not be discussed here.

4. GLOBAL OR LOCAL?

The adiabatic normal modes of a nonmagnetic fluid star form a complete set (cf. Eisenfeld 1969, Dyson and Schutz 1979). Thus any disturbance can be represented as a superposition of these modes, and may be regarded as being in some sense

'global.' Nevertheless, a disturbance initiated by a localized perturbation takes time to communicate with the rest of the sun, and before that time has elapsed the disturbance is genuinely 'local.'

Whether a mode can be genuinely global rests on whether it can survive long enough to propagate around the sun. The modes of low degree are global, since their propagation times are comparable with their periods. But for the modes of high degree the situation is less obvious. In particular, the five minute oscillations, which are p modes of high degree, have group velocities approximately equal to half their horizontal phase velocities, as is apparent from equation (2.2) and the subsequent discussion. Thus a typical mode in the middle of the k-ω power diagram presented, for example, by Deubner, Ulrich and Rhodes (1979) has $k = 0.5$ Mm^{-1} and $\omega = 2 \times 10^{-2}$ s^{-1}, yielding a group velocity of 20 km s^{-1}. To travel a single circumference of the sun would take such a mode a time of about 2×10^5s, which is about 700 periods. Whether the mode survives so long is an open question. Observationally, Deubner, Ulrich and Rhodes (1979) found widths of the ridges in their power spectra consistent with coherence lasting for the entire duration of a day's observing; however that is less than 2×10^5s. Moreover, the theoretical estimates made in the investigation reported by Berthomieu et al. (1980) yielded decay times for some of the modes they selected which were also less than the travel time. This suggests, therefore, that though some of the five minute oscillations may be genuinely global, others may be localized. With sufficiently long and careful observing runs one might hope to resolve the discrete values of the horizontal wavelength k for the global modes. It must be borne in mind, however, that velocity fields associated with convection or other large scale phenomena distort the wave patterns, thus rendering such resolution more difficult than one might at first suspect.

5. EXCITATION

There has been considerable debate concerning the principal source of excitation of the oscillations. Broadly speaking, the driving mechanisms may be divided into two classes: those by which energy is transferred from the mean (horizontally averaged) environment to the oscillations, and those that depend in some intrinsic way on the interaction with the horizontal fluctuations produced by motion other than that associated with the oscillation itself. Of course both forms of energy transfer take place, and the dominant form may be different for different modes. Nevertheless there is mounting evidence that interactions with other motions is important in the overall dynamics of the modes.

It has been argued by Ulrich (1970), Wolff (1972) and Ando and Osaki (1975, 1977) that most of the modes responsible for the five minute oscillations are overstable in linear theory, and thus would grow spontaneously to their present

amplitudes from a presumed initial non-oscillating state. This is the only suggestion implementing one of the first class of driving mechanisms that has been investigated in detail. Ando and Osaki claim that the dominant driving process is the κ-mechanism, whose importance in the dynamics of the radial pulsations of Cepheids and RR Lyrae stars has long been appreciated. An issue that has not been addressed by the advocates of this theory, however, is why it is that the amplitudes of the modes are so low. The mechanisms that limit the amplitude of an overstable oscillator are nonlinear, and it is hard to envisage what they might be in the case of the five minute oscillations. To be sure, the amplitudes of density fluctuations in the low chromosphere may be large enough for nonlinear processes to be extremely important there, as has been pointed out recently for example, by Hill, Rosenwald and Caudell (1978), but aside from the chromospheric modes the energy densities are so small in this region as to make it quite unlikely that such processes can control the energy balance *in situ*. This difficulty must also be faced by anyone who argues that the longer period oscillations are linearly overstable, or that the oscillations are stable in linear theory but are finite-amplitude unstable. There is the possibility, however, that nonlinearities in the chromosphere may modify the structure of the waves to so great an extent as to permit substantial leakage of energy into the corona.

If one is to reject the idea that most of the five minute modes are overstable, one must explain why the linear nonadiabatic analysis came to a contradictory conclusion. The reason presumably lies in the convection-pulsation interaction, which is generally ignored. In these proceedings, however, Berthomieu et al. (1980) report that they found all the modes with $\ell = 200$ and 600 to be stable when convection was taken into account. If these modes are not atypical, most of the five minute modes might therefore be stable. The calculation of Berthomieu et al. employed a generalized mixing-length theory, in the form used by Baker and Gough (1979) to study RR Lyrae models; this method, however, is very uncertain. The result should therefore be regarded not as strong evidence for the stability of the five minute modes, but rather as an indication that one should at least doubt previous claims to the contrary.

The second class of driving mechanisms is now addressed. Here the energy transfer to the modes is nonlinear, and is therefore much more difficult to analyze. It is convenient to divide the transfer into two subclasses, the first of which is transfer from the turbulent convective motion and the second, transfer from other modes of oscillation. In the latter case the energy of the oscillations that drive the mode might come, either directly or indirectly, from the convection or from one or more genuinely overstable modes. Of course there is also the possibility that energy is extracted from other forms of motion, such as meridional circulation, the giant cells and rotation, or from the magnetic field, but it is unlikely that this is

important except possibly for a few exceptional modes.

Random excitation of radial solar oscillations by turbulent convection has been discussed by Goldreich and Keeley (1977b). In this study the modes were presumed to be linearly stable, much of the stabilization coming from a turbulent viscosity provided by those convective eddies of lengthscale L and velocity v whose characteristic timescales L/v fall short of the oscillation period by more than a factor 2π (Goldreich and Keeley 1977a). The mean limiting amplitudes of the oscillations were then computed by balancing against the linear energy losses, which are proportional to the square of the amplitude, the rate at which energy is transferred to the modes via nonlinear interactions with convective fluctuations that are independent of the oscillation amplitude. At the heart of the computation, therefore, is an estimation of the extent to which the normal modes respond to the convective fluctuations, and this is the most uncertain step.

The energy transfer rate between two different components of motion, whether these components be convection and an oscillation or two oscillations, depends not only on the intensity of the motion but also on its geometry. The computation of the rate involves evaluating certain coupling integrals, which are analogous to the matrix elements encountered in quantum theory. To drive a particular mode of oscillation it is necessary to be able to generate a component of the motion that is possessed by that mode. Thus p modes are most efficiently driven by pressure (or dilatation) perturbations, whereas g modes are best generated via their vorticity. Convection may therefore drive p and g modes of similar frequencies to very different amplitudes. Note that the f modes of high degree are almost free of both dilatation and vorticity, which perhaps accounts for the observation (e.g., Deubner, Ulrich and Rhodes 1979) that their amplitudes are rather lower than those of p modes of similar frequency and wavenumber.

Goldreich and Keeley (1977b) made plausible estimates of the order of magnitudes of the terms that contribute to the coupling integrals. It was not possible to take the details of the geometry into account, because the structure of the turbulent convection is not known. From these estimates they concluded that the energy in any particular mode is approximately equal to the energy in a single convective eddy that resonates with the oscillation--that is to say, an eddy with a turnover time comparable to the period of oscillation of the mode. Though this result is only very rough, it predicts amplitudes of radial modes that are so much smaller than the apparent amplitudes quoted by Hill, Stebbins and Brown (1976) and by Brookes, Isaak and van der Raay (1976) that it seems likely that either the observations are not of radial modes or that the excitation of the modes is not predominantly by direct interaction with the convection. Another possibility, which is favored by Goldreich and Keeley, is that the observations have been misinterpreted.

Computations of this kind can easily be performed for other modes of oscillation. In particular, they may be applied to the five minute oscillations with encouraging results. In view of the uncertainties in the procedure it is probably adequate simply to equate the energy of each mode with a constant proportion of that of a resonating convective eddy, provided that such an eddy exists in the propagating region associated with the mode in question. If resonance occurs at more than one level, the two contributions are presumably added, though it makes little difference if one simply chooses the eddy of greatest energy. Using the model solar envelope whose five minute eigenfrequencies are reported by Berthomieu et al. (1980), and assuming the modes to be oscillating with random phases, an rms photospheric velocity amplitude of about 0.2 km s^{-1} is obtained if precise energy equipartition is assumed. This can be adjusted to the observed value of about 0.4 km s^{-1} either by setting the constant of proportionality in the energy relation equal to 4, or by raising above unity the ratio of the convective turnover time to the oscillation period that is considered to define resonance.[2]

A somewhat disturbing property of the outcome of this procedure is that the relative amplitudes of the different modes contributing to the five minute oscillations are not in accord with the observations of Deubner, Ulrich and Rhodes (1979). Aside from predicting excessive f mode amplitudes, as one might expect, the photospheric velocity amplitudes of the p modes are found to increase with increasing wavenumber well into the range in which the observations indicate they should decrease. It is possible that modes of high wavenumber are so highly damped by processes other than direct convective coupling, such as radiation, that the assumed energy balance is no longer valid, though estimates from nonadiabatic calculations suggest this is not the case. Alternatively the high wavenumber modes may be modified substantially by inhomogeneities, especially in the chromosphere.

In these proceedings Keeley (1980) reports an estimate by this method of the amplitude of a quadrupole g mode with a period of 160 minutes, adopting the same estimate for the coupling integral as was used previously for p modes. This is probably a sensible procedure, because the resonating eddies are at a depth of about 1 percent by radius beneath the photosphere, where this g mode locally has the character of a p mode (e.g., Chistensen-Dalsgaard and Gough 1980a). As with the radial modes of low order, the amplitude predicted is far below that quoted by Severny, Kotov and Tsap (1976) and Brookes, Isaak and van der Raay (1976), which strongly suggests that if the oscillation is a quadrupole g mode it is not excited

[2]Keeley (1979) has obtained a similar result using *ab initio* the procedure described by Goldreich and Keeley (1977a,b).

stochastically by the turbulent fluctuations. Keeley's conclusion that therefore the 160 minute oscillation cannot possibly be a quadrupole g mode is perhaps a little premature.

The possibility of excitation by nonlinear interactions with other modes of oscillation will be only briefly mentioned here. Though little work has yet been done on this subject, one can expect considerable progress in the future, partly because the coupling integrals can be evaluated easily and with a reasonable degree of certainty, and partly because we have available a considerable body of related work on plasma turbulence and nonlinear gravity wave interactions. An important difference between an assembly of high quality oscillators and the turbulent convection considered above is that, even if the nonlinear couplings are weak, phase relations between resonating modes can be maintained for long periods of time, thus permitting substantial transfers of energy. Provided the energy in the oscillations is sufficient one might expect the motion to be chaotic on long timescales (cf., for example, Galgani and Vecchio 1979), but over the shorter intervals during which observations have been made a considerable degree of coherence is to be expected. Thus the long period oscillations may all derive their energies, either directly or indirectly, from modes with shorter periods.

Some evidence that the excitation of the modes detected by the solar diameter measurements is intrinsically nonlinear has recently been provided by Perdang (1980). Perdang finds that the fractal dimension of the power spectrum published by Brown, Stebbins and Hill (1978) exceeds unity, and cannot therefore be the spectrum of an assembly of linear oscillators plus random noise. The dimension found is about 3/2, and is close to the value found for the spectrum of turbulent Couette flow. Perdang concludes, therefore, that the power spectrum of the long period solar oscillations is at least compatible with what one would expect from a large number of nonlinearly coupled oscillators. A similar result might be expected if the direct coupling between the modes was negligible and the oscillations were driven directly by the convection, since the dominant eddies driving different oscillation modes are nonlinearly coupled. Note that Perdang's result can also be considered to be further evidence against the suggestion that the SCLERA data is purely random noise.

Finally let us return to the 160 minute oscillation. If this is a g mode, the fact that other modes adjacent to it in the spectrum are not driven to such high amplitude is consistent with the excitation being by direct resonant coupling with other modes. It is claimed that the oscillation has maintained phase for at least three years (Kotov, Severny and Tsap 1978; Scherrer et al. 1979), which suggests that accurate phase coherence between the resonating modes may be necessary. Such resonances are rare, and only a very few low order modes are likely to be excited strongly by this mechanism. The possibility exists, however, that the 160 minute oscillation does not correspond to any linear eigenmode of the sun, but that it is an

essentially nonlinear phenomenon, such as that which appears to arise in cylindrical Couette flow (Swinney and Gollub 1978).

6. PHASE COHERENCE OF THE DIAMETER MEASUREMENTS

The means by which solar oscillations are observed will not be discussed here, as they are described elsewhere in these proceedings. I do, however, wish to address one small point that concerns the solar diameter measurements. The reports of Hill and his colleagues have been doubted by many, but most of the critics would be less skeptical if phase coherence were convincingly demonstrated. In these proceedings Caudell et al. (1980) present a statistical argument supporting phase coherence, but such arguments are sometimes difficult to assimilate when one is not familiar with the statistical tests that are being applied. One is often more likely to feel capable of judging the issue if one can actually see wandering of the phase.

Hill and Caudell (1979) have presented a diagram which shows that the addition of appropriate integral multiples of 2π to the phases of several of the peaks in the power spectrum of the diameter measurements can produce results which are almost linear functions of time. The probability that a random sample of points could have fallen so close to straight lines is quoted to be very small. Thus it is concluded that phase is maintained.

A worry that has been expressed by some people deals with the fact that arbitrary multiples of 2π must be added to the phases, and that only those that yield the best fit to straight lines are included in the diagram. Of course one can argue that this should not matter, because the same procedure was applied to the computation of the random points. Nevertheless, it would perhaps be reassuring if one could see all the possible phases at once.

At this workshop the SCLERA group made available to me all the phase data that had been analyzed. I chose a sample at random. In Figure 1 is plotted the phases in that sample computed from the Fourier spectra of each day's observing as a function of day number. All the factors of 2π that yield points within the confines of the diagram are included. Whether one is to believe that phase is maintained rests on whether one believes that straight nonvertical lines may be drawn almost through the points. It is clear that straight lines of slopes of about 60° and -30° to the abscissa pass close to the points, but are they close enough to be convincing? In other words, if the points on the diagram represent the positions of trees, does the diagram resemble more closely a map of an orange plantation or a map of a natural forest?

To help answer that question one might compare the data with Figure 2, which is a similar diagram constructed on about the same scale from a set of uniformly distributed random numbers in the range $[0, 2\pi)$. It is immediately apparent that pathways between the trees exist, as they do in Figure 1, but this time they are not

straight. Therefore it seems that phase here is not maintained, which is of course the case. It is interesting to notice, however, that had only the second half of the data been available, it would have been difficult to assess on the basis of this test whether or not the phases were random.

Now that one can see the difference between the observed and the random data, it is instructive to measure it. Best fit straight lines were placed through the rows of trees in Figures 1 and 2 and the standard deviations σ of the phases from those lines were computed. In the case of the observations $\sigma = 0.65$, and for the random points $\sigma = 1.26$. One can now refer to the Monte Carlo computation reported by Caudell et al. (1980). The random deviation $\sigma = 1.26$ lies close to the maximum in the computed distribution function, as one should expect, whereas the value $\sigma = 0.65$ is well into the tail. Moreover, a perusal of the remaining SCLERA data revealed that the sample illustrated here is not atypical. Thus one is forced to conclude that Figure 1 resembles an orange plantation, albeit poorly laid out, rather than a forest, and that the diameter measurements do, therefore, maintain phase.[3]

M. Gabriel pointed out during the meeting that rotational splitting of nonaxisymmetrical normal modes would destroy phase coherence over an interval comparable with the beat period. For modes of low degree this period is of the order of the solar rotation period, which is about the same as the time interval over which the phase analysis has been performed. So why is phase maintained? Of course the axisymmetrical normal modes maintain phase, and so do pure runnng nonaxisymmetrical waves. Therefore, if all possible oscillations of a given degree are present with random amplitudes, one should expect some degree of phase maintenance. Just how good the coherence should be has not been calculated, but it is plausible that the standard deviation from perfect coherence that one would expect is not far from that of the observations. If that were the case, most of the scatter in Figure 1 would be the result of rotational splitting, and not of random noise.

7. FIVE MINUTE OSCILLATIONS OF LOW DEGREE

At this workshop Claverie et al. (1980) announced the discovery of a sequence of approximately equally spaced peaks in their power spectra of line shifts measured from light integrated from the entire solar disk, with frequencies between about 2.5 and 4 mHz. Because the instrumental sensitivity to nonradial solar pulsations decreases rapidly with the degree of the mode (Hill 1978, Christensen-Dalsgaard and Gough 1980b), it can immediately be concluded that if indeed solar oscillations are responsible for the data they must be of low degree. Consequently they must be of

[3] After the workshop a similar analysis to that presented here was published by Grec and Fossat (1979). Unfortunately the authors had only 7 day's data available, and could conclude only that the case was not proven.

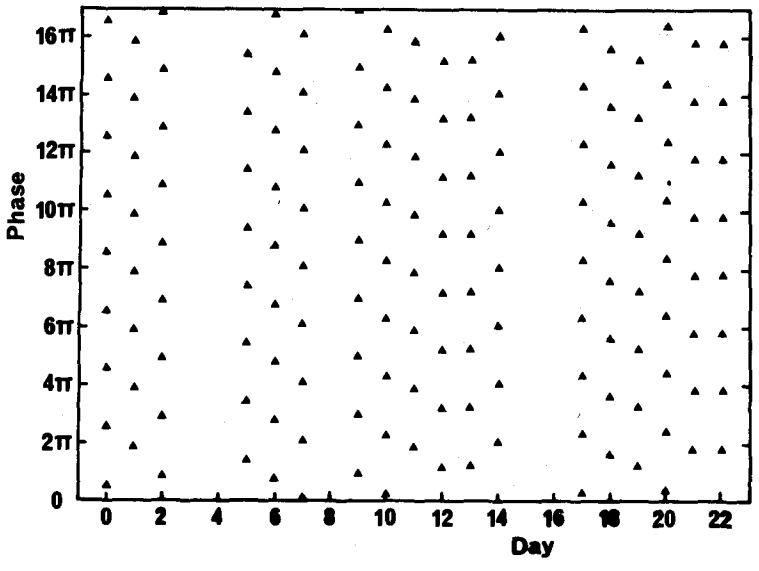

Figure 1. Phases of the x mHz components of Fourier Spectra of individual day's data from diameter measurements taken from y May to y-9 June 1978. The phases are relative to local noon. Included in the diagram are values constructed from the original phases by adding integral multiples of 2π.

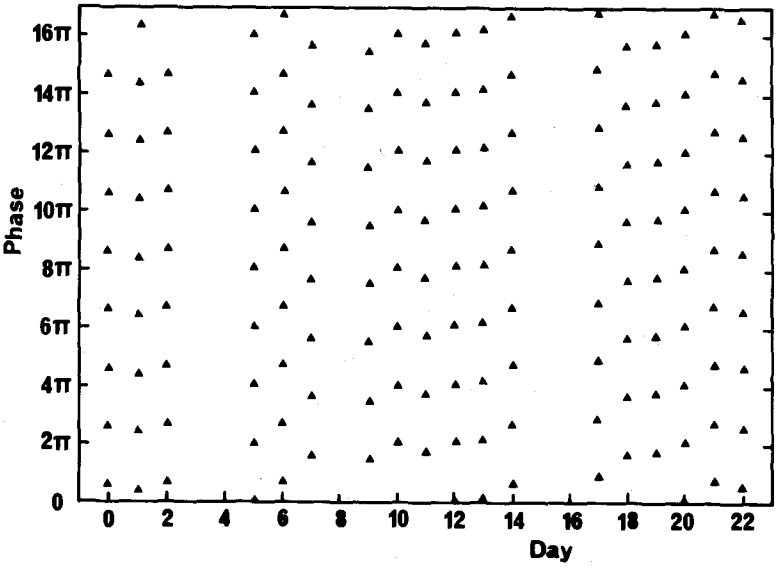

Figure 2. A diagram similar to Figure 1, but constructed from uniformly distributed random numbers.

high order. Specifically, every alternate peak is due probably to a dipole oscillation, and the peaks between to superpositions of monopole and quadrupole modes having almost coincident frequencies.

What are the properties of these oscillations, and to what amplitude would one expect them to be excited? Some results of computations of just the radial modes, carried out in collaboration with N.H. Baker, will be reported here briefly.

A model envelope of the sun was constructed by integrating inwards from the surface, including slightly more than 80 percent by radius (and mass). Turbulent Reynolds stresses were incorporated in the approximate way described by Baker and Gough (1979). The hydrogen and heavy element abundances were $X = 0.745$, $Z = 0.02$ and a mixing length of 1.5 pressure scale heights was chosen. This yields a convection zone 1.99×10^5 km deep, and a k-ω diagram for the five minute oscillations of high degree similar to that reported by Berthomieu et al. (1980). A spectrum of nonadiabatic radial pulsations was then computed, treating convective fluctuations in a manner identical to that used by Baker and Gough (1979) in their Series B of RR Lyrae variables. The frequencies of the modes were subsequently decreased by 6 percent to take into account the replacement of the inner core of the sun in the computations by a rigid sphere. The reduction factor was arrived at by assuming the asymptotic equation (3.1) to be valid for all the modes and, aside from the three lowest order modes, the resulting frequencies differed from the adiabatic eigenfrequencies of the standard model of Christensen-Dalsgaard, Gough and Morgan (1979) by less than 1 percent.

All the modes with frequencies less than 4 mHz were found to be stable. Their stability coefficients are shown in Figure 3. Interestingly, these coefficients are within a factor of 2 of those obtained by Goldreich and Keeley (1977a) for the modes with frequencies in excess of 2.5 mHz. This is rather surprising, since the two calculations made apparently very different assumptions in the treatment of the Reynolds stresses. Some of the modes with frequencies above 4 mHz were found to be unstable, with e-folding times as short as one day. This result should be treated with some caution, however, because the frequencies are close to Lamb's critical frequency for wave propagation in the atmosphere. Energy leakage into the corona, which was ignored in these computations, may add substantially to the damping of these high frequency oscillations. If all the modes are indeed stable, stochastic excitation by turbulence is a likely candidate for the predominant driving mechanism.

Plotted also in Figure 3 is the ratio of the amplitude Δm of the surface luminosity variation, measured in magnitudes, to the surface velocity amplitude v_s (in m s^{-1}) scaled by the factor 2/3, which is the value of the spatial filter function for radial modes appropriate for the whole-disk measurements (e.g., Hill 1978). It is evident that, if these predictions of linear theory are good approximations to reality, the velocity amplitudes of up to 30 cm s^{-1} quoted by

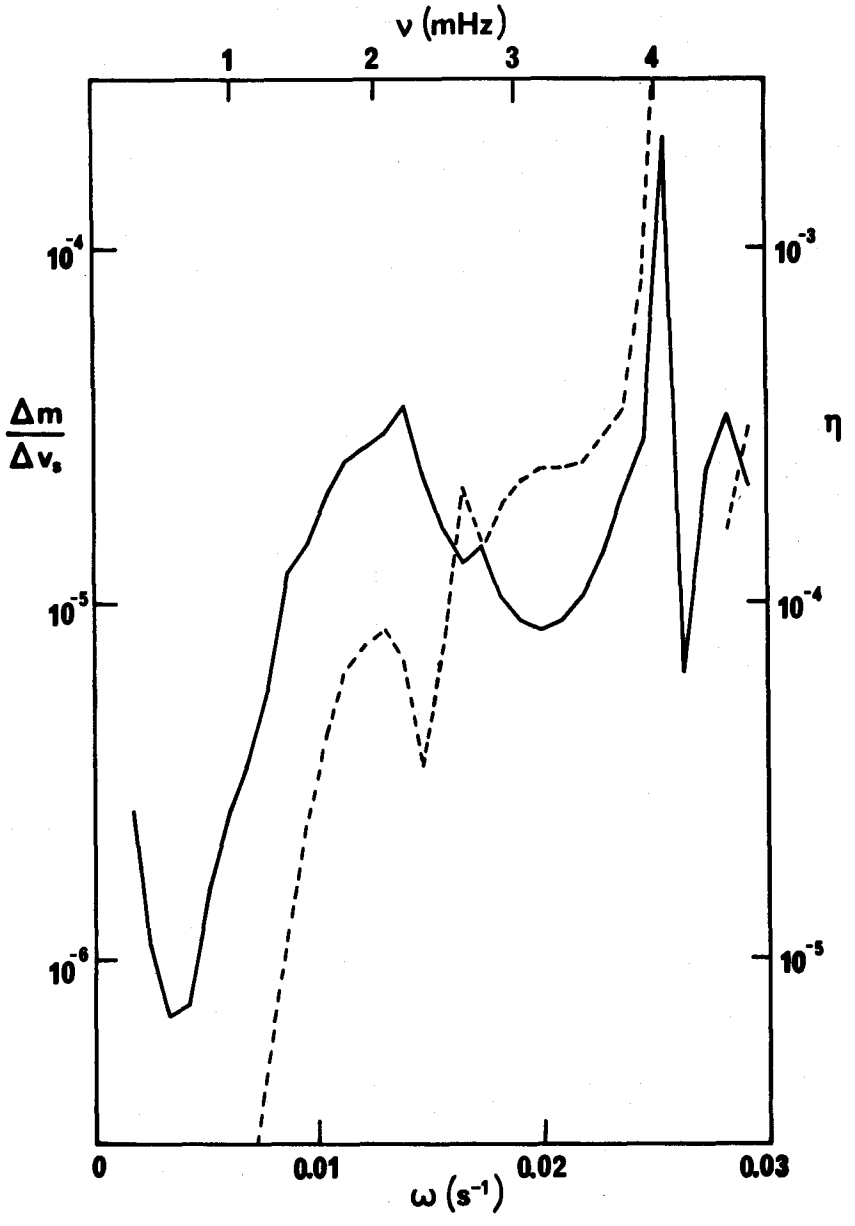

Figure 3. Magnitude-velocity amplitude ratios and stability coefficients of the first 32 radial eigenmodes of a solar model, plotted against frequency. The amplitude ratios $\Delta m/\Delta v_s$ are connected by straight continuous lines; the amplitudes are corrected by the spatial filter functions appropriate for whole-disk measurements (cf. Hill 1978), and velocity is measured in m s^{-1}. The stability coefficients η are the ratios of the decay rates to the angular frequencies of the eigenmodes. Positive values are connected by dashed lines; p_{29} and p_{30} were found to be unstable.

Claverie et al. (1980) imply luminosity amplitudes in the vicinity of 10^{-5} mag. Though luminosity measurements of the sun have not yet been performed with sufficient precision to detect oscillations of such low amplitude, it is feasible that in the frequency range in question they could be made.

It would also be interesting to attempt to detect similar oscillations in other stars. This issue has already been raised in connection with the long period oscillations, though there is at present some disagreement concerning the amplitude of the luminosity variations that should be expected (cf. Severny, Kotov and Tsap 1976, 1978; Deubner 1977). Granted that the presence of the envelope convection zone is likely to be essential for their excitation, one might expect to find low degree oscillations at least in stars of type G and later. Claverie et al. (1980) have already mentioned the possibility of making Doppler measurements from a satellite, but luminosity fluctuations may be easier to detect. Of course it would be best to have both.

Finally, we shall examine the driving of the radial modes, assuming that it takes place through random excitation by the turbulent convection. To obtain a rough estimate of the amplitudes one might expect, the fact has been disregarded that some of the higher frequency modes were found to be overstable; in addition, the simple energy balance of the kind deduced by Goldreich and Keeley will be assumed, calibrated against the local five minute oscillation amplitudes as described above. Thus each mode energy is equated with four times the energy of a single resonating convective cell. The squares of the surface velocity amplitudes, in m^2s^{-2}, are displayed in Figure 4. These should correspond roughly to the contributions to the power spectra obtained by Claverie et al. made by the radial modes alonge. The figure has a superficial resemblance to the observations, showing a maximum amplitude of about $(0.23 \text{ m s}^{-1})^2$ in the vicinity of 3 mHz. In common with the estimates for the five minute oscillations of high degree, the predicted amplitudes of the high frequency modes are too great, but as mentioned above, substantial damping of these modes may result from energy leakage into the corona. The amplitudes of the lower order modes in Figure 4 are greater than the corresponding values quoted by Goldreich and Keeley (1977b). The main reason is probably that the energy balance equation has been scaled upwards to bring the total energy of the five minute oscillations into agreement with the observations. In addition, the equilibrium model is different from that used by Goldreich and Keeley, and so are the surface amplitudes of the eigenmodes at a given mode energy. Though the calculations presented here are much less sophisticated than those of Goldreich and Keeley, and make no pretense to be otherwise, they do suggest that a common process may drive the five minute modes of low and high degree. This is not very surprising, since the eddies that resonate with the five minute oscillations typically have characteristic length scales rather smaller than the wavelengths of the modes, and so the coupling is unlikely to be

sensitive to the global structure of the oscillation eigenfunctions.

8. ON HELIOSEISMOLOGY

One of the most exciting prospects that recent observations have brought into view is the potential diagnosis of certain aspects of the sun's structure. In 1975 Deubner published a k-ω power spectrum of the five minute oscillations that heralded a diagnostic study of the convection zone. Soon afterwards Hill, Stebbins and Brown (1976) announced their discovery of longer period oscillations in the solar diameter that were no doubt associated with modes that penetrate into the radiative interior. Severny, Kotov and Tsap (1976) announced long period oscillations in spectrum line shifts that were immediately confirmed by Brookes, Isaak and van der Raay (1976), and we have learned at this workshop of the five minute oscillations of low degree (Claverie et al. 1980). None of these observations has yet led to any certain inference, but they have stimulated several diagnostic investigations.

Most attention has been devoted to the five minute modes of high degree, because good observations of both their temporal and their spatial structure have been made (e.g., Deubner, Ulrich and Rhodes 1979). Thus it has been possible to identify the modes. Theoretical investigations of the dependence of the corresponding eigenfrequencies of linear modes on the structure of the solar model are reported in these proceedings by Berthomieu et al. (1980) and by Lubow, Rhodes and Ulrich (1980). Because the modes exist in a layer only a few percent of the solar radius deep, they give us no direct information about most of the interior. However, the oscillations do penetrate beyond the upper boundary layer in the convection zone, beneath which we are fairly confident that the stratification is approximately adiabatic. This enables us to extrapolate to the base of the convection zone and so estimate its depth. Both of the studies last mentioned concluded that the observations seem to imply the depth of the convection zone to be about 2×10^5km.

Evidence against so deep a convection zone has been provided by Hill and Caudell (1979), and discussed by Christensen-Dalsgaard, Dziembowski and Gough (1980). Hill and Caudell concluded that oscillations with periods 45 minutes and 66 minutes have horizontal variations with characteristic wavelengths of order $2\pi R/30$, where R is the solar radius. If these are simply interpreted as nonradial modes with $\ell \simeq 30$, the periods imply that they must be g modes trapped beneath the convection zone. This is difficult to reconcile with the models suggested by Berthomieu et al. (1980) and Lubow, Rhodes and Ulrich (1980) because the attenuation of the mode amplitudes through the deep convection zone would be too great for the modes to be observable at the photosphere (Dziembowski and Pamjatnykh 1978). It seems likely that there are solar models with low heavy element abundances of the kind discussed by Christensen-Dalsgaard, Gough and Morgan (1979) that are not subject to this difficulty, but

acceptance of them raises more problems than it solves (Christensen-Dalsgaard, Dziembowski and Gough 1980). In particular, the conclusions already drawn from the five minute oscillations are contradicted.

In an attempt to harmonize the conflicting evidence, Rosenwald and Hill (1980) have proposed that the upper boundary conditions applied in the computations of the five minute eigenfunctions are incorrect. They base their argument on the results of an earlier attempt to determine the spatial structure of the modes observationally (Hill, Rosenwald and Caudell 1978). The implications of their conclusions are so important that some discussion of the analysis is not out of place.

In the adiabatic approximation the pulsation eigenmodes are determined by a second-order linear differential equation. For any given frequency ω there are two independent solutions, which in an isothermal atmosphere under constant gravity either oscillate with height or vary exponentially according to whether ω is above or below some critical value ω_c. For horizontal wavelengths appropriate to the five minute oscillations, the eigenfunctions in the atmosphere resemble those of radial pulsations, and ω_c is approximately Lamb's acoustical cutoff frequency $\gamma g/2c$, which is a decreasing function of temperature. Solutions with ω corresponding to the five minute modes are approximately exponential in the photospheric regions; in the corona they are either exponential or oscillatory, depending on whether the horizontal wavenumber is greater or less than about 0.2 Mm^{-1}. For one of the exponential solutions the energy density in the oscillation decreases with height, while in the other it increases. Hill, Rosenwald and Caudell (1978) refer to these solutions as β_- and β_+ respectively. As is usual for evanescent waves, the β_- solution essentially describes the response of the atmosphere to a disturbance from beneath, and the β_+ solution to a disturbance from above. Of course a normal mode is a superposition of both.

If the physics of the chromosphere and corona were understood, it would be possible at least in principle to determine the five minute eigenfunctions from the condition that there is no inwardly propagating energy at infinity. But unfortunately we are not in a position to carry out that program. Nevertheless, it is hard to imagine how the response of the chromosphere could be such as to generate a solution in the evanescent region that appears to have a large component apparently associated with a downward propagating coronal wave. Accordingly one might naturally expect the amplitude ratio of the β_- and β_+ solutions to be of order unity in the chromosphere-corona transition region. If that were the case, the amplitude of the β_+ solution would be negligible in and below the photosphere, and the reaction of the atmosphere to the waves in the resonating cavity beneath would hardly differ from that calculated by ignoring the β_+ solution entirely. Indeed this was confirmed numerically by Berthomieu et al. (1980), who found that the five minute

eigenfrequencies were extremely insensitive to mild changes in the boundary conditions they imposed at an optical depth of 10^{-8}. Nevertheless, it can be maintained that this result is no more than conjecture based on experience gained in similar but different situations, and that it must not be accepted without question.

The work of Hill, Rosenwald and Caudell (1978) was an attempt to determine the combination of β_- and β_+ solutions observationally. Surprisingly, it was concluded that for the five minute oscillations the displacement amplitude of the β_- solution exceeds that of the β_+ solution by only a factor of about five at an optical depth of 0.1. If the linear solutions were extrapolated into the chromosphere, the β_+ component would be so dominant as to render the measurement hardly plausible. This result has some similarity to a conclusion of Schmieder (1976, 1979) who found from an analysis of phase relations that at some frequencies atmospheric oscillations appear to be downward propagating waves. Nevertheless it has been argued that the increase in amplitude with height produced by the β_+ solution gives rise to nonlinear phenomena, which render linear extrapolation invalid. So drastic a modification to the structure of the eigenfunctions in the solar atmosphere is beyond anything considered by Berthomieu et al., and according to Rosenwald and Hill (1980) could reconcile the observed k-ω power spectra with a convection zone much shallower than that favored by Berthomieu et al. and Lubow.

This conclusion too can be questioned, for the analysis of Hill, Rosenwald and Caudell (1978) depends on several assumptions. It should be realized that the β_- :β_+ amplitude ratio for the five minute oscillations was determined by comparing velocity and radiation intensity amplitudes, and to do this it is necessary to perform a nonadiabatic calculation. Hill, Rosenwald and Caudell did so, using the Eddington approximation to radiative transfer. In this approximation the governing differential equations are of the fourth order, and so admit four independent solutions. Their relative proportions cannot be determined by only two observations, and so it was necessary to restrict the class of admissible solutions by adopting certain boundary conditions. In particular, it was assumed that the heat flux perturbation vanished at the lower boundary of the domain of computation, which was situated in the convection zone at a temperature of 13000 K. It has been argued by Gough (1977) and Baker and Gough (1979) that convection can induce large flux perturbations, and indeed the computations by Baker and myself of radial pulsations that are discussed above predict in all cases that the heat flux perturbation at T = 13000 K is actually greater than it is in the photosphere. Furthermore our temperature perturbations at $\tau = 0.3$, where our outer boundary conditions were applied, are somewhat greater than those found by Hill, Rosenwald and Caudell, which suggests a reduction in the β_+ amplitude. A direct comparison with observation should not be made, because our treatment of both convection and radiative transfer was too crude to describe adequately the oscillations in the photospheric regions.

Nevertheless, the computations do cast doubt on the analysis of Hill, Rosenwald and Caudell (1978), and weaken the case against a deep convection zone.

It is worth noting that perturbations in the convection might also affect similar conclusions(Hill, Rosenwald and Caudell 1978) for the long period oscillations. In particular, the convective activity can modify the limb darkening function, upon which the interpretation of the SCLERA data depends, and the convective blue shift invalidates a naive conversion of spectrum line shifts to mode velocities.

If the β_+ solution is of little significance in determining the eigenfrequencies, so is the T-τ relation in the atmosphere (Berthomieu et al. 1980). In that case the five minute oscillations provide us with a clean diagnostic of the convection zone, as was previously postulated by Gough (1977) and Ulrich and Rhodes (1977). Roughly speaking their frequencies are given by equation (3.2), where γ and μ are to be interpreted as averages of the adiabatic exponent and polytropic index appropriately weighted according to the eigenfunction amplitude. Thus as k decreases and the penetration depth increases, the averages weight more heavily the adiabatic region where $\mu \simeq (\gamma - 1)^{-1}$ and the right hand side of (3.2) increases: the functions $\omega(k)$ defined by the ridges in the k-ω power spectra have smaller gradients than one obtains from equation (3.2) with $\gamma/(\mu+1)$ constant (assuming that $\gamma/(\mu + 1)$ is adjusted to yield about the right value of ω), and the difference between these gradients is a rough measure of the statification in the vicinity of the penetration depth. A more precise measure might in principle be constructed by considering more complicated aspects of the power spectra (cf. Gough 1978) but it would be successful only if the positions of the ridges were defined more precisely. This is likely to be a difficult task, partly because the finite duration of a particular mode may render the determination of its frequency too inaccurate (Berthomieu et al. 1980) and partly because nonlinear interactions with other forms of motion, such as supergranulation, distort the wave patterns in such a way as to broaden the ridges obtained by the current observational techniques. Both these effects yield uncertainties which for some modes are comparable to the ridge widths already achieved by Deubner, Ulrich and Rhodes (1979).

If the convection zone is indeed deep, how is one to explain the results of Hill and Caudell (1979)? Either the horizontal length scale deduced from the observations is in error, or that scale does not measure the horizontal wavelength of the modes. Another possibility is that the amplitudes really are so high in the interior that the estimates of the attenuation through the convection zone made by Dziembowski and Pamjatnykh (1978) and Christensen-Dalsgaard, Dziembowski and Gough (1980) on the basis of linearized theory are incorrect. Alternatively, as has been suggested for the 160 minute oscillation, the oscillations are not the result of normal modes of oscillation of the sun. These possibilities will not be discussed

here, but it is worth recalling that large perturbations to the supergranular velocities induced by modes of low degree (Gough 1977) could give the impression in the photosphere of a mode with a much shorter horizontal wavelength (cf. Gough, Pringle and Spiegel 1976).

The five minute oscillations of low degree discovered by Claverie et al. (1980) provide an additional diagnostic that has a direct bearing on this issue. These modes are particularly interesting because they penetrate to the center of the sun, though the information the frequencies give us weights the outer regions most strongly (see equation 3.1). Moreover, because the orders of the modes are high, it is likely that the objections raised by Rosenwald and Hill (1980) to the analyses of Berthomieu et al. (1980) and Lubow, Rhodes and Ulrich (1980) would be of lesser importance. The reason is that the ratio of the β_- and β_+ amplitudes can be regarded as defining a photospheric boundary condition, and this in turn determines the parameter ε in equation (3.1) and a similar term in the analogue of equation (3.2) that is valid for small n. Accurate comparison of theory with the five minute oscillations of high degree measured by Deubner, Ulrich and Rhodes (1979) is possible when n is of order unity, but for the low degree modes n is about 20. Thus uncertainties in ε should be of lesser importance for the low degree modes, and the eigenfrequencies can be predicted with greater accuracy.

It is too early to assess the implications of these new data. Comparison of the mean frequency separation with those of the modes of a particular sequence of solar models has utilized a model deficient in helium and heavy elements and with a comparatively shallow convection zone (Christensen-Dalsgaard and Gough 1980b). This again contradicts the evidence from the other five minute modes. However, the discrepancies between the observations and the predictions of models of the kind preferred by Berthomieu et al. (1980) and Lubow, Rhodes and Ulrich (1980) is only about 1 percent, and we must await a better estimate of the accuracy of the new data before we take this apparent contradiction seriously.

There are two other classes of modes that deserve brief mention. The first is the chromospheric modes, which are p modes of high degree trapped in the chromospheric minimum of the buoyancy frequency N (e.g., Ando and Osaki 1977), and the second is the atmospheric g modes trapped between the top of the convection zone and the bottom of the corona. Both are insensitive to the structure of the sun beneath the photosphere.

According to the computations of Ando and Osaki (1977) and Ulrich and Rhodes (1977) the chromospheric modes should all have frequencies in the vicinity of 0.027 s^{-1}. Their precise values are sensitive to the buoyancy frequency above the temperature minimum. Adiabatic g-mode eigenfrequencies of the Harvard-Smithsonian Reference Atmosphere (Gingerich, Noyes and Kalkofen 1971) are displayed in Figure 5. As is evident from equation (3.5), they depend both on the value of N in the

atmosphere and on the height of the base of the corona. Because the temperature rise between the chromosphere and corona is very steep, the variation of N is too, and the height h of the resonant cavity is almost independent of frequency. Consequently, unlike the nonchromospheric p modes, the atmospheric g modes all sample conditions in the same region. That is why the g-mode $\omega(k)$ relations plotted in Figure 5 are less curved than those for the f and p modes, as is evident also from the approximate formulae (3.2) and (3.5). Thus, the differences in the information content of the various g-mode eigenfrequencies are less marked than in the cases of p modes, and anything but the crudest inversion is unlikely to be possible.

Another problem with atmospheric diagnostics is the existence of large amplitude inhomogeneities. As Ulrich and Rhodes (1977) have pointed out while discussing the chromospheric modes, and Dziembowski at this workshop regarding the g modes, it may never be possible to isolate ridges of power as has been done for the f and nonchromospheric p modes. Brown (1980) has presented some hint of g-mode ridges, but it may be vain to hope for more than the approximate locus of g_1.

Not only can oscillations measure the temperature and density stratification of the sun, but they can also detect large scale motion. The most obvious form of motion that one might hope to measure is the solar rotation, and already evidence of rotational splitting has been seen in several of the observations (e.g., Deubner, Ulrich and Rhodes 1979; Caudell and Hill 1978). Moreover, other phenomena, such as the periodic change in structure of the 160 minute oscillation reported by Severny, Kotov and Tsap (1978) and the 12.2 day oblateness oscillation reported by Dicke (1976), may be related to rotationally induced precession of normal modes (Gough 1980). Little information is yet available, but what we have all hints that the average of the sun's angular velocity is rather larger than the surface value.

The most detailed data that is available comes from the measurements of five minute oscillations by Deubner, Ulrich and Rhodes (1979). In this work the signal was filtered through an effective N-S slit 192" long placed across the equator. These modes have spatial structures proportional to the sectorial harmonics $P_m^m(\cos\theta)\begin{matrix}\sin\\ \cos\end{matrix} m\phi$ in spherical polar coordinates, where P_ℓ^m is the associated Legendre function. They are therefore confined to an equatorial belt with a total width of about $2(2/m)^{1/2}R$. Since $m \geq 100$ for all modes considered, the belt is no wider than the slit. Indeed, other modes proportional to $P_\ell^m(\cos\theta)\begin{matrix}\sin\\ \cos\end{matrix} m\phi$ with $\ell \simeq m$ also contribute to the signal, but they too extend to latitudes no greater than about the slit length.

Because the modes are confined so closely to the equator they are not affected by the variation of angular velocity with latitude. Moreover, because m is large, Coriolis forces are unimportant. If rotation was the only large scale velocity field present, the wave patterns would simply be advected with the mean angular velocity of the sun weighted by the kinetic energy density of the mode (Gough

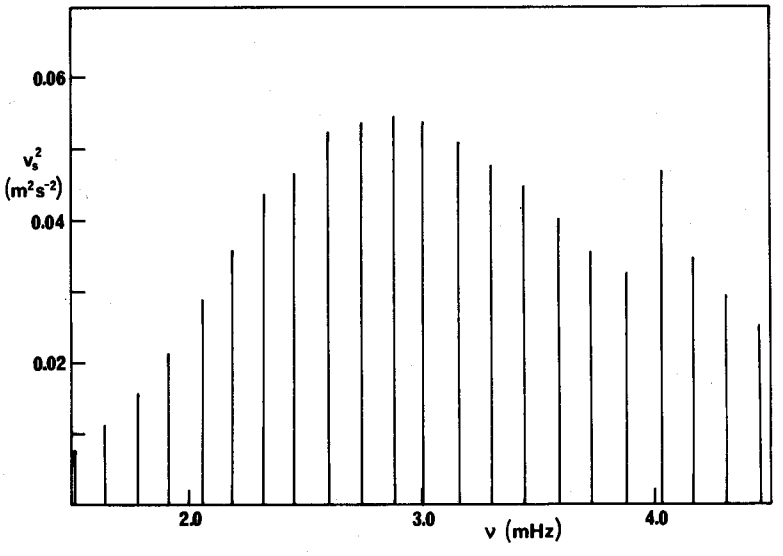

Figure 4. Estimates of the squares of the surface velocity amplitudes of the radial modes p_{10} - p_{31} assuming stochastic excitation by turbulent convection.

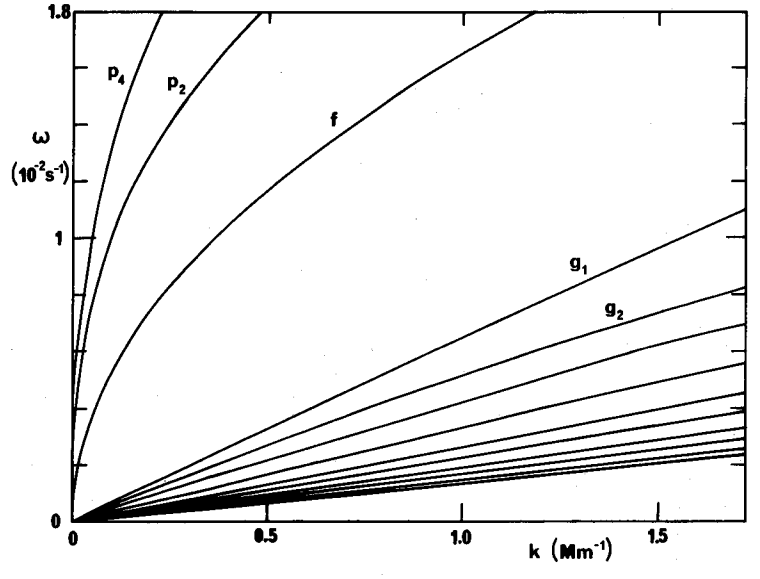

Figure 5. Eigenfrequencies of the first ten adiabatic g modes of the Harvard-Smithsonian Reference Atmosphere, plotted against horizontal wavenumber. The f, p_2 and p_4 modes of the standard model of Berthomieu et al. (1980) are included for comparison.

1978). Thus the measured variation of the pattern speed with horizontal wavenumber would be a genuine reflection of the depth dependence of the angular velocity, almost uncontaminated by latitudinal variations. The procedure could be applied at other latitudes λ too, by similarly selecting appropriate modes with $\ell \simeq m \sec^2\lambda$. Note, however, that the waves are actually influenced by all the other components of the velocity field, including the convection and any large scale circulation. The analysis of the wave patterns is therefore somewhat more complicated than that implied here.

9. CONCLUDING REMARKS

Recent observations of solar oscillations have raised more questions than they have answered. Like the measurements of the neutrino flux and the oblateness of the solar image, they have stimulated much thought on the physics of the sun, which is contributing to our knowledge of stellar physics generally. The subject is still in its infancy, and there is good reason to believe that imminent observations will resolve some of our present confusion, and lead us to a better understanding of the solar interior.

* * * * *

I am very grateful to N.H. Baker, T.M. Brown, T.P. Caudell, J. Christensen-Dalsgaard, G. Contopoulos, W. Dziembowski, M. Gabriel, H.A. Hill, D.A. Keeley, J. Knapp, J.D. Logan, J. Perdang, R.D. Rosenwald, A.B. Severny and R.T. Stebbins for useful and interesting discussions on this subject.

REFERENCES

Ando, H. and Osaki, Y. 1975, Pub. Astr. Soc. Japan, 27, 581.

Ando, H. and Osaki, Y. 1977, Pub. Astr. Soc. Japan, 29, 221.

Baker, N.H. and Gough, D.O. 1979, Astrophys. J., 234, 232.

Berthomieu, G., Cooper, A.J., Gough, D.O., Osaki, Y., Provost, J. and Rocca, A. 1980, these proceedings.

Brookes, J.R., Isaak, G.R. and van der Raay, H.B. 1976, Nature, 259, 92.

Brown, T.M. 1980, these proceedings.

Brown, T.M., Stebbins, R.T. and Hill, H.A. 1978, Astrophys. J., 223, 324.

Caudell, T.P. and Hill, H.A. 1978, Proc. Conf. Current problems in stellar pulsation instabilities (Goddard Space Flight Center, June 1978), in press.

Caudell, T.P., Knapp, J., Hill, H.A. and Logan, J.D. 1980, these proceedings.

Christensen-Dalsgaard, J. 1979, Mon. Not. R. Astr. Soc., in press.

Christensen-Dalsgaard, J. 1980 to be submitted to Mon. Not. R. Astr. Soc.

Christensen-Dalsgaard, J. and Gough, D.O. 1980a, these proceedings.

Christensen-Dalsgaard, J. and Gough, D.O. 1980b, these proceedings.

Christensen-Dalsgaard, J., Dziembowski, W. and Gough, D.O. 1980, these proceedings.

Christensen-Dalsgaard, J., Gough, D.O. and Morgan, J.G. 1979, Astron. Astrophys., 73, 121; 79, 260.

Claverie, A., Isaak, G.R., McLeod, C.P., van der Raay, H.B. and Roca-Cortes, T. 1980, these proceedings.

Cowling, T.G. 1941, Mon. Not. R. Astr. Soc., 101, 367.

Deubner, F.-L. 1975, Astron. Astrophys., 44, 371.

Deubner, F.-L. 1977, Astron. Astrophys., 57, 317.

Deubner, F.-L., Ulrich, R.K. and Rhodes, E.J., Jr. 1979, Astron. Astrophys., 72, 177.

Dicke, R.H. 1976, Solar Phys., 47, 475.

Dyson, J. and Schutz, B.F. 1979, Proc. Roy. Soc., in press.

Dziembowski, W. and Pamjatnykh, A.A. 1978, Pleins feux sur la physique solaire (ed. J. Rosch, CNRS, Paris), p. 135.

Eckart, C. 1960, Hydrodynamics of oceans and atmospheres (London and New York: Pergamon Press).

Eisenfield, J. 1969, J. Math. Analysis Appl., 26, 357.

Galgani, L. and Lo Vecchio, G. 1979, Nuovo Cim., in press.

Gingerich, O., Noyes, R.W. and Kalkofen, W. 1971, Solar Phys., 18, 347.

Goldreich, P. and Keeley, D.A. 1977a, Astrophys. J., 211, 934.

Goldreich, P. and Keeley, D.A. 1977b, Astrophys. J., 212, 243.

Gough, D.O. 1977, Proc. IAU Colloq. 36 (ed. R.M. Bonnet and Ph. Delache; G. de Bussac, Clermont-Ferrand), p. 3.

Gough, D.O. 1978, Proc. Workshop on solar rotation (ed. G. Belvedere and L. Paterno, Univ. Catania Press), p. 255.

Gough, D.O. 1980, Mon. Not. R. Astr. Soc., in press.

Gough, D.O., Pringle, J.E. and Spiegel, E.A. 1976, Nature, 246, 424.

Grec, G. and Fossat, E. 1979, Mon. Not. R. Astr. Soc., 188, 21P.

Hill, H.A. 1978, The new solar physics (ed. J.A. Eddy; AAAS, Washington), Chapter 5.

Hill, H.A. and Caudell, T.P. 1979, Mon. Not. R. Astr. Soc., 186, 327.

Hill, H.A., Rosenwald, R.D. and Caudell, T.P. 1978, Astrophys. J., 225, 304.

Hill, H.A., Stebbins, R.T. and Brown, T.M. 1976 Proc. V Intern. Conf. Atomic Masses and Fundamental Constants (ed. J.H. Sanders and A.H. Wapstra; New York: Plenum), p. 622.

Keeley, D.A. 1979, personal communication.

Keeley, D.A. 1980, these proceedings.

Kotov, V.A., Severny, A.B., Tsap, T.T. 1978, Monthly Notices R. Astr. Soc., 183, 61.

Lubow, S., Rhodes, E. and Ulrich, R. 1980, these proceedings.

Ogura, Y. and Phillips, N.A. 1962, J. Atmos. Sci., 19, 173.

Osaki, Y. 1975, Publ. Astron. Soc. Japan, 27, 237.

Perdang, J. 1980, submitted to Nature.

Rosenwald, R.D. and Hill, H.A. 1980, these proceedings.

Scherrer, P.H., Wilcox, J.M., Kotov, V.A., Severny, A.B. and Tsap, T.T. 1979, Nature, 277, 635.

Schmieder, B. 1976, Solar Phys., 47, 435.

Schmieder, B. 1979, Astron. Astrophys., 74, 273.

Scuflaire, R. 1974, Astron. Astrophys., 36, 101.

Severny, A.B., Kotov, V.A. and Tsap, T.T. 1976, Nature, 259, 87.

Severny, A.B. Kotov, V.A. and Tsap, T.T. 1978, Pleins feux sur la physique solaire (ed. J. Rosch, CNRS, Paris), p. 123.

Swinney, H.L. and Gollub, J.P. 1978, Physics Today, 31 (8), 41.

Ulrich, R.K. 1970, Astrophys. J., 162, 993.

Ulrich, R.K. and Rhodes, E.J., Jr. 1977, Astrophys. J., 218, 521.

Vandakurov, Yu. V. 1967, Astron. Zh., 44, 786.

Wolff, C.A. 1972, Astrophys. J. Lett., 177, L87.

FIVE MINUTE OSCILLATIONS AS A PROBE OF THE SOLAR INTERIOR

S.H. Lubow, E.J. Rhodes, Jr. and R.K. Ulrich
Department of Astronomy
University of California at Los Angeles

ABSTRACT

The solar five minute oscillation has been shown to consist of a large number of nonradial acoustic modes. Observations of these modes provide a probe of the solar interior; specifically tests on models of the solar convection zone.

* * * * *

Among the various types of solar oscillations, the five minute oscillations are the best observed. They provide us with the greatest amount of observational detail for theoretical comparison. As Ulrich (1970a), Wolff (1972), and Ando and Osaki (1975) have described, these oscillations are due to nonradial acoustic modes which can penetrate to depths equaling 20 percent of the solar radius. The currently resolvable modes (see e.g., Deubner, Ulrich and Rhodes 1979) penetrate a few percent of the radius below the solar surface and have ℓ values that range from about one hundred to about one thousand. We can conceptualize these modes as being trapped in two coupled cavities. The first cavity extends from the photosphere to some point below; the second extends from a point in the chromosphere up to the corona. Eigenmodes tunnel their wave energy between the two cavities.

Figure 1 presents evidence that the observed modes are indeed highly nonradial acoustic modes. This figure, taken from a recent paper by Deubner, Ulrich, and Rhodes (1979), plots observed power contours as frequency (ω) versus horizontal wave number (k_h). Dashed lines indicate the results of the linear, nonadiabatic modal analysis of Ulrich and Rhodes (1977) for a solar envelope with a mixing length ratio (ℓ/H) equal to 2.0. The overall agreement speaks for itself. The question that we must address here is the inverse: Can these observations tell us something about the structure of the solar interior? The currently resolvable modes can directly provide information only about the region in which they propagate, a region that extends a few percent of the radius below the solar surface. Information concerning the sun's deep interior can only be inferred by studying complete solar models.

In order to initiate a probe of the solar interior, a theory that is as complete as possible must first be constructed; the sensitivity of the results to the details of the theory must then be tested. We have considered several aspects of

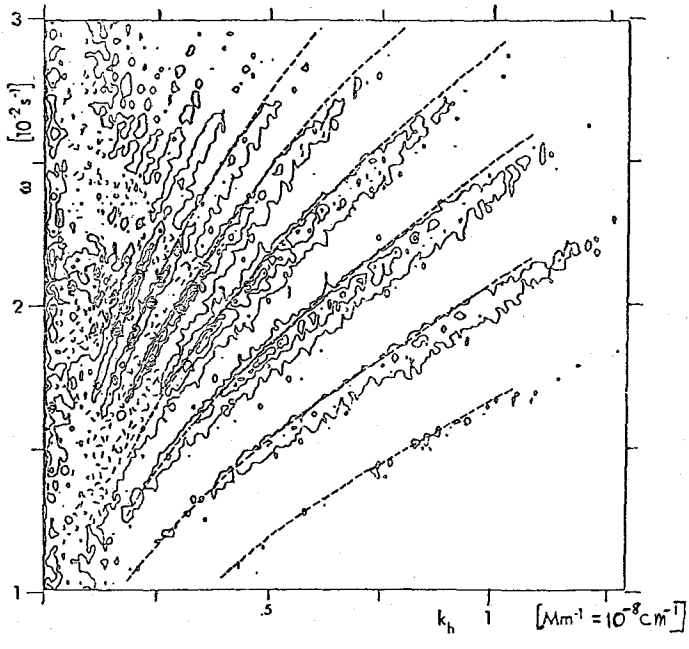

Figure 1. Velocity power spectrum in frequency and horizontal wave number.

these issues. In building upon the theory given in Ulrich and Rhodes (1977), we have included Coulomb corrections to the equation of state via Debye-Huckel theory; the outer solar boundary has also been moved from the chromosphere to the lower corona. An approximation of the model of Avrett, Vernazza, and Linsky (1976) was used to extend the chromospheric model. We have also improved the numerical accuracy of the codes used and have employed updated interior opacities obtained from Huebner. Figure 2 compares the old (dashed line) and new (solid line) results obtained for envelopes with ℓ/H equal to 2.0. The effects of making the Coulomb corrections and moving the outer boundary were similar; both processes acted to lower the frequency at each k_h. The effects of the other improvements implemented were negligible. Frequencies obtained from envelopes with ℓ/H values of 1.5 and 3.0 are represented by the two sets of solid curves in Figure 3. The frequencies for the ℓ/H of the 1.5 model pass a bit above the peak power and those for the ℓ/H of the 3.0 model pass a bit below the peak power. We then computed a complete standard solar model that matches the present solar mass, luminosity, radius, and heavy element distribution; it also makes the usual assumption that the primordial sun was chemically homogeneous. The result is a unique solar model whose convection zone has ℓ/H equal to 1.65. At present, this model appears barely distinguishable from a best possible fit. A more quantitative statement concerning this fit will be made in the future.

We now come to the question of the sensitivity of the results obtained to the details of the model. One possible point to question is the sensitivity of the results to the theory of convection. To answer that question, we considered two envelope models. One was computed with the usual mixing length theory of convection and the other with Ulrich's (1970b) nonlocal convection model. Both envelopes were chosen so as to have the same specific entropy in the adiabatic region, since the value of the specific entropy is provided by a complete solar model. Changes in frequencies were found on the order of 0.5% between the two models, or only about a fifth the frequency separation between the ℓ/H of 1.5 and the ℓ/H of 3.0 models. In order to better understand this result, we then plotted the percent differences of the local sound speed in the two models versus the depth (Figure 4). The full horizontal scale is a typical penetration depth of the modes. We can see from Figure 4 that in only a relatively small region of space can (small) differences arise; this is because only in such a region are the exact values of convective efficiencies important in determining temperature structure. Next, we experimented with the outer boundary condition and found that only negligible ($< 0.1\%$) changes resulted from applying an outgoing wave boundary condition as opposed to a zero boundary condition. This result is not at all surprising, since wave amplitudes are heavily damped by the time the wave penetrates into the corona.

To summarize, a detailed modeling of the five minute oscillations has shown that the standard solar model with standard boundary conditions agrees well with the

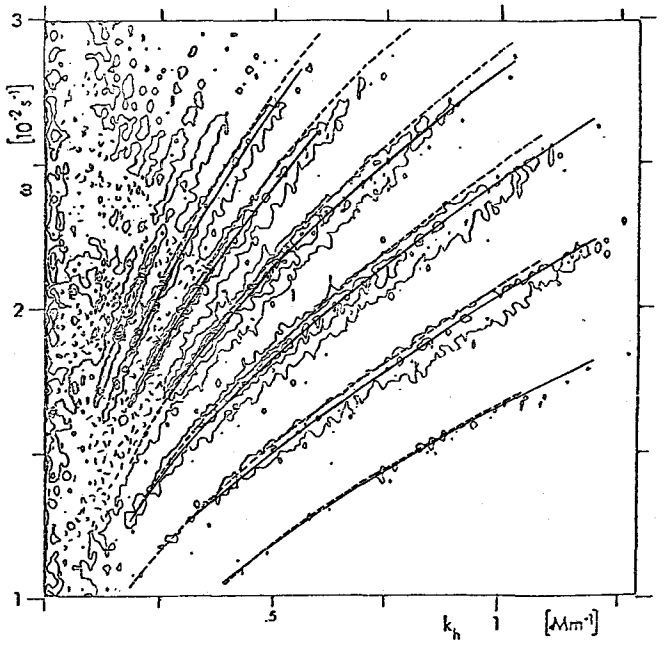

Figure 2. Comparison of two theoretical models with data.

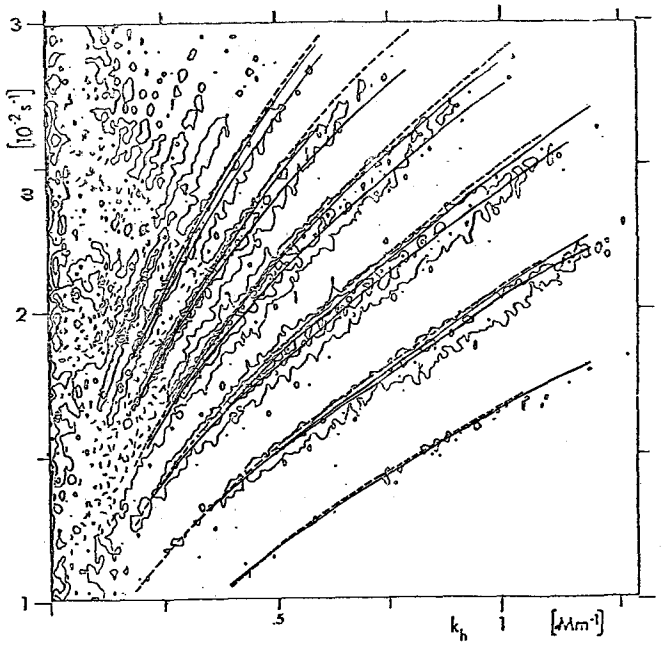

Figure 3. Comparison of three theoretical models with data.

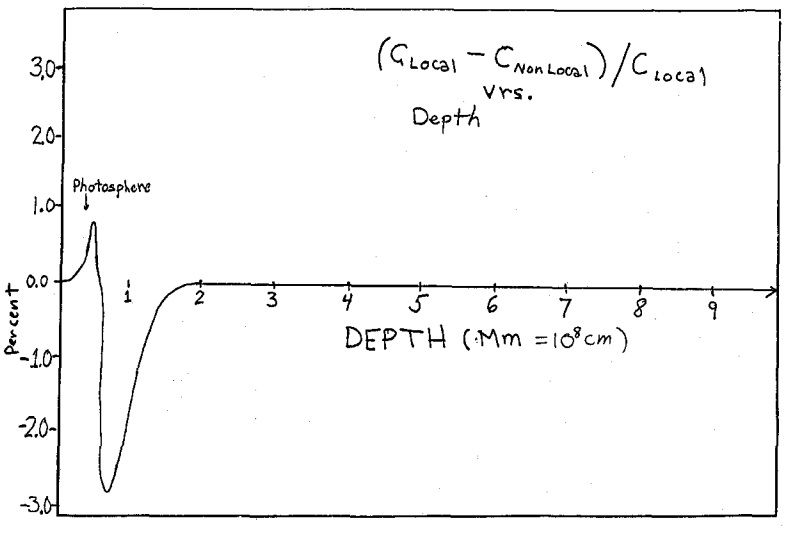

Figure 4. Percentage change in local and nonlocal sound speeds as a function of depth.

observations. In the future, we hope to investigate the effects of the anomalous boundary conditions discussed by Hill, Rosenwald and Caudell (1978), the influence of alternative chromospheric models, and perhaps the question of nonlinear effects.

REFERENCES

Ando, H. and Osaki, Y. 1975, Publ. Astr. Soc. Japan, 27, 581.
Avrett, E.H., Vernazza, J.E. and Linsky, J.L. 1976, Ap. J., 207, L199.
Deubner, F.-L., Ulrich, R.K. and Rhodes, E.J., Jr. 1979, Astr. Ap., 72, 177.
Hill, H.A., Rosenwald, R. and Caudell, T.P. 1978, Ap. J., 225, 304.
Ulrich, R.K. 1970a, Ap. J., 162, 993.
Ulrich, R.K. 1970b, Ap. Sp. Sci., 7, 183.
Ulrich, R.K. and Rhodes, E.J., Jr. 1977, Ap. J., 218, 521.
Wolff, C.L. 1972, Ap. J., 177, L87.

SENSITIVITY OF FIVE MINUTE EIGENFREQUENCIES TO THE STRUCTURE OF THE SUN

G. Berthomieu,(1) A.J. Cooper,(1)(2) D.O. Gough,(1)(2)(3)
Y. Osaki,(1)(4) J. Provost,(1) and A. Rocca (1)

ABSTRACT

The dependence of theoretical eigenfrequencies of five minute oscillation modes on the parameters that determine model solar envelopes has been investigated. It was found that the p mode frequencies are quite strongly correlated with the depth of the convection zone. Comparison of theory with observation suggests that the solar convection zone is about 200,000 km deep.

1. INTRODUCTION

Our investigation was similar to that described by Lubow, Rhodes and Ulrich (1980) though our motivation was somewhat different. Our primary concern was to discover whether the recent observations of solar five minute oscillations (Deubner 1975, 1977; Rhodes, Ulrich and Simon 1977; Deubner, Ulrich and Rhodes 1979) can be used to put useful bounds on the structure of the sun. Thus our quest was to discover how large is the set of solar models that can support normal modes of oscillation with eigenfrequencies that lie on the ridges of the k-ω diagrams constructed from the observations. To achieve this one must study the sensitivity of the computed eigenfrequencies to variations in both the basic solar model and the assumptions of the normal mode theory. This is a necessary first step in any attempt at inversion.

2. THE SOLAR MODELS

The majority of the five minute oscillations penetrate the sun to a depth of no more than a few tens of thousands of kilometers. These modes can supply no direct information from the deep interior. Therefore we have confined our attention to the

---

REFER TO THE AUTHORS AFFILIATIONS
(1) Observatoire de Nice, France
(2) Institute of Astronomy, University of Cambridge, UK
(3) Department of Applied Mathematics and Theoretical Physics, University of Cambridge, UK
(4) Department of Astronomy, University of Tokyo, Japan

envelope, and have constructed models by integrating inwards from a point in the chromosphere to a depth of about 5×10^5 km, paying little attention to whether our models would match onto plausible models of the core.

Above the photosphere we integrated the hydrostatic equation subject to an assumed T-τ relation. Opacities were computed with the routine used for constructing the Harvard-Smithsonian Reference Atmosphere (HSRA), which had been kindly supplied to us by Dr. C.J. Durrant. Beneath the photosphere radiative transfer was treated in the diffusion approximation, with opacities computed by linear interpolation in the tables of Cox and Stewart (1970), and generally the mixing-length formula quoted by Baker and Temesvary (1966) was used to compute the convective heat flux, with mixing length proportional to pressure scale height. For the equation of state it was assumed that the gas was composed of only hydrogen and helium, plus the ten most abundant heavy elements in the relative proportions given by Ross and Aller (1976). Thermodynamic state variables were obtained by minimizing an approximation to the formula for the free energy adopted by Fontaine, Graboske and Van Horn (1977); for this purpose the radii of atomic hydrogen and helium were taken to be 2.2 A and 1.5 A respectively. Normally, turbulent stresses were ignored.

Integrations were performed with a fourth-order accuracy Runge-Kutta algorithm. Typically 600 mesh intervals were used.

3. OSCILLATIONS

Most of the calculations used the adiabatic approximation to the equations of motion, subject to the conditions that the vertical displacement vanished at the base of the envelope and that the Lagrangian pressure perturbation vanished at the upper surface. The governing differential equations were integrated by second-order accuracy centered finite differences using the program described by Baker, Moore and Spiegel (1971), in much the same way as had been done by Ando and Osaki (1975, 1977). Subsequent improvements to the eigenfrequencies were made by substituting the eigenfunctions into variational integrals, which were evaluated to fourth-order accuracy.

4. A REFERENCE MODEL

A model was chosen with eigenfrequencies that reproduced the observations tolerably. It had been constructed with a T-τ relation above $\tau = 2/3$ taken from the HSRA. Its hydrogen abundance was 0.745, its heavy element abundance was 0.02 and the mixing length was 2.5 pressure scale heights. It had a convection zone 230,000 km deep. The frequencies of its lowest order eigenmodes, regarded as continuous functions of the horizontal wavenumber k, are shown in Figure 1 superposed on the power spectrum of Deubner, Ulrich and Rhodes (1979).

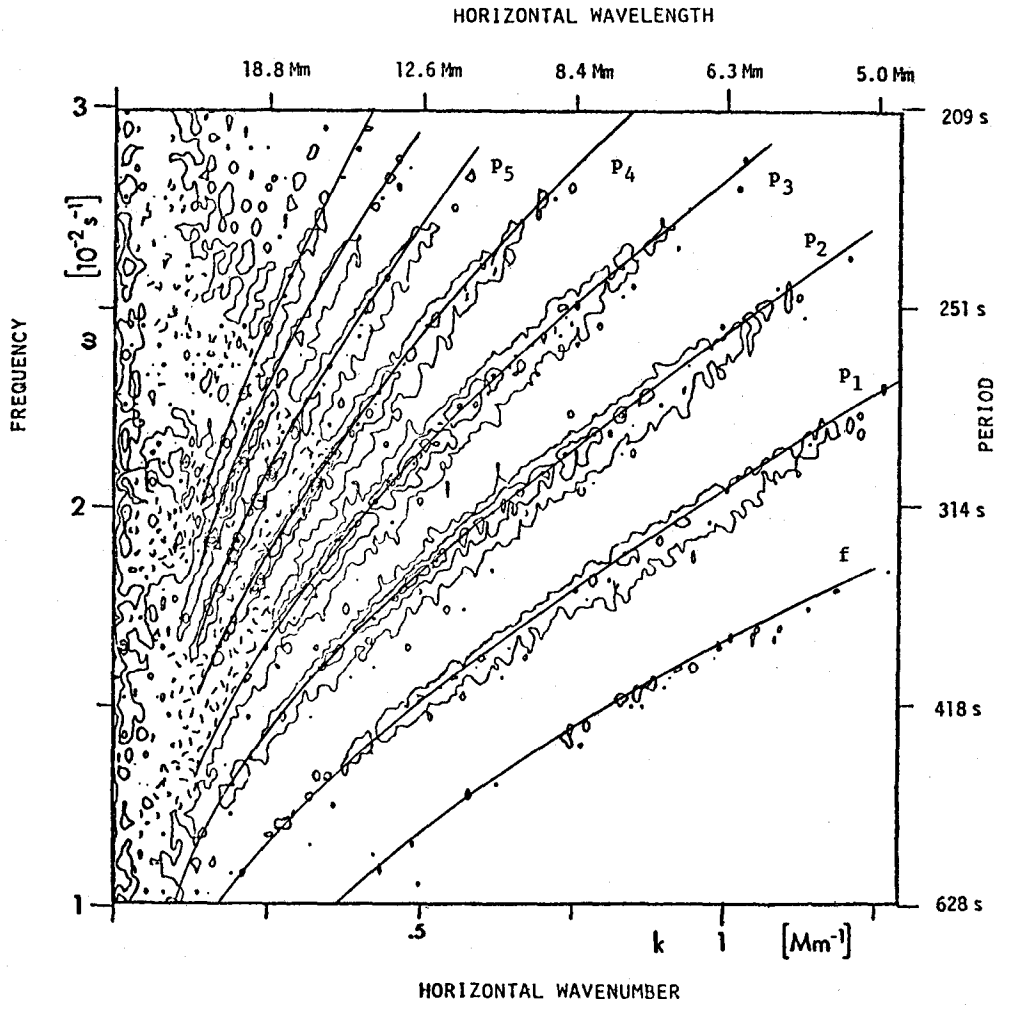

Figure 1. Eigenfrequencies of a model envelope, regarded as continuous functions of the horizontal wavenumber k, superposed on the power spectrum obtained by Deubner, Ulrich and Rhodes (1979).

5. ACCURACY OF THE NORMAL MODE ANALYSIS

Tests were made for numerical accuracy by varying the number of mesh intervals N and using Richardson extrapolation to estimate the limiting eigenfrequencies as $N \to \infty$. The results were compared with nonadiabatic eigenfrequencies computed by treating radiative transfer in the Eddington approximation and estimating the effect of turbulent convective fluxes using the quasiadiabatic approximation. In the latter, horizontal fluxes were ignored and the fluctuations in the vertical fluxes were taken from the latter part of § 5 of Gough (1977a). Also, modes were computed subject to various other upper boundary conditions: vanishing of Eulerian pressure perturbation and of vertical displacement, and matching to a running wave in an isothermal corona. The results depended on the modes selected, but in all cases the deviations from the reference f and p mode adiabatic eigenfrequencies were less than the uncertainties in the corresponding observations.

6. SENSITIVITY ANALYSIS

This analysis was performed by computing the changes in the eigenfrequencies of modes of degree 200 and 600 resulting from variations in the parameters determining the equilibrium model. Composition, the atmospheric T-τ relation, the mixing length and the parameters defining the position of the transition between the two asymptotic branches of the convective flux formula (cf. Gough and Weiss 1976) were varied separately. Also, models were computed using a nonlocal convection theory.

Broadly speaking, the eigenfrequencies were most strongly influenced by the mixing length, which determines the adiabat deep in the convection zone and hence controls the depth of that zone. This result confirms a hypothesis to this effect by Gough (1977b) and Ulrich and Rhodes (1977). Changes in the atmospheric structure had very little effect on the f and p mode eigenfrequencies, except for the chromospheric modes. Thus we conclude that provided the eigenvalue analysis is a good representation of the five minute oscillations, the observations imply that the depth of the solar convection zone is about 2×10^5 km.

7. DISCUSSION

The conclusion of our sensitivity analysis, namely that the k-ω power spectra of the five minute oscillations imply that the convection zone of the sun extends some 30 percent of the solar radius beneath the photosphere, is almost unavoidable. It must be borne in mind, however, that our inference is subject to the validity of the linear normal mode analysis which, we must point out, has been challenged (Rosenwald and Hill 1980).

Because it is difficult to reconcile Hill and Caudell's (1979) g-mode interpretation of the 45^m and 66^m modes of Brown, Stebbins and Hill (1978) with a deep convection zone (Dziembowski and Pamjatnykh 1978), Christensen-Dalsgaard, Dziembowski and Gough (1980) enquired whether a model with a shallow convection zone could be viable. They concluded that such a model might be consistent with Hill and Caudell's (1979) interpretation, though they did not actually construct one that successfully reproduced the observations. However, one cannot entertain the hypothesis that the solar convection zone is shallow without refuting the analysis summarized in this report. Rosenwald and Hill (1980) have gone some way towards doing so, by pointing out that the boundary conditions we apply in the chromosphere may be too poor an approximation to reality. They cite the determination by Hill, Rosenwald and Caudell (1978) of the spatial structure of the modes in the solar atmosphere, and show that this structure is not inconsistent with there being substantial deviations from the frequencies we have calculated. Nevertheless, the case is not proven: Stebbins (1980) has some further observational evidence to support Rosenwald and Hill's hypothesis, but Brown and Harrison (1980) observations seem to suggest a spatial structure more like that of the usual analysis such as that which we have reported here. None of the evidence is conclusive and we must await further observations.

Granted that this gross issue will eventually be resolved, what more might one expect to learn from the five minute oscillations? Of course the oscillations carry information about the large scale motion beneath the photosphere and the convective fluctuations, but one would like also to be able to measure some properties of the stratification in the superadiabatic boundary layer. Our experiments with modified convection formulae have revealed that to render this possible one must improve the resolution of the k-ω power spectra substantially. We have also found that all the p modes of degree 200 and 600, which we presume are not atypical, are stable when their interaction with the convection is taken into account. The decay rates of the nonchromospheric modes yield quality factors as low as 100, which correspond to the current resolution limit of the observations. The required improvements in resolution may not, therefore, be easily obtainable, and hence measurements of subtle features of the temperature and density stratification beneath the photosphere are probably not imminent.

* * * * *

We are grateful to J. Christensen-Dalsgaard, C.J. Durrant, P. Souffrin and J.-P. Zahn for useful discussions.

REFERENCES

Ando, H. and Osaki, Y. 1975, Pub. Astr. Soc. Japan, 27, 581.

Ando, H. and Osaki, Y. 1977, Pub. Astr. Soc. Japan, 29, 221.

Baker, N.H., Moore, D.W. and Spiegel, E.A. 1971, Quart. J. Mech. Appl. Math., 24, 391.

Baker, N.H. and Temesvary, S. 1966, Tables of convective stellar envelopes (Goddard Institute for Space Studies, New York).

Brown, T.M. and Harrison, R.L. 1980, these proceedings.

Brown, T.M., Stebbins, R.T. and Hill, H.A. 1978, Astrophys. J., 223, 324.

Christensen-Dalsgaard, J., Dziembowski, W. and Gough, D.O. 1980, these proceedings.

Cox, A.N. and Stewart, J.M. 1970, Astrophys. J. Suppl., 19, 243.

Deubner, F.-L. 1975, Astron. Astrophys., 44, 371.

Deubner, F.-L. 1977, The energy balance and hydrodynamics of the solar chromosphere and corona (ed. R.-M. Bonnet and Ph. Delache, G. de Bussac, Clermont-Ferrand), p. 45.

Deubner, F.-L., Ulrich, R.K. and Rhodes, E.J., Jr. 1979, Astron. Astrophys., 72, 177.

Dziembowski, W. and Pamjatnykh, A.A. 1978, Pleins feux sur la physique solaire (ed. J. Rösch, CNRS, Paris), p. 135.

Fontaine, G., Graboske, H.C., Jr. and Van Horn, H.M. 1977, Astrophys. J. Suppl., 35, 293.

Gough, D.O. 1977a, Astrophys. J., 214, 196.

Gough, D.O. 1977b, The energy balance and hydrodynamics of the solar chromosphere and corona (ed. R.-M. Bonnet and Ph. Delache, G. de Bussac, Clermont-Ferrand), p. 3.

Gough, D.O. and Weiss, N.O. 1976, Mon. Not. R. Astr. Soc., 176, 589.

Hill, H.A. and Caudell, T.P. 1979, Mon. Not. R. Astr. Soc., 186, 327.

Hill, H.A., Rosenwald, R.D. and Caudell, T.P. 1978, Astrophys. J., 225, 304.

Lubow, S., Rhodes, E.J., Jr., and Ulrich, R. 1980, these proceedings.

Rhodes, E.J., Jr., Ulrich, R.K. and Simon, G.W. 1977, Astrophys. J., 218, 901.

Rosenwald, R.D. and Hill, H.A. 1980, these proceedings.

Ross, J.E. and Aller, L.H. 1976, Science, 191, 1223.

Stebbins, R.T. 1980, these proceedings.

Ulrich, R.K. and Rhodes, E.J., Jr. 1977, Astrophys. J., 218, 521.

HOW DEEP IS THE SOLAR CONVECTION ZONE?

J. Christensen-Dalsgaard
Astronomisk Institut, Aarhus Universitet, Denmark
and Institute d'Astrophysique, Belgium

W. Dziembowski
Department of Physics, University of Arizona
and Copernicus Astronomical Center, Warsaw, Poland

D. Gough
Institute of Astronomy, Cambridge, UK
and Observatoire de Nice, France

ABSTRACT

The interpretation by Hill and Caudell (1979) of some of their solar oscillation data as being due to g modes of degree greater than 20 seems to imply that the solar convection zone is much shallower than that in standard solar models, probably representing only a few per cent of the radius. We attempt here to match the observed periods in models of this nature; the rather complicated spectrum of oscillations in such models can be understood in terms of the asymptotic behavior of modes of large degree. Possible excitation mechanisms for the modes are briefly discussed.

1. INTRODUCTION

Since the initial announcement of observations of large scale solar oscillations (Hill, Stebbins and Brown 1976; Brookes, Isaak and van der Raay 1976; Severny, Kotov and Tsap 1976); it has been clear that such oscillations may represent very powerful probes of the structure of the solar interior (Scuflaire et al. 1975; Christensen-Dalsgaard and Gough 1976; Iben and Mahaffy 1976). For this potential to be realized, however, one must obtain some information about the horizontal structure of the motion as specified by its horizontal wavenumber, k_h, or the degree, ℓ, of the oscillation.

Until recently the five minute oscillations were the only class of solar oscillations for which such information was available. As discussed by Berthomieu et al. (1980) and Lubow, Rhodes and Ulrich (1980), good agreement between the theoretically predicted frequencies as functions of k_h and the ridges of maximum power in the observed k_h - ω diagram can be engineered. On the other hand, these modes are sensitive to the structure of only the outer few percent of the sun; indirectly, through the value of the entropy in the adiabatic part of the convection

zone, they provide information about the depth of the convection zone, but not about the structure of the regions deeper down.

To investigate these deeper parts of the sun one must consider modes of lower degree and for these, mainly because their amplitudes are quite low, the horizontal structure is difficult to determine. Therefore considerable importance is attached to the announcement by Hill and Caudell (1979) of evidence for the nature of the horizontal structure of two of the modes observed by Brown, Stebbins and Hill (1978) (see the review by Hill 1980). By comparing the power at two different scan amplitudes across the solar limb, Hill and Caudell inferred that the modes with periods of about 66 and 45 minutes had ℓ values in excess of 20. This conclusion was based on an analysis of the dependence of detector sensitivity upon ℓ, the details of which may be somewhat uncertain; the basic observational material is yet rather limited, and the statistical significance of the result is probably not yet clear. Nevertheless, the result, if confirmed, may give important information about the solar interior, and it therefore merits some theoretical attention. Furthermore, it is an instructive exercise in helioseismology to take the observations at face value and confront the predicted modes of oscillation of solar models with them.

It was pointed out by Dziembowski and Pamjatnykh (1978) that the observed modes could not be interpreted in terms of a standard solar model. In the inferred range of ℓ the periods of the f and p modes are all shorter than the observed periods. Hence the observed modes must be gravity modes, and such modes are largely confined to regions of the model within which their frequencies are below the local buoyancy frequency. The relatively extensive outer convection zone causes these regions to be deep in the solar model, and the modes are therefore very efficiently trapped, the maximum of the relative displacement being larger than its surface value by a typical factor of 10^5. It is difficult to reconcile this result with the amplitudes observed at the surface, and to envisage an excitation mechanism for the modes. Moreover, it appears very likely that the coherence between the trapping region and the surface would be destroyed by nonlinear effects.

As stressed by Dziembowski and Pamjatnykh (1978) and Gough (1978), these problems may be avoided in solar models with a very thin convection zone. It is therefore interesting that such models have been discussed in a quite different context. To account for the low observed solar neutrino counting rate obtained by Davis (see e.g. Davis 1978), Joss (1974) suggested that the sun had initially a very low abundance Z of heavy elements, and that the convection zone was subsequently enriched with heavy elements by accreted interstellar material to give the present observed value of Z of about 0.02. This hypothesis was tested by Christensen-Dalsgaard, Gough and Morgan (1979) who computed consistent evolution sequences of solar models affected by accretion. Owing to the relatively low opacity in the interior of these models, their convection zones are shallower than those of a

standard solar model and, when Z is sufficiently small in the interior, the buoyancy frequency has a local maximum close to the bottom of the convection zone. This may provide a region that can trap relevant g modes.

Thus it appears possible that these or similar models may have modes of oscillation corresponding to those that appear to have been observed by Hill and Caudell, and the present paper reports an attempt to investigate this possibility. Relevant parts of the asymptotic theory of nonradial oscillations are reviewed in § 2. In § 3 the models computed by Christensen-Dalsgaard et al. are discussed, and § 4 studies in some detail the oscillations of one of these models, comparing them with those of a standard solar model. In § 5 we consider the oscillations of chemically homogeneous envelopes having very thin convection zones. Finally, § 6 contains a summary of the results and a brief discussion of the various possible ways in which the modes might be excited.

2. THE ASYMPTOTIC BEHAVIOR OF NONRADIAL OSCILLATIONS OF LARGE DEGREE

As a background to the numerical results presented later; we review some results from the asymptotic theory of nonradial oscillations with large ℓ. The derivation is discussed by Christensen-Dalsgaard (1979) (see also Shibahashi and Osaki 1976; Dziembowski 1977; Gough 1977; Dziembowski and Pamjatnykh 1978).

Using JWKB analysis one finds that the amplitude ξ_r of the radial component of the displacement has the approximate form

$$\xi_r(r) = r^{-3/2}\rho^{-1/2}\left[|1 - \omega^2/S_\ell^2|/|1 - N^2/\omega^2|\right]^{1/4} \times \left[c_1 \exp(\Phi) + c_2 \exp(-\Phi)\right] \quad . \tag{2.1}$$

Here ω is the frequency of oscillation; S_ℓ and N are local acoustic and buoyancy frequencies, given by

$$S_\ell^2 = \ell(\ell + 1)c^2/r^2 \tag{2.2}$$

and

$$N^2 = g\left(\frac{1}{\Gamma_1}\frac{d\ell n p}{dr} - \frac{d\ell n \rho}{dr}\right) \quad , \tag{2.3}$$

where $c = (\Gamma_1 p/\rho)^{1/2}$ is the adiabatic sound speed, p and ρ are pressure and density, $\Gamma_1 = (d\ell n p/d\ell n \rho)_s$ where s is specific entropy, and g is the gravitational acceleration; furthermore

$$\Phi = i\int^{r} k_r \, dr' \quad , \tag{2.4}$$

where the local radial wavenumber k_r satisfies

$$k_r^2 = \frac{\ell(\ell+1)}{r^2}\left(\frac{N^2}{\omega^2} - 1\right)\left(1 - \frac{\omega^2}{S_\ell^2}\right) \quad . \tag{2.5}$$

Equation (2.1) is not valid close to the turning points where $k_r^2 = 0$, near the singular point at the center, nor near the surface where the equilibrium structure no longer varies on a length scale much greater than that of the oscillations. The eigenfunctions can be expressed in terms of Airy functions near the turning points and Bessel functions near the center, and near the surface in terms of either Bessel functions or confluent hypergeometric functions depending on the value of ℓ. The resulting consistent asymptotic representation leads to the determination of the constants c_1 and c_2 in equation (2.1).

Given ℓ, the model is thus separated into regions where $k_r^2 > 0$ and where ξ_r oscillates as a function of r (these regions are called oscillatory), and regions (called evanescent) where $k_r^2 < 0$ and ξ_r decays or grows exponentially. To each oscillatory region belongs a set of modes whose eigenfunctions are large only in the given region and whose eigenfrequencies can be estimated by considering that region in isolation. These modes, which one may call the local modes of the region, normally correspond approximately to global modes--that is to say, modes of the model as a whole. This correspondence fails to be true only when the frequencies of two local modes belonging to different oscillatory regions are almost identical. In such cases the frequencies of the global modes generally exhibit 'avoided crossings,' and the corresponding eigenfunctions interchange their nature (for a discussion of this phenomenon see, for example, von Neumann and Wigner 1929; Aizenman, Smeyers and Weigert 1977; Christensen-Dalsgaard 1979; Gabriel 1980). Thus it is often useful to classify global modes according to the oscillatory region that controls their behavior. It must be kept in mind, however, that this classification is not invariant under continuous variations of the model (or variations in ℓ), since it changes in the neighborhood of avoided crossings. Specific examples of this are given in § 4.

One may note from equation (2.1) that the ratio between the amplitudes of ξ_r in two adjacent oscillatory regions is of the order of magnitude:

$$\left(\frac{r_2}{r_1}\right)^{3/2}\left[\frac{\rho(r_2)}{\rho(r_1)}\right]^{1/2} \times \exp\left\{\pm\int_{r_1}^{r_2}\left[\ell(\ell+1)\right]^{1/2}\left[\left(1 - \frac{N^2}{\omega^2}\right)\left(1 - \frac{\omega^2}{S_\ell^2}\right)\right]^{1/2}\frac{dr}{r}\right\} \quad , \tag{2}$$

where r_1 and r_2 are the boundaries of the intervening evanescent region. Thus, when

ℓ is large, the degree of trapping of a mode (the ratio between its amplitude in the oscillatory region to which it belongs and its amplitude in the neighboring oscillatory regions) may be extremely large.

For large ℓ the model has an oscillatory region close to the surface; the corresponding modes have frequencies whose squares increase approximately linearly with ℓ. These are the five minute oscillations and gravity waves trapped above the convection zone. Only the latter can have frequencies in the relevant range, but it seems unlikely that these could have values of ℓ appropriate to reproduce the data. In what follows we shall therefore restrict attention to that part of the sun contained beneath the top of the convection zone.

When the model has a convective envelope, $S_\ell^2 > N^2$ everywhere for sufficiently large ℓ. In that case there are oscillatory regions where $\omega^2 < N^2$. The corresponding modes are gravity waves trapped between consecutive zeros of $N^2 - \omega^2$; their frequencies approximately satisfy

$$\left[\ell(\ell+1)\right]^{1/2} \int_{r_1}^{r_2} \left[\left(\frac{N^2}{\omega^2} - 1\right)\left(1 - \frac{\omega^2}{S_\ell^2}\right)\right]^{1/2} \frac{dr}{r} = \pi\left(n - \frac{1}{2}\right) \quad , \tag{2.7}$$

where r_1 and r_2 are consecutive zeros of $N^2 - \omega^2$, with $N^2 > \omega^2$ in (r_1,r_2); and n is a positive integer such that the number of zeros in ξ_r between r_1 and r_2 is $n - 1$. Equation (2.7) is valid only if N^2 is sufficiently smooth (it cannot be used if N^2 is represented by, say, a step function or if N^2 changes very rapidly), and the oscillatory region (r_1,r_2) must not be 'too close' to the singularity at the center and the near singularity at the surface. In particular, if ω^2 is very small, equation (2.7) should be replaced by the expression given by Vandakurov (1967) which properly takes the singularities into account. Furthermore (r_1,r_2) must be well separated from any neighboring oscillatory regions, and $N^2 - \omega^2$ must not become very small in the interior of (r_1,r_2) by, for example, N^2 having a local minimum slightly above ω^2. When (2.7) is valid the local spectrum is considerably simplified, provided that ω^2/S_ℓ^2 is much smaller than 1; in this case the local squared frequency $\omega_{loc}^2(n,\ell)$ is a function of only $(n - 1/2)/[\ell(\ell+1)]^{1/2}$. Thus, if $[\ell(\ell+1)]^{1/2}$ is approximated by $\ell + 1/2$,

$$\omega_{loc}^2(n,\ell) = f\left(\frac{n - \frac{1}{2}}{\ell + \frac{1}{2}}\right) \quad , \tag{2.8}$$

where the function f depends on the behavior of N^2 in the region considered and can be computed from equation (2.7). When ω^2 is close to a local maximum N_m^2 of N^2, $N^2(r)$ may be represented by a parabola in (2.7); if, furthermore, ω^2/S_ℓ^2 is neglected compared with 1, the approximate solution to equation (2.7):

$$1 - \frac{\omega_m^2(n,\ell)}{N_m^2} \simeq 2\beta\frac{n - \frac{1}{2}}{\ell + \frac{1}{2}} \qquad (2.9)$$

is obtained, where

$$\beta^2 = -\frac{1}{2}\frac{r_m^2}{N_m^2}\frac{d^2N}{dr^2}\bigg|_{r=r_m} , \qquad (2.10)$$

r_m being the position of the maximum of N^2. Equation (2.9) is clearly a special instance of the general relation (2.8). Thus each local maximum N_m^2 of N^2 has an associated class of local modes, with squared frequencies tending to N_m^2 like ℓ^{-1} as $\ell \to \infty$. Evidently the global spectrum for models with several local maxima in N^2 could be extremely complicated.

3. PROPERTIES OF THE SOLAR MODELS

The solar models used here were computed using a modified version of Eggleton's (1972) evolution program. Opacities were obtained by linear interpolation from the tables of Cox and Stewart (1970), and the energy generation rate was computed with reaction rates from Fowler, Caughlan and Zimmerman (1975), assuming the p-p chain and the CNO cycle to be always in nuclear equilibrium. The accretion of interstellar material was modelled by increasing Z in the convection zone at such a constant rate as to reproduce the present surface value Z_s, which was taken to be 0.02; the change in the mass of the model due to accretion was neglected. It was assumed that matter enriched with heavy elements was not mixed beneath the base of the convection zone. The initial model was assumed to be in thermal equilibrium and chemically homogeneous, with abundances by mass X_0 and Z_0 of hydrogen and heavy elements respectively. For a given value of Z_0, the model was calibrated by adjusting X_0 and the ratio α of the mixing length to pressure scale height to obtain a luminosity of 3.83×10^{33} erg s^{-1} and a radius of 6.96×10^{10} cm at an age of 4.75×10^9 years. Further information about how the models were calculated was given by Christensen-Dalsgaard, Gough and Morgan (1979).

Three evolutionary sequences were computed. One of these, Model A, is homogeneous in Z and serves as a reference standard model; the other two, Model B and Model C, having values of Z_0 of 0.004 and 0.001 respectively, suffer accretion. Some relevant information about these three models is contained in Table 1. (Note that Table 1 of Christensen-Dalsgaard, Gough and Morgan 1979 contains two misprints: the present central densities of Models B and C should be 135 and 129 g cm^{-3}.)

From Table 1 it can be seen that only Model C has a convection zone that is

Table 1. Properties of Solar Models

	Model A	Model B	Model C
Initial heavy element abundance, Z_o	0.02	0.004	0.001
Initial hydrogen abundance, X_o	0.73	0.81	0.84
Mixing length/pressure scale height, α	1.35	1.11	0.62
Initial mass of convection zone ($M_\odot$)	1.5×10^{-2}	2.9×10^{-3}	3.7×10^{-5}
Present central density, ρ_c (g cm^{-3})	146	135	129
Present central temperature, T_c (^oK)	1.49×10^7	1.43×10^7	1.41×10^7
Present central hydrogen abundance, X_c	0.39	0.47	0.50
Depth of present convection zone, D ($R_\odot$)	0.240	0.172	0.042
Mass in present convection zone ($M_\odot$)	1.0×10^{-2}	1.7×10^{-3}	1.6×10^{-6}
Total neutrino counting rate (SNU)	5.2	2.3	1.7
Values (and locations, x) of maxima of buoyancy frequency (mHz)	0.451 (0.10) 0.415 (0.32)	0.414 (0.11) 0.419 (0.36)	0.398 (0.11) 0.410 (0.35) 0.359 (0.87)
Values (and locations, x) of minima of buoyancy frequency (mHz)	0.406 (0.24)	0.363 (0.25)	0.346 (0.25) 0.277 (0.71)

sufficiently thin as to render it possible for modes trapped in the interior to have observable amplitudes at the surface. This is also the only model considered with a predicted neutrino capture rate which is consistent with the observed value of 1.6 ± 0.4 SNU (Davis 1978). Our subsequent discussion will therefore be devoted mainly to this model.

The asymptotic analysis in § 2 showed that the modes of oscillation are largely shaped by the behavior of the buoyancy and acoustic frequencies. In Figure 1, N^2 and S_{20}^2 in units of g_s/r_s are plotted against $x = r/r_s$ for Model A (dashed lines) and Model C (solid lines). The rather complicated behavior of N^2 is most easily understood by rewriting equation (2.3) as

$$N^2 = \frac{\Gamma_1 g^2}{c^2}\left[(\nabla_{ad} - \nabla)\delta + \left(\frac{\partial \ell n p}{\partial \ell n X}\right)_{p,T}\frac{d\ell n X}{d\ell n p}\right] \quad , \tag{3.1}$$

where $\nabla_{ad} = (\partial\ \ell n\ T/\partial\ \ell n\ p)_s$, $\nabla = d\ \ell n\ T/d\ \ell n\ p$ and $\delta = -(\partial\ \ell n\ \rho/\partial\ \ell n\ T)_p$. In models like those considered here, without convective cores, the term in $d\ \ell n\ X/d\ \ell n\ p$ gives a positive contribution to N^2 in the region where hydrogen has been partly depleted by nuclear burning; this causes the pronounced local maximum in N^2 close to $x = 0.1$ in both models. (The small feature close to $x = 0.17$ is an artifact, probably caused by the use of linear interpolation for the opacity; in fact, in both models it coincides almost exactly with the point where $T = 1.0 \times 10^7$K). Further out the sound speed c decreases with increasing x, whereas g has a fairly broad maximum near $x = 0.2$ and decreases approximately as x^{-2} when $x > 0.4$ (this outer region contributes relatively little to the mass of the model); the rapid decrease in g outweighs the decrease in c for intermediate x, leading to a decrease in N^2. Very near the surface the decrease in c^2 dominates. In the models considered here the maximum in g combined with a decrease in ∇ around $x = 0.3$ causes the second local maximum close to $x = 0.35$. This maximum, however, is absent in some 'standard' models of the sun (e.g. the model considered by Christensen-Dalsgaard 1979).

At the bottom of the convection zone $\nabla_{ad} - \nabla$, and hence N^2, tend to zero. In models with a deep outer convection zone, like Model A, N^2 therefore decreases monotonically from an interior maximum. But in Model C the convection zone is so thin that the rapid decrease in c^2 in the outer parts of the model causes a third local maximum in N^2. The curious shape of N^2 near this maximum results from the retreat of the convection zone during evolution, which produces a zone in which Z, and hence opacity, increases outwards. In fact the position of the maximum in N^2 corresponds, in the mass coordinate, to the base of the convection zone in the zero-age model.

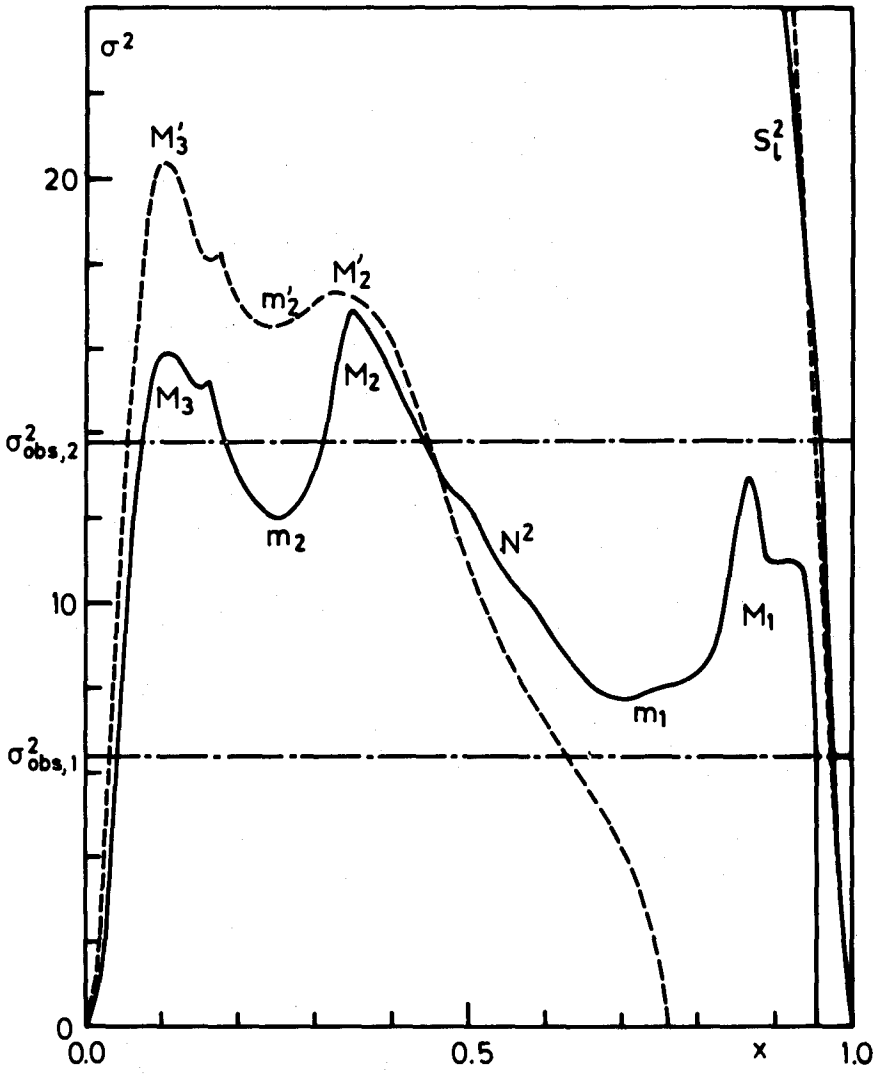

Figure 1. The squared buoyancy frequency N^2 and acoustic frequency $S_{20}{}^2$ in Model A (dashed lines) and Model C (fully drawn lines). The observed squared frequencies are indicated by $\sigma_{obs,1}{}^2$ and $\sigma_{obs,2}{}^2$. For ease of reference the local maxima and minima in N^2 have been labeled.

4. THE OSCILLATIONS OF THE MODELS

The main purpose of the present work is to attempt to understand the observations of solar modes of oscillation with periods of 66 and 45 minutes and values of ℓ in excess of 20. Even so, it is useful to take a wider look at the spectrum of oscillations in order to generally understand the oscillations of these and similar models and thus to consider whether modifications of the models might be able to provide better agreement with the observations.

In the remainder of the paper, frequencies will always be given in dimensionless form, in terms of

$$\sigma^2 = \omega^2 r_2/g_s \quad . \tag{4.1}$$

In this unit the squared frequencies of the observed oscillations are $\sigma^2_{obs,1} = 6.4$ and $\sigma^2_{obs,2} = 13.8$.

Figure 1 shows that N^2 in Model C has three prominent peaks in regions designated M_1, M_2, and M_3, separated by the minima m_1 and m_2. Each of these peaks, M_i, supports a local spectrum of modes for sufficiently large ℓ. These modes we label $g_n^{(i)}(\ell = \ell')$, where as in equation (2.7) n (= 1, 2, . . .) is one higher than the number of zeros of ξ_r in the oscillatory region corresponding to M_i, and ℓ' is the value of ℓ.

The qualitative nature of the spectrum of oscillations in this model at large ℓ thus depends strongly on the value of σ^2. When σ^2 is less than the minimum value $N^2_{m_1}$ of N^2 at m_1 (which is about 7.7), there is just one class of g modes; these possess squared frequencies approximately satisfying (2.7) with r_1 close to the center and r_2 close to the bottom of the convection zone. As σ^2 increases above $N^2_{m_1}$, however, the g modes split into a class of modes trapped beneath m_1 and a class of modes trapped within the region M_1, the latter modes having squared frequencies tending towards the maximum $N^2_{M_1}$ of N^2 at M_1 (which is about 12.9) as ℓ tends to infinity. Finally the interior modes divide into modes trapped within M_2 and M_3 when σ^2 becomes greater than $N^2_{m_2}$ (about 12.0), with squared frequencies tending towards $N^2_{M_2} \approx 16.9$ and $N^2_{M_3} \approx 15.9$ respectively as ℓ tends to infinity.

In Model A, N^2 has only two peaks, M_2' and M_3'; here there is a single class of g modes for $\sigma^2 < N^2_{m_2'}$ (about 16.5). For $\sigma^2 > N^2_{m_2'}$ this splits into modes trapped in the two peaks, with squared frequencies tending to $N^2_{M_2'} \approx 17.3$ and $N^2_{M_3'} \approx 20.4$. This requires ℓ to be sufficiently large to allow M_2' to support the $g_1^{(2)}$ mode; equation (2.7) can be used to estimate that ℓ has to be at least 20. For smaller values of ℓ, the spectrum of this model is presumably very similar to the spectrum of the solar model studied by Christensen-Dalsgaard (1979).

The positions of the observed frequencies are also indicated on Figure 1 with dot-dashed lines. For the higher frequency the evanescent region between the surface and the outermost oscillatory region has about the same geometrical depth in the two

models. In Model C, N^2 is relatively large, greater than $\sigma^2_{obs,2}/2$, in most of the evanescent region. Hence the degree of trapping of a mode at $\sigma^2_{obs,2}$ need not be impossibly large in this model, provided that a mode associated with M_2 could be found. Model A, on the other hand, exhibits the strong trapping of interior g modes found in standard solar models. At the lower frequency the evanescent region in Model C is essentially just the very thin convection zone, and here one expects no problems with trapping; in Model A the evanescent region is still quite deep at this frequency, and the trapping correspondingly strong.

To support these qualitative predictions we have made extensive calculations of modes of Model C. In all cases the Eulerian perturbation in the gravitational potential was neglected, and the differential equations were solved using the constant coefficient method first used by Gabriel and Noels (1976) and described in Christensen-Dalsgaard (1979). The correction to the frequency, caused by the perturbation in the gravitational potential, was found using the Cowling (1941) perturbation approach. The computed squared frequencies are shown on Figure 2, plotted against ℓ, which is here regarded as a continuous variable (this is mathematically permissible, although of course only the integer values of ℓ have physical significance). Some of the modes have been labeled with their Eckart (1960) classification, first used for modes of nonradial stellar oscillation by Scuflaire (1974) and Osaki (1975); this classification has the virtue of being invariant under continuous variations in ℓ (or in any parameter characterizing the model), but it is not directly related to the physical nature of the mode. On the figure are also indicated the observed squared frequencies (dot-dashed lines), the maxima $N^2_{M_1}$, $N^2_{M_2}$ and $N^2_{M_3}$ (dashed lines) and the minima $N^2_{m_1}$ and $N^2_{m_2}$ (dotted lines) of N^2.

The global f mode is evidently always the surface mode of the model. The remaining modes are all gravity modes. We first consider the low-order modes, with frequencies in the neighborhood of $\sigma^2_{obs,2}$. Table 2 gives some properties of these modes at $\ell = 20$; $|\xi_r|_{max}/|\xi_r|_s$ is the ratio of the maximum to the surface value of $|\xi_r|$, x_{max} is the position where $|\xi_r|$ has its maximum, and E is the normalized pulsational energy

$$E = \int_0^{r_s} \left[|\xi_r|^2 + \ell(\ell+1)\,|\xi_h|^2 \right] \rho r^2 dr \Big/ \left[M|\xi_r(r_s)|^2 \right] , \qquad (4.2)$$

where ξ is the amplitude of the horizontal component of the displacement vector. Furthermore, Figure 3 shows ξ_r as a function of x for the same seven modes. From the figure it is evident that the global g_1, g_3 and g_4 modes correspond to the local $g_1^{(3)}$, $g_2^{(3)}$ and $g_3^{(3)}$ modes, whereas the global g_2 mode is the local $g_1^{(2)}$ mode; the global g_5 mode has to some extent the nature of the local $g_2^{(2)}$ mode, although its frequency is too close to N_{m_2} to effectively trap it in M_2. On the other hand the g_6

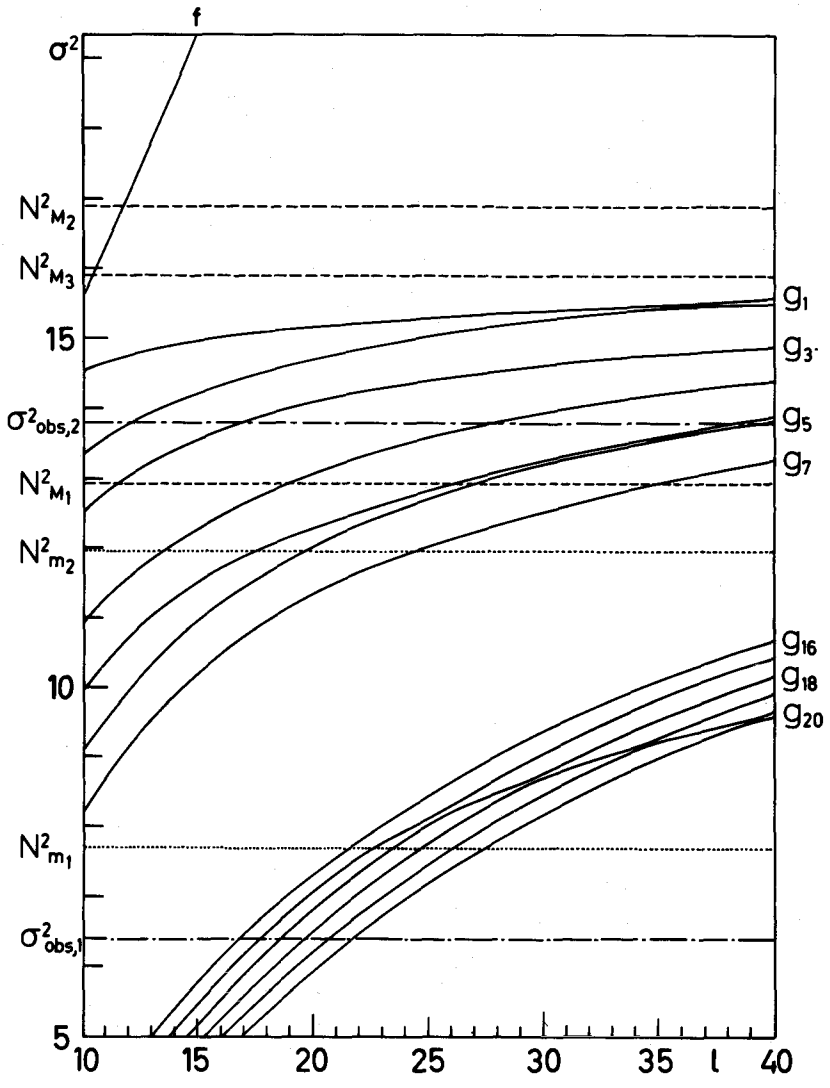

Figure 2. Squared frequencies for selected modes in Model C, as functions of ℓ. The observed values are indicated by $\sigma^2_{obs,1}$ and $\sigma^2_{obs,2}$, and the local maxima $N^2_{M_i}$ (i = 1, 2, 3) and local minima $N^2_{m_i}$ (i = 1, 2) of N^2 are also shown. The distances of closest approach of the curves at the avoided crossings beyond ℓ = 29 have been exaggerated.

and g_7 modes clearly belong to the interior of the model as a whole. The separation of the lowest order modes into two classes is confirmed by Table 2, which furthermore shows that the modes associated with M_2 are much less severely trapped than those belonging to M_3.

Figure 2 shows that the g_1 and g_2 modes engage in an avoided crossing when ℓ is close to 35; for greater values of ℓ, the g_1 mode thus corresponds to the local $g_1^{(2)}$ mode, and the g_2 mode to the local $g_1^{(3)}$ mode. Moreover it is clear that, once above N_{m_2}, the frequencies of the g_5 and g_6 modes begin to approach each other fairly rapidly; however there is no avoided crossing between these two modes, merely an accidental close approach of their frequencies between ℓ = 30 and 40. (On the other hand it is evident that a slight modification of the model to increase the frequencies of the $g^{(3)}$ modes a little could change this behavior into two close avoided crossings; this would almost certainly happen as a consequence of the evolution of the model, if followed to a slightly greater age.)

The pulsational energy E increases rapidly with ℓ, as is shown in Figure 4. For the g_1 and g_2 modes in particular, where ω varies relatively little over the range of ℓ considered, log E increases essentially linearly with ℓ, as might be expected from equation (2.6).

For comparison, Table 3 shows the same quantities as Table 2, but for the lowest order modes in Model A, in addition to a mode close to the second observed frequency. Clearly the modes belonging to M_2 in Model C are much less effectively trapped than the modes with similar frequencies in Model A. Note that although there is no clear separation of modes belonging to M_2' and to M_3', the behavior of the energy of the g_4 mode departs from the general increase in E with decreasing order. This may indicate that this mode is progressing toward an association with M_2'. In fact the g_4 and g_5 modes engage in a weak avoided crossing between ℓ = 25 and 30, and the $g_5(\ell=30)$ mode quite definitely belongs to M_2'.

It appears to be quite difficult to match $\sigma^2_{obs,2}$ in Model C. Since we must require that ℓ be greater than 20, the first possible identification is $g_4(\ell=27)$, but for this mode the energy is implausibly large. The same is true of $g_5(\ell=38)$, even though this is a mode belonging to M_2. If we relax the bound on ℓ somewhat, $g_3(\ell=17)$ might be considered, but equally plausible identifications could be found in a standard model. And one would have to consider values of ℓ as low as 12 (which is probably ruled out by the observations) to identify the observed mode with $g_1^{(2)}$, an identification which might otherwise be attractive. At an only slightly lower value of ℓ one could make the far more natural choice of the envelope f mode in a standard model. However it might be pointed out that by increasing the opacity in the region around M_2, and hence decreasing N^2, it may be possible to reduce the frequency of the $g_1^{(2)}(\ell = 20)$ mode enough to bring it into agreement with $\sigma_{obs,2}$.

Turning now to the 66 minute mode with squared dimensionless frequency

Table 2.

Mode	σ^2	$\frac{\lvert\xi_r\rvert_{max}}{\lvert\xi_r\rvert_s}$	x_{max}	E
g_1	15.19	6.2×10^4	0.10	2.8×10^7
g_2	14.73	1.1×10^2	0.37	2.0×10^2
g_3	14.10	5.8×10^3	0.09	2.7×10^5
g_4	13.08	1.2×10^3	0.08	9.4×10^3
g_5	12.29	22	0.44	11
g_6	12.05	53	0.07	20
g_7	11.36	37	0.07	10

Modes with $\ell = 20$, in Model C. The table shows the Eckart classification, the squared dimensionless frequency, the ratio between maximum and surface displacement, the position of maximum displacement and the normalized pulsational energy (defined in equation 4.2).

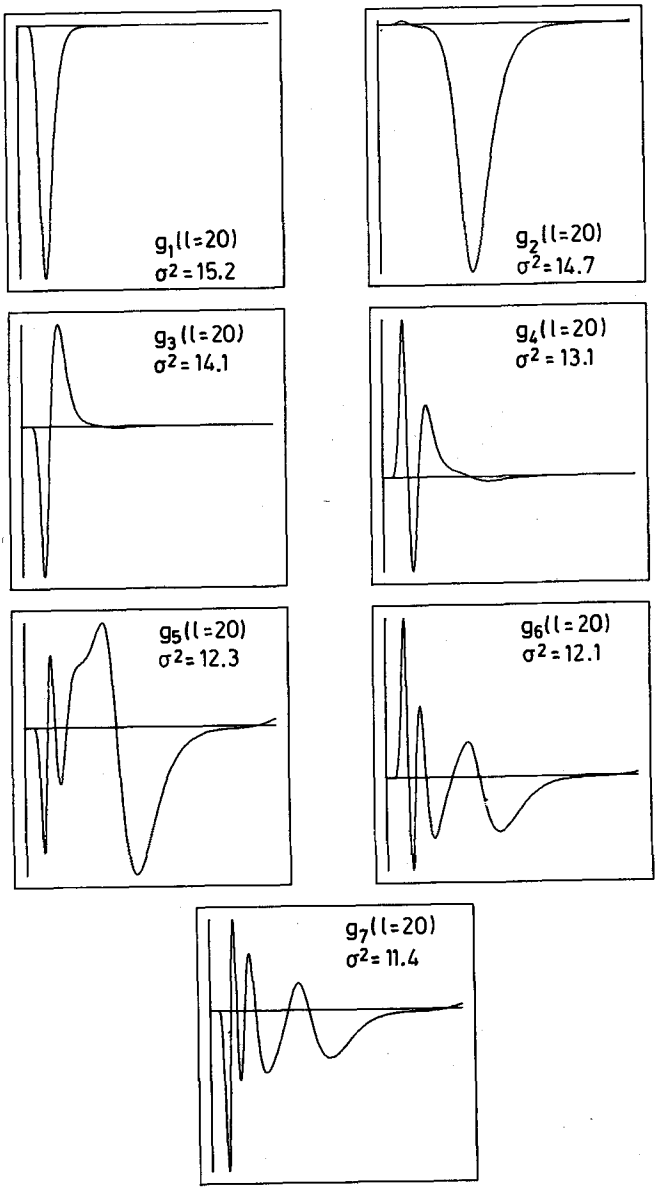

Figure 3. The amplitude $\xi_r(x)$ of the radial displacement for the seven first g modes at $\ell = 20$, in Model C. The abscissa is uniform in x, from o (left) to unity (right). The Eckart classification of the modes is indicated, as well as their squared dimensionless frequencies σ^2.

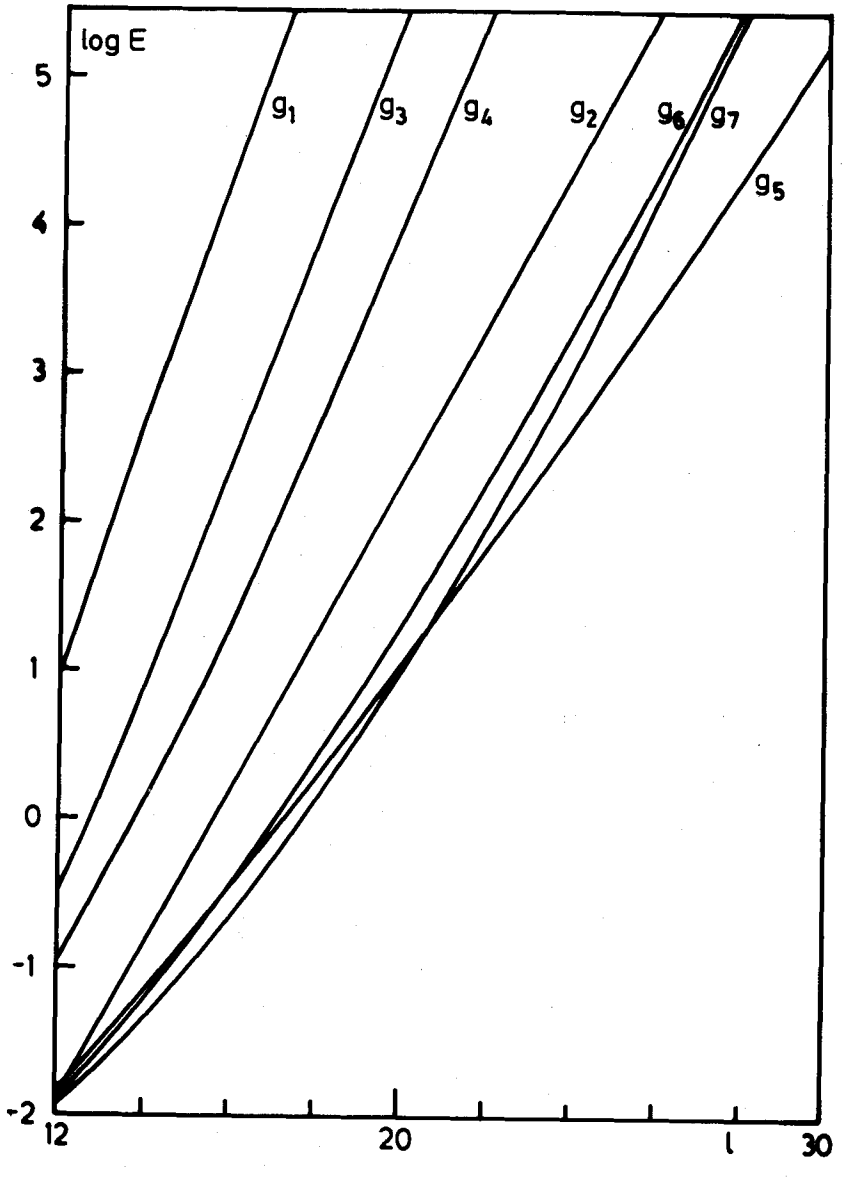

Figure 4. The dependence of $\log_{10}E$ (cf. equation 4.2) on ℓ, for the first seven g modes in Model C.

Table 3.

Mode	σ^2	$\frac{\lvert\xi_r\rvert_{max}}{\lvert\xi_r\rvert_s}$	x_{max}	E
g_1	19.36	4.5×10^{7}	0.10	1.3×10^{13}
g_2	17.79	1.7×10^{6}	0.08	2.2×10^{10}
g_3	16.77	8.8×10^{4}	0.08	8.4×10^{7}
g_4	16.32	1.8×10^{4}	0.08	7.8×10^{6}
g_5	15.61	3.9×10^{4}	0.07	1.1×10^{7}
g_6	14.84	2.3×10^{4}	0.07	4.5×10^{6}
g_7	14.10	2.2×10^{4}	0.06	3.2×10^{6}
g_8	13.36	1.8×10^{4}	0.06	2.0×10^{6}
g_{22}	6.41	2.8×10^{3}	0.04	1.4×10^{4}

Modes with $\ell = 20$, in Model A. The symbols have the same meaning as in Table 2.

$\sigma^2_{obs,1}$ = 6.4, Table 3 shows this mode to be severely trapped in standard solar models, although the degree of trapping is an order of magnitude less than for the 45 minute mode. The situation is quite different in Model C as can be seen from Figure 5. As expected, a number of possible identifications exist here with modes having relatively small energies. Indeed, for frequencies below N_{m_1}, there are many modes with comparable energies.

It is of some interest to consider the variation of σ^2 and log E with ℓ, in the light of the qualitative discussion at the beginning of this section. To facilitate this, circles have been put on the curves in Figure 5 to indicate the values of ℓ where the frequency of the corresponding mode crosses N_{m_1}. When σ^2 is significantly smaller than $N^2_{m_1}$, all modes evidently belong to the same class, with σ^2 increasing at about the same rate and with a rather slowly varying E. For $\sigma^2 > N^2_{m_1}$, however, one clearly distinguishes in Figure 2 the local $g_1^{(1)}$ mode for which σ^2 increases more slowly with ℓ than the remaining modes which are trapped in the interior. The global classification of the $g_1^{(1)}$ mode is changed progressively from $g_{17}(\ell = 23)$ to $g_{21}(\ell = 40)$ in a sequence of avoided crossings between this mode and the interior g modes. This is also evident from Figure 5. Here the bottom envelope of the curves corresponds to the energy of the $g_1^{(1)}$ mode, indicated by a dashed line, and increases slowly with ℓ. In contrast, the energy of the modes trapped in the interior grows very rapidly with ℓ. This is caused by the rapid increase in the width of the evanescent region below M_1 as σ^2 increases above $N^2_{m_1}$; see equation (2.6) and Figure 1. At the points of avoided crossing of the frequencies, where in Figure 5 the log E curves cross, there is an exchange of physical nature between the two modes involved.

Figure 6 shows $\xi_r(x)$ for a few of the modes included in Figure 5. At ℓ = 20 the behavior of ξ_r is qualitatively very similar for the three modes shown, since these modes all have frequencies below N_{m_1}. At ℓ = 30, on the other hand, there is a clear distinction among the modes between interior g modes and modes associated with M_1; this value of ℓ is close to the avoided crossing between g_{18} and g_{19}. The latter mode has the character of the $g_1^{(1)}$ mode, whereas g_{18} is a mixture between this and the interior g modes. The g_{17} and g_{20} modes belong predominantly to the interior.

5. A SEQUENCE OF ENVELOPE MODELS

The preceding section demonstrated the difficulty of explaining the 45 minute mode in terms of the contaminated model considered there. No plausible (in the sense of having a reasonably small pulsational energy) identification of this mode was found for values of ℓ above 20. While it was argued that the structure of the interior of the model could possibly be modified sufficiently to accommodate the 45 minute mode as one trapped in the peak in N^2 designated M_2 on Figure 1, it is clearly more attractive to look for a model where the mode could be trapped in a peak

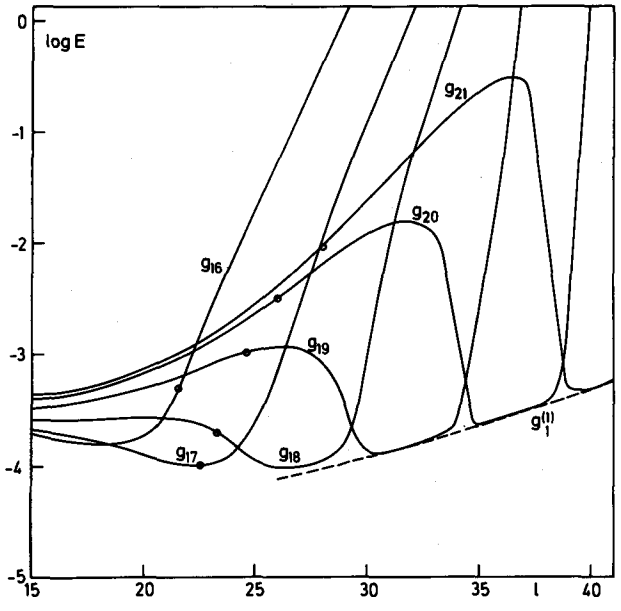

Figure 5. The dependence of $\log_{10}E$ on ℓ, for modes in the neighborhood of $\sigma^2_{obs,1}$ = 6.4, in Model C. The circles indicate the values of ℓ where the frequencies cross the local minimum N_{m_1} in N. The dashed line shows the energy of the local $g_1^{(1)}$ mode, computed in an envelope model extending down to x = 0.68.

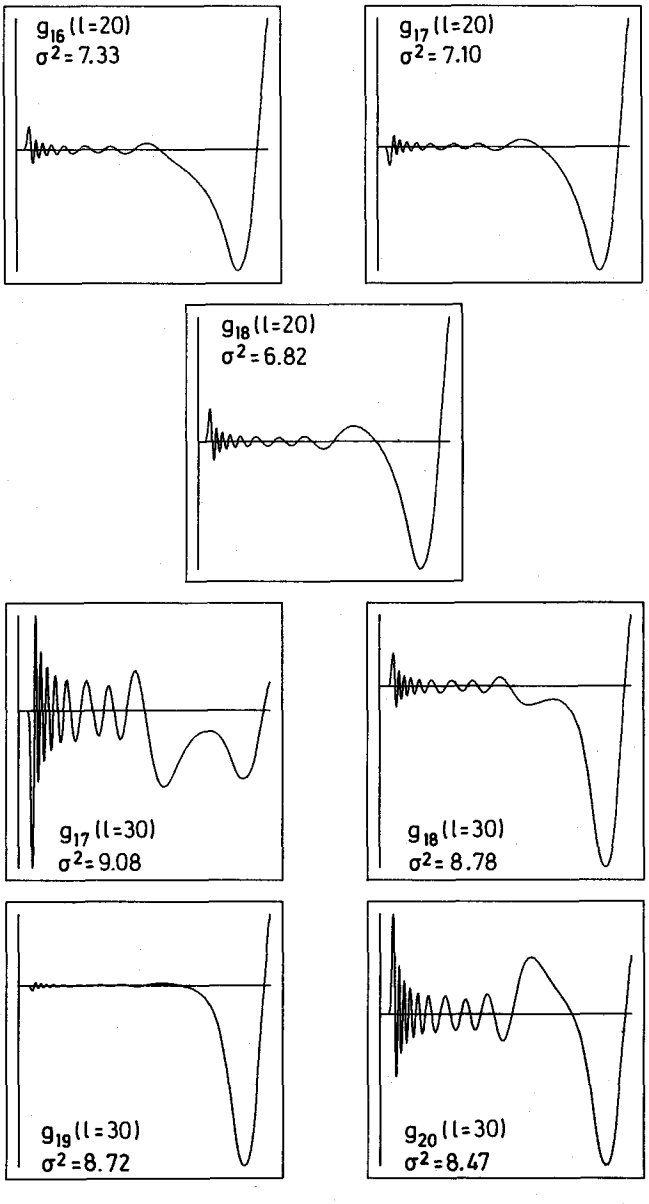

Figure 6. $\xi_r(x)$ for selected modes in Model C; see caption to Figure 3.

corresponding to M_1, close to the bottom of the convection zone. This would require the maximum value $N^2_{M_1}$ of N^2 in this peak to be above 13.8.

In an attempt to investigate this we have computed a sequence of chemically homogeneous solar envelope models, varying the ratio α of mixing length to pressure scale height and hence the depth of the convection zone. In Figure 7 the fully drawn curves show the behavior of N^2 in these models, each curve being labeled with the corresponding value of α. For comparison the dashed curve shows N^2 in Model C, discussed in §§ 3 and 4; as usual the dot-dashed horizontal lines indicate the observed modes.

Clearly the main effect of increasing α is to truncate at progressively greater depth the otherwise rapid increase of N^2 towards the surface. But there is also a general change in the behavior of N^2 beneath the convection zone, due to changes in the structure of the model. For $\alpha > 0.6$, N^2 no longer has a significant local maximum in the region considered.

When $\alpha \leq 0.6$ we can adopt the notation of § 4, by designating the peak in N^2 as M_1. With this is then associated a spectrum of local $g^{(1)}$ modes with frequencies above the minimum N_{m_1} of N beneath the peak, and tending towards the maximum N_{M_1} as ℓ tends to infinity. These modes can be calculated with considerable accuracy in the envelope models by applying a condition at the inner boundary which isolates the solution growing exponentially towards the surface; clearly the inner boundary must be in the evanescent region (see e.g. Dziembowski 1977). However, it should be noticed that $\sigma^2 = 6.4$ is below or close to $N^2_{m_1}$ in all the envelopes. Thus the 66 minute mode cannot be discussed on the basis of the envelope models alone. Like Model C, complete models based on these envelopes would predict a rich spectrum at long periods.

Using the technique sketched above we have computed the $g_1^{(1)}$ and $g_2^{(1)}$ modes in the envelopes with $\alpha = 0.001$, 0.4, 0.45 and 0.5, for values of ℓ up to 100; the results are presented in Figures 8 and 9, the curves being labeled by the value of α and the classification. The observed value of $\sigma^2 = 13.8$ is shown in both figures as a dot-dashed line. For $\alpha = 0.001$ and 0.4 it is possible to find a mode with $\sigma^2 = 13.8$, but only for values of ℓ close to or considerably in excess of 100, whereas when $\alpha \geq 0.45$ the maximum of N^2, and hence the squared frequencies of the $g^{(1)}$ modes, are below 13.8.

On the other hand the envelope models considered here are probably not realistic outer regions of complete solar models. Any solar model with a very thin outer convection zone must presumably have abnormally low opacities in the interior (otherwise the nuclear energy generation rate would not balance the observed luminosity). Excluding the possibility of gross errors in the opacity tables this would then imply a model with a structure similar to that of Model C. It is obviously impossible to predict the detailed behavior of N^2 below the convection zone

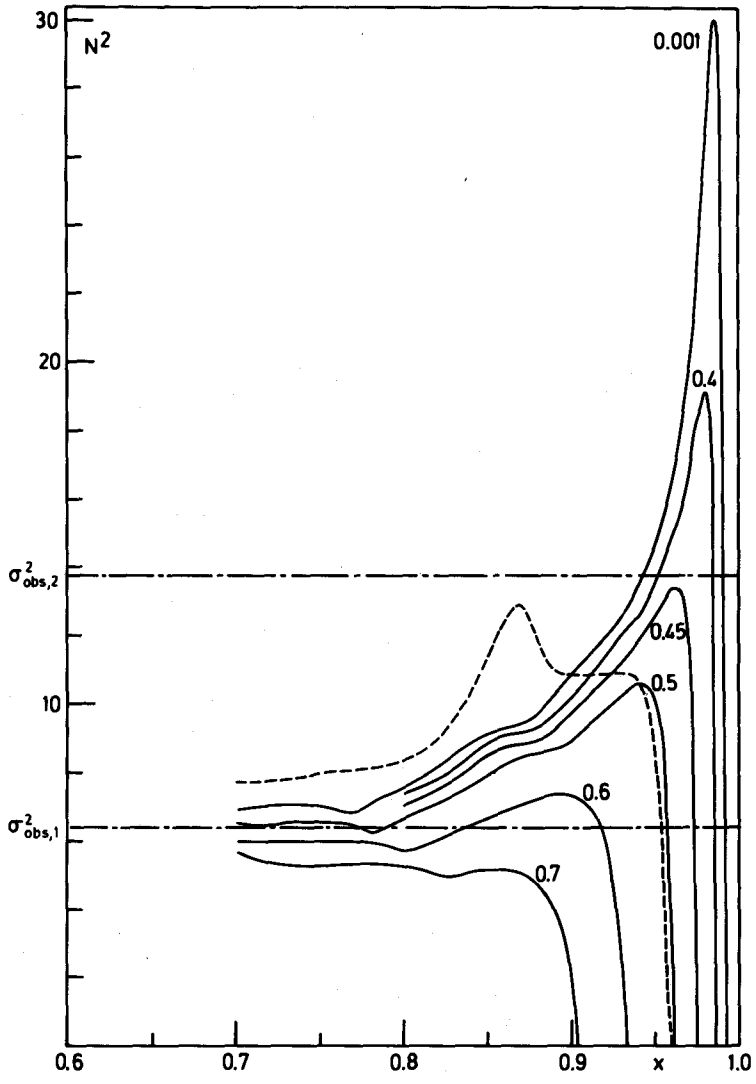

Figure 7. The squared buoyancy frequency N^2 in a sequence of envelope models (fully drawn lines) and in Model C (dashed line). The fully drawn curves are labelled with the ratio between the mixing length and the pressure scale height. $\sigma^2_{obs,1}$ and $\sigma^2_{obs,2}$ indicate the observed modes.

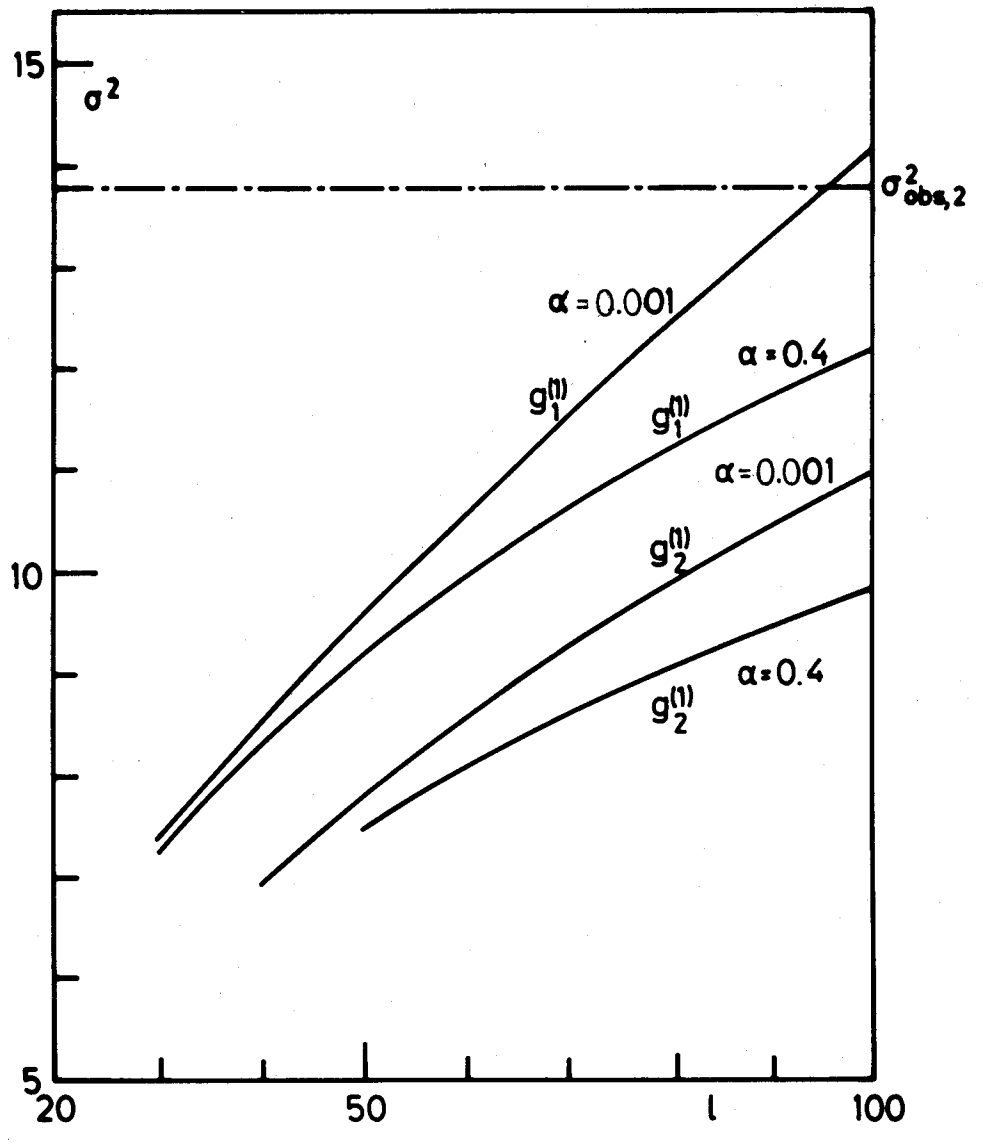

Figure 8. Squared dimensionless frequencies, against ℓ, for the local $g_1^{(1)}$ and $g_2^{(2)}$ modes in the envelopes with $\alpha = 0.001$ and 0.4. The curves are labelled with the value of α and the name of the mode. $\sigma^2_{obs,2}$ indicate the observed 45 minute mode.

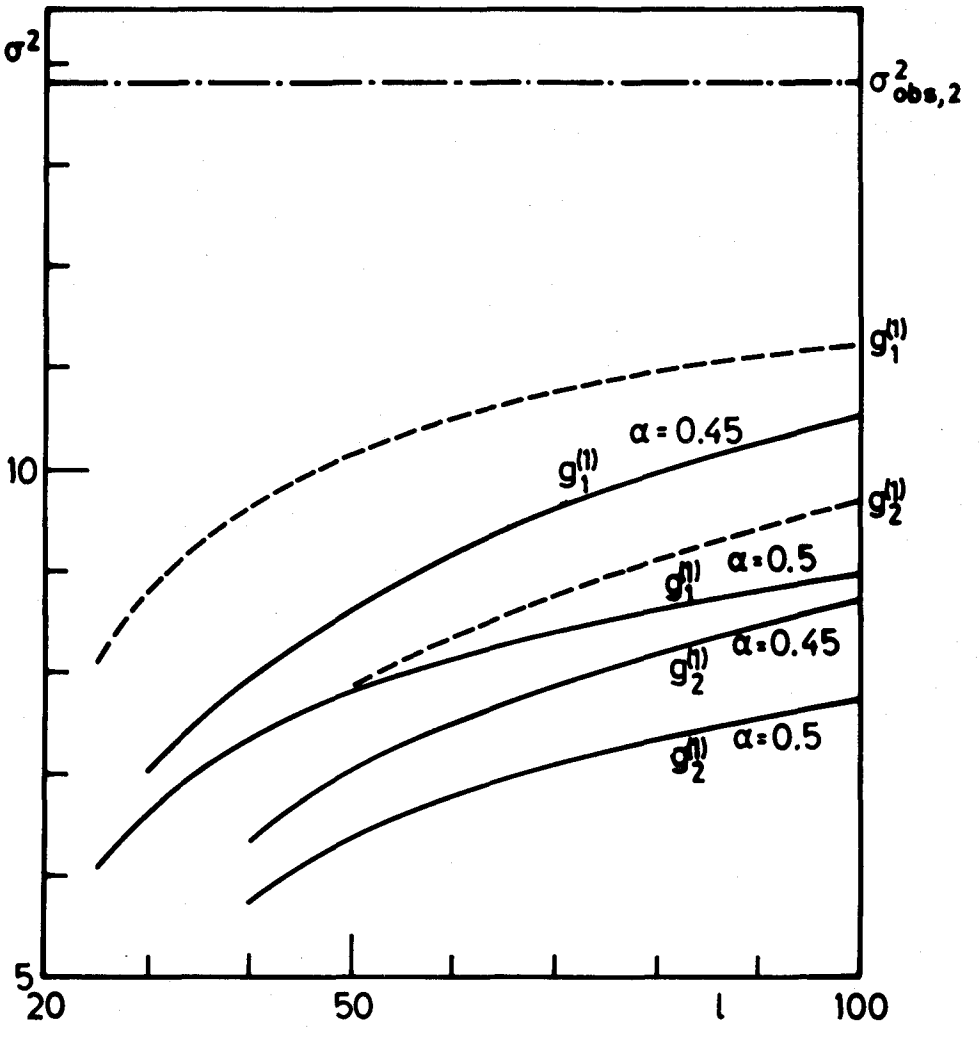

Figure 9. Squared dimensionless frequencies, against ℓ, for the local g_1 and g_2 modes in the envelopes with α = 0.45 and 0.5 (fully drawn lines) and in Model C (dashed line). All curves are labelled with the name of the mode and the fully drawn curves in addition with the value of α. The observed 45 minute mode is indicated by $\sigma^2_{obs,2}$.

in such a model without an evolution calculation for the whole model, but some indication of the effect of low Z in the interior can be seen by comparing Model C with the envelope computed with $\alpha = 0.5$, whose convection zone has approximately the same depth. As seen from Figure 7 there is a general increase in N^2, caused by the decrease in the opacity and the corresponding increase in $\nabla_{ad} - \nabla$; consequently the maximum in N^2 is both higher and considerably wider. The effect on the frequencies can be seen on Figure 9, where the dashed curves show σ^2 in Model C. These frequencies are considerably greater than those of the homogeneous envelope with the same depth of convection zone, and for given ℓ, σ^2 is also significantly larger than the value for the envelope with $\alpha = 0.45$ (where the maximum value of N^2 is about the same as in Model C); this is due to the increased width of the trapping region.

Thus it appears possible that a solar model with a sufficiently shallow convection zone may have a $g^{(1)}$ mode with $\sigma^2 = 13.8$, particularly if the interior of the model is very deficient in heavy elements. But it should be noticed that the $g_2^{(1)}$ mode would almost certainly have a fairly high σ^2, thus raising the problem of why this mode is not observed.

6. DISCUSSION AND CONCLUSION

Hill and Caudell (1979) concluded that two of the observed solar modes of oscillation, with periods of 45 and 66 minutes, had values of ℓ in excess of 20. This interpretation of the observations almost certainly cannot be reconciled with standard models of solar structure, which predict an unacceptably large ratio between the maximum and surface displacement for modes corresponding to the observed periods. The main reason for this is the relatively deep outer convection zones of such models. We have thus been led to study solar models whose convection zones are shallow.

The present work has analyzed the oscillations of one such model of the whole sun, originally computed by Christensen-Dalsgaard, Gough and Morgan (1979) in an attempt to produce a model with a low neutrino flux; a sequence of envelope models was also examined. In no case was there difficulty in reproducing the 66 minute mode; indeed all the models considered have a large number of modes with periods larger than about 60 minutes and with relatively small pulsational energies.

The 45 minute mode could not be identified in the complete solar model studied in § 4. However, it appeared likely that a similar model could be made to trap such a mode at the principal maximum of N^2 for reasonably small values of ℓ, after only a relatively modest modification to its structure. The maximum relative displacement would still be rather large, of the order of a few hundred times the surface displacement, but not so large as to rule out such an identification a priori. Alternatively, as was shown in § 5, this mode could be trapped close to the surface of a chemically homogeneous envelope, but only for values of ℓ above 100 and

only if the depth of the convection zone were less than 1 percent of the solar radius. Taking into account the fact that a complete model with a very thin convection zone probably has a highly Z-deficient interior, the depth of the convection zone in a model reproducing the observed mode can perhaps be increased to 0.02 - 0.03 r_s, but the required values of ℓ are probably still close to 100. The sensitivity of the observational technique to oscillations with such high ℓ is relatively low, however (cf. Hill 1978; Hill and Caudell 1979), and it is not clear that they would be detectable.

We have so far tried only to match the observed periods and ignored the question of the excitation of the modes. It appears rather unlikely that the modes considered here are self-excited. This is certainly true if the modes are trapped in the deep interior of the model, as considered above for the 45 minute mode; in this case the radiative damping is very strong, due to the short horizontal wavelength of the mode. If the modes are trapped near the base of a very thin convection zone there remains a slight possibility that they may be destabilized by the κ - mechanism operating in the hydrogen ionization zone, though convective damping is likely to dominate (cf. Berthomieu et al. 1980). In any case this possibility is unlikely to be realized for the 66 minute mode, which has comparable amplitudes throughout the entire model and is therefore presumably quite heavily damped in the radiative interior. The issue deserves further study, even though this would be beset by the inevitable problems encountered in treating the convective fluxes.

If the linear modes are not self-excited, they must be driven by some nonlinear mechanism. Gravity modes trapped close to the base of a thin convection zone might be excited stochastically by the turbulence. Their amplitudes are relatively large throughout the entire convection zone, and can therefore be reasonably expected to interact with convective motions having turnover times comparable with their periods. However, it would be hard to explain why only modes with periods close to 45 and 66 minutes are excited. To be sure, there may be several modes contributing to Hill and Caudell's data, especially near or above the 66 minute period where many low frequency modes may be present, but it is apparent that the range of frequencies of 'possible' modes is greater than that observed.

A more promising possibility in this respect, perhaps, is resonant excitation by the five minute oscillations, arising principally from three-mode interactions. For modes trapped close to the surface this kind of excitation appears to be energetically possible, and might explain why only selected modes are observed. But it does not seem plausible for modes trapped beneath the prinicipal maximum of N^2 because of the large energy of such modes, unless phase is maintained with the exciting modes for very long periods of time. In this connection it is of some interest that Severny, Kotov and Tsap (1978) point out that the structure of the 160 minute solar oscillation changes on a time scale of a year, pointing strongly to

nonlinear effects: the linear time scale for the growth or decay of a low degree g mode with such a period is probably in excess of 100 years.

Quite apart from the obvious difficulties in explaining the observed modes, the models considered here face other problems. From the contributions of Berthomieu et al. (1980) and Lubow, Rhodes and Ulrich (1980) to these proceedings it is clear that the thin convection zones of those models would ruin the impressive agreement between theory and observation for the five minute oscillations (see also Gough 1977; Ulrich and Rhodes 1977); however, Rosenwald and Hill (1980) suggest that the resulting discrepancy might be removed by a modification of the outer boundary conditions possibly due to nonlinear effects. Furthermore, it might be pointed out that the discovery by Claverie et al. (1980) of discrete frequencies in the whole-disk Doppler data close to a period of five minutes seems to favor models with convection zones that are somewhat thinner than in a standard model, although perhaps not as shallow as in the models considered here (cf. Christensen-Dalsgaard and Gough 1980). An objection which is unrelated to solar oscillations comes from the fact that the proposed models need convection zones rich in heavy elements overlying interiors with very low Z. Such a configuration is liable to be destroyed by the fingering instability (e.g. Turner 1973), which is known to occur in similar oceanographic and laboratory circumstances. This would cause mixing of heavy elements into the interior of the model, thus modifying its structure and increasing the amount of interstellar material which must be accreted to account for the observed surface Z. Accepting a model with a thin convection zone also aggravates the problem of explaining the photospheric lithium abundance. Finally, the calibration of the model discussed in §§ 3 and 4 requires a helium abundance Y = 0.16, which is somewhat below estimates of the cosmic abundance (Danziger 1970), and below the abundances fashionable in current cosmological theories.

It is obvious from the discussion above that interpreting the observations as having resulted from g modes with large ℓ gives rise to serious theoretical problems. It is not easy to find models that exhibit the observed modes. Furthermore the models proposed here may contain internal inconsistencies, and they depart considerably from those computed with the standard theories of stellar evolution, implying perhaps a need for revision of this theory. Although such theoretical difficulties cannot by themselves falsify the interpretation by Hill and Caudell (1979), they would seem to indicate that a close look for possible alternative explanations is needed, as well as much more extensive observational material. On the theoretical side there is an evident need to understand the excitation of the proposed modes; it may also be of some interest to synthesize theoretical power spectra at different scan amplitudes on the basis of a given solar model and some reasonable hypothesis regarding the excitation mechanism, to try to understand why only two modes (or groups of modes) at large ℓ appear to be observed. There is a

similar need to understand the isolated 160 minute oscillation discovered by Severny, Kotov and Tsap (1976) and Brookes, Isaak and van der Raay (1976).

If the observations of g modes with large ℓ are confirmed, they would be highly valuable as a probe of the solar interior. Indeed, the discussion in § 3 of the behavior of the buoyancy frequency shows this to be very sensitive to details of the structure of the sun's radiative interior. Section 2 then shows the same to be the case for the spectrum of g modes. On the other hand, p modes depend predominantly on only the outer layers. Therefore g modes can provide data that is superior to those from the p modes for diagnosing the deep interior of the sun.

* * * * *

We thank T.P. Caudell, H.A. Hill, J. Knapp, J.D. Logan and R.D. Rosenwald for useful and interesting discussions on this subject, and Y. Osaki for checking some of the early computations. Part of this work was done at the Department of Physics and Atmospheric Science, University of Arizona; we are very grateful to H.A. Hill and R.H. Parmenter for their hospitality. J.C.-D. thanks P. Ledoux for the hospitality of the Institut d'Astrophysique, Universite de Liege, and D.O.G. thanks J.-P. Zahn for the hospitality of the Observatoire de Nice.

REFERENCES

Aizenman, M., Smeyers, P. and Weigert, A. 1977, Astron. Astrophys., 58, 41.

Berthomieu, G., Cooper, A.J., Gough, D.O., Osaki, Y. and Rocca, A. 1980, these proceedings.

Brookes, J.R., Isaak, G.R. and van der Raay, H.B. 1976, Nature, 259, 92.

Brown, T.M., Stebbins, R.T. and Hill, H.A. 1978, Astrophys. J., 223, 324.

Christensen-Dalsgaard, J. 1979, Mon. Not. R. Astr. Soc., in press.

Christensen-Dalsgaard, J. and Gough, D.O. 1976, Nature, 259, 89.

Christensen-Dalsgaard, J. and Gough, D.O. 1980, these proceedings.

Christensen-Dalsgaard, J., Gough, D.O. and Morgan, J.G. 1979, Astron. Astrophys., 73, 121.

Claverie, A., Isaak, G.R. McLeod, C.P., van der Raay, H.B. and Roca-Cortes, T. 1980, these proceedings.

Cowling, T.G. 1941, Mon. Not. R. Astr. Soc., 101, 367.

Cox, A.N. and Stewart, J.N. 1970, Astrophys. J. Suppl., 19, 243.

Danziger, I.J. 1970, Ann. Rev. Astron. Astrophys., 8, 161.

Davis, R., Jr. 1978, Proc. informal conference on status and future of solar neutrino research (ed. G. Friedlander; US Technical Information Service BNL 50879, Springfield, VA), p. 1.

Dziembowski, W. 1977, Acta. Astron., 27, 95.

Dziembowski, W. and Pamjatnykh, A.A. 1978, Pleins feux sur la physique solaire (ed. J. Rösch, CNRS, Paris), p. 135.

Eckart, C. 1960, Hydrodynamics of oceans and atmospheres, (London and New York: Pergamon Press).

Eggleton, P.P. 1972, Mon. Not. R. Astr. Soc., 156, 361.

Fowler, W.A., Caughlan, G.R. and Zimmerman, B.A. 1975, Ann. Rev. Astron. Astrophys., 13, 69.

Gabriel, M. 1980, these proceedings.

Gabriel, M. and Noels, A. 1976, Astron. Astrophys., 53, 149.

Gough, D.O. 1977, Proc. IAU Colloq. No. 36 (ed. R.M. Bonnet and Ph. Delache, G. de Bussac, Clermont-Ferrand), p. 3.

Gough, D.O. 1978, Pleins feux sur la physique solaire (ed. J. Rösch, CNRS, Paris), p. 81.

Hill, H.A. 1978, The new solar physics (ed. J.A. Eddy; Boulder: Westview), Ch. 5.

Hill, H.A., 1980, these proceedings.

Hill, H.A. and Caudell, T.P. 1979, Mon. Not. R. Astr. Soc., 186, 327.

Hill, H.A., Stebbins, R.T. and Brown, T.M. 1976, Proc. V Intern. Conf. Atomic Masses and Fundamental Constants, (ed. J.H. Sanders and A.H. Wapstra; New York: Plenum), p. 622.

Iben, I., Jr., Mahaffy, J. 1976, Astrophys. J. Lett., 209, L39.

Joss, P.C. 1974, Astrophys. J., 191, 771.

Lubow, S., Rhodes, E. and Ulrich, R. 1980, these proceedings.

Osaki, Y. 1975, Publ. Astron. Soc. Japan, 27, 237.

Rosenwald, R.D. and Hill, H.A. 1980, these proceedings.

Scuflaire, R. 1974, Astron. Astrophys., 36, 101.

Scuflaire, R., Gabriel, M., Noels, A. and Boury, A. 1975, Astron. Astrophys., 45, 15.

Severny, A.B., Kotov, V.A. and Tsap, T.T. 1976, Nature, 259, 87.

Severny, A.B., Kotov, V.A. and Tsap, T.T. 1978, Pleins feux sur la physique solaire (ed. J. Rösch, CNRS, Paris), p. 123.

Shibahashi, H. and Osaki, Y. 1976, Publ. Astron. Soc. Japan, 28, 199.

Turner, J.S. 1973, Buoyancy effects in fluids (Cambridge: Cambridge University Press).

Ulrich, R.K. and Rhodes, E.J., Jr. 1977, Astrophys. J., 218, 521.

Vandakurov, Yu. V. 1967, Astron. Zh., 44, 786.

von Neumann, J. and Wigner, E. 1929, Physik. Zeitschr., 30, 467.

NONRADIAL OSCILLATIONS OF SOLAR MODELS WITH AN INITIAL DISCONTINUITY IN HYDROGEN ABUNDANCE

A. Boury, R. Scuflaire, A. Noels, and M. Gabriel
Institut d'Astrophysique
Universite de Liege, Belgium

ABSTRACT

Solar models are calculated with low central hydrogen abundance. The stability of these models is investigated. The eigenspectrum is computed and compared with the SCLERA observations of solar oscillation.

1. INTRODUCTION

In an attempt to solve the solar neutrino problem, Faulkner, Da Costa and Prentice (1975) followed a suggestion of Prentice (1973) and constructed models of the sun in which the initial hydrogen content in a small central region was much smaller than that in the rest of the star. Although the models which give the observed solar luminosity at the present solar age yield neutrino fluxes that are too large, they are interesting because they exhibit oscillatory modes connected with the discontinuity in density that is associated with the discontinuity in chemical composition. Moreover, the possible observations of the oscillation spectrum of the sun by the SCLERA group (Brown, Stebbins and Hill 1976, 1978) could permit comparison between various solar models (Scuflaire et al. 1976; Christensen-Dalsgaard and Gough 1976; Hill and Caudell 1979).

2. MODELS AND OSCILLATION PERIODS

Following Faulkner, Da Costa and Prentice (1975), an evolutionary sequence was computed by the Henyey method of a 1 $M_\odot$ star of heavy element abundance $Z = 0.02$ and of initial hydrogen abundance $X = X_c = 0.1$ in the region $m(r)/M_\odot \leq 0.03$ and $X = X_s$ elsewhere. The value of X_s necessary to fit the luminosity at evolutionary age 4.7×10^9 years to the present solar luminosity was found to be 0.7813. The evolutionary sequence was constructed with a ratio of mixing length ℓ/H to the pressure scale height equal to 1.5; this ratio had to be adjusted to 2.15 in order to match the present value of the solar radius to within less than 1 percent. A second sequence with $X_c = 0$ for $m(r)/M_\odot \leq 0.03$ and $X_s = 0.794$ elsewhere was also calculated. The behavior of the models of this second sequence being qualitatively the same as that of the models with $X_c = 0.1$, no precise adjustments of X_s and ℓ/H were made to

achieve a precise fit with the present sun.

The properties of the models tested for vibrational instability are listed in Table 2 where x_D, X_{Di} and X_{DO} respectively represent the non-dimensional distance of the discontinuity to the center of the star and the hydrogen abundance on the inner and outer sides of the discontinuity. Models 1, 2, 3, 7, and 8 correspond to the approach to the main sequence; Model 6 corresponds to the present sun.

The integration of the fourth order differential system of nonradial adiabatic oscillations was then performed following the scheme given in Boury et al. (1975). The fourth column of Table 2 gives the periods of the modes g_1 through g_5 for the horizontal wavenumber $\ell = 1$. In the fourth column of Table 3, we list for $\ell = 1$ to 10 the periods of the modes associated with the discontinuity in density. These modes have a very large amplitude in a narrow layer centered on the discontinuity. With respect to solar seismology, Table 4 provides a list of periods of Model 6 corresponding to the present sun; this allows for a comparison with the SCLERA periods. It is immediately seen that the predicted spectrum is much more compact than the observed spectrum. This compactness comes from the high central condensation of the star due to the very low central abundance of hydrogen. In the present state of observations, models with the assumed distribution of hydrogen do not pass the test of solar seismology.

3. VIBRATIONAL STABILITY

The damping coefficient $\sigma'_{k,\ell}$ relative to the k mode associated with the ℓth harmonic is written, as usual, in the following form (Boury et al. 1975):

$$\sigma'_{k,\ell} = - \frac{1}{2} \left[\frac{\int_0^{Ma} \left(\frac{\delta T}{T}\right)_{k,\ell} \delta\varepsilon \, dm - \int_0^{Ma} \left(\frac{\delta T}{T}\right)_{k,\ell} \delta\left(\frac{1}{\rho} \operatorname{div} \vec{F}\right) dm + \int_0^{Ma} \left(\Gamma_3 - \frac{5}{3}\right) \frac{\delta\rho}{\rho} \delta \left(\varepsilon_2 + \frac{1}{\rho} \underset{\sim}{V} \cdot \underset{\sim}{\nabla} p\right) dm}{\sigma^2 \int_0^M |\underset{\sim}{\delta r}|^2 \, dm} \right]_{k,\ell}$$

$$= - \left[\frac{E_N - E_F + E_2}{2\sigma^2 \int_0^M |\underset{\sim}{\delta r}|^2 \, dm} \right]_{k,\ell} \qquad (1)$$

where all the terms are expressed in terms of the adiabatic solution. The third integral in equation (1) expresses the influence of the mechanical effects of convection. $\vec{V}$ is the mean velocity of turbulence and ε_2 stands for the rate per unit mass of dissipation of turbulent kinetic energy into heat (Ledoux and Walraven 1958; Gabriel et al. 1975). All other symbols have their usual meaning. Table 2 gives the

Table 1. Properties of the Models

a) Sequence $X_c = 0.1$, $X_s = 0.7813$

Model Number	ℓ/H	Age (years)	x_D	X_{Di}	X_{Do}	T_c	ρ_c	L	$\rho_c/\bar{\rho}$
1	1.5	4.44(7)	0.06150	0.09987	0.7796	1.392(7)	290.8	2.637(33)	168.3
2	1.5	4.98(7)	0.06508	0.09983	0.7791	1.374(7)	295.9	2.612(33)	170.4
3	1.5	5.75(7)	0.06514	0.09978	0.7785	1.358(7)	302.3	2.622(33)	175.4
4	1.5	8.68(8)	0.05720	0.09640	0.7182	1.343(7)	346.3	2.840(33)	220.3
5	1.5	4.70(9)	0.04652	0.07604	0.4190	1.509(7)	471.9	3.750(33)	419.1
6	2.15	4.70(9)	0.04977	0.07582	0.4168	1.513(7)	472.5	3.809(33)	342.1
			b) Sequence $X_c = 0$, $X_s = 0.794$						
7	1.5	4.83(7)	0.05736	-	0.7919	1.275(7)	507.4	2.546(33)	302.2
8	1.5	5.63(7)	0.06268	-	0.7911	1.275(7)	506.2	2.526(33)	300.3
9	1.5	9.03(8)	0.05152	-	0.7234	1.282(7)	543.3	2.703(33)	351.6
10	1.5	2.50(9)	0.04809	-	0.5951	1.334(7)	589.2	2.994(33)	429.0

Table 2. Periods of Adiabatic Oscillation and Vibrational Stability Results:

g-modes of $\ell = 1$

Mode	Model	ω^2	P(s)	E_N	E_F	E_{ε_2}	σ'^{-1} years*
		a) Sequence $X_c = 0.1$, $X_s = 0.7813$					
g_1	1	7.8780	3.222(3)	6.621(33)	2.005(37)	6.702(36)	3.617(5)
	2	7.8665	3.217(3)	7.055(33)	1.845(37)	6.676(36)	1.728(5)
	3	7.8640	3.230(3)	7.551(33)	1.839(37)	6.132(36)	1.655(5)
	4	7.9046	3.360(3)	1.425(34)	2.267(37)	7.793(36)	1.627(5)
	5	12.696	3.144(3)	5.622(35)	4.512(36)	9.943(35)	9.657(5)
	6	10.425	3.133(3)	5.143(35)	3.720(36)	7.724(35)	1.031(6)
g_2	1	3.2561	5.012(3)	4.805(35)	1.260(36)	1.414(31)	1.080(6)
	2	3.5710	4.774(3)	4.082(35)	1.222(36)	1.278(31)	1.139(6)
	3	3.9404	4.562(3)	3.436(35)	1.204(36)	1.412(31)	1.185(6)
	4	5.8776	3.912(3)	1.818(35)	1.246(36)	5.114(32)	1.289(6)
	5	10.754	3.416(3)	5.943(35)	6.990(36)	2.263(36)	4.350(5)
	6	8.9907	3.374(3)	4.383(35)	8.810(36)	2.953(36)	3.979(5)
g_3	1	2.1934	6.107(3)	2.070(35)	2.123(35)	1.497(33)	1.129(9)
	2	2.2158	6.061(3)	2.243(35)	2.205(35)	4.203(33)	-6.698(7)
	3	2.2795	5.998(3)	2.466(35)	2.311(35)	3.963(33)	-3.576(7)
	4	3.3686	5.167(3)	4.163(35)	3.769(35)	8.044(33)	-1.719(7)
	5	7.9828	3.965(3)	4.918(34)	3.789(37)	1.202(37)	6.913(4)
	6	7.5896	3.672(3)	1.267(35)	1.708(37)	6.405(36)	1.726(5)
g_4	1	1.3049	7.917(3)	2.148(35)	2.775(35)	1.497(33)	5.712(6)
	2	1.3302	7.823(3)	2.022(35)	2.912(35)	1.523(33)	4.067(6)
	3	1.3971	7.662(3)	1.563(35)	8.474(35)	5.851(32)	5.277(5)
	4	2.0993	6.545(3)	7.504(34)	1.308(36)	1.104(32)	4.267(5)
	5	5.0533	4.984(3)	3.404(35)	1.077(36)	9.896(34)	1.791(6)
	6	4.1532	4.964(3)	3.044(35)	7.788(35)	3.196(34)	2.274(6)
g_5	1	1.1075	8.594(3)	1.913(35)	1.175(36)	1.008(31)	2.912(5)
	2	1.2376	8.110(3)	1.553(35)	1.154(36)	4.795(31)	3.214(6)
	3	1.3607	7.764(3)	1.674(35)	5.898(35)	9.837(32)	8.492(5)
	4	1.9029	6.875(3)	1.419(35)	2.713(35)	3.585(33)	3.791(6)
	5	4.4616	5.3040(3)	1.615(35)	2.424(36)	4.345(33)	4.431(5)
	6	3.6414	5.301(3)	1.424(35)	2.147(36)	1.499(33)	4.363(5)

* A negative signs means instability.

Table 2. Cont.

Mode	Model	ω^2	P(s)	E_N	E_F	E_{ε_2}	σ'^{-1} years*
			b) Sequence $X_c = 0$, $X_s = 0.794$				
g_1	7	12.016	2.645(3)	8.246(33)	1.420(33)	1.120(33)	2.179(6)
	8	11.501	2.700(3)	9.665(33)	1.587(37)	6.319(32)	1.876(6)
	9	13.506	2.602(3)	1.229(34)	1.850(36)	4.443(33)	1.840(6)
	10	16.174	2.522(3)	2.259(34)	2.024(36)	7.014(34)	2.009(5)
g_2	7	7.8233	3.280(3)	9.341(33)	1.125(37)	6.111(36)	3.772(5)
	8	7.8062	3.278(3)	1.022(34)	1.739(37)	5.568(36)	1.690(5)
	9	7.8625	3.411(3)	2.077(34)	1.775(37)	6.621(36)	3.131(5)
	10	8.1235	3.559(3)	1.738(35)	2.059(37)	6.793(36)	1.436(5)
g_3	7	4.6159	4.272(3)	2.205(33)	1.600(36)	2.180(31)	7.385(5)
	8	4.3704	4.380(3)	2.927(33)	1.652(36)	3.393(31)	6.805(5)
	9	5.1462	4.216(3)	1.169(34)	2.061(36)	6.063(32)	6.271(5)
	10	6.9676	3.843(3)	5.438(35)	3.287(36)	9.102(35)	9.375(5)
g_4	7	2.4960	5.808(3)	4.135(33)	4.497(35)	3.301(33)	2.040(7)
	8	3.0155	5.273(3)	5.231(35)	4.776(35)	2.856(33)	-1.617(7)
	9	4.3921	4.564(3)	5.694(35)	5.628(35)	1.355(34)	-4.828(7)
	10	6.1229	4.100(3)	1.723(34)	1.897(36)	4.739(33)	4.449(5)
g_5	7	2.3755	5.953(3)	2.503(33)	1.536(36)	2.708(33)	4.021(5)
	8	2.2827	6.063(3)	8.904(32)	1.813(36)	1.128(31)	3.232(5)
	9	2.6827	5.839(3)	8.637(32)	2.203(36)	2.045(31)	3.037(5)
	10	3.3025	5.582(3)	2.358(35)	6.273(35)	9.362(33)	4.030(5)

* A negative signs means instability.

Table 3. Periods of Adiabatic Oscillations and Vibrational Stability :

Discontinuity Modes

a) Model 1

1	Mode	ω^2	P(s)	E_N	E_F	$E_R^r(D)$	$E_{\epsilon 2}$	$\dot{\sigma}$-1 years
1	p_1	18.605	2.097(3)	6.094(34)	2.289(38)	8.775(34)	7.990(37)	4.901(4)
	p_2	21.825	1.936(3)	5.488(34)	3.998(38)	1.270(35)	1.462(38)	3.008(4)
2	p_4	69.615	1.084(3)	6.168(35)	9.731(37)	1.390(36)	3.886(37)	3.117(5)
3	p_5	113.65	8.483(2)	1.002(36)	1.788(38)	3.554(36)	7.882(37)	2.958(5)
4	p_6	156.63	7.227(2)	1.228(36)	7.506(37)	6.573(36)	2.386(37)	6.099(5)
5	p_7	198.64	6.417(2)	1.389(36)	8.889(37)	1.058(37)	1.830(37)	8.939(5)
6	p_7	240.26	5.835(2)	1.506(36)	1.726(37)	1.556(37)	5.971(35)	4.209(6)
7	p_8	282.13	5.384(2)	1.651(36)	2.006(37)	2.099(37)	1.187(34)	4.097(6)
8	p_9	323.45	5.029(2)	1.732(36)	2.949(37)	2.762(37)	4.970(35)	3.195(6)
9	p_9	364.68	4.736(2)	1.800(36)	3.431(37)	3.513(37)	1.800(31)	3.022(6)
10	p_{10}	405.86	4.489(2)	1.858(36)	4.427(37)	4.352(37)	1.435(35)	2.601(6)

b) Model 8

1	p_2	260.54	1.794(3)	1.013(35)	3.035(38)	2.280(33)	1.179(38)	3.150(4)
2	p_5	119.35	8.382(2)	6.820(35)	6.243(39)	3.190(35)	2.313(39)	7.852(3)
4	p_9	277.24	5.500(2)	1.714(36)	5.922(39)	3.121(36)	1.714(39)	1.781(4)
8	p_{13}	573.71	3.823(2)	2.729(36)	2.801(39)	1.774(37)	7.096(34)	6.342(6)

Table 4.

l=0	l=2	l=4	l=6	l=8	Observed
	70.7 (g_6)		71.1		
65.9	61.2 (g_5)	67.3 (g_{11}) 64.7 (g_{10}) 62.9 (g_9)	67.4 (g_{16}) 65.2 (g_{15}) 61.3 (g_{14})		66.25
	59.4 (g_4) 51.3 (g_3)	56.2 (g_8) 53.0 (g_7)	58.9 (g_{13}) 57.6 (g_{12}) 56.5 (g_{11}) 51.8 (g_{10}) 51.1 (g_9)	59.1 (g_{17}) 55.2 (g_{16}) 55.0 (g_{15}) 52.9 (g_{14}) 51.1 (g_{13})	
41.7	44.8 (g_2)	49.6 (g_6) 43.8 (g_5) 41.5 (g_4)	46.3 (g_8) 42.8 (g_7) 42.0 (g_6)	49.6 (g_{12}) 48.5 (g_{11}) 45.5 (g_{10}) 44.2 (g_9) 42.0 (g_8)	44.66
31.4	39.1 (g_1) 35.5 (f) 32.7 (p_1)	38.4 (g_3) 36.6 (g_2)	37.1 (g_5) 34.9 (g_4) 34.3 (g_3)D 31.3 (g_2)	38.0 (g_7) 37.6 (g_6) 33.1 (g_5) 31.4 (g_4) 31.3 (g_3)	39.00 32.1
24.7	25.4 (p_2) 20.8 (p_3)	29.9 (g_1) 28.1 (f) 27.9 (p_1) 22.3 (p_2)	26.5 (g_1) 25.3 (f) 24.7 (p_1) 20.3 (p_2)	28.3 (g_2) 24.7 (g_1) 23.3 (f) 23.2 (p_1)	28.7 24.8 21.0
17.4 15.0 13.3 12.0	17.6 (p_4) 16.3 (p_5)D 15.3 (p_6) 13.5 (p_7) 12.1 (p_8) 11.0 (p_9) 10.1 (p_{10})	18.5 (p_3) 15.9 (p_4) 14.0 (p_5) 12.8 (p_6) 11.4 (p_7)D 11.3 (p_8) 10.3 (p_9) 9.53(p_{10})	17.1 (p_3) 14.8 (p_4) 13.1 (p_5) 9.46(p_9)	18.8 (p_2) 16.0 (p_3) 13.9 (p_4) 12.4 (p_5) 11.1 (p_6) 10.2 (p_7) 9.40(p_8)	19.5 13.3 12.1 11.4 10.7 9.9

Periods (in minutes) of model 6 ("present sun") for radial (l=0) and non-radial (l=2,4,6,8) modes. The identification of the modes is given in parentheses. D indicates a discontinuity mode. Last column gives solar periods observed by Brown et al. (1978) in the range 10m-70m.

values of E_N, E_F, E_2, and the e-folding time $1/\sigma'$ for the low order g modes corresponding to $\ell = 1$. A negative sign for $1/\sigma'$ means instability and growth of the oscillation amplitude. For the models with $X_c = 0.1$, the g_3 mode becomes unstable in the approach to the main sequence in Model 2 close to the temporary minimum in the ratio ρ_c/ρ, due to the slight expansion of the central regions accompanying the onset of nuclear reactions. The instability subsists more than 10^9 years, until the central condensation has reincreased enough to produce a corresponding increase in amplitude in the envelope which is large enough to damp the oscillation. The "present sun" is stable. The differences in the results for Models 5 and 6 are due to the difference in radii of the two models, the large difference in their ratios of ℓ_c/ρ, and from the high sensitivity of the eigenvalues and eigenfunctions to ρ_c/ρ.

In the sequence $X_c = 0$, the instability appears in the g_4 mode. Let us recall here that in the standard solar evolution of models less condensed than the present ones, a phase of instability towards the g_2 and g_3 modes occurs (Boury et al. 1975). The modes associated with the discontinuity turn out to be very stable (Table 3). The destabilizing effect of the nuclear energy term is largely overcome by the large perturbation of the temperature gradient, which appears as the radial part $\frac{d\delta L}{dm}$ of the term $\delta(\frac{1}{\rho} \text{ div } \vec{F})$. The seventh column of Table 3 shows the contribution $E_R^r(D)$ of the discontinuity to the integral $\int \frac{\delta T}{T} d\delta L$. A steep change in density would have the same stabilizing effect as a strict discontinuity.

In conclusion, the evolution of the sun when starting with a small (or zero) hydrogen abundance in a small central region presents the same instability as the standard evolution towards low-order g nonradial modes for $\ell = 1$; however, the spectrum of the model corresponding to the present solar age is not compatible with the observations.

REFERENCES

Boury, A., Gabriel, M., Noels, A., Scuflaire, R. and Ledoux, P. 1975, Astron. Astrophys., 41, 279.

Brown, T.M., Stebbins, R.T. and Hill, H.A. 1976, in Proceedings of the Solar and Stellar Pulsation Conf., Los Alamos, N. Mex., ed. A.N. Cox and R.G. Deupree, Los Alamos Report No. LA-6544-C, 1.

Brown, T.M., Stebbins, R.T. and Hill, H.A. 1978, Ap. J., 223, 234.

Christensen-Dalsgaard, J. and Gough, D.O. 1976, Nature, 259, 89.

Faulkner, D.J., Da Costa, G.S., and Prentice, A.J.R. 1975, Mon. Not. R. Astr. Soc., 170, 589.

Gabriel, M., Scuflaire, R., Noels, A. and Boury, A., 1975, Astron. Astrophys., 40, 33.

Hill, H.A. and Caudell, T.P. 1979, Mon. Not. R. Astr. Soc., 186, 327.

Ledoux, P. and Walraven, T. 1958, Hdb. der Phys., 51, 353.

Prentice, A.J.R. 1973, Mon. Not. R. Astr. Soc., 163, 331.

Scuflaire, R., Gabriel, M., Noels, A. and Boury, A. 1976, Astron. Astrophys., 45, 15.

NONRADIAL OSCILLATIONS WITH HIGH ℓ-VALUES

C.A. Rouse
General Atomic Company
San Diego, California

ABSTRACT

A few eigenfunctions with high ℓ-values for nonradial oscillations of the 1968 nonstandard solar model (Rouse 1977, 1979 and references therein) are discussed. Particular attention is given to eigenfunctions for periods near 45.5 and 67.2 minutes (Brown, Stebbins and Hill 1978). The Unno theory of stability of the solar core (Unno 1975) is used to delineate the regions where the waves propagate as acoustic waves, gravity waves, or are evanescent. Of particular interest is that the eigenfunction with $\ell = 20$ indicates that a relative displacement at the solar surface of 10^{-7} is consistent with a relative displacement of about 2×10^{-2} in the gravity wave propagation region of the solar interior for this mode of oscillation.

1. INTRODUCTION

The fundamental interest in the calculation of a few eigenfunctions with high ℓ-values for nonradial modes of oscillation of the 1968 nonstandard solar model (Rouse 1977, 1979 and references therein) is that it provides yet another test of the limitations of that model.

By way of a brief background to the 1968 solar model, it was developed as a part of a project at the Naval Research Lab, Washington, D.C., to study the determination of the helium abundance of the solar photosphere by the theoretical prediction of line and continuum radiation from a solar-model photosphere where the envelope and photosphere were calculated with an assumed abundance of helium (Rouse 1968b, 1969, 1971). This project itself was one phase of a program for calculating an accurate model of the solar interior that I formulated in 1963-64, after I came to the conclusion in the fall of 1963 that the interior structure of the sun was not understood (Rouse 1964, 1968a, 1972). By this approach, the abundance of helium in the solar photosphere is removed as a free parameter in solar evolution calculations.

The next phase, had the work been funded from 1969 on, was to look into the problem of the temperature gradient in the convection region of the sun (four unpublished proposals). In 1976, after I heard of the SCLERA observations of solar oscillations, I realized that the prediction of his observed spectrum and the comparison of my predictions with those based upon the standard model of the sun

could be a test of the 1968 model as it stood. The results for radial oscillations are reported in Rouse (1977) and the results for nonradial oscillations with $\ell \leq 11$ are reported in Rouse (1979). Except for the P_0 and P_1 periods of the radial modes of oscillation, the agreements of the other radial periods and of the nonradial p-mode periods with those predicted with the standard model indicates that, since I used a real-gas adiabatic temperature gradient in the envelope and photosphere, an accurate mixing length theory is only needed to approximate second-order effects in the solar convective region.

2. RESULTS

Now we have the exciting possibility that the SCLERA program may be able to determine the ℓ-index of some of their observed periods of solar oscillation (Hill and Caudell 1979; Brown, Stebbins and Hill 1978). In order to determine the consistency of the 1968 model predictions with their interpretation of possible observations of nonradial modes with ℓ between about 20 and 25 or so, a few eigenfunctions were calculated with high ℓ-values. The results for ℓ = 8, 11, 20, 24, and 28 are given in Figures 1 through 5, respectively. A few calculations were also performed with $28 < \ell \leq 100$. The results with ℓ = 100 will be described later.

In the figures are shown the ℓ, g_k, period Π in minutes, ν in mHz, the peaks of the $\frac{\delta r}{r}$ eigenfunctions, nodes, and values at x = 1.0, regions where $A \lesseqgtr 0$, and the regions where the waves can propagate as acoustic waves (a), gravity waves (g), or are evanescent (e) (Unno 1975). For ℓ values to 24, eigenvalues to 18 digits were required. For ℓ = 28 in Figure 5, an eigenvalue to 18 digits was not quite accurate enough to satisfy the boundary conditions at x = 1.0, doing so at $x \approx 0.986$. However, for nonradial oscillations with periods near 45.5 minutes, an f or g_1 mode is possible for ℓ = 100. To 18 digits with $\Pi \approx 46.6957$ minutes, either mode is possible. A computer with more digits in double or quadruple precision is needed.

Of particular interest is the ℓ = 20, g_3 eigenfunction shown in Figure 3. Regarding the relative displacement, $\delta r/r$, at x = 1.0 and the three peaks between x = 0.345 and x = 0.520, a relative displacement at the solar surface of 10^{-7}, a value consistent with observations, would imply relative displacements of about 2×10^{-2} or less in the g-propagation region of this solar model. This supports the Hill and Caudell (1979) interpretation of two oscillations found in the 1973 observations as possible g-modes of oscillation with ℓ in the range 20 to 25 in that the interior amplitude is not unphysical as with other models.

As a test of the limitations of the 1968 model or any solar model, as the SCLERA observations are narrowed to specific ℓ-modes of oscillation, an agreement in oscillation period with an eigenfunction such as in Figure 3, would indicate that the structure of that solar model in the g-propagation zone would be close to physical reality. If true in the present case, the structure of the 1968 solar model from

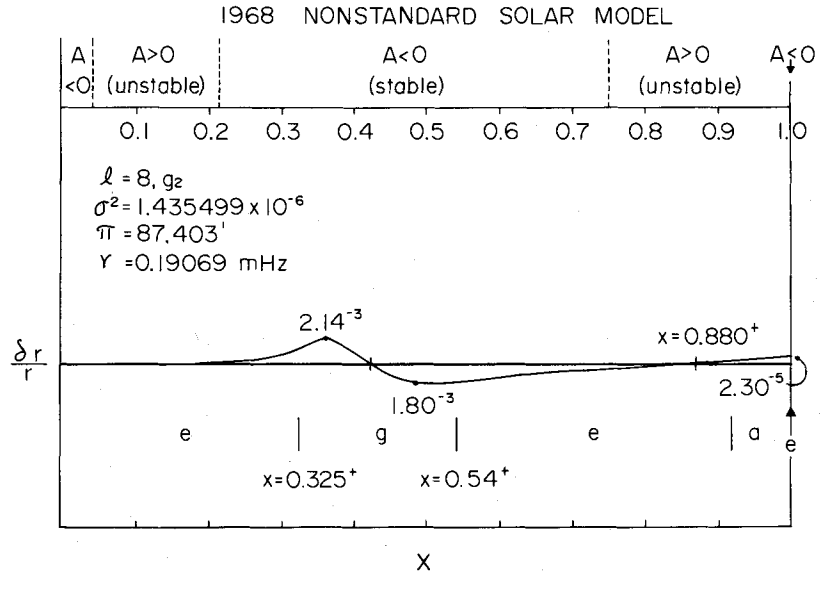

Figure 1. Eigenfunction calculated for the 1968 nonstandard solar model with $\ell = 8$.

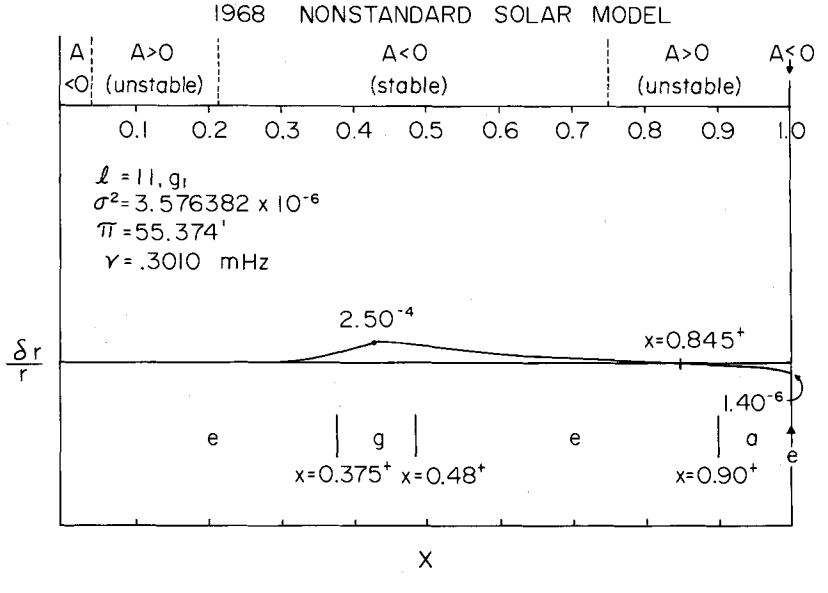

Figure 2. Eigenfunction calculated for the 1968 nonstandard solar model with $\ell = 11$.

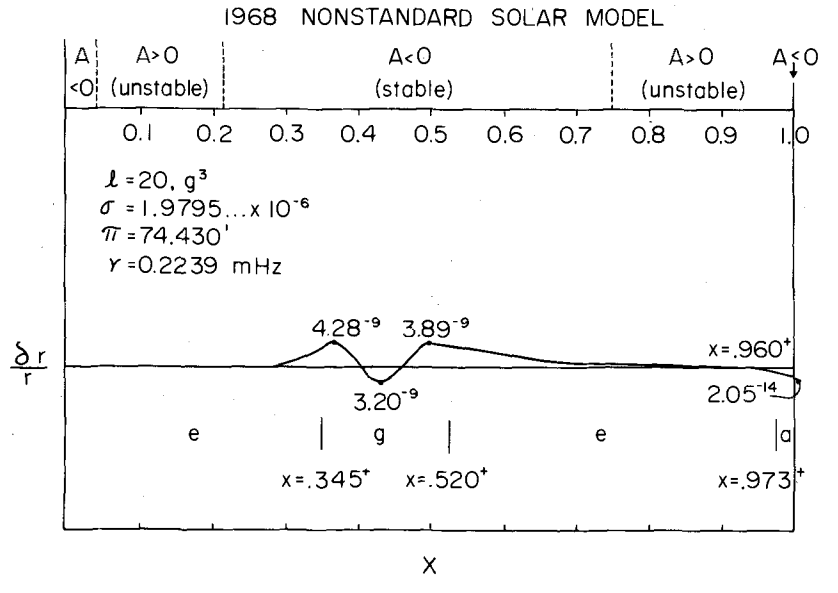

Figure 3. Eigenfunction calculated for the 1968 nonstandard solar model with ℓ = 20.

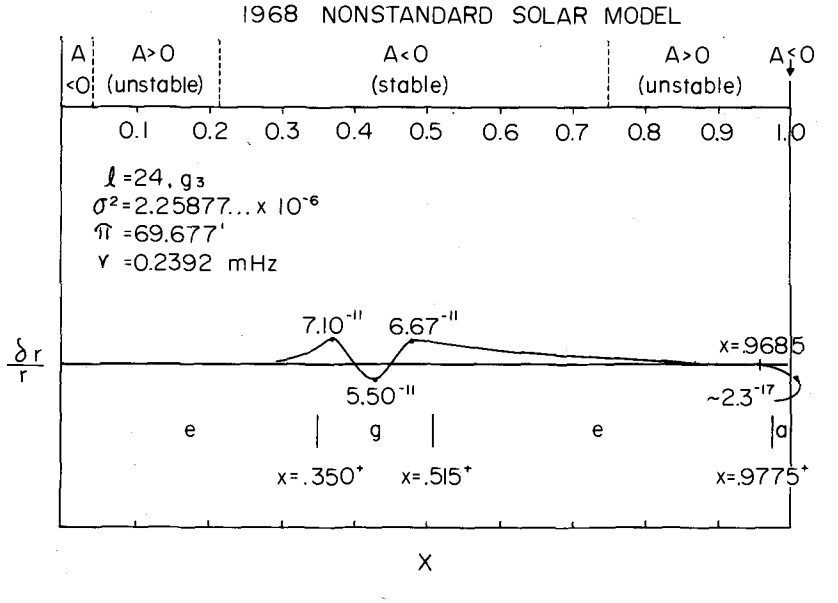

Figure 4. Eigenfunction calculated for the 1968 nonstandard model with ℓ = 24.

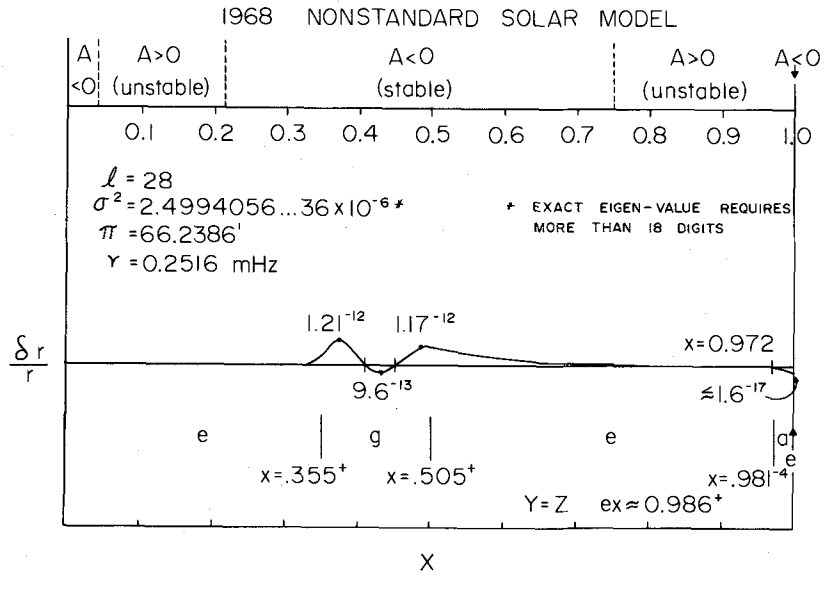

Figure 5. Eigenfunction calculated for the 1968 nonstandard model with $\ell = 28$.

about x = 0.34 to the photosphere would be supported by the above as well as by other observational results. This would put another constraint on the model of the solar core: it must not only be consistent with a positive solar neutrino measurement, but must also be consistent with the basic aspects of the model of the envelope and photosphere derived in the 1968 solar model, photospheric helium abundance study.

Now, what is given up by my 1963-64 approach to solar model calculation? The answer is that nothing basic is given up at all. What is retained is the principle of the scientific method. My use of real-gas physics from the start (in 1962) (see Rouse 1964), my effort to remove the photospheric helium abundance as a free parameter, and my test calculations of periods of solar oscillation to demonstrate the accuracy of my 1968 envelope and photosphere calculations--they all were designed to put these aspects of solar model calculation on a firm physical and mathematical footing. In this way, attention can be focused on the problems of the solar curve--which is precisely how I viewed the solar problem in 1963, a view strongly supported by the subsequent solar neutrino experiment results.

REFERENCES

Brown, T.M., Stebbins, R.T., and Hill, H.A. 1978, Ap. J., 223, 324.

Hill, H.A. and Caudell, T.P. 1979, Mon. Not. R. Astr. Soc., 186, 327.

Rouse, C.A. 1964, UCRL Report 7820-T, dated April 1964. Published as part of (Rouse 1968a).

Rouse, C.A. 1968a, in Progress in High Temperature Physics and Chemistry, Vol. 2, ed. C.A. Rouse, Pergamon Press, Oxford, p. 97.

Rouse, C.A. 1968b, Hydrogen to Helium Ratio in the Solar Photosphere, Univ. of Calif., Space Sciences Lab Series 9, Issue 36, July 1968.

Rouse, C.A. 1969, Astron. & Astrophys., 3, 122.

Rouse, C.A. 1971, in Progress in High Temperature Physics and Chemistry, Vol. 4, ed. C.A. Rouse, Pergamon Press, Oxford, p. 139.

Rouse, C.A. 1972, Gulf-RT-A-12372, dated June 9 and October 30, 1972.

Rouse, C.A. 1977, Astron. & Astrophys., 55, 477-480.

Rouse, C.A. 1979, Astron. & Astrophys., 71, 95.

Unno, W. 1975, Publ. Astron. Soc. Japan, 27, 81.

TIME-VARYING GRAVITATIONAL MULTIPOLE MOMENTS CORRESPONDING TO NONRADIAL SOLAR OSCILLATIONS

W.W. Johnson, D.E. Winget, D.H. Douglass and H.M. Van Horn
Department of Physics and Astronomy
University of Rochester
Rochester, New York

ABSTRACT

Hill (1978) and Severny, Kotov and Tsap (1976) and others have reported oscillations in the apparent radius of the sun of amplitude $\delta R_\odot$ which have been interpreted as arising from mechanical vibrations of various normal modes. A future space mission is being discussed whereby a probe will pass within 4 $R_\odot$ of the sun. This probe would have sufficient sensitivity to measure an oscillating (dimensionless) quadrupole moment J_2' at the 10^{-7} level. In this paper we consider the relationship between various multipoles and $\delta R_\odot/R_\odot$. We calculate the multipole moments for the Cowling polytropic model and an approximate solar model. We find $J_2'/(\delta R_\odot/R_\odot)$ to be $\sim 10^{-3}$ for both models.

1. INTRODUCTION

Hill and co-workers and others, (Hill 1978; Severny, Kotov and Tsap 1976) have published observations which they have interpreted in terms of oscillations of the sun. One of us has recently proposed using a satellite to measure any associated oscillating gravitational multipole moments (Douglass 1978). NASA currently has under consideration a proposal to fly such a "Solar Probe" satellite to within about $4R_\odot$ sometime in the 1980's (see Bender 1978 and Roxburgh 1978). The purpose of this paper is to report preliminary calculations of the time-varying multipole moments associated with several of the nonradial modes of solar oscillation. Such calculations are necessary in order to assess the feasibility of spacecraft measurements of the oscillating multipoles.

The importance of direct measurements of the gravitational moments associated with solar oscillations derives from the fact that they provide direct probes of the solar interior, somewhat analogous to seismic measurements on the earth. The continuing inability of theory to achieve a generally accepted resolution of the solar neutrino problem (cf. Fowler 1974, Bahcall 1978) is a clear demonstration that the interior of the sun is more mysterious than had been recognized previously. In

these circumstances, additional information is essential to improve our understanding, and space probe measurements of the time-dependent gravitational potential provide one of the few ways of obtaining such information.

The plan of this paper is as follows. In § 2 we first define the multipole moments of the gravitational potential, and we relate our definitions of the multipole moments to other conventions (especially for the static quadrupole). We also outline briefly the elements of nonradial stellar oscillaton theory and relate them to the gravitational multipoles. In § 3 we describe the approximate solar models used for these calculations, and we give a brief description of the numerical techniques used to solve the eigenvalue problem for the oscillations. The results of our calculations for several of the nonradial oscillation modes are tabulated, and graphs of some quantities of interest are presented. A discussion of the results, in § 4, concludes the paper.

2. FORMULATION OF THE PROBLEM

2.1. Gravitational Multipole Moments

The gravitational potential $\Phi(r,t)$ external to a given time varying density distribution $\rho(r,t)$ is given by the usual integral

$$\Phi(\vec{r},t) = -G\int \frac{\rho(\vec{r}',t)d^3r'}{|\vec{r} - \vec{r}'|} \quad . \tag{1}$$

With the aid of the Legendre polynomial expansion for $|\vec{r}-\vec{r}'|^{-1}$ and the spherical harmonics addition theorem, (1) may be rewritten in the form

$$\Phi(r,\theta,\phi,t) = -\frac{GM_\odot}{r}\sum_{\ell\geq 0}\sum_{m=-\ell}^{\ell} Y_{\ell m}(\theta,\phi)\left(\frac{R_\odot}{r}\right)^\ell J_{\ell m}(t) \tag{2}$$

where the instantaneous dimensionless multipole moment is defined by

$$J_{\ell m}(t) \equiv \frac{1}{M_\odot R_\odot^{\ell}} \cdot \frac{4\pi}{2\ell + 1}\int (r')^2 dr' d\Omega' \rho(r',\theta',\phi',t)(r')^\ell \, Y_{\ell m}^*(\theta',\phi') \quad . \tag{3}$$

Here we have specialized to the sun, with $M_\odot$ and $R_\odot$ being the solar mass and radius, respectively, $d\Omega'$ the differential element of solar angle, and we have used the definition of the spherical harmonics given by Messiah (1958 pp. 492ff). Note that with these definitions, $J_{00}(t) = (4\pi)^{-1/2}$.

As a special case, we must have $J_{1m} \equiv 0$, because it is proportional to the location of the center of mass of the star.

For infinitesimal oscillations, we take

$$\Phi(\vec{r},t) = \Phi^{(o)}(\vec{r}) + \Phi'(\vec{r},t) \quad ,$$

and for an eigenmode of given (ℓ,m), we write

$$\Phi_{\ell m}'(\vec{r},t) \equiv \hat{\Phi}_{\ell m}(r)\, Y_{\ell m}(\theta,\phi)\, e^{i\sigma t} \quad , \tag{4}$$

where σ is the oscillation eigenfrequency.

Similar relations hold for the density perturbations. When these relations are inserted in (2) and (3) and the angular integrals are evaluated, we obtain

$$\Phi(\vec{r},t) = \sum_{\ell\geq 0} \sum_{m=-\ell}^{\ell} \hat{\Phi}_{\ell m}(r)\, Y_{\ell m}(\theta,\phi)\, e^{i\sigma t}$$

$$= \sum_{\ell\geq 0} \sum_{m=-\ell}^{\ell} \frac{GM_\odot}{r}\left(\frac{R_\odot}{r}\right)^{\ell} \hat{J}_{\ell m}\, Y_{\ell m}(\theta,\phi)\, e^{i\sigma t} \tag{5}$$

where

$$\hat{J}_{\ell m} \equiv \frac{1}{M_\odot R_\odot^{\ell}} \cdot \frac{4\pi}{2\ell+1} \int_0^{R_\odot} \hat{\rho}_{\ell m}(r')(r')^{\ell+2} dr' \quad . \tag{6}$$

The orthogonality of the spherical harmonics requires that all contributions to $\hat{J}_{\ell m}$ come only from oscillations with the same (ℓ,m). Further, in this expansion $\ell = 0$ corresponds to the unperturbed state.

Other definitions of the dimensionless quadrupole moment are also in use (cf. Kaula 1968, especially p. 67). For example if the potential is expanded as

$$\Phi = -\frac{GM_\odot}{r}\left[1 + J_2'\left(\frac{R_\odot}{r}\right)^2\left(\frac{3\cos^2\theta - 1}{2}\right)\right]$$

then our moment is related to the J_2' by

$$J_2' = \left(\frac{5}{4\pi}\right)^{1/2} J_{20} \approx 0.63 J_{20} \quad .$$

2.2 Nonradial Stellar Oscillations

Nonradial spheroidal oscillations of stars are described by a fourth-order system of linear differential equations, which may be written in the form (cf. Osaki and Hansen 1973)

$$\frac{1}{r^2}\frac{d}{dr}\left(r^2 \frac{d\hat{\Phi}}{dr}\right) - \frac{\ell(\ell+1)}{r^2}\hat{\Phi} = -4\pi G\left(\hat{\xi}_r \frac{d\rho}{dr} + \hat{\alpha}\right) \tag{7a}$$

$$-\frac{\Gamma_1 P}{\rho}\hat{\alpha} = \hat{\chi} - \hat{\Phi} + \hat{\zeta}_r \frac{1}{\rho}\frac{dP}{dr} \tag{7b}$$

$$\sigma^2 \hat{\zeta}_r = \frac{d\hat{\chi}}{dr} - A\frac{\Gamma_1 P}{\rho}\hat{\alpha} \tag{7c}$$

$$\sigma^2 \hat{\zeta}_t = \frac{\hat{\chi}}{r} \tag{7d}$$

$$\hat{\alpha} = \frac{1}{r^2}\frac{d}{dr}\left(r^2 \hat{\zeta}_r\right) - \frac{\ell(\ell+1)}{r}\hat{\zeta}_t \quad . \tag{7e}$$

Here Φ is the r-dependent part of the gravitational potential perturbation, as in (4); ζ_r and ζ_t are the radial and transverse amplitudes of the displacement eigenvector ζ (related to the velocity perturbation by $\vec{V}' = i\omega\vec{\zeta}$); $\hat{\alpha}$ is the r-dependent part of div $\vec{\zeta}$; and $\hat{\chi}$ is defined by

$$\hat{\chi} = \frac{\hat{P}}{\rho} + \hat{\Phi} \quad , \tag{8}$$

where $\hat{P}$ is the pressure perturbation. All quantities in these equations that are not distinguished by a supernumerary carat refer to the unperturbed equilibrium model.

Other quantities we shall find convenient to have at our disposal are the definition of the density perturbation

$$\hat{\rho} = -\hat{\zeta}_r \frac{d\rho}{dr} - \rho\hat{\alpha} \tag{9}$$

and

$$A \equiv \frac{d\ell n\rho}{dr} - \frac{1}{\Gamma_1}\frac{d\ell nP}{dr} \quad . \tag{10}$$

Note that $N^2 \equiv -Ag$ defines the Brunt-Väisälä frequency N; it becomes imaginary in regions of convective instability ($A > 0$).

Specification of the nonradial eigenvalue problem is completed by giving the four spatial boundary conditions, two each at the center and at the surface of the star (cf. Osaki and Hansen 1973).

For purposes of numerical computation it is convenient to rewrite the

eigenvalue problem (7) in terms of the dimensionless Dziembowski (1971) variables:

$$y_1 \equiv \hat{\xi}_r/r \tag{11a}$$

$$y_2 \equiv \hat{\chi}/gr = (\hat{\Phi} + \hat{P}/\rho)/gr \tag{11b}$$

$$y_3 \equiv \hat{\Phi}/gr \tag{11c}$$

and

$$y_4 \equiv (d\hat{\Phi}/dr)/g \quad , \tag{11d}$$

where $g \equiv GM_r/r^2$ is the local acceleration due to gravity. We refer the interested reader to Osaki and Hansen (1973) and to Dziembowski (1971) for the forms of the equations in terms of these variables. For our present purposes it is sufficient merely to give the results in terms of these quantities; for example:

$$\hat{\xi}_r = ry_1 \tag{12a}$$

$$\hat{\xi}_t = \frac{\hat{\chi}}{r\sigma^2} = \frac{gy_2}{\sigma^2} \tag{12b}$$

and

$$\frac{\hat{\rho}}{\rho} = -rAy_1 + \frac{\rho gr}{\Gamma_1 P}(y_2 - y_3) \quad . \tag{12c}$$

Although the oscillation variables are defined only in the interior of a star, the gravitational potential must be continuous across the stellar surface. We can therefore express the dimensionless multipole moments of the potential in terms of these pulsation variables. In particular, at the solar surface, (5) and (11) yield

$$y_3(r=R_\odot) = \hat{\Phi}_{\ell m}(R_\odot)/\frac{GM_\odot}{R_\odot} = -\left[\frac{GM_\odot}{R_\odot}\left(\frac{R_\odot}{R_\odot}\right)^\ell \hat{J}_{\ell m}\right]\Big/\frac{GM_\odot}{R_\odot} = -\hat{J}_{\ell m} \quad . \tag{13}$$

Thus, the gravitational multipole moments are obtained as a trivial byproduct of the nonradial oscillation calculations. Alternatively, of course, one may use (6) to evaluate the $J_{\ell m}$ directly.

We shall express the amplitude of the oscillation (and hence the actual value of $\hat{J}_{\ell m}$) in terms of the fractional radial displacement amplitude $\hat{\xi}_r(r = R_\odot)/R_\odot \equiv \delta R_\odot/R_\odot$.

3. THIS CALCULATION

To solve the nonradial oscillation eigenvalue problem, one must begin with a detailed numerical model for the unperturbed star. We have employed two such models: a polytrope with n = 3 and a model from an evolutionary sequence for the sun.

The first model we used was the polytropic (n = 3, N = $3/2$) model, following Cowling (1941). The most important virtue of this model is that a few eigenfunctions are tabulated (Cowling 1941 and Kopal 1949), so that the moments can be evaluated immediately by equation (6). The results for this model are presented in Tables 1 and 2.

The second, evolutionary model was taken from a sequence constructed to study the deep solar interior. The parameters of this model are given in Table 3. Note that the radius of the model differs significantly from that of the sun. This is a consequence of our use of very crude, purely radiative envelope models in the computation of this evolutionary sequence. In fact, although the outermost $\sim 10^{-7}$ $M_\odot$ of the sun are actually convective, we have forced this region to be radiative. This has little effect on the deep interior of the model because of the well-known convergence of stellar models to the radiative solution at large depths (cf. Schwarzschild 1958). However, use of the incorrect temperature gradient in the surface layers does lead to the incorrect stellar radii and thus affects the pressure and temperature in the outer parts of the model.

Apart from this one aspect, however, the model provides a reasonable approximation of the present sun. In particular, the model calculations have employed a standard Newton-Raphson evolutionary program, and the physics employed to describe the material properties of the stellar matter are the usual ones. The equation of state corresponds to a mixture of ideal gases plus radiation (electron degeneracy is included, although it is never very important). Opacities are interpolated in Los Alamos tables having Z = 0.02 (cf. Cox and Stewart 1970), and nuclear reaction rates for both the P-P chain and the CNO cycle are included as given by Clayton (1968), with the fast reactions all taken to be in equilibrium.

To employ the approximate solar model as a basis for nonradial oscillation calculations, it is necessary to compute detailed distributions of a variety of structural and thermodynamic parameters throughout the star. Most of these quantities are already available from the evolutionary calculations. Because of the crude approximation employed for the solar envelope, however, it was necessary to reconstruct separately the run of parameters appropriate to the outer layers of the model. This was done with a separate program, and care was taken to ensure that the structure variables were as monotonic and smooth as possible across the envelope/interior interface.

This model was then used as input to the Osaki-Hansen nonradial oscillation code (see Osaki and Hansen 1973 for details of the numerical methods used). This

Table 1. The Polytrope Model

Parameter	Value
n	3
N	3/2
$M/M_\odot$	1
$R/R_\odot$	1
$\log \rho_c (gm/cm^3)$	1.88

Table 2. Results ($\ell = 2$)

Mode	Period(min)	Iben (1976)		$\hat{J}_{\ell m}/\frac{\hat{\xi} r}{R_\odot}$
		Period(min)	Freq(Hz)	
f	56.6	49.19	3.39 -4	0.91 -3
g_1	76.9	56.00	2.98 -4	2.04 -3
g_2	105.4	65.21	2.56 -4	2.19 -3

Table 3. Parameters of the Approximate Solar Model

Parameter	Value
$M/M_\odot$	1.000
$L/L_\odot$	1.074
$R/R_\odot$	1.38
age (yrs)	4.201×10^9
log P_c(dynes cm^{-2})	17.387
log T_c ($^\circ$K)	7.193
log ρ_c (g cm^{-3})	2.189
X	0.71
Z	0.02

code employs Newton-Raphson iterations to relax an approximate solution of the eigenvalue problem to a converged solution. Our convergence criterion was that the sum of the absolute values of the corrections to the eigenfunction be less than 10^{-9} times the sum of the absolute values of the eigenfunction itself.

The results of our calculations are given in Tables 4 and 5 for nonradial p-, f-, and g-modes corresponding to $\ell = 2$ and 3. In addition to the actual eigenperiods obtained for our approximate model, we have listed eigenperiods scaled to the correct solar radius according to

$$\pi_{scaled} = \pi_{model}(R_{model}/R_{\odot})^{-3/2} \quad ; \tag{14}$$

this scaling would be exact for the p- and f-modes, if the structure of the pulsation eigenfunctions were invariant. Of course they are not, and we have accordingly included also the solar eigenperiods calculated by Iben (1976) to provide an estimate of the accuracy of these results. The dimensionless multipole moments $\hat{J}_{\ell m}$ and the ratios $\hat{\xi}_t/\hat{\xi}_r$ at the stellar surface are also given in these tables; these dimensionless quantities are expected to be approximately invariant under the scaling. They should thus be correct to about the same degree that the scaled eigenperiods reproduce Iben's results.

4. DISCUSSION

The most obvious advantage of the proposed gravitational measurement is that it is a real whole-body measurement. Only whole-body oscillations could conceivably cause perturbations in the potential, and since a "drag-free" satellite will faithfully follow these perturbations, the only serious impediment to the experiment comes from the Doppler tracking system. For example, no sophisticated knowledge of the time-dependent brightness distribution in the photosphere is necessary to interpret the results. Thus a positive result is likely to be uncontroversial.

A major disadvantage of the method is the limited data collection time available for the proposed mission (10-20 hours up close).

We have presented above the formalism that determines the ratio of two quantities that can, in principle, be measured separately for a solar oscillation, the radial displacement and the gravitational moment. If ground based measurements of the radial displacement were reliable enough and well understood, then their comparison to a moment measurement would provide additional information. This is another way of saying that their ratio is model dependent, as can be seen by comparison of our two calculations. Our first look at this suggests that a major effect is caused by the degree of central condensation: when it is larger, the moment/displacement ratio is smaller. Perhaps other information of this kind can be discovered by further study of different models.

We would like to suggest that in future calculations of solar oscillations it

Table 4. Non-Radial Oscillation Moments of the Approximate Solar Model

$\ell = 2$

Mode	Period(min)	Scaled Period(min)	Iben (1976) Period(min)	Iben (1976) Frequency(Hz)	$\hat{J}_{gm}/\frac{\hat{\xi}r}{R_\odot}$	$\hat{\xi}_t/\hat{\xi}_r$
p_{12}	15.04	9.28	8.77	1.88 -3	1.00 -6	0.00215
p_{11}	16.26	10.03	9.44	1.77 -3	-2.24 -6	0.00267
p_{10}	17.70	10.92	10.21	1.63 -3	1.81 -6	0.00325
p_9	19.39	11.96	11.18	1.49 -3	-3.42 -6	0.00419
p_8	21.42	13.21	12.33	1.35 -3	3.58 -6	0.00531
p_7	23.89	14.74	13.74	1.213 -3	-5.98 -6	0.00683
p_6	26.90	16.59	15.54	1.073 -3	7.73 -6	0.00892
p_5	30.68	18.93	17.88	9.32 -4	-1.30 -5	0.01188
p_4	35.50	21.90	21.10	7.90 -4	2.26 -5	0.0162
p_3	41.60	25.66	25.60	6.51 -4	-5.15 -5	0.0226
p_2	48.72	30.06	32.61	5.11 -4	1.14 -4	0.0314
p_1	56.36	34.77	43.75	3.81 -4	-8.36 -5	0.0423
f	65.53	40.43	49.19	3.39 -4	-2.75 -4	0.0575
g_1	75.65	46.67	56.00	2.98 -4	3.67 -4	0.0769
g_2	89.76	55.37	65.21	2.56 -4	2.02 -3	0.1085
g_3	108.36	66.85	77.16	2.16 -4	3.67 -3	0.1590
g_4	128.78	79.44	90.85	1.835 -4	4.23 -3	0.224
g_5	150.8	93.03	104.7	1.592 -4	4.01 -3	0.308
g_6	172.8	106.6	118.6	1.405 -4	3.45 -3	0.405
g_7	———	———	132.6	1.257 -4	———	———
g_8	217.9	134.4	146.7	1.136 -4	2.25 -3	0.645
g_9	241.0	148.7	160.9	1.036 -4	1.75 -3	0.791
g_{10}	264.8	163.3	174.9	9.53 -5	1.33 -3	0.956

Table 5. Non-Radial Oscillation Moments of the Approximate Solar Model

$\ell = 3$

Mode	Period(min)	Scaled Period(min)	Iben (1976) Period(min)	Iben (1976) Frequency(Hz)	$\hat{J}_{\ell m}/\frac{\hat{\zeta r}}{R_\odot}$	$\hat{\zeta}_t/\hat{\zeta}_r$
p_{12}	14.61	9.01	8.53	1.95 -3	2.24 -7	0.00198
p_{11}	15.77	9.73	9.17	1.82 -3	-9.63 -7	0.00246
p_{10}	17.13	10.57	9.90	1.68 -3	5.06 -7	0.00306
p_9	18.72	11.55	10.76	1.55 -3	-1.43 -6	0.00384
p_8	20.62	12.72	11.82	1.41 -3	1.18 -6	0.00486
p_7	22.92	14.14	13.11	1.27 -3	-2.33 -6	0.00622
p_6	25.73	15.87	14.76	1.129 -3	2.56 -6	0.00808
p_5	29.25	18.04	16.94	9.84 -4	-4.58 -6	0.01071
p_4	33.69	20.78	19.72	8.45 -4	6.69 -6	0.01451
p_3	39.47	24.35	23.91	6.97 -4	-1.34 -5	0.0203
p_2	46.81	28.88	29.95	5.56 -4	2.69 -5	0.0289
p_1*	51.58	31.82	40.45	4.12 -4	5.22 -6	0.0353
f*	59.54	36.73	44.67	3.73 -4	-7.21 -5	0.0473
g_1*	67.29	41.51	51.92	3.21 -4	-2.17 -5	0.0607
g_2	76.97	47.48	57.21	2.91 -4	2.83 -4	0.0819
g_3	87.29	53.85	63.33	2.63 -4	6.13 -4	0.1028
g_4	100.46	61.97	72.17	2.31 -4	9.81 -4	0.1364
g_5	115.49	71.25	81.59	2.04 -4	1.18 -3	0.1806

*Note that the p_1 and g_1 modes for $\ell = 3$ have 3 nodes while the f mode has 2; see Dziembowski (1971) and Robe (1968) for further discussion.

would be useful to include a calculation of the moments for possible later comparison to satellite data.

The next step is to repeat our calculations for a more realistic solar model. These results will be reported in another paper. It is these moments that would be most appropriate for evaluating the feasibility of the satellite experiment.

* * * * *

This research supported in part by the National Science Foundation.

REFERENCES

Bahcall, J.N. 1978, Revs. Mod. Phys., 50, 881.

Bender, D.F. 1978, A Close-Up of the Sun, ed. Neugebauer and Davies, JPL Publication 78-70.

Clayton, D.D. 1968, Principles of Stellar Evolution and Nucleosynthesis, (New York: McGraw-Hill).

Cowling, T.G. 1941, Mon. Not. R. Astr. Soc., 101, 367.

Cox, A.N. and Stewart, J.N. 1970, Ap. J. Suppl., 19, 243.

Douglass, D.H. 1978, A Close-Up of the Sun, ed. Neugebauer and Davies, JPL Publication 78-70.

Dziembowski, W. 1971, Acta Astr., 21, 289.

Fowler, W.A. 1974, in Late Stages of Stellar Evolution, ed. R.J. Tayler and J.E. Hesser (Dordrecht: Reidel), p. 245.

Hill, H. 1978, "Seismic Sounding of the Sun," preprint from The New Solar Physics, ed. J.A. Eddy (Boulder: Westview).

Kaula, W.M. 1968, An Introduction to Planetary Physics, (New York: Wiley).

Kopal,Z. 1949, Ap. J., 109, 509.

Messiah, A. 1958, Quantum Mechanics, (New York: John Wiley and Sons, Inc.).

Osaki, Y. and Hansen, C.J. 1973, Ap. J., 185, 277.

Roxburgh, I.W. 1978, A Close-Up of the Sun, ed. Neugebauer and Davies, JPL Publication 78-70.

Schwarzschild, M. 1958, Structure and Evolution of the Stars, (Princeton, N.J.: Princeton University Press).

Severny, A.B., Kotov, V.A. and Tsap, T.T. 1976, Nature, 256, 87.

PERTURBATIONS IN GRAVITATIONAL POTENTIAL ASSOCIATED WITH SOLAR OSCILLATIONS

J. Christensen-Dalsgaard
Astronomisk Institut, Aarhus Universitet, Denmark
and Institut d'Astrophysique, Universite de Liege, Belgium

D.O. Gough
Institute of Astronomy, and Department of Applied Mathematics
and Theoretical Physics, University of Cambridge, UK

ABSTRACT

The relation between the amplitudes of the gravitational potential perturbation and the displacement eigenfunctions of adiabatic oscillations of a solar model is discussed, and numerical results are tabulated for a selection of modes of low degree. In particular, a solar quadrupole oscillation with period 160^m and rms surface velocity of 1 ms^{-1} would induce a perturbation in the external gravitational potential with an oscillating quadrupole moment of amplitude about one-third that of the static moment that would be produced by a uniform interior rotation of the sun with angular velocity comparable with that observed on the surface. It is concluded that quadrupole oscillations might be detectable gravitationally.

1. INTRODUCTION

The announcement of the detection of global oscillations of the sun (Hill, Stebbins and Brown 1976; Severny, Kotov and Tsap 1976; Brookes, Isaak and van der Raay 1976) immediately raised the question of whether the associated gravitational radiation could be measured. In particular, J. Hough (private communication) and J. Weber (private communication) enquired whether the amplitudes of the variations in the solar quadrupole moment associated with modes that might be responsible for the data are large enough to be detected by ground-based observations. The conclusion at that time was that the amplitudes were too low.

At this workshop, Johnson et al. (1980) have addressed themselves to the issue of whether the quadrupole variations might be detected by future extraterrestrial probes. Their discussion is based on modes of oscillation of a polytrope: they have asked how well their modes approximate those of more realistic solar models and, in particular, whether the latter predict substantially larger fluctuations in the external gravitational potential. We are in a position to give an immediate answer to that question, since the perturbation to the gravitational

potential is one of the eigenfunctions of our normal mode computations (Christensen-Dalsgaard, Dilke and Gough 1974). Here we present a selection of our results, some of which may be compared with those of Johnson et al. (1980). We find that for most modes of the solar model the gravitational potential perturbations are indeed larger than those of their polytropic counterparts, but by how much is dependent on the criterion for comparison.

2. RELATION BETWEEN DISPLACEMENT AND THE PERTURBATION IN THE GRAVITATIONAL POTENTIAL

After the usual separation of variables with respect to spherical polar coordinates (r, θ, ϕ), the displacement eigenfunction $\xi_{n\ell m}$ of a normal mode of order n may be written

$$\vec{\xi}_{n\ell m} = R \begin{Bmatrix} \tilde{\xi}_{n\ell}(x) P_\ell^m(\cos\theta) \begin{matrix}\sin \\ \cos\end{matrix} m\phi \\ \tilde{\eta}_{n\ell}(x) \frac{d}{d\theta} P_\ell^m(\cos\theta) \begin{matrix}\sin \\ \cos\end{matrix} m\phi \\ \pm\tilde{\eta}_{n\ell}(x) \frac{m}{\sin\theta} P_\ell^m(\cos\theta) \begin{matrix}\cos \\ \sin\end{matrix} m\phi \end{Bmatrix} \sin\omega_{n\ell} t \quad , \tag{1}$$

where $x = r/R$, R is the radius of the sun, $\omega_{n\ell}$ is the oscillation eigenfrequency and P_ℓ^m is the associated Legendre function of degree ℓ. The corresponding Eulerian perturbations to density ρ and gravitational potential Φ are

$$\rho'_{n\ell m} = \bar{\rho}\,\tilde{\rho}_{n\ell}(x) P_\ell^m(\cos\theta) \begin{matrix}\sin \\ \cos\end{matrix} m\phi \sin\omega_{n\ell} t \quad , \tag{2}$$

$$\Phi'_{n\ell m} = \frac{GM}{R}\,\tilde{\Phi}_{n\ell}(x) P_\ell^m(\cos\theta) \begin{matrix}\sin \\ \cos\end{matrix} m\phi \sin\omega_{n\ell} t \quad , \tag{3}$$

where M is the solar mass, G is the gravitational constant and $\bar{\rho} = 3M/(4\pi R^3)$ is the mean density of the sun. Since there is a neglible amount of matter in the chromosphere, corona and the solar wind, the perturbation to the gravitational potential outside the sun is determined uniquely by that in the photosphere. Thus it is sufficient to determine $\tilde{\Phi}_{n\ell}(1)$.

The perturbations Φ' and ρ' are related by a Poisson equation. This may be solved to yield the gravitational potential perturbation in the photosphere (e.g. Christensen-Dalsgaard 1976; cf. Cowling 1941):

$$\Phi_{n\ell}(1) = \frac{3}{2\ell+1} \left\{ \rho_0(1)\tilde{\xi}_{n\ell}(1) + \int_0^1 x^{\ell+2} \tilde{\rho}_{n\ell}(x)\,dx \right\} \quad , \tag{4}$$

where $\rho_0(x)$ is the unperturbed density measured in units of $\bar{\rho}$. Elimination of $\tilde{\rho}_{n\ell}$ using the continuity equation

$$\tilde{\rho}_{n\ell} = -x^{-2}\frac{d}{dx}(x^2\rho_0\tilde{\xi}_{n\ell}) + \ell(\ell+1)x^{-1}\rho_0\tilde{\eta}_{n\ell} \qquad (5)$$

yields a direct relation between $\tilde{\Phi}_{n\ell}$ and the displacement amplitudes:

$$\tilde{\Phi}_{n\ell} = \frac{3\ell}{2\ell+1}\int_0^1 x^{\ell+1}\rho_0(x)\left[\tilde{\xi}_{n\ell}(x) + (\ell+1)\tilde{\eta}_{n\ell}(x)\right]dx$$

$$\equiv \int_0^1 K_\ell(x)\left[\tilde{\xi}_{n\ell}(x) + (\ell+1)\tilde{\eta}_{n\ell}(x)\right]dx \quad . \qquad (6)$$

The kernel K_ℓ is displayed in Figure 1 for several values of ℓ. For $r > R$ the perturbed potential is given by equation (3) with

$$\tilde{\Phi}_{n\ell}(r/R) = \tilde{\Phi}_{n\ell}(1)(R/r)^{\ell+1} \quad . \qquad (7)$$

When computing eigenfunctions it is most convenient to specify some amplitude at a fixed point in space. Current observations measure conditions at the surface, and usually our normalization is $\overline{\xi}_{n\ell}(1) = 1$. From a physical point of view this is not necessarily a good choice, since surface amplitudes can be poor reflections of the eigenfunctions in the interior (e.g. Christensen-Dalsgaard, Dziembowski and Gough 1980). It is sometimes more instructive to consider an L^2 norm of the displacement such as $I_{n\ell m}$, defined by

$$I_{n\ell m} = \frac{3}{4\pi R^2}\int \rho_0\, \underset{\sim}{\xi}_{n\ell m}\cdot\underset{\sim}{\xi}_{n\ell m}\, x^2 \sin\theta dx d\theta d\phi \equiv \tilde{I}_{n\ell m}\sin^2\omega_{n\ell}t \quad ; \qquad (8)$$

$$\tilde{I}_{n\ell m} = \tfrac{1}{2}(1+\delta_{m0})\frac{3\pi}{2\ell+1}\frac{(\ell+m)!}{(\ell-m)!}\int_0^1 \rho_0\left[\tilde{\xi}^2_{n\ell} + \ell(\ell+1)\tilde{\eta}^2_{n\ell}\right]x^2dx \quad , \qquad (9)$$

where δ_{ik} is the Kronecker delta. This quantity is related to the total energy $E_{n\ell m}$ of the oscillations through the equation

$$E_{n\ell m} = \tfrac{1}{2}\tilde{I}_{n\ell m} MR^2 \omega^2_{n\ell} \quad . \qquad (10)$$

3. ASYMPTOTIC PROPERTIES OF MODES OF HIGH ORDER OR HIGH DEGREE

We first estimate the gravitational potential perburbation when n or ℓ is large. Not only does this provide us with the asymptotic properties of these extreme modes, but also it should indicate the trends in all but perhaps the modes of lowest order or degree.

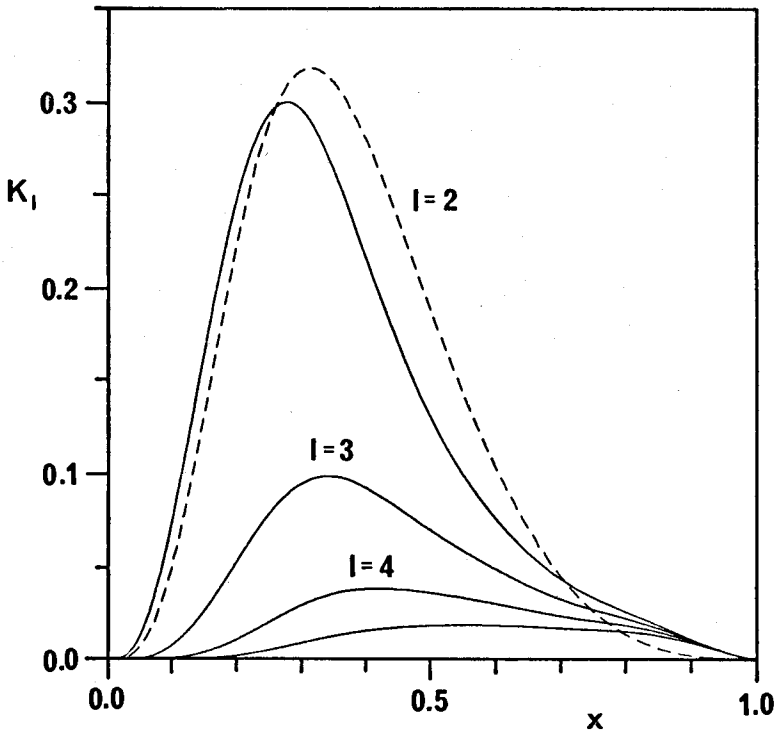

Figure 1. Kernels $K^{\ell}(x) = [3\ell/(2\ell + 1)]\, x^{\ell+1}\ \rho^{o}(x)$ for ℓ = 2,3,4 and 5 for the solar model. The dashed curve is $K_2(x)$ for the polytrope of index 3.

Relative to the mean displacement amplitude, $|\tilde{\Phi}_{n\ell}|$ decreases as n, or ℓ, increases, at least when n, or ℓ, is large: As n increases at constant ℓ, JWKB analysis shows that in the regions of the star where the displacement is significant, the displacement eigenfunctions of both the p and the g modes oscillate spatially with a characteristic wavelength that is inversely proportional to n (e.g., Christensen-Dalsgaard, Dziembowski and Gough 1980). Thus according to Riemann's lemma applied to equation (6) one must expect that for modes normalized with $I_{n\ell m} = 1$, $\tilde{\Phi}_{n\ell}(1) \leq O(n^{-1})$ as $n \to \infty$, and Papaloizou (private communication) has shown that $\tilde{\Phi}_{n\ell}(1) \leq O(n^{-2})$. To determine the actual behavior requires a more careful asymptotic analysis (cf. Zahn, 1970).

The behavior of $\tilde{\Phi}_{n\ell}(1)$ as ℓ increases requires separate discussions for the p and g modes. For the global g modes the dominant factor is the decrease with ℓ of the kernel $K_\ell(x)$ when $x < 1$. When ℓ is large g modes are confined beneath the convection zone, and when ℓ is sufficiently large they are trapped near the maxima of the buoyancy frequency. Thus the displacement amplitudes are significant only when $x < x_c < 1$, for some x_c that is at or beneath the bottom of the convection zone. Taking the axisymmetrical mode as an example, one can see from equations (6) and (9) that at fixed $\tilde{I}_{n\ell o}$, $|\tilde{\Phi}_{n\ell}(1)| \leq O(\ell^{1/2} x_c^{\ell})$ as $\ell \to \infty$. The behavior of the p modes is different. As ℓ increases these modes become more and more severely confined to the surface layers of the star, where the density is low. Consequently they induce smaller and smaller absolute density perturbations. As $\ell \to \infty$, the penetration depth is $O(\ell^{-1} R)$. If the stratification of the upper envelope is approximated by a polytrope of index μ, the mass involved in the oscillation decreases as $\ell^{-\mu-1}$. Hence for the axisymmetrical mode at constant $\tilde{I}_{n\ell o}$, $\tilde{\xi}_{n\ell}$ increases as $\ell^{1+\mu/2}$ and $\tilde{\Phi}^{n\ell}(1) = O(\ell^{-\mu/2})$.

It may be more natural to consider the behavior of $\tilde{\Phi}_{n\ell}(1)$ at constant $E^{n\ell m}$. As $n \to \infty$, $\omega_{n\ell} = O(n^{-1})$ for the g modes, whence $\tilde{\Phi}_{n\ell}(1) = O(n^{-1})$, whereas for the p modes $\omega_{n\ell} = O(n)$ and $\tilde{\Phi}_n(1) \leq O(n^{-3})$. As ℓ increases the g mode frequencies approach the maxima of the buoyancy frequency and the behavior of $\tilde{\Phi}_{n\ell}(1)$ is the same as when the normalization $\tilde{I}_{n\ell m} = 1$ is applied; for the p modes $\omega_{n\ell} = O(\ell^{1/2})$ as $\ell \to \infty$, and $\tilde{\Phi}_{n\ell}(1) = O(\ell^{-(\mu+1)/2})$.

4. GRAVITATIONAL POTENTIAL PERTURBATIONS ASSOCIATED WITH MODES OF LOW ORDER AND DEGREE

Surface amplitudes of the perturbations to the gravitational potential are presented in Table 1 for a selection of the modes of lowest degree. The equilibrium solar model is Model A of Christensen-Dalsgaard, Gough and Morgan (1979), whose properties are summarized in these proceedings by Christensen-Dalsgaard, Dziembowski and Gough (1980). The normal mode analysis was performed in the adiabatic approximation, in a manner similar to that described by Christensen-Dalsgaard, Dilke

and Gough (1974).

The modes of lowest degree that perturb the gravitational potential outside a star are the quadrupole modes. Monopole perturbations in the gravitational potential are not possible because the mass of the star is conserved; oscillatory dipole perturbations are not possible because the external field would be precisely that of a spherically symmetrical mass distribution whose center of mass is moving with respect to the frame of the equilibrium model. Dipole perturbations to Φ are induced inside the star, however. One can see formally from the perturbation equations that the measure of the dipole moment $\tilde{\Phi}_{n1}(1)$ is zero, since when $\ell = 1$ the integral in equation (6) is proportional to the coefficient c_1 of Christensen-Dalsgaard (1976), whose vanishing is equivalent to the stationarity of the center of mass. The essence of an alternative demonstration is given by Zahn (1970). Note however that had Cowling's approximation, which ignores Φ' in the computation of $\underline{\xi}$, been used, the center of mass would have been predicted to move under dipole oscillations. If Φ' were to have been computed subsequently from $\underline{\xi}$ using equation (6), it would have been found not to vanish when $r > R$.

Inspection of Table 1 reveals that the decrease of $|\tilde{\Phi}_{n\ell}(1)|$ with n and ℓ at fixed $\tilde{I}_{n\ell m}$ discussed in the previous section is evident even when n and ℓ are quite low. This is as one might expect, since when the density perturbation oscillates spatially on a shorter and shorter length scale, cancellation amongst its contributions to the gravitational potential from different regions in the star increases.

In trying to gain further insight into the nature of these modes, and to understand the differences between the results presented in Table 1 and those for a polytrope of index 3, one can be guided by JWKB analysis. Though strictly valid only for modes of large order, the results do correctly indicate the qualitative behavior of all but the few lowest order modes. The asymptotic formula for $\tilde{\xi}$ is given, for example, by Christensen-Dalsgaard, Dziembowski and Gough (1980); we omit subscripts on eigenfunctions and eigenvalues from here on. It is evident that the spatial structure of $\tilde{\xi}$ depends crucially on the value of ω compared with the buoyancy frequency N and the acoustic frequency S^{ℓ}; if ω is either greater than or less than both N and S^{ℓ} the eigenfunctions are oscillatory in space, and if ω lies between N and S^{ℓ} they are evanescent. The p modes have frequencies that exceed appropriate averages of S^{ℓ}, and g mode frequencies are less than appropriate averages of N.

In Figure 2, N_2 and S_2^{ℓ} are plotted for the solar model and the polytrope. The major differences between the two models are in the forms of N_2. When $x \leq 0.64$, N_2 is greater for the solar model, a result of the spatial variation in chemical composition produced by nuclear reactions. In the envelope, N_2 changes sign at the base of the convection zone of the solar model, whereas in the polytrope it remains positive and diverges towards the surface where the scale height falls to zero.

Table 1.

ℓ	Mode	Period(min)	$\tilde{I}_{n\ell o}$	$\tilde{\Phi}_{n\ell}(1)$	$\tilde{\Phi}_{n\ell}(1)/\tilde{I}^{1/2}_{n\ell o}$	$J_{n\ell o}$
2	p_5	17.5	1.8×10^{-6}	-3.8×10^{-5}	-2.8×10^{-2}	-2.1×10^{-11}
2	p_2	32.4	4.5×10^{-5}	9.1×10^{-4}	1.3×10^{-1}	9.0×10^{-10}
2	p_1	43.4	3.1×10^{-4}	-4.7×10^{-3}	-2.6×10^{-1}	-6.3×10^{-9}
2	f	48.2	1.3×10^{-3}	-2.7×10^{-3}	-7.4×10^{-2}	-4.0×10^{-9}
2	g_1	57.3	1.1×10^{-3}	4.7×10^{-3}	1.4×10^{-1}	8.4×10^{-9}
2	g_2	65.6	3.8×10^{-2}	1.1×10^{-2}	1.8×10^{-1}	2.2×10^{-9}
2	g_5	102	5.7×10^{-1}	1.7×10^{-2}	7.0×10^{-2}	5.4×10^{-8}
2	g_9	157	4.1×10^{-1}	1.2×10^{-2}	1.8×10^{-2}	5.7×10^{-8}
3	p_5	16.6	9.5×10^{-7}	-1.6×10^{-5}	-1.6×10^{-2}	-9.5×10^{-12}
3	p_2	29.6	2.0×10^{-5}	3.3×10^{-4}	7.2×10^{-2}	3.5×10^{-10}
3	p_1	39.8	9.5×10^{-5}	-1.3×10^{-3}	-1.2×10^{-1}	-1.8×10^{-9}
3	f	43.5	2.0×10^{-3}	-9.3×10^{-4}	-2.0×10^{-2}	-1.5×10^{-9}
3	g_1	50.8	1.7×10^{-3}	1.1×10^{-3}	2.6×10^{-2}	2.0×10^{-9}
3	g_2	57.4	1.5×10^{-3}	3.2×10^{-3}	8.0×10^{-2}	6.7×10^{-9}
3	g_5	79.4	1.1×10^{-2}	7.0×10^{-3}	6.6×10^{-2}	2.0×10^{-8}
3	g_{13}	158	8.1×10^{-1}	5.2×10^{-3}	5.8×10^{-3}	3.0×10^{-8}
4	p_5	15.9	5.7×10^{-7}	-5.9×10^{-6}	-7.8×10^{-3}	-3.9×10^{-12}
4	p_2	27.8	1.1×10^{-5}	1.3×10^{-4}	3.8×10^{-2}	1.5×10^{-10}
4	p_1	37.6	4.8×10^{-5}	-5.0×10^{-4}	-7.0×10^{-2}	-7.7×10^{-10}
4	f	41.5	7.6×10^{-3}	-2.7×10^{-4}	-3.0×10^{-3}	-4.6×10^{-10}
4	g_1	46.9	3.3×10^{-3}	5.1×10^{-4}	8.8×10^{-3}	1.0×10^{-9}
4	g_2	52.3	2.9×10^{-3}	1.5×10^{-3}	2.8×10^{-2}	3.2×10^{-9}
4	g_5	67.9	2.2×10^{-3}	3.5×10^{-3}	7.2×10^{-2}	9.9×10^{-9}
4	g_{17}	159	1.9	3.1×10^{-3}	2.2×10^{-3}	2.0×10^{-8}

Photospheric amplitudes $\tilde{\Phi}_{n\ell}(1)$ of the perturbed gravitational potential for a selection of modes of low degree. Included are the g modes with periods close to 160^m. The amplitudes $\tilde{\Phi}_{n\ell}(1)$ and the norms $\tilde{I}_{n\ell o}$ for the axisymmetrical modes correspond to the normalization $\tilde{\xi}_{n\ell}(1) = 1$. The quantity $J_{n\ell o}$ is the value of $\tilde{\Phi}_{n\ell}(1)$ for the axisymmetrical mode with rms radial velocity amplitude V, averaged over the photosphere, of 1 ms^{-1}. To obtain the corresponding values $J_{n\ell m}$ for values of m greater than zero, multiply $J_{n\ell o}$ by $[2(\ell-m)!/(\ell+m)!]^{1/2}$. $J_{n\ell m}$ scales linearly with V. For comparison, the corresponding measure J_2 of the static gravitational quadrupole moment induced by a uniform rotation of the sun with period $25^d.4$ would be 1.8×10^{-7}.

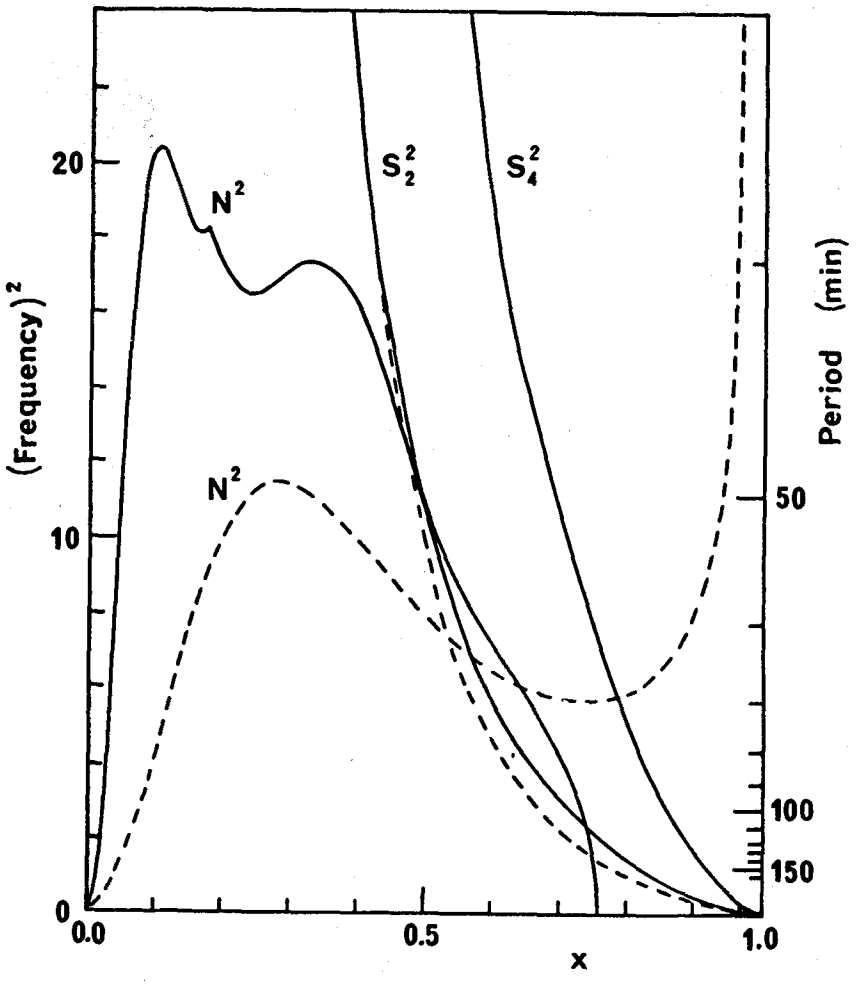

Figure 2. Squares of the buoyancy frequency N and the acoustic frequencies S_2 and S_4 as functions of the fractional radius x. The ordinate scale on the left corresponds to measuring the frequencies in units of $(GM/R^3)^{1/2}$, the ordinate scale on the right indicates the corresponding periods in minutes. Continuous lines are for the solar model, dashed lines for the polytrope of index 3; for the latter it was assumed that the polytrope is composed of a perfect gas with $\gamma = 5/3$. The cusp in N^2 for the solar model at $x \simeq 0.17$ is an artifact which has probably resulted from having interpolated opacity tables linearly.

Consider first the p modes, whose motion is almost radial. These are evanescent in the cores of both models and oscillatory in the envelopes, except in a thin layer near the surface of the polytrope. The greatest contribution to the perturbed gravitational potential associated with such modes comes from near the base of the oscillatory region. This is partly because the sound speed c_s increases with depth, and the wavelength of the spatial oscillations does likewise. Thus the largest coherently moving mass of fluid is that lying beneath the innermost node in $\tilde{\xi}$. One might wonder, of course, whether the decrease with depth of the oscillation amplitude outweighs this factor, but it is not the case. In the JWKB approximation $\tilde{\xi}$ varies approximately as $x^{-1}(\rho c_s)^{-1/2} \sin(\omega \int c_s^{-1} dx)$ in the oscillatory region, so the integrand in equation (6) is approximately proportional to $x^{\ell}(\rho/c_s)^{1/2} \sin(\omega \int c_s^{-1}\, dx)$. Provided ℓ is not too large, the rapid variation of ρ/c_s causes the amplitude of the sinusoid to increase with depth.

It is evident from this argument that at $x = 1$ the phase of the p-mode gravitational potential perturbation is determined by the displacement beneath its innermost node. Thus $\tilde{\Phi}(1)$ is negative for odd order modes and positive for even modes, irrespective of degree. It is also evident that because the densities and sound speeds in the solar model and polytrope are roughly similar throughout most of their interiors, as can be seen from Figures 1 and 2, so must be the eigenfunctions. Consequently the amplitudes $\tilde{\Phi}(1)$ predicted by the two models should be very similar, provided the eigenmodes are normalized to have constant energy; this is indeed the case. There is some difference, however, when the normalization is a constant surface displacement. Because in the polytrope density falls the more steeply with radius near the surface, the displacement eigenfunction rises the more rapidly. Hence at fixed surface amplitude, the polytropic p modes have the lower energy, and perturb Φ less.

The differences between g modes of the solar model and the polytrope are more complicated, and here we shall concentrate on the major aspects that concern Φ. One can see from Figure 2 that in the solar model g-mode eigenfunctions are oscillatory in the interior, where $\omega^2 < N^2$ and $\omega^2 < S_\ell^2$ and the modes behave locally as g modes, and also in the outer regions where $\omega^2 > N^2$ and $\omega^2 > S_\ell^2$ and the modes behave locally as p modes. There is a thin evanescent region between. On the other hand polytropic g modes are oscillatory only in the interior. A second notable difference between the models is that the variation of N^2 in the region where the kernels K^ℓ are substantial is less in the polytrope than it is in the solar model.

The JWKB approximation to the radial displacement for g modes is $(x^3 \rho N)^{-1/2} \sin[\omega^{-1} \sqrt{\ell(\ell+1)} \int x^{-1} N dx]$. Because in the solar model N decreases with x in the region where K^ℓ is relatively large, the wavelengths of the g modes increase with x. In the oscillatory region above $x \simeq 0.3$, the amplitude of the sinusoid in the asymptotic approximation increases with x, almost exactly compensating the decline in

$K^{\ell}(x)$ in the integrand in equation (6) when $\ell = 2$, and overcompensating when $\ell > 2$. Moreover, except for the modes of lowest order, the oscillatory region in the convection zone is too weak to produce a node in the displacement eigenfunctions. Thus one would expect the dominant contribution to $\tilde{\Phi}(1)$ to come from the region above the outermost node, and this is indeed the case for all the g modes listed in Table 1, even though the amplitudes of the oscillations in their eigenfunctions increase with x more slowly than $(x^3 \rho N)^{-1/2}$. In this outer region $\tilde{n} > 0$, being $\omega^{-2}\tilde{\xi}$ at $x = 1$ if ω is measured in units of $(GM/R^3)^{1/2}$, and consequently $\tilde{\Phi}(1) > 0$.

Except for the modes of lowest order, n is equal to the number of nodes in $\tilde{\xi}$. Because the variation of N causes the relative spacing of those nodes to vary with x more widely in the solar model, the uppermost node is deeper in the sun than it is for a mode with the same n and ℓ in a polytrope of index 3. Thus there is a larger mass oscillating in phase where the contribution to $\tilde{\Phi}(1)$ is greatest, and the potential perturbation at constant $\tilde{I}$ is greater for the solar model than for the polytrope. For the $g^5(\ell = 2)$ mode, for example, $\tilde{\Phi}(1)/\tilde{I}^{1/2}$ for the solar model is five times that for the polytrope. This difference is reduced, but not removed, if the comparison is made at constant amplitude of the displacement at the surface, since the larger evanescent region in the polytrope produces a greater reduction in the surface amplitude relative to the amplitude in the interior. The ratio of the potential perturbations in the two models due to $g^5(\ell = 2)$ oscillations with like surface amplitudes is only 2.5. Note, however, that this compensating factor decreases as the period increases above about 140^m, since the evanescent region then increases for the solar model and decreases for the polytrope.

We should remark that if instead comparison between the solar model and the polytrope is made at constant surface amplitude for g modes of the same degree but with about the same frequency, the differences are reduced still further, because in the oscillatory regions N^2 is lower for the polytrope and therefore n is lower for a given frequency. The values of $\tilde{\Phi}(1)$ for quadrupole modes in the solar model with periods near 160^m are only about 30 percent greater than those of polytropic modes with similar periods. We should also note that a solar model with a deeper convection zone, and hence a larger evanescent region at low frequencies, produces higher values of $\tilde{\Phi}(1)$ at fixed surface amplitude. For example, a model with heavy element abundance Z = 0.02 computed with the stellar evolution program described by Christensen-Dalsgaard (1980) has a convection zone 2.0×10^5 km deep, in agreement with conclusions drawn from analyses of the five minute oscillations by Berthomieu et al. (1980) and Lubow (1980). This model supports a $g^{10}(\ell = 2)$ mode (whose period of 166^m is the closest amongst the quadrupole modes to 160^m) which for a given surface amplitude has an associated $\tilde{\Phi}(1)$ some 50 percent greater than that quoted in Table 1 for $g^9(\ell = 2)$.

The discussion above describes all but the solar f, g^1 and g^2 modes. In the

polytrope the g^1 and g^2 modes follow the trends of the g modes of higher order and the f mode is a genuine surface mode; but in the solar model the surface oscillatory region imparts a strong p-mode character to these oscillations, and the f mode has g-mode character in the deep interior where its frequency is below N. Consequently the solar modes tend to have more nodes than their polytropic counterparts, which produces substantial cancellations in the integral in equation (6), reduces $\tilde{\Phi}(1)$ below the polytropic values and, in the case of the f mode, even changes its sign.

5. DISCUSSION

Of the modes of low degree, quadrupole oscillations generate the greatest perturbations to the gravitational potential when normalized to constant photospheric velocity amplitude. Moreover, it is the quadrupole perturbations that decline most gradually with distance from the sun. Therefore the oscillations that extraterrestrial probes are most likely to detect are those with $\ell = 2$.

It is straightforward to show that a solar quadrupole oscillation with rms photospheric radial velocity amplitude V would perturb the velocity of a body in orbit a distance d from the center of the sun by an amount whose component along the line of sight to the earth is about

$$v = \alpha J_{n2m} \left(\frac{R}{d}\right)^2 \frac{GM}{d^2 \omega_{n2m}} V \sin(\omega_{n2m} t + \psi) \quad . \tag{11}$$

Here α is a factor of order unity and the values of α and ψ depend on the elements of the orbit and m. An electromagnetic signal to the earth of frequency ν emitted by such a body would be Doppler shifted by an amount $\Delta\nu = \nu v/c$, where c is the speed of light. In the period range 10^2 - 10^4 s, according to Estabrook et al. (1979), it should be possible to detect oscillations in the Doppler shift of signals from extraterrestrial probes if the amplitudes $\Delta\nu/\nu$ are no less than a few parts in 10^{15}, and one such probe is planned to pass within about 3 solar radii of the sun.

Suppose, for example, we regard the solar $g^9(\ell = 2)$ oscillation as a contender for the cause of the 160^m spectral line shift oscillations discovered by Severny, Kotov and Tsap (1976) and Brookes, Isaak and van der Raay (1976). This mode would induce in a signal from a probe an oscillatory Doppler shift with amplitude $\Delta\nu/\nu \simeq 10^{-10} V(R/d)^4$, where V is measured in ms^{-1}. Though it would be naive to believe that the solar line shifts measured by Brookes, Isaak and van der Raay (1976); and Severny, Kotov and Tsap (1976) are simply the result of a pure Doppler shift from the large scale oscillation velocity of the mode, it is not unreasonable to suspect that the quoted shifts of about 1 ms^{-1} might not be wholly unrepresentative of the oscillation amplitude V. If that were indeed the case, the gravitational field perturbations of at least the 160^m oscillations should be

detectable. Moreover, the amplitude of the oscillatory gravitational quadrupole moment would be only a factor 3 or so less than the static component J_2 induced by centrifugal forces if the solar rotation were approximately uniform.

* * * * *

We are grateful to G.W. Gibbons, J. Hough, J. Papaloizou, J.E. Pringle, R. Scuflaire and J. Weber for interesting conversations on this subject.

REFERENCES

Berthomieu, G., Cooper, A.J., Gough, D.O., Osaki, Y., Provost, J. and Rocca, A. 1980, these proceedings.

Brookes, J.R., Isaak, G.R. and van der Raay, H.B. 1976, Nature, 259, 92.

Christensen-Dalsgaard, J. 1976, Mon. Not. R. Astr. Soc., 174, 87.

Christensen-Dalsgaard, J. 1980, submitted to Mon. Not. R. Astr. Soc.

Christensen-Dalsgaard, J., Dilke, F.W.W. and Gough, D.O. 1974, Mon. Not. R. Astr. Soc., 169, 429.

Christensen-Dalsgaard, J., Dziembowski, W. and Gough, D.O. 1980, these proceedings.

Christensen-Dalsgaard, J., Gough, D.O. and Morgan, J.G. 1979, Astron. Astrophys., 73, 121; 79, 260.

Cowling, T.G. 1941, Mon. Not. R. Astr. Soc., 101, 367.

Estabrook, F.B., Hellings, R.W., Wahlquist, H.D. and Wolff, R.S. 1979, Sources of gravitational radiation (ed. L.L. Smarr; Cambridge: Cambridge University Press), p. 37.

Hill, H.A., Stebbins, R.T. and Brown, T.M. 1976, Proc. V. Intern. Conf. Atomic Masses and Fundamental Constants (ed. J.H. Sanders and A.H. Wapstra; New York: Plenum), p. 622.

Johnson, W.W., Winget, D.E., Douglass, D.H. and Van Horn, H.M. 1980, these proceedings.

Lubow, S. 1980, these proceedings.

Severny, A.B., Kotov, V.A. and Tsap, T.T. 1976, Nature, 259, 87.

Zahn, J.-P. 1970, Astron. Astrophys., 4, 452.

OBSERVATIONAL TESTS OF PULSATION THEORY IN THE SOLAR ENVELOPE

R.T. Stebbins
Sacramento Peak Observatory[1]

H.A. Hill and R. Zanoni[2]
Department of Physics
University of Arizona

R.E. Davis[3]
Department of Physics
University of New Mexico

ABSTRACT

An improved observing technique has been used to look for long period oscillations in the brightness of the extreme solar limb. This technique provides a means for analyzing power spectra to secure a signature characteristic of the signal's origin. Results show significant improvement in the discrimination between solar oscillations, other signals, and noise. Long period intensity oscillations can be seen at the extreme solar limb.

1. INTRODUCTION

In the last few years, interest in stellar and solar pulsation has been growing. Knowledge of solar pulsations in particular has expanded greatly with the identification of the five minute oscillation as the superposition of many low amplitude p-modes (Deubner 1975) and the discovery of longer period (up to 1 hour) oscillations (Hill and Stebbins 1975; Brown, Stebbins and Hill 1978), a very long period (2 hr 40 min) oscillation (Severny, Kotov and Tsap 1976), and short period oscillations (e.g., Deubner 1976). With the exception of the first, all of the others are exceedingly difficult to detect by any method. Naturally, researchers sought stronger confirmation through intercomparison of different observational methods. Such intercomparison (see Hill 1978 for a summary) based on the theory of solar pulsation, did not confirm the difficult observations. Further, the

---

[1]Operated by the Association of Universities for Research in Astronomy, Inc. under contract AST 78-17292 with the National Science Foundation.
[2]Summer Research Assistant 1979, Sacramento Peak Observatory
[3]Summer Research Assistant 1977, Sacramento Peak Observatory

intercomparison revealed contradictions in the easy observations, namely the robust five minute oscillation. This has prompted, in some circles, reexamination of pulsation theory as applied to the solar envelope. The program reported here attempts to provide empirical answers to questions about the theory.

The theory of pulsation begins with the conservation laws, conservation of mass, conservation of momentum, and conservation of energy from which a wave equation can be derived. Sink and source terms must be filled in explicitly; most notably the radiative dissipation is represented by the Eddington approximation. Assuming small amplitudes, the equations are linearized. The particular solutions are computed with the aid of a model atmosphere and physical parameters such as the pressure and temperature derivatives of the opacity. The solutions predict the eigenfunctions, both amplitude and phase, versus height for displacement, velocity, temperature, pressure, etc. In order to arrive at a general solution, some assumption must be made about the boundary conditions so that some linear combination of solutions can be computed. In this paper, nature's solution is examined for insight into the theoretical approach.

The solar five minute oscillation is the most easily observable stellar pulsation known. It is robust. It can be spatially resolved on the sun's surface. It can be resolved, to some extent, in height throughout the photosphere and low chromosphere. The varying superposition of p-modes naturally generates a range of amplitudes from 25 m/sec (lower amplitudes are very uncommon) to 1000 m/sec. Theory (Hill, Caudell and Rosenwald 1979) predicts these modes should have similar eigenfunctions (< 10% maximum, point-to-point variation between displacement eigenfunctions below the temperature minimum). This is important since the changing superposition might otherwise result in a changing solution. One difficulty, common to all observations of spectral lines, is separating line formation effects from the global pulsation effects. This problem will be addressed in future work; the focus in this paper is the observed velocity response, its form and linearity.

2. METHOD

The method used to analyze the velocity response is somewhat intricate. To prepare the reader, it is summarized beforehand. A high resolution spectral line profile is acquired every few seconds for about forty minutes. This time sequence of line profiles is reduced to nine velocity time series by determining the Doppler shift at nine depths in the line. From each velocity time series, a time series of velocity amplitude is then extracted, the collection of which characterize the velocity eigenfunction. A relative eigenfunction is obtained by selecting one string as a reference and computing the ratio of the amplitude at each of the other line depths to the reference depth. An average, relative eigenfunction is obtained by averaging the eight ratios over all time steps and all time strings. Standard

deviations are similarly compiled. The final result is an average velocity amplitude at eight photospheric heights in the units of the amplitude at the reference height. Each average is accompanied by its standard deviation.

In a parallel analysis of the amplitude time series the linearity of the photosphere's response to an oscillation can be tested by comparing the response at each line depth with the response at the reference depth as the amplitude of oscillation changes. To this end, the amplitudes are discretized into 25 m/s ranges, the time strings are searched, and the occurrences of a particular amplitude and associated reference amplitude are counted for each line depth. The result is eight two-dimensional histograms showing the frequency of occurrence of an amplitude at one depth when a given amplitude is found at the reference depth. The ridges in these functions are straight in the event of linear response, and curved in the presence of non-linearities. So much for the summary.

An Fe I spectral line, 5434A, was chosen for the work reported here; three other Fe I lines were also used, but will be reported elsewhere. This line is distinguished by being the g = 0 line formed at the greatest height (530 km above $\tau_{5000} = 1$, Altrock et al. 1975); it is also unblemished by blends and blessed by a multi-level, non-LTE calculation. The data were acquired using the Vacuum Tower Telescope, the Echelle spectrograph and the Diode Array at Sacramento Peak Observatory. The spectrograph sampled a small patch 1" x 4" at disk center; the line profile and surrounding continuum were digitized into 64 samples, each 14.6 mA wide. In 8.55 seconds the profile was sampled 512 times, averaged and recorded. This procedure was repeated 256 times to form a sequence approximately 37 minutes long.

The data used here, 57 sequences, have been selected to exclude those affected by clouds, instrumental problems, and other non-solar idiosyncrasies--about 35 hours of data. These data were gathered in two observing runs, 7-8 November 1978 and 8-12 February 1979.

Data reduction was begun by interpolating the line profiles on a four-times denser grid using Fourier bandwidth limited interpolation (the Fourier methods used in this study follow the work of Brault and White 1971). High spectral frequencies were suppressed to reduce ringing between original data points. The interpolation was performed in anticipation of determining the bisector of the line between original data points. Fourier interpolation followed by linear interpolation on the denser grid improves the accuracy of bisector determination over simple linear interpolation on the original grid.

Before proceeding with the velocity derivation, it is wise to carefully define the measurement leading to velocity. Generally, an oscillation will affect the spectral line position through the Doppler shift and the spectral line shape through induced, frequency dependent, intensity variations. Ideally, one would like to follow the velocity of one gas element on the sun by tracing the changes at one

depth in a spectral line. However, opacity perturbations may well cause light forming a particular part of a spectral line to emanate from slightly different parts of the solar atmosphere during an oscillation. Rigorous identification of the Doppler shift would require better knowledge of line formation than is presently available, and a very detailed description of the pulsation. Progress can be made, though, through empirical definition of a "velocity-like" signal.

The grid of line depth points is defined by a preselected series of line widths, the first width being the spectral sample size and successive widths being two sample sizes larger than the previous. In this manner, nine depth points are defined which correspond to independent spectral samples. The velocity associated with a preselected width is determined by locating the bisector of the line at that point where the line has that width. Thus the reduction proceeds by analyzing each line profile for a bisector at nine different line widths and forming time strings of these nine quantities. Figure 1 shows a sample line profile and the line depths at which the velocities are determined. Quantities pertaining to the depth points will be referred to by the numbers 1 to 9 ranging from the deepest to the shallowest point in the line, or from the highest to the lowest point in the solar atmosphere.

The nine time strings (see Figure 2) are bandpassed using Fourier methods. Processing removes the average and a linear trend, applies a 10% cosine bell to the end points, Fourier transforms the signals into the frequency domain, and bandpasses the transform. The bandpass filter tapers the transform from zero at 1.125 mHz to its full value at 2.475 mHz and from full value at 4.725 mHz to zero again at 6.075 mHz, the full width at half maximum is 3.60 mHz, centered at 3.60 mHz. The filter parameters were chosen to include all power in the five minute band as manifested in an average of 30 power spectra. The bandpassed transforms are used to generate the oscillatory amplitude as a function of time.

The amplitude A(t) of a time series x(t) can be computed from a complex function called the analytic signal z(t),

$$z(t) = A(t) \exp\left(i\Phi[t]\right) = x(t) + i\hat{x}(t) \quad , \tag{1}$$

where $\Phi(t)$ is the phase and $\hat{x}(t)$ is the quadrature function associated with x(t), the signal under analysis. The signal and its quadrature form a Hilbert transform pair, defined by

$$\hat{x}(t) \equiv \text{principal value of } \left\{\frac{1}{\pi}\int_{-\infty}^{\infty} \frac{x(\tau)d\tau}{\tau - t}\right\} \quad . \tag{2}$$

The amplitude is the magnitude of the analytic function which can be easily computed from the discrete Fourier transform. For further information on the analytic signal and Hilbert transforms, see White and Cha (1973), being leery of sign errors,

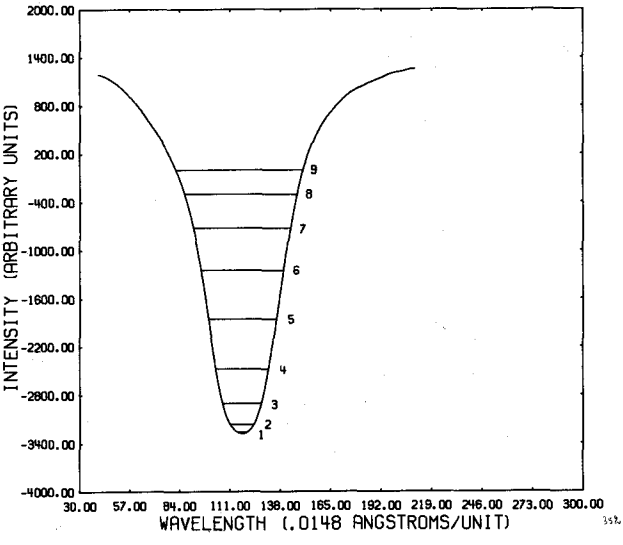

Figure 1. A sample line profile from Fe I 5434 is shown with the locations of the depth points 1-9. Depth point #6 is the reference referred to in the text.

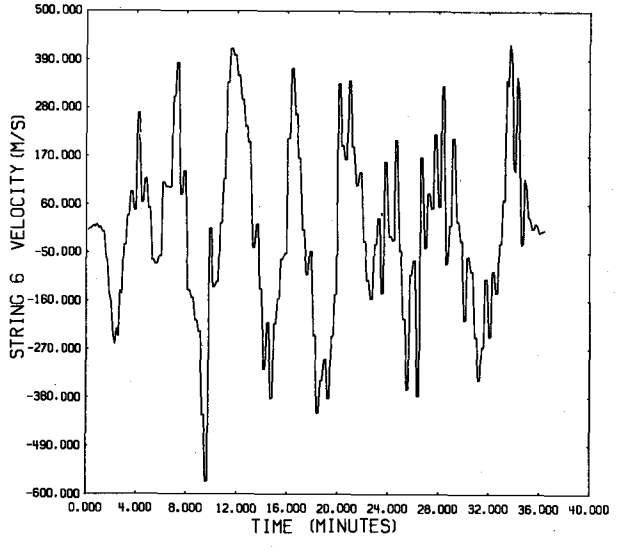

Figure 2. A sample velocity time series is displayed. This is the velocity sequence for the reference string (#6) from a data set starting 8 February 1979, 20:42:28 GMT.

Middleton (1960), and Bracewell (1965). By these means, the velocity amplitudes at nine different heights in the solar atmosphere are obtained at each time step (see Figure 3). Because of the slowly decaying kernel in equation (2), the first and last 10% of the time strings are excluded from the accumulations of averages described below.

The time series are examined time-step-by-time-step wherein the ratios of the velocity amplitude at the comparison depth points to that at the reference depth are computed and accumulated in a running sum for each comparison depth. The squares of the eight ratios are similarly accumulated for later calculation of a standard deviation. Time steps where the reference velocity amplitude is less than 125 m/s were excluded from the accumulations because of the ratio's susceptibility to noise in a small denominator. After all time series have been scanned, the mean and the standard deviation of the mean are computed for each line depth. In all, 9,755 points contributed to the averages.

The result of this procedure is the mean variation of velocity amplitude as a function of height in the solar atmosphere. Velocity amplitude appears in the units of the amplitude at the reference height, i.e., amplitudes are normalized to 1.0 at height #6. The height in the atmosphere is implied through line width. In short, the result is a normalized velocity eigenfunction presented as a peculiar height scale.

The amplitude time series are easily reduced to show the linearity of the photosphere's response to an oscillation. As the time steps are scanned, each line depth, including the reference, is categorized as falling into a 25 m/s amplitude interval. For each line depth, the occurrences of a particular velocity amplitude and corresponding reference amplitude are counted. The result is eight two-dimensional histograms whose independent variables are reference amplitude and amplitude at a particular line depth. When plotted, this function shows the velocity amplitudes occurring at one height in the solar atmosphere for a given reference amplitude.

3. THE EIGENFUNCTION

The normalized velocity eigenfunction derived by the method described above is shown in Figure 4. The function plotted there monotonically decreases from line depth #1 to a minimum near depth #8 followed by a faint upturn at depth #9. The standard deviation of the mean at each depth is equal to or less than .0044, less than the width of the line. By this measure, the means are all systematically and significantly different. Note that the standard deviation need not be due to noise alone, but rather may be due in part to a systematic variance in the signal, as will be discussed in the next section. Using the standard deviation as an indicator of significance is graciously conservative.

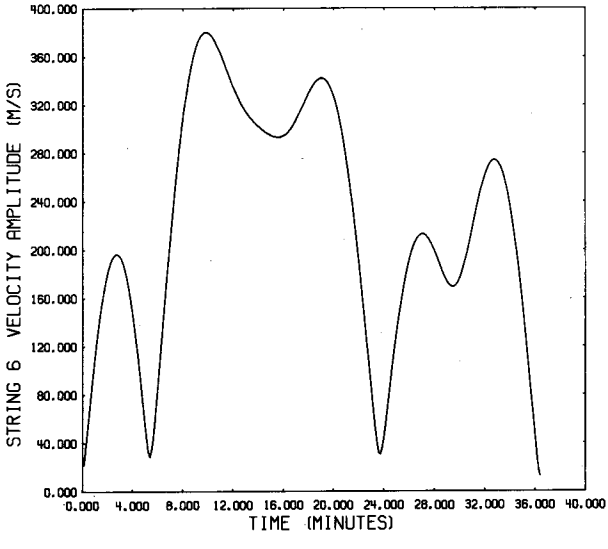

Figure 3. This amplitude time series is derived from the velocity time series in Figure 2 through the Hilbert transform and the analytic function.

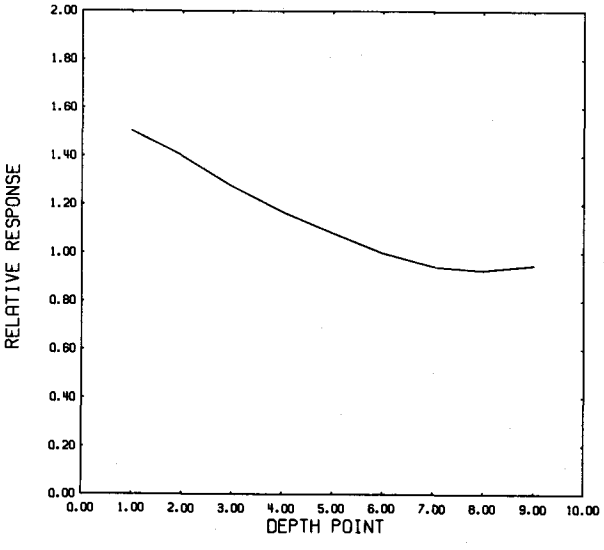

Figure 4. The normalized velocity eigenfunction characterizes the variation of velocity amplitude with height in the photosphere. The abscissa is labeled by the line depth point. Point #1 is approximately the temperature minimum; point #9 is the bottom of the photosphere. The ordinate is relative response normalized to 1.0 at the reference depth, line point #6. The largest standard deviation of the mean for any point is .0044, less than the width of the plotted line.

What can be deduced from this figure? Initially, one might question whether anything at all can be learned from a differential investigation of velocities determined at several points within one spectral line. The spectral sampling relates to an atmospheric height sampling through a contribution function. The contribution functions for the different line depths are not well known, probably overlap, and are likely influenced by the presence of an oscillation. Figure 4 clearly shows that systematic and unique height samples can be obtained. Ultimately, one would like to know what height range was being sampled by a Doppler measurement at one depth in a line. But for the purposes of this paper, this clear demonstration of height resolution will suffice.

The more enlightening feature of Figure 4 comes from a comparison to theoretical eigenfunctions. To do this completely requires associating each line depth with a physical height in the photosphere, via line formation theory. However, the essential deduction can be gotten by noting that the depth samples span the photosphere and comparing the observed and predicted photospheric variation in the eigenfunction. Based on a multi-level, non-LTE model, Altrock et al. (1975) find Fe I 5434 A line center formed at 530 km above $\tau_{5000} = 1$; the same locates the temperature minimum at 555 km. Ninety percent of the contribution function comes between 420 km and 730 km. For all practical purposes, line formation theory predicts that depth point #9 is formed at the bottom. Between these two points, the observed eigenfunction, shown in Figure 4, changes by a factor of 1.62 from minimum to maximum.

There appears to be only two theoretical calculations of photospheric, 5 min eigenfunctions in the literature. The first (Ando and Osaki 1975) is not ideal for this comparison, but fails to show a minimum in the low photosphere and has a minimum-to-maximum change of a factor of 1.2. The second (Hill 1978, Figure 6.1) qualitatively has a very similar form, most notably the minimum in the low photosphere. Though this calculation extends only to $\tau_{5000} = .002$ (about 380 km in the model above), the minimum-to-maximum variation is 2.54. If the theoretical eigenfunction continues to rise beyond $\tau_{5000} = .002$ as the empirical eigenfunction does in its upper reaches, the theoretical variation will be 2-3 times the observed variation. Clearly, either this line is not formed where line formation theory predicts, or pulsation theory is lacking something.

4. NONLINEARITY

Three of the eight two-dimensional histograms are shown in Figure 5. One notices firstly that each plot has a dominant ridge running from lower left to upper right, but that otherwise the plots are different. The histograms for line depth points #1, 4 and 9 vary in width, subordinate ridges and peaks, and slightly in the orientation of the dominant ridge. The first and last have a very complex

topography.

The primary concern is whether the ridges are generally straight or not. If the relative velocity amplitudes between, say, line depth #1 and line depth #6 are constant for all size oscillations, then the ridge should be straight, and the oscillating system is linear. Said another way, the relative eigenfunction does not change with wave amplitude. To test this linearity, a straight line has been fit by eye to the ridge section encircled by the highest contour. [Numerical averaging and/or fitting tends to get confused by the subordinate ridges and peaks. The straight line shown happens to agree with the averages in Figure 4.] If the system is linear, the ridge line extrapolated from low velocities should coincide with the ridge line at high velocities.

These three contour plots show that the dominant ridges have roughly the correct slope and the slope decreases from line depth #1 to line depth #9 as expected. The differences between the plots demonstrate height resolution once again.

The most important deduction from these histograms is the nonlinearity indicated by the straight line. Above 500-600 m/s reference amplitude, the ridge line extrapolated from low amplitudes is systematically below the apparent ridge line. This is most apparent for line depth #1, as expected where the greatest altitude difference lies. This nonlinearity occurs at velocities more than an order of magnitude below the sound speed.

The last observation to be made from these plots is the complex topography in Figures 5a and 5c. The peaks connected to the dominant ridge by low ridges are not likely random noise by virtue of the number and concentration of occurrences of these velocities. They suggest an eigenfunction that is altered occasionally by a recurring change in physical conditions. This variance in the signal contributes to the standard deviation mentioned in the previous section.

5. CONCLUSIONS

The solar five minute oscillation can be a useful diagnostic of pulsations in a stellar atmosphere. The five minute oscillation is readily detectable over a wide amplitude range and, as shown here, the height dependence can be resolved. Further, it is important to solar physics to understand pulsation in this most observed region.

The empirical eigenfunction provides a valuable test of pulsation theories. Of the two theories examined one differs qualitatively in functional form but more closely predicts the quantitative minimum-to-maximum variation. The other agrees well in functional form, but predicts 2-3 times the minimum-to-maximum variation observed. The latter theory incorporates a different approach to boundary conditions which mixes in a solution giving the observed functional form. However, unless the

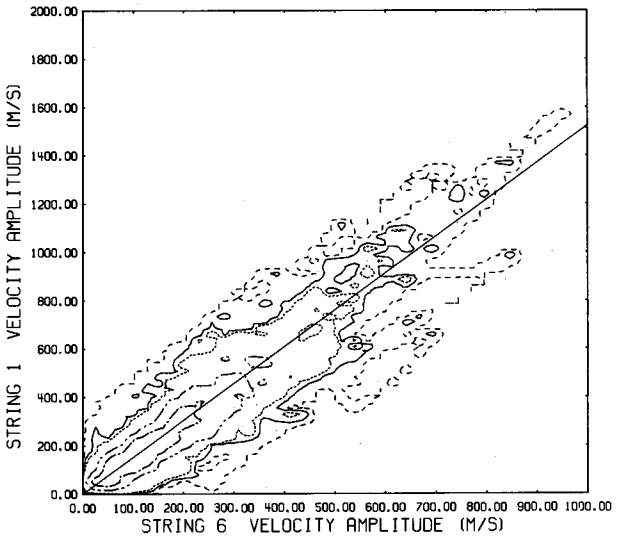
STRING 1 VELOCITY AMPLITUDE (M/S)
2000.00
1800.00
1600.00
1400.00
1200.00
1000.00
800.00
600.00
400.00
200.00
0.00
0.00 100.00 200.00 300.00 400.00 500.00 600.00 700.00 800.00 900.00 1000.00
STRING 6 VELOCITY AMPLITUDE (M/S)

(a)

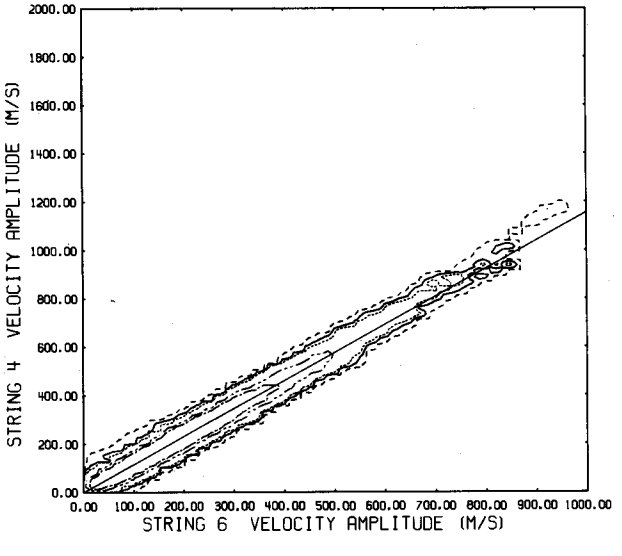
STRING 4 VELOCITY AMPLITUDE (M/S)
2000.00
1800.00
1600.00
1400.00
1200.00
1000.00
800.00
600.00
400.00
200.00
0.00
0.00 100.00 200.00 300.00 400.00 500.00 600.00 700.00 800.00 900.00 1000.00
STRING 6 VELOCITY AMPLITUDE (M/S)

(b)

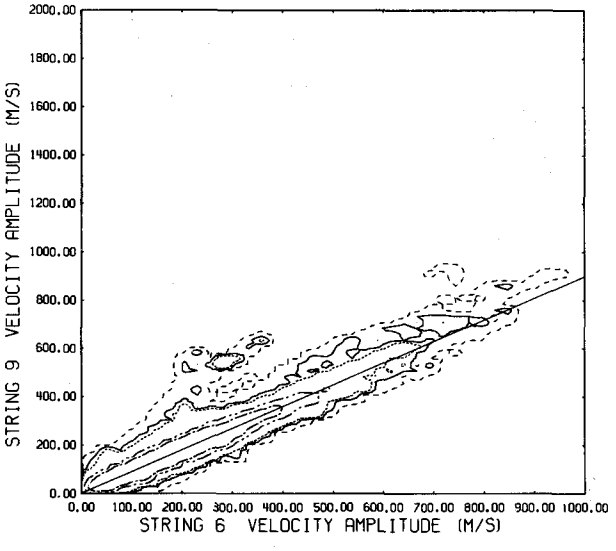

(c)

Figure 5. The two dimensional histograms of velocity amplitude at two line depths are shown in these three contour plots for (a) line depth #1, (b) line depth #4, and (c) line depth #9. The reference is the other line depth, appearing on the horizontal axis, in all cases. The contours are > 1 occurrence (dashed line), > 5 ocurrences (solid line), > 10 occurrences (dotted line), > 50 occurrences (dash-dot-dotted line), and > 100 occurrences (dash-dotted line). The resolution element is 25 m/s x 25 m/s. 11,628 points are shown. The straight line is a fit by eye to the ridge line in the region encircled by the highest contour. Note the peaks and connecting ridges in (a) and (c).

line formation theory is grossly in error, the calculated eigenfunction is not nearly as flat as the observed eigenfunction. A limitation in the treatment of pulsations seems to be indicated.

The evidence for nonlinearity also reveals complications for pulsation theory. The velocity response at mid-altitudes seems to be depressed relative to other heights for velocities greater than 500 m/s. This may be the manifestation of amplitude dependence in line formation processes. This point will be addressed in a later report. If the nonlinearity is truly in the atmosphere's response, then its cause needs to be uncovered and accounted for by the theory.

The complex behavior seen in two of the histograms complicates the picture. The eigenfunction appears to vary in time. Understanding the physics of waves in the solar atmosphere will require understanding this temporal behavior.

* * * * *

We wish to thank Horst Mauter, Dick Mann and Gary Phillis for their observing support on this project. Jacques Beckers, Timothy Brown, Dick White and Lawrence Cram have made helpful comments during the course of this work. Ms. Christy Ott prepared the manuscript and revisions.

REFERENCES

Altrock, R.C., November, L.J., Simon, G.W., Milkey, R.W. and Worden, S.P. 1975, Solar Phys., 43, 33.

Ando, H. and Osaki, Y. 1975, Publ. Astron. Soc. Japan, 27, 581.

Bracewell, R.N. 1965, The Fourier Transform and its Application (New York: McGraw-Hill).

Brault, J. and White, O.R. 1971, Astron. Ap., 13, 169.

Brown, T.M., Stebbins, R.T. and Hill, H.A. 1978, Ap. J., 223, 324.

Deubner, F.-L. 1975, Astr. Ap., 44, 371.

Deubner, F.-L. 1976, Astr. Ap., 51, 189.

Hill, H.A. 1978, The New Solar Physics (ed. J.A. Eddy; Boulder: Westview Press), Chap. 5.

Hill, H.A., Caudell, T.P. and Rosenwald, R.D. 1979, private communication.

Hill, H.A. and Stebbins, R.T. 1975, Ann. N.Y. Acad. Sci., 262, 472.

Middleton, D. 1960, An Introduction to Statistical Communication Theory (New York: McGraw-Hill).

Severny, A.B., Kotov, V.A. and Tsap, T.T. 1976, Nature, 259, 87.

White, O.R. and Cha, M.Y. 1973, Solar Phys., 31, 23.

ON THE STUDY OF GLOBAL OSCILLATIONS OF THE SUN VIA FLUCTUATIONS IN THE SOLAR LIMB DARKENING FUNCTION

J. Knapp, H.A. Hill and T.P. Caudell
Department of Physics
University of Arizona

ABSTRACT

Global solar oscillations have been shown to be primarily observable through changes in the solar limb darkening function. The observational search for these changes is hampered by problems associated with changes in the earth's atmosphere. Attempts by several investigators to deal with these problems are reviewed and the results are reproduced from the most successful of these. The pros and cons of the various techniques used in these observations are brought into focus by an analysis of their individual ability to deal with the earth's atmosphere.

1. INTRODUCTION

One of the more surprising results to come from the study of global solar oscillations with periods between $\sim$ one hour and five minutes is the ability to detect their presence primarily through changes in the solar limb darkening function, I(r) (Hill and Caudell 1979). This property clearly points to a lack of understanding of the processes influencing the photospheric portion of the eigenfunctions of these oscillations (Hill, Rosenwald and Caudell 1978; Keeley 1977). Directly observing the spatial properties of the Eulerian perturbation in radiation intensity, I', near the solar limb, insight germane to the clarification of this problem may be gained. In addition to obtaining a better understanding of the physics in the solar envelope, determination of the spatial properties of a given normal mode could be helpful in ascertaining its modal classification, in designing forthcoming observing programs, and in planning second generation telescopes for the study of solar oscillations.

Identifying the component of I' associated with the global oscillations requires the establishment of an appropriate inertial coordinate system in which to make measurements of I. A means of discriminating against the numerous non-periodic solar phenomena (Keil and Worden 1980) and against the non-periodic fluctuations in the earth's atmospheric column density along the line of sight (Fossat et al. 1977; KenKnight et al. 1977) is also necessary. The need for this inertial coordinate system and the techniques available to address this class of problems are both

generally overlooked. It is with this in mind that in the following we review the origin of these problems and the techniques that can be used to overcome the limitations they pose. In the last section the results from the successful application of these techniques by Hill, Knapp and Caudell (1980) to study the global oscillatory component of I' are summarized. Also presented are the results of their work on the isolation of the atmospheric differential refraction contribution to solar diameter measurements.

2. EULERIAN PERTURBATIONS AND REFERENCE FRAMES

For some time the need has been appreciated for care in theoretical studies of perturbations in, for example, hydrodynamic systems wherein two types of perturbations are commonly used; the Lagrangian and the Eulerian. However, only recently has it become necessary to exercise similar care in theoretically predicting from the eigenfunctions the properties of observed quantities (see Appendix A of Hill, Rosenwald and Caudell 1978). This has consequently required caution in the planning and interpretation of observations on global oscillations of the sun. It is this latter point that we wish to examine here.

Many types of solar observations require no particular care in making the observations relative to, for example, the center of mass of the sun. However, if observations of solar oscillations are being made near the solar limb with reference to a locally defined edge of the solar disk, as is the case in many instances, the fluctuations observed in I are generally being measured in a moving reference frame. The correction term encountered in the transformation back to a coordinate system fixed with respect to the center of mass of the sun is simply the first spatial derivative of the limb darkening function over the region of observation multiplied by the physical displacement of the local coordinate system relative to the center of mass of the sun. This correction term is typically the same size as the fluctuations in I measured in the moving frame. Should the motion of the reference frame not be measured, it is subsequently difficult if not impossible to compare theory and observations of changes in the limb darkening function.

Two examples of this type of difficulty may be found in the solar limb edge work of Brown (1979) and Stebbins (1980). For both cases, measurements were made only on one limb yielding no knowledge of the moving coordinate system with respect to the center of mass of the sun. In the case of the work by Stebbins (1980) wherein the problems arising from the earth's atmosphere (see §§ 1.3 and 1.4) have been overcome, it was possible to identify an important feature of I' but not able to recover I' completely.

An appropriate reference frame may be established in order to study I' by making distance measurements (simultaneous with those of I) from the edge of the sun under study to the diametrically opposite limb of the sun. For the lower values of

ℓ, the principle order number in the spherical harmonic describing the spatial properties of a global mode, the diameter obtained using the finite Fourier transform definition (FFTD) of an edge on the solar limb (Hill, Stebbins and Oleson 1975) is primarily sensitive to even values of ℓ. Thus for even ℓ, the centroid of the measured diameter is expected to coincide with the center of mass of the sun and the amplitude of the diameter changes is twice the displacement of the local coordinate system of measurement. The even ℓ components of I can be projected out by averaging the observed I from the two diametrically opposite limbs. Thus it is possible to establish an appropriate coordinate system for the study of the spatial properties of a global oscillatory component in I', providing the values of ℓ are low. This technique has been used by Hill, Knapp and Caudell (1980) to study I' (this work is reviewed in § 6).

It should be emphasized that the simultaneous measurements of I at diametrically opposite limbs and the associated diameter will permit the establishment of an appropriate coordinate system, but, in itself, does not allow for the removal of seeing effects or fluctuations in the column density of the earth's atmosphere. Other techniques are required for this, as are described in the following sections (§§ 4 and 5).

3. GLOBAL OSCILLATORY COMPONENT OF I': IDENTIFICATION

The spectrum of global oscillations of the sun appears to be quite rich in the spectral range between $\sim$ one hour and five minutes (cf. Brown, Stebbins and Hill 1978). This fact coupled with the small size of the signals associated with the global oscillations makes the process of adequate noise discrimination, as well as the determination of their spatial and temporal properties, quite difficult. There is at this time one technique which far exceeds all the others in its potential to identify a particular global oscillation. This technique exploits the long "lifetime" of the global oscillations as embodied in the phase coherence of the oscillations; it has been used by Hill and Caudell (1979); Caudell and Hill (1980); and Caudell et al. (1980) with particularly impressive results in the latter of these.

4. ATMOSPHERIC SEEING

Efforts to remove the effect of seeing in the study of solar oblateness has led to the development of the finite Fourier transform definition (FFTD) of an edge of the solar limb, mentioned earlier, which is quite insensitive to atmospheric seeing effects (Hill, Stebbins and Oleson 1975). The FFTD can also be used to minimize seeing effects in the study of I'. An example of where the FFTD has been applied to such a study is found in the work of Stebbins (1980); he studied the location of the edge given by the FFTD as a function of the fraction of the limb used in the FFTD. In this manner Stebbins was able to obtain the finite Fourier transform

free of seeing effects of the I' (cf. Hill, Stebbins and Oleson 1975) in an oscillating coordinate system.

The observing program of Stebbins (1980) can be thought of as first using the FFTD to establish a coordinate system not influenced by seeing and then further using the FFTD to study the finite Fourier transform of I' in this moving coordinate system. This procedure requires relatively extensive computations and raises the question: Is it feasible to use the FFTD to only establish a coordinate system not influenced by seeing and then examine directly in those moving coordinate systems the fluctuations in the radiative intensity I'_m (the subscript m denotes I' measured in the moving frame of reference)? An example of this technique is found in the work of Brown (1979).

It is clear in this case that the seeing contribution I'_s to I'_m should manifest itself in the form of

$$I_s = \frac{d^2 I}{dr^2} \cdot \sigma^2 \qquad (1)$$

where σ^2 is the variance of the seeing transfer function. The temporal properties of I_s are essentially given by that of σ^2 while the spatial properties are determined by d^2I/dr^2. A typical I'_m obtained by the technique under discussion at 0.4 mHz is shown in Figure 1 and a sample of d^2I/dr^2 is shown in Figure 2. The signature of d^2I/dr^2 is apparent in Figure 1 and unfortunately, it is not possible to correct the results in Figure 1 for seeing without additional information. This is in fact one of the unresolved problems found in the analysis of Brown and Harrison (1979, 1980).

An alternative approach is available to remove the seeing contribution to fluctuations in I and simultaneously identify the global oscillatory component of I'. This approach taken by Hill, Knapp and Caudell (1980) uses the oscillatory components of the solar diameter (defined with the aid of the FFTD) exhibiting the long term phase stability as a reference signal to "phase sensitive detect" the corresponding phase coherent oscillatory component of I'. This procedure strongly discriminates against the seeing contribution due to the lack of long term phase coherency in the seeing. The work of Hill, Knapp and Caudell (1980) does not show the characteristic seeing signature of Figure 2 and is summarized in § 6.

The framework for a third approach has been constructed. In this work by Hill et al. (1979) a formalism has been developed where, in a systematic convergent procedure, a weighting function different from that used in the FFTD is assembled to define an edge of the sun which possesses a low sensitivity to seeing similar to that in the FFTD. However, the new edge definition will in general exhibit a sensitivity to changes in the limb darkening function different from that of the FFTD. These different sensitivities may be used to infer information on I'. Although no application of this technique has been made to date beyond the preliminary work of Ballard (1978), it may prove quite useful in future work.

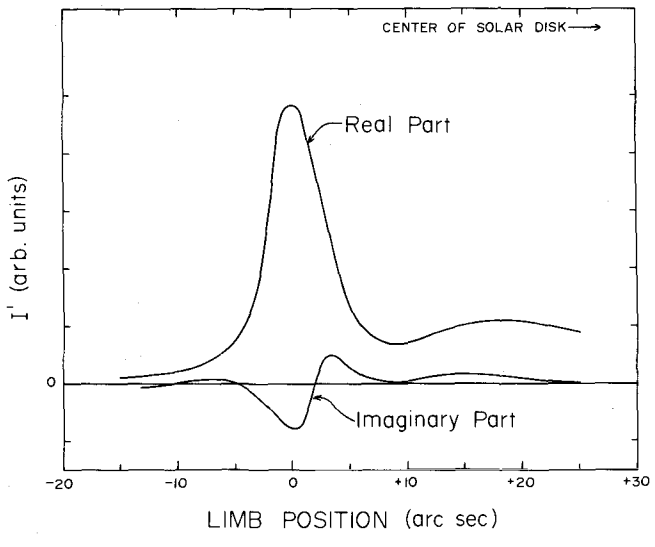

Figure 1. The averaged oscillatory component of the observed limb darkening function I(r) in a band around 0.55 milliHertz measured in the moving coordinate system (Hill, Knapp and Caudell 1980). Both the real and the imaginary components are on the same scale and the zero of the horizontal axis represents the point of intensity onset for I(r).

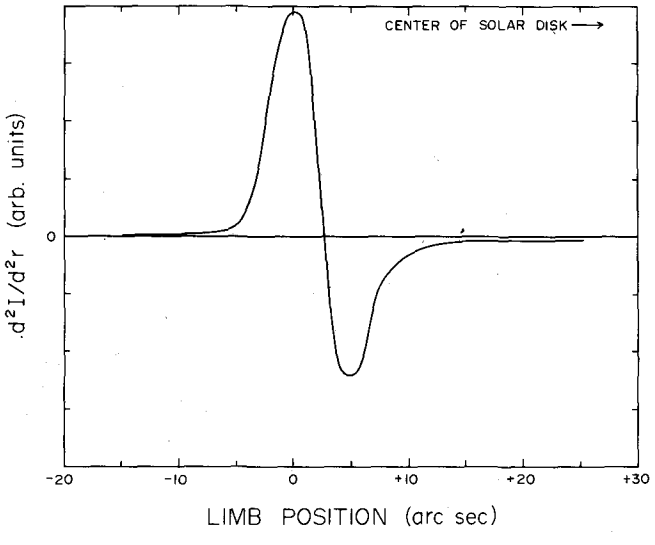

Figure 2. A typical second spatial derivative of the observed limb darkening function I(r) over the region of interest.

5. AIR MASS COLUMN DENSITY FLUCTUATIONS

Fluctuations in the earth's atmospheric column density along the line of sight can introduce problems in two ways: fluctuations in the transparency and fluctuations in the differential refraction. The latter of these two, the differential refraction, has been examined by various people (Fossat et al. 1977; KenKnight et al. 1977) while fluctuations in transparency have not been addressed in the literature per se. It is now possible to address these two aspects of column density fluctuations rather directly instead of by inference or statistical arguments, i.e., a sufficient condition type of study.

The oscillatory power of the fluctuations in atmospheric transparency at the periods of interest (from $\sim$ one hour to five minutes) will in general display a horizontal scale larger than 100 arc second, a typical length in applications of the FFTD. Thus the spatial signature of column density fluctuations will be simply the form of the limb darkening function itself, instead of d^2I/dr^2 as for seeing.

The FFTD is insensitive to simple scale changes. Consequently the column density fluctuations producing transparency changes do not present any complications in the establishment of a moving coordinate system using the FFTD as discussed in § 2. However, observing programs which measure fluctuations in I without any particular precaution to discriminate against column density fluctuations in general are likely to be severely compromised. The work of Hill, Knapp and Caudell (1980) shows that a significant fraction of the I'_m in Figure 1 is not correlated with the phase coherent component of the diameter fluctuations and that this fraction does indeed have the spatial character of the limb darkening function. Therefore this uncorrelated fraction is a prime candidate for the manifestation of column density fluctuations in the measured I'. Brown (1979) introduced a normalizing procedure in an attempt to correct for these effects. However, such a normalizing procedure does not completely remove the effects of column density fluctuations while considerably altering the observed properties of a global oscillatory component of I' and may contribute in part to the discrepancies between his findings and those of Hill, Knapp and Caudell (1980) and Stebbins (1980). Any technique with a spatial resolution < 100 arc second that is not sensitive to scale changes in I will be equally insensitive to fluctuations in the atmospheric column density such as with the FFTD. Thus the third approach discussed in § 3 for discrimination against seeing should also exhibit a similar immunity to atmospheric column density fluctuations.

The phase sensitive detection scheme of Hill, Knapp and Caudell (1980) outlined in § 4 to discriminate against seeing can also be used to study column density fluctuations. It can also be used to discriminate against column density fluctuations just as it was used to discriminate against seeing. There is an exciting possibility to consider here. Instead of asking for the correlation of I'_m with diameters, ask how the diameter fluctuations are correlated with fluctuation in

I'_m. For the first time, we have the opportunity to make a quantitative study of the relationship between differential refraction variation and column density fluctuations. This approach has been pursued by Hill, Knapp and Caudell (1980) which is also briefly examined in § 6.

6. THE GLOBAL OSCILLATORY COMPONENT OF I'

There have been several observational studies of I' with the goal to identify the properties of its global oscillatory component. These works can be ordered according to the degree that provision is made for the points addressed in §§2-5. The papers in particular are by Hill and Caudell (1979); Brown and Harrison (1979, 1980); Stebbins (1980); and Hill, Knapp and Caudell (1980).

The work of Brown and Harrison (1979, 1980) used the FFTD to establish a moving coordinate system in which to make measurements of I. However, adequate techniques were not used to remove the remaining atmospheric seeing effects or the effects of column density fluctuations as noted in §§ 4 and 5. These effects are probably a major contributor to their reported results. Also, the amount of data was sufficiently limited as to render tests for global character quite weak.

Stebbins (1980) used the FFTD extensively and as discussed in §§ 2 and 4, his program can be considered as one establishing a moving coordinate system and in this coordinate system, obtaining a measure of the spatial finite Fourier transform spectrum of I' not contaminated by seeing and column density fluctuation effects. With regard to identification of the global character, he considered properties of the temporal power spectra in the spirit of Brown, Stebbins and Hill (1978).

Information about the spatial finite Fourier transform of I' in a fixed reference frame (vis-a-vis § 2) is available from the work of Hill and Caudell (1979). Here the FFTD was used to establish the moving coordinate system and to obtain measures of the finite Fourier transform with reduced sensitivity to seeing and column density fluctuation effects. Diameters were also simultaneously measured with observation of fluctuations in I permitting the transformation from the moving coordinate system to a coordinate system tied to the center of mass of the sun. The global character of the observed I' was examined via tests for phase coherency (Caudell and Hill 1980) with statistically quite significant results.

A much more complete description of the spatial properties of I' in a reference frame fixed to the center of mass of the sun is now available in the work of Hill, Knapp and Caudell (1980). In the observations of Caudell et al. (1980) which they analyzed, the FFTD was (1) used to establish a moving coordinate system free of seeing and column density fluctuations effects; (2) diameters were measured simultaneously with measures of I allowing the transformation back to a reference frame fixed with respect to the center of mass of the sun; (3) the results of phase coherency tests were used to identify the global component of I', and (4) phase

sensitive detection was used to remove atmospheric seeing and to identify column density fluctuation effects on I'_m (cf. §§ 4 and 5). These results for I', shown in Figure 3, further support the case that the oscillations in the solar diameter are detected through changes in the limb darkening function, a result which questions the validity of the generally expected photospheric eigenfunctions (see Hill, Rosenwald and Caudell 1978; Keeley 1979).

The same techniques have also been used (Hill, Knapp and Caudell 1980) to measure the contribution of fluctuations in differential refraction to solar diameter measurements. They found in the period range of 25 minutes and a band width of 30 mHz, an amplitude in radius of 0.0005 ± 0.00015 arc second for the refractive contribution. This is the first direct measure of the relationship between column density fluctuations and fluctuations in differential refraction. These results bode well for future work on solar oscillations as well as opening up the opportunity for studies in the physics of the earth's atmosphere.

* * * * *

The authors would like to acknowledge the help of Jerry Logan and Randall Bos in preparation of the data for this paper. This work was supported in part by the National Science Foundation and the Air Force Geophysical Laboratory.

Figure 3

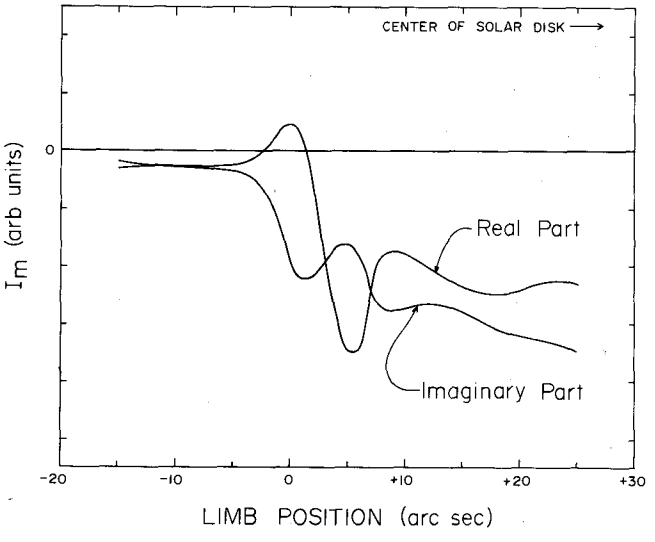

Figure 3. The averaged oscillatory component of the observed limb darkening function I(r) from Figure 1 transformed into the solar center of mass coordinate system (Hill, Knapp and Caudell 1980). Phase sensitive detection based on the measured diameters was used by Hill, Knapp and Caudell (1980) to project out the oscillatory component in phase with the observed global oscillations.

REFERENCES

Ballard, P.T. 1978, Ph.D Dissertation, University of Arizona.

Brown, T.M. and Harrison, R.L. 1979, Ap. J. Letters.

Brown, T.M. and Harrison, R.L. 1980, these proceedings.

Brown, T.M., Stebbins, R.T. and Hill, H.A. 1978, Ap. J., 223, 324.

Caudell, T.P. and Hill, H.A. 1980, Mon. Not. R. Astr. Soc., in press.

Caudell, T.P., Knapp, J., Hill, H.A. and Logan, J.D. 1980, these proceedings.

Fossat, E., Harvey, J., Hausman, M. and Slaughter, C. 1977, Astr. Astrophys., 59, 279.

Hill, H.A., Ballard, P.T., Bryan, S.D. and Rosenwald, R.D. 1979, J. Opt. Soc. Am., 69, 978.

Hill, H.A. and Caudell, T.P. 1979, Mon. Not. R. Astr. Soc., 186, 327.

Hill, H.A., Knapp, J. and Caudell, T.P. 1980, Ap. J. (submitted).

Hill, H.A., Rosenwald, R.D. and Caudell, T.P. 1978, Ap. J., 225, 304.

Hill, H.A., Stebbins, R.T. and Oleson, J.R. 1975, Ap. J., 200, 484.

Keeley, D.A. 1977, Proceedings of the Symposium on Large Scale Motions on the Sun, Sacramento Peak Observatory, 1977 September 1-2.

Keil, S.L. and Worden, S.P. 1980, these proceedings.

KenKnight, D., Gatewood, G.D., Kipp, S.L. and Black, D. 1977, Astr. Astrophys., 59, L27.

Stebbins, R.T. 1980, these proceedings.

SENSITIVITY TO THE APPLIED BOUNDARY CONDITIONS OF THE SOLAR EIGENFREQUENCY SPECTRUM WITH PERIODS NEAR FIVE MINUTES

R.D. Rosenwald
Department of Astronomy
University of Arizona
Tucson,Arizona

H.A. Hill
Department of Physics
University of Arizona
Tucson, Arizona

ABSTRACT

The existence of an anomalous component in the outer solar boundary conditions may cause large deviations from the standard eigenfrequency spectrum. Relaxation of the standard boundary conditions introduces alterations in the eigenfrequencies; for a given mode defined by spherical harmonic of order ℓ and radial number n, a range of frequencies is possible, with the eigenfrequency nonlinearly dependent on the complex ratio between the standard and anomalous solution components. The observed ridges of power in the diagnostic diagram (ℓ abscissa and ω ordinate) lie below the theoretical ridges, i.e., curves defined by constant n and standard boundary conditions. Using a linear nonadiabatic nonradial model for solar oscillations, anomalous boundary conditions were found to extend the standard theoretical ridges upward by roughly 1/3 ridge separation and downward by 2/3 ridge separation, encompassing the location of the observed ridges. The growth rate of a given mode is extremely dependent on the ratio of the anomalous and standard solutions present in the mode. If linear theory is adequate, simultaneous ℓ-ω plots of intensity and velocity may be used to infer the ratio between standard and anomalous solution components.

1. INTRODUCTION

Observational and theoretical studies of the solar eigenfrequency spectrum with periods near five minutes have previously been undertaken. Theoretical studies (Ando and Osaki 1975; Iben and Mahaffy 1976) have assumed the adequacy of linear theory and have imposed standard boundary conditions on the sun's surface. Several discrepancies and problems exist in comparing some theoretically predicted solar properties, under these assumptions, with the observed measurements. An example of

this is the relationship between temperature and displacement perturbations, addressed in Hill, Rosenwald and Caudell (1978) and Hill, Caudell and Rosenwald (1977). A second example, which this paper is concerned with, is the disparity in location of the predicted and observed power maxima in the spectrum of the solar velocity field, as indicated by the spectrum obtained by Deubner, Ulrich and Rhodes (1979). Recent work by Lubow, Rhodes and Ulrich (1980) claims to remove this disparity while retaining standard boundary conditions. This paper addresses the following question: If linear theory is assumed adequate, what effect does modification of the applied boundary conditions have on the solar eigenfrequency spectrum with periods near five minutes?

2. METHOD OF APPROACH

As background to analysis of this question, two general properties of eigenvalue problems will be described, usng a simple harmonic oscillator as an example. These two properties also apply to the solar oscillation problem.

The first property is the following: for a given normalization and set of boundary conditions, a multitude of discrete eigenfrequencies may exist. The differential equation for a simple harmonic oscillator is

$$(d^2/dt^2 + \omega^2)\, x(t) = 0 \quad , \tag{1}$$

Imposed on this equation are the following normalization and boundary conditions:

$$\begin{aligned} &x(0) = 1 \quad , \\ &\frac{dx}{dt}(0) = S \quad , \\ &x(1) = 0 \quad , \end{aligned} \tag{2}$$

respectively. The general solution is known to be

$$x(t) = A \cos \omega t + B \sin \omega t \quad , \tag{3}$$

hence, the following set of equations is obtained:

$$\begin{aligned} &1 = A \\ &s = B\omega \\ &0 = A \cos \omega + B \sin \omega \quad , \end{aligned} \tag{4}$$

The constants of integration, A and B, and the eigenfrequency, ω, are determined by the normalization and boundary conditions. Note that A is uniquely defined, but B and ω may take on many values, so long as $s = -\omega\cot\omega$ and $B = s/\omega$. The different ω's which satisfy equation (4) may be classified by the number of zero crossings of x while t ranges from t = 0 to t = 1.

This multiplicity of eigenfrequencies also occurs in the sun. For a given spherical harmonic number ℓ, a set of eigenfrequencies may be obtained, indexed by the radial number n (which, for the sun, corresponds to the number of zero crossings of the linear displacement, $\delta r/r$, in the radial direction and by the type of mode: pressure, fundamental, or gravity. For some stars, such as Cepheids, the simple correspondence between radial number and zero crossings of $\delta r/r$ does not exist. Dziembowski (1971) was the first to point out this situation.

The second property is the following: relaxation of a boundary condition allows the "discrete" eigenfrequencies to become continuous, i.e., any chosen frequency is an eigenfrequency when an "unmatched" boundary condition is allowed to vary. This is best shown by returning to the example of the simple harmonic oscillator. Use the same frequency, ω_0, for two different initial value integrations:

$$\text{(A):} \quad x(0) = 1 \quad , \quad \frac{dx}{dt}(0) = S_1 \quad ,$$

$$\text{(B):} \quad x(0) = 1 \quad , \quad \frac{dx}{dt}(0) = S_2 \quad . \tag{5}$$

The desired second boundary condition is, for example, $x(1) = 0$, but since ω_0 is not, in general, an eigenfrequency for these two cases, one obtains for integration (A): $x(1) = r_1$ and for integration (B): $x(1) = r_2$. Since the system is linear, a linear combination of solutions (A) and (B) may be constructed which satisfies the boundary condition $x(1) = 0$, namely:

$$\begin{aligned} &x(0) = 1 \quad , \\ &\frac{dx}{dt}(0) = (r_2 s_1 - r_1 s_2)/(r_2 - r_1) \quad , \\ &x(1) = 0 \quad . \end{aligned} \tag{6}$$

Thus, with the freedom to select $dx/dt(0)$, any choice of ω_0 becomes an eigenfrequency and the solutions obtained by the above technique are eigenfunctions.

3. RESULTS

A similar procedure of relaxing an outer solar boundary condition was used to study a portion of the solar eigenfrequency spectrum. Two values of the spherical harmonic number, ℓ, were chosen (100 and 400), together with a range in the frequency, ω, from 0.01 to 0.03 radians/sec; these parameters encompassed the spectral domain of investigation. To obtain information about some of the subtle factors, attention was focused on the p_2 pressure modes with $\ell = 400$.

The set of differential equations used for describing linear, nonadiabatic, nonradial solar oscillations is given in Ando and Osaki (1975). Analogous to the

different initial slopes, s_1 and s_2, of the simple harmonic oscillator example, are the standard and anomalous outer boundary conditions, denoted by β_- and β_+, respectively. Eigenfunctions with anomalous boundary conditions tend to vary on distance scales which are smaller than corresponding eigenfunctions having standard boundary conditions. Further details about the two types of boundary conditions are found in Hill, Rosenwald and Caudell (1978).

Before the relaxation approach was employed, the popular iterative technique of adjusting ω, while keeping boundary conditions fixed, was used to generate eigenfrequencies for comparison purposes. Solar eigenfrequencies corresponding to both purely standard and purely anomalous outer boundary conditions were computed for the p_2, $\ell = 400$ mode. Using a time dependence of $e^{i\omega t}$ and the relation $P = 2\pi/\omega$, a period of (325.5 + 0.1i) seconds was obtained for the standard boundary conditions (β_-) and (313.2 - 1.05i) seconds was obtained for the anomalous boundary conditions (β_+). The difference between these two "eigen-periods" is quite significant. Aside from their quantitative difference in period of greater than 3%, a basic qualitative difference exists: the β_- solution is driven and the β_+ solution is damped. This illustrates the extremely critical role which the applied boundary conditions can play in influencing solar properties.

The "relaxation of boundary conditions" approach was used for a range of real-valued frequencies, given above. Two initial value problems (with pure standard and pure anomalous outer boundary conditions) were integrated and linearly combined to match the unsatisfied inner boundary condition. Table 1 shows the amounts of the β_+ and β_- solutions required to make the given frequency (period) an eigenfrequency. The amounts of β_+ and β_- have been normalized so that they add to unity and the solutions for $\delta r/r$ have been normalized to unity at the optical depth $\tau = 10^{-3}$. Note the strong nonlinearity in the amounts of β_+ and β_- as functions of the period.

For the same set of nine periods, Figure 1 shows the physical location of the nodes (or zero crossings) in $\delta r/r$ for the p_2, $\ell = 400$ mode. There is some ambiguity involved in defining the extent of the period range where this mode is possible. At periods less than 305 seconds a third node will develop at a shallow depth. Similarly, at periods greater than 368 seconds the shallow node will appear at too low an optical depth and not be counted as a node.

Figure 2 shows the results obtained for a more extensive range of frequencies at two ℓ values: 100 and 400. The numbers 1-7 indicate which order pressure mode is considered, while 0 indicates the fundamental mode. The wedges indicate the computationally verified extent of the particular modes. For the p_2, $\ell = 400$ mode the real parts of the two "pure" solutions are also indicated.

For the p_2, $\ell = 400$ modes given in Table 1 it is interesting to note that at the lower end of the frequency range (larger periods) the ratio of β_+ to β_- solutions (denoted by A_+/A_-) is approximately 2 or 4 to 1, with small imaginary component. The

Table 1.

	P (sec)	A_+		A_-	
		real	imag	real	imag
	305	.8346	.0041	.1654	-.0041
	310	.9126	.0177	.0874	-.0177
(+)					
	315	1.0680	.0550	-.0680	-.0550
	320	1.7934	.3966	-.7934	-.3966
(-)	325	-.1346	.0010	1.1346	-.0010
	330	.4369	-.0506	.5631	.0506
	350	.7080	-.0371	.2920	.0371
	362	.7653	-.0338	.2347	.0338
	368	.7959	-.0315	.2041	.0315

This table shows the results of the "relaxation" approach for p_2, ℓ = 400 modes. Certain linear combinations of standard (β_-) and anomalous (β_+) solutions allow the listed periods, P, to become "eigen-periods". A_- and A_+ designate the required amounts of the standard and anomalous solutions, respectively, which must be present to generate this situation. The solutions for $\delta r/r$ have been normalized to unity at $\tau = 10^{-3}$ and the following constraint holds: $(A_+) + (A_-) = 1$. The (+) and (-) under the period column indicate the approximate locations of the "pure" solutions.

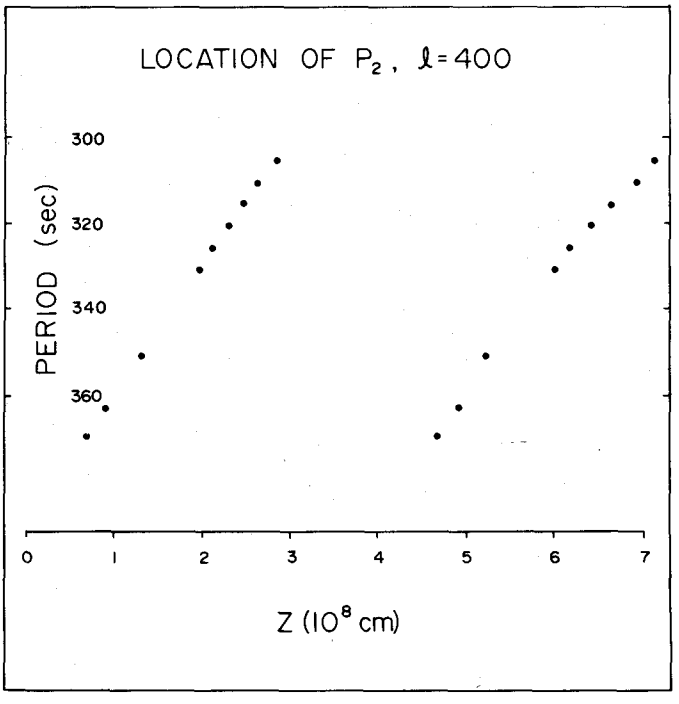

Figure 1. The location of the nodes in $\delta r/r$ for the p_2, ℓ = 400 mode. Z is the distance inward from the solar surface.

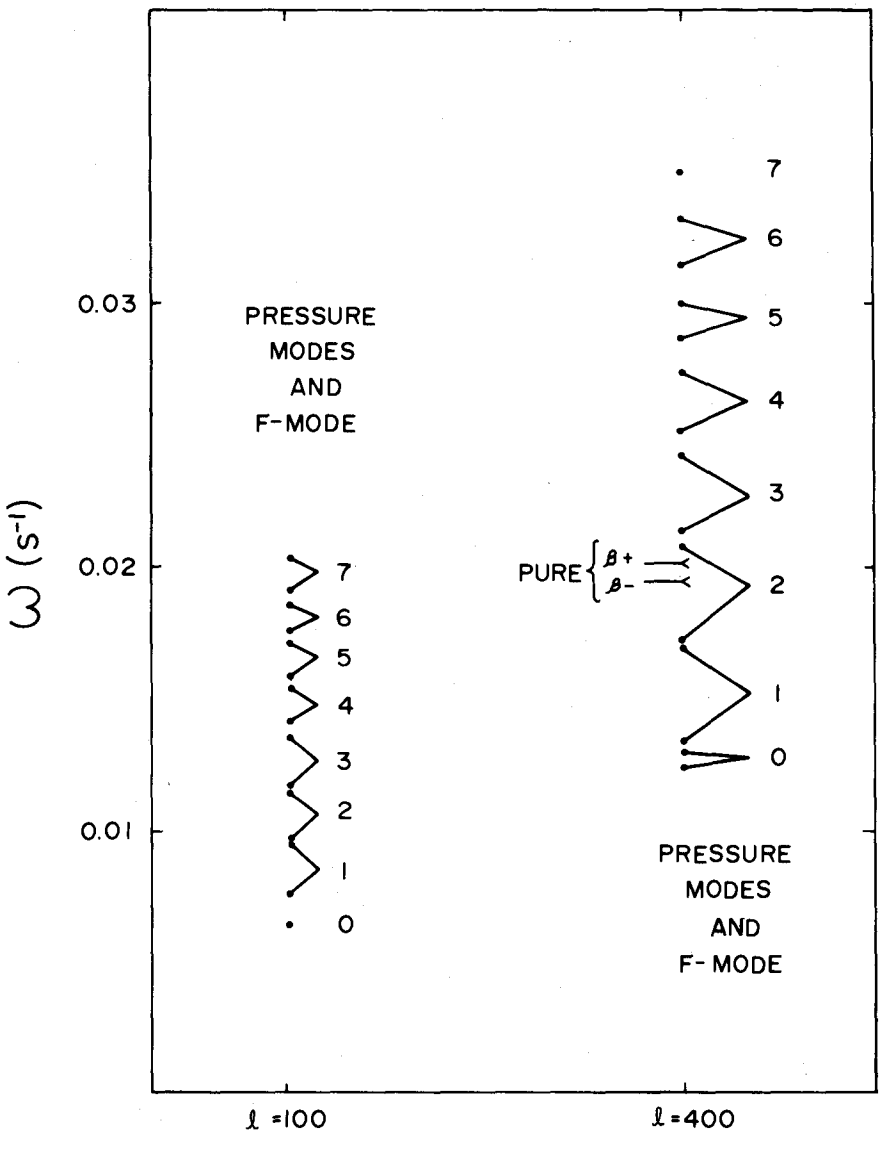

Figure 2. The location of low order pressure modes and fundamental modes in the ℓ-ω plane. Wedges indicate the computationally verified extent of some modes. The real parts of ω are indicated by β_+ and β_- for the two "pure" solutions of the p_2, ℓ = 400 mode.

lower end of the frequency range was chosen because the observed power is at a lower frequency than that predicted by a pure β_- solution. A value of $|A_+/A_-|$ for P ≈ 300 seconds and $\ell \approx 250$ has been published (Hill, Rosenwald and Caudell 1978). Renormalizing the published value of 0.18 at $\tau = 0.1$ to a value at $\tau = 10^{-3}$, one obtains $|A_+/A_-| \approx 3$, not inconsistent with the above number taken from Table 1.

The diagnostic diagram is a graph showing oscillatory power as a function of ℓ and ω. Figure 1 of Lubow, Rhodes and Ulrich (1980) shows observed power ridges in velocity and the curves where they should theoretically lie. The spherical harmonic number, ℓ, is related to k_h by the following formula: $k_h = [\ell(\ell + 1)]^{1/2}/R_0$. At the higher ℓ values the observed ridges of power lie significantly below the theoretical ridges (except for the ridge of fundamental modes). These theoretical ridges were computed using the standard (β_-) outer boundary conditions. Results of the computations in this paper (see Figure 2) show that ridges defined by pure β_- (standard) boundary conditions may be extended upward by roughly 1/3 ridge separation distance and downward by 2/3 ridge separation (easily encompassing the observed power ridges) if linear combinations of both β_+ and β_- solutions are present. With this wide range of power ridges now theoretically available, it becomes more difficult to off-handedly dismiss "exotic" solar models, such as those in Christensen-Dalsgaard and Gough (1980), simply because they have the standard β_- power ridges removed from the observed ridges. Similarly, constraints placed by Rhodes, Ulrich and Simon (1977) on the highly correlated solar quantities of envelope mass, envelope entropy, mixing length parameter (ℓ/H), and convection zone depth may be unnecessary, since modification of the applied boundary conditions alone may bring theoretical power spectra into agreement with observed power spectra.

In conclusion, several important points may be made:

1. The existence of an anomalous (β_+) component in the eigenfunctions, corresponding to the existence of anomalous boundary conditions, may cause large deviations from the standard (β_-) eigenfrequency spectrum.
2. A previously published value of $|A_+/A_-|$ is consistent with the observed power at five minutes. (A_+ and A_- refer to the amounts of anomalous and standard solutions that are present.)
3. Growth (or decay) rates are extremely dependent on A_+/A_-. When the real part of the eigenfrequency depends strongly on the boundary conditions, so also does the imaginary part.
4. If linear theory is adequate, simultaneous ℓ - ω plots (diagnostic diagrams) of intensity and velocity perturbations may be used to infer the ratio A_+/A_- as a function of ℓ and ω along the power ridges. Details of this inference procedure are given in Hill, Rosenwald and Caudell (1978). This ratio has, to date, only been evaluated at sparse points in the diagnostic diagram.

REFERENCES

Ando, H. and Osaki, Y. 1975, Publ. Astron. Soc. Japan, 27, 581.

Christensen-Dalsgaard, J. and Gough, D.O. 1980. These proceedings.

Deubner, F.-L., Ulrich, R.K. and Rhodes, E.J., Jr., 1979, Astron. Astrophys., 72, 177.

Dziembowski, W. 1971, Acta. Astron., 21, 289.

Hill, H.A., Caudell, T.P. and Rosenwald, R.D. 1977, Ap. J. Lett., 213, L81.

Hill, H.A., Rosenwald, R.D. and Caudell, T.P. 1978, Ap. J., 225, 304.

Iben, I., Jr. and Mahaffy, J. 1976, Ap. J. Lett., 209, L39.

Lubow, S., Rhodes, E.J., Jr. and Ulrich, R.K. 1980, these proceedings.

Rhodes, E.J., Jr., Ulrich, R.K. and Simon, G.W. 1977, Ap. J., 218, 901.

SOLAR OSCILLATIONS INTERACTING THROUGH A MEAN FIELD

J.D. Logan, H.A. Hill, and P. Puccio
Department of Physics

R. Rosenwald
Department of Astronomy

University of Arizona
Tucson,Arizona

ABSTRACT

The "mean field" produced by the temperature and opacity fluctuations of the five minute modes in the sun is shown to change the temperature and density spatial structure of the linear 25 minute mode near the top of the photosphere. The effective medium, measured by the coefficients in the differential equation for the linear mode, can be altered by as much as 19 percent by the 5 minute mode "mean field," indicative of possible nontrivial nonlinear processes in the photosphere.

1. INTRODUCTION

Recent observations indicate the presence of nonlinear effects in solar oscillations (Stebbins et al. 1980). Since the observed displacement amplitude for the five minute mode is about 5×10^{-5} of the solar radius at an optical depth of .1, one would reasonably consider nonlinear effects involving the products of such small amplitudes to be insignificant. However, Hill (1978) raised the possibility that the large value of the density and temperature perturbations and even larger value of the opacity perturbation allows nonlinear effects to be important when the collective rms temperature fluctuation is large and Hill, Rosenwald and Caudell (1978a) discuss nonlinear effects appearing at third order as a possible origin of the anomalous boundary conditions implied by the detection of long period solar oscillations (Hill, Rosenwald and Caudell 1978b).

The presence of the pressure and temperature fluctuations of the five minute modes must change the effective medium seen by the other modes. These fluctuations can be appropriately averaged to ascertain the pressure, temperature and opacity of the chosen solar equilibrium model. Each mode can be viewed as an independent linear mode sitting in a medium changed by the "mean field" caused by the existence of all the other modes. A defect in the usual linear analysis would be demonstrated by a significant difference between the computed solution for the linear mode with and

without the mean field.

We ignore in this mean field calculation correlations between the modes and effectively homogenize the influence of the other modes, hence some possible important nonlinear effects (such as parametric resonance, self-excitation, etc.) are not included in this treatment.

2. BASIC EQUATIONS

The basic equations for nonadiabatic radial oscillations in the radiative atmosphere with the radiative transfer treated by the Eddington approximation (as formulated by Ando and Osaki 1975) are

$$\frac{\partial \rho}{\partial t} + \vec{\nabla}.(\rho \vec{v}) = 0 \quad , \tag{1}$$

$$\rho \frac{\partial \vec{v}}{\partial t} = -\vec{\nabla} p + \rho \vec{g} \quad , \tag{2}$$

$$c_p \rho \left(\frac{dT}{dt} - \nabla_{ad} \frac{T}{P} \frac{dP}{dt} \right) = -\pi \vec{\nabla}.\vec{F} \quad , \tag{3}$$

$$\vec{F} = -\frac{4}{3\kappa\rho} \vec{\nabla} J \quad , \tag{4}$$

$$J = \frac{ac}{4\pi} T^4 + \frac{c_p}{4\pi\kappa} \left(\frac{dT}{dt} - \nabla_{ad} \frac{T}{P} \frac{dP}{dt} \right) \quad . \tag{5}$$

where $\nabla_{ad} = (\partial \ell n T / \partial \ell n P)_{ad}$, the adiabatic temperature gradient, and the other symbols have their usual meanings (see Ando and Osaki 1975). We will work exclusively with Eulerian perturbations which will be denoted by primes (').

We assume a real expansion of the physical quantity s of the form

$$s'(r,\theta,\phi,t) = \sum_{n,\ell,m} s^1_{n,\ell,m}(r) f_{\ell,m}(\theta,\phi) \cos\left(\sigma_{n,\ell,m} t + m\phi + \Phi^s_{n,\ell,m}\right) + s^2_{n,\ell,m}(r) f_{\ell,m}(\theta,\phi) \sin\left(\sigma_{n,\ell,m} t + m\phi + \Phi^s_{n,\ell,m}\right) \quad , \tag{6}$$

where

$$f_{\ell,m} = (-1)^m \sqrt{\frac{2\ell + 1}{4\pi} \frac{(\ell - m)!}{(\ell + m)!}} \; P^m_\ell(\cos\theta) \quad , \tag{7}$$

and $P^m_\ell(\cos\theta)$ is an associated Legendre polynomial with the usual angular spherical

harmonic indices ℓ and m. The subscript n stands for the overtone number of the mode. $\Phi^{s}_{n,\ell,m}$ is a random phase associated with the mode (n,ℓ,m) and physical quantity s. The superscripts 1 and 2 refer to the Eulerian perturbations associated with $\cos\sigma t$ and $\sin\sigma t$ respectively. We designate the sets (n,ℓ,m) and (n',ℓ',m') by k and k' for convenience. We define a nondimensional frequency ω and five nondimensional variables y, p, θ, j and f by

$$\theta_k = T_k'/T \quad ,$$

$$\omega_k^2 = (R^3/GM)\sigma_k^2 \quad ,$$

$$y_k = -iv_{rk}'/\sigma_k r \quad ,$$

$$p_k = P_k'/\rho g r \quad ,$$

$$j_k = J_k'/J \quad ,$$

$$f_k = F_{k,r}'/F_s \quad , \tag{8}$$

where F_r is the total energy flux, F_s is the flux at the surface and $i = \sqrt{-1}$ has been introduced as a bookkeeping device for the coupling between the $\cos\sigma t$ and the $\sin\sigma t$ terms and to facilitate comparison with the linear theory. By linearizing equations (1)-(5) and using only Eulerian perturbations for radial oscillations we obtain

$$r\frac{dy}{dr} = (\alpha V - 3 - V\nabla\delta_T)y - \alpha V p + \delta_T\theta \quad , \tag{9}$$

$$r\frac{dp}{dr} = c_1\omega^2 y + (1 - u - V\nabla\delta_T)p + \delta_T\theta \quad , \tag{10}$$

$$r\frac{dj}{dr} = 4V\nabla\left[\psi y - (\alpha + \kappa_p)Vp + (\delta_T - \kappa_T)\theta - f + j\right] \quad , \tag{11}$$

$$r\frac{df}{dr} = -i\omega c_2(\nabla_{ad} - \nabla)Vy + i\omega c_2\nabla_{ad}Vp - i\omega c_2\theta \quad , \tag{12}$$

$$j = i\omega c_4(\nabla_{ad} - \nabla)Vy - i\omega c_4 V\nabla_{ad}p + (4 + i\omega c_4)\theta \quad , \tag{13}$$

where $\psi = \frac{d\ell n(V\nabla)}{d\ell nr} + V(\alpha + \kappa_p + \nabla\kappa_T) + 1 - V\nabla(4 + \delta_T)$, which is identically zero

when the Eddington approximation is valid and was included into equation (11) to make it formally identical to the expression given by Ando and Osaki (1975) when the variables are linearly transformed to their system of variables. The other expressions appearing above are defined by

$$U = \frac{d\ell nM_r}{d\ell nr} = \frac{4\pi r^3}{M_r}\rho \quad , \quad V = -\frac{d\ell nP}{d\ell nr} = \frac{\rho g r}{P} \quad ,$$

$$\alpha = \left(\frac{\partial \ell n\rho}{\partial \ell nP}\right)_T \quad , \quad \delta_T = -\left(\frac{\partial \ell n\rho}{\partial \ell nT}\right)_P \quad ,$$

$$\nabla = \left(\frac{d\ell nT}{d\ell nP}\right)_{eq} \quad , \quad c_1 = \frac{(r/R)^3}{M_r/M} \quad ,$$

$$c_2 = \frac{UM_r c_p T}{L_s}\left(\frac{GM}{R^3}\right)^{1/2} \quad , \quad \nabla_{ad} = \left(\frac{\partial \ell nT}{\partial \ell nP}\right)_{ad} \quad ,$$

$$c_3 = \frac{L_{r,rad}}{L_s} \quad , \quad c_4 = \frac{c_p}{ac\kappa T^3}\left(\frac{GM}{R^3}\right)^{1/2} \quad ,$$

$$\kappa_p = \left(\frac{\partial \ell n\kappa}{\partial \ell nP}\right)_T \quad , \quad \kappa_T = \left(\frac{\partial \ell n\kappa}{\partial \ell nT}\right)_P \quad ,$$

$$c_5 = \frac{4\pi acrT^4}{3\kappa\rho L_s} \quad .$$

and are evaluated using the solar equilibrium model of Bahcall at al. (1973). Turbulence, viscosity, magnetic fields and modifications to the Eddington approximation (Hill, Rosenwald and Robinson 1980) have been neglected.

3. AVERAGING PROCEDURE

We use an ensemble average

$$\langle f \rangle \to \int_{-\pi}^{\pi} f(\Phi)p(\Phi)d\Phi \qquad (15)$$

and assume random phases so that $p(\Phi) = \frac{1}{2\pi}$. Properly speaking we should have a sum over phases, but it is reasonable to replace the sum by an integral since the number of five minute modes is exceedingly large (Rhodes, Ulrich and Simon 1977). Also $p(\Phi_1,\Phi_2) = p(\Phi_1) \cdot p(\Phi_2)$ and similarly for higher order probability distributions due to the assumed statistical independence of the modes.

Some useful averages are

$$\langle\cos(\sigma_k t + m\phi + \Phi_k)\cos(\sigma_{k'} t + m'\phi + \Phi_{k'})\rangle = \frac{1}{2}\delta_{k,k'} \quad ,$$

$$\langle\sin(\sigma_k t + m\phi + \Phi_k)\sin(\sigma_{k'} t + m'\phi + \Phi_{k'})\rangle = \frac{1}{2}\delta_{k,k'} \quad ,$$

$$\langle\sin(\sigma_k t + m\phi + \Phi_k)\cos(\sigma_{k'} t + m'\phi + \Phi_{k'})\rangle = 0 \quad , \qquad (16)$$

as can be shown by trigonometric expansion and application of equation (15). All odd power combinations of $\cos(\sigma_k t + m\phi + \Phi_k)$ and $\sin(\sigma_k t + m\phi + \Phi_k)$ average to zero.

We now take the Eulerian perturbation of equations (1) to (5) exploiting the relationship

$$(ab)' = a'b + ab' + a'b' \qquad (17)$$

and multiplying the resulting equation by $\cos(\sigma_d t + m\phi + \Phi_d)$ and $\sin(\sigma_d t + m\phi + \Phi_d)$ respectively, where the subscript d denotes the selected oscillation of interest, multiply by two and average. The average of three variables after the above multiplication can be expressed as

$$\left\langle\frac{\rho'\kappa'T'}{\rho\kappa T}\right\rangle = \frac{1}{2}\left\{\frac{\rho'_d}{\rho}\left(\left(\frac{\kappa'T'}{\kappa T}\right)\right) + \frac{\kappa'_d}{\kappa}\left(\left(\frac{\rho'T'}{\rho T}\right)\right) + \frac{T'_d}{T}\left(\left(\frac{\rho'\kappa'}{\rho\kappa}\right)\right)\right\} \quad , \qquad (18)$$

where

$$\frac{\rho'_d}{\rho} = \left(\rho^1_d(r) + i\rho^2_d(r)\right)f_d(\theta,\phi)/\rho \qquad (19)$$

and

$$\left(\left(\frac{\kappa'T'}{\kappa T}\right)\right) = \sum_\kappa f^2_\kappa(\theta,\phi)R_e\left[\left(\frac{\kappa'}{\kappa}\right)^*\left(\frac{T'}{T}\right)\right] \quad . \qquad (20)$$

The variables ρ' and κ' must be expanded in terms of our chosen variables. We assume both ρ and κ are functions of T and P. The averages given by equation (20) are rapidly decreasing functions of depth and assume their largest values in the top of the photosphere where a linear expansion for ρ' will suffice

$$\frac{\rho'}{\rho} = \alpha Vp - \delta_T\theta \quad . \qquad (21)$$

However, we need a more general expansion for κ'

$$\frac{\kappa'_S}{\kappa} = \kappa_T\theta_S + \kappa_p Vp_S + \kappa_{TT}\theta^2_S + \kappa_{TP}V\theta_S p_S + \kappa_{PP}V^2p^2_S + \text{higher order} \quad ,$$

$$\text{where} \quad \kappa_T = \left(\frac{\partial \ell n\kappa}{\partial \ell nT}\right)\Big|_P \quad , \quad \kappa_p = \left(\frac{\partial \ell n\kappa}{\partial \ell nP}\right)\Big|_T \quad , \quad \kappa_{TT} = \frac{1}{2}\frac{T^2}{\kappa}\frac{\partial^2\kappa}{\partial T^2} \quad ,$$

$$\kappa_{TP} = \frac{1}{\kappa}\frac{\partial^2\kappa}{\partial \ell n T \partial \ell n P} \quad , \text{ and } \quad \kappa_{PP} = \frac{1}{2}\frac{P^2}{\kappa}\frac{\partial^2\kappa}{\partial P^2} \quad .$$

We do not expand κ to third order because the average of a third order quantity of a single mode is quite small since only the collective sum is taken to be significant.

Fifth order terms involve either a single sum over k of four variables or the product of two terms, each term involving one sum as in equation (20). The fifth order terms that have only one sum over k are smaller than the third order terms by a factor of the square root of the number of modes and the fifth order terms involving products were found to contribute less than 1 percent of the dominant third order term in any particular coefficient.

4. THE MEAN FIELD EQUATIONS

The mean field equations are (see Logan, 1980, for the full derivation of the equations),

$$r\frac{dy_d}{dr} = (\varepsilon - 1)y_d - \alpha V p_d + \delta_T \theta_d \quad , \tag{23}$$

$$r\frac{dp_d}{dr} = \left(c_1\omega_d^2 + \frac{c_1\omega_c\omega_d}{2}\left\{2\varepsilon\alpha V((yp)) + 2\alpha V\delta_T((p\theta)) - 2\varepsilon\delta_T((y\theta))\right.\right.$$
$$\left.\left. - (\alpha V)^2((p^2)) - \delta_T^2((\theta^2))\right\}\right)y_d + \left(1 - U - V\nabla\delta_T\right.$$
$$\left. + \frac{c_1\omega_c\alpha V}{2}\left\{-(\omega_d + \omega_c)\eta_7 + \omega_c\varepsilon((y^2))\right\}\right)P_d + \delta_T\left(1\right.$$
$$\left. + \frac{c_1\omega_c}{2}\left\{(\omega_d + \omega_c)\eta_7 - \omega_c\varepsilon((y^2))\right\}\right)\theta_d$$

$$r\frac{df_d}{dr} = \left\{-i\omega_d c_2 d_4 + \frac{i\omega_d c_2}{2}\left(\alpha\nabla V^3((p^2)) + V\nabla_{ad}\delta_T((\theta^2))\right.\right.$$
$$\left.\left. - V^2\left(\alpha\nabla_{ad} + \nabla\delta_T\right)((p\theta)) + \delta_T\eta_1 - V\left(\alpha + 1\right)\eta_2 + \right.\right.$$
$$\left.\left. \nabla_{ad}\left(1 - \delta_T\right)\eta_4 + \nabla_{ad}\alpha V\eta_s\right) + \frac{i\omega_c c_2}{2}\left(h_{7d}\left(\nabla_{ad}\alpha V((yp))\right.\right.\right.$$

$$+ \nabla_{ad}(1 - \delta_T)((y\theta))\Big) + h_{3d}\Big(\delta_T((y\theta)) - V(\alpha + 1)((yp))\Big)\Big)y_d$$

$$+ \Big\{\frac{i\omega_d c_2 \nabla_{ad}}{2}\Big(2V + \alpha V^2((p\theta)) - V\delta_T((\theta^2))\Big) + \frac{i\omega_c c_2}{2}\Big\{\alpha V^2((p\theta))$$

$$\Big(\nabla_{ad} - 2\Big) + V\delta_T((\theta^2)) + \Big(2\alpha\nabla V^3 - V(\alpha + 1)h_{2d} + h_6\alpha V\nabla_{ad}\Big)((yp))$$

$$+ \Big(h_{2d}\delta_T - \alpha V^2\nabla_{ad} - \nabla\delta_T V^2 + h_6\nabla_{ad}(1 - \delta_T)\Big)((y\theta)) - V(\alpha + 1)\eta_3$$

$$+ \alpha V\nabla_{ad}\eta_6\Big\}\Big\}p_d + \Big\{\frac{i\omega_d c_2}{2}\Big(-2 + V\delta_T((p\theta)) - \alpha V^2((p^2))\Big)$$

$$+ \frac{i\omega_c c_2}{2}\Big(V\delta_T\Big(1 - 2\nabla_{ad}\Big)((p\theta)) + \alpha V^2\nabla_{ad}((p^2)) + \Big(2\delta_T\nabla_{ad}V$$

$$+ h_5\nabla_{ad}(1 - \delta_T) + h_{1d}\delta_T\Big)((y\theta)) + \Big(h_5\nabla_{ad}\alpha V - h_{1d}V(\alpha + 1)$$

$$- \delta_T\nabla V^2 - \alpha V^2\nabla_{ad}\Big)((yp)) + \delta_T\eta_3 + \nabla_{ad}(1 - \delta_T)\eta_6\Big)\Big\}\theta_d$$

$$+ \frac{i\omega_c c_2}{2}h_{4d}\Big(\eta_7 - V((yp))\Big)\Big(f_d - c_3 j_d\Big) \quad , \tag{25}$$

$$r\frac{dj_d}{dr} = 4V\nabla\Big[\psi y_d + p_d\Big(-(\alpha + \kappa_p)V - \frac{1}{2}\Big(2\alpha V^2\kappa_p\frac{((pf))}{c_3} + (\alpha V\kappa_T - \kappa_p V\delta_T)$$

$$\frac{((\theta f))}{c_3}\Big)\Big) + \theta_d\Big(\delta_T - \kappa_T - \frac{1}{2}\Big(((pf))\Big(\frac{\alpha V\kappa_T - \kappa_p V\delta_T}{c_3}\Big) - ((\theta f))$$

$$\Big(\frac{2\delta_T\kappa_T}{c_3}\Big)\Big)\Big) + f_d\Big(-1 + \frac{1}{2}\Big(((p\theta))(\delta_T\kappa_p V - \alpha V\kappa_T) + \delta_T\kappa_T((\theta^2))$$

$$- \alpha V^2\kappa_p((p^2))\Big)\Big) + j_d - \mu(f_d + \alpha V p_d + \delta_T\theta_d)\Big] \quad , \tag{26}$$

$$j_d = \left\{\frac{i\omega_d c_4}{2}\left(2d_4 + V\eta_2 - \nabla_{ad}\eta_4\right) + \frac{i\omega_c c_4}{2}\left(Vh_{3d}((yp)) - \right.\right.$$

$$\left.\left. - \nabla_{ad}h_{7d}((y\theta))\right)\right\}y_d + \left\{\frac{i\omega_d c_4}{2}\left(-2V\nabla_{ad}\right) + \frac{i\omega_c c_4}{2}\left(Vh_{2d}((yp))\right.\right.$$

$$\left. - \nabla_{ad}h_6((y\theta)) + V\eta_3\right) + 4V^2\kappa_p((p\theta)) - \kappa_p V^2((pj)) + V\left(2\kappa_T\right.$$

$$\left.\left. + 3(1 + \kappa_p)\right)((\theta^2)) - \tfrac{1}{2}\kappa_T V((\theta j))\right\}p_d + \left\{4 + i\omega_d c_4\right.$$

$$\left. - \frac{i\omega_c c_4}{2}\left(\nabla_{ad}\eta_6 - Vh_{1d}((yp)) + h_5\nabla_{ad}((y\theta))\right) + (6 + 9\kappa_T)((\theta^2))\right.$$

$$\left. + V(4\kappa_T + 6(\kappa_p + 1))((p\theta)) + 2V^2\kappa_p((p^2)) - \tfrac{1}{2}\kappa_T((pj))\right\}\theta_d$$

$$+ \left\{\frac{i\omega_c c_4}{2}\ Vc_3h_{4d}((yp)) - \tfrac{1}{2}V\left(\kappa_T((p\theta)) + \kappa_p V((p^2))\right)\right\}j_d$$

$$- \frac{i\omega_c c_4}{2}\ Vh_{4d}((yp))f_d + \mu(4\theta_d - j_d) \quad ,$$

with $\quad \varepsilon = \alpha V - 2 - \nabla V\delta_T \quad ,$

$$d_4 = V(\nabla_{ad} - \nabla) \quad ,$$

$$h_{1\kappa} = V\nabla + \frac{1}{4 + i\omega_\kappa c_4}\left\{4V\nabla(\delta_T - \kappa_T) + i\omega c_4 V\nabla\delta_T - i\omega_\kappa \frac{dc_4}{d\ell nr}\right\} \quad ,$$

$$h_{2\kappa} = \frac{1}{4 + i\omega_\kappa c_4}\left\{i\omega_\kappa V\nabla_{ad}\frac{dc_4}{d\ell nr} + i\omega_\kappa c_4\frac{d(V\nabla_{ad})}{d\ell nr} + i\omega_\kappa c_4\alpha V d_4\right.$$

$$\left. + i\omega_\kappa c_4\nabla_{ad}V(1 - U - V\nabla\delta_T)\right\} \quad ,$$

$$h_{3\kappa} = \frac{1}{4 + i\omega_\kappa c_4}\left\{4V\nabla\psi + i\omega c_4\left(\frac{dd_4}{d\ell nr} + c_1\omega^2 V\nabla_{ad} + (1-\varepsilon)d_4\right)\right.$$

$$\left. - i\omega_\kappa d_4\frac{dc_4}{d\ell nr}\right\} \quad ,$$

$$h_{4\kappa} = \frac{4V\nabla}{c_3(4 + i\omega_\kappa c_4)} \quad ,$$

$$h_5 = V\delta_T \quad ,$$

$$h_6 = 2V(1 - U) - \alpha V^2 \quad ,$$

$$h_{7\kappa} = c_1 V\omega_\kappa{}^2 \quad ,$$

$$\eta_1 = h_{1c}((\theta^2)) + h_{2c}((p\theta)) + h_{3c}((y\theta)) + c_3 h_{4c}((j\theta)) - h_{4c}((\lambda\theta)) \quad ,$$

$$\eta_2 = h_{1c}((\theta p)) + h_{2c}((p^2)) + h_{3c}((yp)) + c_3 h_{4c}((jp)) - h_{4c}((\lambda p)) \quad ,$$

$$\eta_3 = h_{1c}((\theta y)) + h_{2c}((py)) + h_{3c}((y^2)) + c_3 h_{4c}((jy)) - h_{4c}((\lambda y)) \quad ,$$

$$\eta_4 = h_5((\theta^2)) + h_6((p\theta)) + h_{7c}((y\theta)) \quad ,$$

$$\eta_5 = h_5((\theta p)) + h_6((p^2)) + h_{7c}((yp)) \quad ,$$

$$\eta_6 = h_5((\theta y)) + h_6((py)) + h_{7c}((y^2)) \quad ,$$

$$\eta_7 = \alpha V((yp)) - \delta_T((y\theta)) \quad .$$

We could write equation (24) as

$$r \frac{dp_d}{dr} = c_1 * \omega_d{}^2 y + (1 - U - V * \nabla\delta_T) p_d + \delta_T * \theta_d \quad ,$$

where the equilibrium constants have been changed by the presence of the mean field. Or we could write the system of equations as

$$r \frac{d}{dr} y_i = T_{ij} y_j$$

and ask about the percentage change

$$\frac{T_{ij_{\text{mean field}}} - T_{ij_o}}{T_{ij_o}} \quad .$$

These percentage changes range from zero to 19 percent near the top of the photosphere.

It should be noted that the second order kappa derivatives only come into the equations in the form

$$\mu = \frac{1}{2}\ \kappa_{TT}((\theta^2)) + \kappa_{Tp}V((\theta p)) + \kappa_{pp}V^2((p^2))$$

which equals 5.8×10^{-2} at an optical depth of 10^{-3}. The other dominant terms involve the temperature and first order kappa fluctuations.

5. EVALUATION OF THE AVERAGES

The ensemble average has terms like $R_e(p_k \cdot \theta_k)$. This involves the solutions to the equations (23) to (27), which unfortunately contain the unknown averages. As a first approximation we take the linear solutions of equations (9) to (13) to insert into the averages. If the solutions to the new linear equations do not differ substantially from the original linear solutions, this procedure is consistent. If the new solutions do differ one can, of course, reiterate the procedure. We assume the major contribution to the ensemble averages comes from the observed five minute modes whose linear variables are predominantly in the radial direction and hence fairly independent of ℓ and m (Hill, Rosenwald and Caudell 1978b). The sum can now be evaluated by invoking the addition theorem which for this case is

$$\sum_m f_\ell^m(\theta,\phi)\ f_\ell^m(\theta,\phi) = \frac{1}{4\pi}\ (2\ell + 1) \quad ,$$

and noting

$$\sum_{n,\ell} (2\ell + 1) = \sum_{n,\ell,m} 1 = N = \text{number of modes} \quad ,$$

so that the ensemble average becomes

$$((p\theta)) \rightarrow \frac{1}{4\pi} R_e\ (p_5{}^*\theta_5) \quad ,$$

where θ_5, etc., is the root mean square of the five minute oscillation. The absolute value of μ in the first integration zone at an optical depth of 10^{-3} was chosen to be 6.86×10^{-5} to give a value of 1 km/sec for the five minute oscillations. The solutions to our linear equations that are of interest are the two that correspond to the two independent solutions of the nonadiabatic wave equation. We denote these two solutions as beta plus and beta minus. The general solution can be written as a combination of these two solutions. In order to match the two solutions at the last zone of integration a ratio of beta plus to beta minus of .93 at an angle of 7° was chosen.

6. METHOD OF COMPUTATION

The numerical integration of the fourth order system of differential equations was treated by a Fehlberg Fourth-Fifth Order Runge-Kutta routine written by

H.A. Watts and L.F. Shampine and utilizing the Godunov-Conte technique of parallel shooting. The opacity derivatives, κ_T, κ_p, κ_{TT}, κ_{Tp} and κ_{pp} were obtained through the use of the equation of state and bicubic spline interpolations (IMSL routines DBCEVU and IBCICU) within the King IVa mixture opacity tables of Cox and Tabor (1976). The imposed boundary conditions are identical to those in Hill, Rosenwald and Caudell (1978b). The computed solutions were not sensitive to the exact value chosen for the outer boundary condition on j. Because of the existence of nonlinear effects reported in this paper, the proper boundary conditions may be difficult to choose.

7. DISCUSSION

The linear differential system of equations (23) - (27) was solved from a depth of $\tau = 10^{-3}$, $T = 4680$ K to $\tau = 3 \times 10^{11}$, $T = 3 \times 10^6$ and a frequency at 25 minutes. A comparison of Figure 1a to Figure 1b depicting the spatial temperature structure of the beta minus 25 minute mode with and without the mean field terms has a qualitatively different shape near the top of the photosphere. The dimensionless displacement variable which can be related to the physical velocity of the oscillation changes by a minuscule amount. Direct measurements of temperature fluctuations and velocities at a certain frequency may give different results. The difference in the mode with and without the mean field is plotted in Figure 1c. This difference has the same form as the beta plus solution for the 25 minute mode plotted in Figure 1d. The collective averaged nonlinear effect of the other modes thus appears to be describable as a change in the mixture of beta plus to beta minus. The effect shown in Figure 1c can be ascribed to a 2 percent admixture of beta plus added to the original beta minus. The most important point to be made is that the change in the coefficients of the linear solutions by these considerations of 10 percent on the whole defaults the cavalier attitude towards nonlinear effects in the solar photosphere.

* * * * *

The authors wish to acknowledge helpful discussions with Wojciech Dziembowski and Thomas P. Caudell.

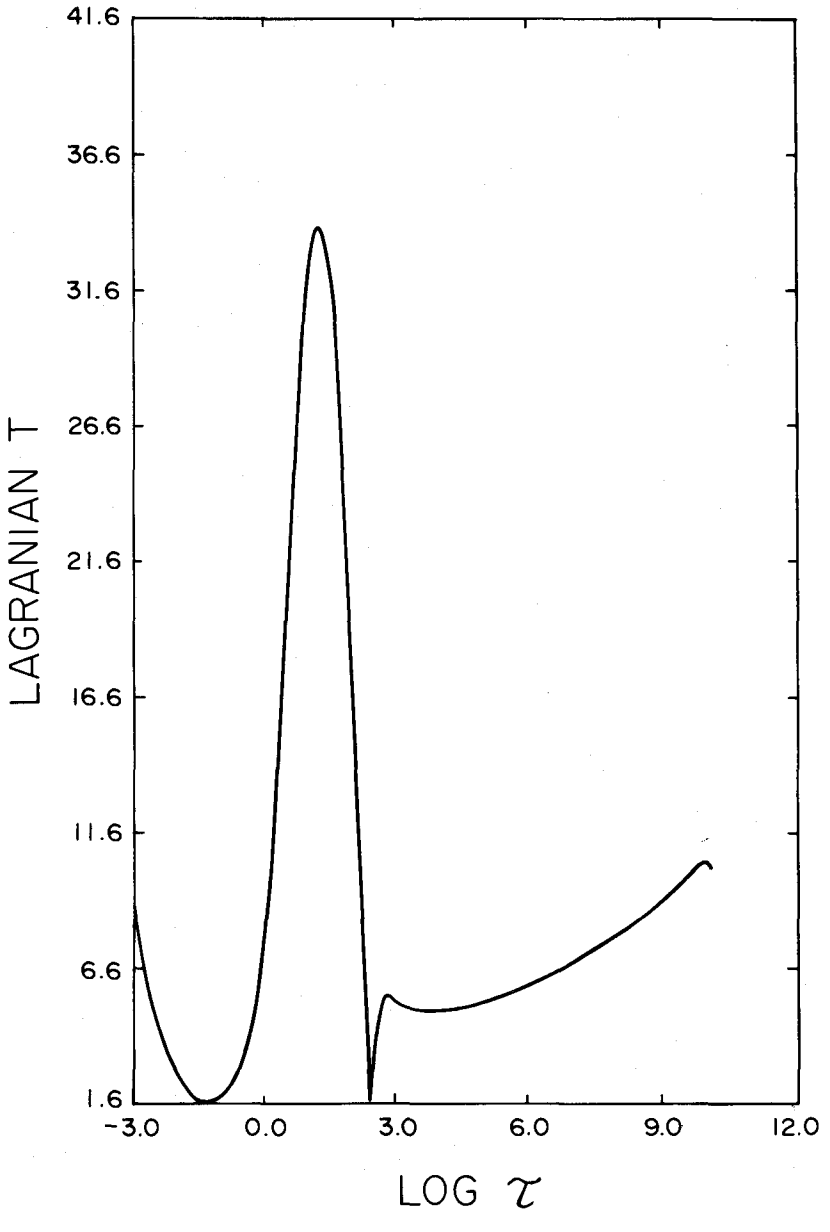

Figure 1a. Dimensionless Lagrangian temperature perturbation (normalized to unit dimensionless Lagrangian radial perturbation at optical depth .001) versus log optical depth for the linear 25 minute β minus mode.

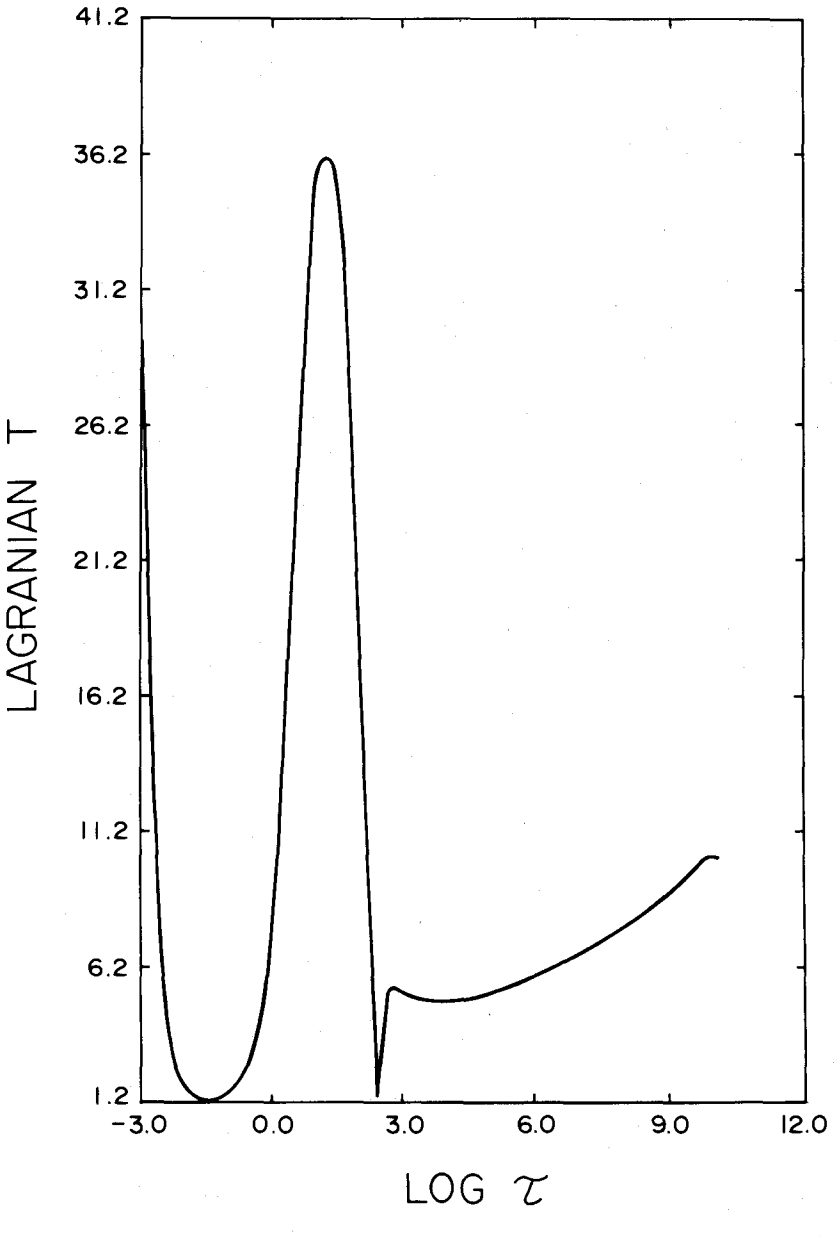

Figure 1b. Dimensionless Lagrangian temperature perturbation versus log optical depth for the nonlinear 25 minute β minus mode.

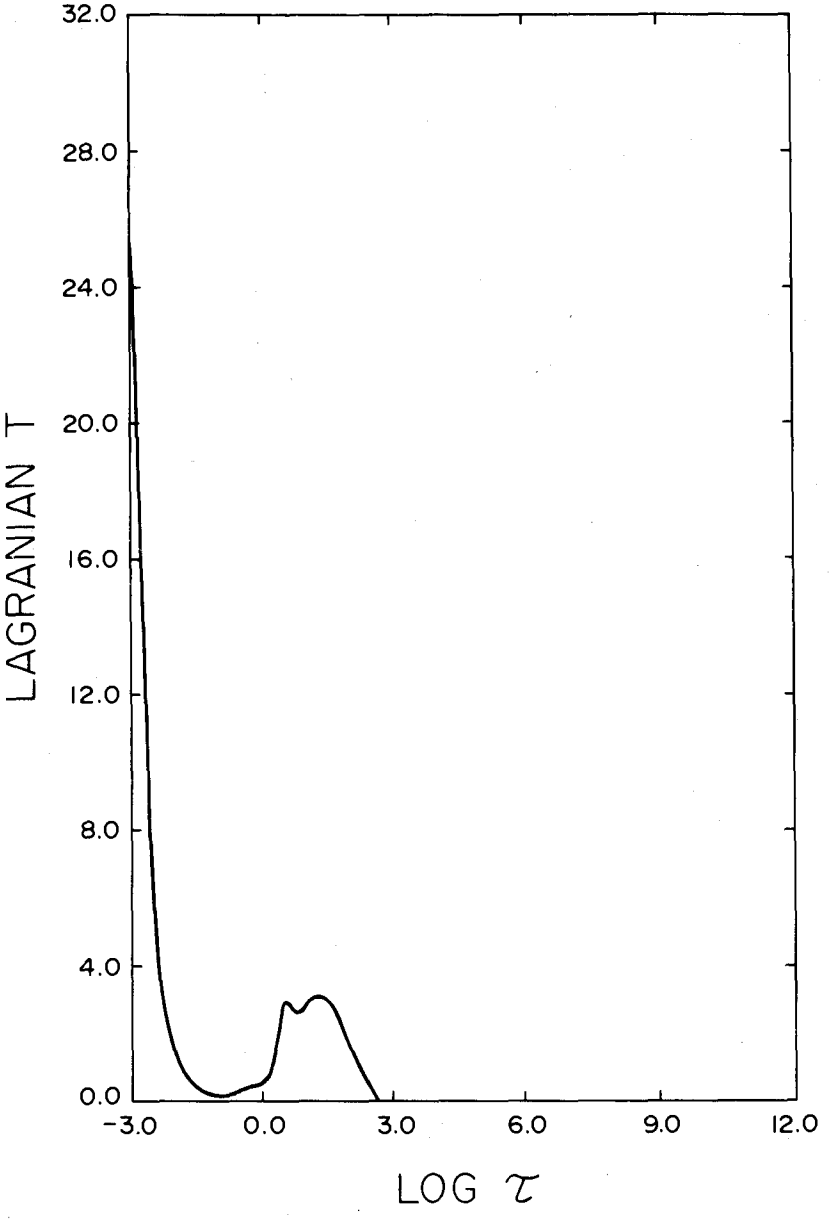

Figure 1c. Difference between linear and nonlinear 25 minute β minus dimensionless Lagrangian temperature perturbation versus log optical depth.

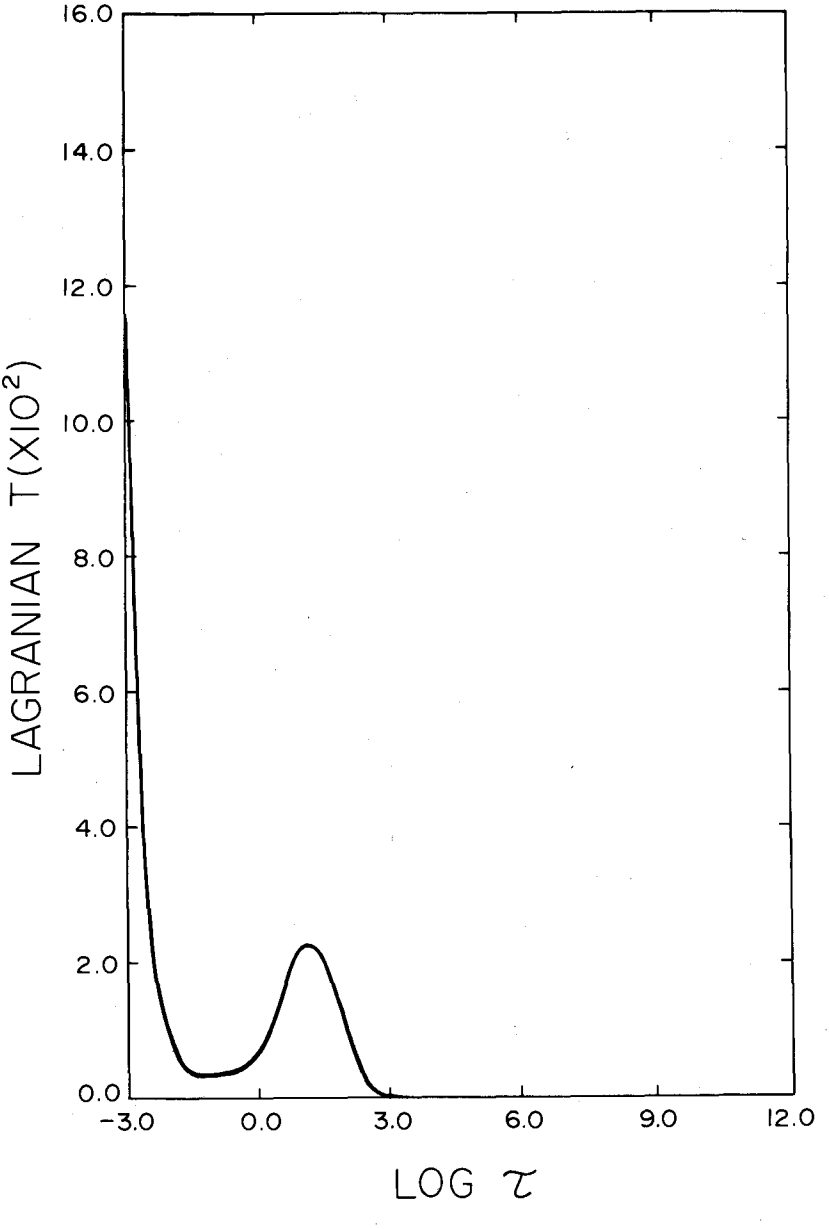

Figure 1d. Dimensionless Lagrangian temperature perturbation versus log optical depth for the linear 25 minute β plus mode.

REFERENCES

Ando, H. and Osaki, Y. 1975, Pub. Astr. Soc. Japan, 27, 581.

Bahcall, J.N., Heubner, W.F., Magee, N.H., Jr., Merts, A.L. and Ulrich, R.K. 1973, Ap. J., 184, 1.

Hill, H.A. 1978, The New Solar Physics, (Boulder: Westview Press), p. 188-9.

Hill, H.A., Rosenwald, R.D. and Caudell, T.P. 1978a, Proceedings of the 2nd European Solar Meeting, Toulouse, France, March 8-10.

Hill, H.A., Rosenwald, R.D. and Caudell, T.P. 1978b, Ap. J., 225, 304.

Hill, H.A., Rosenwald, R.D. and Robinson, S. 1980, these proceedings.

Logan, J.D. 1980, Ph.D Thesis, in progress.

Rhodes, E.J., Jr., Ulrich, R.K. and Simon, G.W. 1977, Ap. J., 218, 901.

Stebbins, R.T., Hill, H.A., Zanoni, R. and Davis, R.E. 1980, these proceedings.

THE ANISOTROPIC RADIATION FIELD APPROXIMATION AND ITS EFFECT ON WAVE EQUATION SOLUTIONS IN THE SOLAR PHOTOSPHERE

H.A. Hill
Department of Physics, University of Arizona

R.D. Rosenwald
Department of Astronomy, University of Arizona

R.S. Robinson
Department of Physics, University of Arizona

ABSTRACT

An approximation is developed which more accurately "solves" the radiative transfer equation than does the standard Eddington approximation. The difference between the two approaches is greatest in the optically thin region of the photosphere, where the new approximation more accurately represents the physics. Solutions of the wave equations for photospheric oscillations in both of the above approximations were generated by a linear, nonadiabatic, radial modeling program. Differences were found to exist between the sets of solutions obtained from the two transfer equation techniques. As to the effect on measurable quantities, such as the Eulerian perturbation in intensity and the radial displacement, the impact of varying the radiative transfer treatment was dependent on the outer solar boundary conditions. A solar model with standard outer boundary conditions produced observables which were less sensitive to the radiative transfer treatment than a solar model having anomalous outer boundary conditions (cf. Hill, Rosenwald and Caudell 1978). Since several observations indicate that the latter model is more realistic, the new approximation may be important in accurately studying the solar photosphere.

1. INTRODUCTION

Various shortcomings and pitfalls exist in current theoretical approaches for studying linear, nonadiabatic, radial solar oscillations. Inadequacies exist in the macroscopic equations usually employed to describe the physical situation. The conservation equations for mass, momentum, and energy are certainly valid, but the Eddington approximation, almost universally used in simplifying the radiative heat equations, is demonstrably inaccurate in the optically thin regions of the solar photosphere.

This paper develops a new approximation for solving the radiative heat

equations. The development of this technique has its foundation in the work of Unno and Spiegel (1966). It takes into account directly the dominant spatial characteristic of a plane-parallel atmosphere in local thermodynamic equilibrium (as in the Milne problem) and incorporates an approximation which, when applied to a nearly isotropic radiation field, leads to the Eddington approximation. It is subsequently referred to as the anisotropic radiation field approximation.

The equilibrium solution obtained using this technique is more accurate in the optically thin region of the photosphere than the solution derived using the Eddington approximation. Section 4 and Table 1 document this higher accuracy in the thin region and the comparable accuracy in the optically thick region. For comparison purposes, a linear, nonadiabatic, radial modeling program generated photospheric solutions of the wave equation using both of the above radiative transfer techniques.

In addition, for each of these techniques both standard and anomalous boundary conditions were imposed on the solutions at the outer solar boundary. For a discussion of the anomalous boundary conditions, and how their existence is implied by observations, see Hill, Rosenwald and Caudell (1978) and Rosenwald and Hill (1980). The solutions with anomalous boundary conditions vary on a distance scale which is smaller than solutions having standard boundary conditions.

The differences in the wave equation solutions derived from the two treatments of radiative transfer were substantial, with the amount of difference dependent on the applied solar boundary conditions. A solar model with anomalous outer boundary conditions produced observable effects which were more dependent on the choice of radiative transfer treatment than did a solar model having standard outer boundary conditions.

2. PROBLEMS ENCOUNTERED WITH THE EDDINGTON APPROXIMATION

In this work the Eddington approximation is taken to be the equation $J = 3K$, where J and K are the usual zeroth and second moments of the radiation intensity, $I(\mu)$, and μ is the cosine of the angle between the direction of propagation and the observer. Sometimes a particular assumed form of $I(\mu)$ is referred to as the Eddington approximation. However, since many different choices of $I(\mu)$ imply $J = 3K$, the relation itself will be called the Eddington approximation. On comparison with the "exact" solution, defined below, it is found that as the optical depth approaches zero, J_{Edd} is 15% larger than J_{exact} and that J_{exact} is less than $3K_{exact}$. The subscripts "Edd" and "exact" refer to the values corresponding to the Eddington approximation and the exact treatment, respectively.

Existing theoretical treatments of the solar atmosphere provide another indicator of trouble in the optically thin region. Various empirical relations between the temperature, T, and the optical depth, τ, have been derived for the solar

atmosphere. The Harvard-Smithsonian reference atmosphere is one of several such examples, obtained from analyses of spectral line observations. For small values of τ (less than unity), these T - τ relations differ quite markedly from both the theoretical T - τ relation implied by the Eddington approximation and the T - τ relation implied by the solution of the Milne problem (radiative transfer in a plane-parallel atmosphere in local thermodynamic equilibrium), the so-called "exact" solution.

Previous approaches (Ando and Osaki 1975) for studying linear, nonadiabatic oscillations in the solar atmosphere with periods near five minutes have used the Eddington approximation as an acceptable assumption in the radiative heat equations; flux is related, using the Eddington approximation, to the divergence of J. Linearizing the equations, the size of the nonadiabatic portion of the energy equation is determined by the linearized flux term, whose accuracy, in turn, is dependent on the accuracy of the Eddington approximation. Since the energy dissipation integral and the eigenfunctions for the five minute oscillation depend strongly on the nonadiabatic energy term near the sun's surface, the question of overall driving or damping and other oscillation properties depend sensitively on the accuracy of the linearized flux term, and hence on the accuracy of the Eddington approximation. This may be a serious weakness in current theories of solar oscillations and may lead to significant errors in the interpretation of observations. In the quest to better understand this topic, the following question is raised: How does a more accurate treatment of the transfer equation affect predicted oscillatory properties, such as eigenfunctions? The answer to this question is pursued in Section 5.

The difficulty with the Eddington approximation may be seen from another viewpoint. Assuming local thermodynamic equilibrium (LTE), which identifies the source function S with the Planck function B, S at an arbitrary point may be expressed as a Taylor series expansion of B at a fixed reference point. Unno and Spiegel (1966), using this approach, developed formal solutions for J and K in terms of infinite series whose terms consist of weighting factors times powers of the photon mean free path length times spatial partial derivatives of the Planck function. At places of high optical depth, the mean free path is small, the series converge rapidly, and the usual relation is obtained: $J = 3K$. For regions of low optical depth, however, the photon mean free path is large, the series are at best very slowly convergent, and large numbers of series terms are needed to evaluate J and K accurately. The same statement also holds for I and S. Unno and Spiegel (1966) formally manipulate the series for J and K, obtaining the usual Eddington approximation but with an additional infinite series of "off-diagonal" terms whose neglect, in their words, "seems closely related to the assumption of near isotropy of the radiation field". At locations in the solar atmosphere where $\tau < 1$, the

radiation field is certainly anisotropic--looking out, the atmosphere is transparent while, looking in, it is opaque. Hence it appears that neglecting the "off-diagonal" terms (equivalent to making the Eddington approximation an identity) introduces critical errors in the optically thin region. A different representation of the radiation intensity used in the anisotropic radiation field approximation is given in the next section; it has few terms and fast convergence properties, even in the optically thin region.

Before proceeding to it, however, mention should be made of another approach to solving the transfer equation, developed by Auer and Mihalas (1970), which is quite independent of the approach described in the next section. They introduce a variable Eddington factor, f, defined as the ratio K/J. Its value is position dependent, tending to 1/3 in the interior and to a larger number in the outer photosphere. In their technique, the exact value of this ratio at a point is determined iteratively. Previous uses of this variable Eddington factor, f, have been independent of the anisotropic radiation field approximation, wherein K is explicitly expressed as a position dependent linear combination of the flux F, and mean intensity J. This expression for K is linearized easily for computer modeling purposes, unlike the iteratively obtained quantity f. The expression for K given by the anisotropic radiation field approximation represents a more careful analysis of the relevant physical properties of the radiative transport than does that for f, a factor defined from the K/J ratio to provide internal consistency of the macroscopic equations.

3. THE ANISOTROPIC RADIATION FIELD APPROXIMATION

Development of this approximation starts with the equation of transfer:

$$\mu \frac{dI}{d\tau} = I - S \quad , \tag{1}$$

where τ is the optical depth and the scattering has been neglected. Assuming LTE, which implies S = B, a solution may be developed iteratively:

$$I = B + \mu \frac{dB}{d\tau} + \mu^2 \frac{d^2B}{d\tau^2} + \ldots \tag{2}$$

(cf. Unno and Speigel 1966; Mihalas 1978). This expansion is most useful in the optically thick region, where the first two terms dominate all others. High order derivative terms contribute the most in the optically thin region, where a different approach works better.

The exact solution for a plane parallel atmosphere is given by

$$I(\tau,\mu) = -\int_0^\tau S(t)\, e^{(\tau-t)/\mu}\, \frac{dt}{\mu} \quad , \tag{3}$$

when looking in the optically thin direction and with τ the vertical optical thickness in that direction. Since S = B, S at an arbitrary point t may be expanded as a Taylor series in B, with the B terms evaluated at a fixed point τ:

$$S(t) = B(\tau) + (t-\tau)\frac{dB}{d\tau} + \frac{(t-\tau)^2}{2}\frac{d^2B}{d\tau^2} + \ldots + \frac{(t-\tau)^n}{n!}\frac{d^nB}{d\tau^n} + \ldots \quad . \tag{4}$$

Substituting this in equation (3), and integrating, we find

$$I = B(1 - e^{\tau/\mu}) + \frac{dB}{d\tau}\left[\mu(1 - e^{\tau/\mu}) + \tau e^{\tau/\mu}\right] + \frac{d^2B}{d\tau^2}\left[\mu^2(1 - e^{\tau/\mu}) + \mu\tau e^{\tau/\mu} - \frac{\tau^2}{2} e^{\tau/\mu}\right] + \ldots \quad . \tag{5}$$

Using equation (2) for $\mu \geq 0$ and equation (5) for $\mu < 0$ and keeping only the first two terms, the moment equations are:

$$J = \left(1 - \frac{E_3}{2} B\right) + \left(\frac{E_3}{2} + \frac{\tau E_2}{2}\right)\frac{dB}{d\tau} \quad , \tag{6}$$

$$\frac{F}{4} = H = \left(\frac{E_3}{2}\right)B + \left(\frac{1}{3} - \frac{E_4}{2} - \frac{\tau E_3}{2}\right)\frac{dB}{d\tau} \quad , \tag{7}$$

$$K = \left(\frac{1}{3} - \frac{E_4}{2}\right)B + \left(\frac{E_5}{2} + \frac{\tau E_4}{2}\right)\frac{dB}{d\tau} \quad , \tag{8}$$

where the symbol E_i represents the "i-th" type of exponential integral function with argument τ. Note that when $\tau \to \infty$, $E_i \to 0$ and the Eddington approximation is an identity. When $\tau \to 0$, however, $3K \neq J$.

For arbitrary values of τ, K may be written, using equations (6-8), as the following linear combination:

$$K(\tau) = g(\tau)\cdot F(\tau) + h(\tau)\cdot J(\tau) \quad , \tag{9}$$

where

$$g(\tau) = \frac{1}{2} \cdot \frac{\left(1 - \frac{E_2}{2}\right)(\tau E_4 + E_5) - \left(\frac{1}{3} - \frac{E_4}{2}\right)(\tau E_2 + E_3)}{\left(1 - \frac{E_2}{2}\right)\left[\frac{4}{3} - 2(\tau E_3 + E_4)\right] - E_3(\tau E_2 + E_3)} \quad , \tag{10}$$

$$h(\tau) = \frac{\left(\frac{1}{3} - \frac{E_4}{2}\right)\left[\frac{4}{3} - 2(\tau E_3 + E_4)\right] - E_3(\tau E_4 + E_5)}{\left(1 - \frac{E_2}{2}\right)\left[\frac{4}{3} - 2(\tau E_3 + E_4)\right] - E_3(\tau E_2 + E_3)} \quad . \tag{11}$$

Note that g and h are explicitly known functions of τ. The Eddington approximation corresponds to $g(\tau) = 0$ and $h(\tau) = 1/3$. Instead of starting with the flux equation

$$F = -\frac{4}{3\kappa\rho}\frac{dJ}{dr} \quad , \tag{12}$$

and deriving its linearized counterpart, the following exact flux equation is used:

$$F = -\frac{4}{\kappa\rho}\frac{dK}{dr} \quad , \tag{13}$$

(κ is the opacity and ρ is the density). Substituting equation (9) into equation (13), this equation for flux is linearized and manipulated to provide one of the four first-order linear differential equations which describe the oscillating system.

4. COMPARISON OF SOLUTION METHODS FOR THE TRANSFER EQUATION

The transfer equation and two of its moment equations are:

$$\mu\frac{dI}{d\tau} = I - S \quad , \tag{14}$$

$$\frac{dH}{d\tau} = J - S \quad , \tag{15}$$

$$\frac{dK}{d\tau} = H \quad , \tag{16}$$

where H is the Eddington flux. The Eddington approximation is: $J_{Edd}(\tau) = 3K_{Edd}(\tau)$, for all τ. Under this assumption and the assumption of radiative equilibrium (J = S), equations (15-16) may be solved exactly, but equation (14) is not satisfied. Using LTE, the following T - τ relation is obtained:

$$T^4 = \frac{3}{4} T_{eff}^4 (\tau + q_{Edd}(\tau)) , \quad q_{Edd}(\tau) \equiv 2/3 , \tag{17}$$

where T_{eff} is the effective temperature. The exact solution, which satisfies all of equations (14-16), is of the following form:

$$T^4 = \frac{3}{4} T_{eff}^4 (\tau + q(\tau)) , \tag{18}$$

where $q(\tau)$ is a known function of τ, first obtained by Mark (1947). The moments of I are given by:

$$J_{exact}(\tau) = \frac{3}{4} F_o (\tau + q(\tau)) , \tag{19}$$

$$F_{exact}(\tau) = F_o , \tag{20}$$

$$K_{exact}(\tau) = \frac{1}{4} F_o (\tau + q(\infty)) , \tag{21}$$

where F_o, the flux, is a constant. When using the anisotropic radiation field approximation, the following definitions apply:

$$J_a(\tau) = \frac{3}{4} F_o (\tau + q_a(\tau)) , \tag{22}$$

$$F_a(\tau) = F_o , \tag{23}$$

$$K_a(\tau) = \frac{1}{4} F_o (\tau + q_a(\infty)) . \tag{24}$$

Imposing equation (9), the following equation is obtained:

$$q_a(\tau) = \frac{\tau + q_a(\infty) - 4g(\tau)}{3h(\tau)} - \tau . \tag{25}$$

At infinite optical depth, $q(\infty) = q_a(\infty) = .710466$. The three sets of q values, $q_{Edd}(\tau)$, $q(\tau)$, and $q_a(\tau)$, are given in Table 1. They represent the Eddington approximation, the exact solution, and the anisotropic radiation field approximation, respectively. The anisotropic radiation field approximation is much closer to the exact solution than is the Eddington approximation.

TABLE 1. Comparison of Eddington, Exact, and Anisotropic Radiation Field Solutions

τ	$q_{Edd}(\tau)$	$q(\tau)$	$q_a(\tau)$	$\frac{g(\tau)F(\tau) + h(\tau)J(\tau)}{K(\tau)} = R(\tau)$	$\frac{J(\tau)}{3K(\tau)} = S(\tau)$
0.00	2/3	.5773	.5790	1.0012	.8126
0.01	2/3	.5882	*	1.0025	.8303
0.02	2/3	.5954	*	1.0033	.8425
0.03	2/3	.6012	*	1.0037	.8524
0.05	2/3	.6107	*	1.0043	.8688
0.1	2/3	.6279	*	1.0048	.8981
0.2	2/3	.6495	.6416	1.0047	.9330
0.3	2/3	.6633	.6568	1.0042	.9533
0.4	2/3	.6731	.6672	1.0039	.9663
0.5	2/3	.6803	.6750	1.0034	.9751
0.6	2/3	.6858	.6809	1.0031	.9812
0.7	2/3	.6901	.6857	1.0027	.9855
0.8	2/3	.6935	.6894	1.0024	.9887
0.9	2/3	.6963	.6925	1.0021	.9912
1.0	2/3	.6985	.6951	1.0018	.9930
1.2	2/3	.7019	.6990	1.0014	.9955
1.5	2/3	.7051	.7028	1.0010	.9976
2.0	2/3	.7079	.7064	1.0005	.9990
2.5	2/3	.7092	.7083	1.0003	.9996
3.0	2/3	.7098	.7092	1.0002	.9998
3.5	2/3	.7101	.7096	1.0001	.9999
4.0	2/3	.7102	.7102	1.0000	.9999
∞	2/3	.710466	.710466	1	1

*indicates that $h(\tau) \sim 0$ and that $q_a(\tau)$, the ratio of two small quantities, is numerically inaccurate.

In the range where τ is small (0.01 to 0.1), $h(\tau)$ is nearly zero and equation (25), which defines $q_a(\tau)$, is indeterminate. This is why asterisks appear in Table 1 in the column of $q_a(\tau)$ values. Because of this, another comparison of the approximations to the exact solution is desirable, a comparison not susceptible to shortcomings such as the one above.

Using values from the exact solution, the following quantities are computed:

$$R(\tau) = (g(\tau)\cdot F(\tau) + h(\tau)\cdot J(\tau))/K(\tau) \quad , \tag{26}$$

$$S(\tau) = J(\tau)/3K(\tau) \quad . \tag{27}$$

If the Eddington approximation is correct, then $S(\tau) \equiv 1$ and if the anisotropic radiation field approximation is correct, then $R(\tau) \equiv 1$. As is evident from the values for $R(\tau)$ and $S(\tau)$ in Table 1, the anisotropic radiation field approximation is superior to the Eddington approximation for the entire range of τ. In fact, the widest deviation of the anisotropic radiation field approximation from the exact solution is less than 1/2% and occurs at $\tau = 0.1$.

5. SOLUTION DEPENDENCE ON RADIATIVE TRANSFER TREATMENT AND OUTER BOUNDARY CONDITIONS

Four sets of wave equation solutions were generated using the equilibrium model and method described in Hill, Rosenwald and Caudell (1978). The two treatments of radiative transfer (Eddington and anisotropic radiation field approximations), combined with the two types of outer boundary conditions define the four sets. All of these sets had a period of 300 seconds. In Figures 1-4, β_- indicates that standard outer boundary conditions were applied and β_+ indicates the use of anomalous outer boundary conditions. The presence of (E) and (A) indicates which radiative transfer treatment was used, the Eddington or anisotropic radiation field approximation, respectively. Figures 1 and 2 show the magnitude and phase of the displacement $\delta r/r$, as a function of log τ for the above four cases. The difference between the β_- (E) and β_- (A) curves for $\delta r/r$ is smaller than the difference between the β_+ (E) and β_+ (A) curves. The differing locations and sharpness of the β_+ minima affect observables more than the differing β_- slopes do.

The method for computing I', the Eulerian perturbation of intensity, is given in Hill, Rosenwald and Caudell (1978). When standard outer boundary conditions are applied, the $\delta r/r$ term, not the $\delta T/T$ term, is the dominant term in computing the value of I'. Thus, even though $\delta T/T$ differs substantially between the β_- (E) and β_- (A) cases (see Figures 3 and 4), its impact on I' is small. For anomalous outer boundary conditions, however, the observables I' and $\delta r/r$ are dependent on the method of treating the radiative transfer physics, and therefore require the more physically correct anisotropic radiation field approximation to be used.

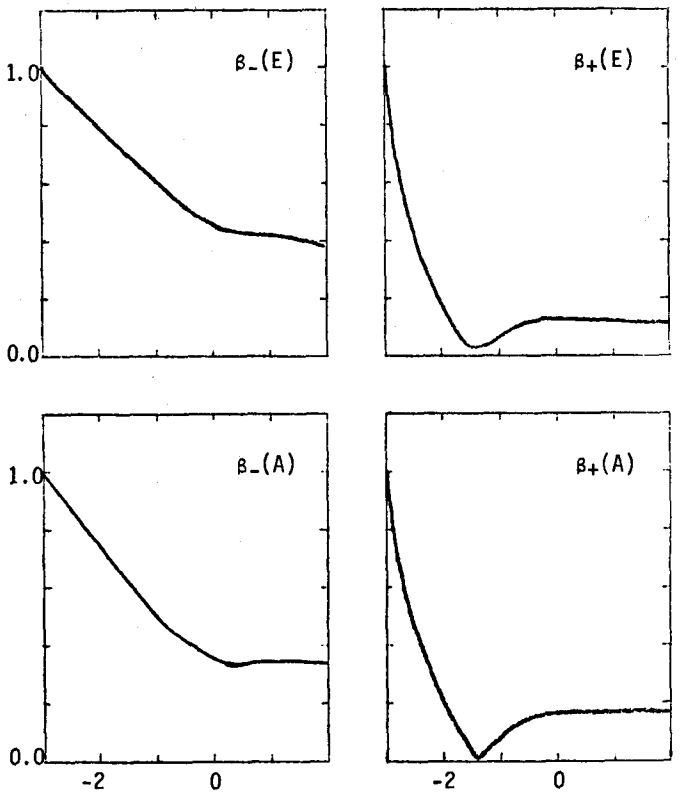

Figure 1. The magnitude of $\delta r/r$ as a function of log τ. β_+ and β_- indicate the use of anomalous and standard outer boundary conditions. (E) and (A) indicate the radiative transfer treatment used: the Eddington or anisotropic radiation field approximation. The period used in the computation is 300^s.

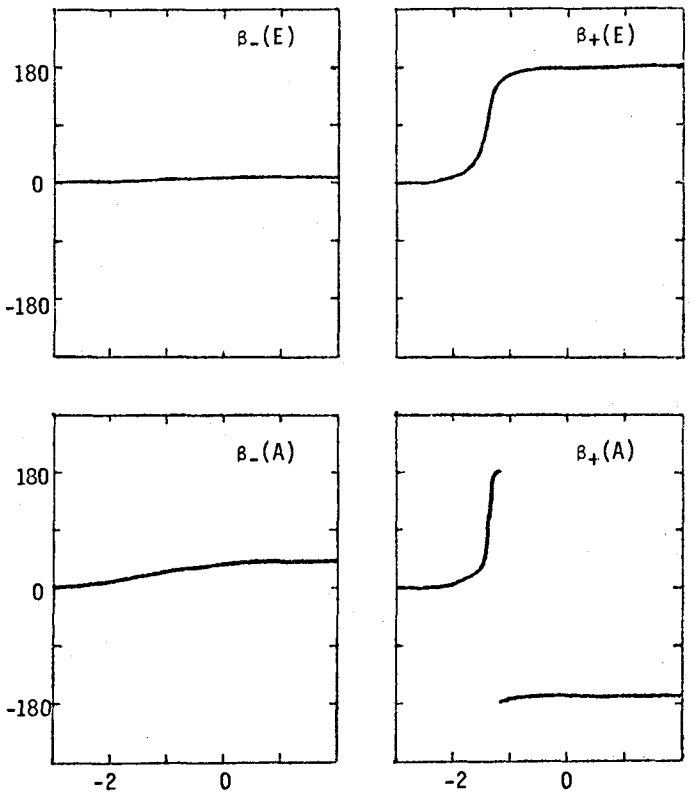

Figure 2. The phase of $\delta r/r$ as a function of $\log \tau$.

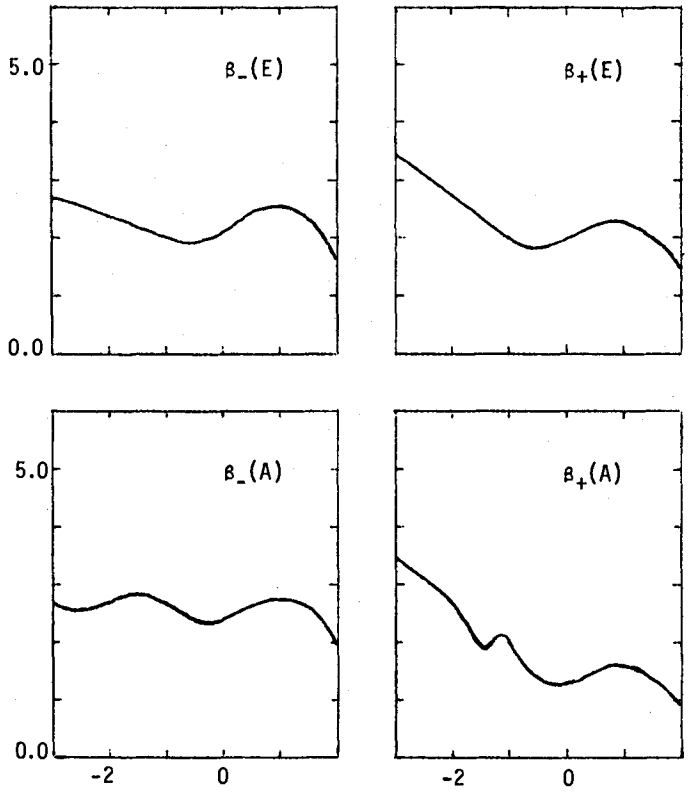

Figure 3. The quantity $\log_{10} |\delta T/T|$ as a function of $\log \tau$.

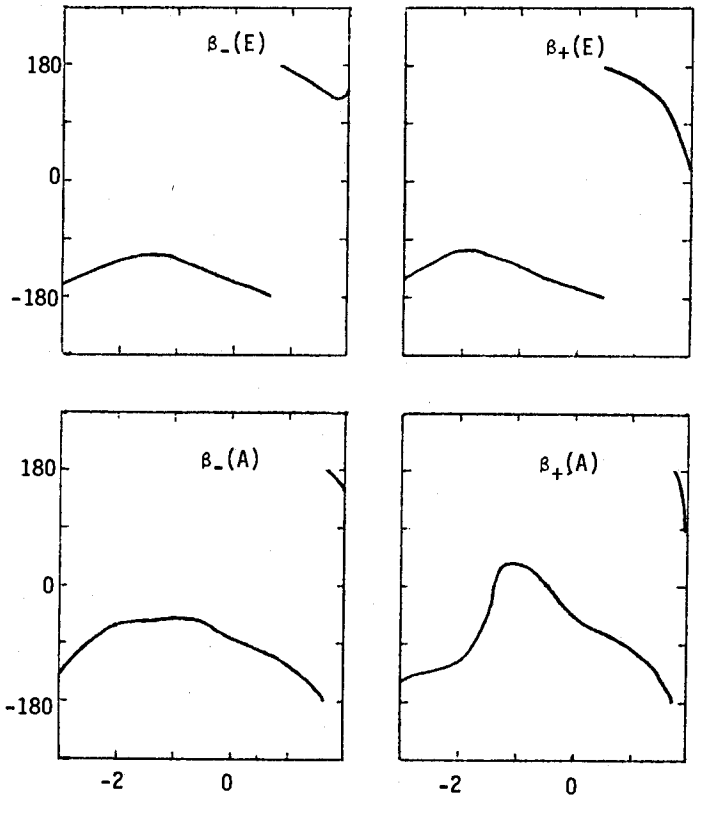

Figure 4. The phase of $\delta T/T$ as a function of $\log \tau$.

* * * * *

This work was supported in part by the National Science Foundation and by the Air Force Geophysical Laboratory.

REFERENCES

Ando, H. and Osaki, Y. 1975, Publ. Astron. Soc. Japan, 27, 581.
Auer, L. and Mihalas, D. 1970, Mon. Not. R. Astr. Soc., 149, 60.
Hill, H.A., Rosenwald, R.D. and Caudell, T.P. 1978, Ap. J., 225, 304.
Mark, C. 1947, Phys. Rev., 72, 558.
Mihalas, D. 1978, Stellar Atmospheres, (2nd edition; San Francisco: Freeman).
Rosenwald, R.D. and Hill, H.A. 1980, these proceedings.
Unno, W. and Spiegel, E.A. 1966, Publ. Astron. Soc. Japan, 18, 85.

THE OBSERVATIONAL PROPERTIES OF THE ZZ CETI STARS*

E.L. Robinson
Department of Astronomy
University of Texas at Austin

ABSTRACT

The ZZ Ceti stars are the pulsating white dwarfs lying within an instability strip on the white dwarf cooling sequence with edges at B-V colors of +0.16 and +0.29. A total of 13 confirmed ZZ Ceti stars have now been found, and all have DA spectral types, all have temperatures between 10500K and 13500K, and all have gravities between log g of 7.8 and 8.1. These properties, like all the properties of the ZZ Ceti stars, are normal for white dwarfs. Indeed, since both pulsating and non-pulsating white dwarfs can be found within the instability strip, at present there is no way to distinguish observationally a pulsator from a non-pulsator other than by the immediate fact of its variability. All of the ZZ Ceti stars are multi-periodic with, in the case of HL Tau-76, more than 20 periods being simultaneously present in the light curve. The periods are always very long, ranging from 100 to 1200 seconds. In at least one variable, R548, the pulsation periods are exceptionally stable, with the upper limit on the rate of change of the periods being $|\dot{P}| < 10^{-12}$, but in other variables the periods appear to change on time scales as short as a few hours. All recent models for the variability of ZZ Ceti stars have invoked nonradial, g-mode pulsations. Qualitatively, the g-mode pulsations easily account for the length of the observed periods and for the occasional close spacing of the periods. While the g-mode interpretation is certainly at least partially correct, the light curve of the ZZ Ceti star GD 154 suggests that other complicating factors are at work. Although it too is multi-periodic, GD 154 has only one strong period, 1186 seconds. This period is so long that if it is a g-mode, it must be a high overtone, $k \sim 20\text{-}30$. Thus, GD 154 seems to have been excited in a single high overtone. It has not been clearly demonstrated that a white dwarf can be excited in such a high overtone without exciting other overtones as well.

---

* The full text of this paper will appear in the proceedings of IAU Symposium No. 53.

THEORETICAL ASPECTS OF NONRADIAL OSCILLATIONS IN WHITE DWARFS: A SUMMARY

C.J. Hansen
Joint Institute for Laboratory Astrophysics[1]
and Department of Physics and Astrophysics
University of Colorado
Boulder, Colorado

ABSTRACT

The present status of nonradial oscillation theory as applied to the ZZ Ceti variables is briefly reviewed as are the author's concerns about what might be the modes of oscillation of these stars.

1. INTRODUCTION

This review shall concentrate on recent theoretical developments concerning nonradial oscillations in otherwise normal white dwarfs; namely, the ZZ Ceti variables. Because the excellent and comprehensive summary by Van Hörn (1978) is generally available, this summary shall, for the most part, be restricted to some special topics and issues which appear to be worthy of future consideration.

The observational aspects of the ZZ Ceti variables as a distinct class of variable star have been most fully put forth in the eminently readable thesis of McGraw (1977); the paper by Robinson (1980) in these proceedings may also be referred to. In Table 1 are listed the photometric properties of the known ZZ Ceti variables (adapted from McGraw 1977 and Nather 1978) in rough order of increasing period of variability. The column labeled "harmonics" indicates whether the power spectrum for that star contains harmonics of a basic frequency. The presence of these is a measure of departures from sinusoidality of the light curve for that basic frequency and is most probably due to nonlinear effects in the pulsing mechanism. Cross coupling, which is the appearance of frequencies corresponding to sums or differences of major frequencies in the spectra, has been interpreted as arising from nonlinear coupling of pulsation modes. The last column, which describes whether major frequencies in the spectra do or do not drift in frequency, is fairly well correlated with the presence of harmonics, cross coupling, and mean pulsation amplitude; in other words, large amplitude and complex, longer period, variable spectra seem to go

[1]Operated jointly by the National Bureau of Standards and the University of Colorado.

together.

Aside from their variability, the ZZ Ceti stars appear to be perfectly normal DA white dwarfs. However, their location on the HR diagram, as shown in Figure 1 (from van Horn 1978), is highly enlightening. We find that they lie in the linearly extended path of the well known Cepheid instability strip in just the temperature range where envelope hydrogen convection (and ionization) zones begin to operate actively in white dwarfs as they cool down from higher temperatures. Thus, the suggestion of Robinson and McGraw (1976) that the usual κ - and γ- mechanisms, which give rise to variability in the Cepheid strip, are also operative in ZZ Ceti stars has prompted investigations along the lines taken for the normal variables (of which more will be said later).

Because of the long periods of the ZZ Ceti stars, it is generally believed that their variable light output is caused by nonradial, gravity (g) mode oscillations. This association comes about as follows. (Two good general references are the reviews of Ledoux 1974 and Cox 1976.) For small amplitude, nonradial oscillations, there are two characteristic frequencies:

1. The Brunt-Väisälä (or buoyancy) frequency σ_g is given by:

$$\sigma_g^2 = N^2 = -Ag$$

where g is the local gravity and A, which is one measure of convective stability ($A < 0$), is:

$$A = \left[\frac{\chi_T}{\chi_\rho}(\nabla-\nabla_{ad}) + \frac{\chi_\mu}{\chi_\rho}\frac{d\ \ell n\ \mu}{d\ \ell n\ P}\right] H_p^{-1} \quad .$$

Here, μ is the mean molecular weight, H_p is the pressure scale height and [for $P = P(\mu,\rho,T)$]

$$\chi_\rho = \left(\frac{d\ \ell n\ P}{d\ \ell n\ \rho}\right)_{\mu,T}$$

with the other χ's being defined by permuting ρ, μ, and T. Other symbols have their usual meanings. In the simple case of a chemically homogeneous star

$$\sigma_g^2 = -\frac{\chi_T}{\chi_\rho}(\nabla-\nabla_{ad})\ H_p^{-1} \quad .$$

An important property of white dwarfs is that χ_T and ∇ are very small in the interior except for the thin nondegenerate envelope.

2. The acoustic frequency is simply related to the sound speed $v^2 = \Gamma_1 P/\rho$ by

Table 1. Photometric Properties of the ZZ Ceti Stars

Star	Basic Periods (Seconds)	Mean Amplitude (Magnitude)	Harmonics	Cross Coupling	Stability
L19-2	114,192	0.03	No	No	High
R548	213,274	0.012	No	No	Very High
G117-B15A	216,312	0.05	No	No	Very High
BPM 31594	310,617	0.21	Yes	No	High
GD 99	260,590	0.07	Yes	Yes	Moderate
G207-9	292,318,557,739	0.06	No	Yes	Moderate
HL Tau-76	494,625,746	0.28	Yes	Yes	Low
BPM 30551	298,823	0.22	No	No	Moderate
R808	833	0.15	Yes	Yes?	Very Low
G29-38	820,930,1020	0.27	Yes	Yes	Low
G38-29	929,1020	0.22	Yes	Yes	Very Low
GD 154	780,1186	0.10	Yes	No	Moderate

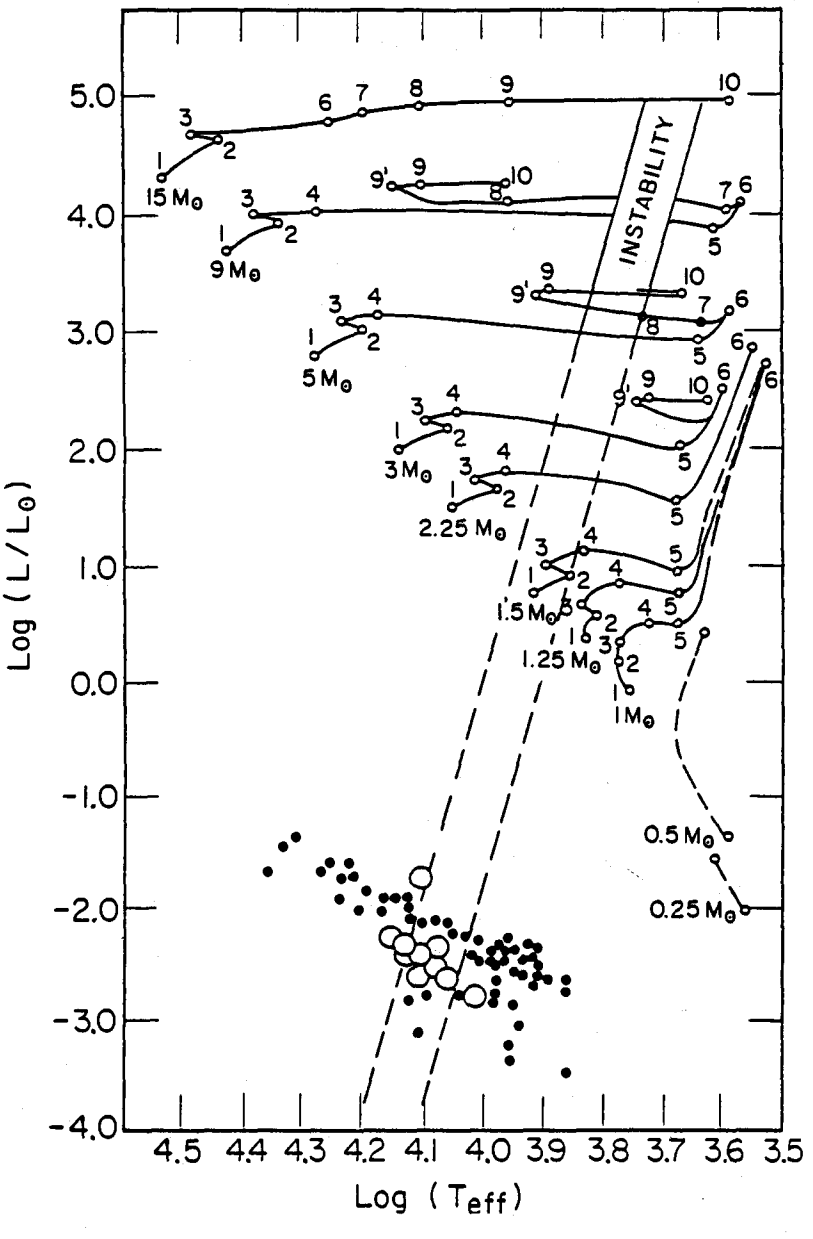

Figure 1. The location of the ZZ Ceti variables on the HR diagram (taken from Van Horn 1978).

$$\sigma_a^2 = S_\ell^2 = \frac{\ell(\ell+1)v_s^2}{r^2}$$

where ℓ is the multipole order of spherical harmonic Y_ℓ^m.

For simple stellar models, there are two types of modes which may be easily distinguished by whether buoyancy or pressure constitute the primary restoring force against displacements in the stellar fluid. These are, respectively, the gravity (g) modes and pressure (p) modes. (The f or Kelvin mode does not concern us here.) They have the following properties:

1. A gravity mode actively propagates (has a sinusoidal behavior for its radial and transverse displacements in a localized region) if its frequency, σ, satisfies the local inequalities

$$\sigma^2 < S_\ell^2 \quad \text{and} \quad \sigma^2 < N^2 \quad .$$

Otherwise, the displacements display evanescent (exponential) behavior.[2] If $N^2 < 0$, implying convective instability, these g-modes are usually given the designation g^-. A radiative region is capable of propagating the variety g^+. Since we shall be concerned with the latter only, the superscript shall be dropped in what follows.

2. Pressure modes propagate in regions where

$$\sigma^2 > S_\ell^2 \quad \text{and} \quad \sigma^2 > N^2 \quad .$$

Otherwise, they too are evanescent.

A sample run of N^2 and S_ℓ^2 (for $\ell = 2$) is shown in Figure 2 for a 1 $M_\odot$, purely radiative white dwarf with $\log L/L_\odot = -4.2$, and $\log T_e = 3.83$. (This model is too cool to correspond to a ZZ Ceti variable but it illustrates the salient points. See also Osaki and Hansen 1973.) Note that the abscissa is $\log (1 - r/R)$, resulting in placement of the model center at the origin (to the right) and emphasis of the outer layers. The boundary of the degenerate core is indicated and it marks (on the well-spread logarithmic scale) that point where N^2 makes its rapid descent into the interior. By inspection, it is clear where p and g modes may propagate. For orientation, however, these are indicated by the positions of the nodes of the radial displacements of the p and g harmonics, p_1, p_2, g_1 through g_3 plotted against frequency for $\ell = 2$. As expected (although this is not strictly necessary), the nodes are confined within the regions of propagation. Also, to our well known chagrin, the g-mode frequencies ($\sim 10^{-3}$ sec^{-2}) are generally too high to account for

[2] Important exceptions to these statements arise when convection reaches out to the stellar surface. See Scuflaire (1974).

those of the ZZ Ceti variables ($\sigma^2 \sim 10^{-5}$-10^{-4} sec^{-2}) unless the harmonic (denoted by k in $g_{\ell k}$) is large. For example, in this (too cool) model the g-mode periods are given closely by

$$P(g_{\ell k}) = \frac{285}{\left[\ell(\ell+1)\right]^{\frac{1}{2}}} \left[1 + \frac{1}{3}(k-1)\right] \text{ sec}; \quad \ell,k=1,2,\ldots \quad .$$

(See also Brickhill 1975.) The observed periods require $k \sim 10$ for the longer period variables even with $\ell = 1$. For a hotter, less evolved model more appropriate to the ZZ Ceti stars the required harmonic is even higher. What about these higher harmonics?

Dziembowski (1977a) has analyzed two 0.6 $M_\odot$ white dwarf models with effective temperatures of $\sim 10^4$ whose distribution of elements corresponds to Paczynski's (1971) planetary nuclei evolutionary sequence. Using a nonadiabatic treatment, he finds that low orders of ℓ and k yield stable g-modes. A destabilizing effect, due mainly to the He II ionization zone, is noted but dissipation in more interior regions overwhelms the effect of that zone. However, unstable modes are encountered for high ℓ and k ($\ell \sim 100$-400, $k \sim 15$-20), but these yield periods of around 10 seconds and are inappropriate for any of the ZZ Ceti stars. Thus, we have the dilemma that the shorter period variables have periods corresponding to low order, but stable, modes and unstable modes have periods which are far too short for any of the variables. A similar result, although for radial modes, has been reported in these proceedings by Cox, Hodson and Starrfield (1980).

A resolution of our difficulties has been suggested by Dziembowski (1977a) for the ~ 1000 second oscillators wherein resonant coupling of the short period unstable modes with low order modes causes the latter to be excited and thus be observed. Unfortunately, it has not yet been demonstrated in detail how this might occur. This is an outstanding problem which impacts on those other variable stars considered at this conference.

Dziembowski (1977b) has also investigated the luminosity amplitudes for many modes and finds that combinations of low ℓ and high k yield the largest excursions in magnitude. Thus, we might expect that longer period ZZ Ceti stars should exhibit larger light amplitudes. Indeed this is generally the case for these stars (see the marvelous sequence of diagrams in Van Horn 1978) although, again, no excitation mechanism seems sufficient except through the coupling of modes.

2. WHAT SHOULD BE DONE NEXT?

Areas which seem to deserve further theoretical attention will be outlined next. Some of these present extraordinary difficulties for the theorist whereas others may remain fundamentally unresolved.

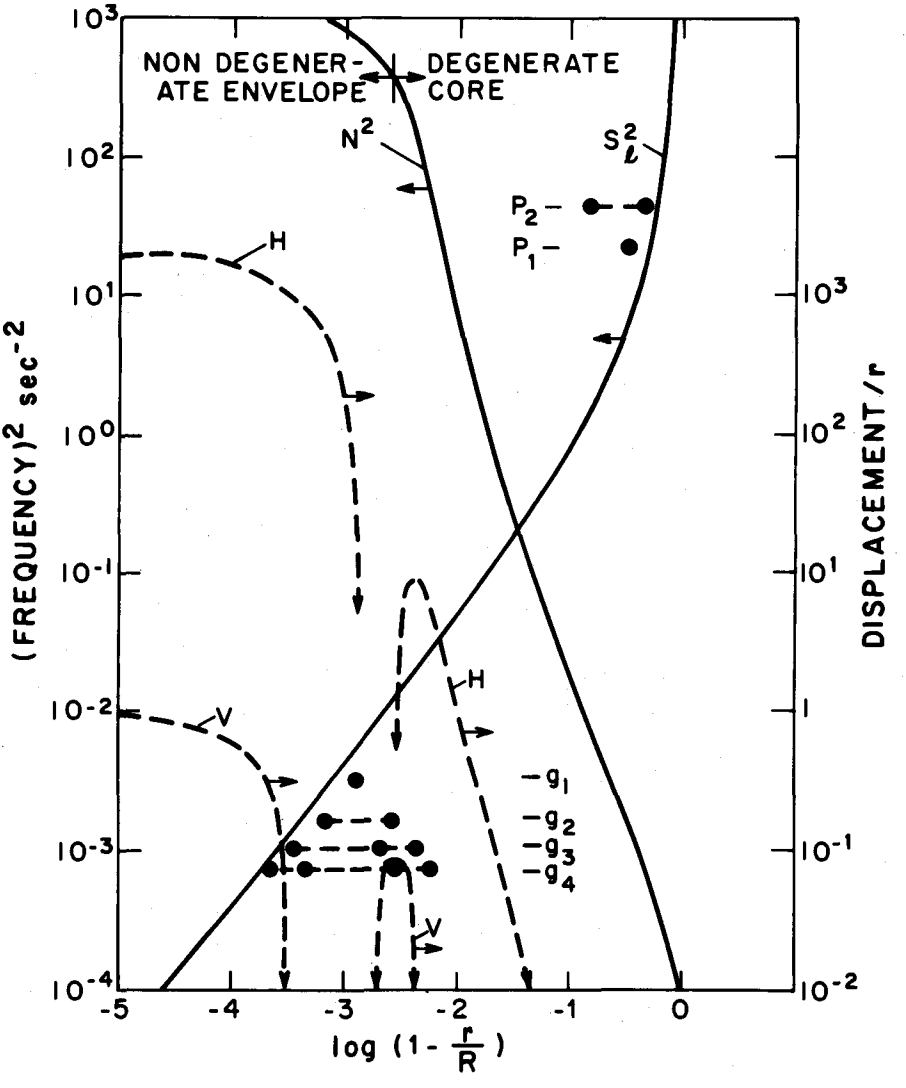

Figure 2. Shown are the run of N^2 and S_ℓ^2 as a function of log (1 - r/R) for a cool, 1 $M_\odot$ ^{56}Fe white dwarf. The location of radial nodes for g and p modes are indicated, as are the radial (V) and horizontal (H) relative displacements for g_3.

2.1. Composition of the Outer Layers

It appears that the atmospheres of DA white dwarfs show abnormal deficiencies in their helium content (Strittmatter and Wickramasinghe 1971, Shipman 1972, for example). If such an effect is due to gravitational settling, then the transition to the helium-rich (for example) interior should take place over roughly a pressure scale height (Baglin 1974, Koester 1976, and Vauclair and Reisse 1977). The depth of such a transition zone is unknown, except that it cannot reach down so far as to ignite hydrogen, and it probably would vary from star to star, but it would have some interesting effects. First, it would change the depth and character of the outer convection zones(s) (see Figure 7 of Fontaine and Van Horn 1976); this effect will be further considered shortly. Second, it introduces a relatively sharp composition discontinuity. The possible importance of the latter has been discussed by Ledoux (1974) who reported calculations of nonradial modes for a heterogeneous incompressible sphere. (See also the paper by Gabriel and Scuflaire 1980, in these proceedings.) It was found that new spectra of g-modes marched out from a reservoir at zero frequency as new density discontinuities were introduced. The modes acted like surface waves with maximum amplitudes at the discontinuities. If these results apply to realistic compressible models, can such modes be found and are they important? This is not an easy task, especially when coupled with evolutionary calculations, since the time behavior of composition profiles as affected by convection can be quite complicated, as shown by Koester (1976) and Vauclair and Reisse (1977). It is interesting to note that the structure of those investigators' model atmospheres changed dramatically as the ZZ Ceti effective temperatures of $\sim$ 10,000 K were reached.

2.2. Effects of Convection

Convection obviously plays a variety of roles in pulsation analysis. It can determine g-mode frequencies as well as influence stability. As a speculative example of the former, an artist's conception of the run of S_ℓ^2 and N^2 in a hypothetical white dwarf (based on Figure 2) is shown in Figure 3. A convective zone is indicated by the well in N^2 in the envelope. Also shown is a "μ-barrier" corresponding to a composition gradient. We can imagine normal g-modes propagating in the cross-hatched region to the right which is labeled "core modes" although we realize that most of the action takes place within a distance of about 10^{-3} of the white dwarf surface. What about the hatched region to the left? Goossens and Smeyers (1974) (see also Tassoul and Tassoul 1968 among others) have effectively shown that, for each interior convective zone (with $N^2 < 0$) present in a stellar model, there are associated families of g-modes which, for the most part, are contained or "trapped" within the surrounding radiative regions with the convective

region acting as a buffer zone. Is this also the case for the white dwarf of Figure 3 or is the buffer zone too thin? If this is true, then we could naively expect to find g-modes which propagate in the very outermost surface layer of the star with a minute amount of mass being involved. By inspection of the figure, their frequencies would be less than $\sim 10^{-5}$ sec^{-1}, corresponding to periods greater than $\sim$ 2,000 sec. However, because nonadiabatic effects for such modes are expected to be very large, it will take much work to establish the relevance of these atmospheric modes to ZZ Ceti stars.

As regards stability, we note from the work of Fontaine and Van Horn (1976, see their Figure 8), for example, that convection in white dwarf envelopes can carry up to all of the energy transported through those zones. In addition, the combination of convective eddy velocities and typical mixing lengths may yield turnover times on the order of seconds to many hundreds of seconds. There is thus the possibility that convective eddies may in some manner keep up with the stellar motion or, at the other extreme, be effectively frozen in. It is not at all clear how these possibilities affect stability. In the calculations of Dziembowski (1977a) the effects of convection (on stability) were ignored, with the inferred meaning that the convective flux (or perhaps its gradient) was held fixed. This would seem to introduce a large measure of uncertainty into those calculations but at the moment such uncertainties appear to be unavoidable. Similarly, large values of ℓ for g-modes imply transverse nodal structures which have dimensions only a few factors of ten larger than eddy sizes in extensive convection zones (assuming those sizes are comparable to local pressure scale heights). Thus, the interaction of pulsation and convection might very well be significant, especially since transverse displacements in g-modes tend to be large (see Figure 2).

Now back to Figure 3, which is a bit of a swindle. The convection zone has been depicted as extending out to a radius fraction of 10^{-5} of the "surface." However, in the temperature regime of the ZZ Ceti variables, the hydrogen convection zone may extend out to optical depths of less than unity (Fontaine and Van Horn 1976). Thus we have the ticklish question of how to apply boundary conditions near or above the photosphere; the spectre may also be raised of β^+ modes, discussed in this conference in the context of solar oscillations. Since, at least in my view, the erratic and complex spectra of light variations in the longer period ZZ Ceti stars most probably arise from surface-like waves involving little total mass, the above questions should be addressed in the future studies.

2.3. Rotation

To my knowledge, no significant new material has appeared since the review of Van Horn (1978) although there are some problems outstanding. Slow rotation is most certainly present in at least some ZZ Ceti stars, as indicated by the extraordinarily

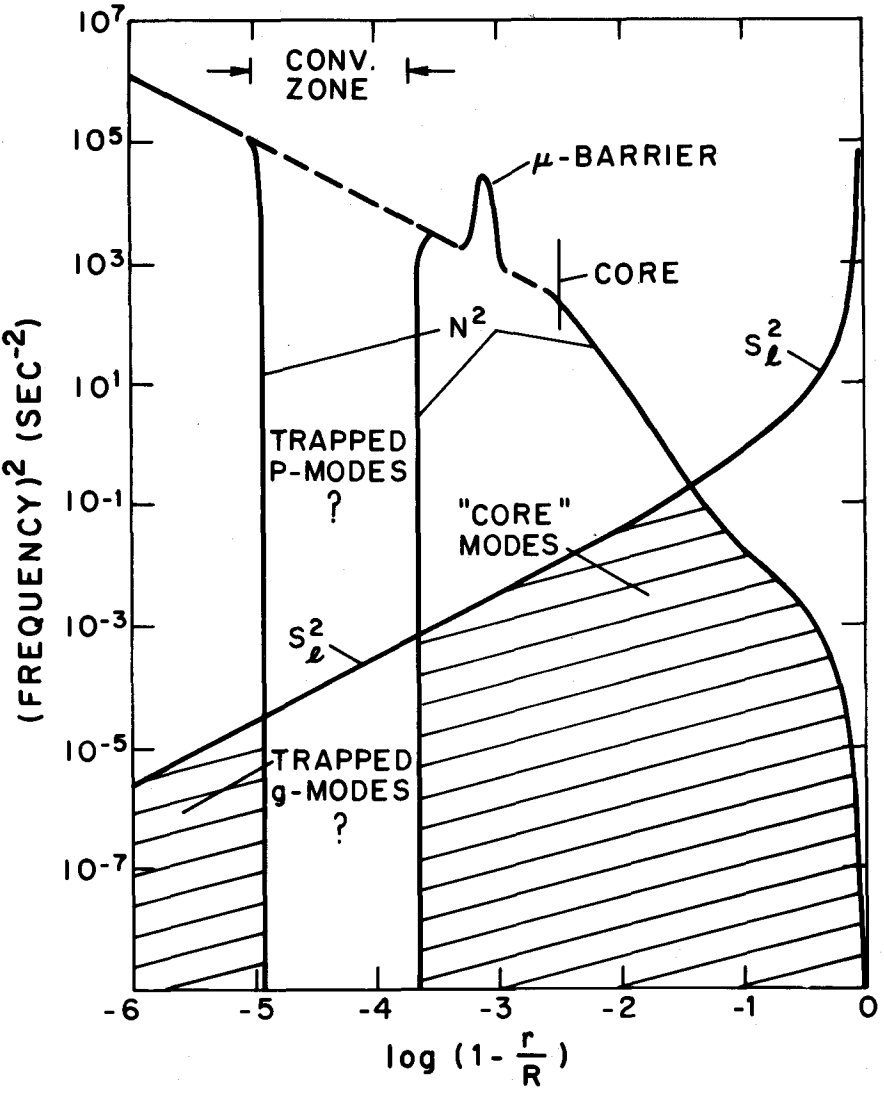

Figure 3. A fanciful run of N^2 and S_ℓ^2 where convection is present in the model of Figure 2. Cross-hatched regions are possible zones of entrapment of g-modes.

stable doublet pair of modes in R548 (Robinson, Nather and McGraw 1976). It is doubtful at this time whether rotational splitting can serve as a really useful diagnostic because of the wide variety of rotation laws which are, in principle, physically acceptable. All that can be said for now is that R548 is slowly rotating. We may contrast this situation with that of the earth where a multitude of oscillation modes are seen, some rotationally split, thus providing numerous cross checks on models.

Rapid rotation, for some variables, has been proposed by Wolff (1977, 1980) in his model of nonlinear beating of rotationally split g-modes. I believe that this theory is still undeveloped and may be contradicted by observations that white dwarfs tend to be slow rotators.

2.4. Solid Core Effects

Van Horn and Savedoff (see Van Horn 1978) have suggested that the crystallized cores of evolved white dwarfs should affect oscillation periods. This may not be directly applicable to the ZZ Ceti variable since, for reasonable masses for these stars ($\sim 0.6\ M_\odot$) and compositions, crystallization may not occur until these stars have cooled down beyond their observed temperatures. However, in a preliminary study, Van Horn and I have calculated low ℓ and k modes for the cool, 1 $M_\odot$ model mentioned previously. The crystalline core for this model is very extensive and comprises all but about 0.1% of the total mass and 5% of the radius. Note, however, that the model is not self-consistent because crystallization was not taken into account during the evolution and was added in only for the pulsation analysis.

The modes calculated were the spheroidal $P_{1,2}$, f and $g_{1,2}$ for $\ell = 1$, 2, and 3. To conform with geophysical usage, these are designated as ${}_{1,2}S_\ell$, ${}_0S_\ell$ and ${}_{-1,-2}S_\ell$ respectively. Toroidal modes, having zero radial displacements and Eulerian pressure variations, were also considered and are denoted by ${}_kT_\ell$ where k counts the number of nodes in the transverse displacement. Our results are summarized in Figure 4. As can be seen, the effects of crystallization on the p and f modes are very small. However, g-mode frequencies increase by nearly a factor of three above their corresponding fluid values, making it still more difficult to reach the low frequencies of the ZZ Ceti variables. Nevertheless, if it can be shown that crystallization does take place in these stars, then pulsation calculations must be modified to account for crystallization effects. The toroidal modes, which have frequencies intermediate between the pressure and gravity modes, are primarily of academic interest because the oscillations are confined to the solid core thus giving no observable surface variations.

* * * * *

I would like to thank Professors J.P. Cox and H.M. Van Horn for numerous

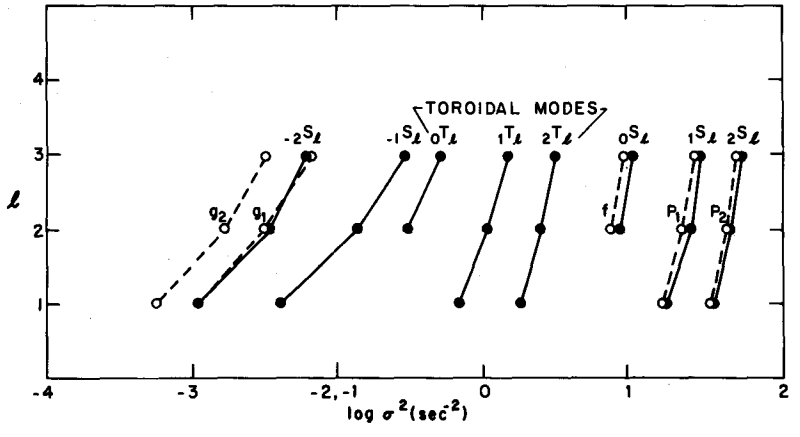

Figure 4. Frequencies of various ℓ and k modes for the well-used model of Figures 2 and 3 where the effects of crystallization have been included. Solid body modes are designated by $_kS_\ell$ (spheroidal) and $_kT_\ell$ (toroidal).

discussions and collaborations down through the years. This work was supported in part by NSF Grant AST 77-23183 through the University of Colorado.

REFERENCES

Baglin, A. 1974, First European Workshop on White Dwarfs, Kiel.

Brickhill, A.J. 1975, Mon. Not. R. Astr. Soc., 170, 405.

Cox, J.P. 1976, Ann. Rev. Astron. Ap., 14, 247.

Cox, J.P., Hodson, S.W. and Starrfield, S.G. 1980, these proceedings.

Dziembowski, W. 1977a, Acta Astron., 27, 1.

Dziembowski, W. 1977b, Acta Astron., 27, 203.

Fontaine, G. and Van Horn, H.M. 1976, Ap. J. Suppl., 31, 467.

Gabriel, M. and Scuflaire, R. 1980, these proceedings.

Goossens, M. and Smeyers, P. 1974, Ap. and Sp. Sci., 26, 137.

Koester, D. 1976, Astron. Ap., 52, 415.

Ledoux, P. 1974, in I.A.U. Symposium No. 59, Stellar Stability and Evolution, ed. P. Ledoux, A. Noels and A.W. Rodgers (Reidel: Dordrecht), p. 135.

McGraw, J.T. 1977, Ph.D. Thesis, University of Texas (Austin).

Nather, E. 1978, Pub. Astron. Soc. Pac., 90, 477.

Osaki, Y. and Hansen, C.J. 1973, Ap. J., 185, 277.

Paczynski, B. 1971, Acta Astron., 21, 417.

Robinson, E.L. 1980, these proceedings.

Robinson, E.L. and McGraw, J.T. 1976, in Proceedings of the Solar and Stellar Pulsation Conference, ed. A.N. Cox and R.G. Deupree, LASL report LA-6544-C, p. 98.

Robinson, E.L., Nather, R.E. and McGraw, J.T. 1976, Ap. J., 210, 211.

Scuflaire, R. 1974, Astron. Ap., 34, 449.

Shipman, H.L. 1972, Ap. J., 177, 723.

Strittmatter, P.A. and Wickramasinghe, D.T. 1971, Mon. Not. R. Astr. Soc., 152, 47.

Tassoul, M. and Tassoul, J.L. 1968, Ann. Ap., 3, 251.

Van Horn, H.M. 1978, in Proceedings of Conference on Current Problems in Stellar Pulsation Instabilities, ed. D. Fischel, J.R. Lesh, and W.M. Sparks, NASA Special Publication.

Vauclair, G. and Reisse, C. 1977, Astron. Ap., 61, 415.

Wolff, C.L. 1977, Ap. J., 216, 784.

Wolff, C.L. 1980, these proceedings.

THE PERIODS OF ZZ CETI VARIABLES

A.N. Cox and S.W. Hodson
Theoretical Division
Los Alamos Scientific Laboratory of the University of California
Los Alamos, New Mexico

S.G. Starrfield
University of Arizona
Tucson, Arizona

ABSTRACT

White dwarf pulsators (ZZ Ceti variables) occur in the extension of the radial pulsation envelope ionization instability strip to the observed luminosities of 3×10^{-3} $L_\odot$ according to van Horn (1979). Investigations have been underway to see if the driving mechanisms of hydrogen and helium ionization can cause radial pulsations as they do for the Cepheids, the RR Lyrae variables, and the δ Scuti variables. Masses used in this study are 0.60 and 0.75 $M_\odot$ and the temperature T_e used ranged between 10,000 K and 14,000 K, the observed range in T_e. Helium rich surface compositions like Y = 0.78, Z = 0.02 as well as Y = 0.28, Z = 0.02 have been used in spite of observations showing only hydrogen lines in the spectrum. The deep layers are pure carbon, and several transition compositions are included. The models show radial pulsation instabilities for many overtone modes at periods between about 0.3 and 3 seconds. The driving mechanism is mostly helium ionization at 40,000 and 150,000 K. The blue edge at about 14,000 K is probably due to the driving region becoming too shallow, and the red edge at 10,000 K is due to so much convection in the pulsation driving region that no radiative luminosity is available for modulation by the γ and κ effects. It is speculated that the very long observed periods (100-1000 sec) of ZZ Ceti variables are not due to nonradial pulsations, but are possibly aliases due to data undersampling.

* * * *

In a recent article on white dwarfs, van Horn (1979) noted that "theoretical calculations have yet to demonstrate the existence of the suspected Cepheid-variable-like driving mechanism for modes that are compatible with the observed pulsations."

He notes that the ZZ Ceti variables, that is those pulsators that are single white dwarfs, occur in the same envelope ionization radial pulsation instability strip as the Cepheids and δ Scuti variables of population I and the RR Lyrae variables and Cepheids of population II. The work reported here on radial pulsation instabilities using the linear nonadiabatic theory will demonstrate that white dwarf

pulsations should occur in a hitherto unexplored frequency domain. We will not predict, unfortunately, the long observed periods of 100-1000 seconds, but only ones of the order of one second.

Observed luminosities for our variables are about 3×10^{-3} $L_\odot$, and the observed T_e range is 10,000 to 14,000 K. The instability strip taken from a review by Nather (1978) who extended the Henden and Cox (1976) instability strip is in the Figure 1. These L and T_e values give radii between 6.5 and 13×10^8 cm or between 0.01-0.02 $R_\odot$. Use of the electron degenerate star relation between mass and radius gives masses between 0.3 and 0.9 $M_\odot$. We have used 0.6 for most of the results here, though some 0.75 $M_\odot$ cases will also be shown.

During the course of this investigation our ideas about the composition of the outer layers of ZZ Ceti stars changed from Y = 0.78 to Y = 0.28, and both compositions will be considered here. Even though only hydrogen lines occur in the spectra of these stars, helium is often invisible and it would not be surprising if Y = 0.78 were indeed found to be correct. Metals which also are absent in the spectra have probably gravitationally settled to deep layers below any well mixed convection zones. In spite of this lack of metals, Z = 0.02 is used in the outer layers of all of our models.

Let's consider the surface layer helium. It appears that there could be an evolutionary settling of helium to deep layers long before T_e falls to 14,000 K. This prevents pulsation because helium really causes most of the driving in pulsating stars except for the cooler RR Lyrae variables and Cepheids where hydrogen ionization plays a small role in pulsation. Now in cooling white dwarfs of our masses, convection cannot mix to very deep layers of $T \geq 10^5$ K until the T_e drops to about the T_e of our blue edge. It may be that the onset of convection to dredge up helium causes the ZZ Ceti instability strip blue edge, though the normal effect of the driving regions becoming too shallow is also operating.

Composition changes cause problems in our stability analyses, the gamma and opacity derivative values have discontinuities at these places and give local damping and driving that does not always cancel to a zero effect. Therefore, our models have transition layers with some residual hydrogen between 1 and 2 million Kelvin, just helium and the normal Z between 2 and 5 million Kelvin, mostly helium but 10 percent carbon to 10 million Kelvin and then half helium and half carbon to a density of 10^4 g/cm^3. Interior to this point is pure carbon which comprises the central 99 percent of the mass.

Our models allow convection by the normal mixing length theory with the ratio, α, of the mixing length to scale height being either 1.0 or 1.5. This gives convection to a level between 10^5 and 10^6 Kelvin depending on this ratio and other parameters such as T_e. The larger α usually puts more mass in the convection zone and makes models more pulsationally unstable. Any spurious convection caused by the

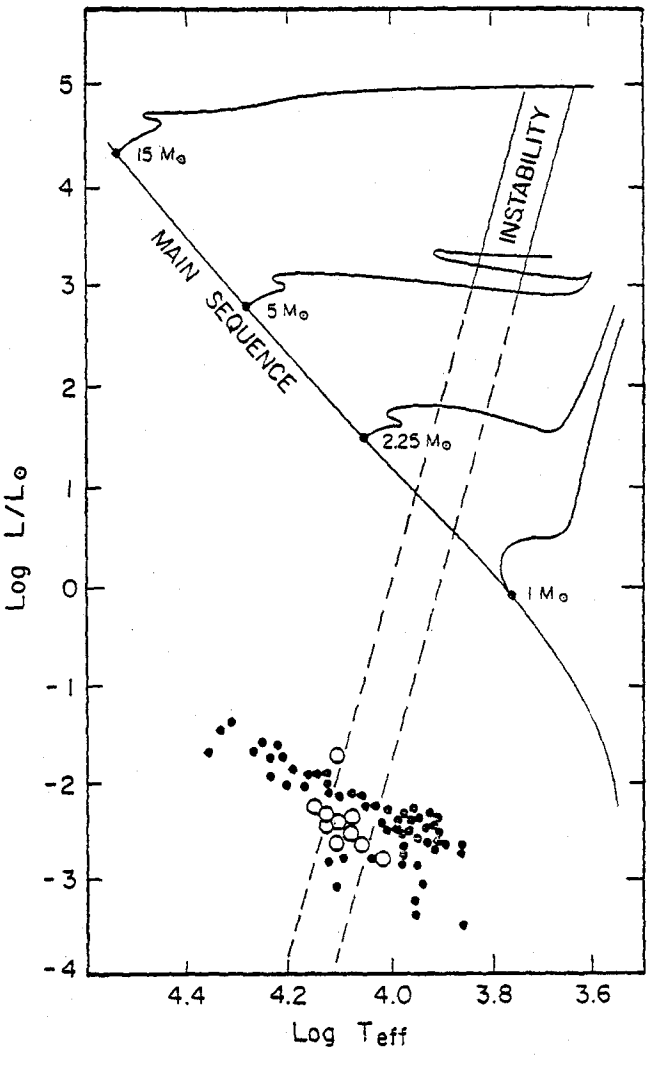

Figure 1. The instability strip taken from a review by Nather (1978).

deep composition transitions is suppressed by us below 10^6 K because the gradient is close to being adiabatic anyway.

The luminosity flowing outward in the models is made proportional to the interior mass according to the behavior of models constructed by van Horn (unpublished). The growth rates of unstable models increase by about a factor of two when a constant surface luminosity is used throughout.

Table 1 gives periods for radial pulsation modes for 0.6 $M_\odot$, 3×10^{-3} $L_\odot$, T_e between 10,000 and 14,000 K and for $Y_s = 0.28$ down to 10^6 K. Hotter models are beyond the blue edge and cooler ones are probably stabilized by convection. The periods are in seconds and unstable modes are marked with U. These have periods from 0.3 to 3 seconds, and the maximum growth rates marked range from 10^{-9} to 4×10^{-8}. These timescales are as short as a few years.

Instability is caused by helium ionization and the γ and κ effects. Consider the models at 12,000 K for 0.75 $M_\odot$ at our luminosity and $Y_s = 0.78$. The internal T, ρ, and opacity are given in Figure 2. Composition variations at a level of 10^{-6} of the mass from the outside at 2 and 5 million degrees show as sudden changes in the opacity. Pulsation eigenfunctions with 12, 14, and 16 nodes, i.e., K = 11, 13, and 15, versus the fractional radius are in Figure 3 where the internal damping is suppressed because of small amplitudes there and the helium driving regions in the outer 7×10^{-4} of the radius can become operative. Thus one gets work plots with more driving than damping, and pulsation is predicted. The work calculated over a pulsation cycle is in Figure 4. The normal driving region at 20,000 K to 50,000 K and the deep region discussed recently by Stellingwerf (1979) at 100,000 K to 250,000 K are shown. Note that all this driving is in the outer 10^{-12} of the white dwarf mass. To what amplitude this driving can lead, is an unknown which awaits full nonlinear calculations which can allow for the possible saturation of the driving and the possible increase of the damping at limiting amplitude.

Let me now discuss the great disparity between the observed periods of 100-1000 seconds, commonly ascribed to g mode pulsation, and our predicted ones around 1 second. Note that the 10,000 K low mode periods are like those for dwarf nova oscillations but the unstable periods are no more than 3 seconds. We suppose that g mode identification for ZZ Ceti variables is correct and maybe our envelope ionization could make them unstable too, just as it does for our radial modes. The g_1 and g_2 modes do have $\delta r/r$ eigenfunctions similar to our high k radial modes. A search for our periods of about 1 second, now being planned by McGraw and Starrfield at Kitt Peak and by Hildebrand from Chicago observing at Mount Lemmon is well justified by our predictions.

Table 1. White Dwarf Radial Pulsation Periods (Seconds) and Growth Rates (Period^{-1})

$0.6\ M_\odot$ $3 \times 10^{-3}\ L_\odot$ $Y_S = 0.28$

k/T_e(K)	10,000	11,000	12,000	13,000	14,000
0	20.1	13.3	9.0	6.4	4.7
1	8.9	6.5	4.8	3.5	2.70
2	6.0	4.5	3.4	2.58	1.98
3	4.8	3.6	2.67	2.02	1.56
4	3.9	3.0	2.26	1.74	1.36
5	3.2	2.46	1.88	1.45	1.14
6	2.82 U	2.13	1.63	1.26	0.98
7	2.50 U	1.89	1.44	1.12	0.87
8	-	1.71 U	1.30	1.01	0.79
9	2.13 U	-	1.19 U	0.91	-
10	1.97 U	1.47 U	1.11 U	0.85	0.66
11	1.84 U	1.37 U	1.04 U	0.80	0.62
12	1.72 U	1.29 U	0.97 U	-	0.58
13	1.60 U	1.21 U	-	0.70 U	0.55
14	1.51 U	1.13 U	0.87 U	-	-
15	1.44 U (6×10^{-9})	1.08 U	0.82 U	-	0.45
16	1.37 U	1.02 U	-	-	-
17	-	-	-	0.51 U	-
18	-	-	-	0.49 U	0.32 U
19	-	0.90 U (1×10^{-9})	-	0.41 U	0.28 U (1×10^{-8})
20	-	-	0.62 U	0.38 U	0.22
21			0.57 U (6×10^{-9})	0.34 U 0.31 U (4×10^{-8})	

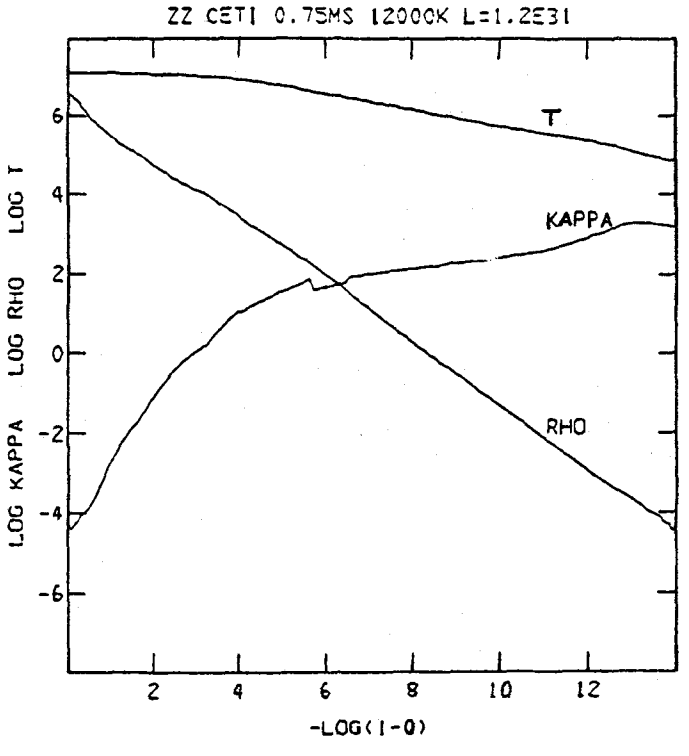

Figure 2. The internal T, ρ and opacity for a 0.75 $M_\odot$ model.

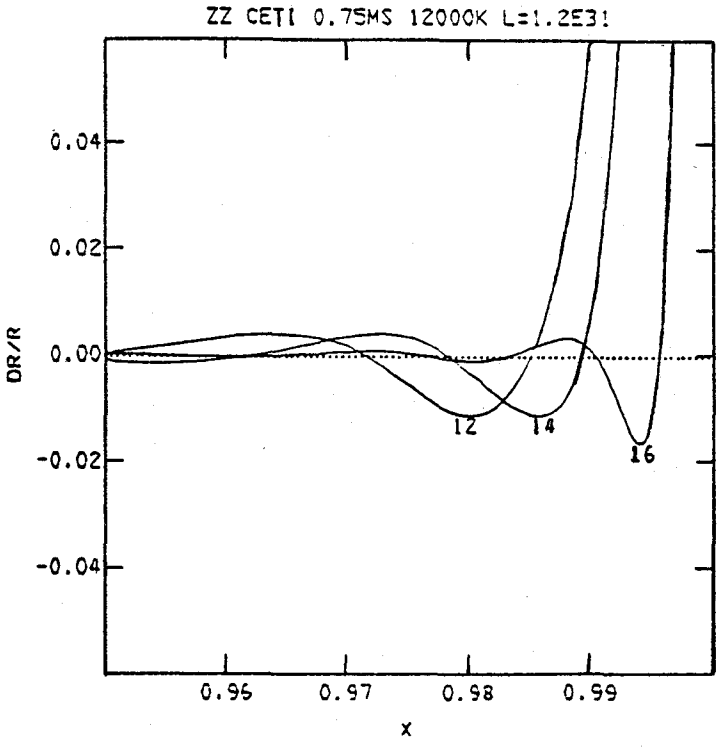

Figure 3. Pulsational eigenfunctions for the 12, 14, and 16th nodes versus the fractional radius.

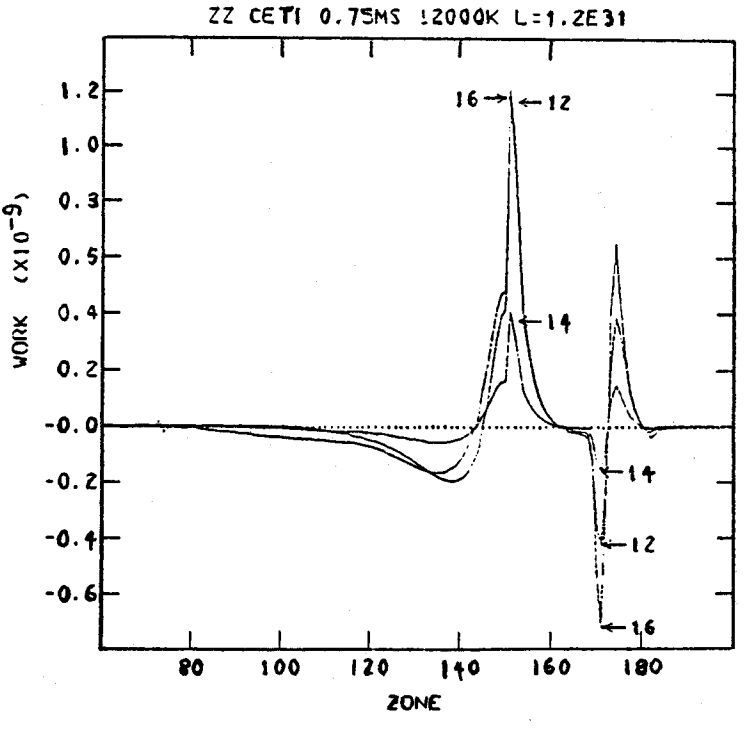

Figure 4. The work calculated over a pulsational cycle.

REFERENCES

Henden, A.A. and Cox, A.N. 1976, in Proceedings of the Solar and Stellar Pulsation Conf., ed. A.N. Cox and R.G. Deupree (LA-6544-C), p. 167.

Nather, E. 1978, Pub. A.S.P., 90, 477.

Stellingwerf, R.F. 1979, Ap. J., 227, 935.

van Horn, H.M. 1979, Physics Today, January 1975, 23.

TWELVE MINUTE LIGHT VARIATIONS IN THE PECULIAR STAR HD 101065

G. Wegner
Department of Physics
University of Delaware
Newark, Delaware

ABSTRACT

The magnetic star HD101065 (Przybylski's star) is known for its peculiar spectrum dominated by rare earth lines. Recently, it has been discovered to exhibit periodic 12.141 ± 0.003 min. light variations of amplitude near ± 0.015 mag. in B (Kurtz and Wegner 1979). Several lines of argument suggest an effective temperature near 7400 K, which could relate HD101065 to the δ Scuti instability strip. Such rapid variability is unprecedented in normal, Am and Ap stars. If HD101065 is near the main sequence, the short timescale of variability seems to create a number of problems, not only for pulsation theory, but also for current ideas on the diffusion mechanism of metal enhancement.

1. INTRODUCTION

The complicated spectrum of HD101065 and its interpretation have been discussed in detail elsewhere. This is a summary of the main points. Przybylski (1961, 1963, 1966) discovered the star's richness in rare earths. Wegner and Petford (1974) concluded that the object has a temperature near spectral class F0 (about 7400 K) and, within the limits of a very difficult atmospheric analysis, obtained near normal abundances for Fe, Ti and Cr while the rare earths were found to be enhanced by nearly five orders of magnitude.

The star's nature depends critically on its effective temperature. Przybylski (1977a,b) argued for a lower value of T_{eff} = 6075 ± 200 K and a corresponding reduction in the Fe abundance by at least 2.4 in the logarithm. Cowley at al. (1977) have shown that Fe lines are present in the spectrum.

Recent progress regarding the effective temperature of HD101065 suggests that the higher value is correct. The determination of T_{eff} is made difficult by the complicated spectrum. In fact, the abnormal Hα and Hβ line profiles (Wegner 1976) could indicate that the temperature structure of the star's atmosphere is perturbed by the abnormally strong line blanketing. The three most reliable temperature indicators are probably as follows: (1) The Hα and Hβ line profiles give T_{eff} = 7500

and 7100 K respectively (Wegner 1976). (2) The infrared (J-K) and (J-L) colors measured by Glass (priv. comm.) indicate temperature near 7000 and 7500°K respectively, almost independent of reddening (Wegner 1976). (3) The Paschen line strengths, in particular that of the P_{12} line, indicate T_{eff} = 7400 ± 300 K (Kurtz and Wegner 1979).

Additional observational results of importance are as follows. Przybylski's star has a ~2200 Gauss magnetic field which strengthens its possible relationship to the Ap stars (Wolf and Hagen 1976). Long period light, spectral and radial velocity variations seem to be ruled out unless they are very small (Wolf and Hagen 1976; Cowley et al. 1977; Przybylski 1978; Wegner, unpublished). From the sharpness of the lines in HD101065, the effects of rotation are small and indicate that vsini $\leq$ 7 km s^{-1}.

Astrometric data (cf. Wegner and Petford 1974) yield little information on the luminosity of HD101065. Churm's (1973) trigonometric measure gives the upper limit, $\pi \leq 0.''025$, or $M_V \leq +5.0$ mag. For T_{eff} = 7400 K, this could place HD101065 near the zero age main sequence and in the δ Scuti instability strip. The lower limit on the star's brightness would probably exclude the possibility that it is a subdwarf unless it is considerably hotter than believed. The low proper motions and radial velocity give weak corroboration that HD101065 is not a member of the halo population.

2. THE LIGHT VARIATIONS

The recent discovery of the light variability of HD101065 provides new insight regarding its nature. The photometric observations made during April to July 1978 using the 1.0 and 0.5 m telescopes at the South African Astronomical Observatory in Sutherland cover over 100 cycles during 22 hours of observation on eight nights spread over 52 days. These have been discussed in detail by Kurtz (1978) and Kurtz and Wegner (1979), so only the main aspects will be presented here.

The data obtained in the B band establish that HD101065 has a principal period near 12.141 ± 0.003 minutes. Table 1 gives a summary of the observations. The frequencies in parentheses were adopted from the more extensive B data set. The U and V data are not adequate for determining possible small phase shifts between light curves of different color. Note the apparent decrease of amplitude in the light variations with wavelength.

There is some suggestion of two low amplitude heat periods, appearing as side lobes of the main peak. In Table 1 these are denoted by f_2 and f_3 while f_1 is the 12.141 min. peak. However, in light of considerations like those of Luomos and Deeming (1978), these should still be labeled as provisional.

Table 1. Summary of Derived Frequencies for HD101065

[After Kurtz and Wegner (1979)]

	f ($hour^{-1}$)	P (minutes)	A (m mag)
(A) All B Data	4.942 ±0.001	12.141 ±0.003	5.8
(B) B Data for JD2443643 and 2443644 only			
$f_1 - f_2 = 0.25\ hr^{-1}$			
$f_3 - f_1 = 0.03\ hr^{-1}$			
(C) V Data	(4.942)		2.3
(D) U Data	(4.942)		7.2

3. DISCUSSION AND CONCLUSIONS

What lessons does HD101065 teach us? How can the 12.141 minute period be understood? These questions can only be answered after making assumptions regarding the star's structure. It must be remembered that nothing definite is known about the luminosity of HD101065. Furthermore, an abnormal He abundance cannot be ruled out because this star is too cool to have He lines in its spectrum.

One entirely plausible hypothesis is to assume that HD101065 is a δ Scuti star. This is certainly consistent with its light variability and the temperature adopted here. However, it should be noted that the dominant single stable frequency observed in the light variations is not a common characteristic among δ Scutis and variable white dwarfs. Nevertheless, if this model is adopted, then very high overtones are needed to explain the 12.141 minute period. For example, as pointed out by Kurtz and Wegner (1979) in a discussion of nonradial pulsation in the $\ell = 2$ mode, the radial quantum number would have to be $k \sim 13$ for a main sequence object while, for a giant star model, $k \approx 35$. It is difficult to understand how a star could oscillate stably in such large overtones. It may be possible to constrain the internal structure by an agent external to the driving force in such a way that only one pulsation mode is allowed. Perhaps the star's -2200 Gauss magnetic field offers a clue.

Lower pulsation modes could be obtained if HD101065 was a subdwarf or had peculiar interior abundances, as would be the case if it was on the He main sequence. In fact, the assumption that HD101065 is a unique pathological object cannot be ruled out and consequently opens up a number of possibilities. For example, the star could have been formed from an interstellar cloud that was greatly enriched in heavy elements by a supernova event.

However, such an extreme view does not appear necessary to explain the spectroscopic properties of HD101065 as outlined above. They are suggestive that it is related to the cool Ap stars. Therefore, it seems more reasonable to question the pulsation theory. This assertion is given additional weight by the other metallic lined objects such as HD52788 that have been found to have light periods nearly as short (Kurtz 1978). It should also be recalled that there are discrepancies of a somewhat similar nature for the variable white dwarfs. They seem to have periods which are much too long, but also vary in high overtones (cf. Robinson 1980).

One additional important question that HD101065 raises regards the relationship between variability, metallicism and magnetic fields. It has generally been considered that variability is not exhibited in the presence of metallicism and a magnetic field because an extremely stable atmosphere is required for the element separation to take place.

Whatever the final outcome, the study of HD101065 and stars like it will probably provide additional new surprises.

* * * * *

This work is partially supported by the A.J. Cannon Fund, the Unidel Foundation and the National Science Foundation.

REFERENCES

Churms, J. 1973, private communication.
Cowley, C.R., Cowley, Aikman, G.C.L. and Crosswhite, H.M. 1977, Ap. J., 216, 37.
Kurtz, D.W. 1978, Mon. Not. R. Astr. Soc., in press.
Kurtz, D. and Wegner, G. 1979, Ap. J., in press.
Luomos, G. and Deeming, T. 1978, Ap. Sp. Sci., 56, 285.
Przybylski, A. 1961, Nature, 189, 739.
Przybylski, A. 1963, Acta. Astr., 13, 217.
Przybylski, A. 1966, Nature, 210, 20.
Przybylski, A. 1977a, Mon. Not. R. Astr. Soc., 178, 71.
Przybylski, A. 1977b, Mon. Not. R. Astr. Soc., 178, 735.
Przybylski, A. 1978, Proc. Astr. Soc. Australia, 3, 143.
Robinson, E.L. 1980, these proceedings.
Wegner, G. 1976, Mon. Not. R. Astr. Soc., 177, 99.
Wegner, G. and Petford, A.D. 1974, Mon. Not. R. Astr. Soc., 168, 557.
Wolf, S.C. and Hagen, W. 1976, P.A.S.P., 88, 119.

ON THE DEFINITION OF CANONICAL ENERGY DENSITY AND OF CANONICAL ENERGY FLUX FOR LINEAR AND ADIABATIC OSCILLATIONS OF A SPHERICAL STAR

P. Smeyers
Katholieke Universiteit Leuven

A. Weigert
Universität Hamburg

ABSTRACT

Two variational principles are known for the problem of stellar oscillations. The meaning of these variational functionals is considered as well as implications for the definition of the canonical energy density and energy flux.

* * * * *

Chandrasekhar and Lebovitz (1964) have shown that the Euler equations of a variational principle are equivalent to the equations that govern the linear adiabatic oscillations of a spherical star. The validity of this variational principle follows from the hermiticity of the linear operator that is applied to the linear adiabatic oscillations of a star.

In geophysics a somewhat different variational principle is applied to the study of waves in a plane atmospheric layer. As far as we know, only a heuristic derivation of the corresponding variational functional has been given (Tolstoy 1963, 1973). It can be verified that the Euler equations of this second variational principle are also equivalent to the equations governing the linear adiabatic oscillations of a spherical star with the exception of the term that represents the perturbation of the gravitational force. This term is commonly neglected in studies of atmospheric waves.

Thus, two variational principles are known for the problem of stellar oscillations. This brings up the question of the meaning of the corresponding variational functionals. We shall examine this question and consider some of its implications for the definition of canonical energy density and canonical energy flux.

We have applied Hamilton's principle explicitly to the linear adiabatic oscillations of a spherical star. The necessary Lagrangian is the difference between the second order change in kinetic energy, T, and the sum of the second order changes in the internal and gravitational potential energies (U and Ω respectively):

$$L_2 = \delta_2 T - (\delta_2 U + \delta_2 \Omega) \quad . \tag{1}$$

It may be noted here that, when the perturbation of the gravitational potential is taken into account, a nonlocal field theory results.

The Lagrangian defined by (1) can be transformed in such a way that one of its terms becomes a volume integral of the divergence of a vector that vanishes together with the pressure at the surface of the equilibrium configuration. Such a term does not contribute to the Lagrangian, so it can be dropped for the purposes of the variational procedure. When this is done, the resulting form of the Lagrangian turns out to be identical to the functional of Chandrasekhar and Lebovitz. Hence, from a physical point of view, this functional is the difference between the second order change in kinetic energy and the sum of the second order changes in the internal and gravitational potential energies for any spherical star with a vanishing surface pressure that is submitted to a linear adiabatic perturbation. Furthermore, the requirement that the Lagrangian of Chandrasekhar and Lebovitz obeys Hamilton's principle allows the generation of both the equations and the associated boundary condition that govern the linear adiabatic perturbations of a spherical star.

It is possible to transform once more the Lagrangian defined by (1), deriving a second term that is also a volume integral of the divergence of a vector. This vector now vanishes at the surface of the equilibrium configuration when the gradient of pressure (or density) vanishes at that surface. Hence, if this condition is satisfied, an additional term can be dropped in the Lagrangian. After this second reduction the Lagrangian becomes identical to Tolstoy's variational functional. Consequently, this functional represents the difference of the second order change in kinetic energy and the sum of the second order changes in the internal and gravitational potential energies for any perturbed star where both the pressure and its gradient vanish at the surface of the equilibrium configuration. Furthermore, when Hamilton's principle is used with Tolstoy's Lagrangian, the equations and the boundary condition can be generated that govern the linear adiabatic perturbations of a spherical star. In this case, however, the boundary condition takes the form to which it reduces when the gradient of pressure vanishes at the equilibrium surface.

At this point we may conclude that both the variational principle of Chandrasekhar and Lebovitz and the variational principle used in geophysics actually stem from Hamilton's principle.

Let us now turn to the definition of canonical energy density and canonical energy flux. Following a procedure of mechanics for continuous systems, one can derive a Hamiltonian H_2 from a Lagrangian density $\mathcal{L}_2$ by putting

$$H_2 = \int_V \left[\frac{\partial \xi^i}{\partial t} \frac{\partial \mathcal{L}_2}{\partial \frac{\partial \xi^i}{\partial t}} - \mathcal{L}_2 \right] dV \quad . \tag{2}$$

Since H_2 represents the second order change in total energy of a spherical star subjected to linear adiabatic perturbation, it is conserved. H_2 can also be considered as a space integral of a canonical energy density $\mathcal{H}_2$ that is defined as

$$\mathcal{H}_2 = \frac{\partial \xi^i}{\partial t} \frac{\partial \mathcal{L}_2}{\partial \frac{\partial \xi^i}{\partial t}} - \mathcal{L}_2 \quad . \tag{3}$$

Definition (3) has been used by Tolstoy (1973) and has been recently applied by Dicke (1978) in a discussion of solar oscillations. Both authors derived a canonical energy density from Tolstoy's Lagrangian density. In this context it is well to keep in mind that, if a Lagrangian density $\mathcal{L}_2$ is associated with one of the simplified forms of the total Lagrangian L_2 as described above, the canonical energy density resulting from definition (3) does not correspond to the second order change in energy density. We may write the second order change in energy density as

$$\begin{aligned} \mathcal{E}_2 = {} & \frac{1}{2} \rho \sum_{i=1}^{3} \left(\frac{\partial \xi^i}{\partial t} \right)^2 - \frac{1}{2} \nabla \cdot \left[(P \nabla \cdot \vec{\xi}) \vec{\xi} + P(\vec{\xi} \times \nabla) \cdot \vec{\xi} \right] \\ & + \frac{1}{2} \Gamma_1 P (\nabla \cdot \vec{\xi})^2 + \frac{1}{2} (\vec{\xi} \cdot \nabla P)(\nabla \cdot \vec{\xi}) \\ & + \frac{1}{2} \rho \, \vec{\xi} \cdot \nabla (\vec{\xi} \cdot \nabla \Phi) + \frac{1}{2} \rho \, \vec{\xi} \cdot \nabla \Phi_1' \quad , \end{aligned} \tag{4}$$

where $\vec{\xi}$ represents the Lagrangian displacement, and Φ_1' the first order Eulerian perturbation of gravitational potential. When $\mathcal{L}_2$ is defined as the Lagrangian density that is associated with the Lagrangian of Chandrasekhar and Lebovitz, canonical energy density is linked to the second order change in energy density by

$$\mathcal{H}_C = \mathcal{E}_2 + \frac{1}{2} \nabla \cdot \left[(P \nabla \cdot \vec{\xi}) \vec{\xi} + P(\vec{\xi} \times \nabla) \cdot \vec{\xi} \right] \quad . \tag{5}$$

In the second case, when $\mathcal{L}_2$ is associated with Tolstoy's Lagrangian, one has for canonical energy density

$$\mathcal{H}_T = \mathcal{H}_C + \frac{1}{2} \nabla \cdot \left[(\vec{\xi} \cdot \nabla P) \vec{\xi} \right] \quad . \tag{6}$$

An equation for the local change of canonical energy density can be obtained by differentiating this density with respect to time. When the Euler equations of the variational principle are taken into account, the equation takes the form

$$\frac{\partial \mathcal{H}_2}{\partial t} + \frac{\partial}{\partial x^j}\left(\frac{\partial \mathcal{L}_2'}{\partial \frac{\partial \xi^i}{\partial x^j}} \frac{\partial \xi^i}{\partial t}\right) = \frac{1}{2}\rho\left(\xi^i \frac{\partial}{\partial t}\frac{\partial \Phi_1'}{\partial x^i} - \frac{\partial \xi^i}{\partial t}\frac{\partial \Phi_1'}{\partial x^i}\right) , \tag{7}$$

where

$$\mathcal{L}_2' = \mathcal{L}_2 + \frac{1}{2}\rho\vec{\xi}\cdot\nabla\Phi_1' . \tag{8}$$

The right-hand member of equation (7) can be interpreted as the local production of canonical energy due to the perturbation of the gravity field. When integrated over the volume of the equilibrium configuration, the energy production is zero, as may be expected since H_2 is conserved. For the important case of displacement fields that vary harmonically in time, the rate of local production of canonical energy is identically zero at all points, and equation (7) becomes a conservation equation for $\mathcal{H}_2$.

Using equation (7) we may also define the components of the flux of canonical energy as

$$\mathcal{F}_2^j = \frac{\partial \mathcal{L}_2'}{\partial \frac{\partial \xi^i}{\partial x^j}} \frac{\partial \xi^i}{\partial t} . \tag{9}$$

When $\mathcal{L}_2$ is derived from the Lagrangian of Chandrasekhar and Lebovitz, the canonical energy flux can be written explicitly as

$$\vec{\mathcal{F}}_C = -\frac{1}{2}\rho\left(\frac{\partial\vec{\xi}}{\partial t}\cdot\nabla\Phi\right)\vec{\xi} - \left[\Gamma_1 P(\nabla\cdot\vec{\xi}) + \frac{1}{2}(\vec{\xi}\cdot\nabla P)\right]\frac{\partial\vec{\xi}}{\partial t} . \tag{10}$$

In particular, the radial component of the flux takes the form

$$\mathcal{F}_C^r = -\Gamma_1 P(\nabla\cdot\vec{\xi})\frac{\partial\vec{\xi}^r}{\partial t} . \tag{11}$$

This component clearly vanishes at the surface of the equilibrium configuration when the boundary condition, which expresses the conservation of momentum, is satisfied. It is interesting to note that, according to expression (10), a displacement field proportional to $\sin\sigma t$ gives rise to a flux of canonical energy that is everywhere opposite to the flux associated with the corresponding displacement field that is proportional to $\cos\sigma t$. This property physically distinguishes the two types of displacement fields.

For displacement fields that vary harmonically in time, expression (10) for canonical energy flux reduces to

$$\vec{\mathcal{F}}_C = - \Gamma_1 P(\nabla \cdot \vec{\xi}) \frac{\partial \vec{\xi}}{\partial t} \quad . \tag{12}$$

On the other hand, when $\mathcal{L}_2$ is derived from Tolstoy's Lagrangian, canonical energy flux is defined as

$$\vec{\mathcal{F}}_T = - \left[\Gamma_1 P(\nabla \cdot \vec{\xi}) + \vec{\xi} \cdot \nabla P\right] \frac{\partial \vec{\xi}}{\partial t} \quad . \tag{13}$$

With this definition, the radial component of the canonical energy flux vanishes at the surface of the equilibrium configuration only if both the pressure and its gradient vanish at that surface.

REFERENCES

Chandrasekhar, S. and Lebovitz, N.R. 1964, Ap. J., 140, 1517.

Dicke, R.H. 1978, Mon. Not. Roy. Astr. Soc., 182, 303.

Tolstoy, I. 1963, Rev. Mod. Phys., 35, 207.

Tolstoy, I. 1973, Wave Propagation, (New York: McGraw-Hill).

PROPERTIES OF NONRADIAL STELLAR OSCILLATIONS

M. Gabriel and R. Scuflaire
Institut d'Astrophysique
Université de Liège, Belgium

ABSTRACT

It is shown that the oscillatory properties of the eigenfunctions can be proved rigorously for the second order problem. Models with discontinuities in density are also considered and "discontinuity modes" are shown to exist. The distribution of amplitudes of these modes is also discussed.

1. INTRODUCTION

The mathematical properties of the eigenvalue problem describing the adiabatic nonradial oscillations of stars are still poorly known and our information rests only on numerical integrations.

Even when the problem is simplified neglecting the Eulerian perturbation of the potential, a rigorous analysis of the eigenvalue problem is still lacking. As early as 1941, Cowling (1941) introduced the distinction between p and g spectra on the basis of an asymptotic discussion of the problem. Owen (1957) was unable to find the f mode and the first p and g modes for polytropes of high central condensation. Robe (1968) showed that these modes still exist but that they acquire extra nodes. Scuflaire (1974) and Osaki (1975) showed that a regularity can be found in all cases provided the nodes are counted in an appropriate way.

We show that a rigorous discussion of the oscillatory properties of the eigenvalue problem can be done when the Eulerian perturbation of the potential is neglected. Full demonstrations are given by Gabriel and Scuflaire (1979).

The discussion is also extended to cases where discontinuities in density are present in the star. For incompressible fluids, it is known that each density discontinuity gives rise to a new mode (called a discontinuity mode). We show that it is not always so in stars.

When a density discontinuity is present in the star, there can nevertheless exist one or more modes having their largest amplitudes in the vicinity of one of the discontinuities. This problem is discussed using a simplified model whose predictions allow the interpretation of numerical results obtained from physical models.

2. OSCILLATORY PROPERTIES OF NONRADIAL OSCILLATIONS

2.1. Equations and Boundary Conditions

The equations for nonradial oscillations neglecting the Eulerian perturbation of the gravitational potential (Cowling's approximation) are

$$\frac{dv}{dr} = a\, w \quad , \tag{1}$$

$$\frac{dw}{dr} = b\, v \quad , \tag{2}$$

where $v = f_1 r^2\, \delta r$, $\quad w = f_2 \frac{p'}{\rho}$,

$$f_1 = \exp\left(\int_o^r \frac{1}{\Gamma_1} \frac{d\ell n p}{dr}\, dr\right) \quad , \tag{3}$$

$$f_2 = \exp\left(\int_o^r A\, dr\right) \quad , \quad A = \frac{d\ell n \rho}{dr} - \frac{1}{\Gamma_1} \frac{d\ell n p}{dr} \quad , \tag{4}$$

$$a = \left(\frac{\sigma_a^2}{\sigma^2} - 1\right) \frac{r^2}{c^2} \frac{f_1}{f_2} \quad , \quad c^2 = \Gamma_1 \frac{\Gamma}{\rho} \quad , \tag{5}$$

$$b = \frac{1}{r^2} (\sigma^2 - n^2) \frac{f_2}{f_1} \quad , \tag{6}$$

ℓ is the degree of surface spherical harmonic, c is the velocity of sound, $n = \sqrt{-Ag}$ is the Brunt-Väisälä frequency and $\sigma_a = [\ell(\ell+1)]^{1/2}\, c/r$ is the critical sound frequency.

Equations (1) and (2) are those given in Ledoux and Walraven (1958) modified to take the non-constancy of Γ_1 into account.

Equation (3) shows that f_1 is continuous throughout the star even when discontinuities in density are present. In such cases, A must be considered as a distribution to maintain the validity of equation (4); f_2 is discontinuous at discontinuities of density and satisfies the equation

$$\frac{f_{2+}}{\rho_+} = \frac{f_{2-}}{\rho_-} \quad , \tag{7}$$

where the subscripts - and + refer to the lower and upper sides of the discontinuity.

For what follows it is useful to represent the solutions in the [v(r), w(r)] plane (Scuflaire 1974) and to introduce the polar coordinates (ψ,θ) defined by

$$v = \psi \cos\theta \quad , \qquad w = \psi \sin\theta \quad . \tag{8}$$

Then equation (1) and (2) become

$$\frac{d\theta}{dr} = b\cos^2\theta - a\sin^2\theta \quad , \tag{9}$$

$$\frac{d\psi}{dr} = (a+b)\psi \sin\theta \cos\theta \quad .$$

The discussion of the properties of the eigenvalue problem is based on the behavior of the solutions of equation (9).

It is readily verified that the regularity condition at the center requires that v and w go to zero respectively as $r^{\ell+1}$ and r^{ℓ}, that $\lim_{r\to 0} \frac{rw}{v} = \frac{\sigma^2}{\ell}$ and $\theta(0,\sigma^2) = \pi/2 + k\pi$.

We may take k = 0 and we have

$$\theta(r,\sigma^2) = \frac{\pi}{2} - \frac{\ell}{\sigma^2} r$$

for sufficiently small r.

The boundary condition to apply at the "surface" is less obvious especially for non-zero surface temperature models. In all cases we are led to a condition of the form $\theta(R) = \alpha + k\pi$ with $0 < \alpha < \pi/2$.

For zero surface temperature models the boundary condition is $\delta p(R) = 0$, which is equivalent to the condition of regularity of the solution, implies that

$$\theta = tg^{-1}\left[\frac{GM}{R^4}\frac{f_2(R)}{f_1(R)}\right] + k\pi = \pi/2 + k\pi \quad .$$

For these models it can be considered that in the outermost layers ($r > r_2$) $m(r) = M$, $r \approx R$ and $P = K\rho^{\gamma}$ with γ constant. Then if $|n^2| >> \sigma^2 >> \sigma_a^2$ the regular solution is

$$\theta = k\pi + tg^{-1}(\beta x^{-m}) \quad , \tag{12}$$

$$\text{with } m = \frac{2\gamma - \Gamma_1}{\Gamma_1(\gamma-1)} \quad , \qquad x = R - r \quad , \qquad \text{and}$$

$$\beta = \frac{m + \sqrt{m^2 - 4a_1b_1}}{2a_1} \quad , \qquad a_1b_1 = \frac{\gamma(\gamma-\Gamma_1)}{\Gamma_1^2(\gamma-1)^2} \quad .$$

At a discontinuity in density δr and δp must be continuous. This implies the continuity of v and a discontinuity in w given by

$$w_+ - w_- = \frac{g}{r^2 f_1}\left(\frac{f_2}{\rho}\right)(\rho_+ - \rho_-)v \quad ,$$

and for θ

$$\operatorname{tg}\theta_+ - \operatorname{tg}\theta_- = \frac{g}{r^2 f_1}\left(\frac{f_2}{\rho}\right)(\rho_+ - \rho_-) \quad . \tag{13}$$

Obviously we may impose that $|\theta_+ - \theta_-| < \pi$ then θ_+ and θ_- belong to the same interval $I_k = (k\pi - \frac{\pi}{2}, k\pi + \frac{\pi}{2})$.

From the definition of a and b it is obvious that they are respectively decreasing and increasing functions of σ^2. Because of this simple property it is possible to demonstrate rigorously the oscillatory properties of the eigenfunctions of nonradial oscillations using exactly the same mathematical techniques as Coddington and Levinson (1955) for the Sturm-Liouville problem. The proofs are given in details by Gabriel and Scuflaire (1979).

If we assign to the nodes the sign of $\frac{d\theta}{dr}$ at that point, the properties are:

(1) All stars have a stable p spectrum of pressure modes, i.e., $\sigma_k^2 > 0$ $k = 1, 2, \ldots$, which has an accumulation point at infinity. The eigenfunction r_k associated to σ_k^2 has k zeros.

(2) There is a fundamental node associated to $k = 0$, with $\sigma_0^2 > 0$. The algebraic sum of the nodes of δr_0 is equal to zero.

(3) If the star has at least one radiative zone there is a stable g^+ spectrum of gravity modes, i.e., $\sigma_k^2 > 0$ $k = -1, -2, \ldots$, which has an accumulation point at zero. The eigenfunction δr_k associated to δ_k^2 has k zeros ($k < 0$).

(4) If the star has at least one convectively unstable zone there is an unstable g^- spectrum of gravity modes, sometimes called convective modes, i.e., $\sigma_k^2 < 0$, $k = +1, +2, \ldots$, which has an accumulation point at zero. The δr_k associated to σ_k^2 has k zeros. The smaller eigenvalue of σ_1^2 is larger than the minimum of the square of Brunt-Väisälä frequency.

(5) If there are N "unstable" discontinuities in the star such that the density below the discontinuity is smaller than above, then N new modes appear in the eigenvalue spectrum provided there is no convectively unstable zone, i.e., if there is no g^- spectrum. We call these modes unstable discontinuity modes. They are all unstable, i.e., $\sigma_j^2 < 0$ $j = 1, \ldots N$.

(6) If there are N "stable" discontinuities in the star such that the density below the discontinuity is larger than above, then N new modes appear in the eigenvalue spectrum provided there is no g^+ spectrum. (The homogeneous model is an example of such a situation.) We call these modes stable discontinuity

modes. They are all stable, i.e., $\sigma_j^2 > 0$ $j = 1, \ldots N$.

3. BEHAVIOR OF EIGENFUNCTIONS NEAR A DISCONTINUITY

From the results of the preceding section we see that under some circumstances the presence of discontinuities in density introduces new modes, i.e., discontinuity modes, while under other circumstances, which are the most common ones, no new mode may be associated with the discontinuities. Nevertheless, it may be that some modes show large amplitudes near the discontinuity and may still be associated with it.

To check this we have searched for such modes in main sequence models of a 1.1 $M_\odot$ with X = 0.6 and Z = 0.044. For $X_c > 0.25$ these models have a small growing convective core on the top of which a "stable" discontinuity develops. As such models are not fully convective, there is no new mode associated to the discontinuity. A few properties of these models are given in Table 1.

Numerical calculations have been performed for values of the degree of spherical harmonic order ℓ equal to 10, 25, 50, and 100. Table 2 shows the results. It gives the eigenvalues ω^2 of the "discontinuity modes" (in unit GM/R^3), the ratio R_a of the value of $\delta r/r$ on the discontinuity to its largest value elsewhere in the star and the identification of the modes.

In all cases but one, only one discontinity mode was found. For model 1 and $\ell = 10$, three modes with $R_a > 1$ were found. All other modes of these models show R_a values much smaller than one.

The existence of one discontinuity mode will not surprise but the presence, in one case, of three of them probably will. This can, however, be explained on the basis of a simple model.

For the amplitude to be large on the discontinuity it is necessary that the eigenfunctions have an exponential behavior on both sides of the discontinuity. Let us suppose that it is so and that the coefficients a and b in equations (1) and (2) may be considered as constant.

Below the discontinuity (subscript 1) the solution is given by

$$v_1 = e^{\lambda_1 (r - r_d)} \quad ,$$

$$w_1 = \sqrt{\frac{b_1}{a_1}}\; e^{\lambda_1 (r - r_d)} \quad ,$$

$$\text{with } \lambda = \sqrt{ab} \quad ,$$

where r_d is the radius on the discontinuity. We have taken $v(r_d) = 1$ and we have also dropped the other independent solution corresponding to the singular one at the

Table 1.

n°	$\frac{\rho_1 - \rho_2}{\rho_1 + \rho_2}$	q	x	X_c
1	$3{,}8\ 10^{-3}$	$3{,}41\ 10^{-2}$	$7{,}13\ 10^{-2}$	0.568
2	$2{,}3\ 10^{-2}$	$4{,}20\ 10^{-2}$	$7{,}15\ 10^{-2}$	0.466
3	$6{,}2\ 10^{-2}$	$4{,}83\ 10^{-2}$	$6{,}9\ 10^{-2}$	0.332

A few properties of the models. q is the mass fraction and x the fractional radius at the discontinuity. X_c is the central hydrogen abundance.

TABLE 2 a

ℓ	10	25	50	100
ω^2	8.747	19,682	38.256	75,42
R_a	11,31	10^7	$8\ 10^6$	10^5
	g_6	g_4	f	f
ω^2	8,626			
R_a	78			
	g_7			
ω^2	7.478			
R_a	2,10			
	g_8			

Dimensionless eigenvalues ω^2 of discontinuity modes, ratio R of amplitudes on the discontinuity to the maximum value in the rest of the star and identification of the modes for model 1.

TABLE 2 b

ℓ	10	25	50	100
ω^2	51,38	120.1	233.8	454.2
R_a	$4\ 10^6$	$2\ 10^{23}$	$4\ 10^{50}$	$4\ 10^{47}$
	P_2	P_3	P_2	P_2

Same as Table 2 a but for model 2.

TABLE 2 c

ℓ	10	25	50	100
ω^2	145.0	340.5	66,2	1317
R_a	$3\ 10^7$	$5\ 10^{22}$	$3\ 10^{49}$	$6\ 10^{44}$
	P_5	P_6	P_6	P_6

Same as Table 2 a but for model 3.

center.

Above the discontinuity (subscript 2) we have

$$v_2 = A\, e^{\lambda_2(r-r_d)} + B\, e^{-\lambda_2(r-r_d)} \quad ,$$

$$w_2 = \sqrt{\frac{b_2}{a_2}}\left(A\, e^{\lambda_2(r-r_d)} + B\, e^{-\lambda_2(r-r_d)}\right) \quad .$$

The continuity of δr and δp give A and B and we have

$$v_2 = \mathrm{ch}\left(\lambda_2(r-r_d)\right) + \mathrm{sh}\left(\lambda_2(r-r_d)\right)\sqrt{\frac{a_2}{b_2}}\left\{\left[\frac{g}{r^2 f_1}\left(\frac{f_2}{\rho}\right)(\rho_+ - \rho_-)\right]_d + \sqrt{\frac{b_1}{a_1}}\right\} \quad ,$$

$$v_2 = \mathrm{ch}\left(\lambda_2(r-r_d)\right) + \mathrm{sh}\left(\lambda_2(r-r_d)\right)\left\{\left[\frac{\sigma_{a,2}^2 - \sigma^2}{\sigma_{a,1}^2 - \sigma^2}\,\frac{\sigma^2 - n_1^2}{\sigma^2 - n_2^2}\right]^{1/2}\frac{\rho_-}{\rho_+}\right.$$

$$\left. - \frac{\rho_+ + \rho_-}{\rho_+}\,\sigma_d^2\sqrt{\frac{\sigma^{-2} - \sigma_{a,2}^{-2}}{\sigma^2 - n_2^2}}\right\} \quad ,$$

$$\text{with } \sigma_d^2 = g\sqrt{\frac{\ell(\ell+1)}{r_d^2}}\,\frac{\rho_- - \rho_+}{\rho_- + \rho_+} \quad . \tag{14}$$

σ_d^2 is the eigenvalue of the discontinuity mode of an infinite incompressible fluid (see for instance Landau and Lifschitz 1969).

If for $r > r_x$ the eigenfunction oscillates, it can have its largest amplitude on the discontinuity only if $v_2(r_x) << 1$. This condition can be fulfilled only if σ^2 is in a narrow range around the value which gives $v_2(r_x) = 0$. Its general form is very complicated. More interesting is its expression when $\sigma_{a,1}^2 \simeq \sigma_{a,2}^2 >> \sigma^2 >> n_1^2$ n_2^2. Then $v(r_x) = 0$ if

$$\sigma^2 = \sigma_c^2 = \frac{\rho_+ + \rho_-}{\rho_+ \coth\left(\lambda_2(r_x - r_d)\right) + \rho_-}\,\sigma_d^2 \simeq \sigma_d^2$$

$$\text{if } \lambda_2(r_x - r_d) >> 1 \quad , \tag{15}$$

and $v(r_x) < 1$ if

$$\left|\frac{\sigma^2 - \sigma_c^2}{\sigma_c^2}\right| < \frac{\sigma_c^2}{\sigma_d^2}\ \frac{\rho_+}{\rho_+ + \rho_-}\ \left[\mathrm{sh}\left(\lambda_2(r_x - r_d)\right)\right]^{-1} \qquad (16)$$

$$\lesssim \frac{\rho_+}{\rho_+\ \mathrm{ch}\left(\lambda_2(r_x - r_d)\right) + \rho_-\ \mathrm{sh}\left(\lambda_2(r_x - r_d)\right)} \approx \frac{2\rho_+\ e^{-\lambda_2(r_x - r_d)}}{\rho_+ + \rho_-} \quad ,$$

$$\text{if } \lambda_2(r_x - r_d) \gg 1 \quad .$$

If several eigenvalues satisfy condition (16) the corresponding modes are likely to have their largest amplitude on the discontinuity, i.e., to be discontinuity modes. This will occur the most easily if σ_c falls in the range of high order p or g modes.

The range of σ^2 defined by condition (16) decreases as $\lambda_2(r_x - r_d)$ increases. Since λ increases with ℓ for a given mode (in the models studied here we have $\lambda r_d \approx \ell$ in all cases), the probability to find several discontinuity modes decreases as ℓ or $(r_x - r_d)$ increases. For all usual models $(r_x - r_d)$ will be larger if σ_c^2 falls among p modes rather than among g^+ modes and more discontinuity modes are found in this later case. It is indeed when the discontinuity modes are g^+ modes of high order that we find several of them.

Since the behavior of the eigenfunction changes very rapidly when σ^2 deviates slightly from σ_c^2 it will always be possible to find at least one discontinuity mode, provided of course that the solutions do not oscillate on the other side of the discontinuity for $\sigma^2 \approx \sigma_c^2$. For this later case no discontinuity mode will be identified.

Even if equation (15) is a very crude one $\sigma_c^2 = \sigma_d^2$ gives a useful order of magnitude for the eigenvalue of discontinuity modes. In all cases we have met so far σ_d^2 predicts always the eigenvalues within less than a factor two.

The very peculiar amplitude distribution of discontinuity modes should be kept in mind when the stability of models with discontinuities is discussed.

REFERENCES

Coddington, E. and Levinson, N. 1955, Theory of Ordinary Differential Equations, (McGraw-Hill).

Cowling, T.C. 1941, Mon. Not. R. Astr. Soc., 101, 367.

Gabriel, M. and Scuflaire, R. 1979, Acta Astr., 29, (in press).

Landau, L. and Lifschitz, E. 1959, Fluid Mechanics, (Pergamon Press).

Ledoux, P. and Walraven, T. 1958, "Variable Stars" in Handbuch der Physik 51, 353, (ed. Flugge; Berlin: Springer).

Osaki, Y. 1975, Publ. Astron. Soc. Japan, 27, 237.

Owen, J.W. 1957, Mon. Not. R. Astr. Soc., 167, 384.

Robe, H. 1968, Ann. Astrophys., 31, 475.
Scuflaire, R. 1974, Astron. Astrophys., 36, 107.

ON MODE INTERACTION OF NONRADIAL OSCILLATIONS

M. Gabriel
Institut d'Astrophysique
Université de Liege, Belgium

ABSTRACT

A method is presented for the discussion of the details of mode interaction. It is shown that during an interaction, two modes exchange their properties and that the two interacting eigenfunctions are weighted means of the eigenfunctions computed when the interaction in negligible.

1. INTRODUCTION

In recent years, several sequences of stellar models showing "mode interaction" have been found, i.e., for a given sequence of models two eigenvalues become close to one another and seem to cross. However detailed consideration of this possibility shows that the eigenvalues do not actually cross because during a sequence the corresponding eigenfunctions exchange their behavior. This phenomenon, called "avoided crossing" by Aizenman et al. (1977), was first found by Osaki (1975) for massive stars during the main sequence phases. It is also found by Boury et al. (1979) for models with a discontinuity in density.

Pekeris et al. (1962, 1963) have also found mode interactions in the oscillations of Bullen's and Gutenberg's earth models in which they vary the rigidity of the inner core. The same kind of problem has also been studied by Denis (1974).

On the other hand, before the discovery of mode interactions, examples of resonances between two regions in a given stellar model had already been found. Resonances between convectively stable core and envelope separated by a convectively unstable zone were found by Goossens and Smeyers (1974). In the case of resonance, not only are two g^+ eigenvalues very close to each other, but the amplitudes of their eigenfunctions are large in both regions. If the parameters of the models had been varied with a small step mode interactions would have been noticed.

Resonances or mode interactions can occur in any sequence of models which have eigenfunctions spatially oscillating in several regions separated by zones where they have an evanescent behavior. The initial tendency has been to call resonance interactions the interaction between two g^+ or g^- modes and to use the name mode interactions when the two interacting modes have a g^+ behavior deep in the star and a p behavior in the envelope. However the two names appear to refer to the same

fundamental phenomenon.

When resonances occur for low order p or g modes the perturbation of the gravitational potential may not be neglected and we may ask if mode degeneracy can, in fact, happen although we know from the theory of catastrophes that this will only happen under special circumstances. Degeneracy will not easily be distinguished numerically from an avoided crossing and therefore a complementary check is useful.

We provide here this check as well as a method to study the details of the interaction.

2. MODE INTERACTION

Let us write the equation of motion

$$\lambda\rho\vec{\xi} = \vec{\nabla}\delta p - \frac{\delta\rho}{\rho}\vec{\nabla}p - \rho\,\vec{\nabla}\,\delta\phi = L(\vec{\xi}) \tag{1}$$

where $\lambda = \sigma^2$ is the eigenvalue, δ the symbol for Eulerian perturbation, ϕ the gravitational potential and ξ the displacement. Since $L(\vec{\xi})$ is an operation operating on $\vec{\xi}$, this means that in equation (1) $\delta\rho$, δp, and $\delta\phi$ are expressed in terms of $\vec{\xi}$ with the relations

$$\frac{\delta\rho}{\rho} = -\,\vec{\nabla}.(\rho\vec{\xi}) \tag{2}$$

$$\delta p = -\,\vec{\xi}.\vec{\nabla}p - \Gamma_1 p\,\vec{\nabla}.\vec{\xi}$$

$$\delta\phi(\vec{r}) = -G\int \frac{\{\vec{\nabla}.\,(\rho\vec{\xi})\}_{r'}}{|\vec{r} - \vec{r}'|}\,dV'$$

Let us consider a sequence of models defined in terms of a parameter ε. Suppose that for $\varepsilon = 0$ the model has two eigenvalues λ_1 and λ_2 very close to one another and that they are eventually degenerate for ε small.

It has been shown by Gabriel (1979) that the eigenvalues of nonradial oscillations are at most double. Therefore we can write

$$\left|\frac{\lambda_1 - \lambda_2}{\lambda_1}\right| << 1 \tag{3}$$

and

$$\left|\frac{\lambda_1 - \lambda_2}{\lambda_1}\right| << \left|\frac{\lambda_1 - \lambda_j}{\lambda_1}\right| \qquad j \neq 1,2$$

Let $\bar{\xi}_1$ and $\bar{\xi}_2$ be the corresponding eigenfunctions for $\varepsilon > 0$.

For ε small it is possible to compute the two interacting modes by a perturbation technique introduced by Wigner and von Neuman (1929).

We write for the eigenfunctions

$$\vec{\xi}(\varepsilon) = c_1(\varepsilon)\,\vec{\xi}_1 + c_2(\varepsilon)\,\vec{\xi}_2 \tag{4}$$

where $\vec{\xi}_1$ and $\vec{\xi}_2$ are considered as functions of a Lagrangian variable, for instance the mass fraction.

Substituting $\vec{\xi}_1$ or $\vec{\xi}_2$ for $\vec{\xi}$ in equation (2), one obtains the corresponding functions $\delta\rho$, δp, and $\delta\phi$ for a given model. Then with equation (1) we define $L_\varepsilon(\vec{\xi}_i)$ for $i = 1,2$. Introducing equation (4) into equation (1), we obtain

$$c_1[\lambda\rho_\varepsilon\vec{\xi}_1 - L_\varepsilon(\vec{\xi}_1)] + c_2[\lambda\rho_\varepsilon\vec{\xi}_2 - L_\varepsilon(\vec{\xi}_2)] = 0$$

After multiplication by $\vec{\xi}_1$ or $\vec{\xi}_2$ and integration over the volume of the star, we find,

$$(\lambda - I_{11})c_1 - I_{12}c_2 = 0 \tag{5}$$

$$-I_{12}c_1 + (\lambda - I_{22})c_2 = 0$$

with

$$I_{ij} = \int \vec{\xi}_1 . L_\varepsilon(\vec{\xi}_j)\, dV$$

where $\vec{\xi}_1$ and $\vec{\xi}_2$ have been normalized. Since $\vec{\xi}_1$ and $\vec{\xi}_2$ satisfy the boundary conditions it can be seen from equation (4) in Gabriel (1979) that

$$I_{12} = I_{21}$$

System (5) is valid in a linear approximation, i.e., we may write

$$L_\varepsilon(\vec{\xi}) = L_o(\vec{\xi}) + \varepsilon\Delta L(\vec{\xi}) \tag{6}$$

and

$$I_{ij} = \lambda_i\delta_{ij} + \varepsilon\Delta I_{ij}$$

where δ_{ij} is the Kronecker delta function.

In this approximation we may expect all the ΔI_{ij} to be different from zero. Therefore system (5) is compatible if λ is an eigenvalue of a two by two hermitian matrix. If $I_{12} \neq 0$ such a matrix may not have a double root and the eigenvalues for nonradial oscillations are single.

Let us now consider the conditions of validity of equation (6). We will, of

course, exclude homologous sequences of models for which $L_\varepsilon(\vec{\xi}) \propto L_0(\vec{\xi})$ and which will show no crossing. Since a crossing is possible only if $I_{11} = I_{22}$, then I_{11} or I_{22} or both must satisfy equation (6). Therefore the linear approximation breaks down only if equation (6) is not valid for I_{12}. Since ε may be chosen as close to zero as we want for the mode giving $I_{11} = I_{22}$, the necessary condition for equation (6) not to be valid for I_{12} is that

$$\lim \frac{d\, I_{12}}{d\varepsilon} = 0$$

as $\varepsilon = 0$ is taken closer and closer to the model for which $I_{11} = I_{22}$. When the linear approach is allowed, it is also possible from equations (5) and (6) to study the details of the interaction.

The compatibility condition for equation (5) is given by

$$\lambda^2 - (\Delta I_{11} + \Delta I_{22})\varepsilon\lambda + (\Delta I_{11}\Delta I_{22} - \Delta I_{12}\Delta I_{21})\varepsilon^2 - \lambda(\lambda_1 + \lambda_2) + (\lambda_1 \Delta I_{22} + \lambda_2 \Delta I_{11})\varepsilon + \lambda_1\lambda_2 = 0 \qquad (7)$$

This conic is a hyperbola since the discriminant of the quadratic members δ given by

$$\delta = -\frac{1}{4}(\Delta I_{11} - \Delta I_{22})^2 - \Delta I_{12}\Delta I_{21}$$

is always negative. It is never degenerate since the discriminant of the conic section $\Delta \neq 0$ with

$$\Delta = (\lambda_1 - \lambda_2)^2\, \Delta I_{12}\Delta I_{21}$$

where $\Delta I_{12} = \Delta I_{21}$. The minimum separation $\Delta\lambda_{min}$ is given by

$$\Delta\lambda_{min} = (-\Delta/\delta)^{1/2} \qquad (8)$$

which occurs for ε given by

$$\varepsilon = \frac{(\lambda_1 - \lambda_2)\,(\Delta I_{11} - \Delta I_{22})}{4\delta} \qquad (9)$$

This value of ε gives also the model where the asymptotes of equation (7) cross each other. It may also be noticed that equation (7) gives real values of λ for all ε and the position of the hyperbola with respect to the asymptotes is known.

From equations (5) and (6) we see that λ is given by

$$\lambda_1 - (\lambda_1 + \lambda_2)/2 = \frac{(\Delta I_{11} + \Delta I_{22})\varepsilon \pm \sqrt{(\lambda_1 - \lambda_2)^2 - 4\delta\varepsilon^2 + 2(\lambda_1 - \lambda_2)(\Delta I_{11} - \Delta I_{22})\varepsilon}}{2}$$

When ε becomes large, i.e., when $\Delta\lambda >> (\lambda_1 - \lambda_2)$, C_1/C_2 is given by

$$\frac{c_2}{c_1} = \frac{-(\Delta I_{11} - \Delta I_{22}) \pm \text{sign}(\varepsilon)\sqrt{-4\delta}}{2\Delta I_{12}}$$

where sign $(\varepsilon) = \pm 1$ according to the sign of ε.

Therefore, asymptotically the eigenfunctions corresponding to the smaller (larger) eigenvalue when $\varepsilon < 0$ is the same as that corresponding to the larger (smaller) one when $\varepsilon > 0$. This means, that during the mode interaction, there is an interchange of the properties of the two eigenfunctions.

Introducing

$$y = \Delta I_{12}(\Delta I_{11} - \Delta I_{22})^{-1}$$

we have

$$\frac{c_2}{c_1} = \frac{-1 \pm k\sqrt{4y^2 + 1}}{2y}$$

with $k = \text{sign}(\varepsilon) \cdot \text{sign}(\Delta I_{11} - \Delta I_{22})$. Equation (8) shows that

$$4y^2 = \left[\left(\frac{\lambda_1 - \lambda_2}{\Delta\lambda_{min}}\right)^2 - 1\right]^{-1}$$

and we get

$$\frac{c_2}{c_1} = \text{sign}(y)[-\alpha \pm k\beta] \qquad (11)$$

with

$$\beta = \left|\frac{\lambda_1 - \lambda_2}{\Delta\lambda_{min}}\right| \quad , \qquad \alpha = \sqrt{\beta^2 - 1}$$

It is then possible to express $\vec{\xi}_1$ and $\vec{\xi}_2$ in terms of the two asymptotic solutions $\vec{\xi}_a$ and $\vec{\xi}_b$ for which $\varepsilon = \infty$. If $\vec{\xi}_a$ corresponds to the plus sign in equation (1), we obtain, taking the normalization conditions into account,

$$\vec{\xi}_1 = \frac{\pm 1}{\sqrt{2\beta}} \left[\sqrt{\beta + k\alpha}\, \vec{\xi}_a \pm \sqrt{\beta - k\alpha}\, \vec{\xi}_b \right]$$

$$\vec{\xi}_2 = \frac{\pm 1}{\sqrt{2\beta}} \left[\sqrt{\beta - k\alpha}\, \vec{\xi}_a \mp \sqrt{\beta + k\alpha}\, \vec{\xi}_b \right]$$

where the ± signs in these expressions appear because the sign of $\xi_{1,r}$, $\xi_{2,r}$, $\xi_{a,r}$, and $\xi_{b,r}$ at the surface is not determined. We see that $\vec{\xi}_1$ and $\vec{\xi}_2$ are weighted averages of $\vec{\xi}_a$ and $\vec{\xi}_b$. These weights are equal if $\varepsilon = 0$ at the minimum separation of the eigenvalues. If $\vec{\xi}_a$ and $\vec{\xi}_b$ were defined at $\varepsilon = \infty$, k would change its sign and their coefficients would be interchanged. This shows again that the two eigenvalues are interchanged. The same interchange of the coefficient occurs when $(\Delta I_{11} - \Delta I_{22})$ changes its sign. If we always take $\lambda_1 > \lambda_2$, equation (9) shows that $(\Delta I_{11} - \Delta I_{22})$ changes sign when the origin of ε, i.e., $\varepsilon = 0$, is taken at one side or the other of the model for which the asymptotes cross. The interaction has a symmetry with respect to that model.

Usually $\vec{\xi}_a$ and $\vec{\xi}_b$ have large amplitudes in only one of the two regions where they have an oscillatory spatial behavior. Then $\vec{\xi}_1$ and $\vec{\xi}_2$ have large amplitudes in both regions. This is the situation met for resonances as well as for mode interaction and they are two names given to the same phenomenon.

2.1. Practical Remark

From the definition of $\Delta L(\vec{\xi}_i)$ it may seem difficult to compute the I_{ij}. However, it is easy to obtain them numerically. Let us compute the interaction of two modes $\vec{\xi}_1$ and $\vec{\xi}_2$ for two models close to each other corresponding to $\varepsilon = 0$ and $\varepsilon = \varepsilon_1$. We have

$$c_i^j(\varepsilon_1) = \int \rho \vec{\xi}_i(0) . \vec{\xi}_j(\varepsilon_1)\, dV$$

Equation (5) written for $\vec{\xi}_1(\varepsilon_1)$ and $\vec{\xi}_2(\varepsilon_1)$ give a 4 by 4 system with the I_{ij} as unknown, the solutions are

$$I_{11} = \frac{\lambda_1(\varepsilon_1) c_1^1 c_2^2 - \lambda_2(\varepsilon_1) c_1^2 c_2^1}{c_1^1 c_2^2 - c_2^1 c_1^2}$$

$$I_{22} = \frac{\lambda_2(\varepsilon_1) c_1^1 c_2^2 - \lambda_1(\varepsilon_1) c_2^1 c_1^2}{c_1^1 c_2^2 - c_2^1 c_1^2}$$

$$I_{12} = \frac{[\lambda_2(\varepsilon_1) - \lambda_1(\varepsilon_1)]\ c_1^1 c_1^2}{c_1^1 c_2^2 - c_2^1 c_1^2}$$

$$I_{21} = \frac{[\lambda_1(\varepsilon_1) - \lambda_2(\varepsilon_1)]\ c_2^2 c_2^1}{c_1^1 c_2^2 - c_2^1 c_1^2}$$

The condition $I_{12} = I_{21}$ implies that

$$\frac{c_1^2}{c_2^2} = -\frac{c_2^1}{c_1^1}$$

$$I_{11} = \lambda_1(\varepsilon_1) + \Delta\lambda \qquad , \qquad I_{22} = \lambda_2(\varepsilon_1) - \Delta\lambda$$

where

$$\Delta\lambda = \frac{[\lambda_1(\varepsilon_1) - \lambda_2(\varepsilon_1)]\ c_1^2 c_2^1}{c_1^1 c_2^2 - c_1^2 c_1^2}$$

$\Delta\lambda$ is a second order term. This expression for I_{11} and I_{22} is in good agreement with another expression obtained from the derivative of equation (7) with respect to ε which shows that, (if $\lambda_1 > \lambda_2$),

$$\Delta I_{11} = \lim_{\varepsilon \to o} \frac{\partial \lambda_+}{\partial \varepsilon}$$

$$\Delta I_{22} = \lim_{\varepsilon \to o} \frac{\partial \lambda_-}{\partial \varepsilon}$$

This procedure allows one to compute easily the details of the interaction.

REFERENCES

Aizenman, M., Smeyers, P. and Weigert, A. 1977, Astron. Astrophys., 58, 41.

Boury, A., Scuflaire, R., Noels, A. and Gabriel, M. 1979 (to be published).

Denis, C. 1974, Ph.D. Thesis, Liege.

Gabriel, M. and Scuflaire, R. 1979, Acta. Astr., 29.

Gabriel, M. 1979, submitted to Astron. Astrophys.

Goossens, M. and Smeyers, P. 1974, Astrophys. Sp. Sc., 26, 139.

Ledoux, P. Handb. Phys., 51, 353.

Osaki, Y. 1975, Publ. Astron. Soc. Japan, 27, 237.

Pekeris, C.L., Alterman, Z. and Jarosch, H. 1962, Proc. Nat. As. Sc., 48, 592.

Pekeris, C.L., Alterman, Z. and Jarosch, H. 1963, J. Geophys. Res., 68, 2887.

KEYWORD INDEX TO PAPERS